**U.S. DEPARTMENT OF COMMERCE**
**National Technical Information Service**

PB-288 511

# Environmental Pathways of Selected Chemicals in Freshwater Systems
# Part II. Laboratory Studies

**SRI International, Menlo Park, CA**

**Prepared for**

**Environmental Research Lab, Athens, GA**

May 78

United States
Environmental Protection
Agency

Environmental Research
Laboratory
Athens GA 30605

EPA-600/7-78-074
May 1978

Research and Development

PB 288511

EPA

# Environmental Pathways of Selected Chemicals in Freshwater Systems: Part II. Laboratory Studies

## Interagency Energy-Environment Research and Development Program Report

REPRODUCED BY
NATIONAL TECHNICAL
INFORMATION SERVICE
U. S. DEPARTMENT OF COMMERCE
SPRINGFIELD, VA. 22161

# RESEARCH REPORTING SERIES

Research reports of the Office of Research and Development, U.S. Environmental Protection Agency, have been grouped into nine series. These nine broad categories were established to facilitate further development and application of environmental technology. Elimination of traditional grouping was consciously planned to foster technology transfer and a maximum interface in related fields. The nine series are:

1. Environmental Health Effects Research
2. Environmental Protection Technology
3. Ecological Research
4. Environmental Monitoring
5. Socioeconomic Environmental Studies
6. Scientific and Technical Assessment Reports (STAR)
7. Interagency Energy-Environment Research and Development
8. "Special" Reports
9. Miscellaneous Reports

This report has been assigned to the INTERAGENCY ENERGY-ENVIRONMENT RESEARCH AND DEVELOPMENT series. Reports in this series result from the effort funded under the 17-agency Federal Energy/Environment Research and Development Program. These studies relate to EPA's mission to protect the public health and welfare from adverse effects of pollutants associated with energy systems. The goal of the Program is to assure the rapid development of domestic energy supplies in an environmentally-compatible manner by providing the necessary environmental data and control technology. Investigations include analyses of the transport of energy-related pollutants and their health and ecological effects, assessments of, and development of, control technologies for energy systems, and integrated assessments of a wide range of energy-related environmental issues.

This document is available to the public through the National Technical Information Service, Springfield, Virginia 22161.

## TECHNICAL REPORT DATA

*(Please read Instructions on the reverse before completing)*

| | | |
|---|---|---|
| 1. REPORT NO.<br>EPA-600/7-78-074 | 2. | 3. RECIPIENT'S ACCESSION NO.<br>PB288511 |
| 4. TITLE AND SUBTITLE<br>ENVIRONMENTAL PATHWAYS OF SELECTED CHEMICALS IN FRESHWATER SYSTEMS Part II: Laboratory Studies | | 5. REPORT DATE<br>May 1978 issuing date<br>6. PERFORMING ORGANIZATION CODE |
| 7. AUTHOR(S)<br>J.H. Smith, W.R. Mabey, N. Bohonos, B.R. Holt, S.S. Lee, T-W. Chou, D.C. Bomberger, and T. Mill | | 8. PERFORMING ORGANIZATION REPORT NO. |
| 9. PERFORMING ORGANIZATION NAME AND ADDRESS<br>SRI International<br>333 Ravenswood Avenue<br>Menlo Park, CA 94025 | | 10. PROGRAM ELEMENT NO.<br>1NE625<br>11. CONTRACT/GRANT NO.<br>68-03-2227 |
| 12. SPONSORING AGENCY NAME AND ADDRESS<br>Environmental Research Laboratory--Athens, GA<br>Office of Research and Development<br>U.S. Environmental Protection Agency<br>Athens, GA 30605 | | 13. TYPE OF REPORT AND PERIOD COVERED<br>Final, 6/30/75 to 4/30/77<br>14. SPONSORING AGENCY CODE<br>EPA/600/01 |

15. SUPPLEMENTARY NOTES

See ENVIRONMENTAL PATHWAYS OF SELECTED CHEMICALS IN FRESHWATER SYSTEMS Part I: Background and Experimental Procedures (EPA-600/7-77-113)

16. ABSTRACT

Environmental exposure assessment models and laboratory procedures for predicting the pathways of potentially harmful chemicals in freshwater environments were described in Part I of this report (EPA-600/7-77-113). Procedures were developed for measuring the rates of volatilization, photolysis, oxidation, hydrolysis, and biotransformations as well as the sorption partition coefficients on natural sediments and on a mixture of four bacteria. The results were integrated with a simple computer model to predict the pathways of chemicals in ponds, rivers, and lakes. This second part of the project report describes the successful application of these procedures to 11 chemicals of environmental interest. The chemicals were p-cresol, benz[a]anthracene, benzo[a]pyrene, quinoline, benzo[f]quinoline, 9H-carbazole, 7H-dibenzo[c,g]carbazole, benzo[b]thiophene, and dibenzothiophene, which might be found in the effluents of plants using or processing fossil fuels, and methyl parathion and mirex, which are agricultural pesticides.

17. KEY WORDS AND DOCUMENT ANALYSIS

| a. DESCRIPTORS | b. IDENTIFIERS/OPEN ENDED TERMS | c. COSATI Field/Group |
|---|---|---|
| Adsorption, Sorption, Oxidation, Hydrolysis, Photolysis, Contaminants, Degradation, Mathematical models, Hydrocarbons, Pesticides, Aromatic polycyclic hydrocarbons. | Environmental Assessment, Volatilization, Microbial degradation, Biodegradation, Transformation, Aquatic systems, Environmental simulations, natural waters, Solar photolysis, Biosorption | 57H<br>99A<br>48G<br>68D |

| | | |
|---|---|---|
| 18. DISTRIBUTION STATEMENT<br>Release to Public | 19. SECURITY CLASS *(This Report)*<br>Unclassified | 21. NO. OF PAGES<br>432 |
| | 20. SECURITY CLASS *(This page)*<br>Unclassified | 22. PRICE |

☆ U. S. GOVERNMENT PRINTING OFFICE: 1978 — 757-140/1302

EPA-600/7-78-074
May 1978

# ENVIRONMENTAL PATHWAYS OF SELECTED CHEMICALS IN FRESHWATER SYSTEMS

## Part II: Laboratory Studies

by

J. H. Smith, W. R. Mabey, N. Bohonos,
B. R. Holt, S. S. Lee, T.-W. Chou,
D. C. Bomberger, and T. Mill
SRI International
Menlo Park, California 94025

Contract No. 68-03-2227

Project Officer
George Baughman
Environmental Processes Branch
Environmental Research Laboratory
Athens, Georgia 30605

ENVIRONMENTAL RESEARCH LABORATORY
OFFICE OF RESEARCH AND DEVELOPMENT
U.S. ENVIRONMENTAL PROTECTION AGENCY
ATHENS, GEORGIA 30605

# DISCLAIMER

This report has been reviewed by the Environmental Research Laboratory, U.S. Environmental Protection Agency, Athens, Georgia, and approved for publication. Approval does not signify that the contents necessarily reflect the views and policies of the U.S. Environmental Protection Agency, nor does mention of trade names or commercial products constitute endorsement or recommendation for use.

# FOREWORD

Environmental protection efforts are increasingly directed towards prevention of adverse health and ecological effects associated with specific compounds of natural or human origin. As part of this Laboratory's research on the occurrence, movement, transformation, impact, and control of environmental contaminants, the Environmental Processes Branch studies the microbiological, chemical, and physico-chemical processes that control the transport, transformation, and impact of pollutants in soil and water.

Delineation of the environmental pathways followed by potentially harmful chemicals in freshwater systems is a key element in predicting the effects of pollutants before extensive damage occurs. Based on concepts developed over a number of years at this Laboratory, the extramural work reported here integrates independent transformation and transport processes with hydrologic parameters in a computer model that provides information on environmental exposure in many kinds of aquatic environments.

David W. Duttweiler
Director
Environmental Research Laboratory
Athens, Georgia

# ABSTRACT

Environmental exposure assessment models and laboratory procedures for predicting the pathways of potentially harmful chemicals in freshwater environments were described in Part I of this report (EPA-600/7-77-113). Procedures were developed for measuring the rates of volatilization, photolysis, oxidation, hydrolysis, and biotransformations as well as the sorption partition coefficients on natural sediments and on a mixture of four bacteria. The results were integrated with a simple computer model to predict the pathways of chemicals in ponds, rivers, and lakes. This second part of the project report describes the successful application of these procedures to 11 chemicals of environmental interest. The chemicals were p-cresol, benz[a]anthracene, benzo[a]pyrene, quinoline, benzo[f]quinoline, 9H-carbazole, 7H-dibenzo-[c,g]carbazole, benzo[b]thiophene, and dibenzothiophene, which might be found in the effluents of plants using or processing fossil fuels, and methyl parathion and mirex, which are agricultural pesticides.

This report was submitted in partial fulfillment of Contract No. 68-03-2227 by SRI International under the sponsorship of the U.S. Environmental Protection Agency. This report covers the period from June 30, 1975, to June 30, 1977.

## CONTENTS

Foreword . . . . . iii
Abstract . . . . . iv
Figures . . . . . vii
Tables . . . . . xiii
Abbreviations and Symbols . . . . . xxiii
Acknowledgments. . . . . xxv

1. Introduction . . . . . 1
2. Conclusions . . . . . 2
3. Recommendations . . . . . 5
4. Laboratory Investigation of p-Cresol. . . . . 6
    4.1 Synopsis. . . . . 6
    4.2 Background. . . . . 6
    4.3 Environmental Assessment. . . . . 9
    4.4 Physical Properties . . . . . 18
    4.5 Chemical Transformation . . . . . 20
    4.6 Biodegradation. . . . . 27
5. Laboratory Investigation of Benz[a]anthracene . . . . . 39
    5.1 Synopsis. . . . . 39
    5.2 Background. . . . . 39
    5.3 Environmental Assessment. . . . . 42
    5.4 Physical Properties . . . . . 46
    5.5 Chemical Transformation . . . . . 57
    5.6 Biodegradation. . . . . 62
6. Laboratory Investigation of Benzo[a]pyrene. . . . . 64
    6.1 Synopsis. . . . . 64
    6.2 Background. . . . . 64
    6.3 Environmental Assessment. . . . . 67
    6.4 Physical Properties . . . . . 75
    6.5 Chemical Transformation . . . . . 81
    6.6 Biodegradation. . . . . 90
7. Laboratory Investigation of Quinoline . . . . . 93
    7.1 Synopsis. . . . . 93
    7.2 Background. . . . . 93
    7.3 Environmental Assessment. . . . . 96
    7.4 Physical Properties . . . . . 104
    7.5 Chemical Transformation . . . . . 106
    7.6 Biodegradation. . . . . 112
8. Laboratory Investigation of Benzo[f]quinoline . . . . . 122
    8.1 Synopsis. . . . . 122
    8.2 Background. . . . . 122
    8.3 Environmental Assessment. . . . . 124

8.4 Physical Properties . . . . . . . . . . . . . . . . . . . . 126
8.5 Chemical Transformation . . . . . . . . . . . . . . . . . . . 134
8.6 Biodegradation . . . . . . . . . . . . . . . . . . . . . . 138
9. Laboratory Investigation of 9H-Carbazole . . . . . . . . . . . 143
9.1 Synopsis . . . . . . . . . . . . . . . . . . . . . . . . . 143
9.2 Background . . . . . . . . . . . . . . . . . . . . . . . . 143
9.3 Environmental Assessment . . . . . . . . . . . . . . . . . . 145
9.4 Physical Properties . . . . . . . . . . . . . . . . . . . . 154
9.5 Chemical Transformation . . . . . . . . . . . . . . . . . . . 156
9.6 Biodegradation . . . . . . . . . . . . . . . . . . . . . . 159
10. Laboratory Investigation of 7H-Dibenzo[c,g]carbazole . . . . . 167
10.1 Synopsis . . . . . . . . . . . . . . . . . . . . . . . . 167
10.2 Background . . . . . . . . . . . . . . . . . . . . . . . 167
10.3 Environmental Assessment . . . . . . . . . . . . . . . . . 171
10.4 Physical Properties . . . . . . . . . . . . . . . . . . . 177
10.5 Chemical Transformation . . . . . . . . . . . . . . . . . . 182
10.6 Biodegradation . . . . . . . . . . . . . . . . . . . . . . 189
11. Laboratory Investigation of Benzo[b]thiophene . . . . . . . . 191
11.1 Synopsis . . . . . . . . . . . . . . . . . . . . . . . . 191
11.2 Background . . . . . . . . . . . . . . . . . . . . . . . 192
11.3 Environmental Assessment . . . . . . . . . . . . . . . . . 193
11.4 Physical Properties . . . . . . . . . . . . . . . . . . . 202
11.5 Chemical Transformation . . . . . . . . . . . . . . . . . . 209
11.6 Biodegradation . . . . . . . . . . . . . . . . . . . . . . 212
12. Laboratory Investigation of Dibenzothiophene . . . . . . . . . 216
12.1 Synopsis . . . . . . . . . . . . . . . . . . . . . . . . 216
12.2 Background . . . . . . . . . . . . . . . . . . . . . . . 216
12.3 Environmental Assessment . . . . . . . . . . . . . . . . . 219
12.4 Physical Properties . . . . . . . . . . . . . . . . . . . 227
12.5 Chemical Transformation . . . . . . . . . . . . . . . . . . 231
12.6 Biodegradation . . . . . . . . . . . . . . . . . . . . . . 234
13. Laboratory Investigation of Methyl Parathion . . . . . . . . . 248
13.1 Synopsis . . . . . . . . . . . . . . . . . . . . . . . . 248
13.2 Background . . . . . . . . . . . . . . . . . . . . . . . 249
13.3 Environmental Assessment . . . . . . . . . . . . . . . . . 252
13.4 Physical Properties . . . . . . . . . . . . . . . . . . . 260
13.5 Chemical Transformation . . . . . . . . . . . . . . . . . . 267
13.6 Biodegradation . . . . . . . . . . . . . . . . . . . . . . 278
14. Laboratory Investigation of Mirex . . . . . . . . . . . . . . 294
14.1 Synopsis . . . . . . . . . . . . . . . . . . . . . . . . 294
14.2 Background . . . . . . . . . . . . . . . . . . . . . . . 294
14.3 Environmental Assessment . . . . . . . . . . . . . . . . . 296
14.4 Physical Properties . . . . . . . . . . . . . . . . . . . 300
14.5 Chemical Transformation . . . . . . . . . . . . . . . . . . 307
14.6 Biodegradation . . . . . . . . . . . . . . . . . . . . . . 312
15. References . . . . . . . . . . . . . . . . . . . . . . . . 316

Appendices

A. Input Data for Nine-Compartment Model . . . . . . . . . . . . 333
B. Experimental Procedures . . . . . . . . . . . . . . . . . . . 376
C. Natural Water Sources . . . . . . . . . . . . . . . . . . . . 404

## FIGURES

| Number | | Page |
|---|---|---|
| 4.1 | Persistence of p-Cresol in a Two-Compartment Pond System . . . | 12 |
| 4.2 | Persistence of p-Cresol in a Partially Mixed River System . . | 14 |
| 4.3 | Persistence of p-Cresol in a Partially Mixed Eutrophic Lake . . . . . . . . . . . . . . . . . . . . . . . . . . . | 15 |
| 4.4 | Persistence of p-Cresol in a Partially Mixed Oligotrophic Lake . . . . . . . . . . . . . . . . . . . . . . . . . . . | 16 |
| 4.5 | Annual Variation of Photolysis Half-Life for p-Cresol . . . . | 24 |
| 4.6 | Biodegradation of p-Cresol in Eutrophic Pond Water . . . . . . | 28 |
| 4.7 | Viable Cell Counts in 0, 3, and 5 $\mu g\ ml^{-1}$ p-Cresol Biodegradation by Batch Fermentation with a Low-Level Inoculum . . . . . . . . . . . . . . . . . . . . . . . . . | 30 |
| 4.8 | Viable Cell Counts in 0, 10, and 20 $\mu g\ ml^{-1}$ p-Cresol Biodegradation by Batch Fermentation with a Low-Level Inoculum . . . . . . . . . . . . . . . . . . . . . . . . . | 31 |
| 4.9 | p-Cresol Biodegradation by Batch Fermentation with a Low-Level Inoculum . . . . . . . . . . . . . . . . . . . . . | 32 |
| 4.10 | Lineweaver-Burk Plot of Data from p-Cresol Biodegradation in a Batch Fermentation Study . . . . . . . . . . . . . . . . | 34 |
| 4.11 | Lineweaver-Burk Plot of Data from p-Cresol Biodegradation in a Continuous Fermentation . . . . . . . . . . . . . . . . . | 37 |
| 5.1 | Persistence of Benz[a]anthracene in a Partially Mixed Oligotrophic Lake . . . . . . . . . . . . . . . . . . . . . | 47 |
| 5.2 | Persistence of Benz[a]anthracene in a Partially Mixed Eutrophic Lake . . . . . . . . . . . . . . . . . . . . . . . . | 48 |
| 5.3 | Persistence of Benz[a]anthracene in a Two-Compartment Pond System . . . . . . . . . . . . . . . . . . . . . . . . . | 49 |
| 5.4 | Persistence of Benz[a]anthracene in a Partially Mixed River System . . . . . . . . . . . . . . . . . . . . . . . . . | 50 |

FIGURES (Continued)

| Number | | Page |
|---|---|---|
| 5.5 | Sorption Isotherms of Benz[a]anthracene on Coyote Creek and Des Moines River Sediments . . . . . . . . . . . . . . . . . | 54 |
| 5.6 | Sorption and Desorption Isotherms of Benz[a]anthracene (Searsville Sediment). . . . . . . . . . . . . . . . . . . . . | 55 |
| 5.7 | Seasonal and Daily Variation of Photolysis Half-Life of Benz[a]anthracene . . . . . . . . . . . . . . . . . . . . | 60 |
| 6.1 | Persistence of Benzo[a]pyrene in a Two-Compartment Pond System . . . . . . . . . . . . . . . . . . . . . . . . . . | 71 |
| 6.2 | Persistence of Benzo[a]pyrene in a Partially Mixed River System . . . . . . . . . . . . . . . . . . . . . . . . | 72 |
| 6.3 | Persistence of Benzo[a]pyrene in a Eutrophic Lake . . . . . . | 73 |
| 6.4 | Persistence of Benzo[a]pyrene in an Oligotrophic Lake . . . . | 74 |
| 6.5 | Sorption Isotherms of Benzo[a]pyrene . . . . . . . . . . . . | 78 |
| 6.6 | Seasonal and Daily Variation of Photolysis Half-Life of Benzo[a]pyrene . . . . . . . . . . . . . . . . . . . . . . | 84 |
| 7.1 | Persistence of Quinoline in a Two-Compartment Pond System . . | 100 |
| 7.2 | Persistence of Quinoline in a Partially Mixed River System . . | 101 |
| 7.3 | Persistence of Quinoline in a Partially Mixed Eutrophic Lake . . . . . . . . . . . . . . . . . . . . . . . . . . . | 102 |
| 7.4 | Persistence of Quinoline in a Partially Mixed Oligotrophic Lake . . . . . . . . . . . . . . . . . . . . . . . . . . . | 103 |
| 7.5 | Direct Photolysis of Quinoline at pH 6.9 and pH 4.4 . . . . . | 109 |
| 7.6 | Annual Variation of Photolysis Half-Life of Quinoline. . . . . | 111 |
| 7.7 | Cascade Batch Fermentations with a Freshly Developed Degrading System Transferred in Fresh Pond Water Media . . . . | 113 |
| 7.8 | Viable Counts in Quinoline Degradation by Batch Fermentations with Low-Level Inocula . . . . . . . . . . . . . . . . . . . . | 115 |
| 7.9 | Quinoline Biodegradation by Batch Fermentations with Low-Level Inocula. . . . . . . . . . . . . . . . . . . . . | 116 |

FIGURES (Continued)

| Number | | Page |
|---|---|---|
| 7.10 | Lineweaver-Burk Plot for Data from Quinoline Biodegradation in a Batch Fermentations with Low-Level Inocula . . . . . . . | 117 |
| 7.11 | Quinoline Utilization in Cascade Batch Fermentations. . . . . | 120 |
| 8.1 | Persistence of Benzo[f]quinoline in a Two-Compartment Pond System . . . . . . . . . . . . . . . . . . . . . . . . | 128 |
| 8.2 | Persistence of Benzo[f]quinoline in a Partially Mixed River System . . . . . . . . . . . . . . . . . . . . . . . . | 129 |
| 8.3 | Persistence of Benzo[f]quinoline in a Eutrophic Lake . . . . | 130 |
| 8.4 | Persistence of Benzo[f]quinoline in an Oligotrophic Lake. . . | 131 |
| 8.5 | Seasonal and Daily Variation of Photolysis Half-Life of Benzo[f]quinoline . . . . . . . . . . . . . . . . . . . . . . | 137 |
| 8.6 | Benzo[f]quinoline Biodegradation in Batch Fermentations with High Cell Counts . . . . . . . . . . . . . . . . . . . | 141 |
| 9.1 | Persistence of 9H-Carbazole in a Partially Mixed Two-Compartment Pond System . . . . . . . . . . . . . . . . . . | 150 |
| 9.2 | Persistence of 9H-Carbazole in a Partially Mixed River System. . . . . . . . . . . . . . . . . . . . . . . . . | 151 |
| 9.3 | Persistence of 9H-Carbazole in a Eutrophic Lake . . . . . . . | 152 |
| 9.4 | Persistence of 9H-Carbazole in an Oligotrophic Lake . . . . . | 153 |
| 9.5 | Seasonal and Daily Variation of Photolysis Half-Life of 9H-Carbazole . . . . . . . . . . . . . . . . . . . . . . . | 160 |
| 9.6 | 9H-Carbazole Biodegradation in Batch Fermentation with High Cell Counts (Experiment 1) . . . . . . . . . . . . . . . | 163 |
| 9.7 | 9H-Carbazole Biodegradation in Batch Fermentation with High Cell Counts (Experiment 2) . . . . . . . . . . . . . . . | 164 |
| 10.1 | Persistence of 7H-Dibenzo[c,g]carbazole in a Partially Mixed Two-Compartment Pond System . . . . . . . . . . . . . . | 173 |
| 10.2 | Persistence of 7H-Dibenzo[c,g]carbazole in a Partially Mixed River System. . . . . . . . . . . . . . . . . . . . . . . | 174 |

FIGURES (Continued)

Number Page

10.3 Persistence of 7H-Dibenzo[c,g]carbazole in a Eutrophic Lake . . . . . . . . . . . . . . . . . . . . . . . . . . . . 175

10.4 Persistence of 7H-Dibenzo[c,g]carbazole in an Oligotrophic Lake. . . . . . . . . . . . . . . . . . . . . . . . . . 176

10.5 Sorption Isotherms of 7H-Dibenzo[c,g]carbazole . . . . . . . . 182

10.6 Seasonal and Daily Variation of Photolysis Half-Life for 7H-Dibenzo[c,g]carbazole . . . . . . . . . . . . . . . . . . 188

11.1 Persistence of Benzo[b]thiophene in a Partially Mixed Two-Compartment Pond System . . . . . . . . . . . . . . . . . 198

11.2 Persistence of Benzo[b]thiophene in a Partially Mixed River System . . . . . . . . . . . . . . . . . . . . . . . . 199

11.3 Persistence of Benzo[b]thiophene in a Partially Mixed Eutrophic Lake . . . . . . . . . . . . . . . . . . . . . . . 200

11.4 Persistence of Benzo[b]thiophene in a Partially Mixed Oligotrophic Lake. . . . . . . . . . . . . . . . . . . . . . . 201

11.5 Volatilization of Benzo[b]thiophene from Aqueous Solution. . . 204

11.6 Annual Variation of Photolysis Half-Life for Benzo[b]thiophene . . . . . . . . . . . . . . . . . . . . . . . 211

12.1 Persistence of Dibenzothiophene in a Two-Compartment Pond System. . . . . . . . . . . . . . . . . . . . . . . . . . 223

12.2 Persistence of Dibenzothiophene in a Partially Mixed River System . . . . . . . . . . . . . . . . . . . . . . . . . 224

12.3 Persistence of Dibenzothiophene in a Eutrophic Lake. . . . . . 225

12.4 Persistence of Dibenzothiophene in an Oligotrophic Lake. . . . 226

12.5 Volatilization of Dibenzothiophene from Aqueous Solution . . . 229

12.6 Annual Variation of Photolysis Half-Life of Dibenzothiophene . . . . . . . . . . . . . . . . . . . . . . . . 233

12.7 Dibenzothiophene Biodegradation in Batch Fermentation with High Cell Counts . . . . . . . . . . . . . . . . . . . . . . . 238

FIGURES (Continued)

Number Page

12.8 Metabolism of Dibenzothiophene . . . . . . . . . . . . . . . . 239

12.9 Mass Spectrum of Compound A, Dibenzothiophene-5-oxide. . . . . 240

12.10 Mass Spectra of Compound B, Bis-trimethylsilyl Ether . . . . . 241

12.11 Mass Spectra of Compound C, Bis-trimethylsilyl Derivative, Isomer 1 . . . . . . . . . . . . . . . . . . . . . 242

12.12 Mass Spectra of Compound D, Bis-trimethylsilyl Derivative, Isomer 2 . . . . . . . . . . . . . . . . . . . . . 243

12.13 Mass Spectrum of Compound E, Trimethylsilyl Ether. . . . . . . 244

12.14 Mass Spectrum of Compound F, Trimethylsilyl Ether. . . . . . . 245

12.15 Mass Spectrum of Compound G. . . . . . . . . . . . . . . . . . 246

13.1 Persistence of Methyl Parathion in a Two-Compartment Pond System. . . . . . . . . . . . . . . . . . . . . . . . . 256

13.2 Persistence of Methyl Parathion in a Partially Mixed River System . . . . . . . . . . . . . . . . . . . . . . . . 257

13.3 Persistence of Methyl Parathion in a Eutrophic Lake . . . . . 258

13.4 Persistence of Methyl Parathion in an Oligotrophic Lake. . . . 259

13.5 Concentration of Methyl Parathion in Supernatant . . . . . . . 264

13.6 Desorption of Methyl Parathion from Coyote Creek Sediment. . . 266

13.7 Annual Variation of Photolysis Half-Life of Methyl Parathion . . . . . . . . . . . . . . . . . . . . . . . . . 270

13.8 pH Rate Profile for Methyl Parathion at 40°C . . . . . . . . . 274

13.9 Cell Counts and MP Concentrations in Batch Fermentations with Low Count Inocula of Rested Cells . . . . . . . . . . . . 282

13.10 Methyl Parathion Utilization in Batch Fermentations with Low Count Inocula of Rested Cells. . . . . . . . . . . . . . . 283

13.11 Methyl Parathion Degradation in Batch Fermentations with Low Inoculum of Rested Cells . . . . . . . . . . . . . . . . . 285

## FIGURES (Concluded)

Number Page

13.12 Lineweaver-Burk Plot of Specific Growth Rates and Substrate Concentrations for Continuous Feed Chemostat Fermentations . . . . . . . . . . . . . . . . . . . . . . . . 287

13.13 Cascade Batch Fermentation of Methyl Parathion . . . . . . 289

13.14 Batch Fermentation with a High Population of MP-Degrading Organisms . . . . . . . . . . . . . . . . . . . . . . . . 290

13.15 Mass Spectrum of the Trimethylsilyl Derivative of *p*-nitrophenol . . . . . . . . . . . . . . . . . . . . . . 293

14.1 Persistence of Mirex in a Two-Compartment Pond System . . . 301

14.2 Persistence of Mirex in a Partially Mixed Lake. . . . . . . 302

14.3 Persistence of Mirex in a Partially Mixed River System. . . 303

# TABLES

| Number | | Page |
|---|---|---|
| 2.1 | Summary of Equilibria and Rate Processes at 25°C | 3 |
| 2.2 | Summary of Environmental Assessments | 4 |
| 4.1 | Physical Properties of p-Cresol | 7 |
| 4.2 | Summary of p-Cresol Laboratory Data | 10 |
| 4.3 | Transformation and Transport of p-Cresol Predicted by the One-Compartment Model | 11 |
| 4.4 | Distribution of p-Cresol in Various Aquatic Systems at Steady State | 13 |
| 4.5 | Absorption Spectra of p-Cresol in Pure Water | 19 |
| 4.6 | Volatilization Rate Constants for p-Cresol | 20 |
| 4.7 | p-Cresol Sorption on Sediments | 21 |
| 4.8 | Rate Constants for Photolysis of 1.0 μg $ml^{-1}$ p-Cresol | 22 |
| 4.9 | Free Radical Oxidation of 0.72 μg $ml^{-1}$ p-Cresol at 50°C and 100 hours | 25 |
| 4.10 | Yield of Cells in a p-Cresol Batch Fermentation with a Low-Level Inoculum | 33 |
| 4.11 | First-Order Rate Constants in a p-Cresol Batch Fermentation with a Low-Level Inoculum | 35 |
| 4.12 | Kinetics of a p-Cresol Biodegradation in a Continuous Fermentation | 36 |
| 4.13 | Comparison of Kinetic Data Obtained on Biodegradation of p-Cresol by Two Procedures | 38 |
| 5.1 | Physical Properties of Benz[a]anthracene | 40 |
| 5.2 | Summary of Benz[a]anthracene Laboratory Data | 42 |
| 5.3 | Transformation and Transport of Benz[a]anthracene Predicted by the One-Compartment Model | 43 |

## TABLES (Continued)

Number | | Page
5.4 Distribution of Benz[a]anthracene in Various Aquatic Systems at Steady State . . . . . . . . . . . . . . . . . . . . 45

5.5 Absorption Spectrum of Benz[a]anthracene in 50% Acetonitrile/50% Water at pH 7 . . . . . . . . . . . . . . . . . . 52

5.6 Benz[a]anthracene Sorption on Sediments . . . . . . . . . . . . 53

5.7 Benz[a]anthracene Sorption and Desorption on a Mixed Bacterial Population. . . . . . . . . . . . . . . . . . . . . . 57

5.8 Benz[a]anthracene Sorption by Viable and Heat-Killed Bacteria . . . . . . . . . . . . . . . . . . . . . . . . . . 57

5.9 Rate Constants for Photolysis of Benz[a]anthracene With Air . . . . . . . . . . . . . . . . . . . . . . . . . . 58

6.1 Physical Properties of Benzo[a]pyrene . . . . . . . . . . . . . 65

6.2 Summary of Benzo[a]pyrene Laboratory Data . . . . . . . . . . . 67

6.3 Transformation and Transport of Benzo[a]pyrene Predicted by the One-Compartment Model. . . . . . . . . . . . . . . . . 68

6.4 Distribution of Benzo[a]pyrene in Various Aquatic Systems at Steady State . . . . . . . . . . . . . . . . . . . . . . . . 70

6.5 Absorption Spectrum of Benzo[a]pyrene in 20% Acetonitrile/ 80% Water at pH 6 . . . . . . . . . . . . . . . . . . . . . . . 77

6.6 Benzo[a]pyrene Sorption on Coyote Creek Sediments . . . . . . . 80

6.7 Benzo[a]pyrene Sorption and Desorption on a Mixed Bacterial Population . . . . . . . . . . . . . . . . . . . . . 81

6.8 Rate Constants for Photolysis of Benzo[a]pyrene . . . . . . . . 82

6.9 Product Yields and Material Balance for Benzo[a]pyrene Photolysis and Free-Radical Oxidation . . . . . . . . . . . . . 86

6.10 Rate Constants for Singlet Oxygen Addition to Benzo[a]pyrene and Benz[a]anthracene . . . . . . . . . . . . . 89

7.1 Physical Properties of Quinoline . . . . . . . . . . . . . . . . 95

7.2 Summary of Quinoline Laboratory Data . . . . . . . . . . . . . 96

TABLES (Continued)

Number Page

7.3 Transformation and Transport of Quinoline Predicted by the One-Compartment Model . . . . . . . . . . . . . . . . . . 97

7.4 Distribution of Quinoline in Various Aquatic Systems at Steady State . . . . . . . . . . . . . . . . . . . . . . . 99

7.5 Absorption Spectra of Quinoline in Water at pH 4.7 and pH 6.8 . . . . . . . . . . . . . . . . . . . . . . . . . 105

7.6 Quinoline Sorption on Sediments . . . . . . . . . . . . . . . . 107

7.7 Rate Constants for Photolysis of Quinoline. . . . . . . . . . 110

7.8 Quinoline Biodegradations in Batch Fermentations with Low-Level Inocula . . . . . . . . . . . . . . . . . . . . . . 118

7.9 Quinoline Degradations in Cascade Batch Fermentations . . . . 121

8.1 Physical Properties of Benzo[f]quinoline. . . . . . . . . . . 123

8.2 Summary of Benzo[f]quinoline Laboratory Data. . . . . . . . . 124

8.3 Transformation and Transport of Benzo[f]quinoline Predicted by the One-Compartment Model . . . . . . . . . . . 125

8.4 Distribution of Benzo[f]quinoline in Various Aquatic Systems at Steady State . . . . . . . . . . . . . . . . . . . . 127

8.5 Absorption Spectra of Benzo[f]quinoline in Water . . . . . . 132

8.6 Sorption of Benzo[f]quinoline on Coyote Creek Sediment. . . . 133

8.7 Biosorption of Benzo[f]quinoline . . . . . . . . . . . . . . 134

8.8 Rate Constants for Photolysis of Benzo[f]quinoline. . . . . . 135

8.9 Development of Benzo[f]quinoline Biodegrading Enrichment Cultures . . . . . . . . . . . . . . . . . . . . . 140

8.10 Viable Cell Counts During Pseudo-First-Order Biodegradation Studies with Benzo[f]quinoline. . . . . . . . . . . . . . . 142

9.1 Physical Properties of 9H-Carbazole . . . . . . . . . . . . . 144

9.2 Summary of 9H-Carbazole Laboratory Data . . . . . . . . . . . 145

TABLES (Continued)

Number Page

9.3 Transformation and Transport of 9H-Carbazole Predicted by the One-Compartment Model . . . . . . . . . . . . . . . . . . 146

9.4 Distribution of 9H-Carbazole in Various Aquatic Systems at Steady State . . . . . . . . . . . . . . . . . . . . . . 148

9.5 Absorption Spectrum of 9H-Carbazole in 26% Acetonitrile/74% Water at pH 7 . . . . . . . . . . . . . . . . . . . . . . 155

9.6 Sorption of 9H-Carbazole on Sediments . . . . . . . . . . . . 157

9.7 Rate Constants for Photolysis of 1.0 $\mu$g ml$^{-1}$ 9H-Carbazole. . . 158

9.8 Development of 9H-Carbazole Biodegradation Enrichment Cultures. . . . . . . . . . . . . . . . . . . . . . . 161

9.9 Cell Counts During Kinetic Studies of the Biodegradation of 9H-Carbazole . . . . . . . . . . . . . . . 162

9.10 Rate Constants for Biodegradation of 9H-Carbazole. . . . . . . 165

10.1 Physical Properties of 7H-Dibenzo[c,g]carbazole. . . . . . . . 168

10.2 Summary of 7H-Dibenzo[c,g]carbazole Laboratory Data. . . . . . 169

10.3 Transformation and Transport of 7H-Dibenzo[c,g]carbazole Predicted by the One-Compartment Model . . . . . . . . . . . . 170

10.4 Distribution of 7H-Dibenzo[c,g]carbazole in Various Aquatic Systems at Steady State. . . . . . . . . . . . . . . . 171

10.5 Absorption Spectrum of 7H-Dibenzo[c,g]carbazole in 5% Acetonitrile/95% Water at pH 4.5. . . . . . . . . . . . . . 178

10.6 Absorption Spectra of 7H-Dibenzo[c,g]carbazole in 50% Acetonitrile/50% Water . . . . . . . . . . . . . . . . . . . 179

10.7 Sorption of 7H-Dibenzo[c,g]carbazole on Sediments. . . . . . . 181

10.8 7H-Dibenzo[c,g]carbazole Sorption and Desorption with Mixed Bacterial Population . . . . . . . . . . . . . . . . . . 184

10.9 Rate Constants for Photolysis of 7H-Dibenzo[c,g]carbazole. . . 186

11.1 Physical Properties of Benzo[b]thiophene . . . . . . . . . . . 192

TABLES (Continued)

Number Page

11.2 Summary of Benzo[b]thiophene Laboratory Data . . . . . . . . . . 194

11.3 Transformation and Transport of Benzo[b]thiophene Predicted by the One-Compartment Model . . . . . . . . . . . . 195

11.4 Distribution of Benzo[b]thiophene in Various Aquatic Systems at Steady State . . . . . . . . . . . . . . . . . . . 197

11.5 Absorption Spectra of Benzo[b]thiophene in Water at pH 6.6 . . . . . . . . . . . . . . . . . . . . . . . 203

11.6 Volatilization Rate Data for Benzo[b]thiophene . . . . . . . . 205

11.7 Sorption of Benzo[b]thiophene on Sediments . . . . . . . . . . 207

11.8 Biosorption of Benzo[b]thiophene by Mixed Bacterial Cultures . . . . . . . . . . . . . . . . . . . . . . . . 208

11.9 Rate Constants for Photolysis of 1.0 μg $ml^{-1}$ Benzo[b]thiophene. 209

12.1 Physical Properties of Dibenzothiophene. . . . . . . . . . . . 217

12.2 Summary of Laboratory Data for Dibenzothiophene. . . . . . . . 220

12.3 Transformation and Transport of Dibenzothiophene Predicted by the One-Compartment Model . . . . . . . . . . . . . . . . . 220

12.4 Distribution of Dibenzothiophene in Various Aquatic Systems at Steady State. . . . . . . . . . . . . . . . . . . 222

12.5 Absorption Spectrum of Dibenzothiophene in 30% Acetonitrile/70% Water at pH 7 . . . . . . . . . . . . . . . . . . . . . 227

12.6 Volatilization Data for Dibenzothiophene . . . . . . . . . . . 228

12.7 Dibenzothiophene Sorption on Coyote Creek Sediment . . . . . . 230

12.8 Biosorption of Dibenzothiophene. . . . . . . . . . . . . . . . 231

12.9 Rate Constants for Photolysis of 0.5 μg $ml^{-1}$ Dibenzothiophene . . . . . . . . . . . . . . . . . . . . . 232

12.10 Development of Dibenzothiophene Biodegrading Enrichment Cultures. . . . . . . . . . . . . . . . . . . . . . . 236

12.11 Viable Cell Counts During Pseudo-First-Order Biodegradation Kinetic Studies with Dibenzothiophene . . . . . . . . . . . . 237

TABLES (Continued)

Number Page

13.1 Physical Properties of Methyl Parathion . . . . . . . . . . . 249

13.2 Summary of Methyl Parathion Laboratory Data . . . . . . . . . . 252

13.3 Transformation and Transport of Methyl Parathion Predicted by the One-Compartment Model. . . . . . . . . . . . . . . . . 253

13.4 Distribution of Methyl Parathion in Various Aquatic Systems at Steady State . . . . . . . . . . . . . . . . . . . 255

13.5 Absorption Spectrum of Methyl Parathion in Water . . . . . . 261

13.6 Methyl Parathion Sorption on Sediments. . . . . . . . . . . . 263

13.7 Sorption Partition Coefficients of Methyl Parathion on a Mixed Bacterial Population. . . . . . . . . . . . . . . . . 267

13.8 Rate Constants for Photolysis of 26 $\mu g\ ml^{-1}$ Methyl Parathion . . . . . . . . . . . . . . . . . . . . 268

13.9 Free Radical Oxidation of Methyl Parathion at 50°C. . . . . . 269

13.10 First-Order Rate Constants $k_H$ for Hydrolysis of Methyl Parathion as a Function of pH . . . . . . . . . . . . . . . 272

13.11 First-Order Rate Constants $k_H$ for Hydrolysis of Methyl Parathion in Natural Waters . . . . . . . . . . . . . . . . 273

13.12 Temperature Dependence of Rate Constants for Neutral ($k_N$) and Base-Catalyzed ($k_B$) Hydrolysis of Methyl Parathion. . . . 275

13.13 Product Balance for Hydrolysis and Photolysis of Methyl Parathion . . . . . . . . . . . . . . . . . . . . . . . . 276

13.14 Cell Counts in Batch Fermentations with Low Count Inocula of Rested Cells . . . . . . . . . . . . . . . . . . 280

13.15 Methyl Parathion Utilization in Batch Fermentations with Low Count Inocula of Rested Cells . . . . . . . . . . . 281

13.16 Summary of Data and Kinetic Constants in Batch Fermentations with Low Count Inocula of Rested Cells . . . . . . . . . . . 284

13.17 Data From Continuous Feed Chemostat Fermentations . . . . . . 286

13.18 Summary of Kinetic Constants for Methyl Parathion Biodegradation. . . . . . . . . . . . . . . . . . . . . . . . 292

TABLES (Continued)

Number Page

14.1 Physical Properties of Mirex . . . . . . . . . . . . . . . . . 295

14.2 Summary of Mirex Laboratory Data . . . . . . . . . . . . . . . 296

14.3 Transformation and Transport of Mirex Predicted by the One-Compartment Model. . . . . . . . . . . . . . . . . . . 297

14.4 Distribution of Mirex in Various Aquatic Systems at Steady State . . . . . . . . . . . . . . . . . . . . . . . . 299

14.5 Sorption of Mirex on Coyote Creek Sediment . . . . . . . . . . 306

14.6 Mirex Sorption and Desorption on a Mixed Bacterial Population . . . . . . . . . . . . . . . . . . . . . . . . 307

14.7 Aerobic Mirex Enrichment Studies with Aeration Effluents . . . 313

A.1 Nine-Compartment Computer Model Inputs for _p_-Cresol: Pond Simulation . . . . . . . . . . . . . . . . . . . . . . . . 333

A.2 Nine-Compartment Computer Model Inputs for _p_-Cresol: River Simulation . . . . . . . . . . . . . . . . . . . . . . . . 334

A.3 Nine-Compartment Computer Model Inputs for _p_-Cresol: Eutrophic Lake Simulation . . . . . . . . . . . . . . . . . . 335

A.4 Nine-Compartment Computer Model Inputs for _p_-Cresol: Oligotrophic Lake Simulation . . . . . . . . . . . . . . . . 336

A.5 Nine-Compartment Computer Model Inputs for Benz[a]anthracene: Pond Simulation . . . . . . . . . . . . . . . . . . . . . . 337

A.6 Nine-Compartment Computer Model Inputs for Benz[a]anthracene: River Simulation . . . . . . . . . . . . . . . . . . . . . . 338

A.7 Nine-Compartment Computer Model Inputs for Benz[a]anthracene: Eutrophic Lake Simulation . . . . . . . . . . . . . . . . . . 339

A.8 Nine-Compartment Computer Model Inputs for Benz[a]anthracene: Oligotrophic Lake Simulation . . . . . . . . . . . . . . . . 340

A.9 Nine-Compartment Computer Model Inputs for Benzo[a]pyrene: Pond Simulation . . . . . . . . . . . . . . . . . . . . . . 341

A.10 Nine-Compartment Computer Model Inputs for Benzo[a]pyrene: River Simulation . . . . . . . . . . . . . . . . . . . . . . 342

TABLES (Continued)

Number Page

A.11 Nine-Compartment Computer Model Inputs for Benzo[a]pyrene: Eutrophic Lake Simulation . . . . . . . . . . . . . . . . . . . . 343

A.12 Nine-Compartment Computer Model Inputs for Benzo[a]pyrene: Oligotrophic Lake Simulation . . . . . . . . . . . . . . . . . 344

A.13 Nine-Compartment Computer Model Inputs for Quinoline: Pond Simulation. . . . . . . . . . . . . . . . . . . . . . . . . 345

A.14 Nine-Compartment Computer Model Inputs for Quinoline: River Simulation . . . . . . . . . . . . . . . . . . . . . . 346

A.15 Nine-Compartment Computer Model Inputs for Quinoline: Eutrophic Lake Simulation . . . . . . . . . . . . . . . . . . . . 347

A.16 Nine-Compartment Computer Model Inputs for Quinoline: Oligotrophic Lake Simulation . . . . . . . . . . . . . . . . . 348

A.17 Nine-Compartment Computer Model Inputs for Benzo[f]quinoline: Pond Simulation . . . . . . . . . . . . . . . . . . . . . . 349

A.18 Nine-Compartment Computer Model Inputs for Benzo[f]quinoline: River Simulation. . . . . . . . . . . . . . . . . . . . . . 350

A.19 Nine-Compartment Computer Model Inputs for Benzo[f]quinoline: Eutrophic Lake Simulation . . . . . . . . . . . . . . . . . . . . 351

A.20 Nine-Compartment Computer Model Inputs for Benzo[f]quinoline: Oligotrophic Lake Simulation . . . . . . . . . . . . . . . . . 352

A.21 Nine-Compartment Computer Model Inputs for Carbazole: Pond Simulation . . . . . . . . . . . . . . . . . . . . . . 353

A.22 Nine-Compartment Computer Model Inputs for Carbazole: River Simulation. . . . . . . . . . . . . . . . . . . . . . 354

A.23 Nine-Compartment Computer Model Inputs for Carbazole: Eutrophic Lake Simulation . . . . . . . . . . . . . . . . . . . . 355

A.24 Nine-Compartment Computer Model Inputs for Carbazole: Oligotrophic Lake Simulation . . . . . . . . . . . . . . . . . 356

A.25 Nine-Compartment Computer Model Inputs for 7H-Dibenzo[c,g]-carbazole: Pond Simulation. . . . . . . . . . . . . . . . . . 357

A.26 Nine-Compartment Computer Model Inputs for 7H-Dibenzo[c,g]-carbazole: River Simulation . . . . . . . . . . . . . . . . . 358

TABLES (Continued)

Number Page

A.27 Nine-Compartment Computer Model Inputs for 7H-Dibenzo[c,g]-carbazole: Eutrophic Lake Simulation . . . . . . . . . . . . . 359

A.28 Nine-Compartment Computer Model Inputs for 7H-Dibenzo[c,g]-carbazole: Oligotrophic Lake Simulation . . . . . . . . . . . 360

A.29 Nine-Compartment Computer Model Inputs for Benzo[b]thiophene: Pond Simulation . . . . . . . . . . . . . . . . . . . . . . . 361

A.30 Nine-Compartment Computer Model Inputs for Benzo[b]thiophene: River Simulation . . . . . . . . . . . . . . . . . . . . . . 362

A.31 Nine-Compartment Computer Model Inputs for Benzo[b]thiophene: Eutrophic Lake Simulation . . . . . . . . . . . . . . . . . . 363

A.32 Nine-Compartment Computer Model Inputs for Benzo[b]thiophene: Oligotrophic Lake Simulation . . . . . . . . . . . . . . . . 364

A.33 Nine-Compartment Computer Model Inputs for Dibenzothiophene: Pond Simulation . . . . . . . . . . . . . . . . . . . . . . . 365

A.34 Nine-Compartment Computer Model Inputs for Dibenzothiophene: River Simulation . . . . . . . . . . . . . . . . . . . . . . 366

A.35 Nine-Compartment Computer Model Inputs for Dibenzothiophene: Eutrophic Lake Simulation . . . . . . . . . . . . . . . . . . 367

A.36 Nine-Compartment Computer Model Inputs for Dibenzothiophene: Oligotrophic Lake Simulation . . . . . . . . . . . . . . . . 368

A.37 Nine-Compartment Computer Model Inputs for Methyl Parathion: Pond Simulation . . . . . . . . . . . . . . . . . . . . . . . 369

A.38 Nine-Compartment Computer Model Inputs for Methyl Parathion: River Simulation . . . . . . . . . . . . . . . . . . . . . . 370

A.39 Nine-Compartment Computer Model Inputs for Methyl Parathion: Eutrophic Lake Simulation . . . . . . . . . . . . . . . . . . 371

A.40 Nine-Compartment Computer Model Inputs for Methyl Parathion: Oligotrophic Lake Simulation . . . . . . . . . . . . . . . . 372

A.41 Nine-Compartment Computer Model Inputs for Mirex: Pond Simulation . . . . . . . . . . . . . . . . . . . . . . . . . . 373

A.42 Nine-Compartment Computer Model Inputs for Mirex: River Simulation . . . . . . . . . . . . . . . . . . . . . . . . . . 374

TABLES (Concluded)

Number Page

A.43 Nine-Compartment Computer Model Inputs for Mirex: Eutrophic and Oligotrophic Lake Simulations . . . . . . . . . . . . . . . . 375

B.1 Nominal Wavelengths and Wavelength Intervals for UV and Visible Absorption Spectra. . . . . . . . . . . . . . . . . . . . . 377

B.2 Sources and Characteristics of Ca-Montmorillonite Clay and Natural Sediments . . . . . . . . . . . . . . . . . . . . . . . 379

B.3 Recommended Experimental Plan for Isotherm Measurements . . . . 380

B.4 Some Water Quality Parameters for 0.22-μm Filtered Water From Searsville Pond, Coyote Creek, and Lake Tahoe . . . . . . 386

B.5 UV Absorbance of 0.22-μm Filtered Natural Waters . . . . . . . 388

# ABBREVIATIONS AND SYMBOLS

| | |
|---|---|
| AA | 4,4'-Azobis(4-cyanovaleric acid) |
| H | Henry's law constant |
| $I_\lambda$ | Light flux (photons $\text{time}^{-1}$ $\text{liter}^{-1}$)[*] |
| $K_b$ | Partition coefficient for sorption on biota or sorption on sediments |
| $K_p$ | Partition coefficient |
| $K_s$ | Concentration of substrate at which $\mu = \frac{1}{2} \mu_m$ |
| M | Moles $\text{liter}^{-1}$ |
| $M_{Bi}$ | Mass of chemical in biota |
| $M_{\ell i}$ | Total mass of substrate in aqueous phase ($\ell$) of compartment i before sorption |
| $M'_{\ell i}$ | Total mass of substrate in aqueous phase ($\ell$) of compartment i after sorption |
| $M_s$ | Mass of suspended sediment |
| $M_{si}$ | Total mass of substrate in the suspended sediment of compartment i before sorption |
| $M'_{si}$ | Total mass of substrate in the suspended sediment of compartment i after sorption |
| $M_w$ | Mass of water |
| $P_s$ | Vapor pressure of pure substrate (torr) |
| R | Gas constant |
| S | Substrate concentration (mass per unit volume)[*] |
| [S] | Substrate concentration (moles per liter) |
| $S_{\ell i}$ | Substrate concentration in the aqueous phase of compartment i |
| T | Temperature (°K) |
| $V_i$ | Volume of compartment i |
| X | Bacterial mass or cell count (cells $\text{ml}^{-1}$) |

---

[*] Specific units of mass, volume, and time used varied.

[‡] Biomass in kinetic studies was generally in cell counts and in units of mass in biosorptions.

| | |
|---|---|
| $X_i$ | Microbial population in compartment i (cells $ml^{-1}$) |
| Y | Biomass or cell yield per mass of substrate utilized[†] (cells $\mu g^{-1}$ substrate) |
| Z | Solar radiance intensity (photons $cm^{-3}$ $sec^{-1}$ $nm^{-1}$) |
| e | Efficiency of production of $RO_2\cdot$ from AA |
| $k_A$ | Rate constant for acid-catalyzed hydrolysis ($M^{-1}$ $sec^{-1}$) |
| $k_B$ | Rate constant for base-catalyzed hydrolysis ($M^{-1}$ $sec^{-1}$) |
| $k_N$ | Rate constant for neutral hydrolysis ($sec^{-1}$) |
| $k_a$ | First-order rate constant for light absorption by chemical ($sec^{-1}$) |
| $k_b$ | $\mu_m/Y$ = Rate constant for biodegradation (mg $cell^{-1}$ $hr^{-1}$) |
| $k_b'$ | Pseudo-first order rate constant for biodegradation ($hr^{-1}$) |
| $k_{b2}$ | Second-order rate constants for biodegradation (ml $cell^{-1}$ $hr^{-1}$) |
| $k_h$ | Rate constant for hydrolysis ($sec^{-1}$) |
| $k_i$ | Rate constant for decomposition of AA ($sec^{-1}$) |
| $k_o$ | Oxygen reaeration rate ($time^{-1}$) |
| $k_{ox}$ | Rate constant for oxidation ($M^{-1}$ $time^{-1}$) |
| $k_p$ | Rate constant for photolysis ($time^{-1}$) |
| $k_v$ | Rate constant for volatilization ($\mu g$ $ml^{-1}$ $time^{-1}$) |
| $m_{bi}$ | Mass of biota |
| $r_b$ | Biodegradation rate ($\mu g$ $ml^{-1}$ $time^{-1}$) |
| $r_h$ | Hydrolysis rate ($\mu g$ $ml^{-1}$ $time^{-1}$) |
| $r_o$ | Oxidation rate ($\mu g$ $ml^{-1}$ $time^{-1}$) |
| $r_p$ | Photolysis rate ($\mu g$ $ml^{-1}$ $time^{-1}$) |
| $r_v$ | Volatilization rate ($\mu g$ $ml^{-1}$ $time^{-1}$) |
| $t_{1/2}$ | Half-life (time) |
| $\varepsilon$ | Absorption coefficient (M $cm^{-1}$) |
| $\lambda$ | Wavelength (nm) |
| $\lambda_{max}$ | Wavelength of an absorption maximum (nm) |
| $\mu$ | Specific growth rate ($hr^{-1}$) |
| $\mu_m$ | $\mu_{max}$ = Maximum specific growth rate ($hr^{-1}$) |
| $\phi$ | Reaction quantum yield |

# ACKNOWLEDGMENTS

The assistance and counsel of the Project Officer for this work, Mr. George Baughman of the Environmental Research Laboratory, Athens, Georgia, has been invaluable in this work, as were the frequent discussions with his staff: Drs. Richard Zepp, Lee Wolfe, David Brown, Charles Steen, and Ms. Doris Paris, as well as Drs. James Hill and Ray Lassiter, who are also located at the Athens, Georgia, laboratory.

The contributions of the SRI International staff members who carried out the laboratory work are gratefully acknowledged. The following persons participated in the following tasks:

Environmental Assessment: T. Peyton, B. Suta, E. C. Waters

Physical Transport: D. Haynes, B. Kingsley, D. Stivers, and M. Zinnecker

Chemical Degradation: D. Hendry, A. Baraze, B. Lan, and H. Richardson

Biodegradation: R. Spanggord, E. Shingai, H. G. Shan, S. Sorenson, G. Shepherd, R. Langley, D. Donaldson, and D. Brajkovich

Substantial assistance in report preparation was provided by C. Reeds.

# 1. INTRODUCTION

The objective of this study was to develop objective, well-documented laboratory and assessment procedures that can be used to predict the pathways of potentially harmful chemicals in freshwater environments. Laboratory procedures were used to measure the sorption partition coefficients on sediments and biomass and the rate constants for volatilization, oxidation, hydrolysis, photolysis, and microbial transformations, using adapted cultures, under conditions that are extrapolatable to environmental conditions. The results of the laboratory procedures were integrated with a simple computer model to predict the pathways for the chemicals in ponds, rivers, and lakes. These procedures are described in detail in Part I of this report (EPA-600/7-77-113).

The results of applying these procedures to eleven chemicals are described in this part of the report. The chemicals were *p*-cresol, benz[a]anthracene, benzo[a]pyrene, quinoline, benzo[f]quinoline, 9H-carbazole, 7H-dibenzo[c,g]-carbazole, benzo[b]thiophene, and dibenzothiophene, which might be found in the effluents of plants using or processing fossil fuels, and methyl parathion and mirex, which are agricultural pesticides.

# 2. CONCLUSIONS

The environmental assessment models and the laboratory procedures described in Part I of this report have been used successfully to predict the environmental pathways of eleven organic chemicals. Nine of the chemicals are representative of those that would be found in the effluents of facilities utilizing fossil fuels. Two pesticides were also tested. The results of these studies are summarized in Tables 2.1 and 2.2.

TABLE 2.1. SUMMARY OF EQUILIBRIA AND RATE PROCESSES AT 25°C

| Chemical | Solubility in water at 22°C | Sorption partition coefficient[a] | Volatilization ratio, $k_v^s/k_v^O$ ($\times 10^3$) | Solar photolysis rate constant, $k_p$ ($sec^{-1}$) | Photolysis quantum yield, $\Phi$ | Oxidation rate constant, $k_{ox}$ ($M^{-1}\ sec^{-1}$) | Biodegradation rate constant, $k_{b2}$ ($ml\ cell^{-1}\ hr^{-1}$) |
|---|---|---|---|---|---|---|---|
| p-Cresol | 1.8[b] mg ml$^{-1}$ | <10 | 1.2 ± 0.3 | $3.3 \times 10^{-8}$[c] | 0.079 | 20 | $5.2 \times 10^{-7}$ |
| Benz[a]anthracene | 5.7 ng ml$^{-1}$ | 26,000 | 1.6 ± 0.6 | $3.3 \times 10^{-4}$[d] | $3.3 \times 10^{-3}$ | 5,000 | 0[e] |
| Benzo[a]pyrene | 1.2 ng ml$^{-1}$ | 76,000 | 3.6 ± 0.6 | $3.6 \times 10^{-4}$[d] | $8.9 \times 10^{-4}$ | 1,900 | 0[e] |
| Quinoline | 6.11[b] mg ml$^{-1}$ | 11 | 2.7 ± 0.4 | $3.5 \times 10^{-7}$[c] | $3.3 \times 10^{-4}$ | <3 | $3.1 \times 10^{-6}$ |
| Benzo[f]quinoline | 76 µg ml$^{-1}$ | 1,300 | 0.22 ± 0.09 | $3.7 \times 10^{-4}$[d] | 0.014 | <3 | $3.6 \times 10^{-8}$ |
| 9H-Carbazole | 1.0 µg ml$^{-1}$ | 175 | <0.1 | $1.9 \times 10^{-4}$[d] | $7.6 \times 10^{-3}$ | 29 | $5.0 \times 10^{-7}$ |
| 7H-Dibenzo[c,g]carbazole | 63 ng ml$^{-1}$ | 20,500 | <0.1 | $5.5 \times 10^{-4}$[d] | $2.8 \times 10^{-3}$ | 830 | 0[e] |
| Benzo[b]thiophene | 130 µg ml$^{-1}$ | 59 | 380 ± 20 | $5.7 \times 10^{-8}$[c] | 0.1[f] | 83 | g |
| Dibenzothiophene | 1.1 µg ml$^{-1}$ | 1,380 | 120 ± 40 | $1.5 \times 10^{-8}$[c] | $5 \times 10^{-4}$ | <3 | $5.3 \times 10^{-7}$ |
| Methyl parathion[h] | 50[b] µg ml$^{-1}$ | 50 | <0.4 | $9.8 \times 10^{-7}$[c] | $1.7 \times 10^{-4}$ | <3 | $2.4 \times 10^{-7}$ |
| Mirex[i] | 70 pg ml$^{-1}$ | 460,000 | 63 ± 18 | $5 \times 10^{-8}$[j] | <1.0[f] | <<1 | 0[e] |
| Rate law | -- | -- | $\frac{k_v^s}{k_v^O} k_v^O[S]$ | $k_p[S]$ | -- | $k_{ox}[RO_2\cdot][S]$ | $k_{b2}[B][S]$ |

[a] Value for a natural sediment collected in Coyote Creek, California.

[b] Literature value.

[c] Rate constant averaged over 24-hr day, June 21.

[d] Instantaneous rate constant for noon, June 21.

[e] Biodegradation was not observed during our enrichment procedures.

[f] Assumed value.

[g] Biodegradation was observed only in the presence of naphthalene; there is no kinetic expression that can be used to express this type of biodegradation.

[h] Rate constant for neutral hydrolysis at 25°C is $9 \times 10^{-8}$ sec$^{-1}$.

[i] Rate constant for neutral hydrolysis is less than $1 \times 10^{-10}$ sec$^{-1}$.

[j] Measured rate constant for a 6-month period.

# TABLE 2.2. SUMMARY OF ENVIRONMENTAL ASSESSMENTS

| | River | | | Pond | | | Eutrophic lake | | | Oligotrophic lake | | |
|---|---|---|---|---|---|---|---|---|---|---|---|---|
| Chemical | Major pathway(s) | Half-life[a] (hr) | Percent sorbed[b] | Major pathway(s) | Half-life[a] (hr) | Percent sorbed[b] | Major pathway(s) | Half-life[a] (hr) | Percent sorbed[b] | Major Pathway(s) | Half-life[a] (hr) | Percent sorbed[b] |
| p -Cresol | Biodegradation | 0.55 | 0.1 | Biodegradation | 12 | 0.3 | Biodegradation | 12 | 0.05 | Biodegradation, photolysis | 2400 | 0.05 |
| Benz[a]-anthracene | Sorption | 0.55 | 71 | Sorption | 22 | 88 | Sorption | 22 | 55 | Sorption | 8 | 55 |
| Benzo[a]-pyrene | Sorption, photolysis | 0.48 | 83 | Sorption, photolysis | 7.3 | 93 | Sorption, photolysis | 7.4 | 71 | Sorption, photolysis | 1.5 | 71 |
| Quinoline | Biodegradation | 0.28 | 0.1 | Biodegradation | 0.5 | 0.3 | Biodegradation | 0.5 | 0.05 | Biodegradation, photolysis | 600 | 0.05 |
| Benzo[f]-quinoline | Photolysis | 0.5 | 12 | Photolysis, biodegradation | 6.9 | 42 | Photolysis, biodegradation | 7.0 | 6.5 | Photolysis | 1.4 | 6.5 |
| 9H-Carbazole | Photolysis, biodegradation | 0.5 | 2.0 | Photolysis, biodegradation | 10 | 5.6 | Photolysis, biodegradation | 10 | 1 | Photolysis, biodegradation | 3 | 1 |
| 7H-Dibenzo[c,g]-carbazole | Photolysis, sorption | 0.36 | 66 | Photolysis, sorption | 1.5 | 82 | Photolysis, sorption | 1.5 | 50 | Photolysis, sorption | 0.5 | 50 |
| Benzo[b]-thiophene | Volatilization | 0.5 | 0.5 | Volatilization | 19 | 1.5 | Volatilization photolysis, biodegradation | 19 | 0.2 | Volatilization, photolysis, biodegradation | 140 | 0.2 |
| Dibenzo-thiophene | Biodegradation | 0.5 | 12 | Biodegradation, sorption | 13 | 42 | Biodegradation | 13 | 6.5 | Photolysis, Volatilization | 140 | 6.5 |
| Methyl parathion | Biodegradation | 0.6 | 0.5 | Biodegradation | 27.3 | 1.5 | Biodegradation | 28.3 | 0.25 | Sorption, photolysis, hydrolysis, biodegradation | 152 | 2.25 |
| Mirex | Sorption, volatilization | 0.83 | 97 | Sorption | 420 | 99 | Sorption | 1480 | 94 | Sorption | 1480 | 94 |

[a] Net half-life for all processes including dilution; predicted by the one-compartment model.

[b] Percent sorbed in bottom sediment; from the compartment nearest the source; predicted by the nine-compartment computer model.

## 3. RECOMMENDATIONS

General recommendations for improving this environmental exposure assessment method were given in Section 3 of Part I of this report. In addition, we offer the following recommendations.

1. These procedures should be verified by ecosystem and field studies, using several of the compounds that were predicted in this report to be persistent.
2. The methodology developed here should be used to improve the strategies for setting effluent guidelines.

# 4. LABORATORY INVESTIGATION OF p-CRESOL

## 4.1 SYNOPSIS

The laboratory data suggest that biodegradation is the major pathway for p-cresol in eutrophic systems. In oligotrophic systems, both biodegradation and photolysis may be important. Volatilization, sorption onto suspended sediments, and oxidation are not significant processes compared with biodegradation and photolysis.

Limited product identification studies were carried out. Two dimeric products of p-cresol were found in small amounts in oxidation experiments. Biodegradation products containing an aromatic ring were not observed; if they were formed, they were degraded by the mixed culture systems at a rate comparable to the degradation rate of p-cresol at the low concentrations of p-cresol tested.

The nine-compartment environmental exposure model predicted the following steady-state concentrations of p-cresol in solution, suspended solids, and sediments near point sources in the presence of a continuous discharge of 1 $\mu g\ ml^{-1}$ (1 ppm) p-cresol:

|  | Half-life* (hr) | Solution ($\mu g\ ml^{-1}$) | Suspended solids ($\mu g\ g^{-1}$) | Sediments ($\mu g\ g^{-1}$) |
|---|---|---|---|---|
| River | 0.55 | 0.980 | 9.80 | 9.65 |
| Pond | 12 | 0.017 | 0.17 | 0.17 |
| Eutrophic lake | 12 | 0.037 | 0.37 | 0.10 |
| Oligotrophic lake | 2400 | 0.0221 | 2.20 | 0.94 |

## 4.2 BACKGROUND

Phenols enter the environment from diverse biological sources, as byproducts from the petroleum and coking industries and as a result of the use of creosote as a wood preservative. Consequently, they may be widely encountered in low concentrations in natural waters. p-Cresol was selected for investigation as being representative of the general class of phenolic compounds. p-Cresol is a constituent of creosote, and the use of creosote probably represents the highest localized concentrations of p-cresol in the environment.

---

*Predicted by one-compartment model for all processes including dilution.

Production of creosote and other coal tar derivatives is concentrated in the Great Lake and Middle Atlantic States with a secondary locus in central Alabama. These products are used throughout the nation, with major concentrations in the Southeast and Pacific Northwest. Approximately 84 plants produce creosote and some 200 use it for wood preservation. Effluents from most of these plants receive biological treatment. The prolonged use of creosote without noticeable adverse effects suggests that releases to the environment are relatively nonhazardous. The physical properties of p-cresol available in the literature are listed in Table 4.1.

TABLE 4.1. PHYSICAL PROPERTIES OF p-CRESOL

| | |
|---|---|
| Structure | 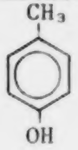 |
| Molecular weight | 108.14 |
| Melting point, °C<br>(CRC Handbook, 54th Ed.) | 34.8 |
| Boiling point, °C, 760 torr<br>(CRC Handbook, 54th Ed.) | 201.9°C |
| Vapor pressure, 25°C | 0.108 torr |
| Solubility in water, 25°C<br>(Lange, 1973) | 1.8 mg $ml^{-1}$ |
| 1 μg $ml^{-1}$ (1 ppm) p-cresol in water = $9.26 \times 10^{-6}$ M | |

Volatilization of p-cresol was not expected to be an important environmental fate. The estimated Henry's law constant is 36 torr and the volatilization half-life from a lake is 167 days, as calculated from equations (5) and (6) of Mackay and Wolkoff (1973).

No literature reference to sorption of p-cresol, phenols, or other cresols on naturally occurring sediments was found in the literature. Cowan and White (1962) report data that fit a Freundlich isotherm of phenols and cresols on complexes of aliphatic amines and bentonite clay.

Phenols are known to oxidize readily under a variety of conditions to give quinones, polyhydroxybenzenes and eventually, carboxylic acids (Wiberg, 1965; Waters, 1964). Dimeric and polymeric products are also obtained under some oxidizing conditions. Chemical oxidations of *p*-cresol have been reported to give the oxidative coupling products Pummerer's ketone (I), 2,2'-dihydroxy-4,4'-dimethylbiphenyl (II), and the trimer III (Musso, 1967).

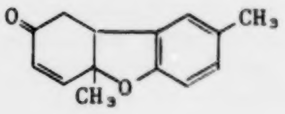

I

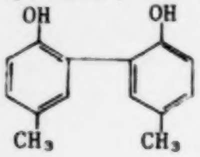

II

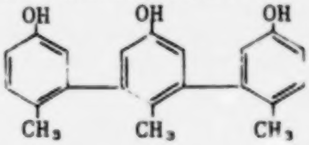

III

Direct photolysis of *p*-cresol in water at 254 nm gave compound II, 2-hydroxy-3,4'-dimethyldiphenyl ether (IV) and 4-methylcatechol (V) (Joschek and Miller, 1966). The analytical method in this experiment provided only qualitative identification for these products and could not identify any nonphenolic products.

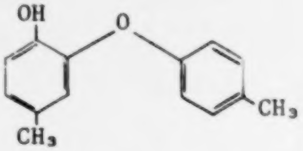

IV

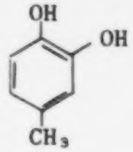

V

Kinetics of free radical oxidations of phenols, including *p*-cresol, have been summarized by Howard (1972) and include rate constants for reactions of alkylperoxyl ($RO_2\cdot$) and alkoxyl ($RO\cdot$) radicals. Land and Porter (1963) showed that dimerization of *p*-methylphenoxy radicals proceeds at nearly diffusion-controlled rate and mostly by *o,o*-coupling to give II. Neither this information nor the limited reports on the direct and photosensitized oxidation of *p*-cresol (Leaver, 1971; Pfoertner and Boese, 1970) or autoxidation of phenolate anion in aqueous alkali (Kirso and Gubergrits, 1972) provide any information useful in assessing the rates of chemical transformation of *p*-cresol in aqueous environments.

Many reports have been published on the biological degradation of phenols, cresols, xylenols, and other "phenolics." A comprehensive review of this subject or of the degradative pathways is not warranted here, but some observations will be reported.

Landa et al. (1953) observed that an *Escherichia coli* cultivated from Moldavian water degraded phenol at 50-100 mg liter$^{-1}$ hr$^{-1}$, which was two to five times as fast as the degradation of *p*-cresol. An *Oospora* culture degraded phenol, cresols, and xylenol, but at 1/3 to 1/7 the rate of the *E. coli*. Phillips and Hinshelwood (1953) adapted *Aerobacter aerogenes* to grow on phenol and alkylated phenols. Oka (1962) found that phenols were absorbed on *E. coli* and *Staphylococcus aureus* at about 22 mM kg$^{-1}$ cells. This is not an unexpected observation when inhibition of the bacteria was occurring. Decomposition of phenol, *o*-cresol, toluene, benzene, and other products by a *Pseudomonas* and an *Achromobacter* was reported by Claus (1964).

The list of types of organisms that will degrade phenolic substances has been expanded, and there have been many reports on the biological purification of coke oven effluents by various procedures. Of particular interest is the publication by Kostenbader and Flecksteiner (1968) in which they reported 99.9% oxidation of 1300 pounds of phenol in a plant processing 112,000 gallons of effluents per day. Kaplin et al. (1968), in a study carried out on samples of 5 liters of river water containing 50 ml of effluent from a coking plant, observed that phenol decomposed immediately but that cresols required two days of adaptation. The decomposition of p-cresol could be represented by the equation $C/C_0 = e^{-(kt)^n}$ where n = 1 and k is the reaction rate constant = 0.188.*

Dagley and Patel (1957) found that with a strain of Pseudomonas, degradation of p-cresol was as follows: p-cresol → p-hydroxymethylphenol → p-hydroxybenzaldehyde → p-hydroxybenzoic acid → protocatechuic acid → ring cleavage. Bayly et al. (1966), in the same laboratories, then described a Pseudomonas oxidation of p-cresol to 4-methyl-catechol, which was then cleaved between carbons 2 and 3. These observations and studies with other phenols indicate a multiplicity of degradative pathways, depending on the organisms and compounds.

Although it was apparent that p-cresol was subject to microbial degradation, our objectives in environmental assessment of the fate of p-cresol as a pollutant were to examine different types of waters for their capacities to develop biodegrading systems, to determine with one culture mixture the kinetic rate constants that could be applicable in an assessment model along with rate constants obtained by other disciplines, to determine any major metabolites and, if warranted, to conduct sorption studies.

## 4.3 ENVIRONMENTAL ASSESSMENT

### 4.3.1 Summary of Laboratory Data

The rate constants obtained in the laboratory investigations of the transformation and transport processes for p-cresol are summarized in Table 4.2.

### 4.3.2 Environmental Assessment Using the One-Compartment Model

The half-lives of dissolved p-cresol calculated for individual transformation or removal processes following an acute discharge, such as a spill, are cited in Table 4.3. Biotransformation (biodegradation) is clearly the dominant transformational pathway in eutrophic waters, but is four times slower than photolysis in oligotrophic waters. Dilution is important compared with biotransformation only in rivers. Sorption and volatilization are unimportant in all waters.

---

*The units of k are not specified in the abstract of the reference.

TABLE 4.2. SUMMARY OF p-CRESOL LABORATORY DATA

| Process | Sorption equilibrium | Partition coefficient |
|---|---|---|
| Sorption | $S_s = K_p S_w$ | $K_p = 9.1 \pm 6.5$[a] |
| | Rate expression | Rate constant at 25°C |
| Volatilization[b] | $k_v[C]$ | $k_v^C = (1.2 \pm 0.3) \times 10^{-3} \cdot k_v^0$ |
| Photolysis[c] | $k_p[C] = \Phi(\Sigma Z_\lambda \epsilon_\lambda)[C]$ | $k_p = 6.8 \times 10^{-7}\ \text{sec}^{-1}$ |
| Oxidation | $k_{ox}[RO_2\cdot][C]$ | $k_{ox} = 20\ \text{M}^{-1}\ \text{sec}^{-1}$ |
| Hydrolysis | NA | $k_h = 0$ |
| Biodegradation | $k_{b2} = \frac{\mu_{max}}{YK_s}$ | $k_{b2} = 5.2 \times 10^{-7}\ \text{ml cell}^{-1}\ \text{hr}^{-1}$ |

[a] On Coyote Creek Sediment.

[b] See discussion in Part I, Section 5.3 of the final report.

[c] Overcast weather in April.

### 4.3.3 Persistence

p-Cresol is not persistent, as the term is usually applied with respect to pesticides. Half-lives of p-cresol in oligotrophic waters are predicted to be about three months, but are half a day or less in eutrophic waters. Desorption of p-cresol from sediments is unlikely to be significant as a source of pollution over the long term.

### 4.3.4 Mass and Concentration Distributions Calculated Using Computer Models

The pseudo-first-order rate constants used in these simulations are presented in Appendix A. The distributions of mass and concentration of p-cresol expected at steady state during chronic discharge to each of four types of water bodies are given in Table 4.4.

Steady-state concentrations were not reached in all compartments of any of the simulations because of the delays in transport of the p-cresol

TABLE 4.3. TRANSFORMATION AND TRANSPORT OF p-CRESOL PREDICTED BY THE ONE-COMPARTMENT MODEL

| Process | River | Eutrophic pond | Eutrophic lake | Oligotrophic lake |
|---|---|---|---|---|
| Photolysis, half-life (hr)[a] | 4,800 | > 10,000 | > 10,000 | 2,400 |
| Oxidation, half-life (hr) | | | | |
| Volatilization, half-life (hr) | | | | |
| Hydrolysis, half-life (hr) | | | | |
| Biotransformation, half-life (hr) | 12 | 12 | 12 | > 10,000 |
| Half-life for all processes except dilution (hr) | 12 | 12 | 12 | 2,400 |
| Half-life for all processes including dilution | 0.55 | 12 | 12 | 2,400 |
| Amount p-cresol sorbed (mg/m$^3$)[b] | 1 | 3 | 0.5 | 0.5 |
| Percentage p-cresol sorbed | 0.1% | 0.3% | 0.05% | 0.05% |

[a] Estimates are the average photolysis rates on a summer day at 40° latitude. Photolysis rates in midwinter are at least three times slower.

[b] 1 μg ml$^{-1}$ of p-cresol in aqueous phase and partition coefficient of 10 are assumed.

solution between compartments in the more complex simulations and the large storage capacity of the sediments and larger aqueous compartments. However, extrapolation of the curves suggests that steady-state conditions would be reached in the simulations within days or weeks in the aqueous compartments, although months might be required for attainment of steady state in the sediments. These patterns are clearly seen in the pond simulation (Figure 4.1) in which steady state in the aqueous compartment is nearly reached within 4 days, while the mass of p-cresol in the sediments at the end of 4 days is roughly 3% of the mass expected at steady state (Table 4.4). Steady states are obtained 40 times faster in the river simulation, where dilution is extremely rapid (Figure 4.2), but are obtained 100 to 1000 times more slowly in the stratified lake simulations, in which transport into the deeper waters and sediments is relatively slow (Figures 4.3 to 4.4).

The concentrations of p-cresol observed at steady state varied significantly among simulations and among compartments within each of the simulations (Table 4.4). Concentrations on the sedimented and suspended solids were generally 10 times higher than in solution, and occasionally as little as 3 times higher. Aqueous concentrations are highest in the river simulation since removal from solution is slow relative to the import and export of p-cresol from the simulated river segments. Indeed, under the assumptions of the simulation in which the stream volume remains constant, the concentration of p-cresol decreases only 1% within each kilometer-long segment. In contrast, in the eutrophic lake simulation in which the flows of the p-cresol solution are much slower, there is a 3- to 10-fold difference in concentrations of dissolved p-cresol between adjacent compartments in the surface waters, and nearly a 150-fold decrease in concentration between the surface and bottom waters in the lake center.

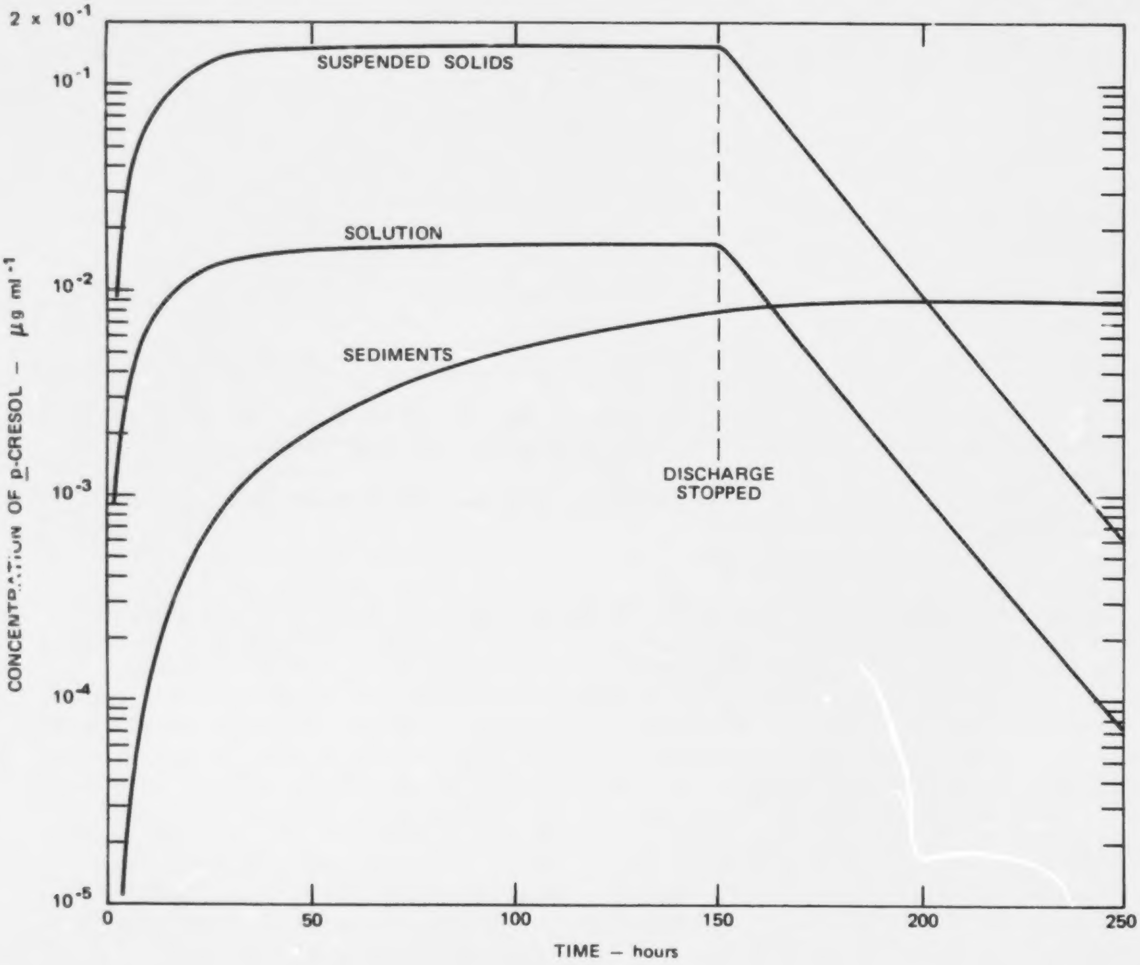

FIGURE 4.1 PERSISTENCE OF p-CRESOL IN A TWO-COMPARTMENT POND SYSTEM

TABLE 4.4. DISTRIBUTION OF p-CRESOL IN VARIOUS AQUATIC SYSTEMS AT STEADY STATE (input concentrations of 1 $\mu g\ ml^{-1}$ p-cresol)

| | Pond | | River | | Eutrophic lake | | Oligotrophic lake | |
|---|---|---|---|---|---|---|---|---|
| | Mass (kg) | Conc. ($\mu g\ g^{-1}$) | Mass (kg) | Conc. ($\mu g\ g^{-1}$) | Mass (kg) | Conc. ($\mu g\ g^{-1}$) | Mass (kg) | Conc. ($\mu g\ g^{-1}$) |
| Compartment 1 (surface water) | | | | | | | | |
| Solution | $3.40 \times 10^{-1}$ | $1.70 \times 10^{-2}$ | $2.94 \times 10^{2}$ | $9.80 \times 10^{-1}$ | 9.44 | $3.77 \times 10^{-2}$ | $5.32 \times 10$ | $2.20 \times 10^{-1}$ |
| Suspended solids | $9.55 \times 10^{-3}$ | $1.70 \times 10^{-1}$ | $2.94 \times 10^{-1}$ | 9.80 | $4.72 \times 10^{-3}$ | $3.77 \times 10^{-1}$ | $2.66 \times 10^{-2}$ | 2.20 |
| Compartment 2 (surface water) | | | | | | | | |
| Solution | -- | -- | $2.89 \times 10^{2}$ | $9.66 \times 10^{-1}$ | 6.02 | $2.40 \times 10^{-3}$ | $3.55 \times 10^{2}$ | $1.28 \times 10^{-1}$ |
| Suspended solids | -- | -- | $2.89 \times 10^{-1}$ | 9.66 | $3.01 \times 10^{-3}$ | $2.40 \times 10^{-2}$ | $1.60 \times 10^{-1}$ | 1.28 |
| Compartment 3 (surface water) | | | | | | | | |
| Solution | -- | -- | $2.85 \times 10^{2}$ | $9.50 \times 10^{-1}$ | $2.49 \times 10^{-1}$ | $9.99 \times 10^{-4}$ | $3.00 \times 10$ | $1.20 \times 10^{-1}$ |
| Suspended solids | -- | -- | $2.85 \times 10^{-1}$ | 9.50 | $1.24 \times 10^{-4}$ | $9.99 \times 10^{-3}$ | $1.50 \times 10^{-2}$ | 1.20 |
| Compartment 5 (bottom water) | | | | | | | | |
| Solution | -- | -- | -- | -- | $7.22 \times 10^{-2}$ | $2.89 \times 10^{-5}$ | $5.25 \times 10$ | $2.10 \times 10^{-2}$ |
| Suspended solids | -- | -- | -- | -- | $3.61 \times 15^{-5}$ | $2.89 \times 10^{-4}$ | $2.62 \times 10^{-2}$ | $2.10 \times 10^{-1}$ |
| Compartments 7-9 (sediment)[a] | | | | | | | | |
| Solution | $4.25 \times 10^{-2}$ | $1.70 \times 10^{-2}$ | 2.41 | $9.65 \times 10^{-1}$ | $8.75 \times 10^{-2}$ | $9.58 \times 10^{-3}$ | $8.29 \times 10^{-1}$ | $9.48 \times 10^{-2}$ |
| Solids | $1.14 \times 10^{-1}$ | $1.70 \times 10^{-1}$ | $1.95 \times 10^{2}$ | 9.65 | 1.30 | $9.58 \times 10^{-2}$ | $1.29 \times 10$ | $9.48 \times 10^{-1}$ |

[a] The amounts given for solid and solution phases in the sediment compartments are estimated from the sorption partition coefficient for suspended solids and may be overestimated because it was assumed that biodegradation of sorbed material does not occur.

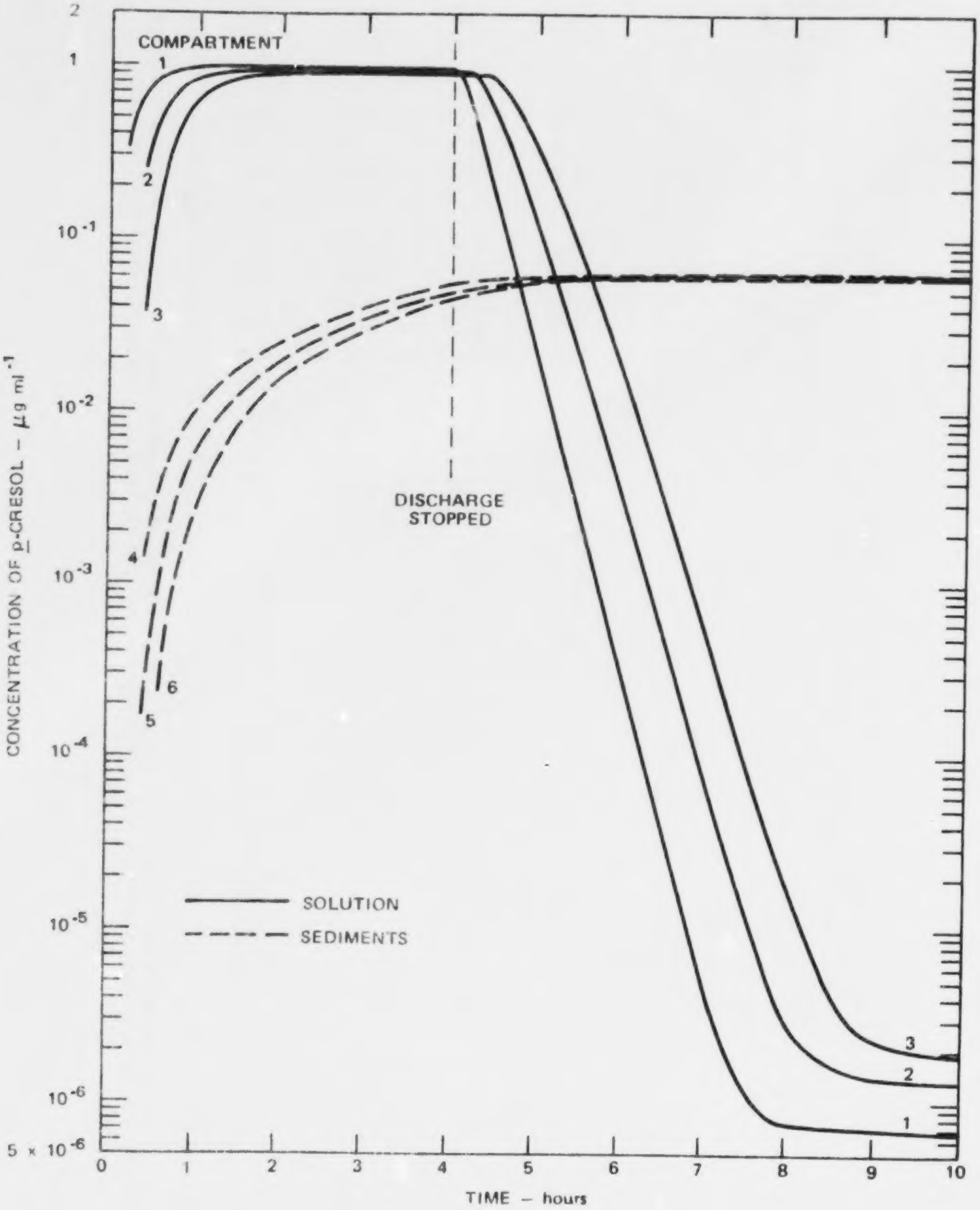

FIGURE 4.2 PERSISTENCE OF p-CRESOL IN A PARTIALLY MIXED RIVER SYSTEM

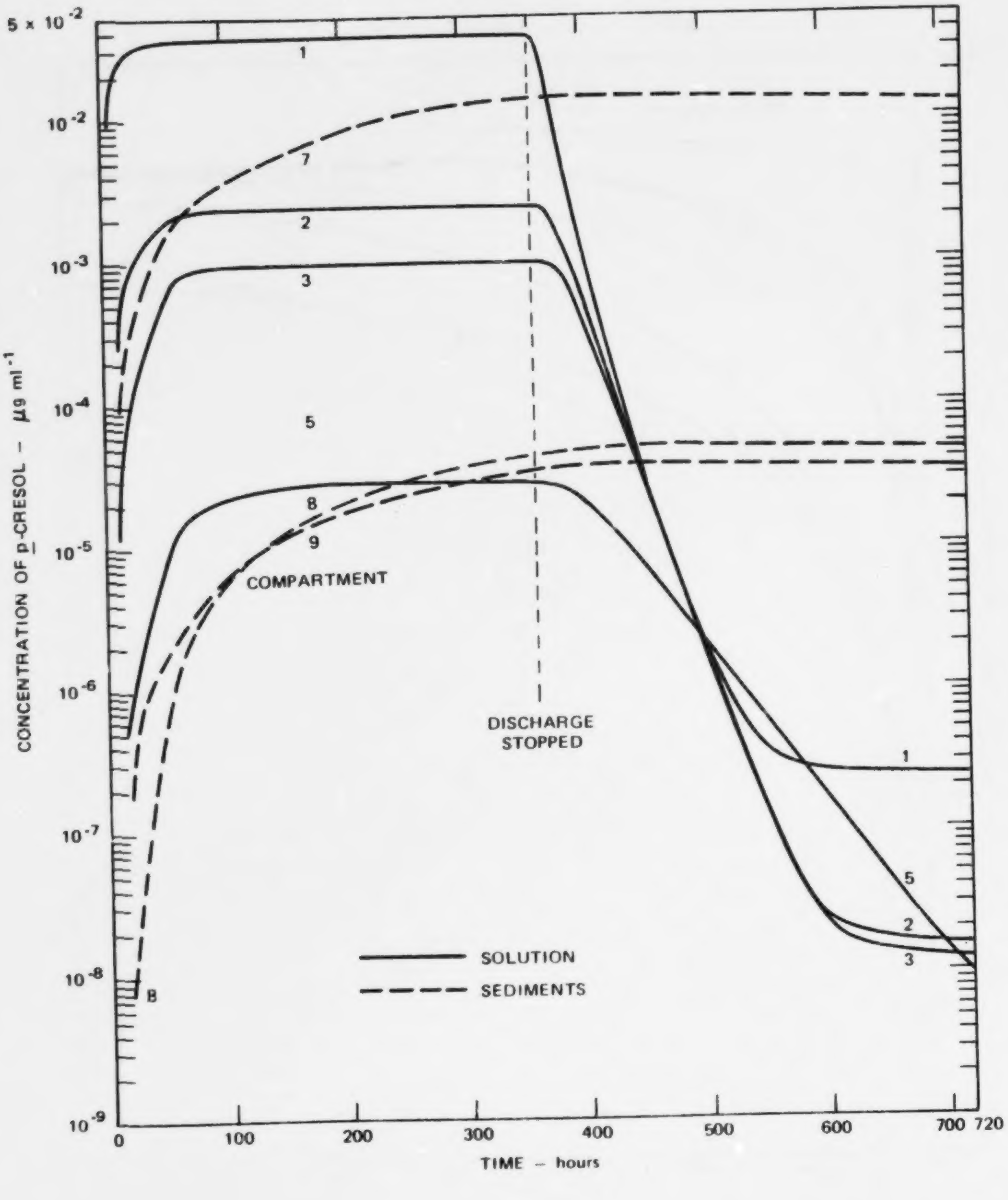

FIGURE 4.3 PERSISTENCE OF p CRESOL IN A PARTIALLY MIXED EUTROPHIC LAKE

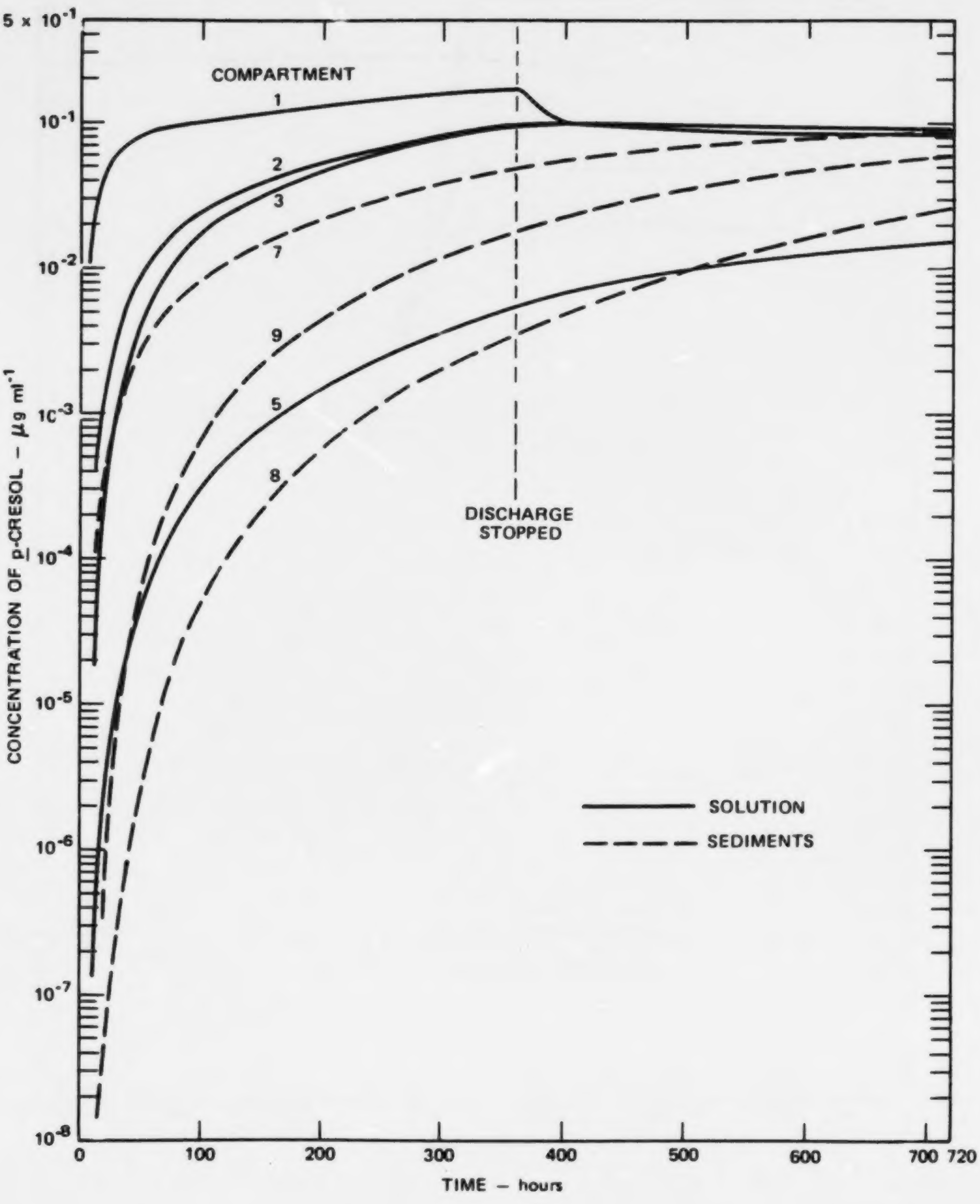

FIGURE 4.4 PERSISTENCE OF p-CRESOL IN A PARTIALLY MIXED OLIGOTROPHIC LAKE

Concentrations in the oligotrophic lake simulation are at least 3 to 10 times those of the eutrophic lake even though the higher of the two photolysis rate constants is assumed. Use of the lower rate constant would increase the difference between the two lake types. Changes in concentration between compartments of the oligotrophic lake are also about 3- to 10-fold in the surface compartments of the oligotrophic lake simulation and about 5-fold between the upper and lower water compartments of the lake center. However, these differences would decrease if the lower rate constant were used, and degradation would be correspondingly slower relative to dispersal by currents.

Once discharges stop, the concentrations of p-cresol in solution decline rapidly by five to six orders of magnitude to new steady states in the river and eutrophic lake simulations. Concentrations in the pond appear to be declining similarly, although the simulation was stopped prematurely. Concentrations of p-cresol on the sediments decline slowly in all simulations because of the slow scouring of sediments.

Patterns of variation for suspended solids are similar to patterns of dissolved p-cresol, but the concentrations are roughly 10 times those of dissolved p-cresol in the same compartments, except in the river simulation. Here concentrations in solution and on suspended solids are about the same. For simplicity, the data for suspended solids are presented graphically only for the pond simulation.

In summary, the steady-state concentrations resulting from an inflow of solution containing 1 $\mu g\ ml^{-1}$ of p-cresol are very nearly 1 $\mu g\ ml^{-1}$ in the initial segments of the simulated stream, roughly 0.1 $\mu g\ ml^{-1}$ in the oligotrophic lake, about 0.04 $\mu g\ ml^{-1}$ in the eutrophic lake, and approximately 0.02 $\mu g\ ml^{-1}$ in the pond. The river can, of course, accommodate a much larger mass of p-cresol without a significant change in concentration due to rapid dilution, but when contaminated by a steady discharge, the concentration downstream changes very slowly indeed, resulting in the contamination of very large volumes of water.

### 4.3.5 Discussion

Biodegradation is likely to be the dominant removal mechanism, accounting for at least 90% of the removal of p-cresol from solution, even if allowance is made for the variability in the importance of photolysis and sorption as a function of variations in turbidity, water color, or temperature. While photolysis may vary as much as tenfold as the pH rises to pH 9 (the upper limits of the values commonly encountered in natural waters), it is unlikely that these high pHs will occur in clear lakes. Hence, biodegradation may be dominant even in these waters.

Hence, the concentration of p-cresol, given constant inflows, should exhibit considerable seasonal variation, with lowest concentrations occurring in the summer months (assuming a constant volume of the water body). Consequently, excluding the effects of changing stream volume, the hypothetical discharge of about 1 metric ton per hour assumed in our simulation would lead to concentrations between 10 and 1000 $ng\ ml^{-1}$ over a 100-km stream segment in the summer months, and roughly the same concentration range over a 1000-km stream segment in the winter. These decreases in concentration may indeed occur due to dilution with inflowing, unpolluted waters, but are unlikely to occur within most streams through transformation.

The risks associated with large discharges of p-cresol in lakes are higher because the potential for dilution is much lower due to slower rates of mixing. However, if the same assumption of a 1 $\mu g\ ml^{-1}$ discharge is made, the concentrations of p-cresol that can be expected in the various compartments of eutrophic and oligotrophic lakes are lower than in the river simulation as long as inputs of solution are of reasonable size. Hence, while the concentrations of p-cresol in lakes should be relatively low, the concentrations in shallow waters, particularly under ice cover, when both photolysis and biodegradation are suppressed, may rise to levels approximating those of the stream simulation.

The biota exposed to the highest concentrations will tend to be organisms that live or feed in streams or shallow waters of lakes. At least some of these organisms are likely to be exposed to toxic concentrations under the conditions assumed in the simulations, since $LD_{50}$s for fish and invertebrates are generally in the range of 5 to 15 ppm (McKee and Wolf, 1963). Hazards to humans and other mammals appear to be low (von Rumker et al., 1975; Christensen and Luginbyhl, 1975), since the $LD_{50}$s for the rat and mouse are 207 and 344 ppm, respectively, for orally ingested p-cresol.

## 4.4 PHYSICAL PROPERTIES

### 4.4.1 Solubility in Water

The solubility of p-cresol in pure water is reported in the literature to be 1.8 $mg\ ml^{-1}$ (Lange, 1973).

### 4.4.2 Absorption Spectra

The ultraviolet (UV) absorption spectra of $4.19 \times 10^{-4}$ M (45.3 $\mu g\ ml^{-1}$) p-cresol in pure water at pH 5, 7, and 9 were measured on a Cary Model 11 spectrophotometer. The absorption coefficients at wavelength intervals from 297.5 to 330 are reported in Table 4.5. The absorption spectrum of p-cresol depends on pH because p-cresol ($pK_a = 10.2$) dissociates at higher pH and the anion is a more strongly absorbing species.

### 4.4.3 Volatilization Rate

The volatilization rate of p-cresol was measured using the method of Hill et al. (1976), which is described in detail in Part I, Section 5.3 of this report. The volatilization half-life of p-cresol in aqueous solution was about 160 hours at a moderate stirring rate. The rate constants were calculated from two experiments as shown in Table 4.6. Although these are measurable volatilization rates, additional measurements were not made because biodegradation was so fast.

TABLE 4.5. ABSORPTION SPECTRA OF p-CRESOL IN PURE WATER[a]

| Center of wavelength interval[b] (nm) | Average absorption coefficient[c] ($M^{-1}$ $cm^{-1}$) | | |
|---|---|---|---|
| | pH 5.1 | pH 7.0 | pH 8.9 |
| 297.5 | 14 | 18 | 193 |
| 300.0 | 3.8 | 7.2 | 173 |
| 302.5 | 2.4 | 3.8 | 150 |
| 305.0 | 2 | 2 | 124 |
| 307.5 | 0 | 2 | 92.6 |
| 310.0 | | 2 | 63.5 |
| 312.5 | | 1 | 40.3 |
| 315.0 | | 0 | 24.1 |
| 317.5 | | | 13.0 |
| 320.0 | | | 6.2 |
| 323.1 | | | 3.8 |
| 330 | | | 0 |

[a] p-Cresol concentration is $4.19 \times 10^{-4}$ M (45.3 μg $ml^{-1}$).

[b] The wavelength intervals are given in Appendix B, Table B.1.

[c] The absorption coefficient at 313.0 nm is 28.6 at pH 8.9.

### 4.4.4 Sorption on Clay and Sediments

The partition coefficients of p-cresol an Ca-contmorillonite clay and on Coyote Creek sediment were measured. The data were fitted to a Freundlich isotherm; from the literature data (Cowan and White, 1962), we assumed that n was equal to 1 (see Part I, Section 5.4.2.3).

The experiments consisted of duplicate flasks at one p-cresol concentration and two clay loadings (for the calcium clay), and at two p-cresol con-

TABLE 4.6. VOLATILIZATION RATE CONSTANTS FOR p-CRESOL

| | Oxygen reaeration rate, $k_v^O$ ($hr^{-1}$) | p-Cresol volatilization rate, $k_v^C$ ($hr^{-1}$) | Ratio $k_v^C/k_v^O$ |
|---|---|---|---|
| Experiment 1 | 3.55 ± 0.24 | $(3.38 \pm 0.67) \times 10^{-3}$ | $(0.95 \pm 0.25) \times 10^{-3}$ |
| Experiment 2 | 2.97 ± 0.21 | $(4.50 \pm 0.39) \times 10^{-3}$ | $(1.5 \pm 0.24) \times 10^{-3}$ |
| Average | | | $(1.2 \pm .3) \times 10^{-3}$ |

centration and two sediment loadings (for the Coyote Creek sediment). The pH was adjusted to 6.0 ± 0.2 with dilute hydrochloric acid. The equilibration time for the initial experiments was 18 hours.

The initial experiments with natural sediments suggested that the partition coefficient $K_p$ was between 50 and 300. However, we suspected that biodegradation might be occurring, which would lead to erroneously high $K_p$ values. Therefore, to minimize biological activity, all solutions were sparged with nitrogen before the p-cresol was added and the p-cresol was exposed to the sediment for only 1 hour. The 1-hour exposure was selected because the cascade experiments using natural water, showed that the time required for acclimation to p-cresol was about 6 hours (Section 4.6). While it would have been possible to sterilize the samples by autoclaving or adding ethylene oxide, we chose not to do this because the nature of the sediment might have been altered. The results are summarized in Table 4.7.

The studies described in Section 4.6 showed that biodegradation of p-cresol is very fast. Therefore, we did not pursue the sorption studies.

### 4.4.5 Biosorption

Because p-cresol so readily biodegraded (Section 4.6), biosorption studies were not undertaken.

## 4.5 CHEMICAL TRANSFORMATION

### 4.5.1 Photolysis Rate

Data for the photolysis of p-cresol in pure water and in water containing 9.5 $\mu g\ ml^{-1}$ humic acid are given in Table 4.8. The initial concentrations of p-cresol in these experiments ranged from 0.80 to 0.60 $\mu g\ ml^{-1}$. With one exception, solutions maintained in the dark as controls during the time period of the photolyses showed less than 2% loss of p-cresol if the glassware and water were sterilized before use. The rate constants in Table

TABLE 4.7. p-CRESOL SORPTION ON SEDIMENTS

| Sediments | Total organic carbon (percent) | Sediment concentration ($\mu g\ ml^{-1}$) | p-Cresol concentration in supernatant ($\mu g\ ml^{-1}$)[a] | p-Cresol concentration on sediment ($\mu g\ ml^{-1}$)[b] | Partition coefficient[c], $K_p$ | |
|---|---|---|---|---|---|---|
| | | | | | $a_o = 0$ | $a_o \neq 0$ |
| Ca-Montmorillonite clay sorption | 0.06 | 0.30 | 0.12 ± 0.00 | 2.14 ± 4.62 | 16 ± 14 | -490 ± 740 |
| | | 3.0 | 0.12 ± 0.00 | 1.55 ± 0.29 | | ($a_o$ = 60 ± 87) |
| Coyote Creek sorption[d] | 1.4 | 4.2 | 4.3 ± 0.1 | 0.0 ± 0.2 | -1.7 ± 2.4 | 9.1 ± 6.5 |
| | | 12 | 4.1 ± 0.1 | 8.0 ± 6.2 | | ($a_o$ = -41 ± 62) |
| | | 7.8 | 7.3 ± 0.3 | 56 ± 31 | | |
| | | 24 | 7.6 ± 0.1 | 6.5 ± 6.0 | | |

[a] Concentration measured in supernatant with population standard deviation.

[b] Concentration on sediment calculated from supernatant concentration with population standard deviation.

[c] Calculated by linear least squares method; see Appendix B, Section B.1.4. for description of regressions. Limits are 95% confidence limits.

[d] 1-hour equilibration time.

4.8 were calculated assuming that the reactions were first order in p-cresol, which was found for photolyses beyond two half-lives using the borosilicate filter system. The quantum yield for p-cresol disappearance, 0.079, was calculated from the rate constant $k_p$ measured for the direct photolysis of p-cresol at 313 nm.

The higher photolysis rate of p-cresol in the experiment using the borosilicate glass (immersion well only) filter system is consistent with the greater light intensity transmitted by this filter compared with the 313-nm filter system. From the data for photolyses conducted in April sunlight, the measured half-lives of p-cresol are 35 days in pure water and about 3 days in solutions containing humic acid.

The half-life for direct photolysis of p-cresol in sunlight as a function of the time of the year was calculated by the procedure of Zepp and Cline (1977) using the quantum yield of 0.079 and the measured UV absorption spectrum of p-cresol (Section 4.4.2). These data are plotted in Figure 4.5.

TABLE 4.8. RATE CONSTANTS FOR PHOTOLYSIS OF 1.0 $\mu g\ ml^{-1}$ p-CRESOL[a]

| Irradiation source | Solution | Extent of reaction (%) | Rate constant $k_p \times 10^6\ sec^{-1}$ | Ratio of $k_p$ with humic acid to that in pure water |
|---|---|---|---|---|
| 313 nm | Pure water | 28 | $0.72 \pm 0.04^{b,c}$ | 2.6 |
| | Pure water with 9.5 $\mu g\ ml^{-1}$ humic acid | 40 | $1.84 \pm 0.04$ | |
| Pyrex filter only | Pure water | 81 | $11.7 \pm 1.6$ | 4.8 |
| | Pure water with 9.5 $\mu g\ ml^{-1}$ humic acid | 93 | $56 \pm 1$ | |
| Solar, in April | Pure water | 32 | $0.68 \pm 0.12^{d,e}$ | 12 |
| | Pure water with 9.5 $\mu g\ ml^{-1}$ humic acid | 93 | $8.0 \pm 0.2^{d,f}$ | |

[a] 1.0 $\mu g\ ml^{-1}$ p-cresol in water = $9.2\ 10^{-6}$ M.

[b] Standard deviation.

[c] Quantum yield for p-cresol disappearance was 0.079.

[d] Calculated assuming 8 hours of sunlight per day; weather was mostly overcast during the two-week reaction period. To obtain average ratio constant for full calendar day (24 hours), divide rate constant by three.

[e] Half-life of 35 days.

[f] Half-life of 3.0 days.

Figure 4.5 shows that the computer-calculated half-life for direct solar photolysis of p-cresol in April is about 400 days, based on a UV spectrum with a cutoff at 315 nm (see Table 4.5). However, a hand calculation including the absorption tail beyond 315 nm estimates a half-life of about 200 days. The experimentally measured half-life for the solar photolysis of p-cresol (Table 4.8) is about 35 days. The difference between the calculated and measured half-lives cannot be explained by a pH effect on the absorption coefficient, since the measured half-life was obtained in a solution that was pH 6.3 and the calculation is based on a UV spectrum measured in pH 7.0 solution (Table 4.5).

Since some loss of p-cresol (7% in 8 days*) was found in the dark control solution for the direct photolysis in sunlight, some biodegradation may have occurred in spite of the precautions taken to maintain sterile conditions. If it is assumed that biodegradation was occurring simultaneously with the direct photolysis and that both processes are first order in p-cresol (and that the organism count remains constant), subtracting out the contribution from biodegradation gives a corrected photolysis half-life of about 70 days. This value is still a factor of three less than the calculated 200 day half-life. It is important to note that the computer calculation method has been shown to be quite reliable for other compounds where the tail of the absorption spectrum does not contribute significantly to the absorption rate constant, $k_a$.

The data in Table 4.8 show that the presence of humic acid in solution accelerates the photolyses of p-cresol by factors of 2 to 12 over those in pure water. Humic acid absorbs essentially all the light that leads to transformation of p-cresol in these photolyses; the absorbance of humic acid at 313 nm is about 0.6, compared with $10^{-5}$ calculated for 1 $\mu$g ml$^{-1}$ p-cresol, assuming a 1-cm effective path length in the reaction tube. The difference in the rate factors for the three experiments is certainly due in part to the different spectral distributions of the light sources used and to the capacity of humic acid to absorb light to beyond 400 nm. It may also be due to a wavelength dependence for the quantum efficiency for the sensitized photolyses. Wavelength dependence has been observed for photolyses of parathion in natural waters containing humic substances (N. L. Wolfe, private communication, 1976).

The acceleration in rate by humic acid may be due to a sensitized photolysis in which humic acid serves to transfer excitation energy to p-cresol; humic acid could act as a photoinitiator, a triplet diradical for example, which initiates a radical oxidation process. Other possible roles for humic acid, such as a screening agent or quencher, are apparently not as important in this system. The data do not permit any distinction between these possible reaction pathways.

---

*The actual elapsed time was 8.0 days, corresponding to 64 sunlight hours. Using $k_p = 6.81 \times 10^{-7}$ sec$^{-1}$ (Table 4.8), the calculated loss of p-cresol is 15%.

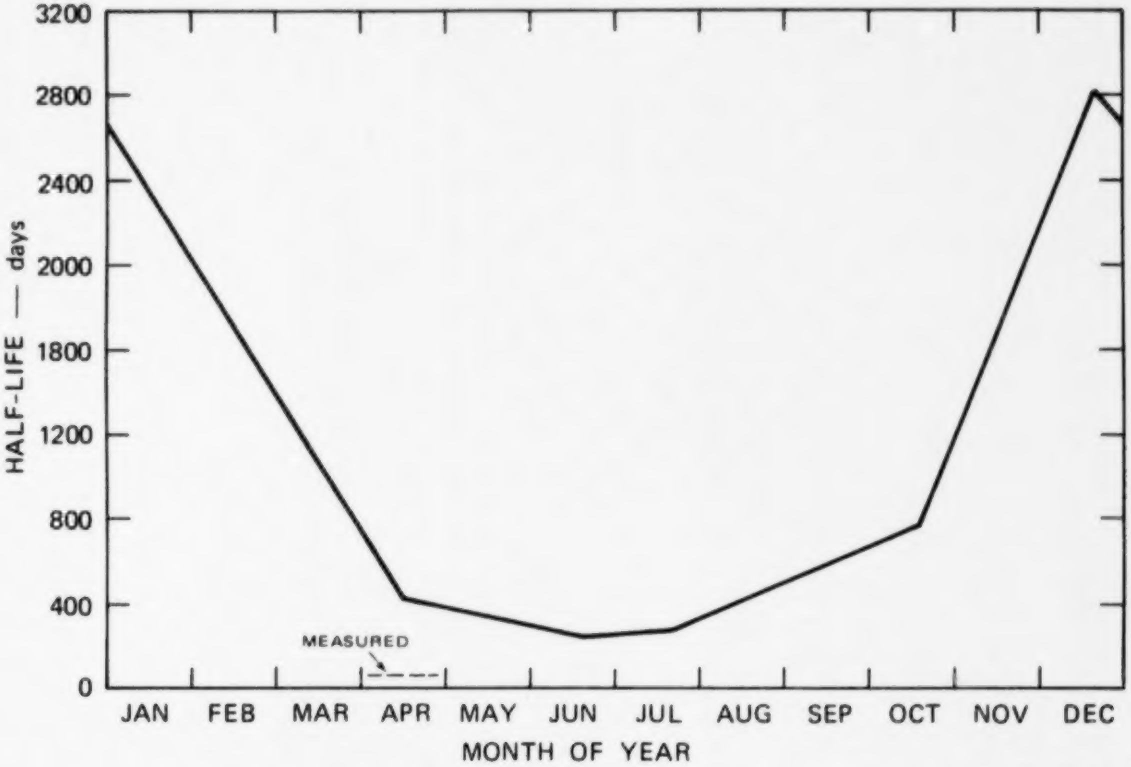

SA-4396-38

FIGURE 4.5 ANNUAL VARIATION OF PHOTOLYSIS HALF-LIFE FOR p-CRESOL

### 4.5.2 Oxidation Rate

The susceptibility of p-cresol to free radical oxidation was examined using the oxidation reaction initiated by 4,4'-azo bis(4-cyanovaleric acid) (AA) (see Appendix B for discussion and procedure). Oxidation reactions with 1.0 x $10^{-4}$ M AA were carried out both in pure water and in pure water that contained 9.5 μg ml$^{-1}$ humic acid; the data are presented in Table 4.9.

TABLE 4.9. FREE RADICAL OXIDATION OF 0.72 μg ml$^{-1}$ p-CRESOL AT 50°C AND 100 HOURS[a]

| Solution | Initial conc. p-cresol (μg ml$^{-1}$)[b] | Final conc. p-cresol (μg ml$^{-1}$)[b] | % Reaction |
|---|---|---|---|
| Water with $10^{-4}$ M AA | 0.72 | 0.58 (0.71)[c] | 20 |
| Water with 9.5 g ml$^{-1}$ humic acid and $10^{-4}$ M AA | 0.73 | 0.53 (0.72)[c] | 27 |

[a] Based on one analysis of reaction at 100 hours.

[b] 1.0 μg ml$^{-1}$ p-cresol in water = 9.2 x $10^{-6}$ M.

[c] Control solution without AA initiator maintained under identical reaction conditions.

From the data in Table 4.9, we obtained a rate constant term ($k_{ox}[RO_2\cdot]$) of 6.0 x $10^{-7}$ sec$^{-1}$ for oxidation of p-cresol in water under the reaction conditions. Under these conditions (see Part I, Section 6.3), this corresponds to a second-order rate constant $k_{ox}$ of 180 M$^{-1}$ sec$^{-1}$. At 25°C, $k_{ox}$ would then be 20 M$^{-1}$ sec$^{-1}$, and with the assumption that $[RO_2\cdot] = 10^{-9}$ M in the environment, the half-life of p-cresol toward oxidation is about 1 year (first-order rate constant of 2 x $10^{-8}$ sec$^{-1}$).

This value of $k_{ox}$ is considerably less than $\sim 10^4$ M$^{-1}$ sec$^{-1}$ observed for a number of phenols in organic media (Howard, 1972). The difference may be due to the hydrogen bonding ability of water, which could reduce the reactivity of the phenolic hydrogen towards abstraction. Alternatively, because of the low radical concentrations, the difference may be due to a more complex reaction sequence than anticipated.

Another important observation is the ineffectiveness of 9 μg ml$^{-1}$ humic acid in the radical oxidation process. Phenolic OH, usually present in humic acids, would be expected to compete with p-cresol for $RO_2\cdot$ and inhibit the rate of p-cresol oxidation. The simplest explanation for lack of a retarding effect is that phenolic OH in humic acid is internally bound (H-bonds or metal complex) and is unreactive or inaccessible to $RO_2\cdot$.

In a separate study of the AA-initiated oxidation of cumene (i-propylbenzene) in water from Coyote Creek, cumene was oxidized readily, indicating that dissolved natural organics did not scavenge all the radicals (Mill et al., 1977). Additional studies of oxidations in natural waters, supported by NSF-RANN are now under way.

### 4.5.3 Hydrolysis Rate

p-Cresol contains no functional groups that are hydrolyzable; therefore, no hydrolysis studies were carried out.

### 4.5.4 Products from Chemical Transformations

Although oxidation and photolysis both showed transformation of p-cresol, only limited studies of these processes were conducted. Biodegradation was obviously the dominant transformation process, as was evident by the biodegradation problems that interferred with the initial chemical transformation studies (Section 4.6). Detailed product studies would have required significant experimental work and therefore were not undertaken.

Information on products was not available from kinetic experiments since some products could not be extracted and others would not elute in the GLPC work-up used for analysis of the p-cresol solutions. One exploratory experiment to analyze for products from oxidation of $7 \times 10^{-5}$ M p-cresol (8 $\mu$g $ml^{-1}$) containing $10^{-4}$ M AA was carried out and analyzed by high pressure liquid chromatography (HPLC). A photoinitiated free radical oxidation was induced by photolyzing AA with 366 nm light (where only AA absorbs). The only products identified were Pummerer's ketone (I) and 2,2'-dihydroxybiphenyl (II); these were identified by comparing retention time with those of samples prepared by literature procedures (Haynes et al., 1956).

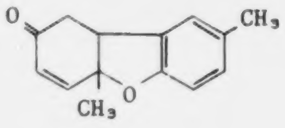

I

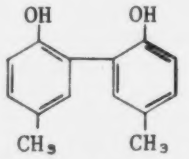

II

These two products accounted for only about 25% of the reacted p-cresol, and after an initial photoperiod, the biphenyl (II) began to decrease with longer irradiation.

More polar products were evident in the HPLC traces but could not be separated for certain identification. These may be the more polar hydroxylated and ring cleavage products and [$RO_2\cdot$] adducts of p-cresol.

## 4.6 BIODEGRADATION

### 4.6.1 Development of Biodegrading Cultures

p-Cresol was one of the first and also the most readily degraded of the compounds studied. For these reasons, there was considerable experimentation with the enrichment and kinetic techniques. Enrichments were first initiated in the 9-liter bottle fermentors containing 4 liters of water, p-cresol, and 1 liter of sterile 0.05% $NH_4NO_3$ or $(NH_4)_2SO_4$ and 0.2% $KH_2PO_4$-$K_2HPO_4$ mixture that maintained the pH of the fermentation at approximately 7.0. When it became obvious that enrichment p-cresol biodegrading systems could be developed readily, initial studies with water samples were sometimes conducted in Erlenmeyer or Fernbach flasks and the water samples were diluted as much as 100%. Incubations were at 25°C except for the Lake Tahoe water samples, which were incubated at 15°C. Initial p-cresol concentrations were 3 $\mu g\ ml^{-1}$ or 10 $\mu g\ ml^{-1}$. For some ancillary studies, the initial levels were as high as 1000 $\mu g\ ml^{-1}$.

A very simple, rapid preliminary test to monitor p-cresol biodegradation consisted of adding 1 drop of 10% aqueous $H_3PO_4$ to a 1- or 2-ml sample, adding 2 ml ethyl acetate, vortexing these contents in a test tube, removing the clear solvent layer, and determining the UV absorbance at 260, 280 and 300 nm. The differences in absorptions at 280 nm and those at 260 and 300 nm were compared with those obtained with standard p-cresol solutions. These wavelengths were chosen because p-cresol has an absorption maximum at 280 nm, aromatic metabolites are expected to absorb at 260 nm, and neither should absorb significantly at 300 nm.

We were unable to obtain water samples from two western coking plants or a wood-creosoting plant. Enrichment biodegrading systems were readily obtained with the water samples from Coyote Creek, the pond near Searsville Lake, aeration effluents from the Palo Alto and South San Francisco sewage plants, the aeration effluent from the Shell Oil Refinery wastewater treatment plant, and Lake Tahoe.

There were invariably induction or lag periods before p-cresol biodegradation began. In one series of experiments with pond water diluted to contain 45% pond water with 3 and 10 $\mu g\ ml^{-1}$ p-cresol, no significant biodegradation occurred until 5.5 and 6 hours incubation of the respective concentrations of pollutant, and degradation was completed at 7 and 8.5 hours, respectively (Figure 4.6). With a 40% v/v dilution of aeration effluent from the Palo Alto sewage plant, total degradation at the 3 and 10 $\mu g\ ml^{-1}$ p-cresol levels occurred at <4 and 6 hours, respectively. In one experiment with 75% pond water and extreme levels of 100, 300, and 1000 $\mu g\ ml^{-1}$ p-cresol, the respective degradations and times were 100% at <24 hours, 100% at approximately 32 hours, and 30% at 72 hours. Undoubtedly, at levels approaching 1000 $\mu g\ ml^{-1}$ p-cresol, many organisms were totally inhibited or killed and some were retarded in growth. No significant degradation was observed in the 1000 $\mu g\ ml^{-1}$ flasks until they had been incubated for 48 hours.

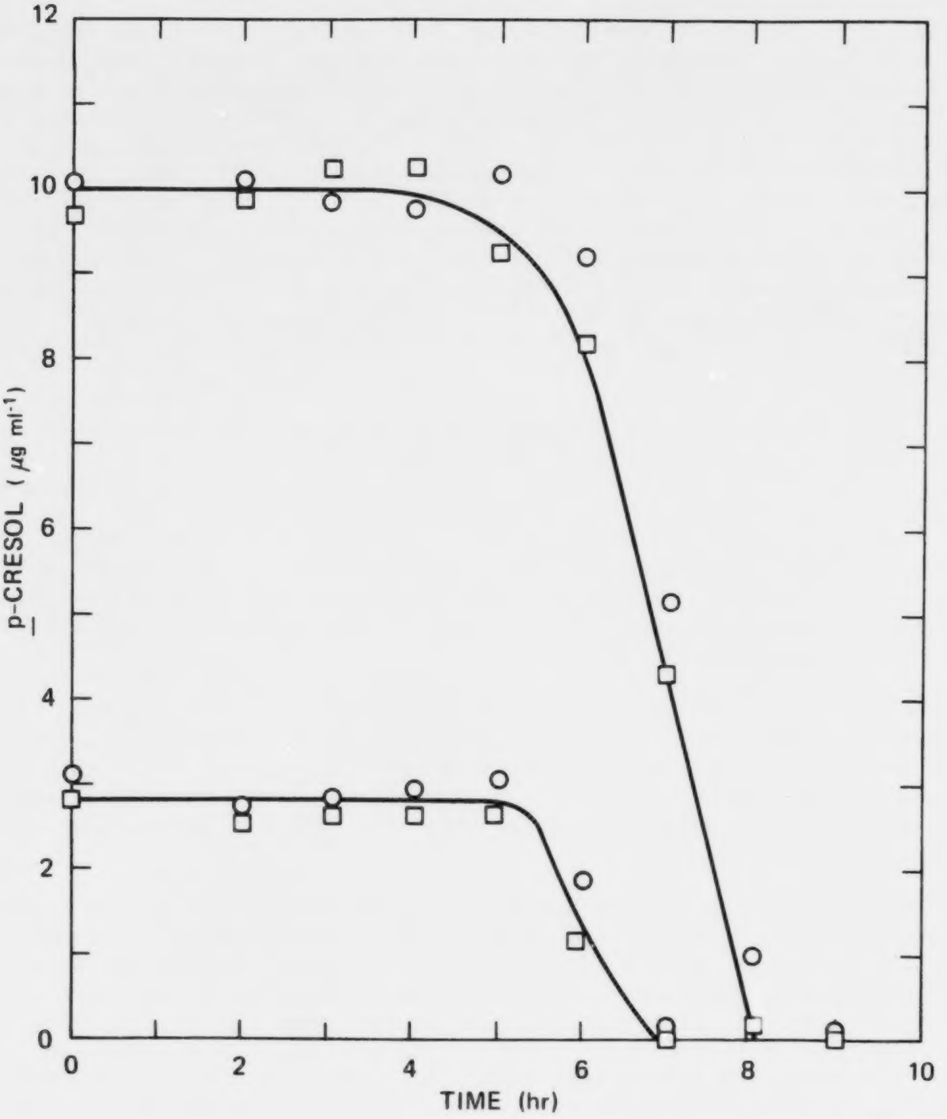

SA-4396-32

FIGURE 4.6 BIODEGRADATION OF p-CRESOL IN EUTROPHIC POND WATER

Initial concentrations of p-cresol were 3 and 10 $\mu$g ml$^{-1}$. Degradation was monitored by uv (○) and gc (□) assays.

With 80% Lake Tahoe water and with 80% Lake Tahoe water that had been mixed with sediment and the sediment was allowed to settle, there was total decomposition of 10 $\mu g\ ml^{-1}$ p-cresol in $<144$ and $<96$ hours, respectively. The respective bacterial counts for these Lake Tahoe samples were 12 and 61 cells $ml^{-1}$. We believe that these counts were too low and that other procedures such as MPN* should have been used.

In subtransferring initial culture mixtures, no problems were encountered in using p-cresol as the only carbon source. There was also no difficulty in developing the pond water culture mixtures to the level that they decomposed 600 $\mu g\ ml^{-1}$ p-cresol in 24 hours. Culture mixtures from other enrichments were not subtransferred in media containing more than 100 $\mu g\ ml^{-1}$ p-cresol. In fact, as will be discussed later, because of the rapid degradation of p-cresol at lower levels, there could be many organisms that grow on release or autolysis products or other bacteria that are primary or secondary utilizers of p-cresol.

A multitransferred p-cresol enrichment culture was streaked out on basal salts/p-cresol agar, and many types of cells were observed. Seven very obvious types were selected from a larger number of variants, and after transfers, they were tested for growth rates on 600 $\mu g\ ml^{-1}$ p-cresol media by optical density measurements at 600 nm. All seven isolates had comparable growth rates.

### 4.6.2 Biodegradation Kinetics

Two types of kinetic studies were conducted: batch fermentations with low-level inocula and continuous fermentations in chemostats.

Batch Fermentations with Low-Level Inocula--Figures 4.7, 4.8, and 4.9 present the data from a batch fermentation with a low-level of inoculum of p-cresol decomposing organisms developed from a eutrophic pond. Figures 4.7 and 4.8 are plots of viable counts in flasks with initial p-cresol levels of 0, 3, 5, and 0, 10, 20 $\mu g\ ml^{-1}$, respectively. The increase in counts in the control flask with no p-cresol is attributed to the fact that the viable organisms were metabolizing and excreting products, and dead cells or cells that were dying in this mixed culture were autolysing and releasing products that other organisms could use for survival and multiplication. The possibility also exists that trace quantities of metabolizable organic matter may be introduced in the distilled water or from the atmosphere (Kayser et al., 1975). Because p-cresol is so readily metabolized, increases in cell counts in media with this compound are most likely due to good survival and growth of p-cresol utilizers (primary and secondary).

The specific growth rate ($\mu$) in each medium was determined by measuring the slope of the curves in the logarithmic phase of growth. For the media initially containing 3, 5, 10, and 20 $\mu g\ ml^{-1}$ p-cresol, $\mu$ values were 0.58,

---

*Most Probable Number, as defined in "Standard Methods for Examination of Water and Wastewater," 13th edition, p. 635.

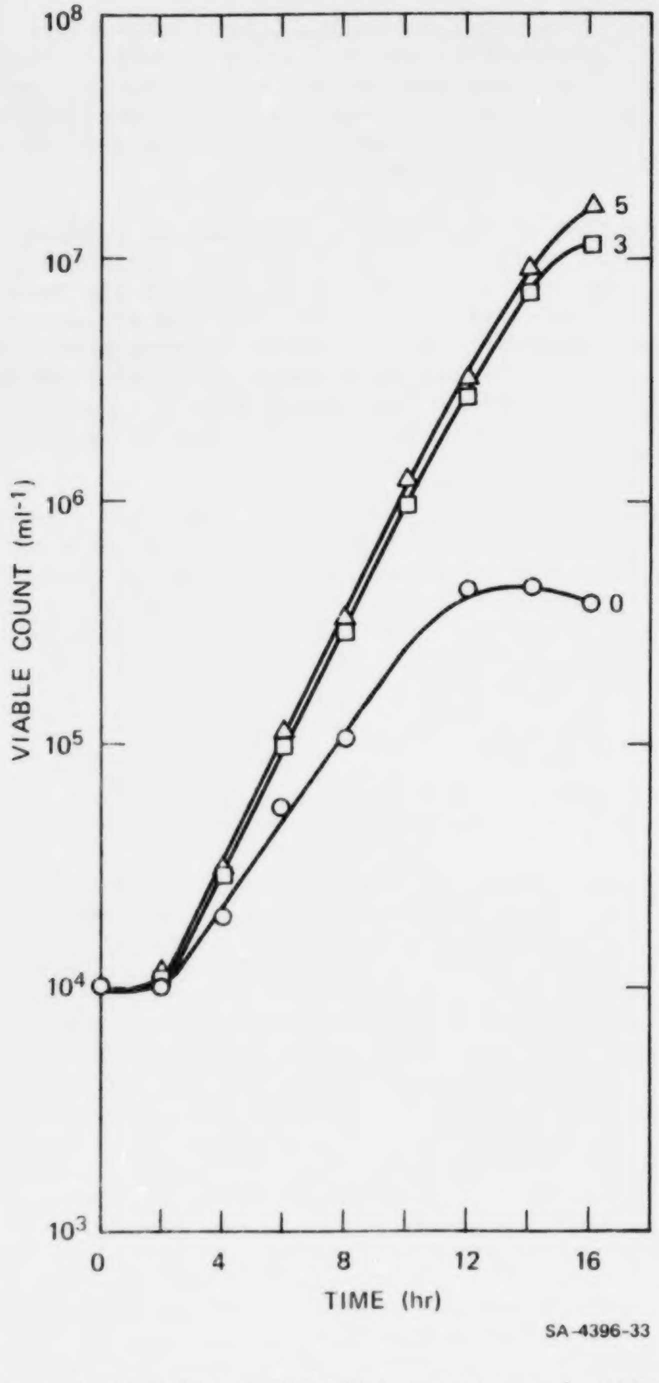

FIGURE 4.7 VIABLE CELL COUNTS IN 0, 3, and 5 $\mu$g ml$^{-1}$ p-CRESOL BIODEGRADATION BY BATCH FERMENTATION WITH A LOW-LEVEL INOCULUM

Initial p-cresol concentrations: 0 (○), 3 (□) and 5 (△) $\mu$g ml$^{-1}$.

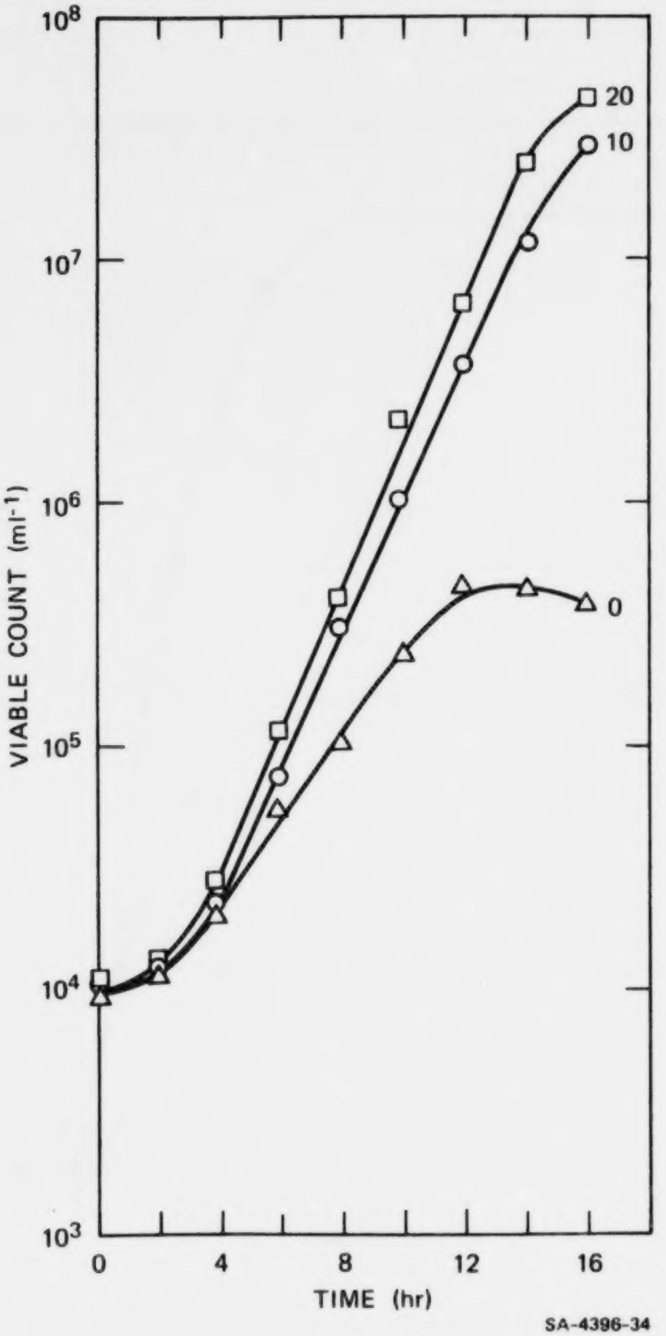

FIGURE 4.8 VIABLE CELL COUNTS IN 0, 10, AND 20 $\mu$g ml$^{-1}$ p-CRESOL BIODEGRADATION BY BATCH FERMENTATION WITH A LOW-LEVEL INOCULUM

Initial p-cresol concentration: 0 (△), 10 (○) and 20 (□) $\mu$g ml$^{-1}$.

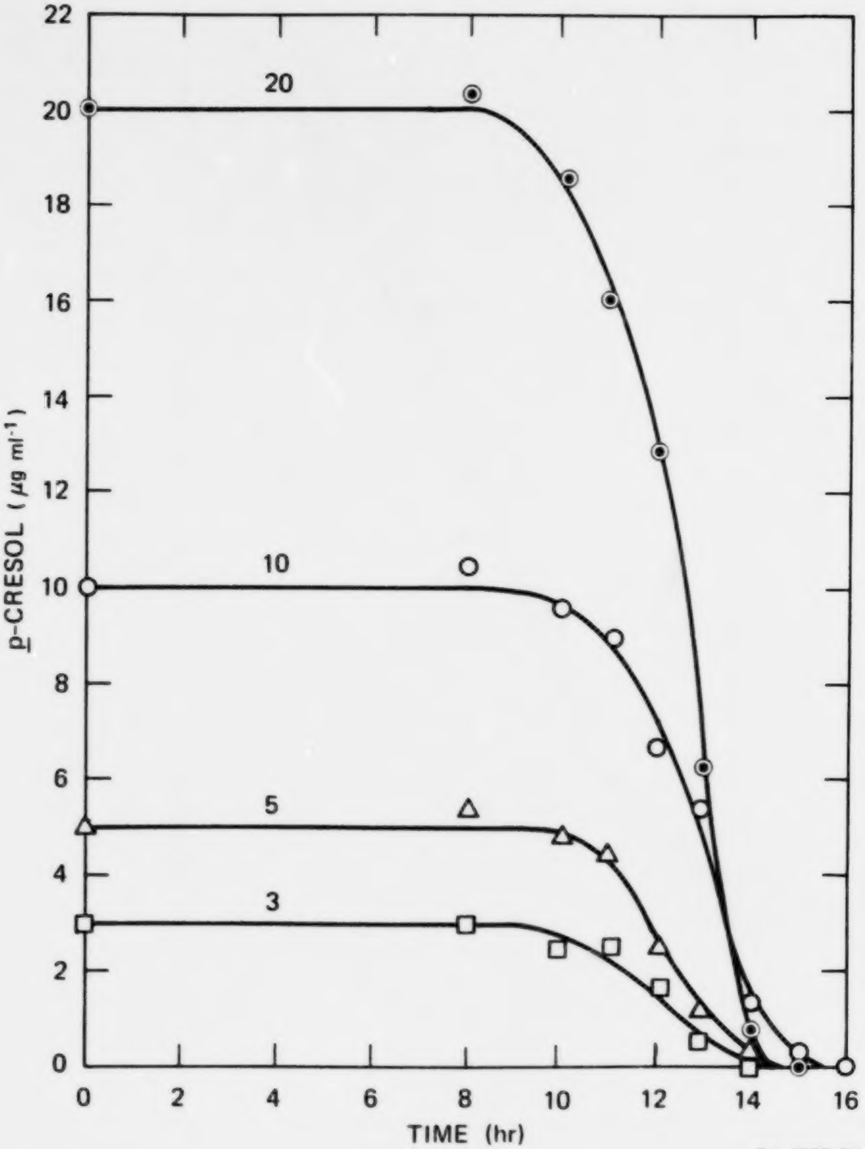

SA-4396-35

FIGURE 4.9 p-CRESOL BIODEGRADATION BY BATCH FERMENTATION WITH A LOW-LEVEL INOCULUM

Initial p-cresol concentration: 3 (□), 5 (△), 10 (○) and 20 (◉) $\mu$g ml$^{-1}$

0.61, 0.63, and 0.67 $hr^{-1}$, respectively. Figure 4.9 shows that most of the p-cresol has been utilized by 14 hours, even though Figures 4.7 and 4.8 indicate significant increases in cell counts between 14 and 16 hours.

Table 4.10 gives the calculated cell yield (Y) values for cell growths in media with different initial p-cresol concentrations and at different periods in the fermentations. The average Y values obtained from the time significant utilization of p-cresol could be measured up to 14 hours of incubation were used in subsequent calculations of rate constants. Figure 4.10 is a Lineweaver-Burk plot developed by the least squares method. The values of $K_s$ and $\mu_m$, determined by the intercept of the ordinate axis and the slope of the curve in Figure 4.10, were calculated as 0.69 μg $ml^{-1}$ and 0.69 $hr^{-1}$, respectively.

TABLE 4.10. YIELD OF CELLS IN A p-CRESOL BATCH FERMENTATION WITH A LOW-LEVEL INOCULUM[a]

| | Incubation time 10 hr | 12 hr | 14 hr | Average yield |
|---|---|---|---|---|
| $S_o$ = 3 μg $ml^{-1}$ | | | | |
| ΔS (μg $ml^{-1}$) | -- | 1.4 | 2.7 | |
| X (cells x $10^{-6}$ $ml^{-1}$) | -- | 2.5 | 7.4 | |
| Y (cells x $10^{-6}$ $\mu g^{-1}$ p-cresol) | -- | 1.8 | 2.7 | 2.2 |
| $S_o$ = 5 μg $ml^{-1}$ | | | | |
| ΔS (μg $ml^{-1}$) | -- | 2.5 | 4.6 | |
| X (cells x $10^{-6}$ $ml^{-1}$) | -- | 3.5 | 9.0 | |
| Y (cells x $10^{-6}$ $\mu g^{-1}$ p-cresol) | -- | 1.4 | 2.0 | 1.7 |
| $S_o$ = 10 μg $ml^{-1}$ | | | | |
| ΔS (μg $ml^{-1}$) | -- | 3.2 | 8.6 | |
| X (cells x $10^{-6}$ $ml^{-1}$) | -- | 3.7 | 12 | |
| Y (cells x $10^{-6}$ $\mu g^{-1}$ p-cresol) | -- | 1.2 | 1.4 | 1.3 |
| $S_o$ = 20 μg $ml^{-1}$ | | | | |
| ΔS (μg $ml^{-1}$) | 1.5 | 7.0 | 19.3 | |
| X (cells x $10^{-6}$ $ml^{-1}$) | 2.0 | 6.5 | 25 | |
| Y (cells x $10^{-6}$ $\mu g^{-1}$ p-cresol) | 1.3 | 0.9 | 1.3 | 1.2 |

[a] 9.8 x $10^3$ cells $ml^{-1}$ of a biodegrading system developed from eutrophic pond water. $S_o$ is initial concentration of p-cresol, ΔS is difference in concentration after incubation, X is bacterial cell count, and Y is the cell yield.

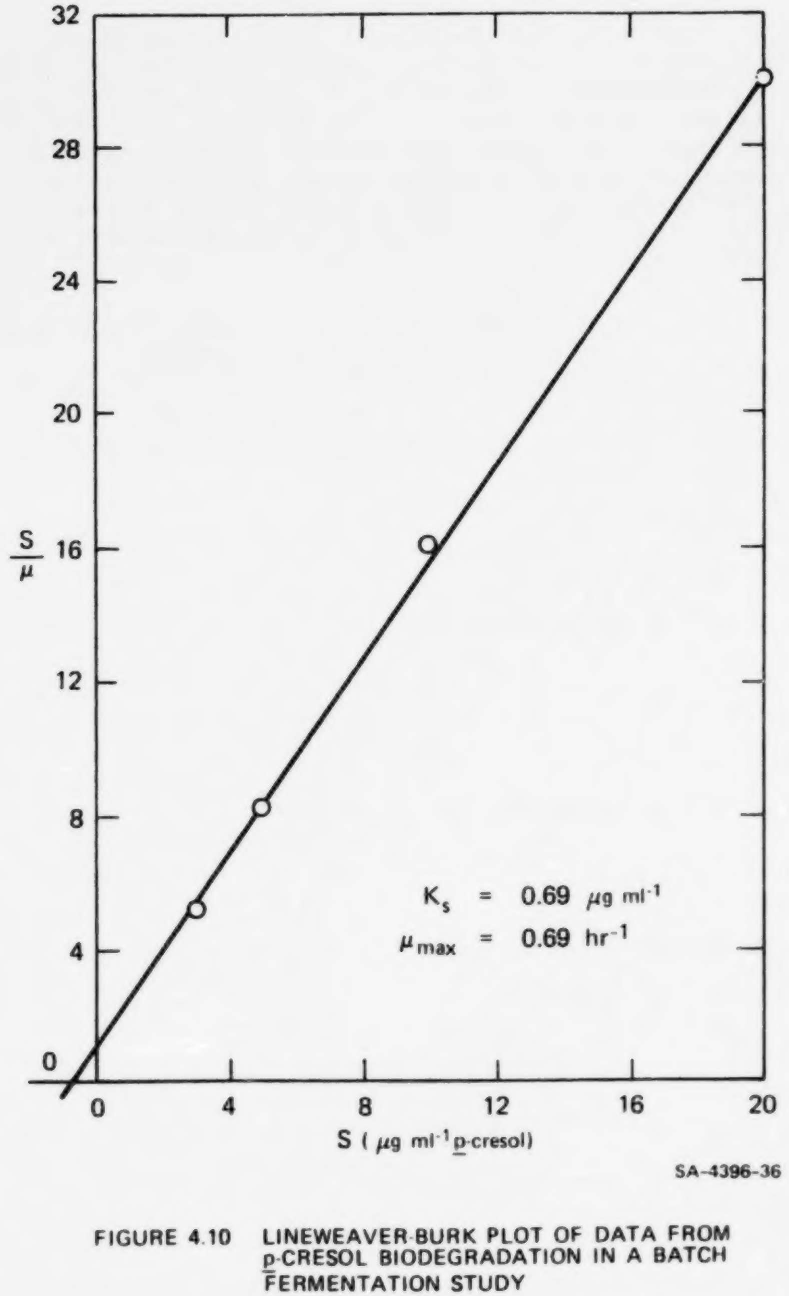

FIGURE 4.10 LINEWEAVER-BURK PLOT OF DATA FROM p-CRESOL BIODEGRADATION IN A BATCH FERMENTATION STUDY

Table 4.11 presents the calculated Y and first-order rate constant ($k_b$) values obtained in this batch fermentation study with low levels of inoculum of a p-cresol degrading system. The second-order rate constant $k_{b2} = k_{b1}/K_s$ equals $6.7 \times 10^{-7}$ ml cell$^{-1}$ hr$^{-1}$.

TABLE 4.11. FIRST-ORDER RATE CONSTANTS ($k_b$) IN A p-CRESOL BATCH FERMENTATION WITH A LOW-LEVEL INOCULUM[a]

| Initial conc. $S_o$ ($\mu$g ml$^{-1}$) | Cell yield (Y) (cells $\mu$g$^{-1}$) | $k_b = \mu_m/Y$ ($\mu$g cell$^{-1}$ hr$^{-1}$) |
|---|---|---|
| 3 | $2.2 \times 10^6$ | $3.1 \times 10^{-7}$ |
| 5 | $1.7 \times 10^6$ | $4.1 \times 10^{-7}$ |
| 10 | $1.3 \times 10^6$ | $5.3 \times 10^{-7}$ |
| 20 | $1.2 \times 10^6$ | $5.8 \times 10^{-7}$ |
| Average | $(1.6 \pm 0.5) \times 10^6$ | $(4.6 \pm 1.2) \times 10^{-7}$ |

[a] $9.8 \times 10^3$ cells ml$^{-1}$ of a biodegrading system developed from eutrophic pond water.

Biodegradation in a p-Cresol Continuous Feed Fermentation in a Chemostat--Table 4.12 presents data from a fermentation in which a basal inorganic salts/100-$\mu$g ml$^{-1}$ p-cresol medium was continuously fed to a fermentation in a chemostat. The Lineweaver-Burk plot determined by the least squares method is presented in Figure 4.11. From these data, $K_s$ was calculated as 0.99 $\mu$g ml$^{-1}$ and $\mu_m$ was calculated as 0.56 hr$^{-1}$. The second-order rate constant $k_{b2}$ is $3.7 \times 10^{-7}$ ml cell$^{-1}$ hr$^{-1}$.

The $\mu_m$, $K_s$, Y, $k_b$, and $k_{b2}$ values obtained by the two procedures are compared in Table 4.13.

### 4.6.3 Metabolites

The p-cresol degradation took place so rapidly that no metabolites were observed.

### 4.6.4 Discussion

Enrichment culture systems that would biodegrade p-cresol were readily obtained from all waters after relatively short induction periods. It was also relatively easy to develop culture systems that could decompose high concentrations of p-cresol when it was the only carbon source. Under microscopic

TABLE 4.12. KINETICS OF A p-CRESOL BIODEGRADATION IN A CONTINUOUS FERMENTATION

| Specific growth rate ($\mu$) (hr$^{-1}$) | Outflow conc. (S) ($\mu$g ml$^{-1}$) | S/$\mu$ (calculated) | Microbial count (X) (cells ml$^{-1}$) | Cell yield (Y) (cells $\mu$g$^{-1}$ MP) | $k_b = u_m/Y$ ($\mu$g cell$^{-1}$ hr$^{-1}$) |
|---|---|---|---|---|---|
| 0.56 | 46.4 | 82.9 | $4.0 \times 10^7$ | $7.4 \times 10^6$ | $7.6 \times 10^{-7}$ |
| 0.53 | 26.9 | 50.8 | | | |
| 0.50 | 18.0 | 36.0 | $9.0 \times 10^7$ | $1.1 \times 10^6$ | $5.1 \times 10^{-7}$ |
| 0.48 | 14.9 | 31.1 | | | |
| 0.47 | 9.72 | 20.7 | $1.8 \times 10^8$ | $2.0 \times 10^6$ | $2.8 \times 10^{-7}$ |
| 0.45 | 5.84 | 13.0 | $2.0 \times 10^8$ | $2.1 \times 10^6$ | $2.7 \times 10^{-7}$ |
| 0.44 | 1.76 | 4.0 | $2.8 \times 10^8$ | $2.9 \times 10^6$ | $1.9 \times 10^{-7}$ |
| 0.42 | 1.24 | 2.95 | | | |
| 0.40 | 0.76 | 1.90 | $2.6 \times 10^8$ | $2.6 \times 10^6$ | $2.2 \times 10^{-7}$ |
| 0.38 | 0.26 | 0.68 | $3.2 \times 10^8$ | $3.2 \times 10^6$ | $1.75 \times 10^{-7}$ |
| | | | Average | $(2.1 \pm 0.9) \times 10^6$ | $(3.4 \pm 2.2) \times 10^{-7}$ |

examination and in a plating-out study it was obvious that many types of cultures were present after many passages on liquid media. It is not known how many of these were primary utilizers of p-cresol, or secondary utilizers that grew on metabolites, or how many grew on excretion products associated with living or dying p-cresol metabolizers.

The agreement in the $\mu_m$, $K_s$, Y, $k_b$, and $k_{b2}$ values obtained by the two kinetic procedures (Table 4.13) is excellent for mixed and even pure cultures. There were difficulties with film formation (Atkinson and Fowler, 1974) in the continuous feed studies. Also, these kinetic studies were conducted at such different periods that there could have been changes in proportions of different strains in the microbial mixture, particularly in the prolonged chemostat fermentations. These values cannot be compared with those reported for phenol by Yang and Humphrey (1975) because, although p-cresol and phenol have similar structures, they would obviously have different metabolic processes and because Yang and Humphrey's studies with phenol were conducted at levels that were inhibitory to the microorganisms they used.

No attempts were made to determine optimal degradation conditions or to develop or select strains or mixtures of strains with high degradation rates. The development of degrading culture mixtures that are more exclusively asso-

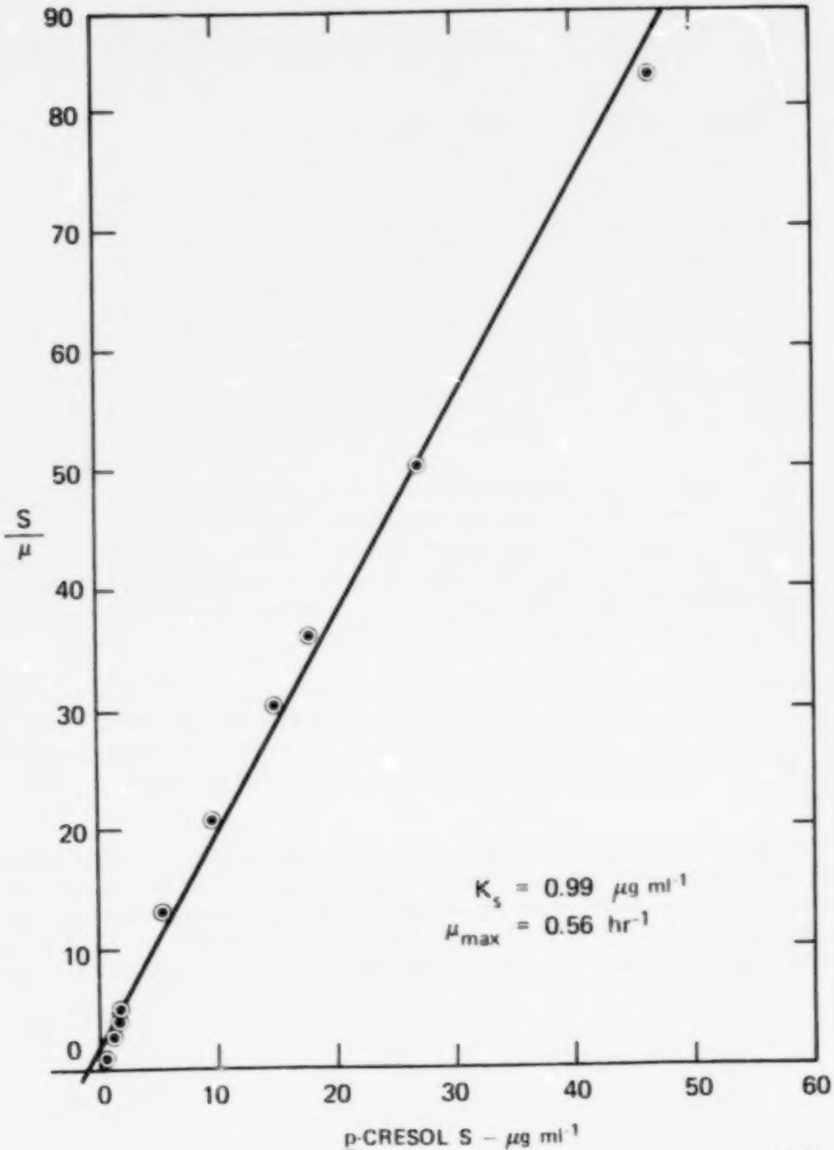

SA-4396-37

FIGURE 4.11 LINEWEAVER-BURK PLOT OF DATA FROM p-CRESOL BIODEGRADATION IN A CONTINUOUS FERMENTATION

TABLE 4.13. COMPARISON OF KINETIC DATA OBTAINED ON BIODEGRADATION OF p-CRESOL BY TWO PROCEDURES

| | $\mu_m$ ($hr^{-1}$) | $K_s$ ($\mu g\ ml^{-1}$) | $Y$ (cells $\mu g^{-1}$) | $k_{b1}$ ($\mu g\ cell^{-1}\ hr^{-1}$) | $k_{b2}$ ($ml\ cell^{-1}\ hr^{-1}$) |
|---|---|---|---|---|---|
| Batch fermentation with low inoculum | 0.69 | 0.69 | $1.6 \times 10^{6}$ | $4.6 \times 10^{-7}$ | $6.7 \times 10^{-7}$ |
| Continuous chemostat fermentation | 0.56 | 0.99 | $2.1 \times 10^{6}$ | $3.7 \times 10^{-7}$ | $3.7 \times 10^{-7}$ |
| Average | 0.62 | 0.84 | $1.8 \times 10^{6}$ | $4.2 \times 10^{-7}$ | $5.2 \times 10^{-7}$ |

ciated with the primary and secondary utilization of p-cresol would have required very frequent, short-interval transfers before all p-cresol had degraded, but this would have been impossible without continuous 24-hour monitoring. This could be avoided, however, by using a continuous fermentation in which a desired level is maintained, similar to the phenol-stat chemostat used by Yang and Humphrey (1975).

During the course of our p-cresol degradations, no breakdown products were detected. This suggests that, with our complex mixuture of cultures, the growth limiting step was the primary attack on p-cresol. However, we were working with very low levels of compound and frequently close to the limits of detection.

Undoubtedly, if single isolates had been obtained, if the fermentations had been appropriately regulated, and if higher levels of p-cresol had been used, metabolites would have been observed with characteristics of those reported by Dagley and Patel (1957), and Bayly et al. (1966). The mixed culture fermentations are, however, more representative of conditions in nature.

## 5. LABORATORY INVESTIGATION OF BENZ[a]ANTHRACENE

### 5.1 SYNOPSIS

The results of the laboratory investigations suggest that benz[a]anthracene (BA) will accumulate in the sediment and biota portions of an aquatic environment. A small amount of BA will be dissolved and will be transformed by photolysis and, to a lesser extent, by oxidation. One primary photolysis product is the 7,12-quinone, which is photostable at 366 nm. Other products are also formed as a result of photolysis in the presence of both water and oxygen. Biotransformation of BA was not observed in our enrichment cultures; however, reports in the literature suggest that biotransformation of BA might occur under environmental conditions.

The nine-compartment environmental exposure assessment model predicted the following steady-state concentrations of BA in solution, suspended solids, and sediments near point sources in the presence of a continuous discharge of 1 ng $ml^{-1}$ (1 ppb) BA.

| | Half-life[*] (hr) | Solution (ng $ml^{-1}$) | Suspended solids (ng $g^{-1}$) | Sediments[†] (ng $g^{-1}$) |
|---|---|---|---|---|
| River | 0.55 | $2.6 \times 10^{-1}$ | $6.6 \times 10^{3}$ | $6.1 \times 10^{3}$ |
| Pond | 22 | $3.2 \times 10^{-3}$ | $7.2 \times 10^{1}$ | $7.2 \times 10^{1}$ |
| Eutrophic lake | 22 | $3.2 \times 10^{-2}$ | $8.0 \times 10^{2}$ | $2.7 \times 10^{2}$ |
| Oligotrophic lake | 8 | $1.8 \times 10^{-2}$ | $4.4 \times 10^{2}$ | $1.2 \times 10^{2}$ |

### 5.2 BACKGROUND

Benz[a]anthracene (BA) is a polynuclear aromatic hydrocarbon (PAH) that is known to be carcinogenic to animals and probably also to humans. Excellent reviews on the occurrence of BA and other PAH in various environments are available (Radding et al., 1976; Harrison et al., 1975; National Academy of Sciences, 1972; Andelman and Suess, 1970).

---

[*] Predicted by one-compartment model.

[†] Average concentration in sediments.

Benz[a]anthracene (BA) is ubiquitous in the environment. Typical sources are engine exhaust, cigarette smoke, coal-tar pitch, and the soot and smoke of industrial and domestic origin. High concentrations of BA have been found in air and in soil near industrial centers and transportation routes. BA concentrations of 1 to 23 pg $ml^{-1}$ have been found in drinking waters, with 4.3 to 185 pg $ml^{-1}$ found in surface waters. Concentrations as high as 31.4 ng $ml^{-1}$ have been found in sewage water, and concentrations ranging from 25 to 10,360 pg $ml^{-1}$ have been found in industrial effluents and waters contaminated by bituminous substances (IARC, 1973).

The general physical properties of BA that were found in the literature are given in Table 5.1.

TABLE 5.1. PHYSICAL PROPERTIES OF BENZ[a]ANTHRACENE

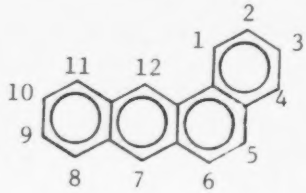

| | |
|---|---|
| Molecular weight | 228.28 |
| Melting point (°C) | 155-7 (160)(162)(167) |
| Boiling point at 760 torr (°C) | 435 (sublimes) |
| Vapor pressure at 20°C (torr) (Pupp et al., 1974) | $5 \times 10^{-9}$ |
| Solubility in water at 27°C (ng $ml^{-1}$) (Davis and Parke, 1942) | 11 |

1.00 ng $ml^{-1}$ (1 ppb) BA in water = $4.38 \times 10^{-9}$ M

The oxidation and photochemistry of PAH were reviewed by SRI as part of a task report for EPA-OTS (Radding et al., 1976). McGinnes and Snoeyink (1974) have reported the direct photolysis of BA; their data indicate that the half-life for photolysis in sunlight is less than a day. They tentatively identified one BA photoproduct as benz[a]anthracene-7,12-quinone and a second major product only as a complex organic acid.

Microbial oxidations of benzo[a]pyrene, benz[a]anthracene, and dibenz[a]-anthracene have been reported by Sisler and Zobell (1947), Fedoseeva et al. (1968), and Poglazova et al. (1967a,b; 1968). However, little was known about the metabolic products of these compounds until recently.

Gibson et al. (1975), using enrichment techniques with biphenyl as a sole carbon source, isolated a Beijerinckia from a polluted stream. This organism completely degraded biphenyl, but a mutant obtained from this parent could only oxidize biphenyl to cis-2,3-dihydroxy-1-phenylcyclohexa-4,6-diene when the mutant was grown in an inorganic-salt medium containing succinate (0.2%) and biphenyl (0.1%) and the washed cells were incubated with biphenyl.

Under these growth conditions, succinate provided all the carbon for growth. These two strains have been very useful in metabolic studies with such chemically related compounds as BA, benzo[a]pyrene, and dibenzothiophene (Gibson, 1975; Gibson et al., 1975). The mutant converted BA to four dihydrodiols (Gibson et al., 1975; Gibson, 1975), and the parent strain could oxidize this compound to cause ring fission and form organic acids that were not identified (Gibson, 1975).

This excellent work from Gibson's laboratories indicates the value of using chemically related products for development of enrichment cultures and the utility of this procedure in transformation or degradation studies with more complex products.

In totally different studies with sediments from an oil-polluted creek, Walker and Colwell (1975) concluded that the susceptibility of aromatic components to degradation decreases with increase in the number of rings, i.e., in order from monoaromatics through diaromatics, triaromatics, tetraaromatics, and pentaaromatics.

Wodzinski and Johnson (1968) reported that the generation times of the bacteria isolated on aromatic hydrocarbon were related to the solubilities of the aromatic hydrocarbons on which they were grown. The more insoluble aromatic hydrocarbons resulted in slower growth.

Wodzinski and Bertolini (1972) and Wodzinski and Coyle (1974) showed that bacteria utilize naphthalene and phenanthrene in the dissolved state and that the growth rates were independent of the amount of solid, undissolved hydrocarbon presented, which suggests that bacteria do not utilize hydrocarbons directly at the surface of a solid particle suspended in the medium. They predicted that very insoluble aromatic hydrocarbons would not be utilized readily.

Wodzinski and Larocca (1977) reported that bacteria can also utilize liquid state aromatic hydrocarbons and solid aromatic hydrocarbons dissolved in liquid hydrocarbons at the water-hydrocarbon interfaces, but not at the solid particle surface.

A personal communication from J. J. Perry (1977) indicated that a number of fungi could transform benzo[a]pyrene to complex mixtures of organic acids. A comparable situation could exist in the biodegradation of BA.

These results suggest that biodegradation of BA might occur under certain conditions. However, there have been no reports on the development of BA-biodegrading enrichment systems or on the rate of metabolism of BA in aquatic environments.

We anticipated that photolysis and sorption onto sediments and biota would probably be important pathways for BA. The literature data on these processes were, however, insufficient to allow us to quantitatively estimate the importance of these processes in relation to biodegradation, volatilization, and oxidation. Screening studies were therefore conducted for all of these processes.

## 5.3 ENVIRONMENTAL ASSESSMENT

### 5.3.1 Summary of Laboratory Data

The rate constants obtained in the laboratory investigations of the transformation and transport processes for BA are summarized in Table 5.2.

TABLE 5.2. SUMMARY OF BENZ[a]ANTHRACENE LABORATORY DATA

| Process | Sorption equilibrium | Partition coefficient |
|---|---|---|
| Sorption | $S_s = K_p S_w$ | $K_p = 26{,}200 \pm 1{,}700$[a] |
| | Rate expression | Rate constant at 25°C |
| Volatilization[b] | $k_v[BA]$ | $k_v = (0.0016 \pm 0.0006)k_v^0$ |
| Photolysis[c] | $k_p[BA] = \Phi(\Sigma Z_\lambda \varepsilon_\lambda)[BA]$ | $k_p = (5.91 \pm 0.07) \times 10^{-5}\ sec^{-1}$ |
| Oxidation | $k_{ox}[RO_2\cdot][BA]$ | $k_{ox} = 5.0 \times 10^3\ M^{-1}\ sec^{-1}$ |
| Hydrolysis | NA | $k_h = 0$ |
| Biodegradation[d] | $k_{b2} = \frac{\mu_{max}}{Y K_s}$ | $k_{b2} = 0$ |

[a] On Coyote Creek sediment.

[b] See discussion in Part I, Section 5.3 of the final report.

[c] Midday on a cloudy day in early March.

[d] Biodegradation was not observed during our enrichment procedures.

### 5.3.2 Environmental Assessment Using the One-Compartment Model

The half-lives of dissolved BA calculated for individual transformation or removal processes following a spill are listed in Table 5.3. Although these half-lives vary among water bodies, photolysis and sorption consistently dominate the transformation and removal processes. Loss by oxidation is about 4 times slower than loss by photolysis, and loss by volatilization is 20 to 100 times slower than photolysis.

As discussed in detail in Section 5.5, the half-life of photolysis as measured at noon was approximately 3 hours. Allowing for variations in light intensity during a 24-hour cycle, the average photolysis rate constant is estimated to be $6.93 \times 10^{-1}$ per hour in oligotrophic waters, giving an estimated half-life of 40 hours.

TABLE 5.3. TRANSFORMATION AND TRANSPORT OF BENZ[a]ANTHRACENE PREDICTED BY THE ONE-COMPARTMENT MODEL

| Process | Stream | Eutrophic pond | Eutrophic lake | Oligotrophic lake |
|---|---|---|---|---|
| Photolysis, half-life (hr) | 20 | 50 | 50 | 10 |
| Oxidation, half-life[a] (hr) | 38 | 38 | 38 | 38 |
| Volatilization, half-life (hr) | >1000 | >1000 | >1000 | >1000 |
| Hydrolysis, half-life (hr) | NA | NA | NA | NA |
| Biodegradation, half-life (hr) | Slow | Slow | Slow | Slow |
| Half-life for all processes, except dilution (hr) | 13 | 22 | 22 | 8 |
| Half-life for all processes, including dilution (hr) | 0.55 | 22 | 22 | 8 |
| Amount BA sorbed[b] (mg $m^{-3}$) | 2.5 | 7.5 | 1.25 | 1.25 |
| Percentage BA sorbed | 71% | 88% | 55% | 55% |

[a] Based on peroxy radical concentration of $10^{-9}$ M.

[b] 1 ng $ml^{-1}$ BA is assumed in the solution phase.

The oxidation rate of BA may also vary during a 24-hour period, since the formation of the peroxy radical, which is at least partially responsible for the oxidation of BA, may be governed by light intensity. Hence the oxidation half-life of 38 hours estimated from the laboratory data, when adjusted to account for diurnal variations, gives an estimated half-life of about 160 hours in an aquatic environment.

Sorption half-lives have not been measured, but the times needed to reach equilibrium are generally less than half an hour for those compounds for which the rates have been measured.

The partition coefficient of BA was measured as $2.5 \times 10^4$. As shown in Table 5.3, ranges of 55% to 88% BA are sorbed on the solid phase. This means that less than half of the total BA in the water body is available for photolytic and oxidative reactions.

Half-lives are estimated to range from 10 to 50 hours in rivers, ponds, and lakes as wholes, but the half-life of BA in specific river segments should be an order of magnitude less, the precise value depending on the flow rates and geometry of that river segment.

### 5.3.3 Persistence

The persistence of concentrations that approximate the initial concentrations following an acute discharge should be largely a function of the dilution rate in fast flowing streams. Persistence of relatively high concentrations in lakes and ponds is expected to be determined by rates of sorption and photolysis within the aqueous phase. In both cases, "high" concentrations should be transient, lasting only a few hours. However, low concentrations of BA caused by desorption from contaminated sediments can be expected indefinitely.

BA may be more persistent in eutrophic water than in oligotrophic waters, since the major transformation pathway, photolysis, would be less effective in such waters, as indicated in Table 5.3. Moreover, since the sediment loading is typically higher in eutrophic waters, the amount of BA sorbed to solids should be greater than in oligotrophic waters, creating a larger reservoir of BA that is subject to later desorption. This pattern is borne out by the more elaborate simulations reported below.

### 5.3.4 Mass and Concentration Distributions Calculated Using Computer Models

The pseudo-first-order rate constants used in these simulations are presented in Appendix A. The distributions of mass and concentration of BA expected at steady state during chronic discharge to each of four types of water bodies (Table 5.4) are typical of most of the chemicals studied to date. At most, 20%, and generally less than 0.5%, of the BA is in solution under steady-state conditions. The steady-state concentrations of BA in solution or sorbed to suspended solids differ about 100-fold between compartments in each of the multicompartment simulations, but are generally at least 100 times less than in the inflowing waters, with the highest concentrations occurring near the source.

TABLE 5.4. DISTRIBUTION OF BENZ[a]ANTHRACENE IN VARIOUS AQUATIC SYSTEMS AT STEADY STATE
(input concentrations of 1 ng ml$^{-1}$ benz[a]anthracene)

| | Pond | | River | | Eutrophic Lake | | Oligotrophic Lake | |
|---|---|---|---|---|---|---|---|---|
| | Mass (kg) | Conc. (ng g$^{-1}$) | Mass (kg) | Conc. (ng g$^{-1}$) | Mass (kg) | Conc. (ng g$^{-1}$) | Mass (kg) | Conc. (ng g$^{-1}$) |
| Compartment 1 (surface water) | | | | | | | | |
| Solution | $6.30 \times 10^{-5}$ | $3.2 \times 10^{-3}$ | $7.93 \times 10^{-2}$ | $2.64 \times 10^{-1}$ | $7.98 \times 10^{-3}$ | $3.19 \times 10^{-2}$ | $4.40 \times 10^{-3}$ | $1.76 \times 10^{-2}$ |
| Suspended solids | $4.4 \times 10^{-4}$ | 72.0 | $1.98 \times 10^{-1}$ | $6.60 \times 10^{3}$ | $9.98 \times 10^{-3}$ | $7.98 \times 10^{2}$ | $5.50 \times 10^{-3}$ | $4.4 \times 10^{2}$ |
| Compartment 2 (surface water) | | | | | | | | |
| Solution | -- | -- | $7.35 \times 10^{-2}$ | $2.45 \times 10^{-1}$ | $2.74 \times 10^{-2}$ | $1.09 \times 10^{-2}$ | $5.18 \times 10^{-3}$ | $2.07 \times 10^{-3}$ |
| Suspended solids | -- | -- | $1.83 \times 10^{-1}$ | $6.10 \times 10^{3}$ | $3.42 \times 10^{-2}$ | $2.73 \times 10^{2}$ | $6.48 \times 10^{-3}$ | 51.8 |
| Compartment 3 (surface water) | | | | | | | | |
| Solution | -- | -- | $6.81 \times 10^{-2}$ | $2.27 \times 10^{-1}$ | $1.79 \times 10^{-3}$ | $7.16 \times 10^{-3}$ | $2.47 \times 10^{-4}$ | $9.83 \times 10^{-4}$ |
| Suspended solids | -- | -- | $1.70 \times 10^{-1}$ | $5.66 \times 10^{3}$ | $2.24 \times 10^{-3}$ | $1.79 \times 10^{2}$ | $3.09 \times 10^{-4}$ | 24.7 |
| Compartment 5 (bottom water) | | | | | | | | |
| Solution | -- | -- | -- | -- | $4.93 \times 10^{-3}$ | $1.97 \times 10^{-4}$ | $3.47 \times 10^{-5}$ | $1.38 \times 10^{-5}$ |
| Suspended solids | -- | -- | -- | -- | $6.17 \times 10^{-3}$ | 49.3 | $4.33 \times 10^{-5}$ | 3.46 |
| Compartments 7-9 (sediment)[a] | | | | | | | | |
| Solution | $8.0 \times 10^{-7}$ | $3.2 \times 10^{-3}$ | $1.83 \times 10^{-2}$ | $2.65 \times 10^{-1}$ | $4.99 \times 10^{-5}$ | $5.71 \times 10^{-3}$ | $2.33 \times 10^{-5}$ | $2.66 \times 10^{-3}$ |
| Solids | $4.9 \times 10^{-4}$ | 72.0 | $1.24 \times 10^{3}$ | $6.12 \times 10^{3}$ | 3.63 | $2.66 \times 10^{2}$ | 1.59 | $1.16 \times 10^{2}$ |

[a] The amounts given for solid and solution phases in the sediment compartments are estimated from the sorption partition coefficient for suspended solids and may be overestimated because it was assumed that biodegradation of sorbed material does not occur.

The most interesting patterns occur during the approaches to steady states before and just after the simulated chronic discharges are stopped in the oligotrophic and eutrophic lake simulations (Figures 5.1 and 5.2). After discharge stops in the oligotrophic lake simulation, concentrations of dissolved BA decline rapidly by one to two orders of magnitude, reaching new steady states in each aqueous compartment in a week to ten days. New steady states are approached more slowly in the eutrophic lake simulation, apparently requiring at least two weeks, and possibly one or more months. In addition, the range of concentrations between compartments is an order of magnitude smaller in the eutrophic than in the oligotrophic lake, and the concentrations of dissolved BA are two to four times higher. The net effects are higher concentrations and much slower loss of BA from solution in eutrophic waters and a wider distribution of relatively high concentrations.

Changes in the concentrations of suspended sediments are not shown in Figures 5.1 and 5.2 but can be inferred from the changes in the concentrations of dissolved BA, which they parallel, as seen in the pond simulation shown in Figure 5.3, which closely resembles compartment 1 of the eutrophic lake simulation.

Changes in concentrations of dissolved BA are most dramatic in the river simulation (Figure 5.4) where the high rates of dilution result in very low concentrations of dissolved BA in individual compartments and minimize the difference in concentration between compartments. As observed in other river simulations, the zone of peak concentration of dissolved BA moves downstream as increasing concentrations reach the successive downstream compartments. While this effect is accentuated by the absence of tributaries in the model stream, this pattern of downstream shift in peak concentrations might occur in actual streams and could obscure the location of sources of contaminants.

### 5.3.5 Discussion

The significance of the concentrations simulated in this study cannot be readily appraised with the available toxicological data, which are based on experiments with somewhat higher concentrations than we used. Although acute exposures to concentrations of 1 ng $ml^{-1}$ are apparently not toxic to fish (McKee and Wolf, 1963) and are within the range reported for some drinking waters, BA is a carcinogen (IARC, 1973), and as such, must be assumed to be hazardous at these low concentrations until demonstrated to be otherwise.

## 5.4 PHYSICAL PROPERTIES

### 5.4.1 Solubility in Water

Two reports of the solubility of BA in water were found in the literature. Davis and Parke (1942) give the solubility as 11 ng $ml^{-1}$ at 27°C and Klevens (1950) gives a value of 10 ng $ml^{-1}$ at 25°C. We also measured the solubility of BA in water using the method described in Section 5 of Part I of this report and obtained a value of $5.7 \pm 0.5$ ng $ml^{-1}$ [$2.5 (\pm 0.2) \times 10^{-8}$ M] at $20.0 \pm 0.1$°C based on replicate analyses. Some of the solutions were centrifuged after equilibration to make sure they were free of suspended solid BA.

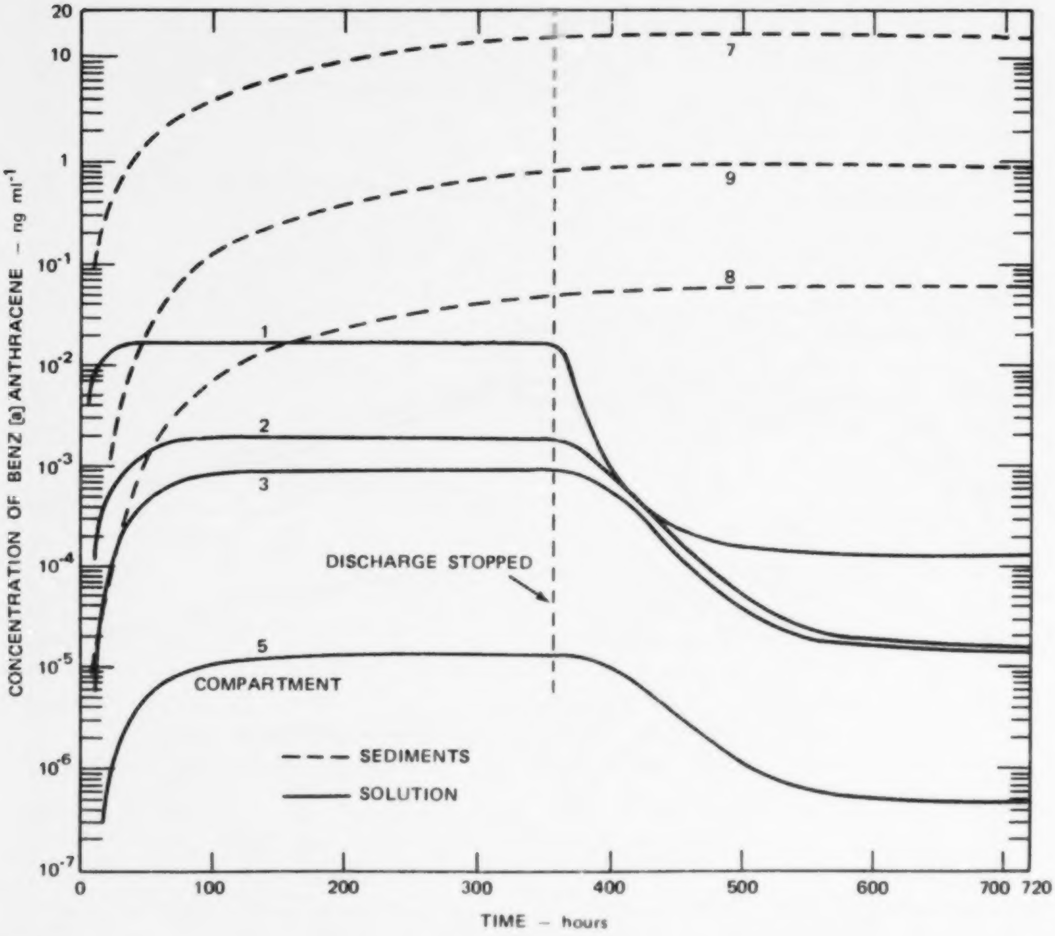

FIGURE 5.1 PERSISTENCE OF BENZ [a] ANTHRACENE IN A PARTIALLY MIXED OLIGOTROPHIC LAKE

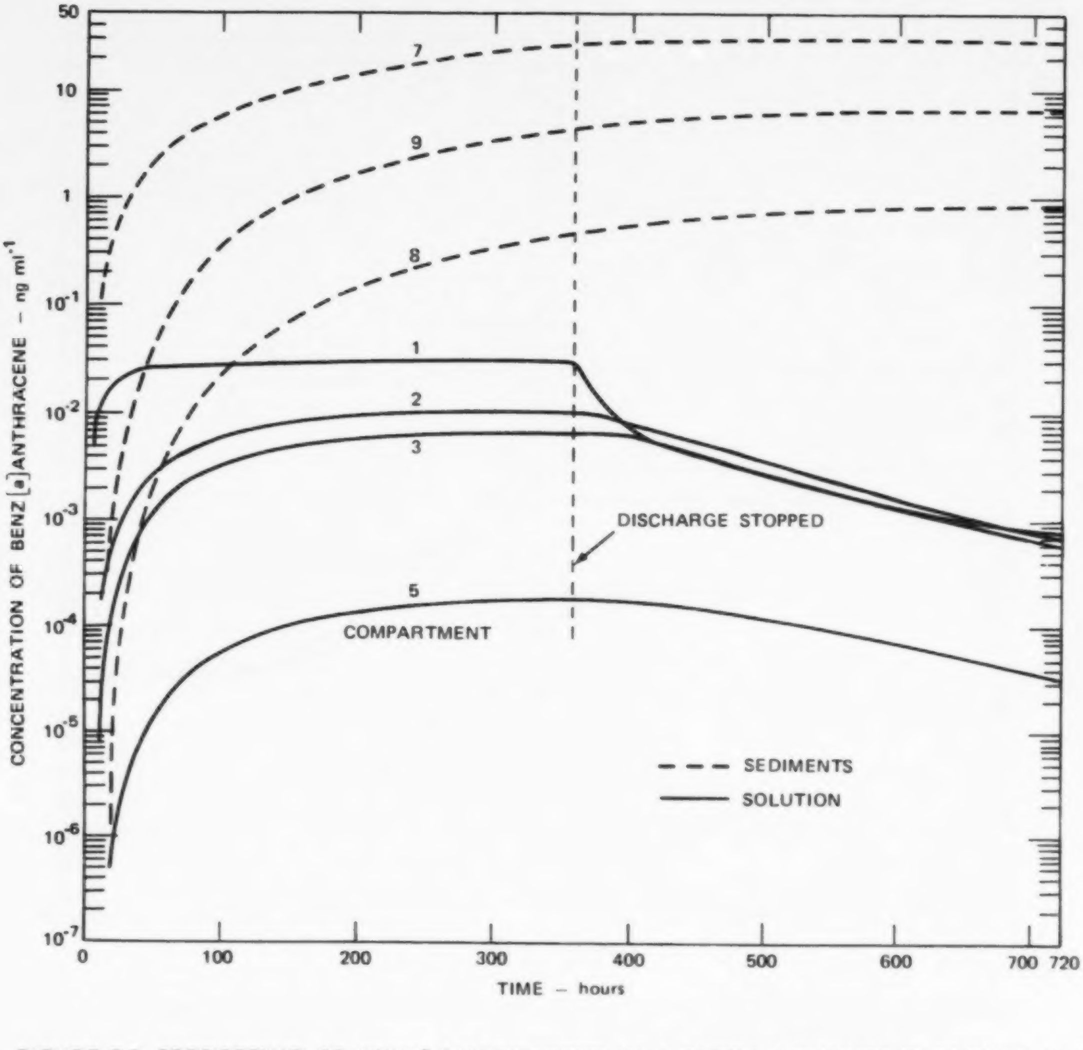

FIGURE 5.2 PERSISTENCE OF BENZ[a]ANTHRACENE IN A PARTIALLY MIXED EUTROPHIC LAKE

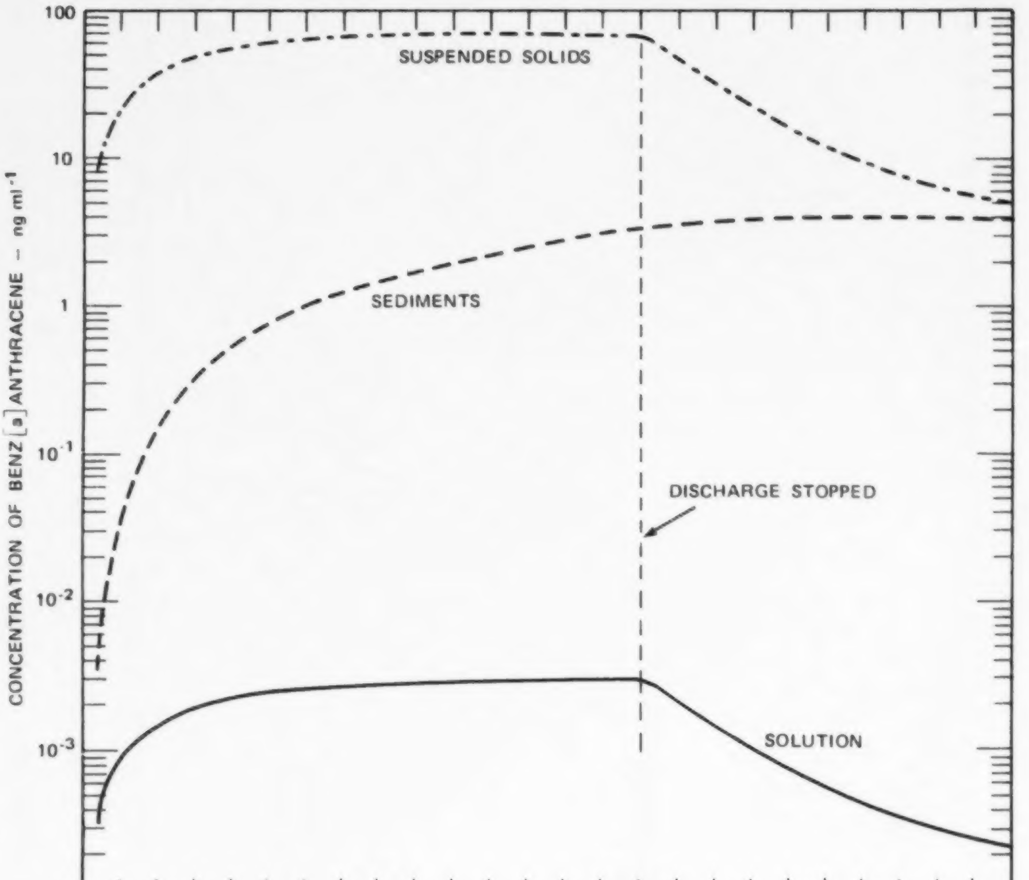

FIGURE 5.3 PERSISTENCE OF BENZ [a] ANTHRACENE IN A TWO-COMPARTMENT POND SYSTEM

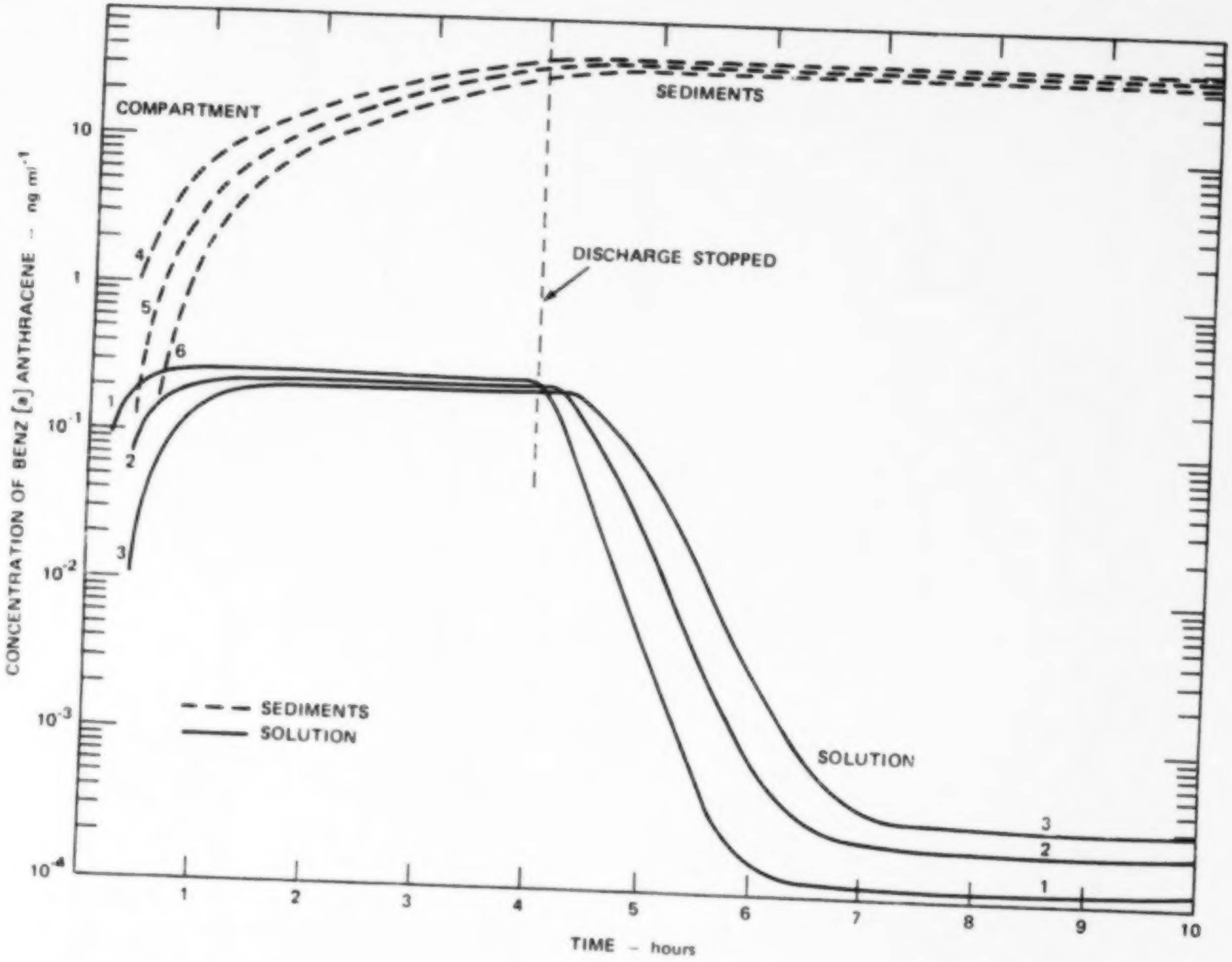

FIGURE 5.4 PERSISTENCE OF BENZ [a] ANTHRACENE IN A PARTIALLY MIXED RIVER SYSTEM

### 5.4.2 Absorption Spectrum

BA absorbs light strongly in the solar region to 390 nm, then weakly to 490 nm. The absorption spectrum was measured in 50% acetonitrile/50% water. The high percentage of acetonitrile was necessary to give a solution concentration that was adequate for measurement on the Cary 15 spectrophotometer. The solutions were tested for cloudiness with collimated beam of light to make sure that they did not contain undissolved BA. Since BA contains no functional groups, the effect of changes in pH on the absorption spectrum was not investigated. All measurements were made at pH 7. The absorption spectra for BA at wavelength intervals from 297.5 to 500 nm and at wavelengths of 313 and 366 nm are reported in Table 5.5.

### 5.4.3 Volatilization Rate

The volatilization rate for BA was measured by the method of Hill et al. (1976), which is described in detail in Part I, Section 5.3.3. The volatilization half-life of BA in an aqueous solution was about 89 hours under the experimental conditions used for this measurement. The rate constants for BA volatilization and oxygen reaeration were measured to be:

Oxygen reaeration rate:* $k_v^O = 4.92 \pm 1.09\ \text{hr}^{-1}$

BA volatilization rate: $k_v^{BA} = 0.00789 \pm 0.00093\ \text{hr}^{-1}$

Ratio: $k_v^{BA}/k_v^O = 0.00160 \pm 0.00057$

### 5.4.4 Sorption on Clay and Sediments

The sorption partition coefficients of BA were measured on three natural sediments: Coyote Creek, Des Moines, and Searsville Pond. In addition, a desorption partition coefficient was measured for the Searsville Pond sediment. Care was taken to assure that the samples were protected from light at all times to minimize photooxidation of the BA. The initial concentration of BA in each sample was always less than the saturation concentration of 5.7 $\mu g\ ml^{-1}$ ($2.5 \times 10^{-5}$ M). Each experiment consisted of triplicate analyses of replicate flasks at two BA concentrations and two sediment loadings plus suitable blanks, as described in Appendix B. Periodic checks were made for sorption of BA onto the glassware; since none of the glassware extracts contained BA, we presumed that no sorption onto the glassware took place.

The data, summarized in Table 5.6 and Figures 5.5 and 5.6, were fitted to a Freundlich isotherm, where $n \cong 1$, using several statistical procedures.

---

*This value represents the average and standard deviation of six reaeration measurements taken over the period of the experiment.

TABLE 5.5. ABSORPTION SPECTRUM OF BENZ[a]ANTHRACENE IN 50% ACETONITRILE/50% WATER AT pH 7[a]

| Center of wavelength interval[b] (nm) | Average absorption coefficient[c] ($M^{-1}$ $cm^{-1}$) |
|---|---|
| 297.5 | 7930 |
| 300.0 | 7070 |
| 302.5 | 5880 |
| 305.0 | 3790 |
| 307.5 | 3200 |
| 310.0 | 3480 |
| 312.5 | 3900 |
| 315.0 | 4200 |
| 317.5 | 4170 |
| 320.0 | 4120 |
| 323.1 | 4800 |
| 330.0 | 5450 |
| 340.0 | 5390 |
| 350.0 | 4850 |
| 360.0 | 3350 |
| 370.0 | 1560 |
| 380.0 | 662 |
| 390.0 | 417 |
| 400.0 | 17.2 |
| 410.0 | 18.1 |
| 420.0 | 18.1 |
| 430.0 | 13.6 |
| 440.0 | 33.6 |
| 450.0 | 15.4 |
| 460.0 | 11.8 |
| 470.0 | 36.3 |
| 480.0 | 8.2 |
| 490.0 | 1.8 |
| 500.0 | 0 |

[a] Benz[a]anthracene concentration was 25.16 μg $ml^{-1}$ ($1.102 \times 10^{-4}$ M).

[b] The wavelength intervals are given in Appendix B, Table B.1.

[c] The absorption coefficients at 313.0 and 366.0 are 4010 and 2410 $M^{-1}$ $cm^{-1}$, respectively.

The column labeled LLS, $a_o = 0$ gives the results of using the linear least squares (LLS) equations* for the equation

$$S_s = K_p S_w \tag{5.1}$$

where $S_s$ and $S_w$ are the substrate concentrations on sediments and supernatant, respectively, and $K_p$ is the sorption partition coefficient.

---

* The regression equations are given in Appendix B, Section B.1. The Hewlett-Packard Model 65 calculator was programmed to carry out these calculations.

TABLE 5.6. BENZ[a]ANTHRACENE SORPTION ON SEDIMENTS

| Sediment | Total organic carbon (percent) | Sediment concentration ($\mu g\ ml^{-1}$) | BA concentration in supernatant[a] ($ng\ ml^{-1}$) | BA concentration on sediment[b] ($ng\ g^{-1} \times 10^{-3}$) | Recovery[c] (percent) | Partition coefficient, $K_p$ ($\times 10^{-3}$)[d] | | | |
|---|---|---|---|---|---|---|---|---|---|
| | | | | | | LLS | | NLLS | |
| | | | | | | $a_o = 0$ | $a_o \neq 0$ | $S_w$ only | $S_s$ and $S_w$ |
| Coyote Creek sorption | 1.4 | 19 | 2.7 ± 0.4 | 82 ± 5 | 91 | 29.3 ± 4.7 | 27.3 ± 5.3 | - | 26.2 ± 1.7 |
| | | 35 | 2.6 ± 0.2 | 63 ± 6 | 103 | | ($a_o$ = 4.3 ± 27) | | |
| | | 19 | 2.0 ± 0.3 | 39 ± 15 | 87 | | | | |
| | | 50 | 1.4 ± 0.2 | 33 ± 2 | 95 | | | | |
| Des Moines River sorption | 0.6 | 20 | 4.4 ± 0.2 | 51 ± 10 | 101 | 9.8 ± 2.0 | 15.0 ± 6.6 | 8.75 ± 0.55 | 8.30 ± 0.70 |
| | | 60 | 3.3 ± 0.2 | 23 ± 3 | 87 | | ($a_o$ = -18 ± 43) | | |
| | | 20 | 3.0 ± 0.3 | 30 ± 4 | 103 | | | | |
| | | 60 | 2.1 ± 0.3 | 16 ± 2 | 88 | | | | |
| Searsville Pond sorption | 3.8 | 16 | 3.5 ± 0.3 | 75 ± 25 | 97 | 20.0 ± 5.1 | 15.0 ± 20.0 | 20.6 ± 0.9 | 20.7 ± 1.0 |
| | | 32 | 2.8 ± 0.2 | 55 ± 11 | 92 | | ($a_o$ = 14 ± 52) | | |
| | | 16 | 2.0 ± 0.5 | 50 ± 6 | 92 | | | | |
| | | 32 | 1.6 ± 0.2 | 33 ± 4 | 89 | | | | |
| Searsville Pond desorption | 3.8 | 31 | 1.4 ± 0.1 | 29 ± 10 | 97 | 19.0 ± 5.3 | 13.0 ± 23.0 | - | 20.6 ± 1.3 |
| | | 63 | 1.3 ± 0.1 | 24 ± 6 | 81 | | ($a_o$ = 7.7 ± 26) | | |
| | | 31 | 1.0 ± 0.2 | 13 ± 5 | 89 | | | | |
| | | 63 | 0.8 ± 0.3 | 22 ± 1 | 103 | | | | |

[a] Concentration measured in supernatant with population standard deviation.

[b] Concentration measured on sediment with population standard deviation.

[c] Based on using blank flasks to determine total material added to each flask.

[d] LLS = linear least squares; NLLS = nonlinear least squares. See text for description of regressions. Limits are 95% confidence limit.

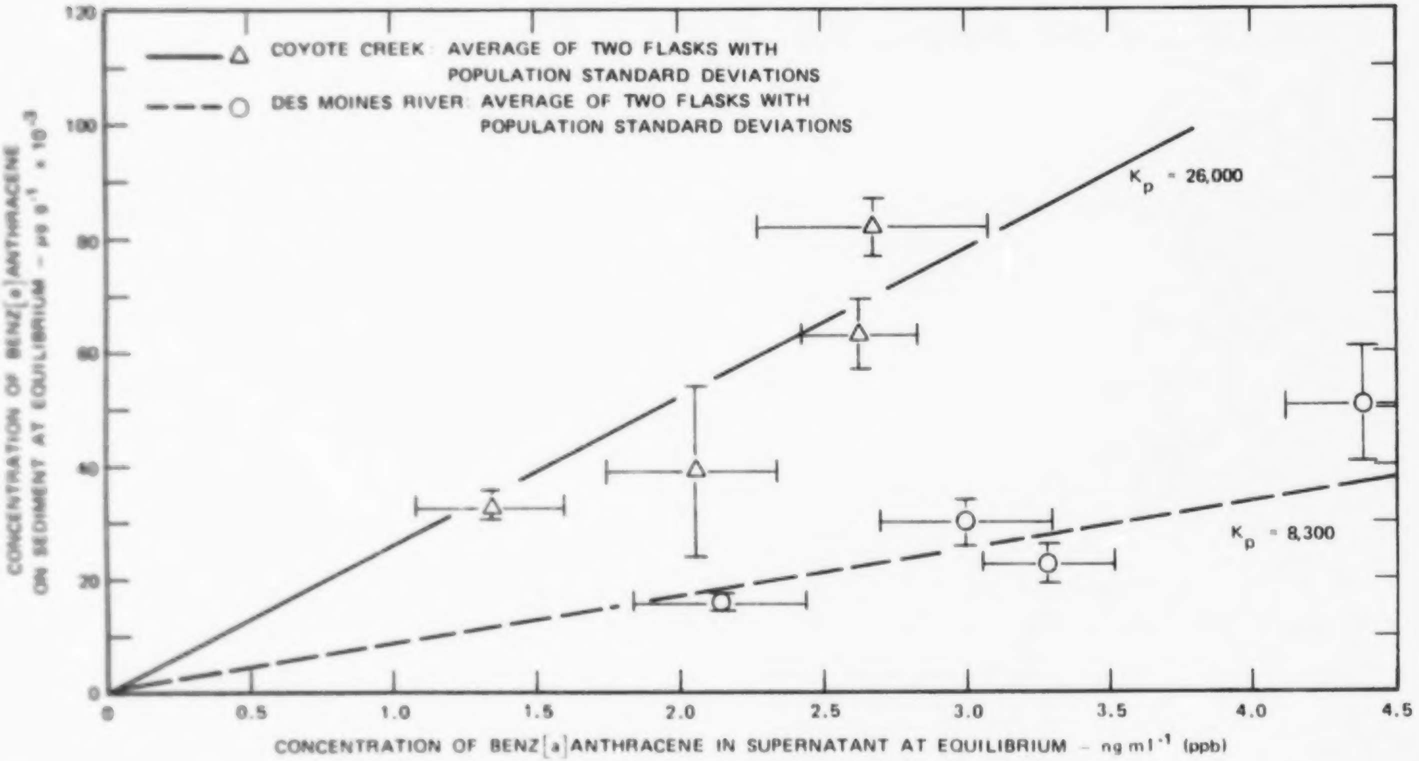

FIGURE 5.5 SORPTION ISOTHERMS OF BENZ[a]ANTHRACENE ON COYOTE CREEK AND DES MOINES RIVER SEDIMENTS.

$K_p$ was estimated by nonlinear least squares using supernatant and sediment concentrations from sorption experiment.

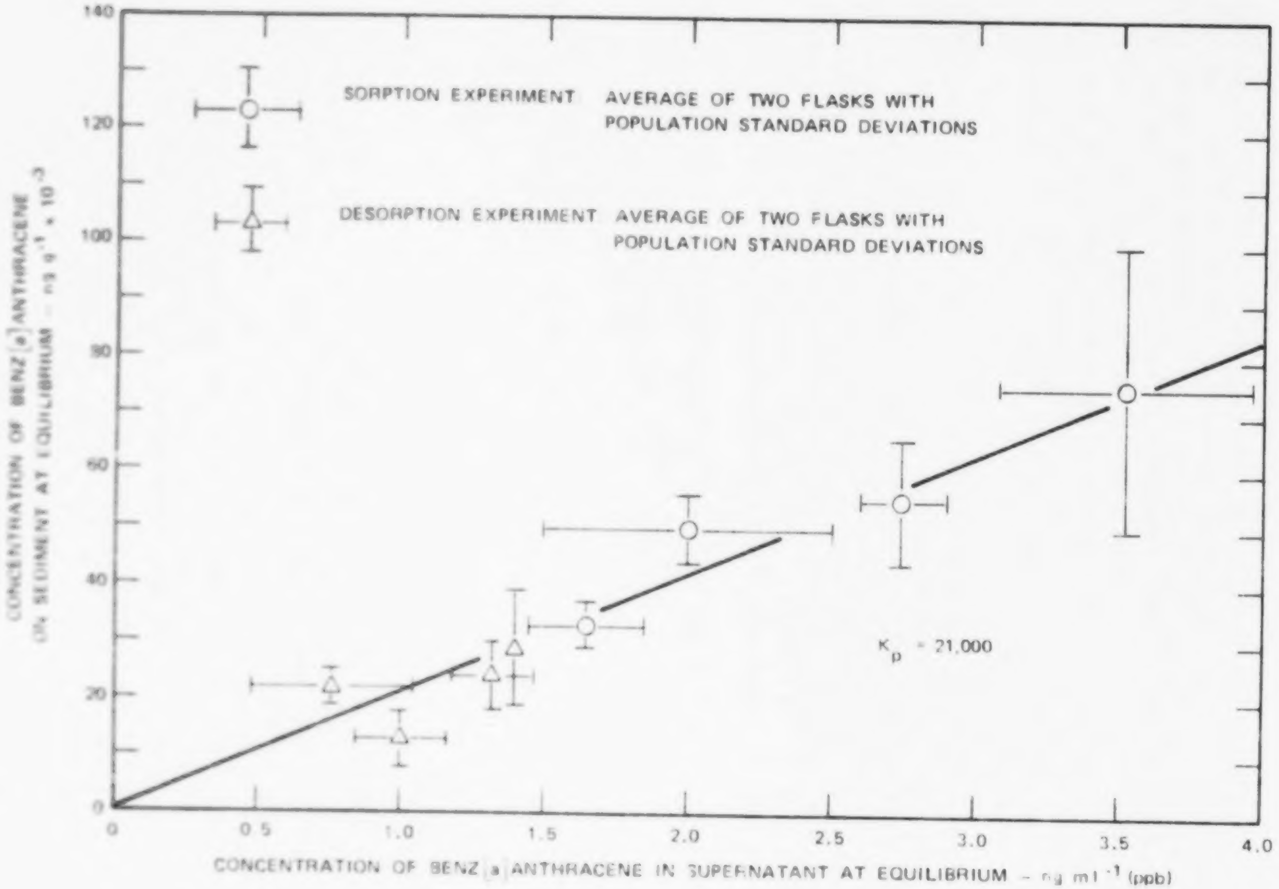

FIGURE 5.6 SORPTION AND DESORPTION ISOTHERMS OF BENZ[a]ANTHRACENE (SEARSVILLE SEDIMENT).

$K_p$ was estimated by nonlinear least squares using supernatant and sediment concentrations from sorption experiment.

The column labeled LLS, $a_o \neq 0$ gives the results of using linear least squares equations* for the equation

$$S_s = K_p S_w + a_o \qquad (5.2)$$

where $a_o$ is the intercept. In both cases, the average $S_s$ and $S_w$ for each flask were used as input data to the regression equations. These calculations show that the intercept of the regression equation is the origin within experimental error. The $K_p$ values in the columns labeled NLLS were calculated using the nonlinear least squares (NLLS) techniques described in Appendix B, Section B.1.4. The $K_p$ values in the column labeled $S_w$ only were calculated from supernatant concentrations only. The "best" estimates of $K_p$ are the values reported in the last column, labeled $S_s$ and $S_w$. These estimates were obtained from the measurements of $S_s$ and $S_w$.

Several conclusions can be made from these results. First, the nonlinear least squares technique gives the best estimate of $K_p$, since the 95% confidence limits are less than the LLS method. Second, the estimates of $K_p$ are virtually identical when calculated from $S_w$ data only or when calculated from values of $S_s$ and $S_w$. Third, the LLS method, where $a_o = 0$, also gives a good estimate, since the range of $K_p$ overlaps the NLLS estimates. However, the 95% confidence limits are much wider for the LLS, $a_o = 0$, method than for the NLLS methods because the error due to flask effects is included in the LLS methods.

The results from the desorption isotherm measurement on Searsville Pond sediment are summarized in Table 5.6 and Figure 5.6. These data show that the value of $K_p$ is, within experimental error, the same for sorption and desorption. Therefore, for a sorption time of 12 hr sorption of BA is reversible on this sediment.

The correlation of $K_p$ with sediment organic content is poor ($r^2 = 0.45$). However, only three points are available and the correlation might improve if $K_p$ were measured on more sediments.

### 5.4.5 Biosorption

Because of the low solubility of BA, biosorption studies were conducted at BA concentrations of 12.8 and 7.5 ng $ml^{-1}$. The density of the mixture of the four bacterial cultures used in sorption studies was reduced to an optical density of 0.2. The results from the one-hour sorption and three-hour desorptions are presented in Table 5.7. The cell dry weights were equivalent to 96 μg $ml^{-1}$. The adjustments for sorption of BA on glassware in Table 5.7 were 3.4% and 1.6% for sorption studies with 12.8 and 7.5 mg $ml^{-1}$ BA, respectively. The corresponding adjustments for glassware sorption in the desorption were 2.6% and 1.7%, respectively.

---

*Calculated using the Hewlett-Packard Model 65 calculator and the Stat-Pac 1 routines.

TABLE 5.7. BENZ[a]ANTHRACENE SORPTION AND DESORPTION ON A MIXED BACTERIAL POPULATION

| Initial BA concentration (ng ml$^{-1}$) | Sorption (S) or desorption (D) | Amount in supernatant (%) | Amount in cells (%)[a] | Sorption coefficient (x $10^{-4}$) |
|---|---|---|---|---|
| 12.8 | S | 21 ± 1 | 78 ± 2 | 3.9 ± 0.2 |
| | D | 22 + 2 | 59 ± 1 | 2.9 ± 0.3 |
| 7.5 | S | 23 ± 3 | 72 ± 3 | 3.3 ± 0.4 |
| | D | 21 ± 3 | 50 ± 1 | 2.5 ± 0.2 |

[a] The dry weight equivalent to 96 µg ml$^{-1}$.

Sorption coefficients of viable cells and heat-killed cells were also compared. The sorption coefficients with initial BA concentration of 11.4 ng ml$^{-1}$ are shown in Table 5.8. Heat-killed cells had a higher sorption coefficient.

TABLE 5.8. BENZ[a]ANTHRACENE SORPTION BY VIABLE AND HEAT-KILLED BACTERIA[a]

| Condition of cells | Cells dry weight (mg-liter$^{-1}$) | Amount in supernatant (%) | Amount in cells (%) | Sorption coefficient (x $10^{-4}$) |
|---|---|---|---|---|
| Viable cells | 91 | 22 ± 1 | 71 ± 5 | 3.6 ± 0.3 |
| Heat-killed cells | 76 | 11 ± 1 | 86 ± 1 | 9.9 ± 0.7 |

[a] The initial concentration of BA was 11.4 ng ml$^{-1}$.

As expected, BA sorption coefficient data were lower than those for BaP, but they are still very high. These high sorption coefficients with bacterial cells would reduce the BA in the aqueous phase "available" for development of biodegradable organisms. These data also suggest that sorption could be important in biomagnification up the food chain ladder.

## 5.5 CHEMICAL TRANSFORMATION

### 5.5.1 Photolysis Rate

Photolysis of BA is rapid in the solar region with half-lives of several hours. Data for the photolysis of BA with air in sunlight and at 313 and 366 nm are given in Table 5.9. Acetonitrile was used as the cosolvent to enhance

TABLE 5.9. RATE CONSTANTS FOR PHOTOLYSIS OF BENZ[a]ANTHRACENE

| Light source | BA concentration[a] (ng ml$^{-1}$) | Solution[b] | % Reaction | Rate constant ($K_p$ x $10^5$ sec$^{-1}$) |
|---|---|---|---|---|
| 313 nm | 19.6 | 0.1% AN in pure water | 63 | 2.59 ± 0.09[c,d] |
| 313 nm | 18.0 | 1.0% AN in pure water | 38 | 1.98 ± 0.08[e] |
| 366 nm | 17.4 | 0.1% AN in pure water | 83 | 14.5 ± 0.4[d] |
| 366 nm | 9.8 | 1.0% AN in pure water | 67 | 12.3 ± 0.3[e] |
| 366 nm | 19.6 | 0.1% AN in Lake Tahoe water | 88 | 8.10 ± 0.65 |
| 366 nm | 9.8 | 1.0% AN in Lake Tahoe water | 62 | 10.8 ± 0.2 |
| 366 nm | 22.4 | 0.1% AN in Coyote Creek water | 84 | 8.80 ± 0.48 |
| 366 nm | 9.3 | 1.0% AN in Coyote Creek water | 58 | 9.55 ± 0.15 |
| 366 nm | 19.6 | 0.1% AN in Searsville Pond water | 85 | 7.47 ± 0.30 |
| 366 nm | 222 | 1.0% AN in Searsville Pond water | 56 | 6.55 ± 0.09 |
| 366 nm | 17.3 | Humic acid (8 μg ml$^{-1}$) in 1% AN in pure water | 57 | 3.9[f] |
| Midday sunlight, early March | 19.6 | 0.1% AN in pure water | 66 | 5.91 ± 0.078 |

[a] 1.00 ng ml$^{-1}$ BA in water = 4.38 x $10^{-9}$ M.

[b] AN = acetonitrile.

[c] Standard deviation.

[d] Quantum yield of 3.2 x $10^{-3}$.

[e] Quantum yield of 3.4 x $10^{-3}$.

[f] Rate constant for initial photolysis; data do not follow first-order kinetic law.

[g] Half-life of 3.3 hours.

the solubility of BA in water from the sources indicated because of the low solubility of BA in pure water. (See Section 5.4.1.) Except for the photolysis reaction in the solution containing 8 $\mu g\ ml^{-1}$ humic acid, good first-order kinetic behavior was found for photolyses carried out to beyond two half-lives of BA under laboratory conditions.

In experiments using 9.3 to 222 $ng\ ml^{-1}$ BA, the photolysis rate constant was independent of BA concentration, again confirming first-order kinetic behavior. The quantum yields for direct photolysis at 313 and 366 nm were $(3.3 \pm 0.1) \times 10^{-3}$. The data in Table 5.9 also indicate that the photolysis experiments in the same water are not reproducible to within two standard deviations (~ 95% confidence limits) of each experiment; the average deviation between the two experiments in the same water ranged from 4% to 14%. Beyond these limits, however, the photolysis rates in Lake Tahoe or Coyote Creek water is about 70% of that in pure water, and in the water from the pond near Searsville Lake, the rate is half as fast as in pure water. Since the absorbance of the natural waters at 366 nm is less than 0.02 (in a 1-cm cell), the lower photolysis rates observed in natural waters are not due to light screening effects.

It was also found that photolysis at 366 nm of a 9.3 $ng\ ml^{-1}$ BA solution (1% acetonitrile in water) containing 8 $\mu g\ ml^{-1}$ humic acid did not follow a first-order kinetic law, since the rate decreased as the photolysis proceeded; we have no explanation for this behavior. While not a first-order reaction, a first-order rate constant calculated from the initial two data points is $4 \times 10^{-5}\ sec^{-1}$, which is at least three times slower than the reaction in pure water. Since the absorbance of the humic acid solution is 0.43 (1-cm cell), the light screening effect of the humic acid should only reduce the reaction rate by 37% (e.g., 0.63 times the rate in pure water). Some process other than screening appears to be retarding the photolysis rates in the three natural waters. Discussion of some possible explanations is given in the section on BaP (Section 6.5.1).

The half-life for direct photolysis of BA in sunlight as a function of the time of day was calculated by the procedure of Zepp and Cline (1977) using a quantum yield of $3.3 \times 10^{-3}$ and the measured UV spectrum of BA (Section 5.4.2). The data for summer and winter seasons are plotted in Figure 5.7. A calculated half-life of 1 to 2 hours for midday photolysis is in good agreement with the 3-hour half-life measured for midday on a cloudy day in early March.

### 5.5.2 Oxidation Rate

The susceptibility of 19.6 $ng\ ml^{-1}$ ($8.59 \times 10^{-8}$ M) BA to free radical oxidation was examined using an AA-initiated oxidation reaction, as described in Part I and Appendix B. The experiment was performed at 50.0°C in 1% acetonitrile in water containing $9.6 \times 10^{-5}$ M AA.

Analysis of controls (BA solutions without AA maintained under identical reaction conditions) at reaction times of 3.0 and 5.4 hours showed a 36% loss of BA compared with the original solutions; this was apparently due to sorption

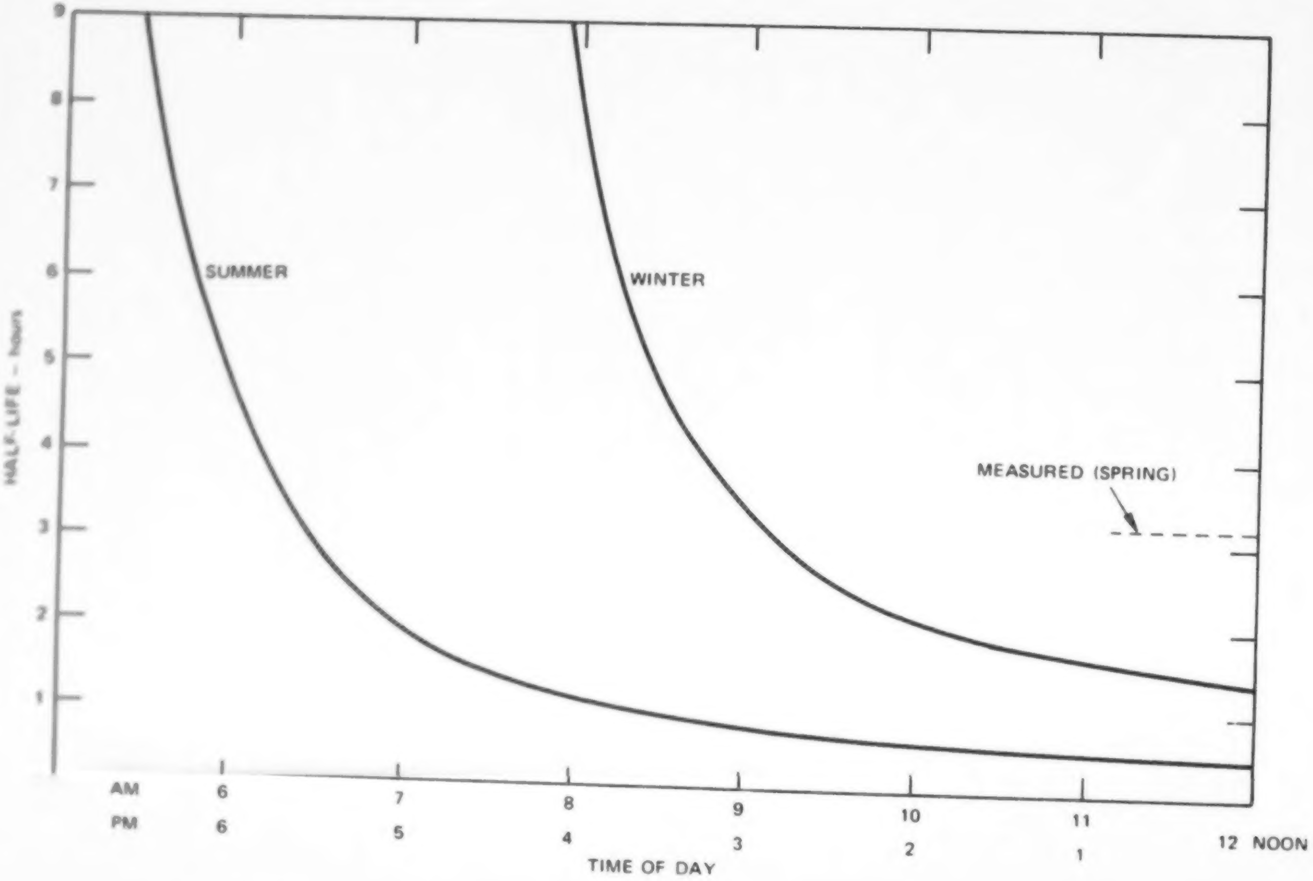

FIGURE 5.7 SEASONAL AND DAILY VARIATION OF PHOTOLYSIS HALF-LIFE OF BENZ [a] ANTHRACENE

of BA on glassware. Correcting for this sorption, we obtained a pseudo-first-order rate constant ($k_{ox}[RO_2\cdot]$) of $(1.53 \pm 0.18) \times 10^{-4}$ $sec^{-1}$ for oxidation of BA under the reaction conditions. This rate constant corresponds to a half-life of 1.3 hours. Under these conditions (Part I, Section 6.3), this corresponds to a second-order rate constant $k_{ox}$ of $4.5 \times 10^4$ $M^{-1}$ $sec^{-1}$ at 50.0°C. At 25°C, $k_{ox}$ would then be $5.0 \times 10^3$ $M^{-1}$ $sec^{-1}$.

Assuming that $[RO_2\cdot] = 10^{-9}$ M in the aquatic environment, the half-life of BA toward oxidation is estimated to be about 38 hours. The free-radical oxidation of BA in the environment is rapid and could be competitive with photolysis or sorption processes.

### 5.5.3 Hydrolysis Rate

BA contains no groups that are hydrolyzable; therefore, no hydrolysis studies were conducted.

### 5.5.4 Products from Chemical Transformation

One product from the photolysis of BA at 366 nm in air-saturated, acetonitrile-water solvent was identified as benz[a]anthracene-7,12-quinone (7,12-BAQ) by comparing the HPLC retention time and UV spectrum with that of an authentic quinone sample.

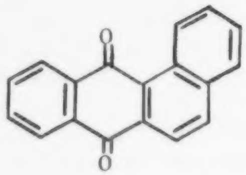

At times when BA was 15%, 26%, and 46% reacted, 7,12-BAQ was present in about 26% yield based on the amount of BA reacted. The quinone was stable to photolysis at 366 nm at these reaction times.

At low conversions of BA, we found that two other products peaks were also present in photolysis reaction mixtures from experiments under a variety of conditions. At higher conversions of BA, at least four additional, but smaller, peaks were found in the HPLC traces of the reaction mixtures. These products eluted earlier than BA or 7,12-BAQ on reverse-phase HPLC. Since these products could not be separated and identified, their yields could not be determined. These more polar, unknown products could account for the balance (74%) of the reacted BA.

In an attempt to identify the photochemical processes responsible for the complex product mixtures, we performed several additional experiments. The photolysis of BA at 366 nm in 1:1 acetonitrile:water that had been purged of oxygen with nitrogen gave a photolysis rate that was about one-third of that found when oxygen was present. The same three major product peaks were present in this reaction mixture.

It was also found that the photolysis of BA in oxygen-saturated, pure acetonitrile solvent was slower than in the aqueous solutions. In this experiment, less than 2% 7,12-BAQ was formed and one of the other two major products significantly increased in yield. In nitrogen-purged, pure acetonitrile solvent the photolysis of BA did not occur.

In another experiment it was also found that photooxygenation in methanol, using rose bengal as the singlet oxygen sensitizer, produced the same mixture of products that was found in the air-saturated aqueous solutions.

The effects of water and oxygen on the BA photolysis rates and the finding that 7,12-BAQ is formed in water in the absence of oxygen is surprising and indicates that the photolyses are more complicated than the simple photooxygenation process expected on the basis of literature information. In photolysis studies on BA, McGinnes and Snoeyink (1974) found a product that they tentatively identified as 7,12-BAQ, in agreement with our work. They also found a major product that they described as a complex organic acid with the empirical formula $C_{18}H_{13}O_3$, which was not further characterized.

This polar, acidic compound could correspond to any of the products that eluted early in our reverse-phase HPLC analysis. However, it is difficult to rationalize how any product containing three oxygens could be a primary BA transformation product. Since 7,12-BAQ is stable to photolysis in water, we expect that such acid product(s) would be derived from other primary product(s), which are rapidly photolyzed (or possibly hydrolyzed or oxidized). Evidence for such unstable primary products, which could be other quinones or endoperoxides, could not be found in any of the HPLC traces of the reaction mixtures.

These findings indicate that the photoreactions of BA and possibly other polynuclear aromatics are complex and require more detailed studies, especially in aqueous sytems. Such investigations will be necessary in order to understand the chemistry of these processes and the identity of the primary products. The kinetic data obtained for the air-saturated, aqueous solutions presented in Table 5.9 are, however, still reliable for environmental assessment purposes.

## 5.6 BIODEGRADATION

### 5.6.1 Development of Enrichment Cultures

Screening for enrichment cultures for BA degrading systems was conducted with water samples in 9-liter aerated fermentors with 10 μg $ml^{-1}$ of BA. The samples were initiated with and without 10 μg $ml^{-1}$ of phenanthracene added as an analog inducer in conjunction with the BA. The water samples tested were from Searsville Pond in Woodside, CA; Coyote Creek water; aeration effluents from sewage plants in Palo Alto and South San Francisco, and from the Shell Oil Refinery in Martinez, CA; and a composite sample of waters from ponds that are part of the storm and emergency drainage system of the Shell Oil Refinery.

Transfers were made from these 9-liter fermentors into shaker flasks containing BA and basal salts with and without phenanthracene. Samples from South San Francisco and Shell ponds were also transferred into shaker flasks containing basal salts medium, BA, and naphthalene. Neither the 9-liter fermentors nor subsequent transfers into flasks indicated the development of BA degrading cultures within the specified six-week period.

Additionally, five single bacterial isolates obtained in other studies from biphenyl and phenanthracene degrading systems were tested for BA degradation with 10 $\mu$g ml$^{-1}$ of BA in the presence of the respective 10 $\mu$g ml$^{-1}$ of biphenyl or phenanthracene substrate with and without 100 ppm of Tripticase Soy broth. No BA degradation was observed.

To test the possibility that polyaromatic carcinogens can affect metabolism or viability of bacteria, we examined the inhibition activity of 10 $\mu$g ml$^{-1}$ of BA on growth of p-cresol and on quinoline degrading systems. No significant effects were observed.

### 5.6.2 Biodegradation Kinetics

Since enrichment cultures that degraded BA were not obtained, biodegradation kinetic studies were not performed.

### 5.6.3 Discussion

The discussion about the biodegradability of benzo[a]pyrene (Section 6) can be applied to BA. Enrichment procedures tend to favor certain types of organisms. With the high sorption coefficients and the low solubility of BA, it is possible that conventional enrichment procedures do not provide enough "available" BA for organisms to utilize this substrate for growth in competition with other organisms that have a more favorable predator-prey relationship under the conditions of the primary enrichment process.

The bacteria that can utilize BA may be too slow to develop within the six-week limit because the growth rates of bacteria in aromatic hydrocarbon media are regulated by amount of dissolved substrates (Wodzinski et al., 1968, 1972, 1974). The fact that enrichment systems did not develop BA biodegrading culture mixtures within the time limit does not unequivocally classify BA as a recalcitrant compound. BA biodegradation may also take place slowly on sediments.

# 6. LABORATORY INVESTIGATION OF BENZO[a]PYRENE

## 6.1 SYNOPSIS

The results of the laboratory investigations suggest that benzo[a]pyrene (BaP) will accumulate in the sediment and biota portions of an aquatic environment. A small amount of BaP will be dissolved and will photolyse rapidly. The estimated half-lives of BaP dissolved in different types of water bodies and the percent sorbed on suspended sediments are:

| | Half-life[*] (hr) | Solution ($ng\ ml^{-1}$) | Suspended solids ($ng\ g^{-1}$) | Sediments ($ng\ g^{-1}$) |
|---|---|---|---|---|
| River | 0.48 | $1.5 \times 10^{-3}$ | 7.4 | 9.9 |
| Pond | 7.3 | $1.5 \times 10^{-6}$ | $7.0 \times 10^{-2}$ | $7.0 \times 10^{-2}$ |
| Eutrophic lake | 7.4 | $1.1 \times 10^{-5}$ | $5.4 \times 10^{-1}$ | $1.4 \times 10^{-1}$ |
| Oligotrophic lake | 1.5 | $1.9 \times 10^{-6}$ | $9.3 \times 10^{-2}$ | $2.3 \times 10^{-2}$ |

Several problems were encountered in these studies. Experimental difficulties were encountered because BaP sorbed on glassware, and its low solubility in water made it difficult to prepare and work with aqueous solutions. We suspect that sorbed BaP may be transformed by photochemical and chemical oxidation as well as by biodegradation processes, but the extent of these processes could not be evaluated by our laboratory procedures. Finally, there is literature evidence that biodegradation of BaP may take place under different conditions and with different organisms than those used in these studies. Therefore, the general conclusion is that BaP will accumulate in sediments and microorganisms and may degrade slowly in sediments with half-lives of a few years.

## 6.2 BACKGROUND

Benzo[a]pyrene is a polynuclear aromatic hydrocarbon (PAH) that is known t be carcinogenic to animals and probably also to man. The time from exposure to BaP to observation of cancer (referred to as the latent period) is o the order of years, so the persistence and pathways for BaP in the aquatic environment are subtle but important issues. Excellent reviews on the occurrence of BaP and other PAH in various environments have recently appeared in literature (Radding et al., 1976; Harrison et al., 1975; National Academy of Science, 1972; Andelman and Snodgrass, 1974; Andelman and Suess, 1970). Most studies of PAH in natural waters do not discriminate between material that is sorbed on particulate matter and that in "true" solution. As several reviews have pointed out, however, the low solubility of BaP (and all PAH) in water does not necessarily mean that all BaP is sorbed, since many natural waters and industrial effluents also contain other more soluble organic material that may increase the solubility of BaP.

---

[*] redicted by one-compartment model.

BaP is widespread in the environment, having been found in soils, airborne articulates, and plant materials as well as in natural, waste, and drinking waters. In a 1970 review, Andelman and Suess reported that BaP concentrations of over 300 ng $ml^{-1}$ are present in some effluents from the coke and shale-oil industries. Concentrations to 0.15 ng $ml^{-1}$ BaP have been found in surface waters. A review prepared by the International Agency for Research on Cancer (1973) reported that concentrations of BaP in drinking waters ranged from 0.0001 to 0.023 ng $ml^{-1}$. A concentration of 56 μg $kg^{-1}$ total PAH has been found in river sediments; values of several thousand μg $kg^{-1}$ BaP have been found in analyses of marine sediments (Andelman and Suess, 1970).

The general physical properties of BaP that were found in literature are given in Table 6.1.

TABLE 6.1. PHYSICAL PROPERTIES OF BENZO[a]PYRENE

| | |
|---|---|
| Structure | 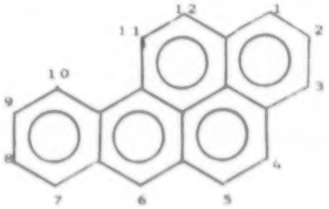 |
| Molecular weight | 252.30 |
| Melting point (°C) | 179 |
| Boiling point at 10 torr (°C) | 311 |
| Vapor pressure at 25°C (torr) | $5 \times 10^{-9}$ |
| Solubility in water (ng $ml^{-1}$)[a] | 1.2 ± 0.1 |
| 1.00 ng $ml^{-1}$ (1 ppb) BaP = $3.96 \times 10^{-9}$ M | |

[a] Measured in this study (Section 6.4.1).

The reported concentrations of BaP in sediments suggest that sorption onto sediments and particulates is an important environmental fate. Although reliable data were not available for the solubility of BaP, it is known that the solubility is extremely low in pure water.

The oxidation and photochemistry of polynuclear aromatic compounds were reviewed as part of a recent task report for EPA-OTS (Radding et al., 1976). Autoxidation of BaP by peroxy radicals appears to be slow. Photooxygenation (reaction with singlet oxygen) to produce quinones is expected to be an important degradative process in the environment. BaP appears to serve as both the sensitizer and the reactant hydrocarbon.

The extreme insolubility of BaP in water has made it necessary to conduct the laboratory work in organic or mixed organic-aqueous solvent systems. The photodegradation of BaP has been carried out in solution and sorbed on calcium carbonate (Andelman and Suess, 1971) and on kaolinite (McGinnes and Snoeyink, 1974). When corrected to environmental solar flux values, these data indicate that BaP may have a half-life of less than a day both in solution and in the sorbed state. BaP has been reported to show an increased half-life beyond about 60% photodegradation when sorbed on kaolinite) the authors ascribe this reduction of the rate of photodegradation to competitive light sorption by the quinone products. Since only small yields of these quinones are isolated, this explanation is plausible. The solution photochemistry shows no such retardation of rate.

Gibson (1975, 1976) and Gibson et al. (1975) reported on the microbial conversion of BaP to *cis*-9,10-dihydroxy-9,10-dihydrobenzo[a]pyrene and more extensive degradation by *Beijerenckia* bacteria isolated from a polluted stream. The wild strain was obtained by enrichment procedures using biphenyl as the sole source of carbon for growth, and a mutant, B-836, was prepared by treating the parent with N-methyl-N-nitrosguanidine (Gibson et al., 1973). The wild strain oxidized BaP to acid products (Gibson, 1975, 1976; Gibson et al., 1975). Gibson et al., 1975, reported a 1.7% yield of a fraction from B-856 conversion of BaP that was primarily the *cis*-9,10-dihydroxy-9,10-dihydrobenzo[a]pyrene and possibly a small amount of the 7,8-dihydrodiol isomer.

Shabad et al. (1971), in a continuation of many studies on the analysis, presence, and degradation of BaP in the environment, demonstrated some of the intricacies of research with this carcinogen. They found that some soils from oil refinery plants contained up to 200,000 μg BaP $kg^{-1}$, and from some BaP-contaminated soils they isolated strains of bacteria that could decompose polyaromatic. Some strains that could not decompose BaP in their liquid medium decomposed 40% to 86% of the BaP when added to sterilized BaP-contaminated soils.

Other studies further indicate the many characteristics of BaP degradation research (Fedoseeva et al., 1968; Khesina et al., 1969; Lohrbacher et al., 1971; Malaney et al., 1967; Niaussat and Ottenwalder, 1969; Poglazova and Meisel, 1971; Poglazova et al., 1966. 1967a,b, 1968, 1971, 1972; Shabad, 1968; Sisler and Zobell, 1947).

To a large degree the source of the BaP metabolizing cultures has been material with long exposure to relatively high concentrations of BaP. Single cell isolates have been used, the level of BaP available to the microorganisms has been on the order of $\mu g\ ml^{-1}$, other nutrients were present, and many species of organisms have been implicated. Included in the identified degrading organisms are the yeasts *Endomyces magnusii* and *Candida lipolytica* and bacteria such as strains of *Bacillus megaterium*, *Mycobacterium flavum*, *M. rubrum*, *M. smegmatis*, *Bacillus sphaericus*, *Pseudomonas aeruginosa*, *Azobacter chrococcus*, and *Escherichia coli*.

While we anticipated that sorption onto sediments and photolysis were probably the most important pathways for BaP, the literature data were insufficient to allow us to quantitatively estimate the importance of these processes in comparison to biodegradation, volatilization, and oxidation. Therefore, we decided that screening studies should be conducted for each of these processes.

## 6.3 ENVIRONMENTAL ASSESSMENT

### 6.3.1 Summary of Laboratory Data

The rate constants obtained in the laboratory investigations of the transformation and transport processes for BaP are summarized in Table 6.2.

TABLE 6.2. SUMMARY OF BENZ[a]PYRENE LABORATORY DATA

| Process | Sorption equilibrium | Partition coefficient[a] |
|---|---|---|
| Sorption | $S_s = K_p S_w$ | $K_p = (7.6 \pm 2.4) \times 10^4$ |
| | Rate expression | Rate constant at 25°C |
| Volatilization | $k_v[BaP]^b$ | $k_v = k_v^0 \times (0.0036 \pm 0.0006)$ |
| Photolysis | $k_p[BaP] = \phi(\Sigma Z_\lambda \epsilon_\lambda)[BaP]$ | $k_p = (2.8 \pm 0.2) \times 10^{-4}\ sec^{-1}$ [c] |
| Oxidation | $k_{ox}[RO_2\cdot][BaP]$ | $k_{ox} = 1.86 \times 10^3\ M^{-1}\ sec^{-1}$ |
| Hydrolysis | NA | $k_h = 0$ |
| Biodegradation | $k_{b2} = \frac{\mu_{max}}{Y\ K_s}$ | $k_{b2} = 0^d$ |

[a] On Coyote Creek sediment.

[b] See discussion in Part I, Section 5.3, and Appendix B.

[c] Noonday sunlight, in mid-December.

[d] Biodegradation was not observed in the enrichment procedures.

### 6.3.2 Environmental Assessment Using the One-Compartment Model

The half-lives of dissolved BaP calculated for individual transformation or removal processes are listed in Table 6.3. Although these half-lives generally change from one water body to another, the half-life for photolysis is an order of magnitude smaller than the half-lives of the other transformation pathways. Sorption half-lives have not been measured, but they are probably at least 100 times smaller than the half-lives for photolysis (Section 6.5.1). Moreover, since the sorption partition coefficient is at least 50,000 (Section 6.4.4), it is probable that most of the BaP entering natural waters is trapped in sediments. Subsequent loss from the sediments cannot be assessed with our data, although loss by biodegradation is plausible (Section 6.6).

TABLE 6.3. TRANSFORMATION AND TRANSPORT OF BENZO[a]PYRENE PREDICTED BY THE ONE-COMPARTMENT MODEL

| Process | River | Eutrophic pond | Eutrophic lake | Oligotrophic lake |
|---|---|---|---|---|
| Photolysis, half-life (hr)[a] | 3.0 | 7.5 | 7.5 | 1.5 |
| Oxidation, half-life (hr) | >340 | >340 | >340 | >340 |
| Volatilization, half-life (hr) | 140 | 350 | 700 | 700 |
| Hydrolysis, half-life (hr) | NA | NA | NA | NA |
| Biodegradation, half-life (hr)[b] | $>10^4$ | $>10^4$ | $>10^4$ | $>10^4$ |
| Half-life for all processes, except dilution (hr) | 2.9 | 7.3 | 7.4 | 1.5 |
| Half-life for all processes, including dilution (hr) | 0.48 | 7.3 | 7.4 | 1.5 |
| Amount BaP sorbed[c] (mg $m^{-3}$) | 5 | 15 | 2.5 | 2.5 |
| Percentage BaP sorbed | 83% | 93% | 71% | 71% |

[a] Based on the photolysis rates estimated for summer sunlight.

[b] Biodegradation of BaP was not observed in our enrichment procedure. However, the literature suggests that biodegradation of BaP may occur in the environment (see Sections 6.3.5 and 6.6).

[c] 1 ng $ml^{-1}$ BaP is assumed in the solution phase.

### 6.3.3 Persistence

The half-life, and hence the residence time, of BaP in the water column attributable to transformation and volatilization is expected to be independent of the dilution rate in lakes and ponds (Table 6.3). However, dilution may account for as much as a tenfold reduction time in short river segments, perhaps 1-20 km in length, since the major portion of the sorbed BaP should be in the slowly settling, small particles. Effects of dilution should be less for longer river reaches due to the sedimentation of BaP-contaminated particles.

### 6.3.4 Mass and Concentration Distributions Calculated Using Computer Models

Table 6.4 summarizes the distribution of mass and concentration of BaP expected at steady state within each of four types of water bodies, as calculated with the aid of the computer model. The pseudo-first-order rate constants used in these simulations are presented in Appendix A.

The sediments and suspended solids clearly dominate the distribution of BaP in the pond and lake simulations, with at least 98% of the BaP in the bottom sediments and at least 70% of the remainder in the suspended fraction.

The quantities of BaP predicted to be in solution are on the order of $10^{-5}$ to $10^{-6}$ ng $ml^{-1}$ in the pond and lake simulations. Only the river simulation predicts concentrations approximating those encountered in natural waters ($1.5 \times 10^{-3}$ ng $ml^{-1}$), and even these concentrations are much lower than the concentrations typical of surface waters (Suess, 1976; Andelman and Snodgrass, 1974). Three explanations are possible: either the field data include the BaP on the very fine suspended particulates as well as dissolved BaP, or there are processes operative under natural conditions that were not included in our study and that enhance the solubility of BaP or increase its stability (such as complexation with humic acids), or the BaP concentrations that we assumed for the inflows in the simulations are much too low. We cannot discriminate among these three sources of disagreement with the data in hand, but the first one is the simplest and most plausible.

However, these differences do not alter the conclusions that follow from the simulations. Even if the BaP concentration were raised by two or three orders of magnitude, the predicted distribution and transformation half-lives would be the same, because the rate expressions would still be pseudo-first order. That is, adjusting the concentration in the simulation's inflows will proportionately change the concentration in each compartment.

The effects of incomplete mixing are also illustrated quantitatively by Figures 6.1 through 6.4, which show the patterns of buildup and decline of BaP in the pond, river, and lake simulations. Figures 6.1 and 6.2 show the trends in the concentration of BaP on suspended solids in the pond and river, but these paralleled the trends of dissolved BaP and are omitted from Figures 6.3 and 6.4 for simplicity. In all four simulations the concentrations of dissolved BaP rapidly approach steady states both before and after stoppage

TABLE 6.4. DISTRIBUTION OF BENZO[a]PYRENE IN VARIOUS AQUATIC SYSTEMS AT STEADY STATE (input concentrations of 1 ng $ml^{-1}$ benzo[a]pyrene)

| | Pond | | River | | Eutrophic Lake | | Oligotrophic Lake | |
|---|---|---|---|---|---|---|---|---|
| | Mass (g) | Conc. (ng $ml^{-1}$) | Mass (g) | Conc. (ng $ml^{-1}$) | Mass (g) | Conc. (ng $ml^{-1}$) | Mass (g) | Conc. (ng $ml^{-1}$) |
| Compartment 1 (surface water) | | | | | | | | |
| Solution | $2.9 \times 10^{-5}$ | $1.5 \times 10^{-6}$ | $4.5 \times 10^{-2}$ | $1.5 \times 10^{-3}$ | $2.7 \times 10^{-3}$ | $1.1 \times 10^{-5}$ | $4.7 \times 10^{-4}$ | $1.9 \times 10^{-6}$ |
| Suspended solids | $4.2 \times 10^{-4}$ | $7.0 \times 10^{-2}$ | $2.2 \times 10^{-1}$ | 7.4 | $6.7 \times 10^{-3}$ | $5.4 \times 10^{-1}$ | $1.2 \times 10^{-3}$ | $9.3 \times 10^{-2}$ |
| Compartment 2 (surface water) | | | | | | | | |
| Solution | -- | -- | $4.2 \times 10^{-2}$ | $1.4 \times 10^{-3}$ | $3.7 \times 10^{-3}$ | $1.5 \times 10^{-6}$ | $2.0 \times 10^{-4}$ | $7.9 \times 10^{-8}$ |
| Suspended solids | -- | -- | $2.0 \times 10^{-1}$ | 6.7 | $9.4 \times 10^{-3}$ | $7.5 \times 10^{-2}$ | $4.9 \times 10^{-4}$ | $3.9 \times 10^{-3}$ |
| Compartment 3 (surface water) | | | | | | | | |
| Solution | -- | -- | $3.7 \times 10^{-2}$ | $1.2 \times 10^{-3}$ | $1.8 \times 10^{-4}$ | $7.4 \times 10^{-6}$ | $5.2 \times 10^{-6}$ | $2.1 \times 10^{-8}$ |
| Suspended solids | -- | -- | $1.8 \times 10^{-1}$ | 6.1 | $4.6 \times 10^{-4}$ | $3.7 \times 10^{-2}$ | $1.3 \times 10^{-5}$ | $1.0 \times 10^{-3}$ |
| Compartment 5 (bottom water) | | | | | | | | |
| Solution | -- | -- | -- | -- | $5.5 \times 10^{-5}$ | $2.2 \times 10^{-8}$ | $5.2 \times 10^{-7}$ | $2.1 \times 10^{-10}$ |
| Suspended solids | -- | -- | -- | -- | $1.4 \times 10^{-4}$ | $1.1 \times 10^{-3}$ | $1.3 \times 10^{-6}$ | $1.0 \times 10^{-5}$ |
| Compartments 7-9 (sediment)[a] | | | | | | | | |
| Solution | $3.6 \times 10^{-7}$ | $1.4 \times 10^{-6}$ | $1.0 \times 10^{-3}$ | $1.35 \times 10^{-4}$ | $2.2 \times 10^{-5}$ | $2.6 \times 10^{-6}$ | $2.3 \times 10^{-6}$ | $2.7 \times 10^{-7}$ |
| Solids | $4.7 \times 10^{-2}$ | $7.0 \times 10^{-2}$ | $1.4 \times 10^{-2}$ | 6.7 | 1.9 | $1.4 \times 10^{-1}$ | $3.1 \times 10^{-1}$ | $2.3 \times 10^{-2}$ |
| Total mass | $4.7 \times 10^{-2}$ | | 140 | | 2.0 | | $3.2 \times 10^{-1}$ | |

[a] The amounts given for solid and solution phases in the sediment compartments are estimated from the sorption partition coefficient for suspended solids and may be overestimated because it was assumed that biodegradation of sorbed material does not occur.

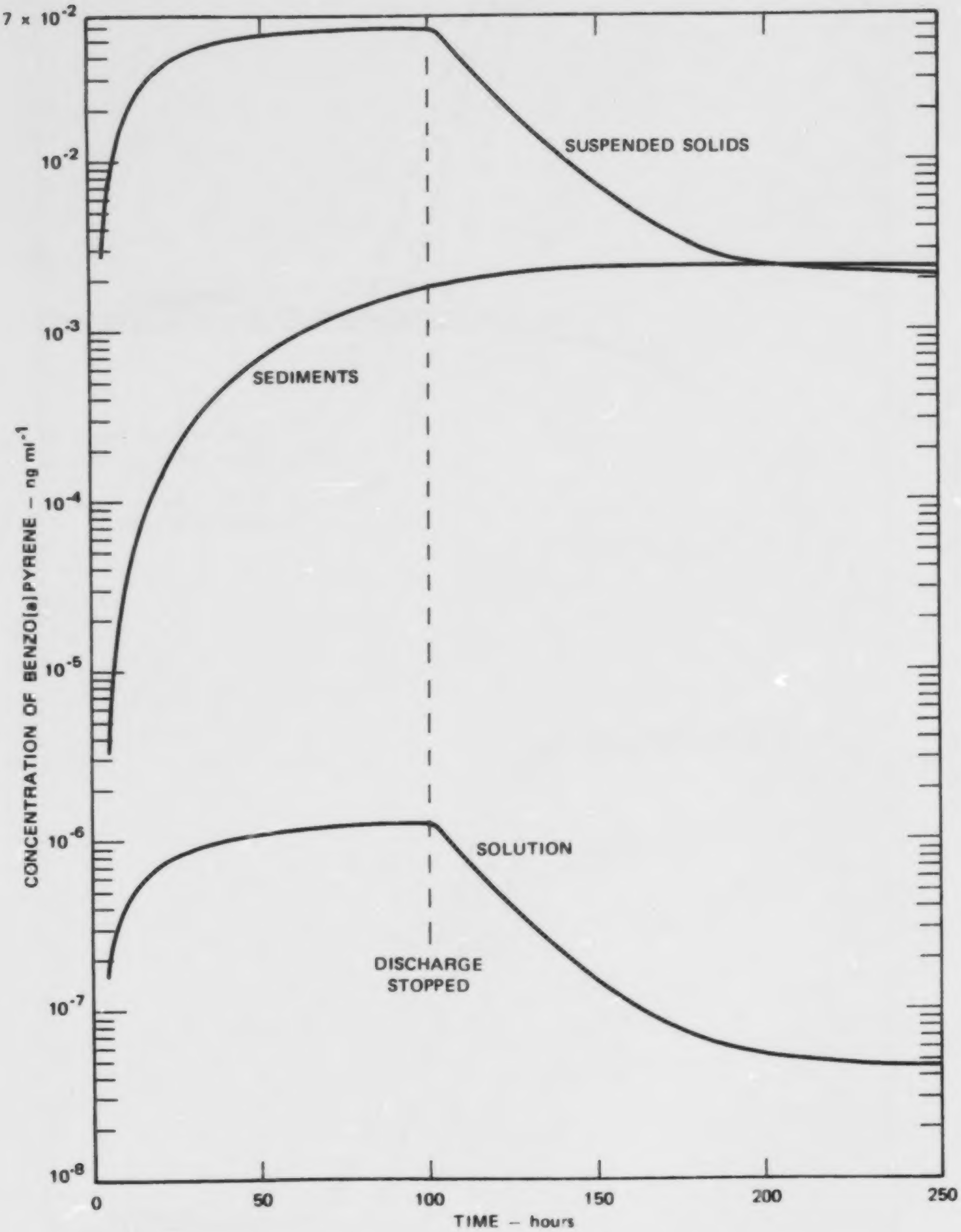

FIGURE 6.1 PERSISTENCE OF BENZO[a]PYRENE IN A TWO-COMPARTMENT POND SYSTEM

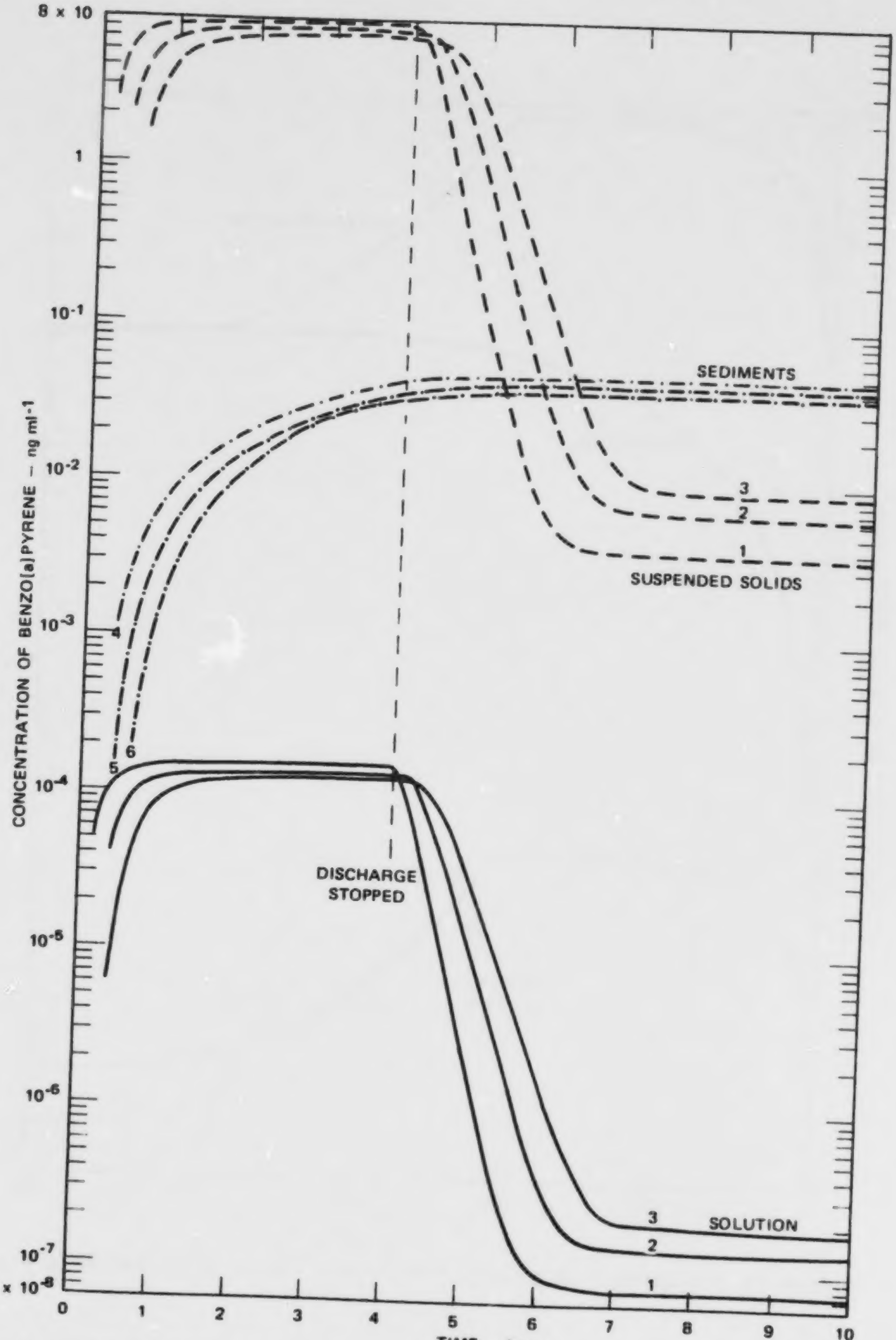

FIGURE 6.2 PERSISTENCE OF BENZO[a]PYRENE IN A PARTIALLY MIXED RIVER SYSTEM

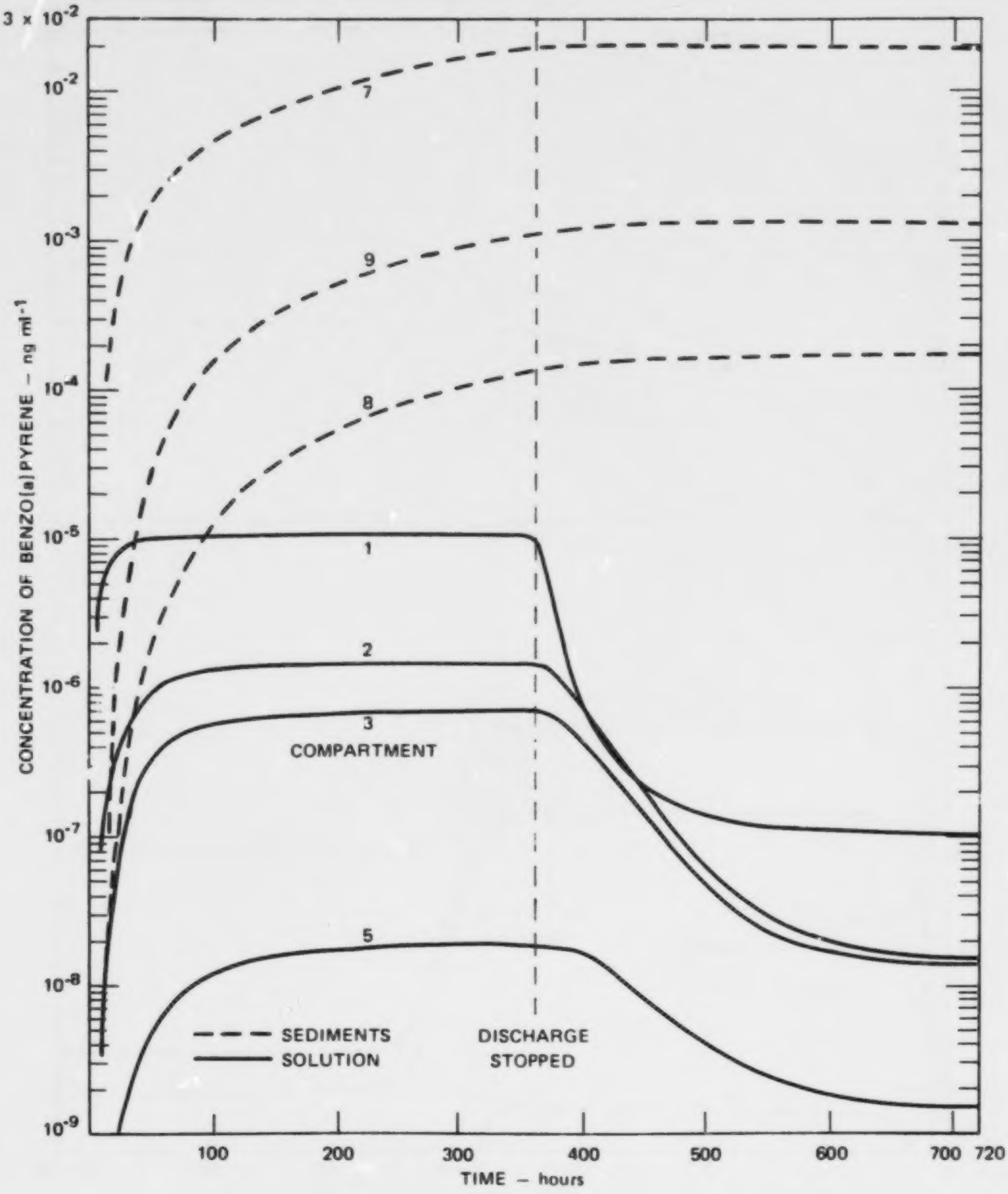

FIGURE 6.3 PERSISTENCE OF BENZO[a] PYRENE IN A EUTROPHIC LAKE

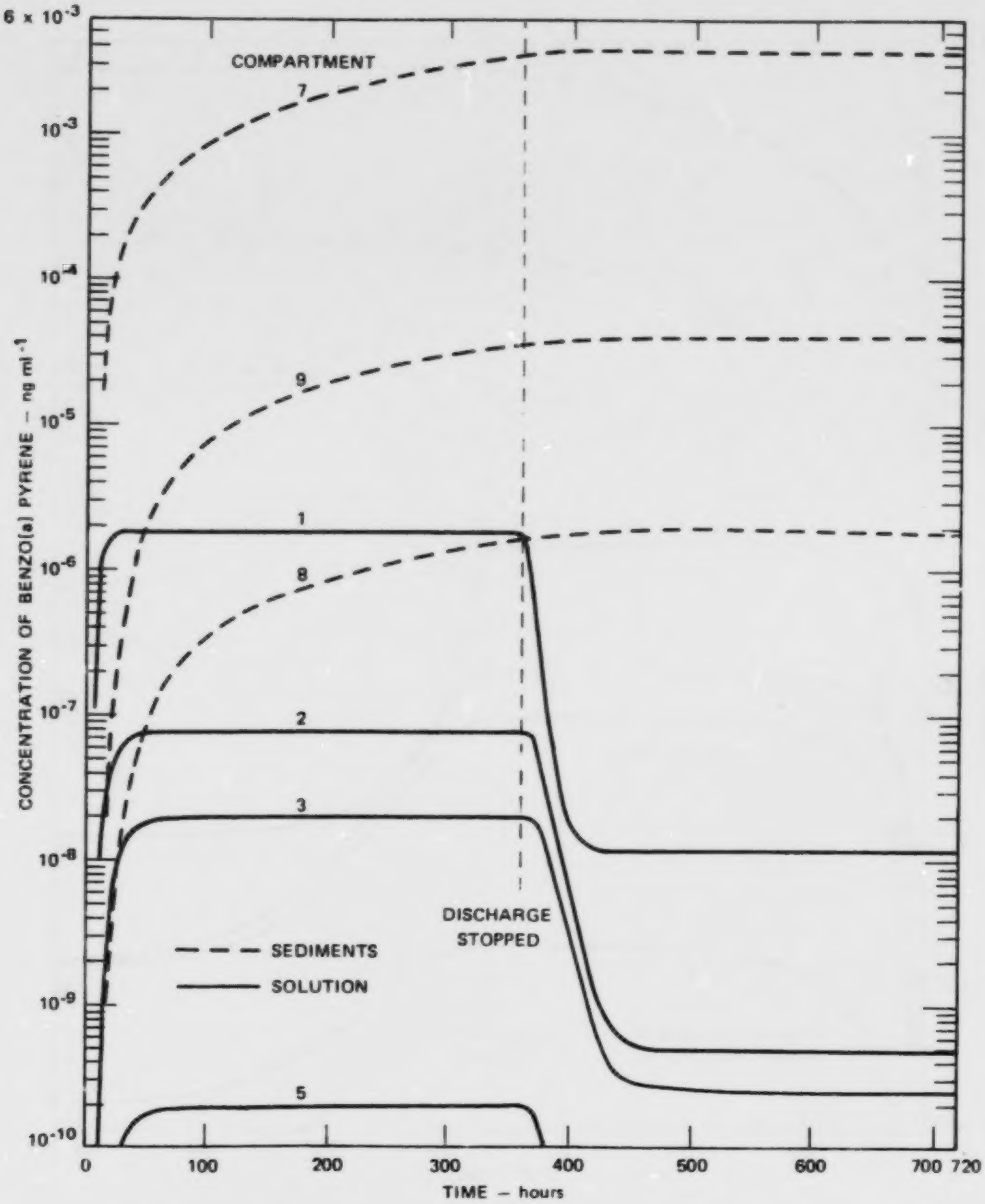

FIGURE 6.4 PERSISTENCE OF BENZO[a]PYRENE IN AN OLIGOTROPHIC LAKE

of discharge. Sediment concentrations in each simulation rise relatively slowly and decline exceedingly slowly after discharge stops. Stoppage of discharge causes a consistent 100- to 1000-fold decrease in the concentration of dissolved BaP, but in all cases desorption from the sediments is sufficient to maintain a very low concentration of BaP in solution, roughly equal to the concentrations in unpolluted groundwaters (Suess, 1976; Andelman and Snodgrass, 1974).

### 6.3.5 Discussion

The greatest uncertainty in the foregoing analyses, the transformational pathway of sorbed BaP, is less easily resolved. The stability of BaP is clearly affected by the presence of other organic compounds (Suess, 1972), but the net effect of other organic pollutants, and hence the role of chemical transformation, cannot be assessed with confidence. It is quite possible that the presence of other organics in polluted waters will increase the solubility of BaP, but waters that are polluted enough for this to occur will probably be too turbid for significant photolytic degradation (Andelman and Snodgrass, 1974).

Shabad et al. (1971) obtained some field data from experimentally contaminated agricultural fields and from industrially contaminated urban and suburban sites that suggest that biodegradation of BaP may occur in soils. Granting that these data appear to include minor losses due to leaching as well as degradation and were obtained from aerobic environments, it is reasonable to presume that they are within an order of magnitude of the rates to be expected in aquatic sediments. If this assumption is indeed true, it is probable that the half-life of BaP in aquatic sediments is one to ten years, probably at least three to four years.

Thus it appears probable that virtually all the BaP entering all but the cleanest natural waters is already sorbed on, or will rapidly sorb on suspended sediments and will accumulate in the bottom sediments. It will be lost from the sediments by biodegradation with a half-life of five to ten years.

## 6.4 PHYSICAL PROPERTIES

### 6.4.1 Solubility in Water

The solubility of BaP in water at room temperature (about 22 ± 2°C) was measured using the methods described by Haque and Schmedding (1975). The average solubility was 1.2 ± 0.1 ng $ml^{-1}$ (4.8 x $10^{-}$[illegible] M), based on replicate determinations.

### 6.4.2 Absorption Spectrum

BaP absorbs light strongly in the solar region to 420 nm.

The absorption spectrum of BaP in 20% acetonitrile/80% water was measured from 295 to 650 nm. The pH of the solution was 6 and was not adjusted. Care was taken to assure that the BaP was in solution and not a suspension. No particulate could be observed by light scattered by a collimated beam of green light (the green filter absorbed light below about 450 nm and eliminated the strong fluorescence observed in a beam of white light that obscured the scattered light).

The absorption coefficients at wavelength intervals from 297.5 to 420 nm and at wavelengths of 313 and 366 nm are reported in Table 6.5.

### 6.4.3 Volatilization Rate

The volatilization rate of BaP was measured using the method of Hill et al. (1976), which is described in detail in Part I, Section 5.3. The volatilization half-life of BaP in aqueous solution was about 22 hours at a fast stirring rate. The rate constants were calculated as follows:

Oxygen reaeration rate:* $k_v^O = 8.41 \pm 1.51\ \mathrm{hr}^{-1}$

BaP volatilization rate: $k_v^{BaP} = 0.030 \pm 0.002\ \mathrm{hr}^{-1}$

Ratio: $k_v^{BaP}/k_v^O = 0.0036 \pm 0.0006$

While this is an appreciable volatilization rate, the estimates reported in Table 6.3 show that volatilization of BaP is slow compared with photooxidation. This is largely because most of the BaP is sorbed on sediment, and volatilization of sorbed material is presumed to be very slow.

### 6.4.4 Sorption on Clay and Sediments

The sorption partition coefficients of BaP were measured on four sediments: Ca-montmorillonite, Des Moines River sediment, Coyote Creek sediment, and Searsville Pond sediment. Care was taken to assure that the samples were protected from light at all times to minimize photooxidation of the BaP. The initial concentration of BaP in each sample was always less than the saturation concentration of 1.2 ng $\mathrm{ml}^{-1}$ ($4.76 \times 10^{-9}$ M). Each experiment consisted of samples at one BaP concentration and two of three sediment loadings, plus blanks that contained only BaP. Duplicate flasks were analyzed for all sediment except clay. Periodic checks were made for sorption of BaP onto the glassware; since none of the glassware extracts contained BaP, we presumed that no sorption onto the glassware took place. The data, summarized in Table 6.6, were fitted to a Freundlich isotherm.

Graphs of the data are shown in Figure 6.5 with the partition coefficients ($K_p$). The calculation of the partition coefficient was based on the

---

*This value represents the average and standard deviation of five reaeration measurements taken over the period of the experiment.

TABLE 6.5. ABSORPTION SPECTRUM OF BENZO[a]PYRENE IN 20% ACETONITRILE/80% WATER AT pH 6[a]

| Center of wavelength interval[b] (nm) | Average absorption coefficient[c] ($M^{-1}$ $cm^{-1}$) |
|---|---|
| 297.5 | 46,600 |
| 300.0 | 27,700 |
| 302.5 | 13,900 |
| 305.0 | 6,670 |
| 307.5 | 4,840 |
| 310.0 | 3,970 |
| 312.5 | 3,890 |
| 315.0 | 3,650 |
| 317.5 | 3,730 |
| 320.0 | 3,570 |
| 323.1 | 3,650 |
| 330.0 | 5,400 |
| 340.0 | 8,330 |
| 350.0 | 12,300 |
| 360.0 | 18,100 |
| 370.0 | 19,680 |
| 380.0 | 21,910 |
| 390.0 | 15,160 |
| 400.0 | 2,100 |
| 410.0 | 1,100 |
| 420.0 | 0 |

[a] Benzo[a]pyrene concentration was 0.318 μg $ml^{-1}$ ($1.26 \times 10^{-6}$ M).

[b] The wavelength intervals are given in Appendix B Table B.1.

[c] The absorption coefficients at 313.0 and 366.0 nm are 3,730 and 23,650 $M^{-1}$ $cm^{-1}$, respectively.

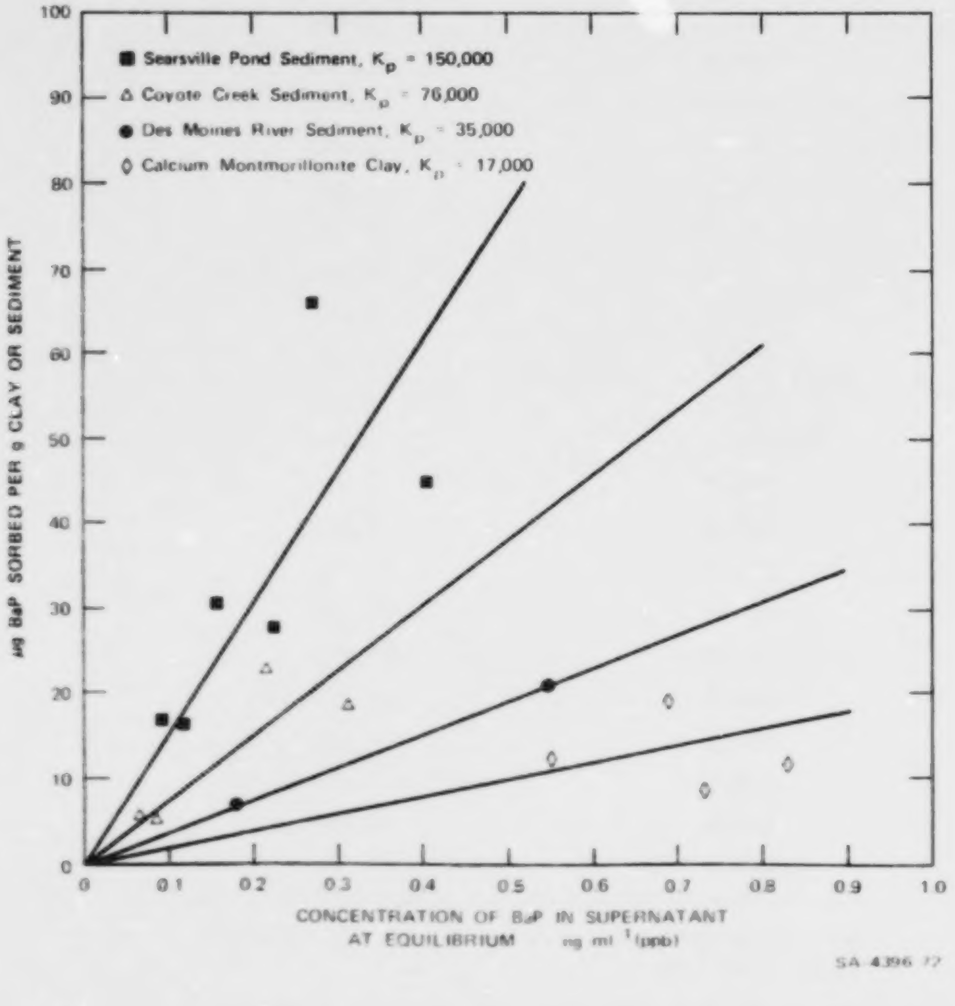

FIGURE 6.5. SORPTION ISOTHERMS OF BENZO[a]PYRENE

results of the analysis of the supernatant at equilibrium. The amount of BaP sorbed on the sediments was calculated by the difference between the amount that was added and the amount that was found in the supernatant. To check for material balance, sediment analyses were performed for these isotherms; however, the data are much more scattered than those from the supernatant. Recoveries of BaP from the supernatant plus the sediment ranged from approximately 70% to 110% (Table 6.6).

The relatively large experimental error in these data resulted from a combination of three factors. First, the concentration of BaP in the supernatant was less than 1 ng $ml^{-1}$. Second, the extraction and concentration of the samples required concentration of the extract of 100 ml of supernatant to less than 1 ml of sample. Third, materials that interfered with the BaP analysis were extracted from the water and from the sediment. There is, however, no doubt that sorption of BaP on sediments is very strong and that sorption will be an important physical process for BaP in the environment.

BaP sorption onto sediments is strongly correlated with the organic carbon levels in the sediments and is not related to the cation exchange capacity. A regression of the partition coefficient versus the sediment organic carbon levels was significant at the 0.5% level. The correlation coefficient was 0.996. Since the Ca-montmorillonite clay, which has essentially 0% carbon, did show sorption of BaP, it appears that BaP sorption involves both a weak interaction with solid surfaces and a strong interaction with organic material.

### 6.4.5 Biosorption

Biosorption studies were conducted with ng $ml^{-1}$ BaP solutions and 0.05% potassium phosphate buffer. Experiments using BaP solutions that did not contain cells showed that significant amounts of BaP were sorbed onto the glassware. These experiments are described in Appendix B. A correction was made for sorption of BaP on glass walls by determining the recovery of BaP from the centrifuge tubes when the cell suspensions were poured out of control tubes.

Because of the low level of BaP, the optical densities of solutions containing equal density concentrations of the four test bacteria (Azotobacter beijerinkii ATCC 19366, Bacillus cereus ATCC 11778, Escherichia coli ATCC 9637, and Serratia marcescens ATCC 13880) were reduced to 0.2. These solutions were combined immediately before the experiment was carried out. The results from the one-hour sorption and three-hour desorption studies are presented in Table 6.7.

The high sorption coefficients were anticipated on the basis of our earlier sorption studies with bacterial cell mixtures, the sorptive characteristics on glass, and the technique that was necessary to extract BaP quantitatively from wet cells. This strong sorptive capacity of cells for BaP is also discussed by Lohrbacher et al. (1974) and by Poglazova and Meisel (1971), and accounts for the drop in interest in producing biomass for feed and food pur-

TABLE 6.6. BENZO[a]PYRENE SORPTION ON COYOTE CREEK SEDIMENTS

| Sediment | Total organic carbon (%) | Sediment concentration ($\mu g\ ml^{-1}$) | BaP concentration in supernatant[a] ($\mu g\ ml^{-1} \times 10^3$) | BaP concentration on sediment[b] ($\mu g\ g^{-1}$) | Partition coefficient[c] $K_p \times 10^{-4}$ | | |
|---|---|---|---|---|---|---|---|
| | | | | | LSS | | NLLS |
| | | | | | $a_o = 0$ | $a_o \neq 0$ | $S_w$ and $S_s$ |
| Ca-montmorillonite clay | 0.06 | 19 | 0.77 ± 0.15 | 16 ± 8 | 1.7 ± 0.5 | -2.7 ± 1.6 | 1.7 ± 0.5 |
| | | 38 | 0.65 ± 0.10 | 11 ± 3 | | ($a_o$ = 32 ± 12) | |
| Coyote Creek | 1.4 | 23 | 0.27 ± 0.06 | 21 ± 3 | 7.6 ± 2.4 | 6.0 ± 5.1 | 7.6 ± 4.0 |
| | | 120 | 0.69 ± 0.013 | 6.0 ± 0.1 | | ($a_o$ = 4 ± 11) | |
| Des Moines River | 0.6 | 19 | 0.56 ± 0.11 | 22 ± 6 | 3.5 ± 2.7 | 2.5 ± 8.1 | 4.2 ± 2.6 |
| | | 96 | 0.18 ± 0.15 | 7.4 ± 1.6 | | ($a_o$ = 5 ± 35) | |
| Searsville Pond | 3.8 | 7.7 | 0.33 ± 0.09 | 55 ± 11 | 15 ± 2 | 9.7 ± 0.4 | 16.5 ± 2.7 |
| | | 19 | 0.19 ± 0.04 | 30 ± 2 | | ($a_o$ = 14 ± 10) | |
| | | 38 | 0.10 ± 0.03 | 17 ± 1 | | | |

[a] Concentration measured in supernatant with population standard deviation.

[b] Concentration on sediment calculated from supernatant concentration with population standard deviation.

[c] LLS = linear least squares; NLLS = nonlinear least squares; see Appendix B, Section B.1.4 for description of regressions. Limits are 95% confidence limit.

poses from liquid petroleum fractions. The elimination of BaP in activated sludge of sewage plants is also attributed to this characteristic.

TABLE 6.7. BENZO[a]PYRENE SORPTION AND DESORPTION ON A MIXED BACTERIAL POPULATION[a]

| Initial BaP concentration (ng ml$^{-1}$) | Sorption (S) or desorption (D) | Sorption coefficient (x 10$^{-4}$) |
|---|---|---|
| 1.01 | S | 33.6 ± 6.3 |
| | D | 36.9 ± 7.0 |
| 0.55 | S | 44.8 ± 5.4 |
| | D | 49.5 ± 5.0 |

[a] Dry weight of bacterial mixture equivalent to 97 mg liter$^{-1}$.

The adjustments in results in Table 6.7 for sorption of BaP on glassware in sorption studies were 1.8% and 3.6%, and in desorption studies they were 3.6% and 4.0% for initial BaP concentrations of 1.01 and 0.55 ng ml$^{-1}$, respectively.

## 6.5 CHEMICAL TRANSFORMATION

### 6.5.1 Photolysis Rate

Photolysis of BaP in air-saturated water is rapid in the solar region and gives a mixture of three quinones. Data for the photolysis of BaP are given in Table 6.8. Acetonitrile was used as the cosolvent with water from the sources indicated since the solubility of BaP in water alone is very low (see Section 6.4.1). In sunlight the half-life of BaP was only 0.7 to 1.1 hour. Good first-order kinetic behavior was found for photolyses carried to beyond two half-lives of BaP under laboratory conditions.

In the experiments using 260 and 13 ng ml$^{-1}$, the photolysis rate was independent of the BaP concentration. The quantum yields for direct photolysis of BaP measured at 313 and 366 nm were 8.9 x 10$^{-4}$ and 5.4 x 10$^{-4}$, respectively. These data indicate that there may be a slight dependence of the quantum yield on wavelength, but this conclusion must be treated cautiously in view of the number of variables that might affect these measurements and the limited number of experiments. Similar cautions apply also to the possible small solvent effect shown in Table 6.8. For the photolysis of BaP at 366 nm in the acetonitrile-pure water solvents, the standard deviation of the photolysis rate constant among experiments is about 15% from the average of 3.77 x 10$^{-4}$ sec$^{-1}$.

TABLE 6.8. RATE CONSTANTS FOR PHOTOLYSIS OF BENZO[a]PYRENE

| Irradiation source | Solution[a] | BaP concentration (ng ml$^{-1}$)[b] | Extent of reaction (%) | Rate constant $k_p \times 10^4$ sec$^{-1}$ |
|---|---|---|---|---|
| 313 nm | 20% AN in PW | 270 | 71 | 0.105 ± 0.009[c,d] |
| 366 nm | 20% AN in PW | 260 | 84 | 3.47 ± 0.12[e] |
| 366 nm | 20% AN in PW | 13 | 77 | 3.36 ± 0.22 |
| 366 nm | 1% AN in PW | 13 | 87 | 4.37 ± 0.30<br>2.9[f] |
| 366 nm | 1% AN in PW with humic acid | 13 | 43 | 0.690 ± 0.041 |
| 366 nm | 1% AN in Lake Tahoe water | 13 | 54 | 1.76 ± 0.10<br>1.8[f] |
| 366 nm | 1% AN in Searsville Pond water | 13 | 76 | 3.98 ± 0.13 |
| 366 nm | 1% AN in Coyote Creek water | 13 | 46 | 1.70 ± 0.07<br>1.2[f] |
| Mid-morning sunlight, late January | 20% AN in PW | 270 | 86 | 1.79 ± 0.39[g,h] |
| Noon sunlight mid-December | 20% AN in PW | 270 | 91 | 2.79 ± 0.23[g,i] |

[a] AN = acetonitrile; PW = pure water.

[b] 1.00 ng ml$^{-1}$ BaP in water = $3.96 \times 10^{-9}$ M.

[c] Standard deviation.

[d] Quantum yield for BaP disappearance at 313 nm is $8.9 \times 10^{-4}$.

[e] Quantum yield for BaP disappearance at 366 nm is $5.4 \times 10^{-4}$.

[f] One data point for each photolysis experiment. Reactions were photolyzed simultaneously in merry-go-round reactor for direct comparison of the effect of the three waters indicated.

[g] Rate constant not corrected for variation in sunlight intensity during experiment.

[h] Half-life of 1.1 hour.

[i] Half-life of 0.7 hour.

While these differences are considered negligible in an environmental assessment, the small variations in data between experiments may be subtle, but real, phenomenological effects and not experimental error. Further studies to elucidate the mechanism would clarify these effects, but such studies are beyond the scope of this project.

The photolyses of BaP conducted in natural waters or in pure water containing humic acid showed slower photolysis rates than photolyses conducted in pure water alone. Photolysis of 13 ng $ml^{-1}$ BaP in the presence of humic acid in pure water (absorbance at 366 nm is 0.11) is five times slower than the photolysis in pure water; the other natural waters showed intermediate but definite retardation of the BaP photolysis. It is not known why the water from Lake Tahoe shows greater inhibition of BaP photolysis than the water from the Searsville Pond. It is unlikely that a light screening effect is responsible for the slowed photolysis rates since the absorbance of the natural waters at 366 nm is very small ($< 0.02$); the 0.11 absorbance of the humic acid solution at 366 nm should reduce the photolysis rate 13% if light screening is the only effect operative.

The reason for the slower photolyses in natural waters can only be speculated upon at this time. It is not known how much or what types of organic material are present in these natural waters. It is possible that substances present in the natural waters (either organic or inorganic) may quench a BaP excited state, singlet oxygen (if it is an intermediate oxidant), or any excited state complex that occurs in the reaction.

Another possible process by which photolysis in natural waters may be inhibited is by formation of a complex of BaP and natural substances (organic or inorganic) in solution, which would alter the reactivity of ground state BaP itself. Evidence for complex formation was found in an experiment with approximately 30 $\mu g\ ml^{-1}$ humic acid and 270 ng $ml^{-1}$ BaP in which about 50% of the BaP could not be recovered from the aqueous solution by hexane extraction.

An example of possible inhibition of BaP photolysis on kaolinite clay caused by complex formation during photolysis was reported by McGinnes and Snoeyink (1974); products formed during photolysis are apparently responsible for this effect. Such effects may be occurring by several mechanisms, including competitive reactions of the associated organic material with the oxidizing agent(s) formed during the BaP photolysis. If lipophilic/hydrophoic compounds such as BaP do form such complexes, the photolysis rates of BaP in lakes and streams may be much slower than in pure water solutions.

The half-life for direct photolysis of BaP in sunlight as a function of the time of day was calculated by the procedure of Zepp and Cline (1977) using a quantum yield of $8.9 \times 10^{-4}$ and the measured UV spectrum of BaP (Section 6.4.2). The data for the summer and winter seasons are plotted in Figure 6.6. The calculated half-life of 1.2 hour for midday photolysis in winter is in excellent agreement with the measured half-lives of 1.1 and 0.7 hours measured during the same season.

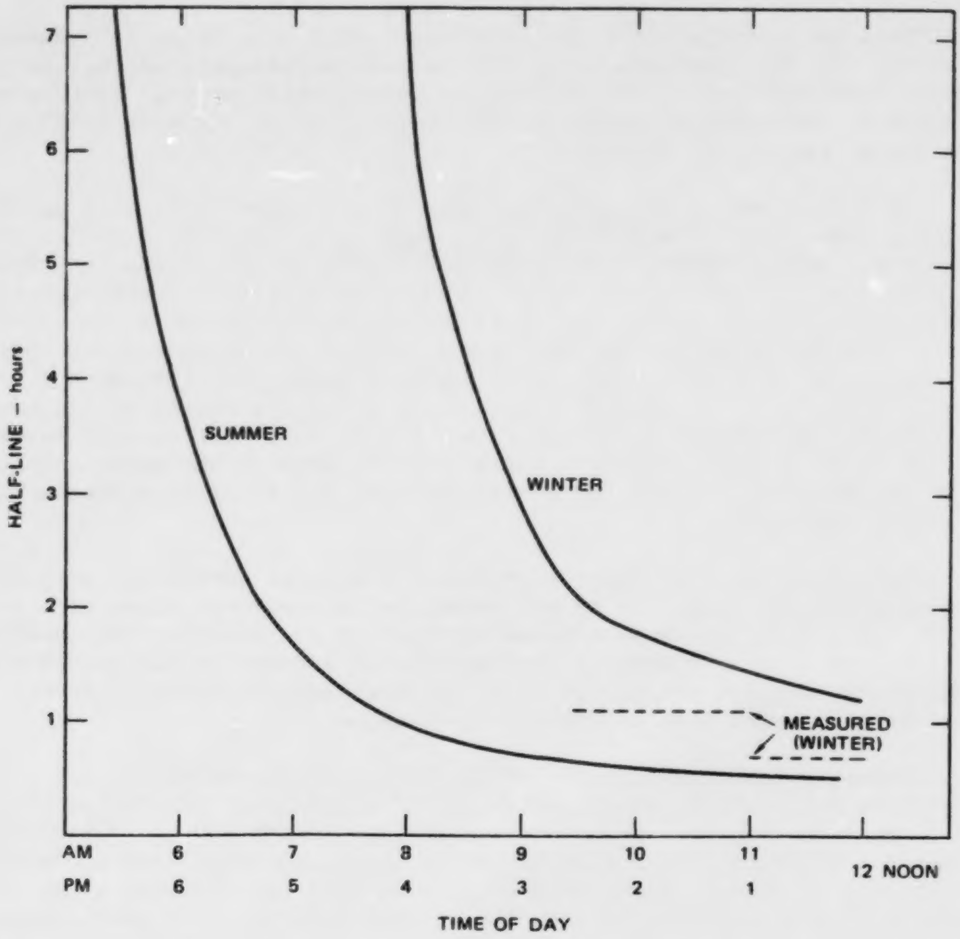

FIGURE 6.6 SEASONAL AND DAILY VARIATION OF PHOTOLYSIS HALF-LIFE OF BENZO[a]PYRENE

### 6.5.2 Oxidation Rate

When the susceptibility of BaP to free radical oxidation was examined using the AA-initiated oxidation reaction, BaP was found to be completely consumed after the usual 100-hour reaction time. The oxidation experiment was then repeated using a 270 ng $ml^{-1}$ ($1.0 \times 10^{-6}$ M) BaP solution (20% acetonitrile in water) containing $1.0 \times 10^{-4}$ M AA, and analyzed for BaP at reaction times of 4.5 and 6.0 hours. The data from this experiment gave a first-order rate constant term ($k_{ox}[RO_2^\cdot]$) of $(5.7 \pm 1.1) \times 10^{-5}$ $sec^{-1}$. Under the reaction conditions at 50°C (see Appendix B, Section B.2), this corresponds to a second-order rate constant $k_{ox}$ of $1.68 \times 10^{4}$ $M^{-1}$ $sec^{-1}$. At 25°C, $k_{ox}$ would then be $1.86 \times 10^{3}$ $M^{-1}$ $sec^{-1}$, and assuming a $[RO_2^\cdot] = 10^{-9}$ M, the half-life for oxidation of BaP in aquatic environments would be 4.3 days. While this is a reasonably fast process, the nonphotolytic oxidation of BaP is clearly not competitive with photolysis or sorption of BaP under environmental conditions.

### 6.5.3 Hydrolysis Rate

BaP contains no groups that are hydrolyzable. Therefore, no hydrolysis studies were carried out.

### 6.5.4 Products from Chemical Transformation

Products from the oxidation and photolysis of BaP have been reported to be quinones of the BaP structure (Radding, 1976); however, no material balances for the reactions have been reported. In our studies, the primary products resulting from oxidation and photolyses of BaP were tentatively identified as quinones by comparing their HPLC retention times with those of authentic samples obtained from the National Cancer Institute. The quinones found are shown below:

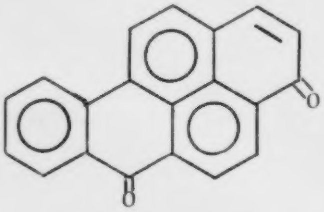

BaP-3,6-quinone

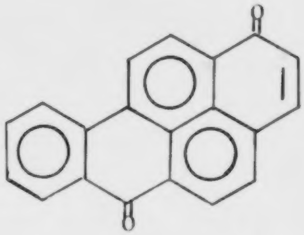

BaP-1,6-quinone

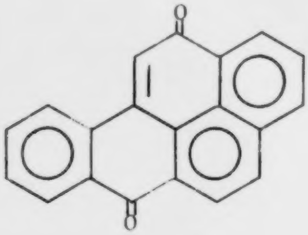

BaP-6,12-quinone

The yield of quinones and the material balances for the free radical oxidation and the photolyses at 366 nm and in the sunlight are listed in Table 6.9. The material balances for the oxidation and photolyses are good. This is contrary to what would be expected from the work of McGinnes and Snoeyink (1974), who reported that the quinone products are more photolabile than BaP itself. The material balances in Table 6.9 show that the chemical transformation products are accounted for by the three quinones.

The data in Table 6.9 are interesting in several respects. The product ratio of the 1,6-quinone and the 3,6-quinone is about 3 to 1 in both the sunlight and the 366 nm photolyses; only traces of the 6,12-quinone were found. This result suggests that the formation of the products of BaP photolysis is independent of wavelength.

The mechanism for the photolytic transformation is not known. While singlet oxygen may be involved, it is doubtful that there is an endoperoxide intermediate involved; an alternative mechanism of electron-transfer/superperoxide radical anion oxidation is also a possibility. It is also inter-

TABLE 6.9 PRODUCT YIELDS AND MATERIAL BALANCE FOR BENZO[a]PYRENE PHOTOLYSES AND FREE-RADICAL OXIDATION

| Reaction | % BaP reacted | % Yield[a] 1,6-quinone | % Yield[a] 3,6-quinone | % Yield[a] 6,12-quinone | Material balance[b] (%) |
|---|---|---|---|---|---|
| AA-initiated oxidation of 2700 ng $\text{ml}^{-1}$ BaP in 20% AN | 50 | 36 | 22 | 32 | 90 |
| | 74 | 35 | 18 | 27 | 80 |
| | 100 | 40 | 24 | 40 | 104 |
| Average | | 37 | 21 | 33 | |
| Sunlight photolysis of 270 ng $\text{ml}^{-1}$ BaP in 20% AN | 50 | 54 | 16 | Trace[c] | 70 |
| | 55 | 78 | 24 | Trace | 102 |
| | 74 | 81 | 26 | Trace | 107 |
| Average | | 71 | 22 | Trace | |
| Photolysis at 366 nm of 270 ng $\text{ml}^{-1}$ BaP in 20% AN | 25 | 80 | 20 | Trace | 100 |
| | 56 | 77 | 20 | Trace | 96 |
| Photolysis at 366 nm of 270 nm $\text{ml}^{-1}$ BaP in 50% AN | 8.5 | 71 | 24 | Trace | 95 |
| | 19 | 66 | 18 | Trace | 84 |

---

[a] Based on BaP reacted.

[b] Material balance = (BaP consumed/quinones formed) x 100.

[c] Trace, discernible peak in HPLC, but less than 5% yield.

esting to note that the same quinone products in about the same product ratio (3 to 1 ratio of 1,6-Q to 3,6-Q) have been reported for the ozonolysis of BaP (Moriconi et al., 1961).

Table 6.9 shows that free radical oxidation of BaP also produces the 6,12-quinone in significant yield. The mechanism of the oxidation reaction is unknown, probably involving $RO_2\cdot$ radicals and other oxidizing species, and is likely different from that of the BaP photolysis. However, oxidation at the 6-position on the BaP skeleton appears to be a common feature in both types of reaction. It may be that a primary reaction occurs at the 6-position of BaP, with the nature of the oxidant then determining the selectivity of attack at other carbons on the ring (e.g., positions 1, 3, or 12).

### 6.5.5 Reaction with Singlet Oxygen

Several studies of the photolysis of polynuclear aromatic compounds (PAHs) have implicated singlet oxygen ($^1O_2$) as the oxidant in the formation of quinone products (National Academy of Sciences, 1972). One suggested mechanism is that the PAH serves as a singlet oxygen sensitizer and as a reactant with $^1O_2$ (Stevens and Algar, 1968).

$$\mathrm{PAH} \xrightarrow{h\nu} {}^1\mathrm{PAH}^* \tag{6.1}$$

$${}^1\mathrm{PAH}^* \longrightarrow \mathrm{PAH} \tag{6.2}$$

$${}^1\mathrm{PAH}^* \dashrightarrow {}^3\mathrm{PAH}^* \tag{6.3}$$

$${}^3\mathrm{PAH}^* + {}^3O_2 \longrightarrow \mathrm{PAH} + {}^1O_2 \tag{6.4}$$

$${}^3\mathrm{PAH}^* \longrightarrow \mathrm{PAH} \tag{6.5}$$

$${}^3\mathrm{PAH} + {}^3O_2 \longrightarrow \mathrm{MO_2} \tag{6.6}$$

$${}^1O_2 + \mathrm{PAH} \xrightarrow{k_7} \mathrm{MO_2} \tag{6.7}$$

$${}^1O_2 \xrightarrow{k_8} {}^3O_2 \tag{6.8}$$

where the asterisk denotes an electronic excited state; $^3O_2$ and $^1O_2$ are the triplet (the ground state) and singlet oxygen; PAH, $^1PAH^*$, and $^3PAH^*$ are the ground state, singlet, and triplet excited states of PAH; and $MO_2$ is the oxidized PAH product or products. Reaction of $^3PAH$ with $^3O_2$ to form a complex (exciplex) that gives products directly without formation of free $^1O_2$ is also a reasonable alternative mechanism.

$${}^3\mathrm{PAH}^* + {}^3O_2 \longrightarrow (\mathrm{PAH},\ {}^1O_2)^* \tag{6.9}$$

$$(\mathrm{PAH},\ {}^1O_2)^* \longrightarrow \mathrm{MO_2} \tag{6.10}$$

Since photolysis of BaP was found to be rapid in aqueous solution giving quinone products (see Section 6.5.4), it was of interest to determine the reactivity of ground-state BaP with $^1O_2$. One measure of such reactivity is the ratio of the rate constant $k_8$ for the decay of $^1O_2$ to ground state ($^3O_2$) to the rate constant $k_7$ for the reaction of $^1O_2$ with substrate (in this system the BaP). This ratio is referred to as the β value:

$$\beta = (k_8/k_7)M^{-1} \tag{6.11}$$

β is also equal to the concentration of substrate required to trap half of the singlet oxygen in the reaction system. Values of β are solvent dependent because $k_8$ changes with solvent while $k_7$ does not (Stevens et al., 1974). The value for $k_8$ in different solvents has been measured by Merkel and Kearns (1972).

To evaluate $k_7$ for BaP, ($k_{BaP}$), we used a competitive reaction technique in which BaP and a reference compound, for which $k_7$ and β are known, were exposed to singlet oxygen in the same reaction solution. Methanol was used as the solvent for this study. Since the same concentration of singlet oxygen is available to both reactants in solution, the ratio of the first-order rate constants $k'_{BaP}$ and $k'_{RC}$, corresponding to the disappearance of BaP and reference compound, respectively, gives the relative reactivity of BaP to the reference compound. With this reactivity ratio and the known absolute value of $k_7$ for the reference compound ($k_{RC}$), the value of $k_{BaP}$ in water can be calculated.

$$\left[\frac{k'_{BaP}}{k'_{RC}}\right] \times k_{RC} = k_{BaP} \tag{6.12}$$

From the value for $k_{BaP}$ and the known value for $k_8$ in water, the β value for BaP in water can be calculated.

Singlet oxygen was generated in our experiments using the sensitizer rose bengal. This sensitizer absorbs light above 500 nm, well beyond the highest wavelength absorption of BaP or other PAHs.

$$\text{Sens} \xrightarrow{h\nu} {}^1\text{Sens}^* \tag{6.13}$$

$${}^1\text{Sens}^* \rightsquigarrow {}^3\text{Sens}^* \tag{6.14}$$

$${}^3\text{Sens}^* + {}^3O_2 \longrightarrow \text{Sens} + {}^1O_2 \tag{6.15}$$

Thus singlet oxygen is formed independently of the PAH, and the β values are then related to the true bimolecular reaction (6.7) and without any contribution to oxidation due to the possible PAH-$^1O_2$ complexes, reactions (6.9) and (6.10). Photolyses were conducted using two 750-watt tungsten lamps and a Corning 3-71 filter to cut off all light below 450 nm.

Initial experiments to measure the β value for BaP found that it reacted much slower with singlet oxygen than a reference compound, 1,3-diphenylisobenzofuran (β = 0.06). Benza[a]anthracene (BA) was then chosen as a reference compound because its β value was known (870 ± 250 at 25°C in benzene solvent), because it reacted at a rate comparable to BaP, and because HPLC analysis clearly resolved both PAHs ($k_7$ for BA = $4.8 \times 10^4$; Stevens et al., 1974). The data for the rose bengal sensitized, singlet oxygen reaction (also called photooxygenation) of BA and BaP in 10% acetonitrile in water are given in Table 6.10. Rate constants for loss of BA and BaP ($k'_{RC}$ and $k'_{BaP}$, respectively) were evaluated from first-order plots of ln[PAH] versus time.

TABLE 6.10. RATE CONSTANTS FOR SINGLET OXYGEN ADDITION
TO BENZO[a]PYRENE AND BENZ[a]ANTHRACENE[a]

| | Concentration of PAH ($M \times 10^5$) | | $k' \times 10^5$ sec$^{-1}$ | | Ratio |
|---|---|---|---|---|---|
| Experiment | BaP | BA | BaP | BA | $k'_{BA}/k'_{BaP}$ |
| 1 | 1.00 | 1.00 | 0.97 ± 0.02 | 2.04 ± 0.05 | 2.11 |
| 2 | 1.00 | 1.20 | 0.94 ± 0.09 | 2.28 ± 0.18 | 2.42 |
| | | | | Average | 2.26 |

[a] Solvent was 10% acetonitrile in methanol with $2 \times 10^{-5}$ M rose bengal sensitizer.

The averaged value of 2.3 for the ratio of the reactivity of BA to BaP is in accord with the similar polycyclic structure of the two PAHs. It is also interesting that the quantum yield for direct photolysis of BA at 366 nm was $3.3 \times 10^{-4}$ (Section 5.5.1), slightly more than three times larger than that of BaP ($8.9 \times 10^{-4}$ at 366 nm). While perhaps fortuitous, the close agreement between the relative reactivity of BA and BaP to singlet oxygen and the ratio of direct photolysis quantum yields suggests that the direct photolysis of these PAHs may involve reaction with $^1O_2$ [reactions (6.4), (6.7), or (6.9), (6.10)].

As discussed above, the value of $k_7$ for reaction between a substrate and $^1O_2$ is independent of solvent. Using BA as the reference compound, $k_{RC}$ is then equal to $4.8 \times 10^4$ $M^{-1}$ sec$^{-1}$ at 25°C. From this rate constant and the ratio $k'_{BaP}/k'_{RC} = 0.44$, $k_{BaP}$ is calculated as $2.1 \times 10^4$ $M^{-1}$ sec$^{-1}$ at 25°C. Based on a value for $k_8$ in water solvent = $5 \times 10^5$ sec$^{-1}$ (Merkel and Kearns, 1972), the β value for BaP is calculated to be 24 $M^{-1}$. For comparison, the β value for BA in water is 10 $M^{-1}$.

## 6.6 BIODEGRADATION

### 6.6.1 Development of Enrichment Cultures

The three sets of experimental conditions used in attempting to develop BaP degrading enrichment cultures failed to yield systems indicating any significant breakdown of this carcinogen.

In one series, BaP was ground to a small particle size in a suspension by the use of a low-clearance Potter-Elvehjem homogenizer. The BaP was added at 3 $\mu g\ ml^{-1}$ concentrations to the original 100 ml of water samples plus buffer and ammonium salts in 500-ml Erlenmeyer shaker flasks, and to the basal salts media used in subsequent transfers in 250-ml Erlenmeyer shaker flasks.

The first transfers from the flasks containing water samples from the eutrophic pond near Searsville Lake in Woodside, California, and aeration effluents from the wastewater treatment plants of Palo Alto, South San Francisco, the Shell Oil Refinery in Martinez, California, and the Monsanto Chemical Company, Anniston, Alabama, were arbitrarily made after 4 days incubation at 25°C in a rotatory shaker. Subsequent transfers (2% vol) to fresh media with suspended BaP appeared to develop 30% to 40% reduction of BaP, but these results were obtained before fermentation broths were frozen and thawed three times in the presence of some solvent before the final extractions were made. At the time of the seventh transfer from each water sample, transfers were also made to basal salts media with no added organic substrate. After 4 days of incubation, microbial counts in all flasks were all in the range of $(2.7\ to\ 5.8) \times 10^6\ ml^{-1}$. The freeze-thaw (3 times) extraction procedure resulted in complete recovery of the 3 $\mu g\ ml^{-1}$ BaP, indicating no biodegradation of BaP. Because there was an increase in numbers of organisms when new media were inoculated, but there was no degradation of BaP, the organic material for growth of the organisms had to originate from the distilled water used in the preparation of the media and/or from the atmosphere.

The second series of enrichment studies was initiated with naphthalene and pyrene as added organic substrates. The concept was that BaP may be so highly sorbed by the organisms and particulate matter in the water samples that there was insufficient free BaP for the growth of organisms that could or would develop the capacity to degrade BaP. It was possible that cultures could develop that would degrade naphthalene and/or pyrene, and then because of the similarities of these compounds to parts of the structure of BaP, a BaP-biodegrading enrichment culture might develop if BaP were present in subsequent transfer media.

To the 9-liter aerated bottles with eutrophic pond water and the aeration effluents from the South San Francisco, Shell Oil Refinery (Martinez, CA), and Monsanto Company Plant (Anniston, AL), naphthalene and pyrene were added in DMSO equivalent to 50 and 1 $\mu g\ ml^{-1}$, respectively, at days 1 and 2, and 100 and 1 $\mu g\ ml^{-1}$, respectively, at days 3 and 4. On day 5, a transfer was made into shaker flasks containing basal salts medium to which naphthalene (300 $\mu g\ ml^{-1}$) and pyrene (6 $\mu g\ ml^{-1}$) had been added.

Subsequent repeated transfers, made into shaker flasks every three days into media containing naphthalene (600 $\mu$g ml$^{-1}$), pyrene (12 $\mu$g ml$^{-1}$), and BaP (3 $\mu$g ml$^{-1}$) all developed good growth as had been expected with naphthalene providing organic carbon for growth. The fermented broths, after up to 11 days of fermentation, did not indicate any loss of BaP in the shaker flasks when the broths were subjected to three freeze-thaw cycles in the presence of ethyl acetate used for the first extraction.

The third series of enrichment studies was initiated with BaP (1 $\mu$gml$^{-1}$) and naphthalene (10 $\mu$g ml$^{-1}$) and a weekly addition of naphthalene (10 $\mu$g ml$^{-1}$) to the contrary 9-liter first-stage enrichment fermentors with a water sample from Coyote Creek and aeration effluent from the Palo Alto sewage plant. During the six weeks of this study, degradation of BaP was not observed.

### 6.6.2 Biodegradation Kinetics

Since enrichment cultures that degraded BaP were not obtained, biodegradation kinetic studies were not performed.

### 6.6.3 Discussion

The literature results summarized in Section 6.2suggest that, with long exposure of microorganisms in the environment to BaP or other polyaromatic hydrocarbons, there is a natural preselection and induction process that did not occur within the time limitations of our enrichment studies. Our inability to develop BaP degrading systems may also be due to the characteristics of the water samples. Several of the reports from the laboratories of Poglazova and Shabad used levels of BaP far above the level of solubility. With the high sorption coefficientsof BaP on microorganisms and particulate matter and the low water solubility of BaP, there is little BaP in solution for the growth of specific microorganisms that may be able to metabolize or adapt to the metabolism of BaP when it is the only available carbon nutrient. These conditions could put such microorganisms at a disadvantage with organisms having more favorable predator-prey or microbial interaction relationships. To date, no BaP biodegrading culture systems have been developed when BaP was used as a sole carbon source.

The phenomena of microbial interactions or predator-prey relationships depend on many factors including the species of organisms; rates of growth; availabilities and characteristics of nutrients present as natural contaminants or released by excretion or autolysis of other organisms; symbiosis or antagonisms by modifying pH, oxygen tensions, and/or production of new substrates; growth of inhibitory substances; dilution rates of constitutive organisms; and phagocytosis.

It is also possible that some of the degradations reported were conclusions based on observations made as a consequence of artifacts of analytical procedures. However, with the many reports and analogies with microbial attack on other aromatic compounds, it is reasonable to conclude that BaP can be microbially metabolized. In aquatic systems this is probably most important in sediments and may be the major pathway for degradation of BaP that is deposited by sedimentation of microbes and other solids to which it is sorbed when it enters a water body and escapes photolytic or oxidative degradation. Additional discussion is given in Section 6.3.5.

# 7. LABORATORY INVESTIGATION OF QUINOLINE

## 7.1 SYNOPSIS

The laboratory data suggest that the major degradation pathway for quinoline in eutrophic systems is biodegradation. In oligotrophic systems, both biodegradation and photolysis may be important. In rivers, volatilization may be important during the winter; in other water bodies, volatilization is slow compared with biodegradation and photolysis. Oxidation and sorption by suspended sediments are not significant compared with biodegradation and photolysis.

The nine-compartment environmental exposure model predicted the following steady-state concentrations of quinoline in solution, suspended solids, and sediments near point sources in the presence of a continuous discharge of 1 μg $ml^{-1}$ (1 ppm) quinoline.

| | Half-life* (hr) | Solution (μg $ml^{-1}$) | Suspended solids (μg $g^{-1}$) | Sediments† (μg $g^{-1}$) |
|---|---|---|---|---|
| River | 0.28 | $9.6 \times 10^{-1}$ | 9.6 | 9.2 |
| Pond | 0.5 | $6.6 \times 10^{-3}$ | $6.6 \times 10^{-2}$ | $6.6 \times 10^{-2}$ |
| Eutrophic lake | 0.5 | $1.8 \times 10^{-2}$ | $1.8 \times 10^{-2}$ | $1.4 \times 10^{-4}$ |
| Oligotrophic lake | 600 | $1.7 \times 10^{-1}$ | 1.7 | $6.7 \times 10^{-1}$ |

## 7.2 BACKGROUND

Quinoline, isoquinoline, alkylated quinolines, and other derivatives of quinoline are present in coal and coal products (Hayatsu et al., 1975; Vymetal, 1974a,b; Clemo, 1973), in diesel fuel or other petroleum products (Ben'kovskii et al., 1974; Brodskii et al., 1975), in slightly decomposed sphagnum peats (Naucke et al., 1972), and as components of a whole class of alkaloids. They may be emitted to the atmosphere as a by-product of petroleum refining and coal mining, coking, and the like. Since heterocyclic compounds containing O, S, and N in the ring systems are particularly difficult to remove from the effluents from coal gasification and liquefaction plants (Hayatsu et al.,

---

[*] Predicted by one-compartment model.

[†] Average concentration in sediments.

1975), the environmental exposure to these compounds, including quinoline and its derivatives, may increase.

Doehler and Young (1960) reported the sorption of quinoline on a Na- and Ca-montmorillonite, illite, and kaolinite in water as a function of quinoline concentration, pH, salinity, time, and temperature. The general trend found for clays was that: reducing the pH increased the partition coefficient, temperature had a very small effect on sorption, and the sorption equilibrium was reached in less than 200 minutes and was not completely reversible. Although Doehler and Young did not use the Freundlich isotherm, their data for Ca-montmorillonite suggest that $n = 1$ at quinoline concentrations below about 50 $\mu g\ ml^{-1}$. The value of the partition coefficients calculated from their data for their Ca-montmorillonite at 25°C was 10.4 at pH 7.3 and 16.8 at pH 6.3. No data on sorption of quinoline by natural sediments were available in the literature.

Quinoline will not hydrolyze in environmental aquatic systems. No data were available to evaluate the importance of the chemical oxidation of quinoline in the environment. While it is known that quinoline absorbs strongly in the solar spectrum to about 350 nm, no data on the rates or products of photolysis were available for assessing its transformation in aquatic environments.

Several electron spin resonance studies on the photolysis of quinoline and its derivatives, using the full spectrum of the Hg lamp, have been reported. Castellano et al. (1975) detected the semiquinone radical derived from reaction of the photoexcited quinoline with methanol solvent. Kataoka et al. (1966) noted only that "Almost all the [quinoline] compounds were completely destroyed by UV irradiation." No products were isolated and identified in these studies, and it is not known how much of the photoreaction can be attributed to photolysis at wavelengths greater than 290 nm. Photolysis of pyridine at 256 nm in aqueous solution is reported to give an aminoaldehyde with a product quantum yield of 0.07 (Joussot-Dubien and Houdard, 1967).

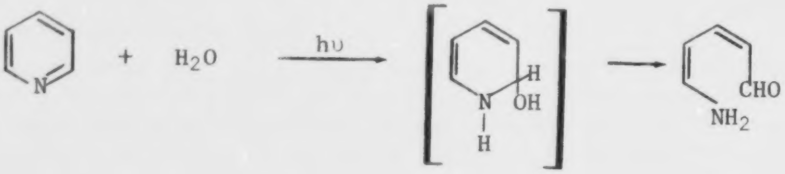

It is not known whether quinoline reacts in a similar manner.

There is no information on the biodegradability of quinoline in aqueous systems. Robbins (1916, 1917) and Funchess (1917) reported on the degradability of quinoline in soils. More recently, Robbins (1971) reported using enrichment procedures to isolate organisms that would degrade 2-hydroxyquinoline. In this preliminary study, Robbins obtained an organism that would grow on 2-hydroxyquinoline, quinoline, glucose, or yeast extract as the only carbon sources, but would not grow on coumarin, 2-methylquinoline, acridine, naphthalene, naphthols, phenol, salicylate, anthranilate, o-aminophenol, or pyridine. Respirometry studies, although reportedly poorly reproducible, indicated some oxygen consumption with quinoline, 2-hydroxyquinoline, and coumarin.

The physical properties of quinoline are summarized in Table 7.1.

TABLE 7.1. PHYSICAL PROPERTIES OF QUINOLINE

| | |
|---|---|
| Structure | 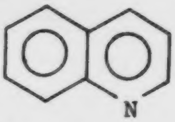 |
| Molecular weight<br>(CRC Handbook, 1974) | 129.15 |
| Melting point (°C)<br>(CRC Handbook, 1974) | -15.6 |
| Boiling point (°C)<br>(CRC Handbook, 1974) | 238.05 |
| Vapor pressure[a] at 25°C (torr) | $9.1 \times 10^{-3}$ |
| Solubility in water at 25°C<br>(mg $ml^{-1}$)<br>(Albersmeyer, 1958) | 6.11 |
| $pK_a$<br>(Perrin, 1965) | 4.8[b] |
| Ultraviolet spectrum in ethanol<br>[$\lambda_{max}$ (log $\varepsilon$)]<br>(CRC Handbook, 1974) | 275 (3.51)<br>299 (3.46)<br>312 (3.52) |
| 1 $\mu g\ ml^{-1}$ is equivalent to $7.72 \times 10^{-6}$ M | |

---

[a] Extrapolated from data between 180° and 240°C (Maczynski and Maczynska, 1965).

[b] Quinoline is 98%, 39%, and 0.6% protonated at pH 3, 5, and 7, respectively.

## 7.3 ENVIRONMENTAL ASSESSMENT

### 7.3.1 Summary of Laboratory Data

The rate constants obtained in the laboratory studies of the transformation and transport processes for quinoline are summarized in Table 7.2.

TABLE 7.2. SUMMARY OF QUINOLINE LABORATORY DATA

| Process | Sorption equilibrium | Partition coefficient[a] |
|---|---|---|
| Sorption | $S_s = K_p S_w$ | $K_p = 11$ |
| | Rate expression | Rate constant at 25°C |
| Volatilization[b] | $k_v[Q]$ | $k_v = (2.7 \pm 0.4) \times 10^{-3}\ k_v^0$ |
| Photolysis[c] | $k_p[Q] = \Phi(\Sigma Z_\lambda \varepsilon_\lambda)[Q]$ | $k_p = 7.8 \times 10^{-7}\ \text{sec}^{-1}$ |
| Oxidation | $k_{ox}[RO_2\cdot]\ [Q]$ | $k_{ox} = 2.8\ M^{-1}\ \text{sec}^{-1}$ |
| Hydrolysis | NA | $k_h = 0$ |
| Biodegradation | $k_{b2} = \frac{\mu_{max}}{Y\ K_s}$ | $k_{b2} = 3.1 \times 10^{-6}\ \text{ml cell}^{-1}\ \text{hr}^{-1}$ |

[a] On Coyote Creek sediment having an organic content of 1.9%.

[b] See discussion in Part I, Section 5.3 of the final report.

[c] Assumes 12 hours of sunlight per day in late June.

### 7.3.2 Environmental Assessment Using the One-Compartment Model

The half-lives of dissolved quinoline calculated for individual transformation or removal processes following a spill are listed in Table 7.3. The half-lives in eutrophic and oligotrophic waters differ by roughly a factor of 1000, but among the three eutrophic systems half-lives differ by only a factor of 2. Biodegradation is the dominant pathway in the eutrophic waters, and the much slower photolytic pathway dominates in oligotrophic waters. Sorption is relatively unimportant, and oxidation, volatilization, and hydrolysis are unimportant in all water bodies.

TABLE 7.3. TRANSFORMATION AND TRANSPORT OF QUINOLINE PREDICTED BY THE ONE-COMPARTMENT MODEL

| Process | Stream | Eutrophic pond | Eutrophic lake | Oligotrophic lake |
|---|---|---|---|---|
| Photolysis, half-life (hr) | 1,200 | 3,000 | 3,000 | 600 |
| Oxidation, half-life[a] (hr) | $>10^4$ | $>10^4$ | $>10^4$ | $>10^4$ |
| Volatilization, half-life (hr) | $7.0 \times 10^3$ | $3.5 \times 10^4$ | $2.8 \times 10^4$ | $2.8 \times 10^4$ |
| Hydrolysis, half-life (hr) | NA | NA | NA | NA |
| Biodegradation, half-life (hr) | 0.5 | 0.5 | 0.5 | 10,000 |
| Half-life for all processes, except dilution (hr) | 0.5 | 0.5 | 0.5 | 600 |
| Half-life for all processes, including dilution (hr) | 0.28 | 0.5 | 0.5 | 600 |
| Amount quinoline sorbed[b] (mg $m^{-3}$) | 1 | 3 | 0.5 | 0.5 |
| Percentage quinoline sorbed | 0.1% | 0.3% | 0.05% | 0.05% |

[a] Based on peroxy radical concentration of $10^{-9}$ M.

[b] 1 μg $ml^{-1}$ is assumed in the solution phase.

### 7.3.3 Persistence

The persistence of quinoline following an acute discharge should be virtually independent of dilution because the biotransformation rate of quinoline is very fast. Even in the river simulation, which assumes a relatively rapidly flowing stream, the apparent half-life at a given location is only halved by the effects of dilution (Table 7.3). In the oligotrophic lake, where biodegradation is expected to be relatively slow, the half-life is 25 days.

### 7.3.4 Mass Concentration Distributions Calculated Using Computer Models

The pseudo-first-order rate constants used in these simulations are presented in Appendix A. The distributions of mass and concentration of quinoline expected at steady state during chronic discharge to each of four types of water bodies are given in Table 7.4. The changes in concentration as discharge begins and ends are shown in Figures 7.1 through 7.4.

The concentrations at steady state varied 100-fold between the water bodies, as indicated by concentrations near the sources. Concentrations varied 10,000-fold among compartments within the eutrophic lake simulation but varied only 10-fold or less within the simulation in the oligotrophic lake, where transformation is slow, and in the river, where dilution is rapid (Table 7.4).

The approaches to steady-state concentrations were rapid in all water bodies following start of the simulated discharge, as generally were the transitions to new steady states after discharge stopped (Figures 7.1 through 7.4). The oligotrophic lake was an exception to the general pattern of rapid decline, rising rapidly to concentrations approximating steady-state concentrations during discharge, but declining very slowly when discharge stopped. Concentrations of quinoline on sediments declined slowly in all simulations because of the long half-life for scouring of the sediments. Concentrations on suspended solids paralleled concentrations in solution.

Despite the higher concentrations of quinoline on suspended solids than in solution, virtually all the quinoline remained in solution because of the much larger mass of water than suspended solids assumed in all the simulations (see Part I of the final report). This pattern might be reversed in actual water bodies if sediments are contaminated to depths greater than those assumed in these simulations, but a substantial fraction of the quinoline present in any water body can nonetheless be expected to be in the water column and most of that fraction will be in solution.

These patterns were not changed in a sensitivity test by reducing the concentration of quinoline in the inflow to 10 $\mu$g ml$^{-1}$ and 10 $\mu$g ml$^{-1}$. Furthermore, since the steady-state concentrations in the pond simulation, which are 7 x 10$^{-3}$ $\mu$g ml$^{-1}$ and 7 x 10$^{-5}$ $\mu$g ml$^{-1}$ for the 1 $\mu$g ml$^{-1}$ and 10 $\mu$g ml$^{-1}$ inflows, respectively, are much less than the value of $K_s$ measured in the laboratory (0.16 $\mu$g ml$^{-1}$), the biodegradation kinetics can consistently be expressed as:

$$R_b = \frac{\mu_{max}[S][X]}{Y\ K_s} \qquad K_s \gg [S] \tag{7.1}$$

$$= k_{b2}[S][X]$$

### 7.3.5 Discussion

Quinoline appears to be toxic to aquatic organisms at concentrations above 1 $\mu$g ml$^{-1}$. For vertebrates LD$_{50}$s range from 5 to 50 $\mu$g ml$^{-1}$, and for phyto- and zoo-plankton from 50 to 140 $\mu$g ml$^{-1}$. Mammals appear to be more resistant, with LD$_{50}$s of 460 or more for oral and dermal exposures (Merck, 1960; Christensen and Lyginbyhl, 1975; McKee and Wolf, 1963). Consequently, toxic concentrations are unlikely to be widespread even if concentrations in discharges are as high as 1 $\mu$g ml$^{-1}$.

TABLE 7.4. DISTRIBUTION OF QUINOLINE IN VARIOUS AQUATIC SYSTEMS AT STEADY STATE (input concentrations at 1 μg $ml^{-1}$ quinoline)

| | Pond | | River | | Eutrophic Lake | | Oligotrophic Lake | |
|---|---|---|---|---|---|---|---|---|
| | Mass (kg) | Conc. (μg $g^{-1}$) | Mass (kg) | Conc. (μg $g^{-1}$) | Mass (kg) | Conc. (μg $g^{-1}$) | Mass (kg) | Conc. (μg $g^{-1}$) |
| Compartment 1 (surface water) | | | | | | | | |
| Solution | $1.3 \times 10^{-1}$ | $6.6 \times 10^{-3}$ | $2.9 \times 10^{2}$ | $9.6 \times 10^{-1}$ | 4.5 | $1.8 \times 10^{-2}$ | $4.2 \times 10$ | $1.7 \times 10^{-1}$ |
| Suspended solids | $3.9 \times 10^{-1}$ | $6.6 \times 10^{-2}$ | $2.9 \times 10^{-1}$ | 9.6 | $2.2 \times 10^{-3}$ | $1.8 \times 10^{-1}$ | $2.1 \times 10^{-2}$ | 1.7 |
| Compartment 2 (surface water) | | | | | | | | |
| Solution | -- | -- | $2.8 \times 10^{2}$ | $9.2 \times 10^{-1}$ | 1.1 | $4.3 \times 10^{-4}$ | $2.4 \times 10^{2}$ | $9.7 \times 10^{-2}$ |
| Suspended solids | -- | -- | $2.8 \times 10^{-1}$ | 9.2 | $5.4 \times 10^{-4}$ | $4.3 \times 10^{-3}$ | $1.2 \times 10^{-1}$ | $9.7 \times 10^{-1}$ |
| Compartment 3 (surface water) | | | | | | | | |
| Solution | -- | -- | $2.7 \times 10^{2}$ | $8.8 \times 10^{-1}$ | $2.1 \times 10^{-2}$ | $8.6 \times 10^{-4}$ | $2.0 \times 10$ | $8.0 \times 10^{-2}$ |
| Suspended solids | -- | -- | $2.7 \times 10^{-1}$ | 8.8 | $1.1 \times 10^{-1}$ | $8.6 \times 10^{-3}$ | $1.0 \times 10^{-2}$ | $8.0 \times 10^{-1}$ |
| Compartment 5 (surface water) | | | | | | | | |
| Solution | -- | -- | -- | -- | $4.9 \times 10^{-3}$ | $2.0 \times 10^{-6}$ | $2.7 \times 10$ | $1.1 \times 10^{-2}$ |
| Suspended solids | -- | -- | -- | -- | $2.5 \times 10^{-6}$ | $2.0 \times 10^{-5}$ | $1.4 \times 10^{-2}$ | $1.1 \times 10^{-1}$ |
| Compartments 7-9 (Sediment)[a] | | | | | | | | |
| Solution | $1.7 \times 10^{-3}$ | $6.6 \times 10^{-3}$ | $6.9 \times 10^{-1}$ | $9.2 \times 10^{-1}$ | $1.2 \times 10^{-5}$ | $1.4 \times 10^{-5}$ | $5.8 \times 10^{-1}$ | $6.7 \times 10^{-2}$ |
| Solids | $4.5 \times 10^{-2}$ | $6.6 \times 10^{-2}$ | $1.9 \times 10^{2}$ | 9.2 | $6.3 \times 10^{-1}$ | $1.4 \times 10^{-4}$ | 9.0 | $6.7 \times 10^{-1}$ |

[a] The amounts given for solid and solution phases in the sediment compartments are estimated from the sorption partition coefficient for suspended solids and may be overestimated because it was assumed that biodegradation of sorbed material does not occur.

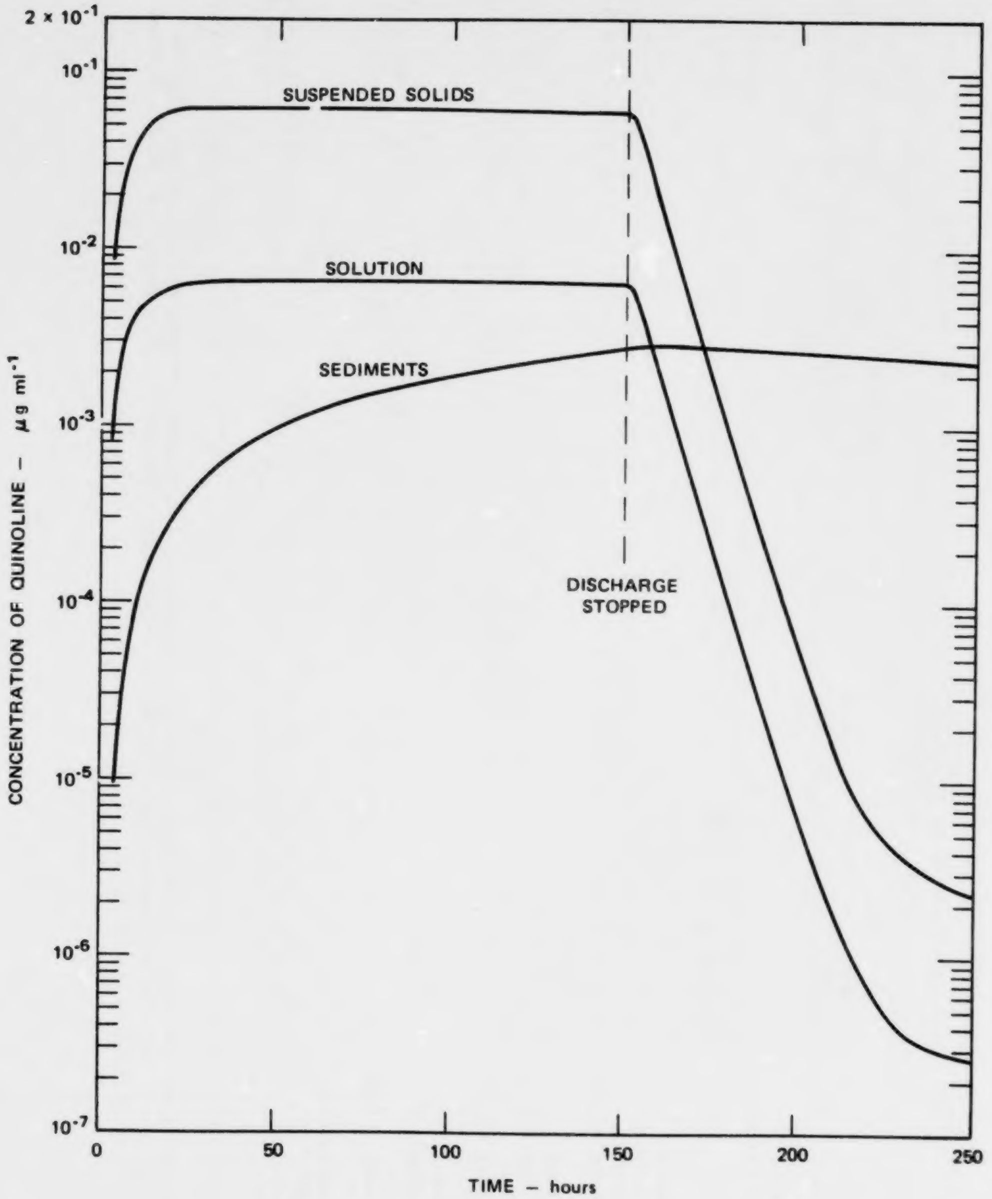

FIGURE 7.1 PERSISTENCE OF QUINOLINE IN A TWO-COMPARTMENT POND SYSTEM

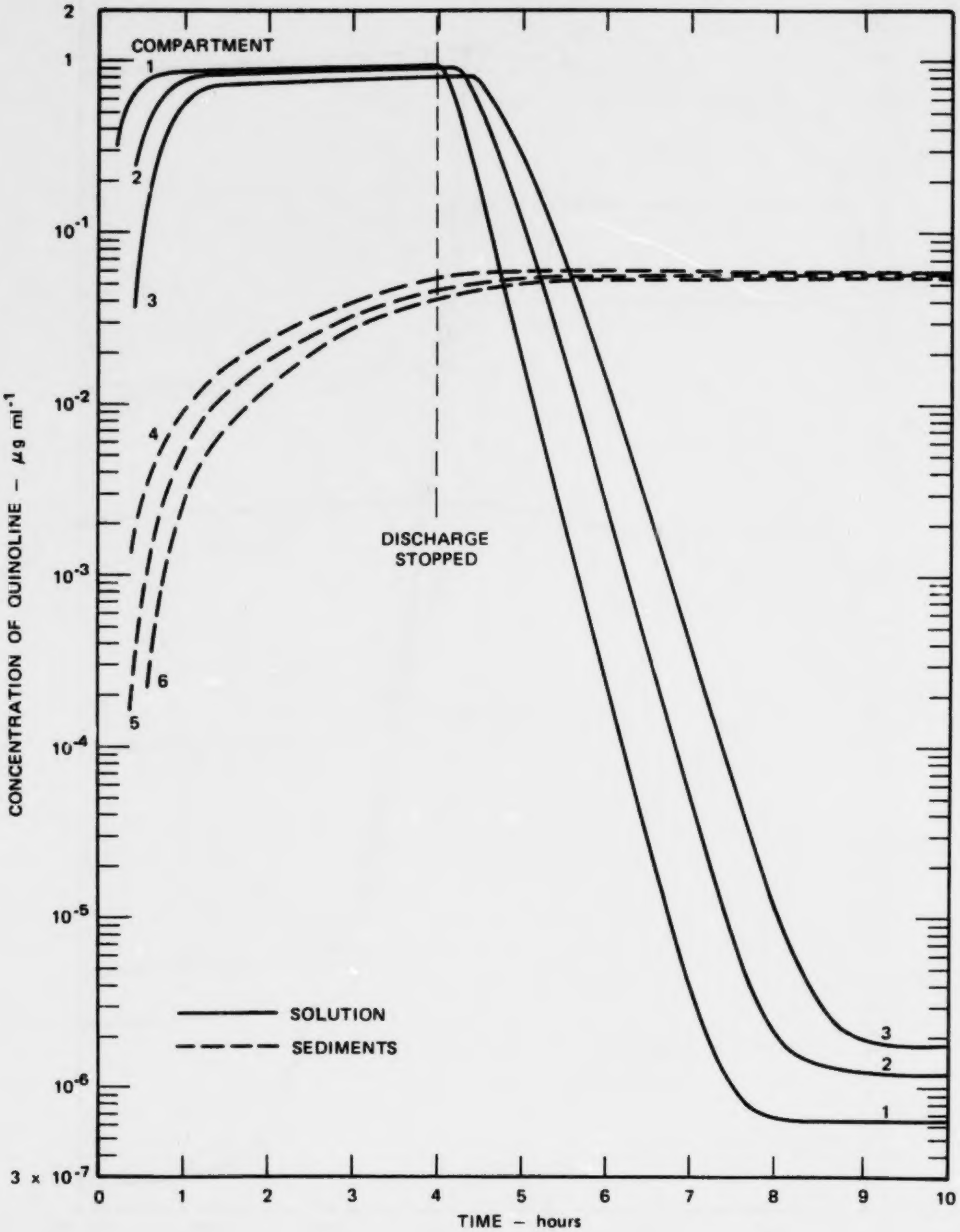

FIGURE 7.2 PERSISTENCE OF QUINOLINE IN A PARTIALLY MIXED RIVER SYSTEM

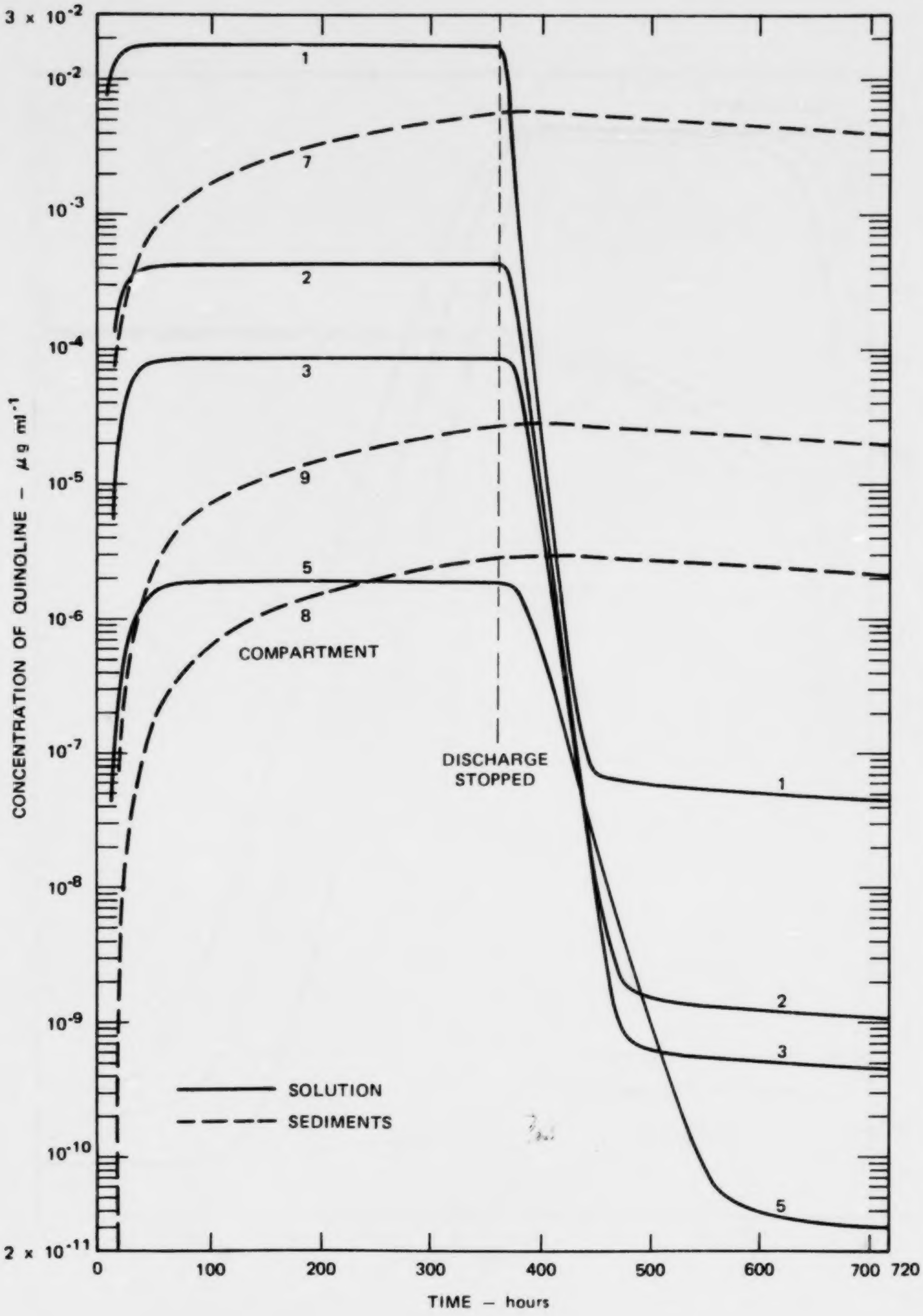

FIGURE 7.3 PERSISTENCE OF QUINOLINE IN A PARTIALLY MIXED EUTROPHIC LAKE

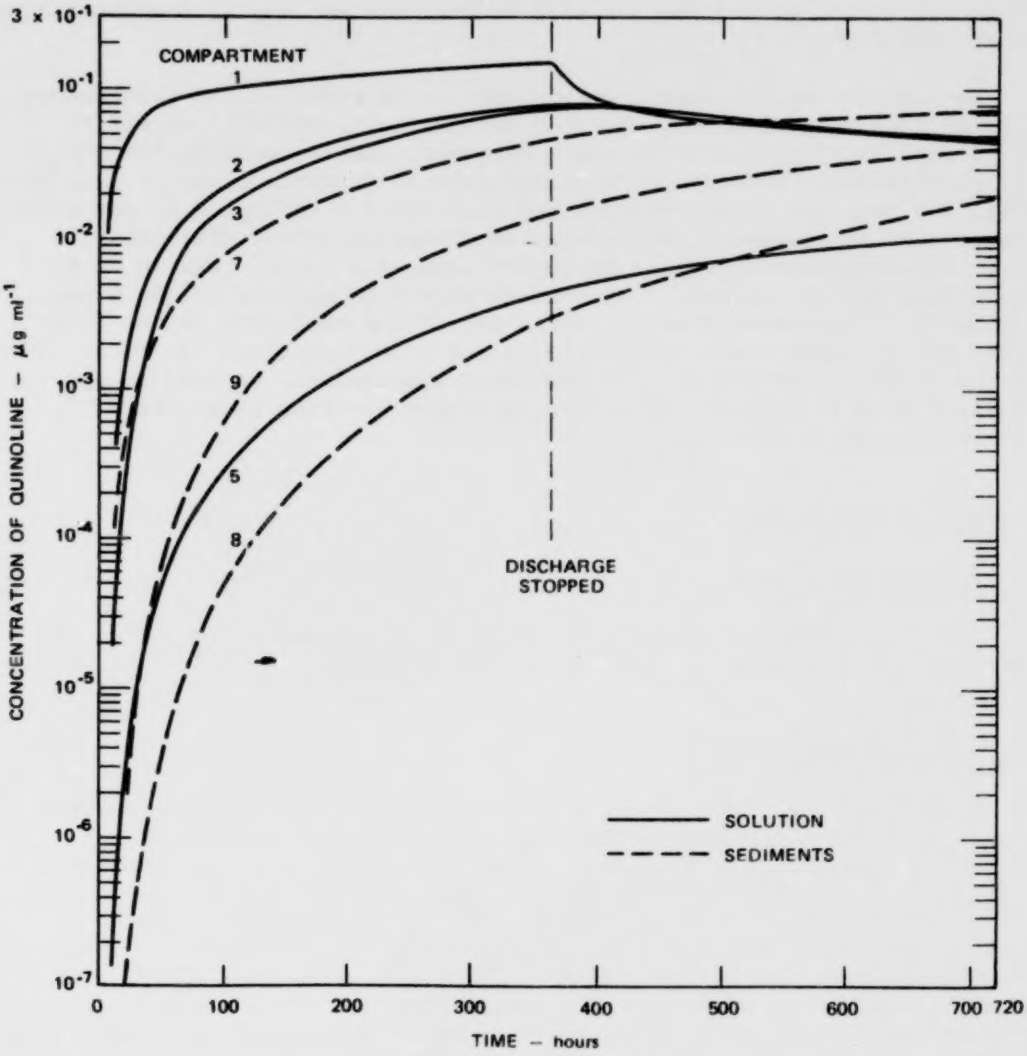

FIGURE 7.4 PERSISTENCE OF QUINOLINE IN A PARTIALLY MIXED OLIGOTROPHIC LAKE

Degradation in all but the most oligotrophic waters will probably be dominated by biodegradation; however, the effective bacteria populations assumed in the oligotrophic lake simulations are very low, and merely doubling or tripling bacterial population in the oligotrophic lake simulation would put biodegradation and photolysis on an equal level. Moreover, since cometabolism is omitted from all the simulations, our predictions of biodegradation rates may be much too low. If so, biodegradation should be expected to be dominant in all natural waters except in the coldest months.

During winter months in the Northeast, the Midwest, and the mountain states, volatilization and photolysis rates may exceed biodegradation. Indeed, it is probably that volatilization will be dominant as long as the water surfaces are ice-free.

In summary, we can expect degradation to be rapid in all freshwaters, with half-lives ranging from 5 hours or less in warm eutrophic waters to about 25 days in oligotrophic waters. Moreover, unless cometabolism occurs and is significantly affected by concentration at concentrations of 1 $\mu g\ ml^{-1}$ or less, the patterns of degradation and distribution estimated by our simulations should be generally applicable, as indicated by the similarity of results of simulations using the concentrations of 1 $\mu g\ ml^{-1}$ and 10 $ng\ ml^{-1}$ for quinoline in the inflows. Degradation should be slowest in the winter, particularly in ice-covered waters where the 25-day half-life may be greatly exceeded due to suppression of photolysis and volatilization. At worst, under thick ice cover, quinoline may not degrade. Nonetheless, as long as the concentrations of quinoline in the inflowing waters are less than 1 $\mu g\ ml^{-1}$, the hazard should be low.

## 7.4 PHYSICAL PROPERTIES

### 7.4.1 Solubility in Water

The solubility of quinoline in water at room temperature (25°C) is reported in the literature as 6.11 $mg\ ml^{-1}$ (Albersmeyer, 1958).

### 7.4.2 Absorption Spectrum

A small sample of quinoline was purified by preparative gas chromatography. A portion of this purified material was used to prepare a $1.5 \times 10^{-4}$ M solution of quinoline in distilled deionized water. The pH of this solution was adjusted to pH 4.7 and 6.8 with dilute HCl or NaOH, and the UV absorption spectra were measured. The absorption coefficients at wavelength intervals from 297.5 to 370 nm are reported in Table 7.5. The $pK_a$ of quinoline is 4.8 (Perrin, 1965). Therefore, quinoline is 98%, 39%, and 0.6% protonated at pH 3, 5, and 7, respectively. The increase in the absorption coefficient with the decrease in pH is undoubtedly a result of the increase in the fraction of protonated quinoline.

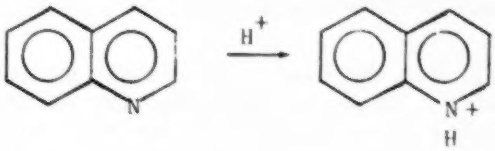

### 7.4.3 Volatilization Rate

The volatilization rate of quinoline from water was measured using the method of Hill et al. (1976), which is described in detail in Part I, Section 5.3.3 of this report.

## TABLE 7.5. ABSORPTION SPECTRA OF QUINOLINE IN WATER[a] at pH 4.7 and pH 6.8

| Center of wavelength interval[b] (nm) | Average absorption coefficient[c] ($M^{-1}$ $cm^{-1}$) | |
|---|---|---|
| | pH 4.7 | pH 6.8 |
| 297.5 | 4320 | 2910 |
| 300.0 | 4660 | 3050 |
| 302.5 | 4850 | 2740 |
| 305.0 | 5070 | 2480 |
| 307.5 | 4980 | 2050 |
| 310.0 | 5220 | 2440 |
| 312.5 | 5720 | 2920 |
| 315.0 | 4880 | 1680 |
| 317.5 | 3820 | 622 |
| 320.0 | 2920 | 269 |
| 323.1 | 2270 | 119 |
| 330.0 | 1370 | 26 |
| 340.0 | 529 | 9 |
| 350.0 | 143 | 0 |
| 360.0 | 9.3 | 0 |
| 370.0 | 0 | 0 |

[a] Quinoline concentration 1.61 x $10^{-4}$ mole $liter^{-1}$.

[b] The wavelength intervals are given in Appendix B, Table B.1.

[c] The absorption coefficients at 313.0 and 366.0 nm are 5690 and 0 at pH 4.7.

The volatilization half-life of quinoline in aqueous solution was about 69 hours at a moderate stirring rate. The rate constants were calculated as follows:

| | | |
|---|---|---|
| Oxygen reaeration rate constant: | $k_v^O$ | $= 4.01 \pm 0.22\ \text{hr}^{-1}$ |
| Quinoline volatilization rate constant: | $k_v^Q$ | $= 0.011 \pm 0.001\ \text{hr}^{-1}$ |
| Ratio: | $k_v^Q/k_v^O$ | $= 0.0027 \pm 0.0004$ |

Additional measurements were not made because biodegradation was found, in separate experiments, to be so rapid (see Section 7.6.2).

### 7.4.4 Sorption on Clay and Sediments

Sorption isotherms were measured on Ca-montmorillonite clay and Coyote Creek sediment. Each experiment consisted of duplicate samples at two quinoline concentrations and two sediment loadings, in addition to blanks containing quinoline only and sediment only. All samples were adjusted to pH 6.0 ± 0.2 with dilute HCl. The data, summarized in Table 7.6, were fitted to a Freundlich isotherm where $n = 1$ and in which either the regression line was forced through the origin ($\alpha = 0$) or a non-zero intercept was calculated.

Calculation of the partition coefficients was based on analysis of the supernatant at equilibrium, and the initial amount present, as determined by analysis of samples containing no sediment. The estimated values of $K_p$ reported in Table 7.6 indicate that sediment sorption is not an important pathway for the disappearance of quinoline; thus, no further sorption studies were conducted.

### 7.4.5 Biosorption

Since biodegradation of quinoline was so rapid and sediment sorption so weak, no biosorption studies were conducted.

## 7.5 CHEMICAL TRANSFORMATION

### 7.5.1 Photolysis Rate

Data for the photolysis of quinoline in pure water and in water containing 9.5 $\mu g\ ml^{-1}$ humic acid are given in Table 7.7. The photolyses at 313 nm were carried out to 50% to 70% conversion of quinoline with good first-order kinetic behavior found. The rate constant for direct photolysis of quinoline at pH 6.9 was unaffected by the presence of oxygen. From the rate constant $k_p$ measured for the direct photolysis, the quantum yield for quinoline conversion was calculated as $3.3 \times 10^{-4}$.

## TABLE 7.6. QUINOLINE SORPTION ON SEDIMENTS

| Sediment | Total organic carbon (percent) | Sediment concentration (mg ml$^{-1}$) | Quinoline concentration in Supernatant (μg ml$^{-1}$)[a] | Quinoline concentration on Sediment (μg g$^{-1}$)[b] | Partition coefficients, $K_p$ LLS[c] $a_o = 0$ | Partition coefficients, $K_p$ LLS[c] $a_o \neq 0$ |
|---|---|---|---|---|---|---|
| Ca-montmorillonite clay | 0.06 | 39 | 4.3 ± 0.20 | 37 ± 5 | 7.3 ± 0.5 | 5.8 ± 15<br>(a = 11 ± 10) |
|  |  | 80 | 3.7 ± 0.10 | 26 ± 1 |  |  |
|  |  | 39 | 9.0 ± 0.40 | 62 ± 10 |  |  |
|  |  | 78 | 7.0 ± 0.60 | 57 ± 7 |  |  |
| Coyote Creek | 1.4 | 38 | 4.0 ± 0.2 | 44 ± 5 | 10.9 ± 0.4 | 9.7 ± 1.1<br>(a = 7.7 ± 6.1) |
|  |  | 77 | 2.9 ± 0.1 | 36 ± 2 |  |  |
|  |  | 38 | 8.5 ± 0.2 | 87 ± 5 |  |  |
|  |  | 77 | 6.2 ± 0.1 | 74 ± 2 |  |  |

---

[a] Concentration measured in supernatant with population standard deviation.

[b] Concentration on sediment calculated from supernatant concentration with population standard deviation.

[c] Calculated by linear least squares statistical treatment, as described in Appendix B, Section B.1.4. Limits are 95% confidence limit.

Since quinoline is a weak base ($pK_b = 9.2$) and will be mostly in the conjugate acid form at low pH, an experiment on the direct photolysis at pH 4.4 was carried out. At this pH, quinoline is 71% protonated; less than 1% is protonated at pH 6.9.

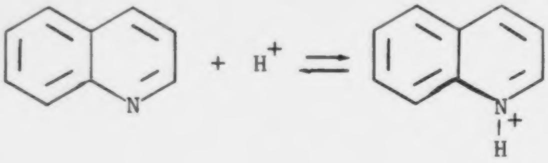

Figure 7.5 plots the log of quinoline concentration at pH 6.9 and pH 4.4 as a function of time. Although the pH 6.9 data show good first-order kinetic behavior, the pH 4.4 data indicate that the reaction is progressively inhibited as the photolysis proceeds. The pH 4.4 data are not correlated by any simple integral or half integral kinetic rate law for quinoline conversion. The reason for this behavior is not known. The effect of pH may be to produce two different mechanisms for photolysis. It is unlikely that the products from the reaction affect the photolysis at pH 4.4, since their concentrations are less than 1 $\mu g\ ml^{-1}$. The total absorbance of the solution is so low that it does not affect the total light intensity passing through the solution. Any product that acts as a triplet quencher could not compete with the oxygen (about $10^{-3}$ M) in the air-saturated solution. There is insufficient data for determining the processes that are taking place.

The data in Table 7.7 show that in the photolyses at 313 nm, the presence of humic acid reduced the photolysis rate of quinoline by 56%. The absorbance of the humic acid solution was 0.56 (compared with 0.01 calculated for 0.7 $\mu g\ ml^{-1}$ quinoline) so that the humic material absorbed about half of the incident light. The effect of humic acid in slowing the photolysis of quinoline can then be mostly accounted for by a screening effect. As discussed previously, the slower rate may also be due partially to the low pH of the solution (5.25); at this pH quinoline would be 20% in the protonated form. The photolyses in humic acid solutions, however, showed no deviation from first-order kinetics for disappearance for quinoline.

Evidence for the absence of any photoinitiated radical reaction or photosensitized processes involving humic acid was provided by the photolysis at 366 nm. At this wavelength, quinoline has no absorption, whereas humic acid absorbs appreciably. Correcting for the difference in light intensity and the humic acid absorbance at 313 nm versus 366 nm, we calculated from the experiments at 366 nm that any sensitized photolysis with 9.5 $\mu g\ ml^{-1}$ humic acid must have a rate constant less than 10 times that of the direct photolysis. This calculation assumed that the quantum efficiency for any humic acid sensitized photolysis was independent of wavelength.

The half-life for direct photolysis of quinoline in sunlight was calculated according to the procedure of Zepp and Cline (1977) using the quantum yield of $3.3 \times 10^{-4}$ and the absorption spectrum (Section 7.4.2). As shown in Figure 7.6, the half-life for direct photolysis of quinoline will vary from 160 days in winter to about 23 days in summer. The latter value is in excellent agreement with the measured half-life of 21 days during June (Table 7.7).

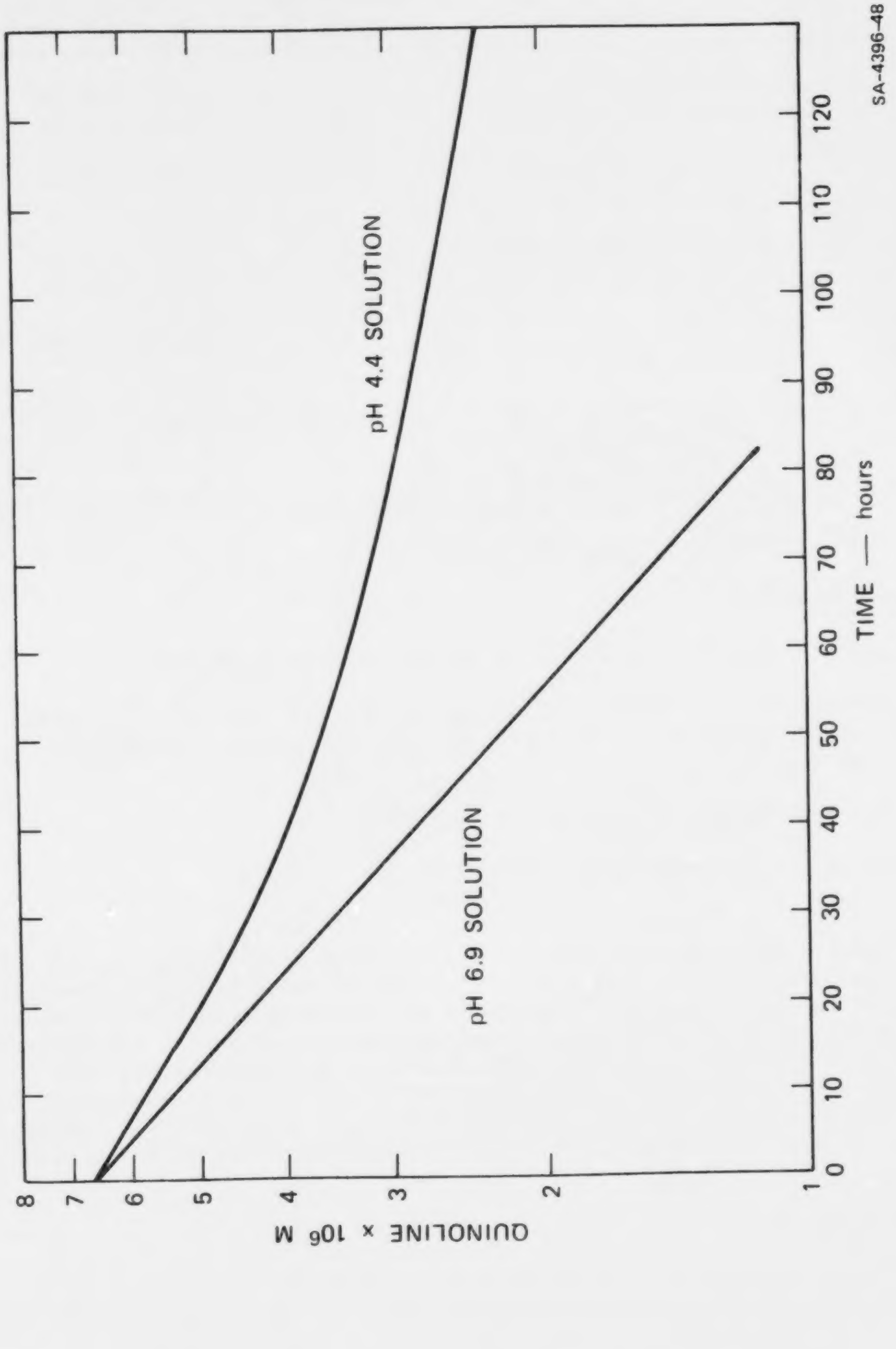

FIGURE 7.5 DIRECT PHOTOLYSIS OF QUINOLINE AT pH 6.9 AND pH 4.4

TABLE 7.7. RATE CONSTANTS FOR PHOTOLYSIS OF QUINOLINE

| Irradiation source | Solution | Quinoline concentration[a] (μg $ml^{-1}$) | Rate constant ($k_p \times 10^6$ $sec^{-1}$) |
|---|---|---|---|
| 313 nm | Pure water, air saturated, pH 6.9 | 0.82<br>0.69 | 6.07 ± 0.00[b]<br>5.85 ± 0.14 |
| 313 nm | Pure water, nitrogen sparged, pH 6.9 | 0.69 | 5.71 ± 0.36 |
| 313 nm | 9.5 μg $ml^{-1}$ humic acid in pure water,[c] pH 5.4 | 0.67<br>0.68 | 2.60 ± 0.18<br>2.52 ± 0.21 |
| Sunlight, late June | Pure water, air saturated, pH 6.9 | 0.82 | 0.770 ± 0.060[d,e] |
| Sunlight, late June | 9.5 μg $ml^{-1}$ humic acid in pure water, pH 5.4 | 0.67 | 3.04 ± 0.10[d,f] |

[a] 1.00 μg $ml^{-1}$ quinoline in water = $7.74 \times 10^{-6}$ M.

[b] Standard deviation.

[c] Absorbance of humic acid solution at 313 nm is 0.56 (1-cm cells).

[d] Calculated assuming 12 hours of sunlight per day in late June; to obtain average rate constant for a fall calendar day (24 hours), divide rate constant by two.

[e] Half-life of 21 calendar days.

[f] Half-life of 5.3 calendar days.

The data of Table 7.7 for the solar photolysis of quinoline in the 9.5 μg $ml^{-1}$ humic acid solution indicate a half-life of about 5.3 days, about four times faster than for the direct photolysis of quinoline at the same time of year. This result is contrary to what was expected based on the laboratory photolyses at 313 and 366 nm, which indicated that humic acid acted only as a light screen and gave no evidence of a photoinitiated or photosensitized reaction. We have no explanation for the difference in results for the laboratory and the field experiments; the problem deserves further investigation.

### 7.5.2 Oxidation Rate

The susceptibility of 0.83 μg $ml^{-1}$ ($6.4 \times 10^{-6}$ M) quinoline to free radical oxidation was examined using the AA-initiated oxidation reaction. See

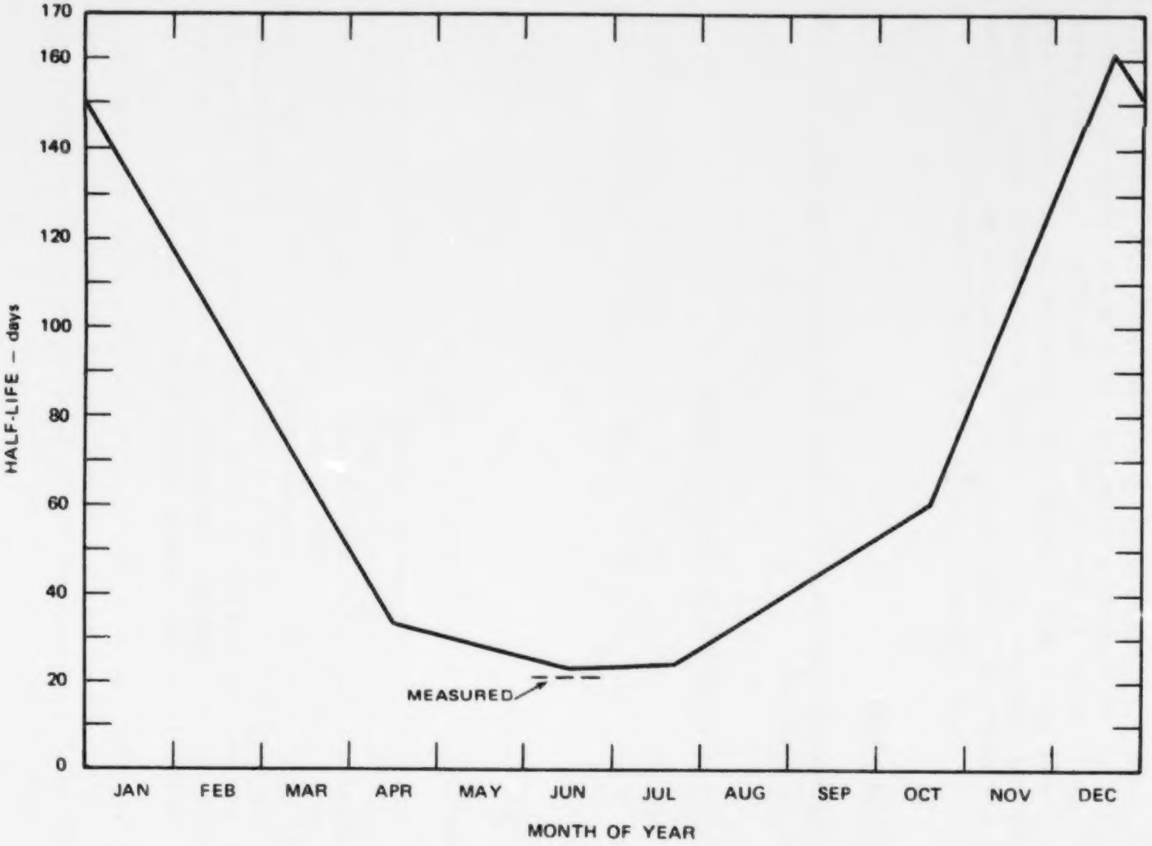

FIGURE 7.6 ANNUAL VARIATION OF PHOTOLYSIS HALF-LIFE OF QUINOLINE

Appendix B, Section B.2 for discussion and procedure. This experiment was carried out at 50°C in pure water containing $1.0 \times 10^{-4}$ M AA. At the end of 100 hours reaction time, only 3% of the quinoline had been consumed. A control solution without AA under identical reaction conditions showed no change (± 1% in the quinoline concentration.

A pseudo-first-order oxidation rate constant ($k_{ox}$ $[RO_2^{\cdot}]$) of $8.5 \times 10^{-8}$ $sec^{-1}$ was obtained for oxidation of quinoline under the reaction conditions. For the reaction at 50°C, this corresponds to a second-order rate constant $k_{ox}$ of 25 $M^{-1}$ $sec^{-1}$ (Part I, Section 5.4.2). At 25°C, $k_{ox}$ would then be 2.8 $M^{-1}$ $sec^{-1}$, and for a $RO_2^{\cdot}$ radical concentration in the aqueous environment of $10^{-9}$ M, the half-life of quinoline toward oxidation is about 8 years. The free radical oxidation of quinoline by $RO_2^{\cdot}$ is clearly not competitive with biodegradation or even photolysis under aquatic environmental conditions.

### 7.5.3 Hydrolysis Rate

Since quinoline contains no groups that are hydrolyzable, no hydrolysis studies were carried out.

### 7.5.4. Products from Chemical Transformation

Since screening studies determined that photolysis and oxidation were not competitive with biodegradation, detailed kinetic studies and product studies were not performed for quinoline.

## 7.6 BIODEGRADATION

### 7.6.1 Development of Biodegrading Cultures

Screening for quinoline-biodegrading cultures developed by an enrichment process was initiated with quinoline levels of 10 $\mu g$ $ml^{-1}$. The 9-liter aerated fermentors were used for water samples from Searsville Pond near Woodside, California; water from Coyote Creek in San Jose, California; aeration effluent from the Palo Alto, California, sewage plant; and water from Lake Tahoe. Fernbach flasks with 1.5 liters of 4:5 diluted aeration effluents were used with samples of aeration effluents from the South San Francisco and Shell Oil Refinery (Martinez, California) wastewater treatment plants. The Fernbach flasks were placed in a Psycrotherm Shaker with rotary action.

All incubations were at 25°C except the Lake Tahoe samples, which were incubated at 15°C. Progress in the development of quinoline biodegradation was monitored by GC analyses and by UV absorptions of ethyl acetate extracts at 308, 312, and 320 nm.

Quinoline biodegrading systems were obtained from all waters. The general pattern of quinoline disappearance was similar to the adaptation period indicated in Figure 7.7, which also includes cascade series breakdowns of quinoline. Degradation, once initiated, was rapid. Greater than 95% break-

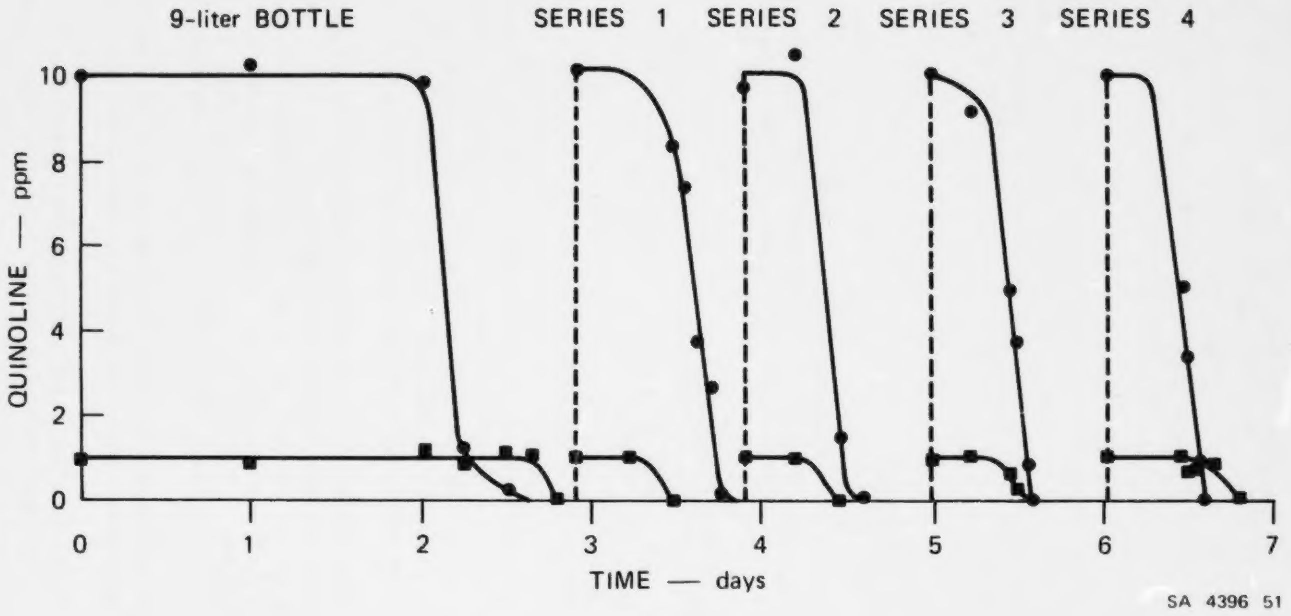

FIGURE 7.7 CASCADE BATCH FERMENTATIONS WITH A FRESHLY DEVELOPED DEGRADING SYSTEM TRANSFERRED IN FRESH POND WATER MEDIA

down of quinoline occurred with samples from Coyote Creek, Palo Alto Sewage Plant aeration effluent, Searsville Pond and Lake Tahoe in 48 hours, 40 hours, 60 hours, and 11 days, respectively. It is of interest that with the adaptation in Lake Tahoe water, the time for greater than 95% breakdown of 10 µg ml$^{-1}$ quinoline after start of degradation was 8 hours. The samples of aeration effluent waters from the South San Francisco and Shell Oil Refinery treatment plants contained substances that interfered with UV monitoring for quinoline and, arbitrarily, at 48 hours, a 2% transfer was made to flasks containing basal salts/10 µg ml$^{-1}$ quinoline medium. Degradation of quinoline in these flasks was observed in 24 hours.

In subtransferring from the original water sample mixtures in 9-liter bottles to 50 ml of basal salts media in 250-ml Erlenmeyer flasks, no problems were encountered in using quinoline as the only carbon source or in stepping up quinoline to 30 and 100 µg ml$^{-1}$ levels. A pink color developed in some of the degrading systems.

### 7.6.2 Biodegradation Kinetics

Two types of kinetic studies were conducted: batch fermentations with low-level inocula and cascade batch fermentations with a freshly developed degrading system serially transferred in fresh pond water media.

*Batch Fermentations with Low-Level Inocula*--Figures 7.8 and 7.9 present data from batch fermentations with low-level inocula of quinoline decomposing organisms developed from a eutrophic pond. Figure 7.8 plots viable cell counts in flasks with initial quinoline levels of 0, 1, 3, 5, and 10 µg ml$^{-1}$ respectively. The increase in counts in the control flask with no quinoline is attributable to the growth of some organisms or secretion products of other viable cells and/or autolysis products of dead cells. It is also possible that trace quantities of metabolizable organic compounds were introduced into the media by the distilled water or air during shaker flask agitation (Kayser, 1975). Because quinoline is so readily metabolized, increases in cell counts in flasks with quinoline are most likely due to good survival and growth of quinoline utilizers (primary and secondary).

The specific growth rate ($\mu$) in each medium was determined by measuring the slope of the curves in the logarithmic phase of growth. For the media initially containing 1, 3, 5, and 10 µg ml$^{-1}$ quinoline, $\mu$ values were 0.65, 0.69, 0.73, and 0.73 hr$^{-1}$, respectively. Comparing counts and residual quinoline data in Figures 7.8 and 7.9, it is apparent that significant increases in cell counts occurred after quinoline was essentially all degraded.

Figure 7.10 is a Lineweaver-Burk plot developed by the least squares method. $K_s$ and $\mu_m$ were calculated as 0.16 ppm and 0.74 hour$^{-1}$, respectively.

Table 7.8 presents the data and calculated values for Y and $k_b$ obtained in one low-inoculum batch fermentation study with one biodegrading system. The average yield (Y) was 1.9(±1.0) x 10$^{6}$ cells µg quinoline$^{-1}$ and the first-order rate constant in X is 4.9(±2.5) x 10$^{-7}$ µg quinoline cell$^{-1}$ hr$^{-1}$. The second-order rate constant $k_{b2}$, first order in X and S, is $k_b/K_s = 3.1 \times 10^{-6}$ ml cell$^{-1}$ hr$^{-1}$.

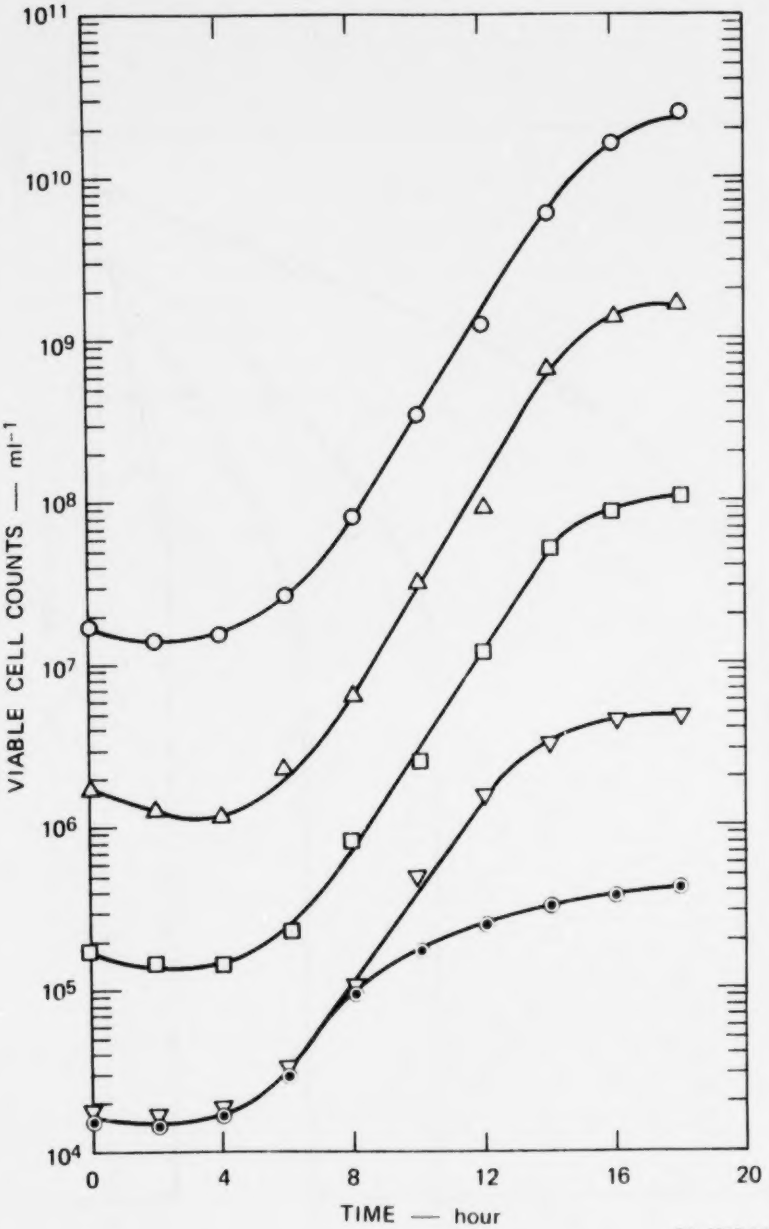

SA-4396-52

**FIGURE 7.8** VIABLE COUNTS IN QUINOLINE DEGRADATION BY BATCH FERMENTATIONS WITH LOW-LEVEL INOCULA

Counts for initial concentrations: 0 (◉); 1 $\mu$g ml$^{-1}$ (▽); $10\chi$ counts for 3 $\mu$g ml$^{-1}$ (□); $10^2\chi$ counts for 5 $\mu$g ml$^{-1}$ (△); $10^3\chi$ counts for 10 $\mu$g ml$^{-1}$ quinoline (○).

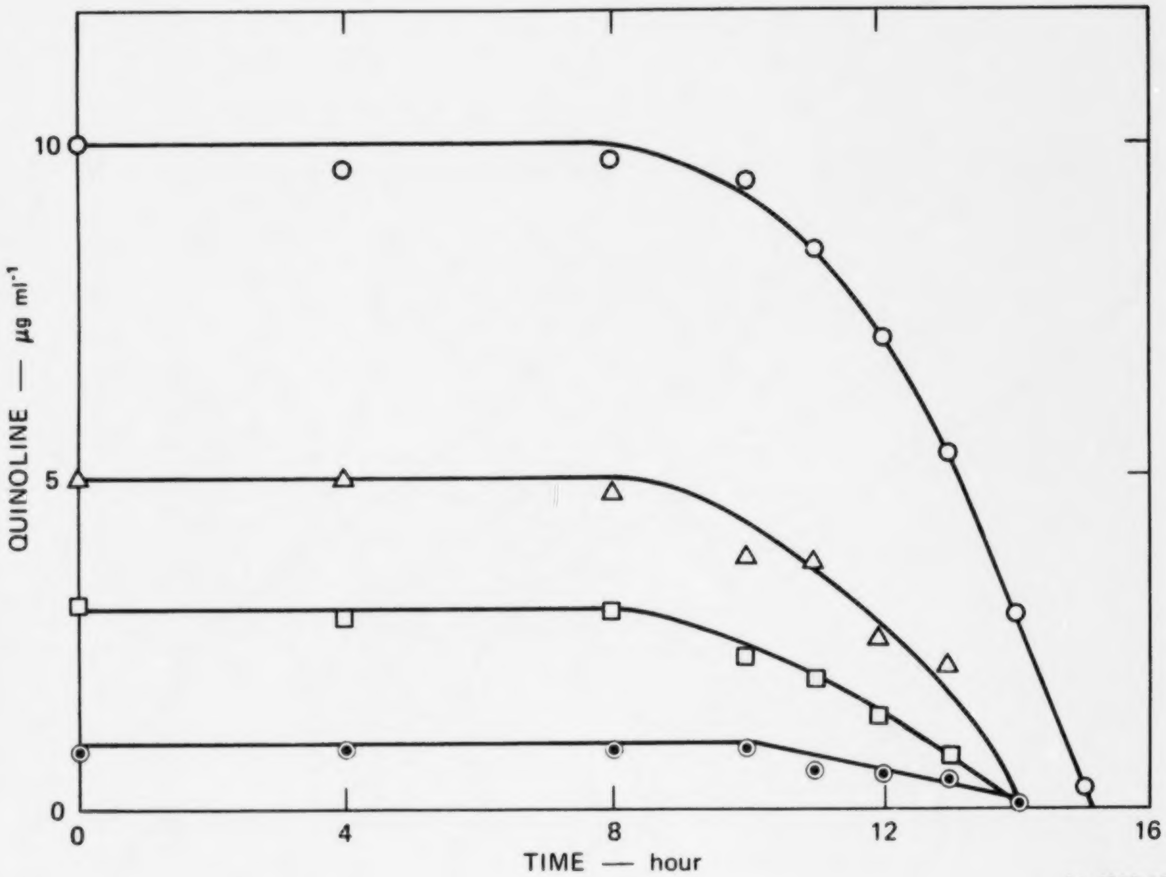

SA-4396-53

FIGURE 7.9 QUINOLINE BIODEGRADATION BY BATCH FERMENTATIONS WITH LOW-LEVEL INOCULA

Initial quinoline concentrations = 1 (◉), 3 (□), 5 (△) and 10 (○) $\mu$g ml$^{-1}$

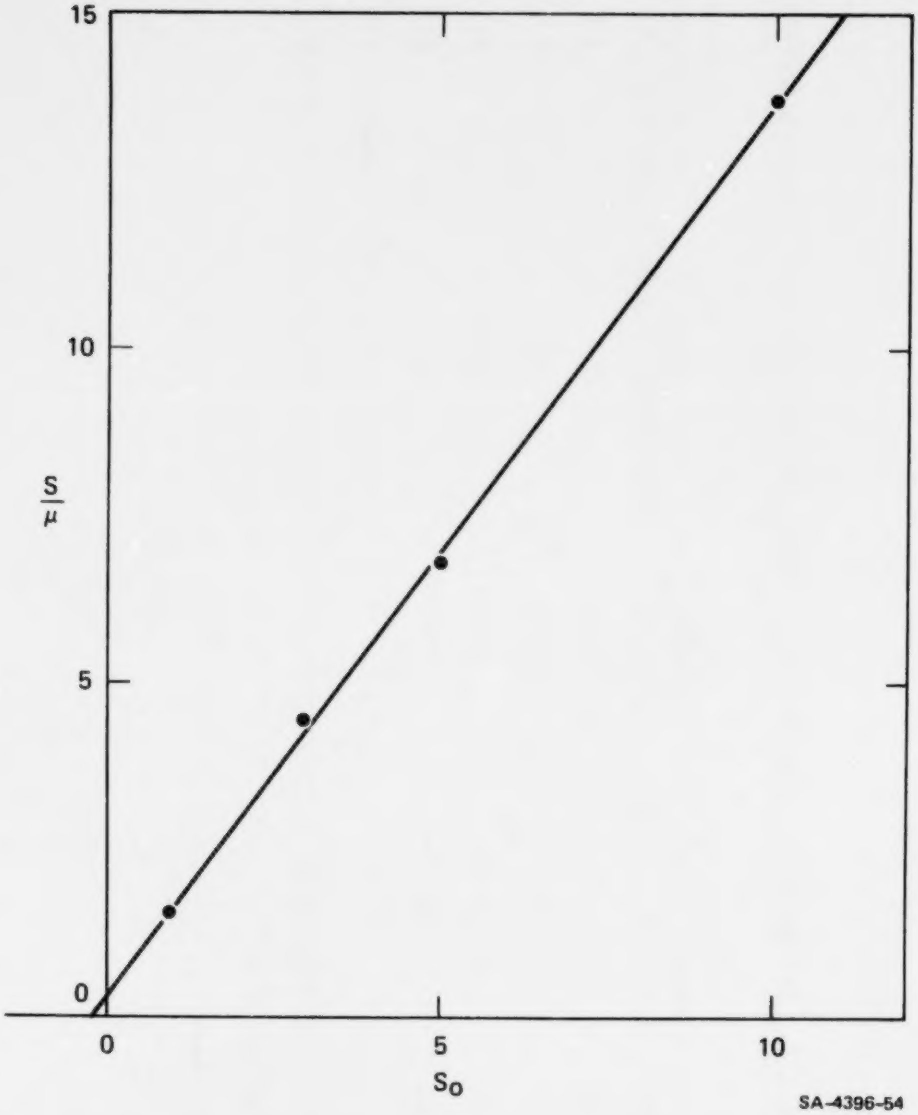

FIGURE 7.10 LINEWEAVER-BURK PLOT FOR DATA FROM QUINOLINE BIODEGRADATION IN BATCH FERMENTATIONS WITH LOW-LEVEL INOCULA

TABLE 7.8. QUINOLINE BIODEGRADATIONS IN BATCH FERMENTATIONS WITH LOW-LEVEL INOCULA[a]

| Initial quinoline conc. ($\mu g\ ml^{-1}$) | Time (hr) | Change in bacterial counts ($\Delta X$) (cells $ml^{-1} \times 10^{6}$) | Quinoline degraded ($\Delta S$) ($\mu g\ ml^{-1}$) | Cell yield (Y) (cells $\mu g^{-1}$ S $\times 10^{6}$) | First-order rate constant ($k_b$) ($\mu g\ cell^{-1}\ hr^{-1} \times 10^{-7}$) |
|---|---|---|---|---|---|
| 1 | 12 | 1.5 | 0.45 | 3.3 | 2.2 |
| 3 | 14 | 5.5 | 2.90 | 1.9 | 3.9 |
| 5 | 14 | 6.7 | 4.90 | 1.4 | 5.3 |
| 10 | 14 | 6.1 | 7.10 | 0.9 | 8.2 |
| | | | | Average 1.9 ± 1.0[b] | Average 4.9 ± 2.5[b] |

[a] $X_o = 1.75 \times 10^{4}$ cells $ml^{-1}$.

[b] Standard deviations.

The decreasing value of Y with increasing initial concentrations of quinoline may reflect an increasing accumulation of a metabolite that has an inhibitory effect.

Cascade Batch Fermentations with a Freshly Developed Degrading System Transferred in Fresh Pond Water Media--The data obtained for quinoline levels and viable cell counts in a cascade study with water from a eutrophic pond are presented in Figures 7.7 and 7.11 and in Table 7.9. Because the samplings were limited, only the data from the 10 μg ml$^{-1}$ quinoline series were analyzed for determination of the yield factor and the first-order rate constant. The initial viable counts ($X_o$) after 0.2% inoculation from the previous degradation culture mixture ranged from 0.6 x 10$^5$ to 2.2 x 10$^5$ cells ml$^{-1}$. These counts were at least two orders magnitude smaller than the cell counts used in calculations of Y, and they were neglected in the change in population used to calculate this factor. The values of $\mu_m$ were determined from the slopes of the slots of ln $\Delta S$ versus t in Figure 7.11 (see Section 7.3, Part I of this report for the details of this kinetic analysis). Since $Y = \Delta S/\Delta X$, $k_b$ could be calculated (Table 7.9). Data from series 2 in the cascade studies were not used in these calculations because of insufficient data points in the critical time periods. When the $K_s$ value of 0.16 μg ml$^{-1}$ from batch fermentations with low-level inocula is used, the second-order rate constant $k_{b2} = k_b/K_s$ is (2.4 ± 1.5) x 10$^{-6}$ ml cell$^{-1}$ hr$^{-1}$.

### 7.6.3 Identification of Metabolites

Quinoline metabolites were observed during the kinetic studies. Two intermediates were found after they were converted to the corresponding trimethylsilyl derivatives and examined by gas chromatography/mass spectrometry. The major metabolite was identified as 2-hydroxyquinoline (I) based on comparative spectra of an authentic standard (supplied by Pfaltz and Bauer company).

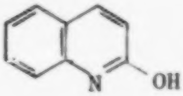

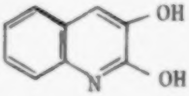

The mass spectrum of the second metabolite corresponded to the ditrimethylsilyl ether of a dihydroxylated quinoline [M/e = 305 ($M^+$)]. This metabolite is expected to be 2,3-dihydroxyquinoline (D). However, this structure has not been verified because an authentic standard is not available.

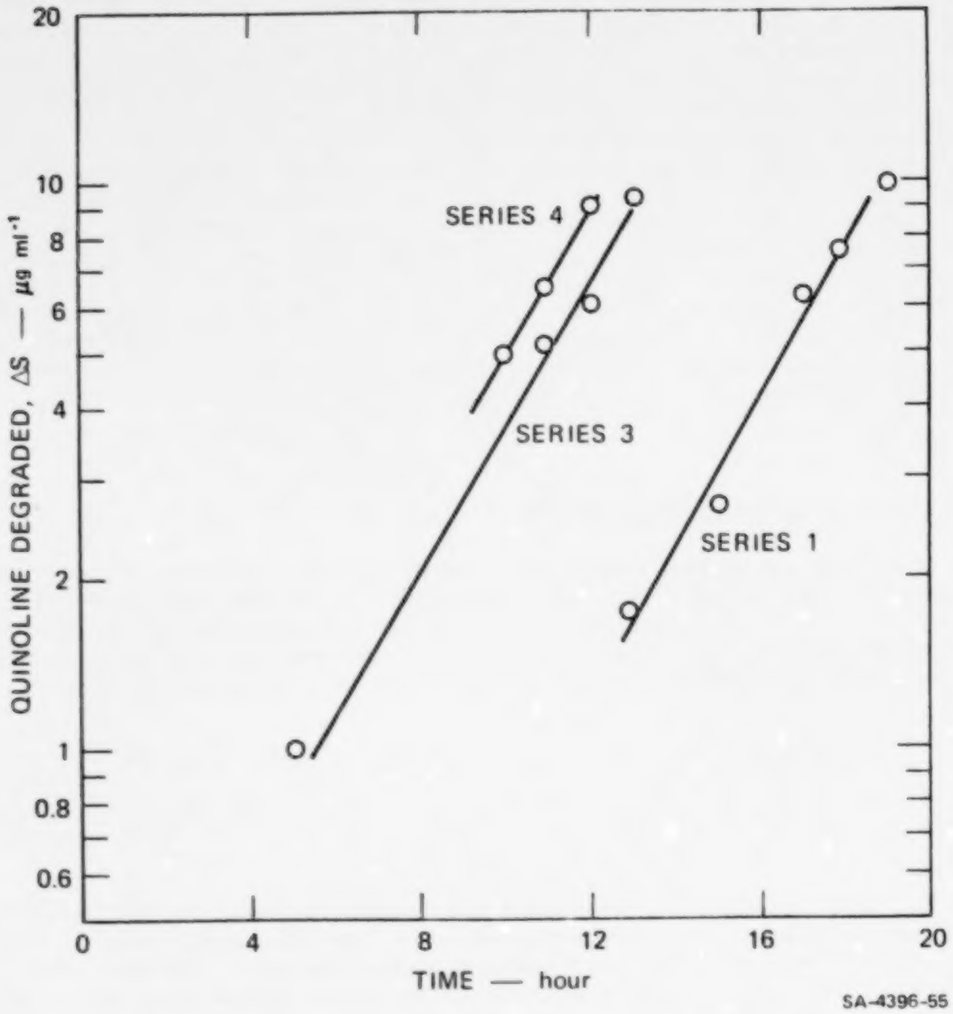

FIGURE 7.11 QUINOLINE UTILIZATION IN CASCADE BATCH FERMENTATIONS

TABLE 7.9. QUINOLINE DEGRADATIONS IN CASCADE BATCH FERMENTATIONS[a]

| Flask series | Time (t) (hr) | Cell counts (X) (cells $ml^{-1} \times 10^6$) | Quinoline degraded ($\Delta S$) ($\mu g\ ml^{-1}$) | Cell yield (Y) (cells $\mu g^{-1}$ S $\times 10^6$) | $\mu_{\underline{m}}$ ($hr^{-1}$) | First-order rate constant ($k_{bl}$) ($\mu g\ cell^{-1}\ hr^{-1} \times 10^{-7}$) |
|---|---|---|---|---|---|---|
| 1 | 16 | 4.6 | 4.0 | 1.15 | 0.301 | 2.6 |
| 2 | 14 | 4.3 | 9.9 | 0.43 | 0.289 | 6.7 |
| 4 | 14 | 14.0 | 10.0 | 1.40 | 0.289 | 2.1 |
|  |  |  |  | Average 1.0 ± 0.5[b] |  | Average 3.8 ± 2.5[b] |

[a] Freshly developed quinoline biodegrading system sequentially transferred (0.2% inoculum) into fresh pond water sample media.

[b] Standard deviations.

# 8. LABORATORY INVESTIGATION OF BENZO[f]QUINOLINE

## 8.1 SYNOPSIS

The results of the laboratory investigations suggest that photolysis is the major transformation pathway for benzo[f]quinoline (BQ) in all types of water bodies. Biodegradation may occur slowly in eutrophic waters. Sorption by sediments may be significant in turbid waters.

The nine-compartment model predicted the following steady-state concentrations of BQ in solution, suspended solids, and sediments near point sources in the presence of a continuous discharge of 10 ng $ml^{-1}$ (10 ppb) BQ:

| | Half-life* (hr) | Solution ($\mu g\ ml^{-1}$) | Suspended solids ($\mu g\ g^{-1}$) | Sediments ($\mu g\ g^{-1}$) |
|---|---|---|---|---|
| River | 0.5 | $8.1 \times 10^{-1}$ | $1.1 \times 10^{3}$ | $1.0 \times 10^{3}$ |
| Pond | 6.9 | $7.8 \times 10^{-3}$ | $1.1 \times 10^{1}$ | $1.1 \times 10^{1}$ |
| Eutrophic lake | 7.0 | $2.4 \times 10^{-2}$ | $3.3 \times 10^{1}$ | 8.3 |
| Oligotrophic lake | 1.4 | $4.3 \times 10^{-3}$ | 6.0 | 1.5 |

## 8.2 BACKGROUND

Benzoquinolines have been identified in various crude oils (Brodeskii et al., 1975; Snyder, 1969; Ball, 1962) and are produced in the low-temperature carbonization of coal (Karr and Ta-Chung, 1958).

Brodeskii et al. (1975) reported that the acridines and benzoquinolines constituted 12% to 20% of the basic components in Sakhalim petroleums; the concentrations of the quinolines were 50% to 60% of these same fractions. Snyder (1969) observed that in a California crude oil the total benzoquinoline content in two distillate fractions was approximately one-sixth that of the quinolines. It is apparent that the quinolines and benzoquinolines are usually found together and should be present in both petroleum and coal processing wastes. Benzoquinolines have been found in airborne particulates in urban atmospheres (Sawicki et al., 1965; Brocco et al., 1973; Ray and Frei, 1972). Benzo[f]quinoline (BQ) has been selected for this study; its physical properties are listed in Table 8.1.

---

*Predicted by the one-compartment model.

TABLE 8.1. PHYSICAL PROPERTIES OF BENZO[f]QUINOLINE

| | |
|---|---|
| Structure | 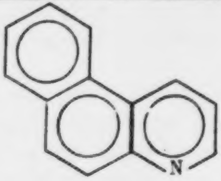 |
| Molecular weight | 179.22 |
| Melting point (°C) | 93.5 |
| Boiling point (°C) (Lange's Handbook of Chemistry, 1973) | 350 (721 torr)<br>202-5 (8 torr) |
| Vapor pressure at 20°C (torr) (McEachern et al., 1975) | $2.8 \times 10^{-5}$ |
| Solubility in water ($\mu g\ ml^{-1}$)[a] | 76.1 ± 2.2 |
| UV spectrum (ethanol) $\lambda_{max}$ nm (log $\varepsilon$) (CRC Handbook) | 316 (3.34)<br>323 (3.26)<br>330 (3.62)<br>338 (3.28)<br>346 (3.71) |
| $pK_a$[b] (Ray and Frei, 1972) 1 $\mu g\ ml^{-1}$ BQ = $5.58 \times 10^{-6}$ M | 5.15 |

[a] Measured in this study (Section 8.4.1).

[b] $pK_b = 8.85$; $pK_b$ for quinoline is 9.5.

No information was found concerning the water solubility, volatilization, or sorption properties of BQ on soils or sediments. Doehler and Young (1960) studied the sorption of quinoline on Na and Ca-montmorillonite. They reported that the partition coefficient is pH dependent; sorption increases as the pH decreases.

BQ should not hydrolyze under the conditions of environmental aquatic systems.

Data were not available for evaluating the importance of free radical oxidation of BQ under environmental conditions. In the study of the free radical oxidation of quinoline, an environmental half-life of at least 100 years was estimated.

As seen from the UV spectral data (see Table 8.1), BQ absorbs strongly in the solar region out to 350 nm. Although no information on the photolysis of

BQ was available, our studies on quinoline indicated a half-life of about 21 days for direct photolysis; in the presence of humic acid, the photolysis half-life of quinoline was about 6 days (See Section 7.5.1).

No reports were found regarding the biodegradation of the benzoquinolines. In Section 7, we reported that quinoline biodegrading systems could be readily obtained by enrichment processes with oligotrophic and eutrophic waters and with aeration effluents from sewage plants. BQ also has structural similarities with phenanthrene, which can be biodegraded.

In summary, the literature information and our data from quinoline suggested that photolysis and biodegradation might be important processes in the removal of BQ from natural waters.

## 8.3 ENVIRONMENTAL ASSESSMENT

### 8.3.1 Summary of Laboratory Data

The rate constants obtained in the laboratory investigations of the transformation and transport processes for BQ are summarized in Table 8.2.

TABLE 8.2. SUMMARY OF BENZO[f]QUINOLINE LABORATORY DATA

| Process | Sorption equilibrium | Partition coefficient |
|---|---|---|
| Sorption | $S_s = K_p S_w$ | $K_p = 1300$[a] |
| | Rate expression | Rate constant at 25°C |
| Volatilization[b] | $k_v[BQ]$ | $k_v = (2.2 \pm 0.9) \times 10^{-4} k_v^0$ |
| Photolysis [c] | $k_p[BQ] = \Phi (\Sigma Z_\lambda \varepsilon_\lambda)[BQ]$ | $k_p = (1.4 \pm 0.7) \times 10^{-4}\ \mathrm{sec}^{-1}$ |
| Oxidation | $k_{ox}[RO_2\cdot][BQ]$ | $k_{ox} < 2.8\ \mathrm{M}^{-1}\ \mathrm{sec}^{-1}$ |
| Hydrolysis | NA | NA |
| Biodegradation | $k_{b2} = \frac{\mu_m}{Y K_s}$ | $k_{b2} = (3.6 \pm 0.01) \times 10^{-8}\ \mathrm{ml}\ \mathrm{cell}^{-1}\ \mathrm{hr}^{-1}$ |

[a] Measured on Coyote Creek sediment.

[b] See Part I, Section 5.3.

[c] Assumes 12 hours of sunlight in mid-June.

### 8.3.2 Environmental Assessment Using the One-Compartment Model

The half-lives of dissolved BQ calculated for individual transformation or removal processes following a single, brief input are listed in Table 8.3.

Photolysis is the dominant pathway in all standing waters, but is roughly five times slower than dilution under the assumed conditions of rapid river flow. Sorption is important only in the most turbid waters, but even in these waters it is unlikely to account for more than 40% of the BQ lost from solution. In all waters, biodegradation is slow, and volatilization and oxidation are exceedingly slow. The half-lives in eutrophic and oligotrophic waters differ by roughly a factor of 4.

TABLE 8.3. TRANSFORMATION AND TRANSPORT OF BENZO[f]QUINOLINE PREDICTED BY THE ONE-COMPARTMENT MODEL

| | River | Eutrophic pond | Eutrophic lake | Oligotrophic lake |
|---|---|---|---|---|
| Photolysis, half-life (hr)[a] | 2.8 | 7.0 | 7.0 | 1.4 |
| Oxidation, half-life (hr) | $>10^5$ | $>10^5$ | $>10^5$ | $>10^5$ |
| Volatilization, half-life (hr) | $>10^4$ | $>10^5$ | $>10^5$ | $>10^5$ |
| Hydrolysis, half-life (hr) | -- | -- | -- | -- |
| Biodegradation, half-life (hr) | 190 | 190 | 190 | $>10^6$ |
| Half-life for all processes except dilution (hr) | 2.8 | 7.0 | 7.0 | 1.4 |
| Half-life for all processes including dilution (hr) | 0.48 | 6.9 | 7.0 | 1.4 |
| Amount BQ sorbed (mg $m^{-3}$)[b] | 140 | 720 | 70 | 70 |
| Percentage BQ sorbed | 12% | 42% | 6.5% | 6.5% |

[a] Estimates are the average photolysis rates on a summer day at 40° latitude. Photolysis rates in midwinter are at least three times slower.

[b] Assumes 1 $\mu$g $ml^{-1}$ of BQ in aqueous phase and partition coefficient of 200.

### 8.3.3 Persistence

Benzo[f]quinoline should not be "persistent" in any shallow or thoroughly mixed natural waters. However, in lakes such as Lake Superior and Lake Tahoe, which are so deep as to be unproductive and poorly lit throughout much of their depth, benzo[f]quinoline may persist at relatively high concentrations for decades or centuries. The persistence of concentrations that approximate the initial concentrations following an acute discharge should be virtually independent of dilution except in all but the largest streams, such as the hypothetical river assumed in the river simulation of Table 8.3.

### 8.3.4 Mass and Concentration Distributions Calculated Using Computer Models

The distributions of mass and concentration of BQ expected at steady state during chronic discharge to each of four types of water bodies are shown in Table 8.4. The changes in concentration as discharge begins and ends are shown in Figures 8.1 through 8.4. The pseudo-first-order rate constants used in the simulations are presented in Appendix A. Under our assumptions regarding the geometries of the water bodies and the flow rates within them, roughly 95% of the BQ is in the sediments at steady state and roughly 90% of the remainder is in solution.

The concentrations of dissolved BQ at steady state varied 100-fold among the four simulated water bodies, the highest concentrations being in the eutrophic waters where photolysis is slower than in the oligotrophic lake. Concentrations within individual waters varied 10,000-fold among aqueous compartments of the oligotrophic lake, 1,000-fold within the eutrophic lake, and about 15% in the river, where dilution is very rapid (Table 8.4). Average concentrations in the sediments differ by roughly a factor of 10 or less from the concentrations in the aqueous compartment that receives the inflowing waters (Compartment 1 in each simulation). Concentrations of BQ on solids in the water columns and in the sediments tend to be 1,000 times higher than concentrations in solution.

The approaches to steady-state concentrations were rapid in all water bodies following start of the simulated discharge, and the transitions to new steady states after discharge stopped were very rapid in the surface waters of the lake simulations (Figures 8.3 and 8.4). Concentrations of BQ in the sediments declined slowly in each simulation, reflecting the large mass of BQ in the sediments and the relatively slow rates of exchange between the sediments and the water column.

## 8.4 PHYSICAL PROPERTIES

### 8.4.1 Solubility in Water

The solubility of BQ in water at 25°C, measured using the method of Campbell (1930), was 76.1 ± 2.2 $\mu$g ml$^{-1}$.

### 8.4.2 Absorption Spectra

The absorption spectra of BQ in water were measured at pH 7.1 (adjusted and 6.3 (nonadjusted). The absorption coefficients at wavelength intervals from 297 to 400 nm and at 313 and 366 nm are given in Table 8.5. The absorption coefficients at pH 6.3 were slightly higher than at pH 7.1, probably due to the higher concentration of protonated BQ. (BQ is 1.1% protonated at pH 7.1 and 7.1% at pH 6.3.)

TABLE 8.4. DISTRIBUTION OF BENZO[f]QUINOLINE IN VARIOUS AQUATIC SYSTEMS AT STEADY STATE

(input concentrations of 1 μg ml$^{-1}$ benzo[f]quinoline)

| | Pond | | River | | Eutrophic Lake | | Oligotrophic Lake | |
|---|---|---|---|---|---|---|---|---|
| | Mass (kg) | Conc. (μg ml$^{-1}$) | Mass (kg) | Conc. (μg ml$^{-1}$) | Mass (kg) | Conc. (μg ml$^{-1}$) | Mass (kg) | Conc. (μg ml$^{-1}$) |
| Compartment 1 (surface water) | | | | | | | | |
| Solution | $1.55 \times 10^{-1}$ | $7.75 \times 10^{-3}$ | $2.43 \times 10^{2}$ | $8.10 \times 10^{-1}$ | 5.93 | $2.37 \times 10^{-2}$ | 1.07 | $4.30 \times 10^{-3}$ |
| Suspended solids | $6.50 \times 10^{-2}$ | $1.08 \times 10$ | $3.40 \times 10$ | $1.13 \times 10^{3}$ | $4.15 \times 10^{-1}$ | $3.32 \times 10$ | $7.53 \times 10^{-2}$ | 6.02 |
| Compartment 2 (surface water) | | | | | | | | |
| Solution | -- | -- | $2.25 \times 10^{2}$ | $7.50 \times 10^{-1}$ | 2.28 | $9.13 \times 10^{-4}$ | $6.54 \times 10^{-2}$ | $2.61 \times 10^{-5}$ |
| Suspended solids | -- | -- | $3.15 \times 10$ | $1.05 \times 10^{3}$ | $1.59 \times 10^{-1}$ | 1.27 | $4.58 \times 10^{-3}$ | $3.66 \times 10^{-2}$ |
| Compartment 3 (surface water) | | | | | | | | |
| Solution | -- | -- | $2.08 \times 10^{2}$ | $6.95 \times 10^{-1}$ | $6.56 \times 10^{-1}$ | $2.62 \times 10^{-4}$ | $3.76 \times 10^{-4}$ | $1.50 \times 10^{-6}$ |
| Suspended solids | -- | -- | $2.92 \times 10$ | $9.73 \times 10^{2}$ | $4.59 \times 10^{-2}$ | $3.67 \times 10^{-1}$ | $2.63 \times 10^{-5}$ | $2.10 \times 10^{-3}$ |
| Compartment 5 (bottom water) | | | | | | | | |
| Solution | -- | -- | -- | -- | $5.40 \times 10^{-2}$ | $2.16 \times 10^{-5}$ | $4.15 \times 10^{-4}$ | $1.66 \times 10^{-7}$ |
| Suspended solids | -- | -- | -- | -- | $3.78 \times 10^{-3}$ | $3.02 \times 10^{-2}$ | $2.92 \times 10^{-5}$ | $2.32 \times 10^{-4}$ |
| Compartments 7-9 (sediment)[a] | | | | | | | | |
| Solution | $1.94 \times 10^{-3}$ | $7.75 \times 10^{-3}$ | 5.63 | $7.51 \times 10^{-1}$ | $5.20 \times 10^{-2}$ | $5.94 \times 10^{-3}$ | $8.87 \times 10^{-2}$ | $1.06 \times 10^{-3}$ |
| Solids | 7.29 | $1.08 \times 10$ | $2.13 \times 10^{4}$ | $1.05 \times 10^{3}$ | $1.13 \times 10^{2}$ | 8.32 | $2.03 \times 10$ | 1.49 |

[a] The amounts given for solid and solution phases in the sediment compartments are estimated from the sorption partition coefficient for suspended solids and may be overestimated because it was assumed that biodegradation of sorbed material does not occur.

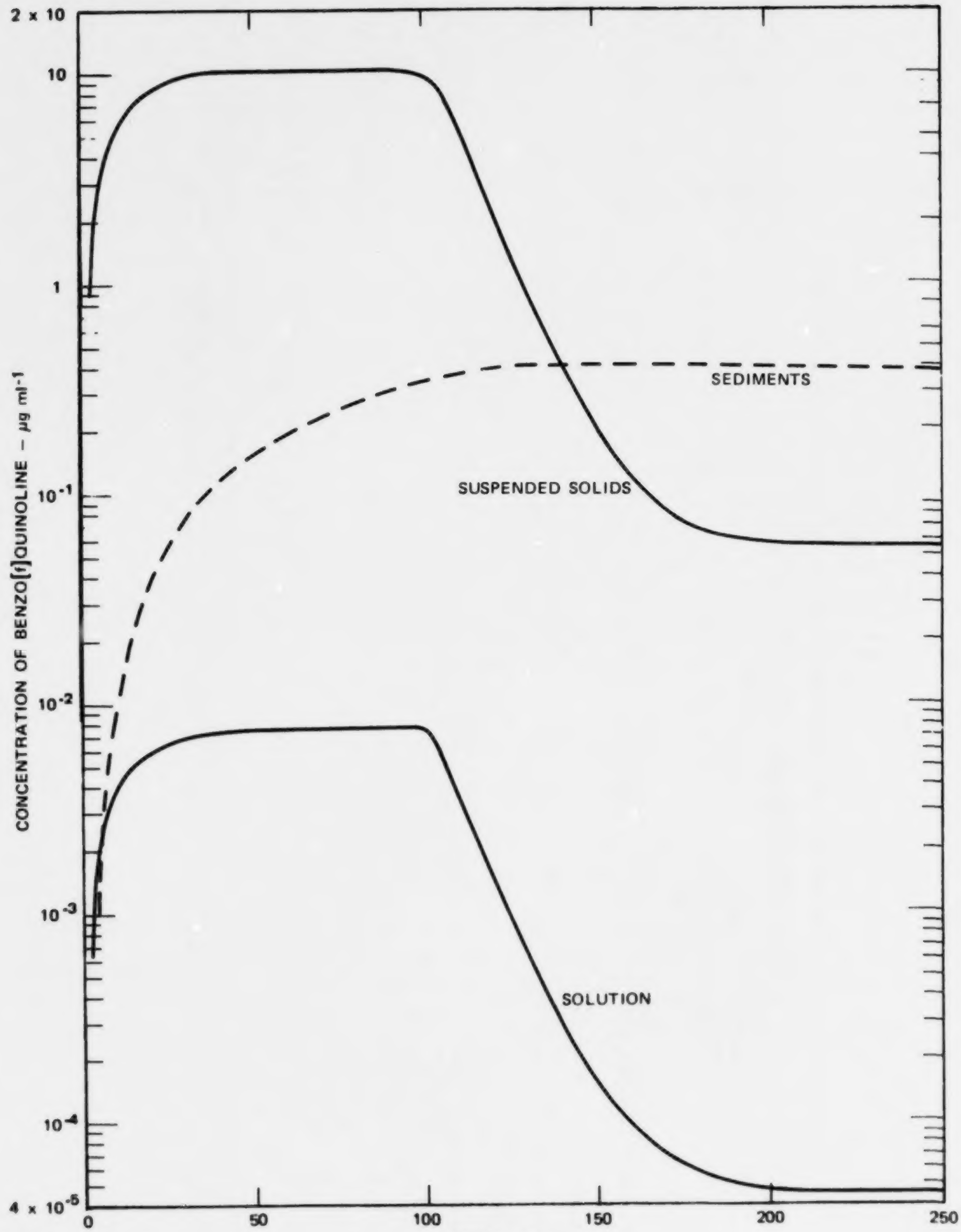

FIGURE 8.1. PERSISTENCE OF BENZO[f]QUINOLINE IN A TWO-COMPARTMENT POND SYSTEM

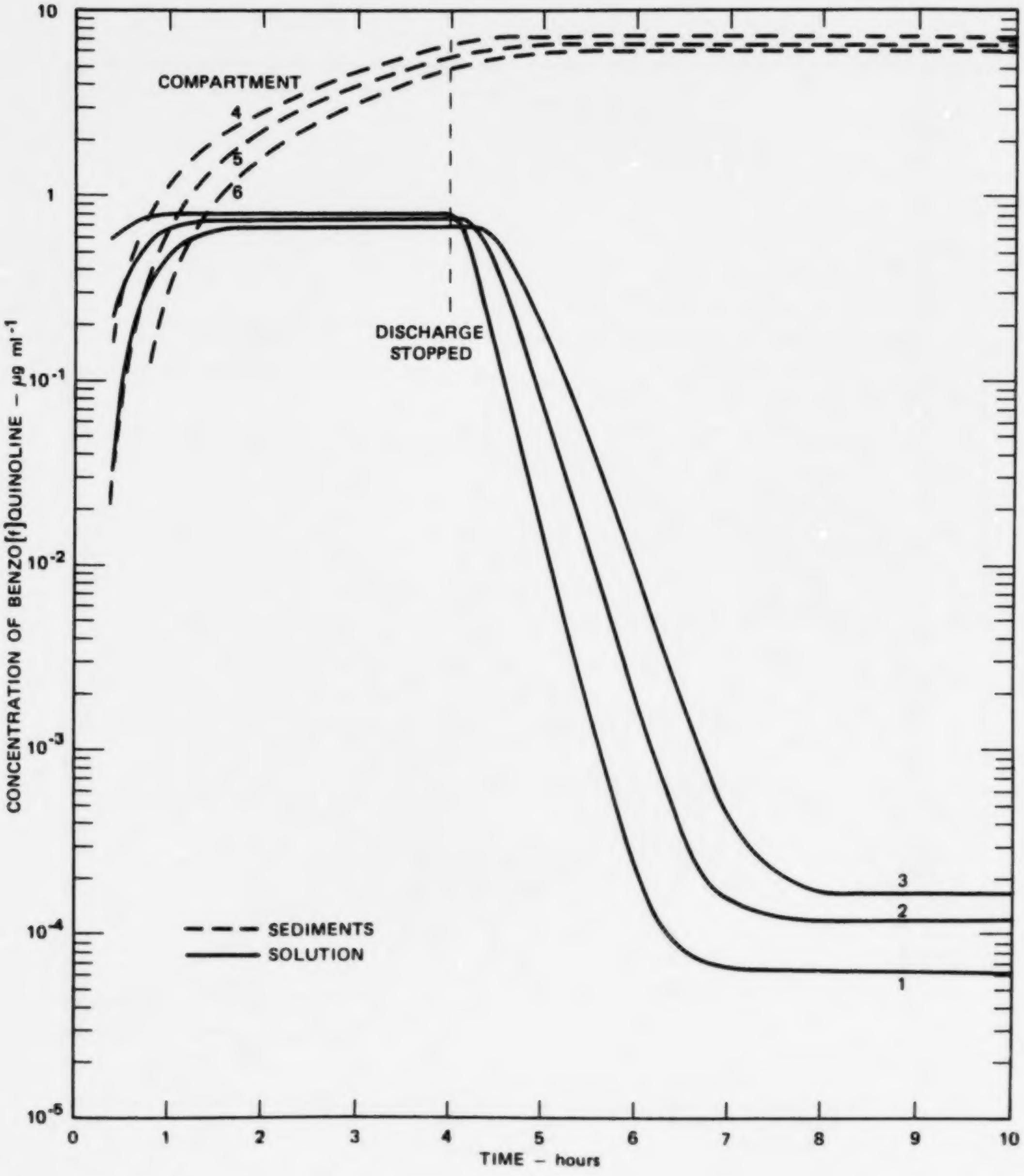

FIGURE 8.2 PERSISTENCE OF BENZO[f]QUINOLINE IN A PARTIALLY MIXED RIVER SYSTEM

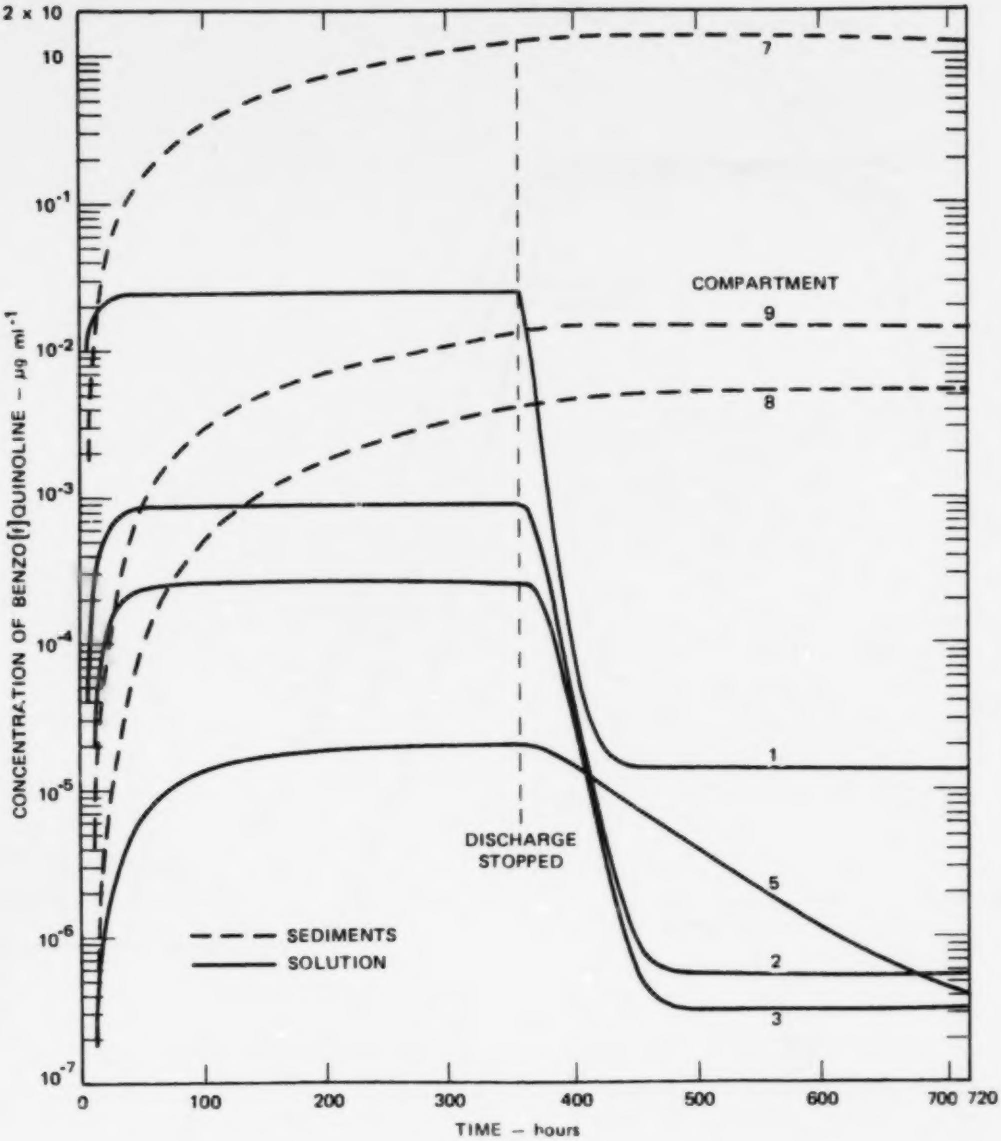

FIGURE 8.3. PERSISTENCE OF BENZO[f]QUINOLINE IN A EUTROPHIC LAKE

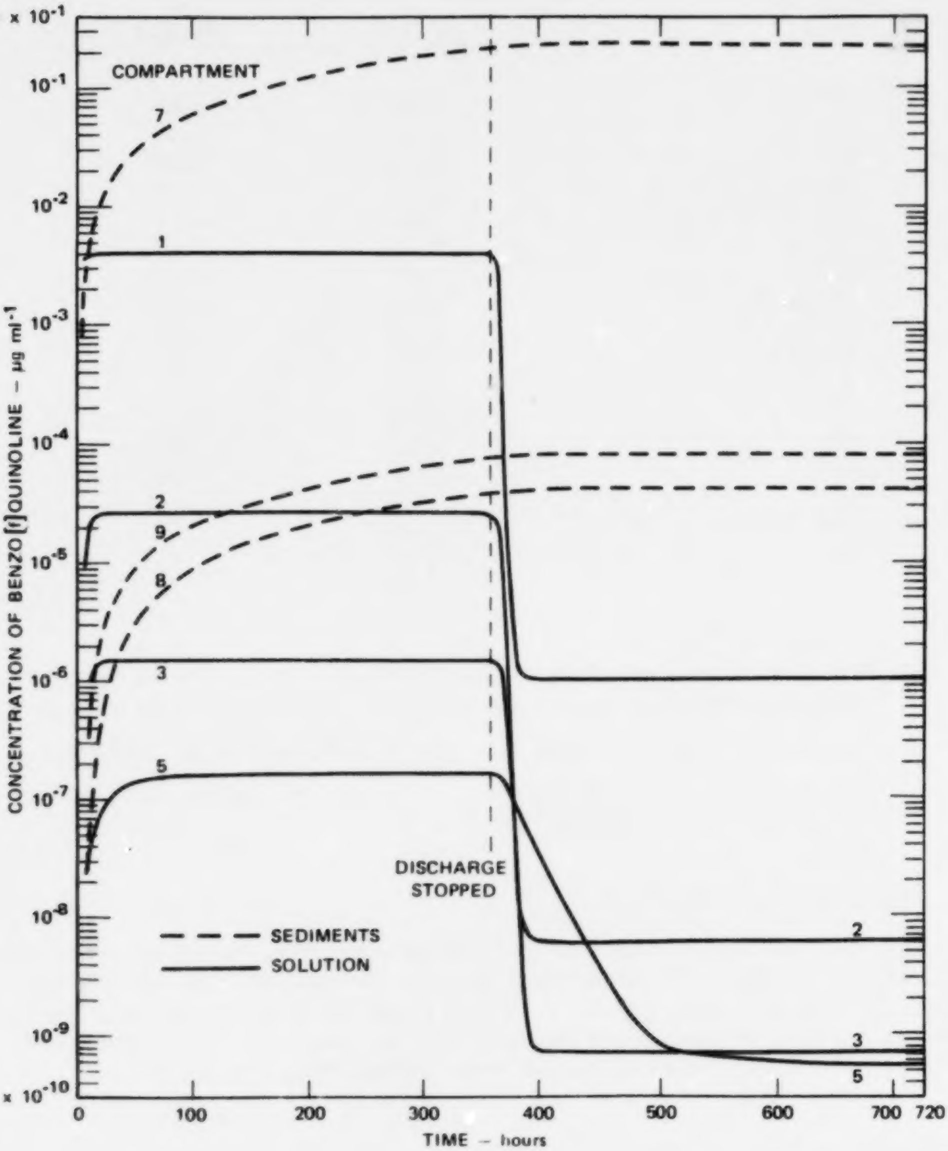

FIGURE 8.4. PERSISTENCE OF BENZO[f]QUINOLINE IN AN OLIGOTROPHIC LAKE

TABLE 8.5. ABSORPTION SPECTRA OF BENZO[f]QUINOLINE IN WATER[a]

| Center of wavelength interval[b] (nm) | Absorption coefficients[c] ($M^{-1}$ $cm^{-1}$) | |
|---|---|---|
| | pH 7.1 | pH 6.3 |
| 297.5 | 3980 | 3960 |
| 300.0 | 3910 | 3910 |
| 302.5 | 2070 | 2140 |
| 305.0 | 1400 | 1500 |
| 307.5 | 1140 | 1240 |
| 310.0 | 1070 | 1180 |
| 312.5 | 1330 | 1430 |
| 315.0 | 1600 | 1670 |
| 317.5 | 1410 | 1480 |
| 320.0 | 1340 | 1380 |
| 323.1 | 1460 | 1490 |
| 330 | 3010 | 3020 |
| 340 | 1600 | 1680 |
| 350 | 1380 | 1530 |
| 360 | 89 | 250 |
| 370 | 44 | 185 |
| 380 | 30 | 96 |
| 390 | 0 | 37 |
| 400 | 0 | 0 |

[a] Benzo[f]quinoline concentration was $1.35 \times 10^{-4}$ M in a 1-cm cell.

[b] The wavelength intervals are given in Appendix B, Table B.1.

[c] The absorption coefficients at 313 and 366 nm are 1361 and 37 at pH 7.1 and 1479 and 207 at pH 6.3.

### 8.4.3 Volatilization Rate

The rate of volatilization of BQ from water was measured using the method of Hill et al. (1976). At an average oxygen reaeration rate $k_v^0 = 4.00 \pm 1.51$ $hr^{-1}$, the ratio $k_v^{BQ}/k_v^0$ was $(2.2 \pm 0.9) \times 10^{-4}$. Since this ratio is very small, volatilization was not an important pathway for BQ compared with photolysis; therefore, no further volatilization experiments were conducted.

### 8.4.4 Sorption on a Sediment

The sorption partition coefficient of BQ on Coyote Creek sediment was measured. Replicate samples were run at two BQ concentrations and two sediment loadings as well as blanks. All solutions were buffered to maintain pH 7. Table 8.6 summarizes the results.

## TABLE 8.6. SORPTION OF BENZO[f]QUINOLINE ON COYOTE CREEK SEDIMENT[a]

| Sediment concentration (mg ml$^{-1}$) | BQ concentration in supernatant[a,b] (μg ml$^{-1}$) | BQ concentration on sediment[c] (μg g$^{-1}$ x 10$^{-2}$) | Partition coefficient, $K_p$ LLS[d] | |
|---|---|---|---|---|
| | | | $a_o = 0$ | $a_o \neq 0$ |
| 4.8 | 0.99 ± 0.19 | 12.04 ± 0.39[e] | | |
| 14.5 | 0.61 ± 0.02 | 4.27 ± 0.01 | | |
| 4.8 | 1.35 ± 0.17 | 22.95 ± 0.34[f] | 1313 ± 170 | 2150 ± 440 |
| 14.5 | 0.84 ± 0.01 | 8.01 ± 0.01 | | ($a_o$ = -856 ± 433) |

---

[a] Total organic content = 1.4%

[b] Concentration measured in supernatant with population standard deviation.

[c] Concentration on sediment calculated from supernatant concentration with population standard deviation.

[d] LLS = linear least squares regression; see Part I, Section 5.4.2.3.

[e] Measured concentration on sediment for one of the flasks was 8.80 ± 0.10 μg g$^{-1}$.

[f] Measured concentration on sediment for one of the flasks was 17.63 ± 0.10 μg g$^{-1}$.

### 8.4.5 Biosorption

Benzo[f]quinoline was dissolved in phosphate buffer and added to a suspension of the four types of bacteria prepared as described in Part I of this report. The sorptions were conducted with suspensions of viable (optical density of 2) and heat-killed cells at 25°C for 1 hr in 10-ml volumes in 15-ml Corex tubes agitated in a Rotor drum. All sorptions were conducted in triplicate. The centrifuged cell pellets and clear supernatants were extracted with ethyl acetate and analyzed for BQ by HPLC.

The sorption coefficients developed with two levels of BQ had a greater difference between those for heat-killed and viable cells (Table 8.7) than were observed for any other compound examined under this contract. The higher sorption coefficient for the heat-killed cells suggests that the sorption is not a receptor or enzymatic phenomenon.

TABLE 8.7. BIOSORPTION OF BENZO[f]QUINOLINE

| Condition of cells[a] | Initial BQ concentration ($ng\ ml^{-1}$) | Sorption coefficient[b] |
|---|---|---|
| Viable | 115 | 158 ± 8 |
| Viable | 390 | 139 ± 7 |
| Heat-killed | 115 | 560 ± 67 |
| Heat-killed | 390 | 520 ± 19 |

[a] Dry weights of bacterial cell mixture in viable-cell sorptions = 1.05 g $liter^{-1}$, and in heat-killed cells = 0.847 g $liter^{-1}$.

[b] $\frac{\mu g\ BQ}{g\ cells}$ / $\mu g$ BQ $ml^{-1}$ supernatant after 1 hr equilibration.

## 8.5 CHEMICAL TRANSFORMATION

### 8.5.1 Photolysis Rate

In air-saturated water, the direct photolysis half-life of BQ in sunlight is less than a day. Photolysis experiments were conducted with BQ in pure water and in natural waters from several sources. These solutions also contained 1% methanol to increase the solubility of BQ. Data for photolysis of BQ in sunlight and at 313 nm are summarized in Table 8.8. The quantum yield measured at 313 nm for photolysis of BQ in air-saturated pure water containing 1% methanol is $1.4 \times 10^{-2}$.

Photolysis of BQ in water that had been purged of air by nitrogen showed a rate acceleration of 70%, indicating that oxygen may be quenching a photoexcited state of BQ and that the reaction observed is a photohydrolysis or rearrangement. The data in Table 8.8 also show that, while the photolysis rate

TABLE 8.8. RATE CONSTANTS FOR PHOTOLYSIS OF BENZO[f]QUINOLINE[a]

| Irradiation source | BQ concentration ($\mu g\ ml^{-1}$) | Solution[b] | Extent of reaction (%) | Rate constant ($k_p \times 10^5\ sec^{-1}$) |
|---|---|---|---|---|
| 313 nm | 7.3 | Pure water, air saturated | 39 | 1.73 ± 0.15[c,d] |
| 313 | 7.3 | Pure water, $N_2$ purged | 55 | 2.90 ± 0.27 |
| 313 | 9.1 | Lake Tahoe water | 51 | 1.92 ± 0.10 |
| 313 | 9.1 | Searsville Pond water | 29 | 0.748 ± 0.071 |
| 313 | 9.1 | Coyote Creek water | 49 | 1.34 ± 0.12 |
| 313 | 12.1 | 8.0 $\mu g\ ml^{-1}$ humic acid in pure water | 14 | 0.275 ± 0.055 |
| 313 | 9.1 | Methanol | 21 | 0.475 ± 0.031 |
| 313 | 9.1 | Acetonitrile | 17 | 0.372 ± 0.040 |
| Sunlight, midday mid-June | 10.2 | Pure water | 87 | 14.0 ± 0.66[e] |
| Sunlight, midday mid-June | 9.1 | Pure water | 83 | 18[f] |

[a] 1.00 $\mu g\ ml^{-1}$ benzo[f]quinoline in water = $5.59 \times 10^{-6}$ M.

[b] Solutions contained 1% methanol as cosolvent.

[c] Standard deviation.

[d] Quantum yield for disappearance of BQ was $1.4 \times 10^{-2}$.

[e] Half-life of 1.4 hours.

[f] Half-life of 1.1 hours; based on one datum point at 83% reaction.

of BQ in Lake Tahoe water is the same as that in the pure water solvent, the rates in the waters from Coyote Creek and Searsville Pond are 28% and 57% slower, respectively. Since the absorbances of the creek and pond waters (both about 0.07 at 313 nm) would account for less than a 10% reduction in rate due to light screening effects, other processes must also be contributing to the rate decrease in these waters.

A similar conclusion applies to the photoreaction in the water containing 8.0 μg $ml^{-1}$ humic acid where the rate constant is only 16% of that in pure water. Light screening by humic acid because of the absorbance at 313 nm of 0.81 would account for a rate constant 45% of that in pure water. The apparent sensitivity of BQ triplet state (probably) to quenching by oxygen makes it probable that BQ triplet is also quenched efficiently by other materials including those present in natural waters.

Photolyses were also carried out using methanol and acetonitrile as the solvents. The data in Table 8.8 show that the rates in these solvents are less than 25% of the rate in water. Based on the limited number of experiments, it is impossible to determine whether the rate difference was due to a change in lifetime of the excited state owing to solvent interaction, to quenching by the probable higher concentration of oxygen in organic solvents, or to reaction of excited state BQ with solvent (that is, water versus methanol rates). The solvent effects and the apparent quenching effects of oxygen and natural substances pose many questions regarding the chemistry of these reactions, and further studies on the phototransformation of BQ in water seem indicated.

The half-lives for direct photolysis of BQ in sunlight as a function of the time of day and season were calculated by the procedure of Zepp and Cline (1977), using a quantum yield of $1.4 \times 10^{-2}$ measured at 313 nm and the measured UV spectrum of BQ. These data are plotted in Figure 8.5. The half-life of less than an hour calculated for midday in summer is in good agreement with measured half-lives of 1.1 and 1.4 hours measured in midday in mid-June. As discussed above, the presence of naturally occurring substances in water may slow the photolyses significantly, so application of the direct photolysis data to environmental assessments should be used with some caution.

### 8.5.2 Oxidation Rate

The susceptibility of 9.1 μg $ml^{-1}$ ($5.1 \times 10^{-5}$ M) BQ to free radical oxidation was examined using the AA-initiated oxidation reaction. (See Part I, Section 6.3, of this report and Appendix B for discussion and procedure for this experiment.) The BQ oxidation experiment was conducted at 50.0°C in 1% methanol in water containing $1.0 \times 10^{-4}$ M AA. At the end of 96 hours reaction, less than 1% of the BQ had been consumed. Similar lack of reactivity toward oxidation was found for quinoline (Section 7.5.2), where only 3% loss of quinoline was found for a 100-hour reaction time. If a 3% experimental error in the analysis of BQ is assumed, the second-order rate constant $k_{ox}$ at 25°C is the same as that for quinoline, or less than 2.8 $M^{-1}$ $sec^{-1}$. Assuming $[RO_2\cdot] = 10^{-9}$ M in the aquatic environment, the half-life of BQ toward oxidation is more than 8 years. The free radical oxidation of BQ by $RO_2\cdot$ radicals is then not competitive with photolysis under environmental conditions.

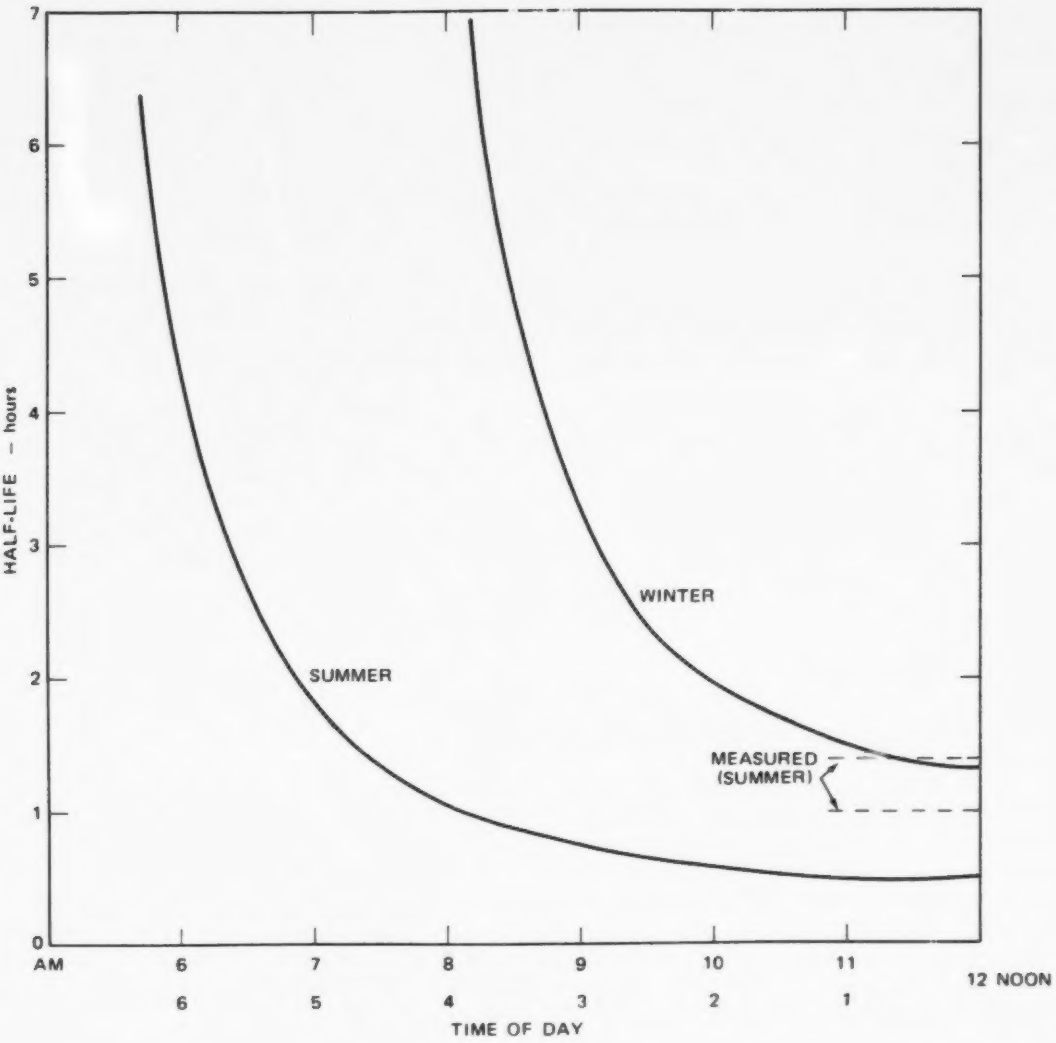

FIGURE 8.5. SEASONAL AND DAILY VARIATION OF PHOTOLYSIS HALF-LIFE OF BENZO[f]QUINOLINE

### 8.5.3 Hydrolysis Rate

BQ contains no groups that are hydrolyzable; therefore, no hydrolysis studies were performed.

### 8.5.4 Products from Chemical Transformations

Two early eluting primary product peaks were found in the HPLC traces of photolyzed BQ solutions. The relative size of these peaks was not affected by the presence of oxygen during photolyses, although the photolysis did proceed more slowly (by a factor of over 2) when oxygen was present (see Section 8.5.1). The result suggests that oxygen serves to quench a BQ excited state (probably triplet) during the photoreaction.

Different products were observed when the photolyses were carried out in acetonitrile or methanol rather than in water. The rate in deoxygenated acetonitrile was only one-eighth the rate in deoxygenated water (Table 8.8) and there was no significant effect of oxygen on rate or products.

These observations indicate that the photoreaction of BQ in water is some kind of photohydrolysis process. Attempts to identify products by concentration and characterization by silylation and GC-MS were unsuccessful. Assuming that the HPLC response factors are about equal to those of the BQ, these peaks accounted for approximately 50% of the reacted BQ. In view of the importance of photolysis of BQ in aquatic systems, more information is needed on the structure of the photolysis products.

## 8.6 BIODEGRADATION

### 8.6.1. Development of Encrichment Cultures

Because BQ is frequently found in the presence of quinoline and quinoline is readily biodegraded (see Section 7.6), enrichment procedures for BQ biodegrading cultures were conducted with BQ as the sole carbon compound added to the water samples and with BQ plus quinoline as carbon source, each at 10 $\mu g\ ml^{-1}$. All enrichments were initiated in 9-liter fermentors, and when BQ was being degraded, transfers were made to shaker flasks containing basal salts medium containing BQ alone or BQ plus quinoline. As with other compounds, when inducers were used, attempts were made to grow the various mixed cultures, derived from BQ plus quinoline enrichments, on basal salts/BQ medium.

The development of BQ biodegrading cultures was monitored by determining the differences in UV absorptions at 345 and 355 nm of ethyl acetate extracts prepared from fermentation broths with 2 volumes of ethyl acetate at pH 7. Although BQ has a UV absorption peak at 345 nm and a larger peak at 266 nm, too much interference was observed at this lower wavelength to make this practical in our rapid assays. Quinoline has UV absorption maximum at 312-320 nm. Critical analysis were confirmed by HPLC with a fluorescence detector.

Table 8.9 indicates the times (days) at which biodegradations of BQ were observed in the 9-liter fermentors when BQ alone, or BQ plus quinoline were the organic substrates added to the diluted (4:5) water samples. Table 8.9 also shows our success in developing culture systems that would biodegrade BQ in basal salts medium with BQ, or BQ plus quinoline, as the only carbon substrates. With every water sample, BQ-degrading systems were readily developed when quinoline was present, but with only three of these six water samples was a culture system developed that could utilize BQ as the sole carbon substrate in the basal salts medium. All biodegrading cultures derived with the BQ plus quinoline mixture rapidly adapted to growth on media with 50 $\mu g\ ml^{-1}$ BQ and 20 $\mu g$ quinoline $ml^{-1}$, and transfers were made daily.

The enrichment studies initiated with Coyote Creek water to which only BQ was added developed a BQ-degrading system in 15 days. With the eutrophic pond water, BQ degradation was observed at 43 days. All other 9-liter fermentors with only BQ did not have any detectible BQ degradation during this period.

The culture system derived from Coyote Creek water (with BQ as the only added carbon substrate) degraded BQ in basal salts/BQ (10 $\mu g\ ml^{-1}$) and Trypticase soy broth (100 $\mu g\ ml^{-1}$)/BQ (10 $\mu g\ ml^{-1}$) media. The BQ-degrading mixed culture derived from aeration effluent from the Shell Oil Refinery treatment plant could degrade BQ only if quinoline were present in the basal salts medium. It also failed to degrade BQ when transferred to Trypticase soy broth (100 $\mu g\ ml^{-1}$)/BQ (10 $\mu g\ ml^{-1}$) medium or basal salts medium to which glucose (20 $\mu g\ ml^{-1}$), Difco yeast extract (2 $\mu g\ ml^{-1}$), and BQ (10 $\mu g\ ml^{-1}$) were added; but it grew well on these two media. This indicated that with this culture system, BQ degradation was dependent on cometabolism with quinoline.

### 8.6.2 Biodegradation Kinetics

Pseudo-first-order kinetic studies were conducted with a BQ-degrading culture developed by original enrichment of Coyote Creek water with BQ. The inoculum was first grown with shaking for 2 days in basal salts/BQ (10 $\mu g\ ml^{-1}$) medium, 600 ml/2-liter Erlenmeyer flask, diluted to 2.8 liters and distributed in four sterile 2-liter Erlenmeyer flasks and incubated with shaking for 18 hours. The combined broths were centrifuged, washed twice with basal salts medium, suspended in 100 ml basal salts medium and shaken for 4 hours, centrifuged again and suspended to appropriate volumes for kinetic studies with BQ at 1000 $ng\ ml^{-1}$ in basal salts medium. The data in Table 8.10 indicate the constancy of cell counts throughout the kinetic studies.

Figure 8.6 plots ln BQ concentrations versus time. The pseudo-first-order rate constants ($k_b^1$) calculated from the slopes of the plots are 1.04 and 0.56 $hr^{-1}$ for series 1 and 2, respectively. Consequently, the respective second-order rate constants are $3.5 \times 10^{-8}$ and $3.7 \times 10^{-8}$ $ml\ cell^{-1}\ hr^{-1}$. These data correspond to a half-life ($\ln 2/k_b'$) of 193 hours assuming $10^5$ degrading organisms in a total population of $10^6$ organisms per milliliter. Since all enrichment cultures grown on BQ plus quinoline degraded BQ more rapidly than when BQ was the sole carbon source, these rate constants should be considered lower limits. The degradation rates under cometabolic conditions in the environment should be significantly higher.

TABLE 8.9. DEVELOPMENT OF BENZO[f]QUINOLINE BIODEGRADING ENRICHMENT CULTURES

| Source of water sample[a] | Compounds added to water sample | Days for first biodegradation | Development of culture on salts medium with | |
|---|---|---|---|---|
| | | | BQ[b] | BQ + Q[b] |
| Aeration effluent from Palo Alto Sewage Plant | BQ + Q | 3 | No | Yes |
| | BQ | --[c] | No | |
| Eutrophic pond, Woodside, CA | BQ + Q | 3 | Yes | Yes |
| | BQ | 43 | | |
| Coyote Creek, San Jose, CA | BQ + Q | 2 | Yes | Yes |
| | BQ | 15 | Yes | |
| Aeration effluent from South San Francisco plant | BQ + Q | 2 | Yes | Yes |
| | BQ | --[c] | No | |
| Aeration effluent from Shell Oil Refinery, Martinez, CA | BQ + Q | 3 | No | Yes |
| | BQ | --[c] | No | |
| Lake Tahoe, CA | BQ + Q | 8 | No | Yes |
| | BQ | --[c] | No | |

[a] Water samples diluted 4:5 with buffer and $(NH_4)_2SO_4$ solution.

[b] BQ = benzo[f]quinoline, Q = quinoline.

[c] No degradation observed in 42 days.

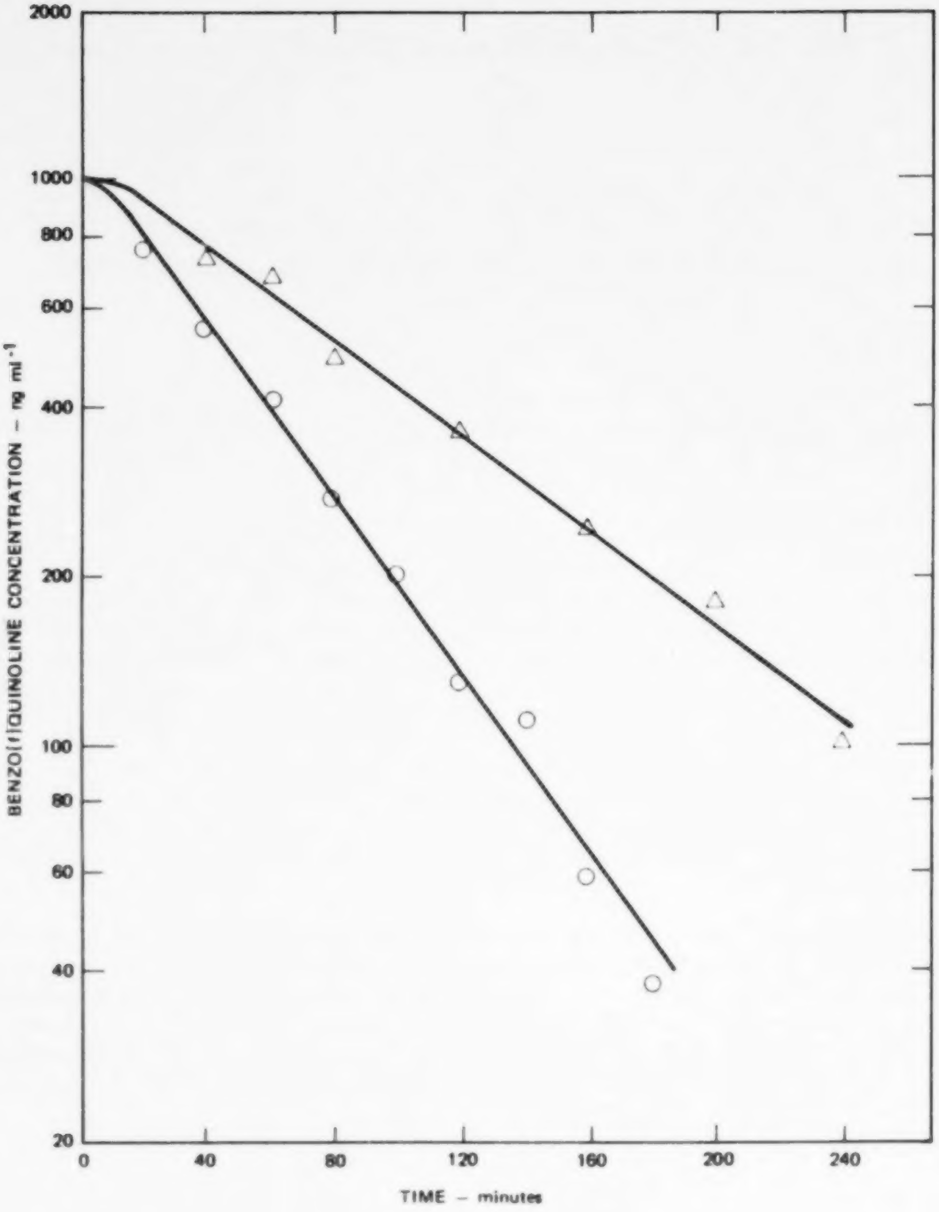

FIGURE 8.6. BENZO[f]QUINOLINE BIODEGRADATION IN BATCH FERMENTATIONS WITH HIGH CELL COUNTS

Initial cell concentration: ○ $3.0 \times 10^7$ cells ml$^{-1}$
△ $1.5 \times 10^7$ cells ml$^{-1}$

TABLE 8.10. VIABLE CELL COUNTS DURING PSEUDO-FIRST-ORDER BIODEGRADATION STUDIES WITH BENZO[f]QUINOLINE

| Time (hr) | Counts x $10^7$ $ml^{-1}$ Series 1 | Series 2 |
|---|---|---|
| 0 | 3.0 | 1.5 |
| 60 | 2.9 | 1.42 |
| 120 | 2.8 | 1.51 |
| 180 | 2.9 | 1.46 |
| 210 | 3.0 | 1.51 |
| 240 | -- | 1.41 |

### 8.6.3 Metabolites

HPLC analyses of an extract prepared during biodegradation kinetic studies revealed that one metabolite was formed. This product was not identified.

### 8.6.4 Discussion

The results of the enrichment studies illustrate the strong influence that closely related products can have on the development of biodegrading culture systems. The effluents of coal processing or petroleum plants would contain series of structurally related heteroaromatics such as the quinolines. These conditions would favor biodegradation processes similar to those observed with BQ plus quinoline. BQ would not be expected to persist for prolonged periods, but the susceptibility of derivatives of BQ cannot be estimated at this time. The development of a cometabolic system from the aeration effluent of the Shell Oil Refinery clearly indicated that the mixed culture would grow in media containing conventional nutrients plus BQ but would not degrade BQ unless quinoline were present. In nature, it is possible that other products could function in cometabolism of BQ.

The half-life indicated in the above pseudo-first-order kinetic studies was measured for a culture developed when only BQ was added to the diluted buffered Coyote Creek water. For these studies, transfers on basal salts/BQ were made at three- to four-day intervals. However, when cometabolic cultures were developed with BQ plus quinoline, transfers could be made daily and the half-life for BQ under these conditions would probably be reduced.

# 9. LABORATORY INVESTIGATION OF 9H-CARBAZOLE

## 9.1 SYNOPSIS

The results of the laboratory investigation suggest that 9H-carbazole should not be a significant environmental hazard. Both photolysis and biodegradation are rapid. Carbazole* is not sorbed strongly, and it will not accumulate in either sediments or biota. The volatilization and oxidation rates are slow. The photolysis transformation products appear to be coupling products containing one or two oxygen atoms, but their structures were not positively identified. No biodegradation products were observed, and it is likely that complete degradation occurs.

The nine-compartment environmental exposure model predicted that the steady-state concentrations of carbazole in solution, suspended solids, and sediments near point sources in the presence of a continuous discharge of 1 $\mu g\ ml^{-1}$ (1 ppm) carbazole are expected to be:

| | Half-life† (hr) | Solution ($\mu g\ ml^{-1}$) | Suspended solids ($\mu g\ g^{-1}$) | Sediments‡ ($\mu g\ g^{-1}$) |
|---|---|---|---|---|
| River | 0.5 | $9.3 \times 10^{-1}$ | 190 | 180 |
| Pond | 10 | $1.3 \times 10^{-2}$ | 2.5 | 2.5 |
| Eutrophic lake | 10 | $3.1 \times 10^{-2}$ | 6.2 | 0.88 |
| Oligotrophic lake | 3 | $4.0 \times 10^{-2}$ | 8.0 | 1.2 |

## 9.2 BACKGROUND

The pyrrole nucleus of carbazole is found in natural products and in products derived from natural substances. Carbazoles are present in coal, petroleum, peat, and the smoke from combustion of these materials (Wu and Storch, 1967; Utkina, 1965; Poulsen et al., 1974; Snyder, 1969; Braids et al.,

---

*Carbazole and 9H-carbazole are used interchangeably in this section.

†Predicted by the one-compartment model.

‡Average concentration in sediments.

1967; Hartung and Jewell, 1962; Filatova et al., 1973). Carbazoles have also been found in tobacco smoke (Hoffman et al. 1968, 1969). Carbazoles and indoles (including alkylated derivatives) have been found in the effluents from the coal processing industry (Schmidt et al., 1974; Karr et al., 1967).

9H-Carbazole was chosen for study because it is the simplest carbazole-type nitrogen heterocycle found in energy-related effluents. The results are also interesting for comparison with the results from the 7H-dibenzo [c,g] - carbazole study (Section 10) to assess the relative importance of increasing the number of aromatic rings of a basic molecular nucleus in terms of effects on the transport and transformation processes. No information on the physical transport or chemical transformation of carbazole in the environment was available when our laboratory studies began. One report was found regarding the biodegradation of carbazole. Medvedev et al. (1973) reported that carbazole was less readily degraded by soil organisms than cresols, aniline, fluorene, acenaphthene, or acridine but more readily degraded than β-naphthylamine, β-naphthol, pyrene, or chrysene.

The general physical properties of carbazole are given in Table 9.1.

TABLE 9.1. PHYSICAL PROPERTIES OF 9H-CARBAZOLE

| | |
|---|---|
| Structure | 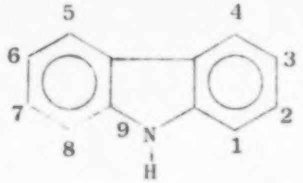 |
| Molecular weight<br>(CRC handbook, 1976-1977) | 167.21 |
| Melting point (°C)<br>(CRC handbook, 1976-1977) | 247-248 |
| Vapor pressure at 20°C (torr) | $7 \times 10^{-4}$[a] |
| Solubility in water 20°C ($\mu g\ ml^{-1}$) | $1.03 \pm 0.05$[b] |
| $pK_a$ (see text) | $\sim -3$ |
| $1.00\ \mu g\ ml^{-1}$ (1 ppm) carbazole in water = $5.98 \times 10^{-6}$ M | |

[a] Estimated using vapor pressure data from CRC Handbook, 1976-77, and Clausius-Clapeyron equation.

[b] Measured in this study, see Section 9.3.1

Carbazole is reported to have a $pK_a$ intermediate between those of indole and pyrrole (Zherebtsov and Lopatinskii, 1970). The $pK_a$ values of the compounds are -2.4 and -3.8, respectively (Perrin, 1965). This indicates that carbazole would be less than 1% in the protonated form at pH 1 and that the environmental chemistry of carbazole will involve only the free base.

The literature information on carbazole was insufficient for making preliminary assessment of the relative importance of the various transport and transformation processes in the aquatic environment. Therefore, screening studies were conducted for each of these processes.

## 9.3 ENVIRONMENTAL ASSESSMENT

### 9.3.1 Summary of Laboratory Data

The rate constants obtained in the laboratory investigation of the transformation and transport processes for 9H-carbazole are summarized in Table 9.2.

TABLE 9.2. SUMMARY OF 9H-CARBAZOLE LABORATORY DATA

| Process | Sorption equilibrium | Partition coefficient |
|---|---|---|
| Sorption[a] | $S_s = K_p S_w$ | $K_p = 175 \pm 21$ |
| | Rate expression | Rate constant at 25°C |
| Volatilization[b] | $k_v [C]$ | $k_v < k_v^0 \times 10^{-4}$ |
| Photolysis[c] | $k_p [C] = \Phi (\Sigma Z_\lambda \varepsilon_\lambda) [C]$ | $k_p = 6.6 \times 10^{-5}\ \text{sec}^{-1}$ |
| Oxidation | $k_{ox} [RO_2 \cdot] [C]$ | $k_{ox} = 29\ (M^{-1}\ \text{sec}^{-1})$ |
| Hydrolysis | NA | $k_h = 0$ |
| Biodegradation | $k_{b2} = \frac{\mu_{max}}{Y\ K_s}$ | $k_{b2} = 5 \times 10^{-7} (\text{ml cell}^{-1}\ \text{hr}^{-1})$ |

[a] On Coyote Creek sediment.

[b] See discussion in Part I, Section 5.3 of the final report.

[c] Midday sunlight in late January.

### 9.3.2 Environmental Assessment Using the One-Compartment Model

The half-lives of dissolved 9H-carbazole calculated for individual transformation of removal processes following a spill are listed in Table 9.3. Although these half-lives vary among water bodies, photolysis consistently dominates the transformation and removal processes. Biodegradation is at least 2 to 5 times slower even in the presence of large acclimated microbial populations. Oxidation half-lives are expected to be an order of magnitude greater than biodegradation half-lives except in oligotrophic lakes, where oxidation is roughly 5 times faster than biodegradation. Sorption half-lives have not been measured, but the times needed to reach equilibrium are generally less than half an hour for those compounds for which the rates have been measured. Nonetheless, since the partition coefficients were generally low, the amount of carbazole removed from the water by sorption is expected to be low, perhaps 1% to 6% of the amount entering the water body.

Thus, excluding the effects of dilution, the half-life for removal of carbazole from natural waters may be as short as 3 hours in oligotrophic lakes during the day in the summer, and a long as 4 days in eutrophic lakes during the winter.

TABLE 9.3. TRANSFORMATION AND TRANSPORT OF 9H-CARBAZOLE PREDICTED BY THE ONE-COMPARTMENT MODEL

| | River | Eutrophic pond | Eutrophic lake | Oligotrophic lake |
|---|---|---|---|---|
| Photolysis, half-life (hr)[a] | 6 | 15 | 15 | 3 |
| Oxidation, half-life (hr) | >240 | >240 | >240 | >240 |
| Volatilization, half-life (hr) | $> 10^5$ | $> 10^5$ | $> 10^5$ | $> 10^5$ |
| Hydrolysis, half-life (hr) | -- | -- | -- | -- |
| Biodegradation, half-life (hr) | 14 | 14 | 14 | >1000 |
| Half-life for all processes except dilution (hr) | 5 | 10 | 10 | 3 |
| Half-life for all processes including dilution (hr) | 0.5 | 10 | 10 | 3 |
| Amount carbazole sorbed (mg $m^{-3}$)[b] | 20 | 60 | 10 | 10 |
| Percentage carbazole sorbed | 2.0% | 5.6% | 1% | 1% |

[a] Estimates are the average photolysis rates on a summer day at 40° latitude. Photolysis rates in midwinter are at least three times slower.

[b] 1 $\mu g\ ml^{-1}$ of 9H-carbazole in aqueous phase and partition coefficient of 200 are assumed.

### 9.3.3 Persistence

The persistence of concentrations that approximate the initial concentrations following an acute discharge should largely be a function of the dilution rate in fast flowing streams. Persistence of relatively high concentrations in lakes and ponds is expected to be determined by rates of transformation within the aqueous phase. Sorption is not expected to significantly affect the persistence of concentrations approximating those prevailing immediately after a spill, but it will be a major determinant of the relatively low concentrations of carbazole to be expected in ensuing weeks as desorption from contaminated sediments becomes the major source of carbazole in solution.

Carbazole may be more persistent in eutrophic water than in oligotropic waters if the major transformation pathway, photolysis, is less effective in such waters, as assumed in Table 9.3. This tendency is unlikely to be present except in frequently contaminated waters. Even in these waters there may be a lag of several hours before biodegradation begins. Moreover, since the sediment loading is typically higher in eutrophic waters, the amount of carbazole sorbed to suspended solids should be greater than in oligotrophic waters, creating a larger reservoir of carbazole that is subject to later desorption and therefore the presence of low concentrations of carbazole for long periods.

### 9.3.4 Mass and Concentration Distributions Calculated Using Computer Models

Table 9.4 summarizes the distribution of mass and concentration of carbazole expected at steady state during chronic discharge to each of four types of water bodies, as calculated with the aid of the computer model. The pseudo-first-order rate constants used in these simulations are presented in Appendix A.

The steady-state concentrations of carbazole in solution in the simulated stream segments imply a removal from solution of approximately 3% per kilometer. However, in smaller, and hence more slowly flowing rivers than we have assumed in the simulations, 10% to 20% of carbazole may be removed within the same river reach.

The steady-state concentrations of carbazole in solution are roughly $10^{-2}$ to $10^{-4}$ $\mu$g ml$^{-1}$ in pond and lake simulations. This is roughly 100 to 10,000 times less than the input concentrations (Table 9.4). In the pond simulation, the steady-state concentration of carbazole is estimated to be 1% of the concentration in inflowing waters. Within the lake simulations, the concentrations of dissolved carbazole in the surface waters decrease 100-fold with increasing distance from the source, and concentrations in the hypolimnion are predicted to be 1,000 times lower than the concentrations in inflowing waters.

The model predicts that virtually all the carbazole is in the bottom sediments at steady state, because it is assumed that carbazole concentration in sediments equals the concentrations on suspended solids at steady state and that carbazole does not undergo transformation following sorption. We suspect, however, that biodegradation of carbazole may take place in the sediment layers. Hence, the estimated values of carbazole in sediment are probably upper limits

TABLE 9.4. DISTRIBUTION OF 9H-CARBAZOLE IN VARIOUS AQUATIC SYSTEMS AT STEADY STATE
(input concentrations of 1 $\mu g\ ml^{-1}$ 9H-carbazole)

| | Pond | | River | | Eutrophic Lake | | Oligotrophic Lake | |
|---|---|---|---|---|---|---|---|---|
| | Mass (kg) | Conc. ($\mu g\ g^{-1}$) | Mass (kg) | Conc. ($\mu g\ g^{-1}$) | Mass (kg) | Conc. ($\mu g\ g^{-1}$) | Mass (kg) | Conc. ($\mu g\ g^{-1}$) |
| Compartment 1 (surface water) | | | | | | | | |
| Solution | $2.6 \times 10^{-1}$ | $1.3 \times 10^{-2}$ | $2.8 \times 10^{2}$ | $9.3 \times 10^{-1}$ | 7.8 | $3.1 \times 10^{-2}$ | $1.0 \times 10$ | $4 \times 10^{-2}$ |
| Suspended solids | $1.5 \times 10^{-2}$ | 2.5 | 5.6 | $1.9 \times 10^{2}$ | $7.8 \times 10^{-2}$ | 6.24 | $1.0 \times 10^{-1}$ | 8 |
| Compartment 2 (surface water) | | | | | | | | |
| Solution | -- | -- | $2.7 \times 10^{2}$ | $9.0 \times 10^{-1}$ | 2.3 | $9.2 \times 10^{-4}$ | 3.8 | $1.5 \times 10^{-3}$ |
| Suspended solids | -- | -- | 5.4 | $1.8 \times 10^{2}$ | $2.3 \times 10^{-2}$ | $1.8 \times 10^{-1}$ | $3.8 \times 10^{-2}$ | $3.0 \times 10^{-1}$ |
| Compartment 3 (surface water) | | | | | | | | |
| Solution | -- | -- | $2.6 \times 10^{2}$ | $8.6 \times 10^{-1}$ | $8.2 \times 10^{-2}$ | $3.3 \times 10^{-4}$ | $1.7 \times 10^{-1}$ | $6.8 \times 10^{-4}$ |
| Suspended solids | -- | -- | 5.2 | $1.7 \times 10^{2}$ | $8.2 \times 10^{-4}$ | $6.6 \times 10^{-2}$ | $1.7 \times 10^{-3}$ | $1.4 \times 10^{-1}$ |
| Compartment 5 (bottom water) | | | | | | | | |
| Solution | -- | -- | -- | -- | $2.9 \times 10^{-2}$ | $1.1 \times 10^{-5}$ | $1.4 \times 10^{-1}$ | $5.6 \times 10^{-5}$ |
| Suspended solids | -- | -- | -- | -- | $2.9 \times 10^{-4}$ | $2.3 \times 10^{-3}$ | $1.4 \times 10^{-3}$ | $1.1 \times 10^{-2}$ |
| Compartments 7-9 (sediment)[a] | | | | | | | | |
| Solution | $3.3 \times 10^{-3}$ | $1.3 \times 10^{-2}$ | $6.8 \times 10$ | $9.0 \times 10^{-1}$ | $3.84 \times 10^{-2}$ | $4.4 \times 10^{-3}$ | $5.12 \times 10^{-2}$ | $5.8 \times 10^{-3}$ |
| solids | 1.7 | 2.5 | $3.7 \times 10^{3}$ | $1.8 \times 10^{2}$ | 12 | $8.8 \times 10^{-1}$ | 16 | 1.2 |
| Total mass | 2.0 | | $4.4 \times 10^{3}$ | | 22 | | 21 | |

[a] The amounts given for solid and solution phases in the sediment compartments (7, 8, and 9) are based on the assumption that the carbazole concentration in the solution phases of these compartments at steady state is the same as the concentrations in the solution phases of the adjacent water compartments (2, 5, and 3, respectively). These concentrations may be overestimated because it was assumed sorbed material is not biodegraded.

for the concentrations that may be expected in natural environments. Values shown in Table 9.4 for sediments are estimated from the above assumption. Note that the interchanges between water compartments and sediment compartments are slow processes. Sediment compartments may require very long times before steady-state conditions are established.

If an acclimated microbial culture is developed in the receiving water bodies, biodegradation may contribute significantly to carbazole removal. Figure 9.1 illustrates the effects of varied assumptions regarding metabolic activity in a partially mixed two-compartment pond system. Steady-state concentrations of carbazole in the pond simulations vary 1.5 to 3.0-fold in response to a 30-fold variation in biotransformation rates. Variations in the steady-state concentrations following termination of discharge are as much as 20-fold, roughly the range by which the biotransformation rates varied.

Figure 9.1 also shows the buildup and decline of carbazole in the pond simulation during and following discharge. Steady states are reached within two days for the solution and suspended solid phases, but concentrations in the sediments are still increasing slowly when discharge is stopped on the seventh day. Predicted carbazole concentrations in the suspended solid and solution fractions decline fairly rapidly after discharge stops and approach a new steady state in about four days. Desorption then provides a lower limit to the decreases in the concentrations of carbazole in the dissolved and suspended solids fractions, giving a relatively long-lived loading in the water column of roughly $10^{-7}$ $\mu g\ ml^{-1}$. The half-life of carbazole following a spill, as estimated from the rate of decline in the pond simulation, is approximately the same as that predicted by the one-compartment model.

Similar patterns prevail in the river simulation (Figure 9.2) except that steady-state conditions are obtained far more rapidly (within hours instead of days). Because of the high dilution rates in the stream and the presence of multiple compartments, the concentration of carbazole in solution changes abruptly in the first compartment after discharge is stopped, since from then on it receives only uncontaminated water. Successively less abrupt changes occur in the downstream compartments because they receive water that is increasingly contaminated by carbazole desorbed from the sediments of the previous compartment. This downstream movement of the area of highest concentration of dissolved carbazole conceals the role of the initial source, which is now 2 km upstream from the area of maximum concentration. Similar shifts occur in the concentrations of carbazole on suspended solids, but are omitted from the figure for the sake of clarity.

Buildup and declines in the lake simulations (Figures 9.3 and 9.4) most nearly resembled the pond simulations. During the period of accumulation of carbazole, large amounts of carbazole appear in the compartment receiving the discharge, little in the distant surface compartments, and even less in the bottom waters because of the slow transports between hypolimnion and epilimnion. However, during the fall and spring overturns, rapid vertical mixing of the lake waters should result in significant transport of carbazole to the lower portions of the lake, causing relatively high concentrations in the hypolimnion for one to three weeks. After discharge stops, the concentration of carbazole in the hypolimnion is predicted to be higher than that in the surface compartment furtherest from the source.

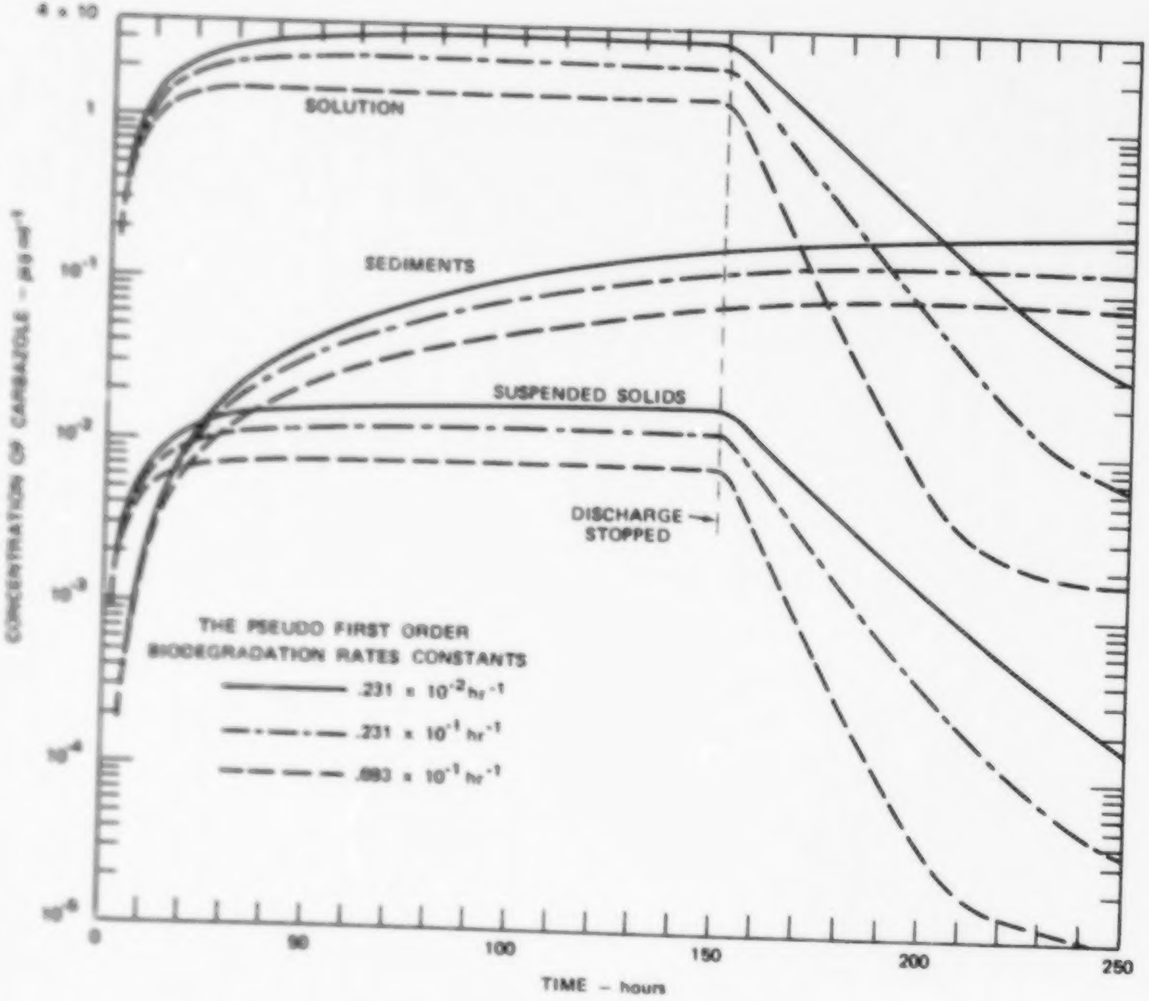

FIGURE 9.1 PERSISTENCE OF 9H-CARBAZOLE IN A PARTIALLY MIXED TWO-COMPARTMENT POND SYSTEM

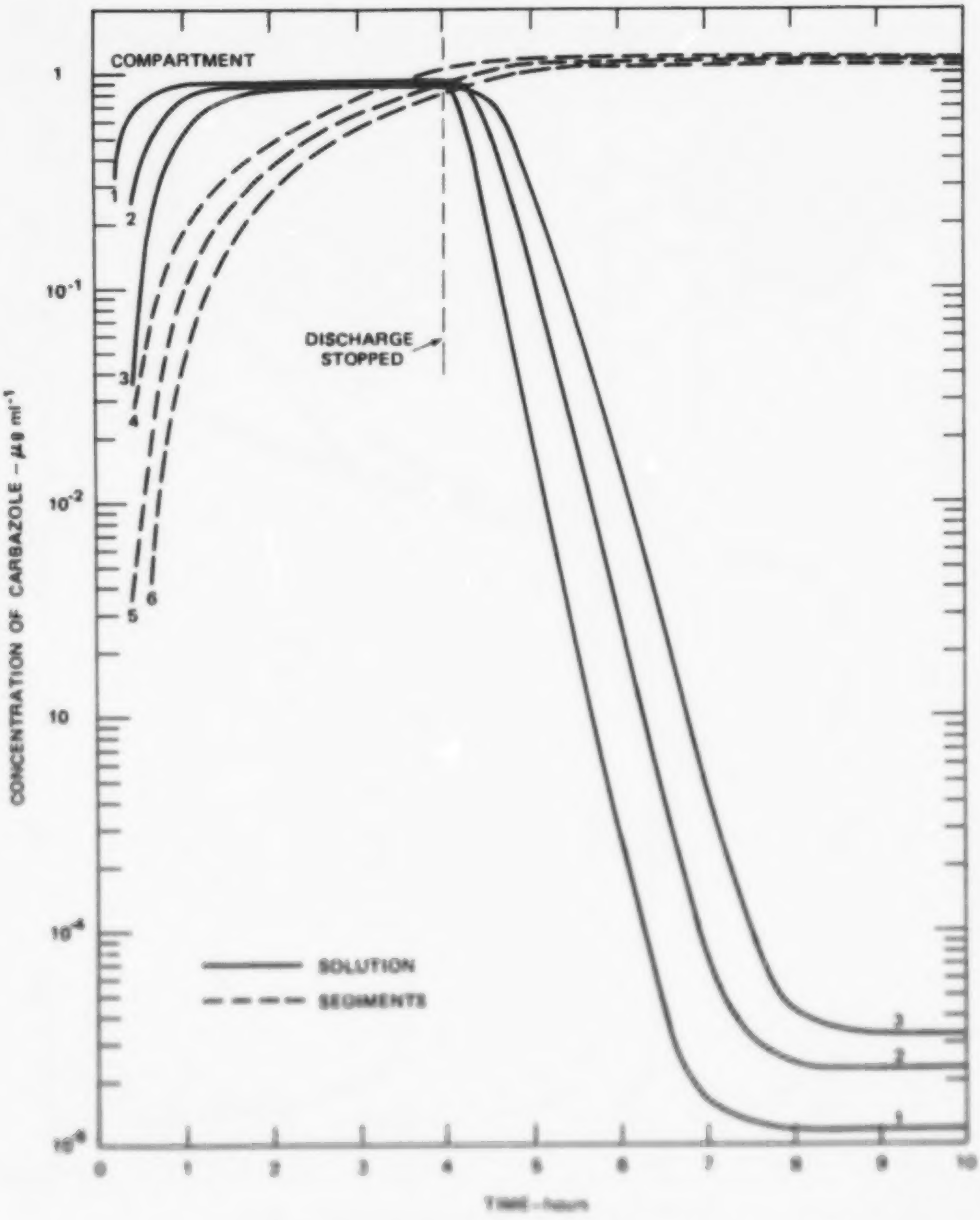

FIGURE 6.2 PERSISTENCE OF 9H-CARBAZOLE IN A PARTIALLY MIXED RIVER SYSTEM

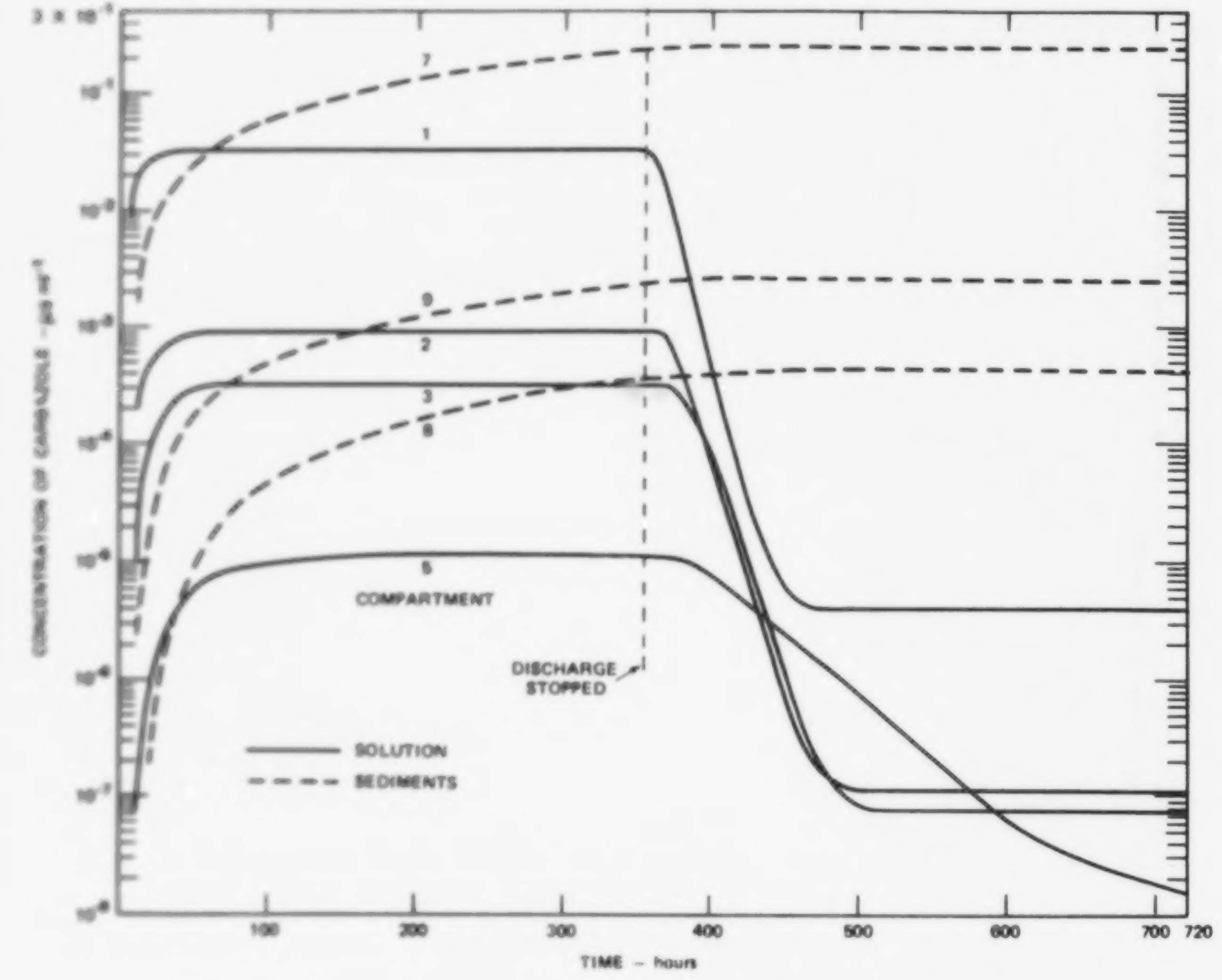

FIGURE 9.3 PERSISTENCE OF 9H-CARBAZOLE IN A EUTROPHIC LAKE

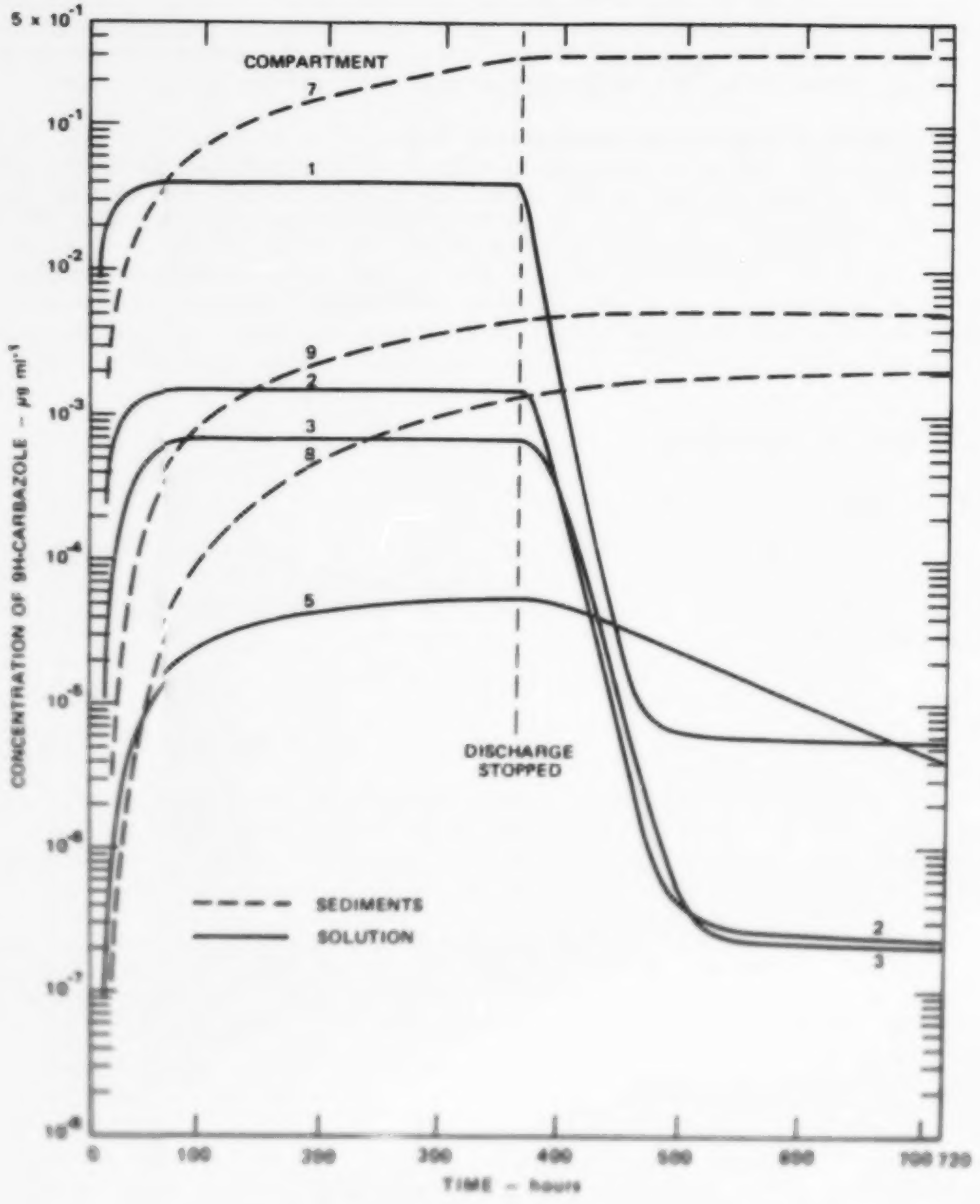

FIGURE 9.4 PERSISTENCE OF 9H-CARBAZOLE IN AN OLIGOTROPHIC LAKE

### 9.3.5 Discussion

Despite the uncertainties inherent in extrapolating laboratory data to the field, it is evident that the concentrations of carbazole should rapidly decline by 5 to 6 orders of magnitude after discharges to the water are stopped. The concentrations of carbazole in lakes should reach a new steady state within one to two weeks after discharges are stopped and within hours in rivers.

The most significant uncertainty lies in the estimation of the ultimate concentration of the carbazole, since this is determined largely by the properties of the sediments, and in the potential biological effects. Since the partition coefficient of carbazole is sensitive to the composition of the sediments, the ultimate concentration of carbazole in water bodies with a long history of pollution with carbazole may vary by one or two orders of magnitude even if discharges are stopped. However, the significance of the variations cannot be appraised with the available toxicological data. We can only say that the concentrations will be quite low shortly after discharges stop.

## 9.4 PHYSICAL PROPERTIES

### 9.4.1 Solubility in Water

The solubility of 9H-carbazole in water at room temperature (20.0 ± 0.1°C) was measured using the method described by Campbell (1930). The average solubility was 1.03 ± 0.05 $\mu g\ ml^{-1}$ [6.16(± 0.30) x $10^{-6}$ M], based on replicate determinations.

### 9.4.2 Absorption Spectrum

9H-Carbazole absorbs light strongly in the solar region to 400 nm.

The absorption spectrum of 9H-carbazole in 26% acetonitrile/74% water was measured from 210 to 500 nm. The pH of the solution was 7 and was not adjusted. The absorption coefficients at wavelength intervals from 297.5 to 400 nm and at wavelengths of 313 and 366 nm are reported in Table 9.5.

The pH-dependence of the absorption spectrum was not measured because our estimate of the $pK_a$ of 9H-carbazole (∿ -3, Section 9.2), indicated that less than 1% would be in the protonated form even at pH 1. The environmental chemistry of carbazole will involve only the free base form.

### 9.4.3 Volatilization Rate

The volatilization rate of 9H-carbazole was measured using the method of Hill et al. (1976), which is described in detail in Appendix B of this report. The concentration of carbazole did not change measurably over the four-day period of the experiment. The average oxygen reaeration rate was 3.76 ± 1.82 $hr^{-1}$.* An upper limit for the volatilization rate

---

* This value represents the average and standard deviation of four reaeration measurements taken over the period of the experiment.

TABLE 9.5. ABSORPTION SPECTRUM OF 9H-CARBAZOLE IN 26% ACETONITRILE/74% WATER (V/V) AT pH 7[a]

| Center of wavelength interval[b] | Average absorption coefficient[c] ($M^{-1}$ $cm^{-1}$) |
|---|---|
| 297.5 | 5540 |
| 300.0 | 3100 |
| 302.5 | 2440 |
| 305.0 | 2270 |
| 307.5 | 2390 |
| 310.0 | 2530 |
| 312.5 | 2600 |
| 315.0 | 2700 |
| 317.5 | 2920 |
| 320.0 | 3190 |
| 323.1 | 3170 |
| 330 | 2900 |
| 340 | 1520 |
| 350 | 166 |
| 360 | 23 |
| 370 | 13 |
| 380 | 12 |
| 390 | 2 |
| 400 | 0 |

[a] 9H-Carbazole concentration was 40.8 μg $ml^{-1}$ ($2.44 \times 10^{-4}$ M).

[b] The wavelength intervals are given in Appendix B, Table B.1.

[c] The absorption coefficients at 313.0 and 366.0 nm are 2600 and 12 $M^{-1}$ $cm^{-1}$, respectively.

constant was therefore estimated based on the measurement error. The 95% confidence limit (two times the average standard deviation) of the measurements of the carbazole concentration was 0.654 ± 0.24 μg $ml^{-1}$. Therefore, the lowest possible final concentration of carbazole at the end of the experiment was about 0.63 μg $ml^{-1}$. Therefore

$$k_v^C < [-\ln(0.63/0.654)]/94 = 4 \times 10^{-4} \text{ hr}^{-1} \tag{9.1}$$

and

$$\frac{k_v^C}{k_v^O} < 1 \times 10^{-4} \tag{9.2}$$

### 9.4.4 Sorption on Clay and Sediments

The sorption partition coefficients of 9H-carbazole were measured on Ca-montmorillonite clay and Coyote Creek sediment. Care was taken to assure that the samples were protected from light at all times to minimize photolysis of the carbazole (Section 9.5.1). The initial concentration of carbazole in each sample was always less than the saturation concentration of 1.0 μg $ml^{-1}$. Each experiment consisted of replicate samples at one carbazole concentration and two sediment loadings, plus blanks that contained only carbazole. The data are summarized in Table 9.6.

The calculation of the partition coefficient was based on the results of the analysis of the supernatant at equilibrium. The amount of carbazole sorbed on the sediments was calculated by finding the difference betwen the initial amount and the amount that was found in the supernatant afterequilibration with the sediment. The estimates reported in Table 9.6 show hat sediment sorption is not an important environmental pathway for 9H-cabazole compared with photo-oxidation and biodegradation. Therefore, no furter studies of the sorption of carbazole by either sediments or microorganisms wee carried out.

### 9.4.5 Biosorption

Because of the rapid development of enrichment cultures, rapi photolysis, and low sorption coefficients on clays and sediments, biosorpton studies did not appear to be warranted and were not conducted.

## 9.5 CHEMICAL TRANSFORMATIONS

### 9.5.1 Photolysis Rate

The photolysis of 9H-carbazole is rapid and unaffected by oxygen; in sunlight the half-life for direct photolysis is less than a day. Photolysis experiments were conducted with 1.0 μg $ml^{-1}$ concentrations of 9H-carbazole in pure water and in natural waters from several sources. These waters also con-

## TABLE 9.6. SORPTION OF 9H-CARBAZOLE ON SEDIMENTS

| Sediment | Total organic carbon (percent) | Sediment concentration ($\mu g\ ml^{-1}$) | Carbazole concentration in supernatant ($\mu g\ ml^{-1}$)$^{a}$ | Carbazole concentration on sediment ($\mu g\ g^{-1}$)$^{b}$ | Partition Coefficient, $k_p$ LLS$^{c}$ |  |
|---|---|---|---|---|---|---|
|  |  |  |  |  | $a_o = 0$ | $a_o \neq 0$ |
| Ca-montmor-illonite clay | 0.06 | 13<br>25 | 0.52 ± 0.01<br>0.50 ± 0.01 | 1.9 ± 1.1<br>1.7 ± 0.5 | 3.2 ± 1.1 | -3.2 ± 2.4<br>($a_o$ = 18 ± 12) |
| Coyote Creek | 1.4 | 6.8<br>14 | 0.24 ± 0.03<br>0.14 ± 0.01 | 41 ± 4<br>29 ± 1 | 175 ± 21 | 87 ± 52<br>($a_o$ = 18 ± 10) |

---

[a] Concentration measured in supernatant with population standard deviation.

[b] Concentration on sediment calculated from supernatant concentration with population standard deviation.

[c] LLS = linear least squares; see Appendix B, Section B.1.4 for description of regressions. Limits are 95% confidence limit.

tained 1% acetonitrile to increase the solubility of carbazole. Data for photolysis of 9H-carbazole in sunlight and at 313 nm are summarized in Table 9.7. Good first-order kinetic behavior was found for photolyses at 313 nm carried out to beyond two half-lives of carbazole. The quantum yield for 9H-carbazole phototransformation in pure water (containing 1% acetonitrile) is 7.6 ($\pm$ 0.3) x $10^{-3}$.

Photolysis experiments carried out at 313 nm on 1.0 $\mu$g ml$^{-1}$ 9H-carbazole solutions that had been purged with nitrogen showed that oxygen had no effect on the photolysis rate. The photolysis of 9H-carbazole in 100% acetonitrile with 313 nm light was slow. The rate constant was less than 2 x $10^{-6}$ sec$^{-1}$, which is only 3% of the rate constant found for the direct photolysis of 9H-carbazole in 1% acetonitrile in water as solvent (see Table 9.7). The reaction must then be some kind of photohydration process.

The data in Table 9.7 show that the photolysis rates of carbazole in waters from Lake Tahoe or Coyote Creek are the same within experimental error as the rate in pure water. The experiments with Searsville Pond water and in pure water containing 8.0 $\mu$g ml$^{-1}$ humic acid do show retardation of the photolysis rate, but these slower rates are accounted for by screening by the natural substances in the waters. The absorbances of 0.08 for Searsville Pond water and 0.43 for humic acid in water account for the 25% and 66% decrease in rate due to reduced light intensity.

TABLE 9.7. RATE CONSTANTS FOR PHOTOLYSIS OF 1.0 $\mu$g ml$^{-1}$ 9H-CARBAZOLE[a]

| Irradiation source | Solution[b] | Extent of reaction (%) | Rate constant ($k_p$ x $10^5$ sec$^{-1}$) |
|---|---|---|---|
| 313 nm | Pure water | 85 | 7.50 $\pm$ 0.18[c,d] |
| 313 nm | Lake Tahoe water | 87 | 7.69 $\pm$ 0.38 |
| 313 nm | Coyote Creek water | 73 | 7.66 $\pm$ 0.39 |
| 313 nm | Searsville Pond water | 65 | 5.74 $\pm$ 0.23 |
| 313 nm | Humic acid (8 $\mu$g ml$^{-1}$) in pure water | 35 | 2.46 $\pm$ 0.11 |
| Sunlight, midday late January | Pure water | 57 | 6.59 $\pm$ 1.21[e] |

[a] 1.00 $\mu$g ml$^{-1}$ 9H-carbazole in water = 5.98 x $10^{-6}$ M.

[b] Solutions contained 1% acetonitrile as cosolvent.

[c] Standard deviation

[d] Quantum yield for disappearance of 9H-carbazole at 313 nm was 7.6 x $10^{-3}$.

[e] Half-life of 2.9 hours.

The half-life for direct photolysis of carbazole in sunlight as a function of the time of day was calculated by the procedure of Zepp and Cline (1977) using a quantum yield of $7.6 \times 10^{-3}$ measured at 313 nm and the measured uv spectrum of carbazole. The data are plotted in Figure 9.5. The instantaneous half-life of 2.7 hours calculated for midday in winter is in excellent agreement with the measured half-life of 2.9 hours.

### 9.5.2 Oxidation Rate

The susceptibility of 1.0 $\mu g\ ml^{-1}$ ($6.0 \times 10^{-6}$ M) 9H-carbazole to free radical oxidation was examined using the AA-initiated oxidation reaction. See Part I, Section 6.3 of this report and Appendix B for discussion and procedure. This experiment was carried out at 50.0°C in 1% acetonitrile in water containing $1.0 \times 10^{-4}$ M AA. At the end of 136 hours, 32% of the carbazole had been reacted. A rate constant ($k_{ox}[RO_2\cdot]$) of 8.08 (± 0.36) $\times 10^{-7}$ $sec^{-1}$ was obtained for the oxidation of 9H-carbazole under the reaction conditions; this rate constant corresponds to a half-life of 9.9 days. Under these conditions (Part I, Section 6.3), this corresponds to a second-order rate constant $k_{ox}$ of $2.6 \times 10^2\ M^{-1}\ sec^{-1}$. At 25°C, $k_{ox}$ would be 29 $M^{-1}\ sec^{-1}$ and with the assumption that $[RO_2\cdot] = 10^{-9}$ M in the environment, the half-life of carbazole toward oxidation is ~280 days. The free radical oxidation of carbazole by $RO_2\cdot$ is clearly not competitive with photolysis or biodegradation of carbazole under aquatic environmental conditions.

### 9.5.3 Hydrolysis Rate

Carbazole contains no groups that are hydrolyzable; therefore, no hydrolysis studies were carried out.

### 9.5.4 Products from Chemical Transformation

Four compounds were isolated by HPLC from the direct photolysis of carbazole and subjected to mass spectrometry. However, only two products could be identified as being derived from 9H-carbazole, giving apparent molecular ions of m/e 364 and 368 (9H-carbazole has m/e = 167). These values indicate that both products are coupling products of carbazole (molecular weight of 332), with the m/e 364 having two added oxygen atoms. Since the photolysis rate was unaffected by the presence of oxygen and photolysis did not occur except in the presence of water, we assume that the source of the oxygen is water. The m/e 368 product corresponds to addition of two water molecules to a 9H-carbazole coupling product (36 + 332). No further information was provided by the mass spectra. Some additional structure information seems necessary to identify these products.

## 9.6 BIODEGRADATION

### 9.6.1 Development of Enrichment Cultures

Enrichment studies were initiated with 5-liter liquid volumes in 9-liter, aerated bottle-fermentors. 9H-Carbazole (50 $mg\ ml^{-1}$ in DMSO) was added

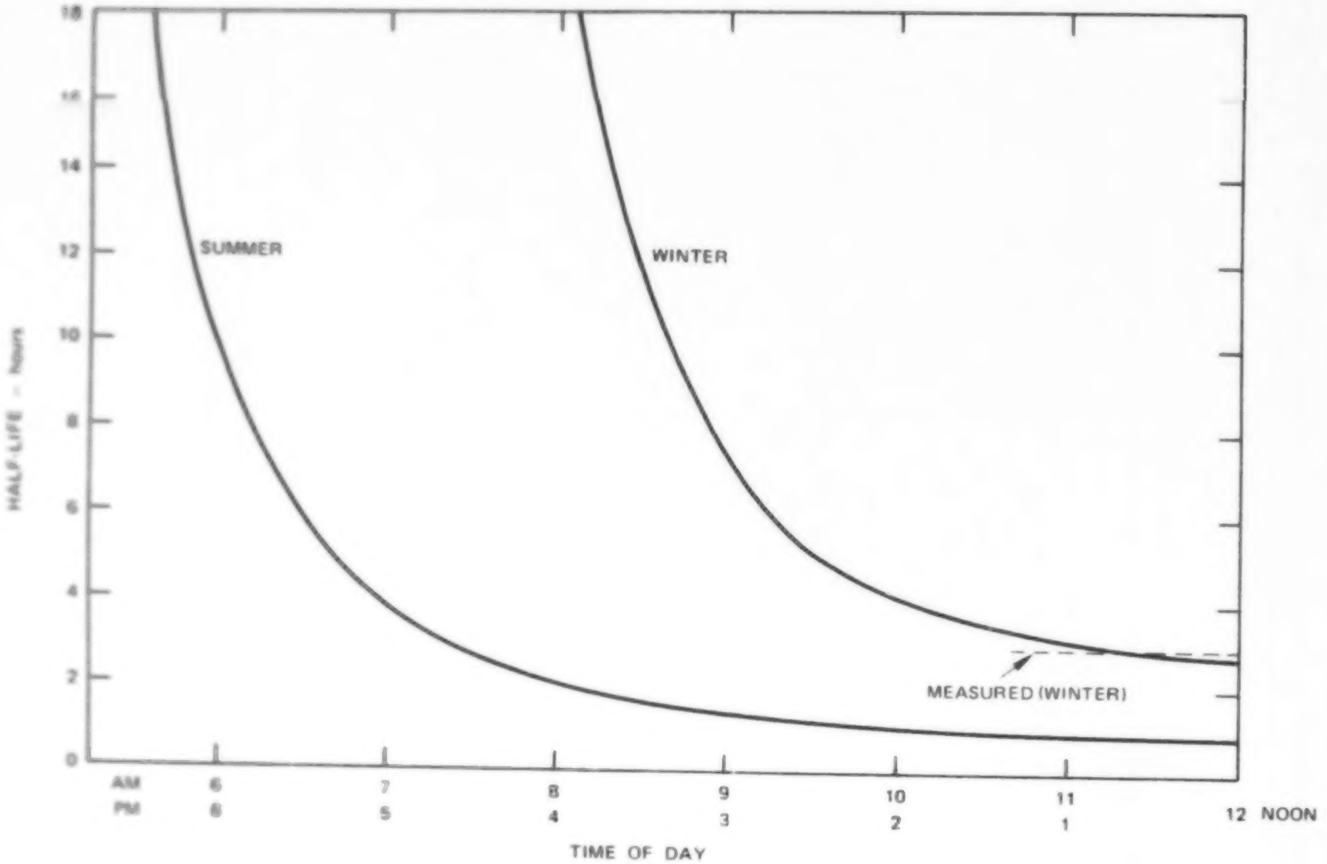

FIGURE 9.5 SEASONAL AND DAILY VARIATION OF PHOTOLYSIS HALF-LIFE OF 9H–CARBAZOLE

to these fermentors to give initial concentrations of 10 μg $ml^{-1}$. This level is about 10 times the solubility of 9H-carbazole (Section 9.4.1) and some precipitation was observed. Water samples used in these enrichment studies and the characteristics of the first observations of 9H-carbazole biodegradations are presented in Table 9.8.

TABLE 9.8. DEVELOPMENT OF 9H-CARBAZOLE BIODEGRADATION ENRICHMENT CULTURES

| | First observations of biodegradations | |
|---|---|---|
| Sources of samples | Days of incubation | Percent degraded[a] |
| Coyote Creek, San Jose, CA | 6 | 70% |
| Pond near Searsville Lake, Woodside, CA | 6 | 90 |
| Palo Alto Sewage Plant, Palo Alto, CA | 5 | 99 |
| South San Francisco Sewage Plant, South San Francisco, CA | 5 | 70 |
| Shell Oil Refinery Industrial Waste Plant, Martinez, CA | 11 | 60 |
| Lake Tahoe, CA | 42 | 0 |

[a] Determined by UV assay.

In all cases, subtransfers were readily adapted to growth on 9H-carbazole/inorganic salts media in shaker flasks incubated at 25°C. The 9H-carbazole concentrations in the media were raised progressively from 10, to 30, and finally to 100 μg $ml^{-1}$. Before the individual culture systems were preserved in the vapor space in a Dewar flask containing liquid nitrogen, > 90% biodegradation of 100 μg $ml^{-1}$ 9H-carbazole media was generally observed in 24 to 48 hours of incubation with 2% (v/v) inocula.

## 9.6.2 Biodegradation Kinetics

Because of the low solubility of carbazole and the lower limits of detection by HPLC (0.1 μg $ml^{-1}$), pseudo-first-order kinetic studies (see Part I, Section 7.2 of this report) were conducted with a biodegrading culture system developed from the Palo Alto sewage plant aeration effluent. These studies involved two series of batch fermentations (experiments 1 and 2, Table 9.9) with initial 9H-carbazole concentrations of 0.7 and 0.8 μg $ml^{-1}$, respectively. Each series of kinetic studies was initiated with two levels of stationary phase cells (a and b, Table 9.9).

The carbazole concentration versus time data are plotted in Figures 9.6 and 9.7. The complete metabolism of 9H-carbazole did not result in any

TABLE 9.9. CELL COUNTS[a] DURING KINETIC STUDIES OF THE BIODEGRADATION OF 9H-CARBAZOLE

| Time (hr) | Experiment | | | |
|---|---|---|---|---|
| | 1a | 1b | 2a | 2b |
| 0 | 4.7 | 1.41 | 1.69 | 0.76 |
| 0.5 | 4.6 | 1.57 | 1.44 | 0.69 |
| 1.0 | 4.7 | 1.51 | 1.63 | 0.70 |
| 1.5 | | 1.65 | 1.62 | 0.78 |
| 2.0 | | | | 0.91 |
| 2.5 | | | | 0.71 |

[a] Cell x $10^{-7}$ $ml^{-1}$.

significant change in microbial mass, as shown by the data in Table 9.9. In the lower cell-count experiment 1b, there was a lag period of approximately 6 minutes before rapid degradation took place. No lag period was observed with the higher cell population.

The pseudo-first-order rate constants, $k'_{b1} = k'_{b2}X_o$ were calculated from the slopes of the plots of ln [carbazole] versus time (Figures 9.6 and 9.7). From these data, the second-order rate constants were calculated by using the following relationship:

$$k'_{b2}\ (\text{ml cells}^{-1}\ \text{hr}^{-1}) = \frac{k'_{b1}}{\text{cells ml}^{-1}} \qquad (9.3)$$

Values obtained for $k'_{b1}$ and $k'_{b2}$ are listed in Table 9.10.

After experiments 1a and 1b, the mixed culture was refrigerated for two days, and three sequential 2% (v/v) transfers were made daily in 100 μg $ml^{-1}$ carbazole/basal salts medium, followed by two daily 10% (v/v) transfers into 50 μg $ml^{-1}$ carbazole/basal salts medium. In contrast with previous observations, the first fermentation with the 10% inoculum resulted in slower degradation of carbazole. However, with the second 10% inoculum, carbazole was completely degraded in 18 hours.

These cells were used for the second kinetic study (experiments 2a and 2b) conducted under conditions similar to those described above; results are presented in Figure 9.7 and Table 9.10. In this study, with both levels of cultures, there were lag periods in which carbazole was slowly degraded. After the lag period, the degradation rates were greater then those in the first kinetic study (experiments 1a and 1b, Figure 9.6). For experiments 2a and 2b the rate constants were calculated from data obtained during the period of rapid degradation. Considering the fact that the mixed culture behaved quite differently in the two experiments during preparation of cells for kinetic

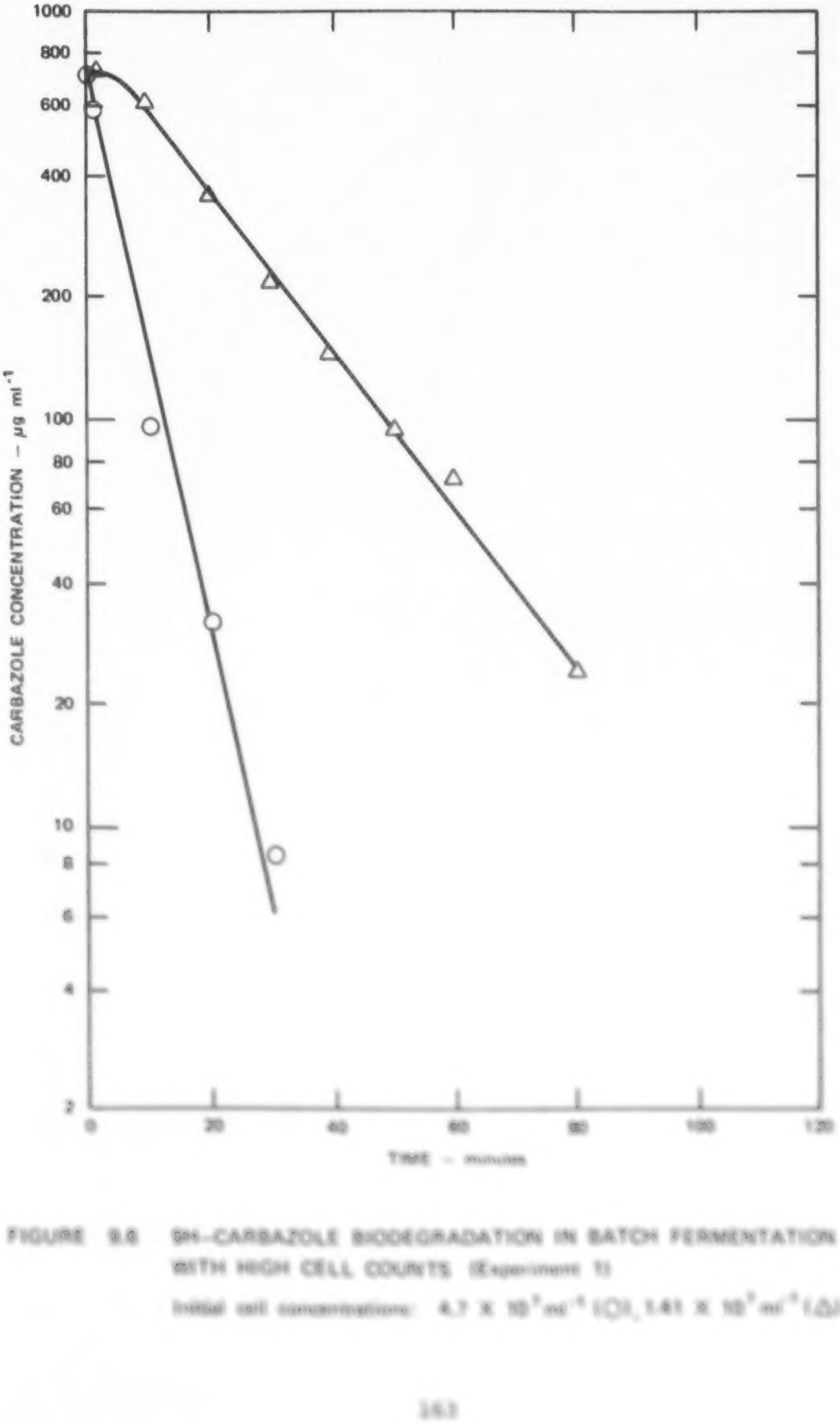

FIGURE 9.6 9H–CARBAZOLE BIODEGRADATION IN BATCH FERMENTATION WITH HIGH CELL COUNTS (Experiment 1)

Initial cell concentrations: 4.7 X $10^7$ $ml^{-1}$ (○), 1.41 X $10^7$ $ml^{-1}$ (△)

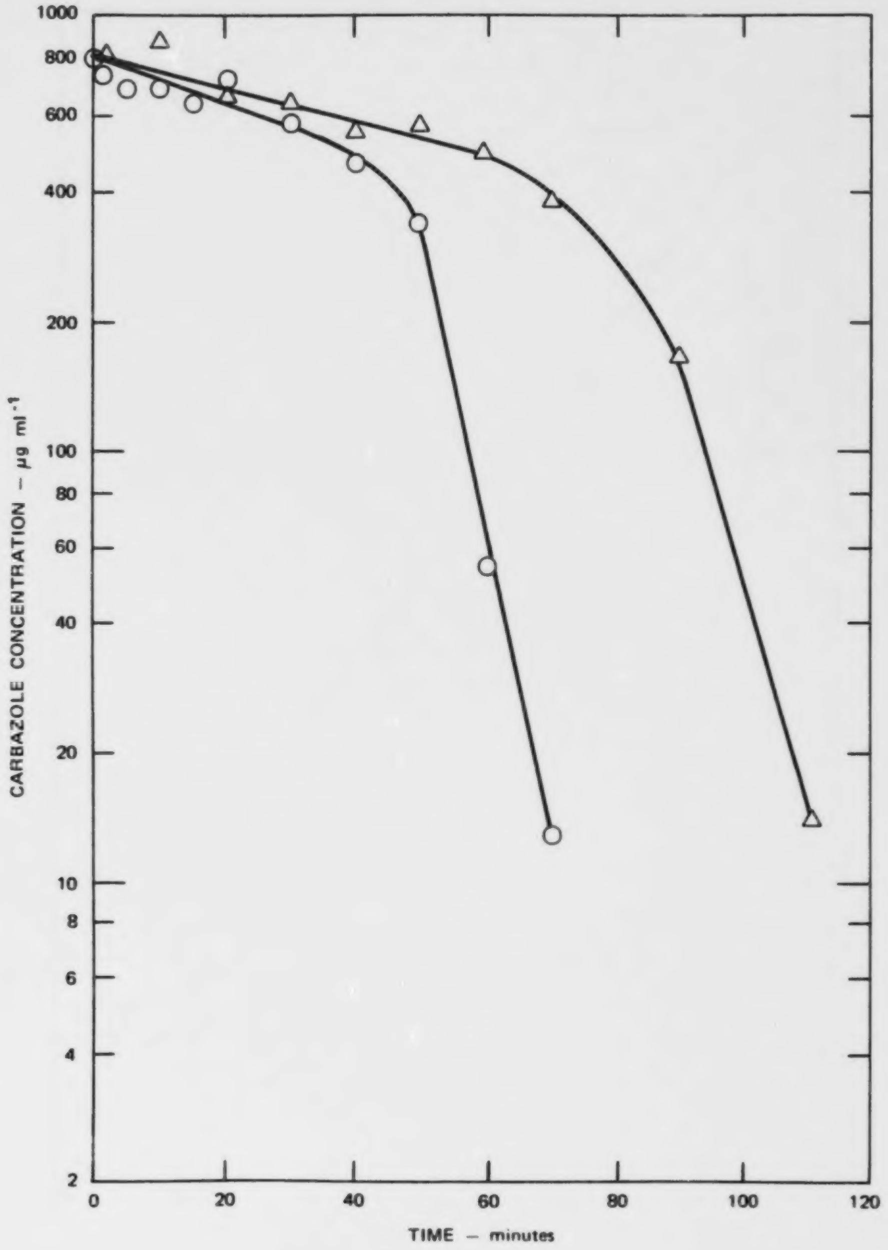

FIGURE 9.7 9H–CARBAZOLE BIODEGRADATION IN BATCH FERMENTATION WITH HIGH CELL COUNTS (Experiment 2)

Initial cell concentrations: $1.69 \times 10^7$ ml$^{-1}$ (○), $0.76 \times 10^7$ ml$^{-1}$ (△)

TABLE 9.10. RATE CONSTANTS FOR BIODEGRADATION OF 9H-CARBAZOLE

| Experiment[a] | Initial cell level (cell $ml^{-1}$) x $10^7$ | Pseudo-first-order rate constants ($hr^{-1}$) | Second-order rate constant (ml $cell^{-1}$ $hr^{-1}$) x $10^7$ |
|---|---|---|---|
| 1a | 1.4 | 2.7 | 1.9 |
| 1b | 4.7 | 9.2 | 2.0 |
| 2a | 0.76 | 7.3 | 9.6 |
| 2b | 1.7 | 9.7 | 5.7 |
| | | Average | 4.8 ± 3.7 |

[a] Data from experiments 1 and 2 are plotted in Figures 9.6 and 9.7, respectively.

studies, this is a surprisingly close agreement. The average value of $k'_{b2}$, $(4.8 \pm 3.7) \times 10^{-7}$ ml $cell^{-1}$ $hr^{-1}$, obtained is probably not significantly different in environmental situations.

### 9.6.3 Major Metabolites in Carbazole Biodegradation

In the many HPLC analyses (fluorescence and UV detectors) performed on concentrated extracts of acidified fermentation samples, no significant evidence for metabolites was observed. These observations suggest that after the initial attack on the carbazole molecule, degradation took place rapidly to products that did not fluoresce or absorb in the ultraviolet. Gas chromatography analyses also gave no evidence of metabolites.

### 9.6.4 Discussion

The ease of development of carbazole biodegrading enrichment cultures was comparable to our experience with methyl parathion. The data suggest that biodegradation of carbazole would probably take place under a variety of environmental conditions and, therefore, carbazole should not present any major pollution problem. n-Alkylated carbazoles would also possibly degrade rapidly.

During the biotransformations of 100 μg $ml^{-1}$/basal salts medium with mixed cultures the biodegrading bacteria were in fact exposed to levels of carbazole equal to the saturation concentration (approximately 1 μg $ml^{-1}$) and not to the total initial concentration in the medium, which included solid carbazole. In the presence of other solutes, it is possible that the saturation concentration of carbazole could be elevated, but there is no available information on the antimicrobial activity of this compound.

The differences in behaviorial patterns of the mixed cultures used in the two sets of kinetic studies illustrated in Figures 9.6 and 9.7 are interesting and undoubtedly reflect the complexities of mixed culture fermentations. No study was made of the component cultures, but the results may be due to relative changes of some strains and/or to the development of mutants during the five days between the two sets of experiments. In ecological studies of microorganisms in aquatic or soil habitats, much more significant behavior changes have been observed over a one-week period (Silvey et al., 1975).

## 10. LABORATORY INVESTIGATION OF 7H-DIBENZO[c,g]CARBAZOLE

### 10.1 SYNOPSIS

The results of the laboratory investigations suggest that 99% of the 7H-dibenzo[c,g]carbazole (DBC) entering natural waters will be sorbed onto the sediment and that the remaining 1% will be rapidly transformed photochemically to yield two products, one of which has added oxygen from reaction with water and is probably phenolic. Photolysis of DBC is expected to be the dominant process in clear waters. In turbid waters, sorption by suspended sediments will be more important. No information was obtained concerning possible phototransformation of DBC sorbed on suspended sediments. Enrichment cultures that could degrade DBC were not obtained. Volatilization of DBC will be extremely slow.

Steady-state concentrations of DBC in solution, suspended solids, and sediments near point sources in the presence of a continuous discharge of 10 ng $ml^{-1}$ (10 ppb) are expected to be:

| | Half-life* (hr) | Solution (ng $ml^{-1}$) | Suspended solids (ng $g^{-1}$) | Sediments (ng $g^{-1}$) |
|---|---|---|---|---|
| River | 0.36 | 2.8 | 55,000 | 49,000 |
| Pond | 1.5 | 0.01 | 180 | 200 |
| Eutrophic lake | 1.5 | $2.9 \times 10^{-2}$ | 580 | 81 |
| Oligotrophic lake | 0.5 | $1.5 \times 10^{-3}$ | 30 | 4.4 |

These concentrations may be hazardous even though they are approximately 1000 times lower than those tested to date under relevant conditions (Christensen et al., 1976). The few toxicity data available suggest that even low concentrations and brief exposures are carcinogenic, and caution certainly is warranted.

### 10.2 BACKGROUND

7H-dibenzo[c,g]carbazole (DBC) is a known carcinogen (Christensen et al., 1976). It has been found in the combustion products of tobacco smoke and is present in the particulate matter of polluted atmospheres. No reports on the distribution of DBC in the aquatic environment were found in our literature search.

---

*Predicted by one-compartment model.

DBC was chosen for study because of its known health hazard and because it is representative of the indole- and carbazole-type nitrogen heterocycles found in energy-related effluents (Schmidt et al., 1974; Karr et al., 1967). The results of the DBC study are also useful for comparison with the results from the carbazole study (Section 9) to assess the relative importance of the transport and transformation processes, which may be affected by the aromatic ring structure. No information on the physical transport or the chemical and microbiological transformation of DBC was available when our laboratory studies began.

The general physical properties of DBC are given in Table 10.1.

TABLE 10.1. PHYSICAL PROPERTIES OF 7H-DIBENZO[c,g]CARBAZOLE

Structure

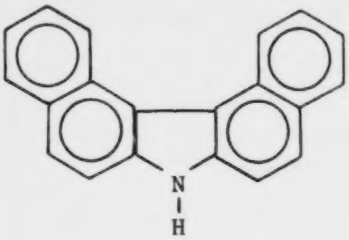

| | |
|---|---|
| Molecular weight | 267.31 |
| Melting point (°C) | 155-159 |
| Vapor pressure at 20°C (torr) | $10^{-9}$[a] |
| Solubility in water (ng $ml^{-1}$) | $63 \pm 3$[b] |

1.00 ng $ml^{-1}$ (1 ppb) DBC in water = $3.74 \times 10^{-9}$ M

---

[a] Estimated by comparison with benzo[a]pyrene, Section 6.

[b] Measured in this study, see Section 10.3.1.

The $pK_a$ of DBC is not known, but by analogy to carbazole (see Section 9), the $pK_a$ of DBC is expected to be less than zero, indicating that DBC would be less than 1% protonated even at pH 1. The environmental chemistry of DBC will then involve only the free base (neutral) form.

While we anticipated that sorption onto sediments and photolysis were probably the most important pathways for DBC, the literature data were insufficient to allow us to quantitatively estimate the importance of these processes in comparison to biodegradation, volatilization, and oxidation. Therefore, we decided that screening studies should be conducted for each of these processes.

## 10.3 ENVIRONMENTAL ASSESSMENT

### 10.3.1 Summary of Laboratory Data

The rate constants obtained in the laboratory investigations of the transformation and transport processes for DBC are summarized in Table 10.2.

TABLE 10.2. SUMMARY OF 7H-DIBENZO[c,g]CARBAZOLE LABORATORY DATA

| Process | Sorption equilibrium | Partition coefficient |
|---|---|---|
| Sorption | $S_s = K_p S_w$ | $K_p = 20,500 \pm 2,000^a$ |
|  | Rate expression | Rate constant at 25°C |
| Volatilization | $k_v[DBC]^b$ | $k_v \leqq (9.4 \times 10^{-5})\ k_v^0$ |
| Photolysis | $k_p[DBC]^c = \Phi\ (\Sigma Z_\lambda \varepsilon_\lambda)[DBC]$ | $k_p = 5.2 \times 10^{-4}\ sec^{-1}$ |
| Oxidation | $k_{ox}[RO_2\cdot][DBC]$ | $k_{ox} = 830\ M^{-1}\ sec^{-1}$ |
| Hydrolysis | NA | $k_h = 0$ |
| Biodegradation[d] | $k_{b2} = \frac{\mu_{max}}{Y\ K_s}$ | $k_{b2} = 0$ |

[a] On Coyote Creek sediment.

[b] See discussion in Part I, Section 5.3 and in text.

[c] Assumes midday sunlight in mid-January.

[d] Biodegradation was not observed during our enrichment procedures.

### 10.3.2 Environmental Assessment Using the One-Compartment Model

The half-lives of dissolved DBC calculated for individual transformation or removal processes following spills or other acute discharges are listed in Table 10.3. Although these half-lives generally change from one water body to another, the half-lives of photolysis and adsorption appear generally shortest. Sorption half-lives have not been measured, but they are probably at least comparable to the half-lives for photolysis. The laboratory estimates of the partition coefficient varied greatly (Section 10.4.4), due to variations in organic content of the sediments. Consequently, since photolysis is rapid, the pathway of DBC in natural waters is likely to be extremely sensitive to the suspended sediment concentration; transformation should dominate in clear waters, and sorption should dominate in turbid waters with an expected range of 50-82% sorption onto suspended solids in most natural waters. Transformation of the sorbed material is expected to be extremely slow, and accumulation large, unless biodegradation in natural environments is significantly faster than was observed in our experiments.

TABLE 10.3 TRANSFORMATION AND TRANSPORT OF 7H-DIBENZO[c,g]CARBAZOLE PREDICTED BY THE ONE-COMPARTMENT MODEL

| Process | River | Eutrophic pond | Eutrophic lake | Oligotrophic lake |
|---|---|---|---|---|
| Photolysis, half-life (hr)[a] | 1.0 | 1.5 | 1.5 | 0.5 |
| Oxidation, half-life (hr) | >700 | >700 | >700 | >700 |
| Volatilization, half-life (hr) | 15,000 | 37,000 | 73,000 | 73,000 |
| Hydrolysis, half-life (hr) | -- | -- | -- | -- |
| Biodegradation,[b] half-life (hr) | Very long | Very long | Very long | Very long |
| Half-life for all processes except dilution (hr) | 1.0 | 1.5 | 1.5 | 0.5 |
| Half-life for all processes including dilution (hr) | 0.36 | 1.5 | 1.5 | 0.5 |
| Amount DBC sorbed ($\mu g\ m^{-3}$)[c] | 20 | 60 | 10 | 10 |
| Percentage DBC sorbed | 66% | 82% | 50% | 50% |

[a] Estimates assume winter insolation.

[b] No acclimated cultures were obtained during the screening studies.

[c] Assumes 10 ng $ml^{-1}$ (10 ppb) of DBC in aqueous phase and sorption partition coefficient of $2 \times 10^4$.

### 10.3.3 Persistence

The persistence of DBC following acute discharges is expected to be largely a function of the dilution rate in large, fast flowing streams. Persistence in lakes and ponds should be dominated by rates of transformation within the sediments. However, very low concentrations can be expected indefinitely in all natural waters if biodegradation is indeed very slow in natural sediments, as is implied by our failure to obtain microbial cultures capable of transforming DBC. If so, desorption from the sediments will maintain low concentrations of DBC in solution indefinitely, the significance of which will probably depend on biological concentration processes, which cannot be appraised with our data.

### 10.3.4 Mass and Concentration Distributions Calculated Using Computer Models

The distributions of mass and concentration of DBC expected at steady state within each of four types of water bodies, as calculated with the aid of the computer model, are summarized in Table 10.4. The pseudo-first-order rate constants used in these simulations are presented in Appendix A.

TABLE 10.4. DISTRIBUTION OF 7H-DIBENZO[c,g]CARBAZOLE IN VARIOUS AQUATIC SYSTEMS AT STEADY STATE (input concentrations of 10 μg $ml^{-1}$ 7H-dibenzo[c,g]carbazole)

| | Pond | | River | | Eutrophic lake | | Oligotrophic lake | |
|---|---|---|---|---|---|---|---|---|
| | Mass (kg) | Conc. (μg $ml^{-1}$) | Mass (kg) | Conc. (μg $ml^{-1}$) | Mass (kg) | Conc. (μg $ml^{-1}$) | Mass (kg) | Conc. (μg $ml^{-1}$) |
| Compartment 1 (surface water) | | | | | | | | |
| Solution | $2.0 \times 10^{-4}$ | $1 \times 10^{-2}$ | $8.4 \times 10^{-1}$ | 2.8 | $7.2 \times 10^{-3}$ | $2.9 \times 10^{-2}$ | $3.9 \times 10^{-4}$ | $1.5 \times 10^{-3}$ |
| Suspended solids | $1.1 \times 10^{-3}$ | 18 | 1.7 | $5.5 \times 10^{4}$ | $7.2 \times 10^{-3}$ | $5.8 \times 10^{2}$ | $3.8 \times 10^{-4}$ | 30 |
| Compartment 2 (surface water) | | | | | | | | |
| Solution | -- | -- | $7.4 \times 10^{-1}$ | 2.5 | $1.5 \times 10^{-3}$ | $6.0 \times 10^{-4}$ | $5.1 \times 10^{-5}$ | $2 \times 10^{-5}$ |
| Suspended solids | -- | -- | 1.5 | $4.9 \times 10^{4}$ | $1.5 \times 10^{-3}$ | 12 | $5.1 \times 10^{-5}$ | 0.4 |
| Compartment 3 (surface water) | | | | | | | | |
| Solution | -- | -- | $6.4 \times 10^{-1}$ | 2.13 | $2.5 \times 10^{-5}$ | $1 \times 10^{-4}$ | $5.6 \times 10^{-7}$ | $1 \times 10^{-6}$ |
| Suspended solids | -- | -- | 1.3 | $4.3 \times 10^{4}$ | $2.5 \times 10^{-5}$ | 2 | $5.6 \times 10^{-7}$ | $4.5 \times 10^{-2}$ |
| Compartment 5 (bottom water) | | | | | | | | |
| Solution | -- | -- | -- | -- | $1.2 \times 10^{-5}$ | $4.3 \times 10^{-5}$ | $1.9 \times 10^{-7}$ | $5.6 \times 10^{-8}$ |
| Suspended solids | -- | -- | -- | -- | $1.2 \times 10^{-5}$ | $1 \times 10^{-5}$ | $1.9 \times 10^{-7}$ | $1.5 \times 10^{-3}$ |
| Compartments 7-9 (sediment)[a] | | | | | | | | |
| Solution | $2.5 \times 10^{-6}$ | 0.01 | $1.8 \times 10^{-1}$ | 2.5 | $3.7 \times 10^{-5}$ | $6.1 \times 10^{-3}$ | $1.9 \times 10^{-2}$ | $2.2 \times 10^{-4}$ |
| Solids | $1.4 \times 10^{-1}$ | $2 \times 10^{2}$ | $1 \times 10^{3}$ | $4.9 \times 10^{4}$ | 1.1 | 81 | $6.0 \times 10^{-2}$ | 4.4 |
| Total mass | $1.4 \times 10^{-1}$ | | $1 \times 10^{3}$ | | 1.1 | | $6.0 \times 10^{-2}$ | |

[a] The amounts given for solid and solution phases in the sediment compartments are estimated from the sorption partition coefficient for suspended solids and may be overestimated because it was assumed that biodegradation of sorbed material does not occur.

The sediments clearly dominate the distribution of DBC in each of these simulations, with virtually all the DBC in the bottom sediments and less than 1% in the suspended fraction. The amounts of DBC sorbed to the suspended solids and in solution are equal in the aqueous compartments of the lake simulations, but the suspended solids dominate in the aqueous compartments of the pond and river simulations. These predictions contrast rather sharply with the results of the one-compartment, acute pollution analyses, given in Section 10.3.2, which ignored interactions with the bottom sediments and the continual replenishment of the suspended solids by exchange with the sediments.

The expected steady-state concentrations of DBC in solution are roughly $10^{-3}$ to $10^{-6}$ ng $ml^{-1}$, which is roughly one thousand to one million times less than the input concentrations (Table 10.4). The highest steady-state concentrations of DBC in solution occurred in the river, with 100-fold lower concentrations in the eutrophic pond and lake simulations, and a 1000-fold lower concentration in the oligotrophic lake simulation. Within the lake simulations, concentrations of dissolved DBC decrease by 100- to 1000-fold with increasing distance from the source. Concentrations in the river simulation decline by 25% in the first 3 kilometers. Concentrations in the sediments are roughly equivalent to the concentration of DBC in the inflowing waters in the river simulation, and roughly one-tenth the concentration of the inflowing rates in the lake simulations.

The buildup and decline of DBC in the pond simulation, shown in Figure 10.1, shows the dynamics of DBC accumulation following initiation and termination of discharge. Steady-state conditions are reached within two days for the solution and suspended solid phases, but the concentration of DBC sediments in Figure 10.1 appears to rise until the ninth day (216 hours), when it declines due to desorption. Desorption then provides a lower limit to the decreases in the concentration of DBC in the dissolved and suspended solids fractions, which began with the cessation of discharge after 150 hours, giving a relatively long-lived loading of roughly 2.5 ng $ml^{-1}$. The half-life of DBC following a spill, estimated from the rate of decline, is much longer than that predicted by the one-compartment model (7 versus 1.5 hours) since the DBC in solution in the computer simulation is continually replenished from the sediments. Half-lives of DBC during actual spills should lie between these two limiting values.

Similar patterns prevail in the river simulation (Figure 10.2), except that steady-state conditions are obtained far more rapidly (within hours instead of days).

Buildup and declines in the lake simulations (Figures 10.3 and 10.4) are rapid, as in the pond simulation, showing the effects of the high partition coefficient in one strong localization of DBC near the source.

### 10.3.5 Discussion

The principal uncertainties in the preceding analyses lie in the estimates of partition coefficients and the extrapolations of the laboratory

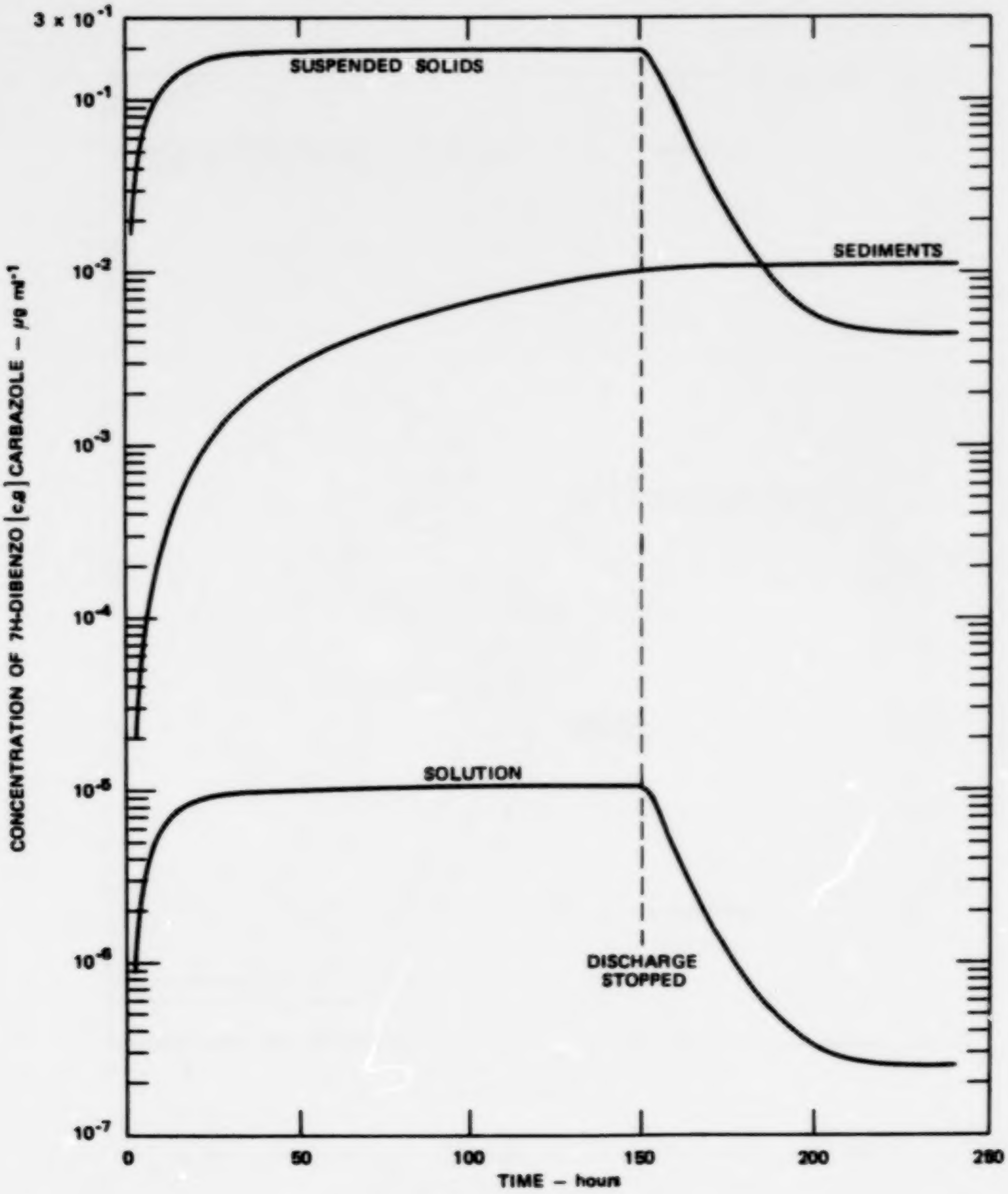

FIGURE 10.1 PERSISTENCE OF 7H-DIBENZO [c,g] CARBAZOLE IN A PARTIALLY MIXED TWO-COMPARTMENT POND SYSTEM

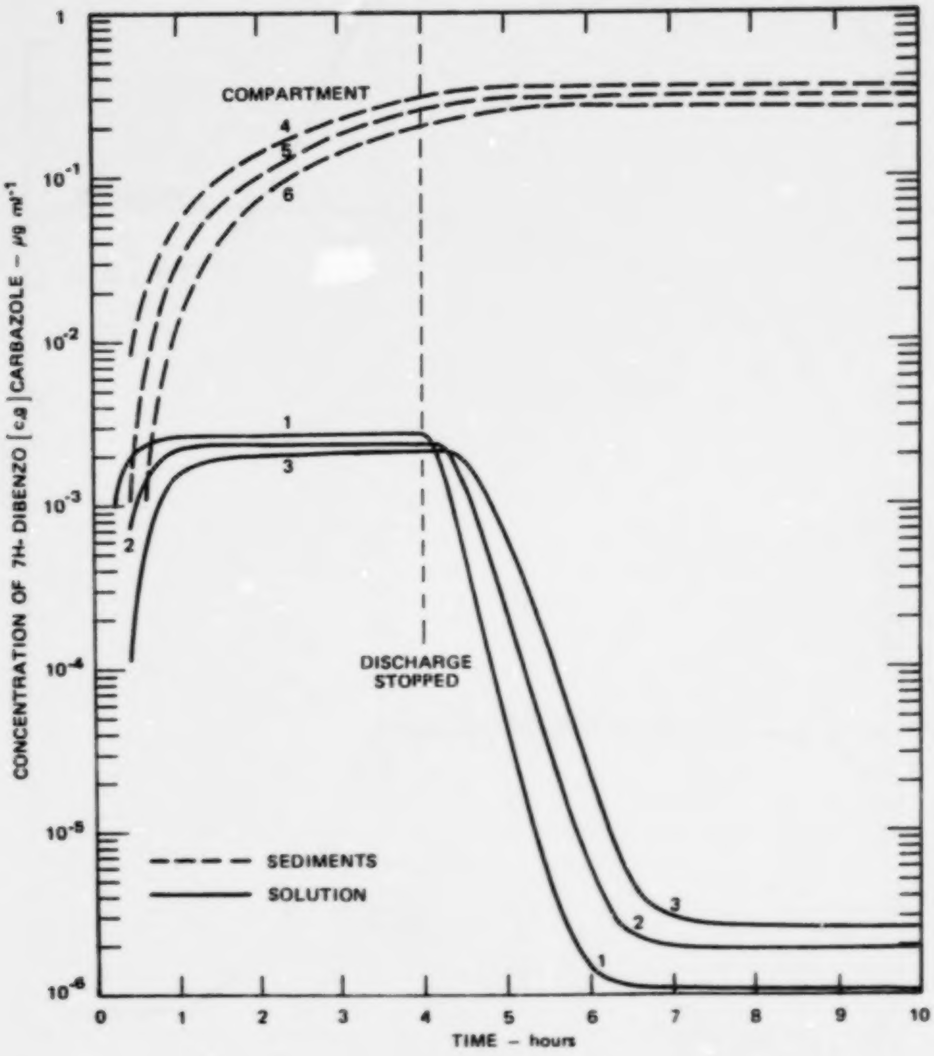

FIGURE 10.2 PERSISTENCE OF 7H-DIBENZO [c,g] CARBAZOLE IN A PARTIALLY MIXED RIVER SYSTEM

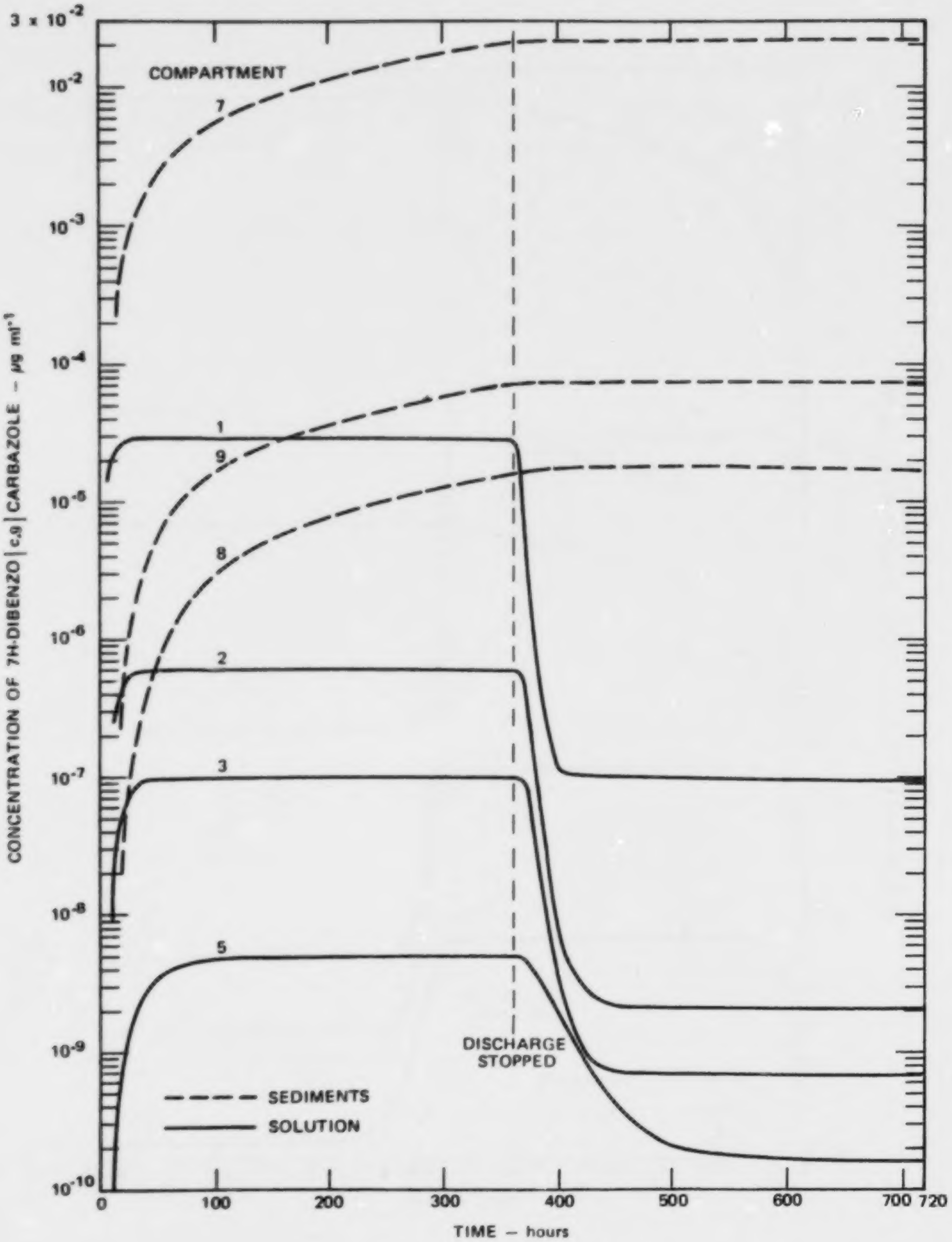

FIGURE 10.3 PERSISTENCE OF 7H-DIBENZO [c,g] CARBAZOLE IN A EUTROPHIC LAKE

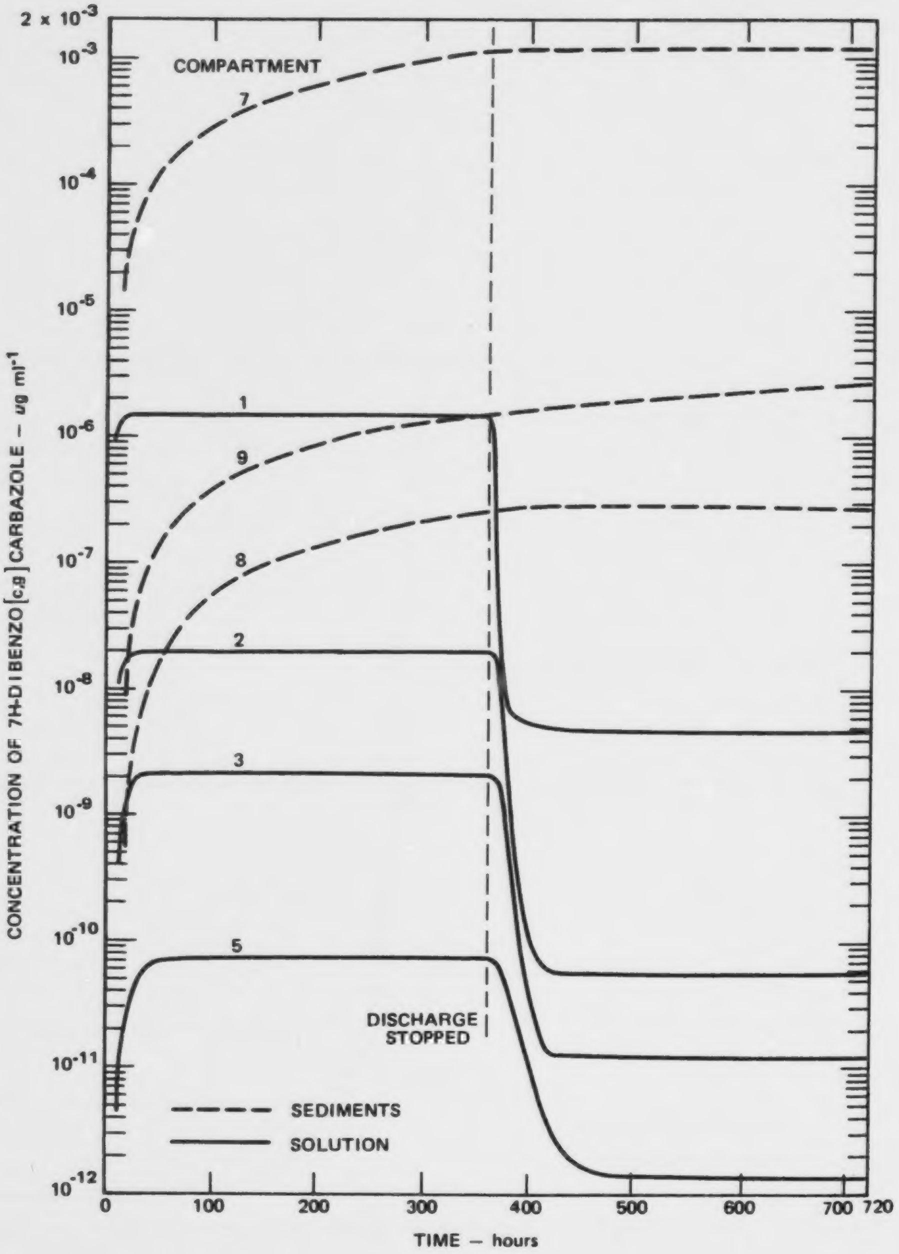

FIGURE 10.4 PERSINSTENCE OF 7H-DIBENZO [c,g] CARBAZOLE IN AN OLIGOTROPHIC LAKE

microbial data to the field. Even though our assumption that biological transformation is unimportant may be wrong, it is probable that most of the DBC released to natural waters will be rapidly sorbed by suspended particulates because of the size of the sorption partition coefficient and the rapidity with which sorption typically occurs. Hence, further research to reduce the uncertainty in our analysis seems unwarranted unless the transformation products of DBC are themselves of interest, or the predicted concentrations are found to be carcinogenic.

## 10.4 PHYSICAL PROPERTIES

### 10.4.1 Solubility in Water

The solubility of DBC in water at room temperature (about 22 ± 2°C) was measured using the methods described by Haque and Schmedding (1975). The average solubility was 63 ± 3 ng $ml^{-1}$ [2.4 (± 0.1) x $10^{-7}$ M], based on replicate determinations of solutions that were subjected to long centrifugation (30 min at 15,000 rpm) until a constant value for the solubility was obtained.

### 10.4.2 Absorption Spectrum

DBC absorbs light strongly in the solar region to 380 nm, weakly to 390 nm. The pH of a solution of DBC in 5% acetonitrile/95% water was adjusted with HCl (Table 10.5). The absorption spectra of DBC in 50% acetonitrile/50% water was also measured from 295 to 650 nm at pH 3.3, 5.2, and 7.2 (Table 10.6). Care was taken to assure that the DBC was in solution and not a suspension. No particulate could be observed by light scattered by a collimated beam of green light (the green filter absorbed light below about 450 nm and eliminated the strong fluorescence observed in a beam of white light that obscured the scattered light).

These data show that pH has no effect on the absorption spectrum in the pH range of environmental interest. However, there is a solvent effect on the absorption coefficient. At 360 nm, it is 12,400 $cm^{-1}$ $M^{-1}$ in 5% acetonitrile and 17,400 $cm^{-1}$ $M^{-1}$ in 50% acetonitrile. This solvent effect was not examined because it would have been necessary to reduce the concentration of DBC to be sure that it remained in solution, and our spectrophotometer does not have the required sensitivity to make the measurement with good precision. Also, the data reported in Table 10.5 in 5% acetonitrile are adequate for estimating the photolysis rate within the precision required for our predictions of the photolysis half-lives. These results do point out the necessity of making the absorption spectra measurements with the minimum amount of cosolvent.

### 10.4.3 Volatilization Rate

The volatilization rate of DBC was measured using the method of Hill et al. (1976), which is described in detail in Part I and Appendix B. Volatilization of DBC in aqueous solution was undetectable, within experimental error, at an average oxygen reaeration rate of 5.7 (± 1.6) $hr^{-1}$ over a 4-day

## TABLE 10.5. ABSORPTION SPECTRUM OF 7H-DIBENZO[c,g]CARBAZOLE IN 5% ACETONITRILE/95% WATER AT pH 4.5[a]

| Center of wavelength interval[b] (nm) | Average absorption coefficient[c] ($M^{-1}$ $cm^{-1}$) |
|---|---|
| 297.5 | 16,500 |
| 300.0 | 15,900 |
| 302.5 | 12,300 |
| 305.0 | 8,760 |
| 307.5 | 6,480 |
| 310.0 | 4,990 |
| 312.5 | 4,340 |
| 315.0 | 4,070 |
| 317.5 | 3,930 |
| 320.0 | 3,960 |
| 323.1 | 4,260 |
| 330.0 | 5,830 |
| 340.0 | 9,220 |
| 350.0 | 11,000 |
| 360.0 | 12,700 |
| 370.0 | 7,890 |
| 380.0 | 770 |
| 390.0 | 10 |
| 400.0 | 0 |

[a] 7H-Dibenzo[c,g]carbazole concentration was 985 ng $ml^{-1}$ ($3.69 \times 10^{-6}$ M).

[b] The wavelength intervals are given in Appendix B, Table B.1.

[c] The absorption coefficients at 313.0 and 366.0 nm are 4,210 and 13,000 $M^{-1}$ $cm^{-1}$, respectively.

TABLE 10.6. ABSORPTION SPECTRUM OF 7H-DIBENZO[c,g]CARBAZOLE IN 50% ACETONITRILE/50% WATER[a]

| Center of wavelength interval[b] (nm) | Absorption coefficient[c] ($M^{-1}$ $cm^{-1}$) | | | Average absorption coefficient ($M^{-1}$ $cm^{-1}$) |
|---|---|---|---|---|
| | pH 3.3 | pH 5.2 | pH 7.2 | |
| 297.5 | 20,400 | 21,000 | 21,200 | 20,900 |
| 300.0 | 21,800 | 21,800 | 22,500 | 22,000 |
| 302.5 | 18,200 | 18,000 | 19,200 | 18,500 |
| 305.0 | 13,400 | 12,800 | 14,400 | 13,500 |
| 307.5 | 9,500 | 8,860 | 9,910 | 9,420 |
| 310.0 | 6,630 | 6,510 | 6,830 | 6,660 |
| 312.5 | 5,380 | 5,410 | 5,670 | 5,490 |
| 315.0 | 4,910 | 4,850 | 5,170 | 4,980 |
| 317.5 | 4,740 | 4,650 | 4,940 | 4,780 |
| 320.0 | 4,500 | 4,500 | 4,850 | 4,620 |
| 323.1 | 5,090 | 5,060 | 5,170 | 5,110 |
| 330 | 7,180 | 6,970 | 6,970 | 7,040 |
| 340 | 12,000 | 12,000 | 12,200 | 12,100 |
| 350 | 14,100 | 14,200 | 14,700 | 14,300 |
| 360 | 17,100 | 17,100 | 18,000 | 17,400 |
| 370 | 11,500 | 11,300 | 12,100 | 11,600 |
| 380 | 619 | 590 | -- | 604 |
| 390 | 0 | 0 | -- | 0 |

[a] 7H-Dibenzo[c,g]carbazole concentration was 9.20 μg $ml^{-1}$ ($3.44 \times 10^{-5}$ M).

[b] The wavelength intervals are given in Appendix B, Table B.1.

[c] The absorption coefficients at 313.0 and 366.0 nm are 5,420 and 19,300 $M^{-1}$ $cm^{-1}$, respectively.

period. The average DBC concentrations at 0, 21, and 96 hours were 15.1 (± 0.8), 15.5 (± 1.5), and 14.3 (± 0.5) ng $ml^{-1}$. We assumed that a 5% loss of DBC in 96 hours is the maximum loss that could have occurred without being detected, within experimental error. The upper bound for the $k_v^S/k_v^O$ ratio was estimated as:

$$\text{DBC volatilization rate:} \quad k_v^S = \frac{\ln(1 - 0.05)}{96} = 5.3 \times 10^{-4}\ \text{hr}^{-1}$$

$$\text{Ratio:} \quad k_v^S/k_v^O < 9.4 \times 10^{-5}$$

This is an extremely low value of the ratio. We concluded that volatilization of DBC would not be a significant pathway in the environment. Therefore, no further volatilization experiments with DBC were performed.

### 10.4.4 Sorption on Clay and Sediments

The sorption partition coefficients of DBC were measure on three sediments: Des Moines River sediment, Coyote Creek sediment, and Searsville Pond sediment. Care was taken to assure that the samples were protected from light at all times to minimize photo-oxidation of the DBC. The initial concentration of DBC in each sample was always less than the saturation concentration of 63 ng $ml^{-1}$ ($2.4 \times 10^{-7}$ M). Each experiment consisted of replicate samples at two DBC concentrations and two sediment loadings, plus blanks that contained only DBC or sediment. Triplicate analyses were made on each flask. Periodic checks were made for sorption of DBC onto the glassware; since none of the glassware extracts contained DBC, we presumed that less than 5% of the DBC was sorbed onto the glassware. The stock solutions of DBC in water were centrifuged at 7500 rpm for 1 hour to remove any suspended DBC before the sediment/DBC mixtures were prepared.

The data, summarized in Table 10.7, were fitted to a Freundlich isotherm with n = 1 (equation B.6 ). Graphs of the isotherm data, calculated on the basis of the supernatant concentrations of DBC, are shown in Figure 10.5 with the partition coefficients ($K_p$). The partition coefficients were calculated two ways. First, we used only the measured values of the supernatant DBC concentrations in the blanks and the sediment/DBC mixtures. The calculation of the partition coefficient was based on the results of the analysis of the supernatant at equilibrium. The amount of DBC sorbed on the sediments was calculated by the difference between the amount that was added and the amount that was found in the supernatant. These data are also plotted in Figure 10.5. Our opinion is that these values are the most valid (the estimated error is ± 10%).

The sediments were also extracted to determine the amount of sorbed DBC. From these data, partition coefficients and material balances were calculated. However, the data are much more scattered than those from the supernatant, and a number of experimental difficulties were encountered. The sediment in one flask at each level of sediment and DBC was extracted with ethyl acetate, and the extract was concentrated and analyzed for DBC. These concentration data are less reliable than the supernatant analyses due to analytical problems encountered (the estimated error is ± 25%).

We experienced several analytical difficulties with the measurement of the DBC isotherms, but we did not attempt to repeat the measurements. The analyses of the supernatant DBC, after centrifugation of the samples for 20 min at 12,000 rpm, were made by direct injection of 0.1 ml (Searsville and Des Moines) or 1 ml (Coyote Creek) of the aqueous solution directly onto the LC. After the isotherms on the Des Moines and Searsville sediments were complete, we discovered that some of the DBC was held up on the sample loop while the loop was being filled. Dilution of the aqueous samples with 25% by volume of acetonitrile eliminated this problem. The Coyote Creek isotherm data were analyzed by this procedure, and the standard deviations calculated from the

TABLE 10.7. SORPTION OF 7H-DIBENZO[c,g]CARBAZOLE ON SEDIMENTS

| Sediment | Total organic carbon (%) | Sediment concentration (μg $ml^{-1}$) | DBC concentration in supernatant[a] (ng $ml^{-1}$) | DBC concentration on sediment[b] (ng $g^{-1}$ x $10^{-3}$) | Recovery[c] (%) | Partition coefficient, $K_p$ (x $10^{-3}$)[d] | | | | | |
|---|---|---|---|---|---|---|---|---|---|---|---|
| | | | | | | LLS | | | | NLLS | |
| | | | | | | $S_w$ only | | $S_w$ and $S_s$ | | $S_w$ only | $S_s$ and $S_w$ |
| | | | | | | a = 0 | a ≠ 0 | a = 0 | a ≠ 0 | | |
| **Des Moines River** sorption | 0.6 | 84.2 | 6.7 ± 0.4 | 95 ± 13 | 65 | 32.6 ± 5.9 | 19.5 ± 7.4 | 14 ± 2.6 | 13 ± 6 | -- | 14.8 ± 1.4 |
| | | 168.0 | 3.6 ± 1.4 | 52 ± 2 | 52 | | a = 56 ± 27 | | a = 9 ± 23 | | |
| | | 84.2 | 2.7 ± 0.6 | 38 ± 5 | 47 | | | | | | |
| | | 168.0 | 1.3 ± 0.3 | 30 ± 4 | 50 | | | | | | |
| **Coyote Creek** sorption | 1.4 | 35.8 | 15.2 ± 1.4 | 198 ± 18 | 94 | 18.5 ± 2.8 | 14.2 ± 4.5 | 15.0 ± 28 | -13 ± 44 | 20.5 ± 2.0 | 12.2 ± 1.4 |
| | | 71.7 | 8.5 ± 0.5 | 89 ± 6 | 63 | | a = 46 ± 44 | | a = 200 ± 28 | | |
| | | 35.8 | 7.9 ± 0.5 | 108 ± 1 | 104 | | | | | | |
| | | 71.7 | 4.8 ± 0.5 | 62 ± 4 | 83 | | | | | | |
| **Searsville Pond** sorption | 3.8 | 27.5 | 13.0 ± 0.4 | 159 ± 9 | 77 | 27.6 ± 5.1 | 17.9 ± 1.1 | 12 ± 7 | 11 ± 28 | | 9.2 ± 1.6 |
| | | 82.5 | 8.6 ± 1.0 | 65 ± 9 | 62 | | a = 96 ± 93 | | a = 12 ± 240 | | |
| | | 27.5 | 6.6 ± 1.4 | 129 ± 30 | 69 | | | | | | |
| | | 82.5 | 3.7 ± 0.1 | 39 ± 10 | 47 | | | | | | |

---

[a] Concentration measured in supernatant with population standard deviation.

[b] Concentration measured on sediment with population standard deviation.

[c] Based on blank flasks to determine total material added to each flask.

[d] LLS = linear least squares; NLLS = nonlinear least squares; $S_w$ = concentration in supernatant; $S_s$ = concentration on sediment. See Appendix B for description of regressions. Limits are 95% confidence limits.

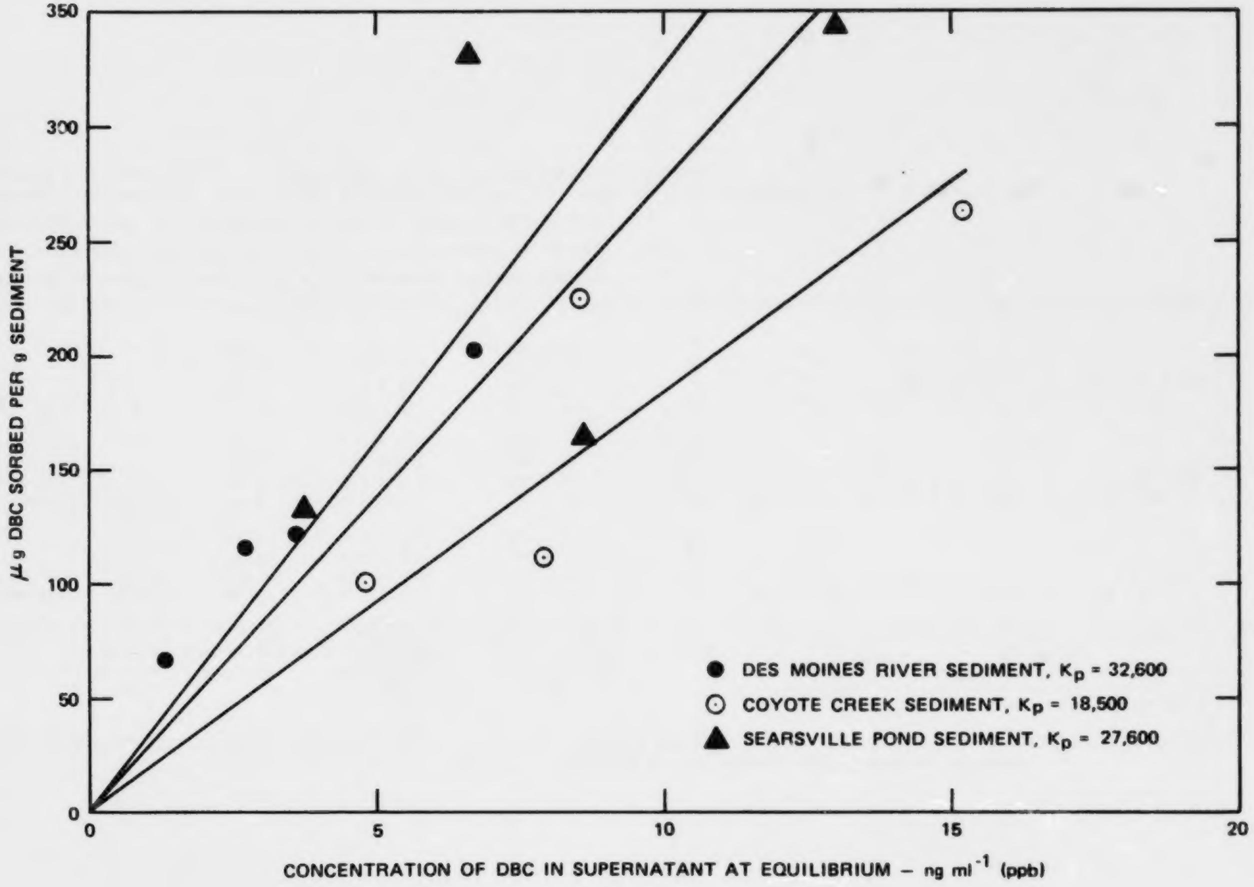

FIGURE 10.5. SORPTION ISOTHERMS OF 7H–DIBENZO[c,g] CARBAZOLE

triplicate analyses are a good estimate of the error associated with these measurements. The error introduced into the Des Moines and Searsville data was about 30%. However, since all flasks for all three sediments were made from the same stock solution of DBC in water, we could correct all the supernatant data because we had analyzed blanks containing only DBC (along with each isotherm measurement). These corrections have been made on the data reported in Table 10.7.

To measure recovery, the sediment from one flask at each level was shaken with ethyl acetate to extract the sorbed DBC. The ethyl acetate extracts from the Coyote Creek sediments were analyzed by injecting 0.1 ml of extract onto the LC. The volume of ethyl acetate extracts injected during the analysis of the Des Moines and Searsville sediment was 1 ml. This sample volume injected was too large, and much of the DBC was eluted with the solvent front. However, some DBC was retained and eluted at the usual elution volume. The overall sensitivity of the method was reduced by about a factor of 10, with a corresponding decrease in precision and accuracy. However, calibration curves could be constructed from data obtained with standards that had been prepared in water-saturated ethyl acetate, and this curve was used to calculate the concentration of DBC in the sediment extracts. Hence, the amount of DBC sorbed on the sediments could be estimated within about ± 20%. Recoveries ranging from 47% to 104% were obtained. Values of $K_p$ were calculated from the measured supernatant and sorbed DBC concentrations. These data are also reported in Table 10.7. However, we have less confidence in the values of $K_p$ and we prefer to use the values calculated from the supernatant concentrations calculated on the basis of these data only.

In spite of the analytical difficulties, a reasonable range of $K_p$ values for DBC is 15,000 to 40,000. The $K_p$ for Coyote Creek, which is the most reliable experiment, gave $K_p$ = 20,500 for the nonlinear least squares fit to the data for the supernatant data, in good agreement with the value of 20,000 used in the environmental assessment.

### 10.4.5 Biosorption

Biosorption studies were conducted with DBC solutions and 0.05% potassium phosphate buffer, pH 7.0. Corrections were made for sorption of DBC on glass walls by determining the recovery of DBC from the centrifuge tubes when the cell suspensions were poured out of the control tubes.

Because of the low levels of DBC that were being used, each suspension of the four test bacteria (*Azotobacter beijerinkii* ATCC 19366, *Bacillus cereus* ATCC 11778, *Escherichia coli* ATCC 9637, and *Serratia marcescens* ATCC 13880) was reduced to an optical density of 0.4. These suspensions were combined immediately before the experiment was initiated. The results from the one-hour sorption and three-hour sorption studies are presented in Table 10.8.

The adjustments for sorption of DBC on glassware in Table 10.8 were 4.6%, 3.7%, and 6.9% for sorption studies conducted in experiment 1 with 22.3 ng DBC $ml^{-1}$ and in experiment 2 with 20 and 6.2 ng DBC $ml^{-1}$, respectively. The corresponding adjustment for glassware sorption values in the desorption

TABLE 10.8. 7H-DIBENZO[c,g]CARBAZOLE SORPTION AND DESORPTION WITH A MIXED BACTERIAL POPULATION

| Experiment[a] | Initial DBC concentration ($ng\ ml^{-1}$) | Sorption(S) or desorption (D) | Sorption coefficient ($x\ 10^{-4}$) |
|---|---|---|---|
| 1 | 22.3 | S | 9.0 ± 2.2 |
| | | D | 10.7 ± 2.3 |
| 2 | 20.0 | S | 9.2 ± 1.3 |
| | | D | 6.4 ± 1.1 |
| 2 | 6.2 | S | 8.0 ± 1.2 |
| | | D | 6.9 ± 1.0 |

[a] Dry weight of bacterial mixture equivalent to 178 and 162 mg liter $liter^{-1}$ in experiments 1 and 2, respectively.

studies were 7.7%, 6.4%, and 5.7%, respectively. The quantities of DBC sorbed on the glassware are very close to the values for DBC in the supernatants and present a problem in definitive interpretations of the sorption coefficients beyond the fact that DBC is highly sorbed by biological and inorganic materials.

These corrections for sorption of DBC on glassware could be in error because some bacterial cells may have remained on the walls of the centrifuge tubes. In preliminary experiments with BaP, it was observed that the presence of microorganisms in a glass vessel resulted in lower residual BaP values on the glassware than in the controls with no microorganisms. However, these results were complicated by the fact that bacteria also sorbed BaP, which lowered the available concentration of BaP for sorption on glassware. As was observed with BaP, DBC was readily sorbed by clean glass surfaces.

This problem could best be resolved by a series of studies using isotopically labeled DBC and bacteria. With the data we have obtained, the sorption coefficient values would have been changed in the range of 5%--a value less than our standard deviations. It would appear that this was a futile exercise, but in view of the high sorbability of DBC on glassware and the low levels of DBC that were to be studied, this adjustment procedure was warranted.

The high sorption coefficient of bacterial cells for DBC would indicate that, in activated sludge sewage treatment facilities, most of the DBC would probably be removed on the sludge. The fate of DBC in flowing streams or stationary waters is more difficult to predict. The high degree of sorption on such a relatively inert surface as glass as well as natural sediments and the high probability that DBC in bacterial mass is more dependent on sorption phenomenon than on surface sorption, probably indicate that, in aquatic systems with low microbial counts, sorption onto suspended sediments may be the prime initial factor in decreasing DBC levels in waters. Subsequently, degradation can take place by microbial and/or chemical/physical phenomena acting on free or available DBC in equilibrium with the sorbed DBC.

## 10.5 CHEMICAL TRANSFORMATION

### 10.5.1 Photolysis Rate

The photolysis of DBC is rapid and is unaffected by oxygen. In sunlight the half-lives are less than a day. Since the solubility of DBC in pure water is 63 ng ml$^{-1}$, we used 0.1% acetonitrile as a cosolvent to enhance the solubility of DBC in waters from the natural sources. Data for photolysis of DBC in sunlight and at 366 nm are given in Table 10.9. Good first-order kinetic behavior was found for photolyses at 366 nm carried out to beyond two half-lives of DBC. The quantum yield for DBC phototransformation in pure water is $(2.8 \pm 0.2) \times 10^{-3}$.

Photolysis experiments carried out at 366 and 313 nm on 9.1 ng ml$^{-1}$ DBC solutions that had been purged with nitrogen showed that oxygen had no effect on the photolysis rate. One experiment at 366 nm found, however, that DBC was stable to photolysis when pure acetonitrile (no water) was the reaction solvent. Therefore water, but not oxygen, is involved in the rate-determining step, and the reaction is probably some type of photohydration process like that found for carbazole (see Sections 9 and 10.5.4).

Photolyses of 9 ng ml$^{-1}$ DBC solution were also carried out at 313 nm but these experiments provided an enigma. In 0.1% acetonitrile solution, a 15% loss of DBC was found in the initial 15-minute photoperiod, but no further loss of DBC was found after 45 additional minutes irradiation. A similar observation was made for 10 ng ml$^{-1}$ DBC in water containing 0.1% methanol, where a 45% loss of DBC was found in the initial 20-minute photoperiod, but no further loss after 60 additional minutes of irradiation. The DBC concentrations of the unphotolyzed solutions were confirmed by the direct-injection HPLC analysis, so the observation is considered a chemical phenomena and not an artifact of the experiment procedure. The possible error introduced by holdup of DBC in the sample loop (Section 10.4.4) is no greater than 5%. It is doubtful that products from the DBC phototransformation could explain the observations either through chemical or physical (quenching) processes, and at this time we can offer no explanation for the unusual photolysis behavior at 313 nm.

The data in Table 10.9. show that the photolysis rate of DBC in water from Lake Tahoe or Searsville Pond is not changed from that in pure water. The water from Coyote Creek (absorbance at 366 is 0.06 in a 1-cm cell) shows only a slight retardation of the photolysis rate. However, the experiment in pure water containing humic acid does show a definite reduction in photolysis rate. The absorbance of the humic acid solution at 366 nm is 0.63, indicating that 75% of the incident light is absorbed by the humic acid. Thus, the screening by humic acid accounts for only a fourfold decrease in rate, and other processes must also be occurring to explain the twelvefold decrease in rate observed. Some possible mechanisms are discussed in Section 9.5.1.

The half-life for direct photolysis of DBC in sunlight was calculated according to the procedure of Zepp and Cline (1977), using the quantum yield of $2.8 \times 10^{-3}$ measured at 366 and the absorption spectrum (Section 10.4.2). The UV spectrum of DBC passes through a minimum at about 320 nm. While the experi-

TABLE 10.9. RATE CONSTANTS FOR PHOTOLYSIS OF 7H-DIBENZO[c,g]CARBAZOLE

| Irradiation source | Solution[a] | DBC concentration[b] (ng ml$^{-1}$) | Extent of reaction (%) | Rate constant ($k_p$ x $10^3$ sec$^{-1}$) |
|---|---|---|---|---|
| 366 nm | Pure water | 9.1 | 84 | 1.52 ± 0.10[c,d] |
| 366 nm | Pure water, $N_2$ purged | 9.1 | 84 | 1.5[e] |
| 366 nm | Lake Tahoe water | 10.3 | 71 | 1.42 ± 0.09 |
| 366 nm | Coyote Creek water | 9.2 | 89 | 1.17 ± 0.13 |
| 366 nm | Searsville Pond water | 8.2 | 78 | 1.80 ± 0.22 |
| 366 nm | Humic acid in pure water | 11.5 | 56 | 0.122 ± 0.005 |
| Noon sunlight, late January | Pure water | 11.3 | 78 | 0.518 ± 0.032[f] |

[a] Solution contained 0.1% acetonitrile as cosolvent.

[b] 1.00 μg ml$^{-1}$ DBC in water = 3.74 x $10^{-9}$ M.

[c] Standard deviation.

[d] Quantum yield of 2.8 x $10^{-3}$ for disappearance of DBC at 366 nm.

[e] One data point at 84% reaction in nitrogen purged solution.

[f] Half-life of 24 minutes.

ments at 313 nm suggest that the rate of photolysis of DBC below 320 nm may be minimal, the calculation was carried out for the entire solar spectral region from 297.5 to 380 nm. Such a procedure is permissible since the major contribution to photolysis will be in the region above 320 nm where the DBC absorbance and sunlight intensity are more intense than in the lower end of the solar spectrum (e.g., 290-320 nm).

Figure 10.6 shows the variation in the photolysis half-life of DBC as a function of the time of day for midsummer and midwinter. The half-life of 51 minutes calculated for midday in midwinter is in good agreement with the measured half-life of 24 minutes on a clear day in late January. While the photolysis half-lives do vary with the time of day, Figure 10.6 shows that photolysis of DBC will be an important process in the environment, with half-lives of less than a day.

### 10.5.1 Oxidation Rate

When the susceptibility of DBC to free radical oxidation was examined using the AA-initiated oxidation screening reaction (see Section 6.3 in Part I and Appendix B for discussion and procedure), DBC was completely oxidized after the usual 100-hour reaction time. The experiment was then repeated using a 9.1 ng $ml^{-1}$ ($3.40 \times 10^{-8}$ M) DBC solution (0.1% acetonitrile in water) containing $1.00 \times 10^{-4}$ M AA. The solution was analyzed for DBC at reaction times of 4.0 and 8.3 hours. A rate constant term ($k_{ox}[RO_2\cdot]$) of $(2.5 \pm 0.4) \times 10^{-5}$ $M^{-1}$ $sec^{-1}$ was calculated from the data. Under the reaction conditions at 50°C, this corresponds to a rate constant $k_{ox}$ of $7.5 \times 10^{3}$ $M^{-1}$ $sec^{-1}$ (see Section 6.3 in Part I). At 25°C, $k_{ox}$ is then 830 $M^{-1}$ $sec^{-1}$, and assuming $[RO_2\cdot] = 10^{-9}$ M in the environment, the half-life for oxidation of DBC is about 10 days. The free radical oxidation of DBC by $RO_2\cdot$ is clearly not competitive with photolysis or sorption under aquatic environmental conditions.

### 10.5.3 Hydrolysis Rate

DBC contains no groups that are hydrolyzable. Therefore, no hydrolysis studies were carried out.

### 10.5.4 Products from Chemical Transformation

Two primary products were found by HPLC analyses of the photolysis of DBC in pure water. Both products were separated by HPLC and subjected to mass spectrometry. The only distinguishing features of the spectrum of the major product were an apparent molecular ion at m/e 299 and peaks at m/e 270 and 271, corresponding to loss of CHO and CO, respectively from the molecular ion; this indicates the presence of at least one phenolic group (McLafferty, 1973). DBC itself has a molecular ion of m/e 267. The spectrum of the major product is compatible with that of a dihydroxylated DBC; however, no silylated derivative of this product could be obtained using O,N-bis(trimethylsilyl)trifluoroacetamide.

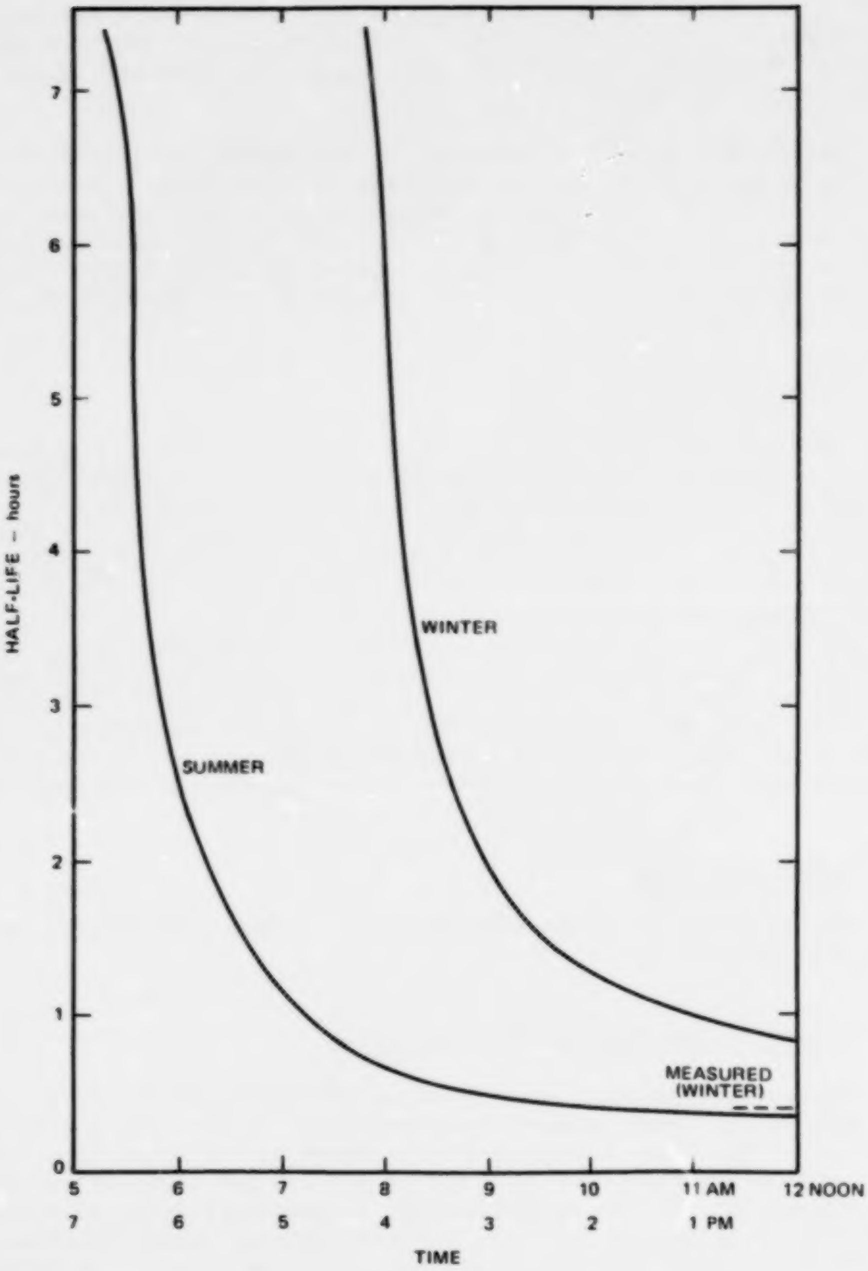

FIGURE 10 6. SEASONAL AND DAILY VARIATION OF PHOTOLYSIS HALF-LIFE OF 7H-DIBENZO[c,g]CARBAZOLE

It is difficult to rationalize why neither hydroxyl nor amine functions would be silylated with this reagent. The rate of photolysis of DBC did depend on water and not on oxygen, but the observed products could depend on a subsequent reaction with oxygen (this possibility was not checked). Unless an (unlikely) termolecular process is occurring involving two water molecules and DBC, the product must be formed by initial reaction of water and the photo-excited DBC, followed by a subsequent rapid reaction of the intermediate with another water molecule or oxygen. Neither of these events seems likely, and some additional structure determination appears necessary.

The second product could not be silylated, and gave an apparent molecular ion of m/e 271 with no characteristic fragmentation pattern to allow further identification. On the basis of the m/e 271 molecular ion, the second product could be a tetrahydro-DBC derivative, but such a photoreduction in water in the presence of oxygen is without precedent. As with the major product, some additional structure determination for the second product seems necessary.

## 10.6 BIODEGRADATION

### 10.6.1 Development of Enrichment Cultures

Enrichment studies were initiated with 1 $\mu g\ ml^{-1}$ of DBC in 5-liter liquid volumes in 9-liter, aerated, bottle-fermentors. We examined water samples from Coyote Creek (eutrophic) and from the aeration effluents from sewage plants in South San Francisco, and at the Shell Oil Refinery in Martinez, California. Since there was a good possibility that the Shell Oil Refinery effluents contained minor discharges of DBC, this source was considered both as a commercial discharge source and as a sewage treatment plant that possibly contained organisms capable of biodegrading DBC.

Thus, studies with the Shell Oil Refinery effluents were initiated with DBC as the sole added carbon source [in addition to the normal components in the samples, phosphate buffer, and $(NH_4)_2SO_4$]. Studies of water samples from all three sources were also initiated with DBC and either carbazole or naphthalene (10 $\mu g\ ml^{-1}$) as an additional source of carbon.

After one week of incubation of the 9-liter fermentors, additional 2-liter volumes of fresh samplings from the South San Francisco sewage effluent and from Coyote Creek were added to the respective bottles to possibly expand the range of types of organisms in the original samplings. Carbazole (10 $\mu g\ ml^{-1}$) was added once a week for three weeks. Naphthalene (10 $\mu g\ ml^{-1}$) was added three times a week for three weeks.

During the six weeks of this study, degradation of DBC was not observed by LC analysis of ethyl acetate extracts of broths that had been subjected to three freeze-thaw cycles.

After three and six weeks of incubation of Shell Oil Refinery and South San Francisco sewage plant samples, transfers were made from the corresponding 9-liter bottles into shaker flasks containing DBC (1 $\mu g\ ml^{-1}$) plus carbazole (10 $\mu g\ ml^{-1}$) and DBC (1 $\mu g\ ml^{-1}$) plus naphthalene (10 $\mu g\ ml^{-1}$). From the

9-liter bottle fermentor with the Shell Oil Refinery sample in which DBC was the only added carbon source, transfers were made to shaker flasks containing basal salts medium with DBC (1 $\mu g\ ml^{-1}$), glucose (50 $\mu g\ ml^{-1}$), and yeast extract (10 $\mu g\ ml^{-1}$).

All shaker flasks developed good growth. However, after up to 10 days of incubation, the fermented broths did not indicate any loss of DBC in the shaker flask media.

### 10.6.2 Biodegradation Kinetics

Since enrichment cultures that degraded DBC were not obtained, biodegradation kinetic studies were not performed.

### 10.6.3 Discussion

It had been previously emphasized (Section 6) that enrichment procedures have a propensity for favoring certain types of organisms. Our inability to obtain enrichment biodegrading systems cannot be accepted as a positive indication of recalcitrance of DBC to microbial biodegradation. With the high sorption coefficients and the low solubility of DBC, it is possible that conventional enrichment procedures do not provide enough "available" DBC for organisms to utilize this substrate for growth in competition with other organisms that have a more favorable predator-prey relationship in the milieu of the primary enrichment process.

A personal communication from J. J. Perry (1977) indicated that a number of fungi could transform benzo[a]pyrene to complex mixtures of organic acids. A comparable situation could exist in the biodegradation of DBC. However, our enrichment procedures do not favor the growth of filamentous fungi, and we would not expect to observe transformation of DBC by fungi. Transformation by fungi are most likely to be important in flowing waters such as streams and may be significant in bottom sediments. In summary, DBC biodegradation may take place slowly under aerobic conditions on sediments, but this pathway was not investigated in these studies.

# 11. LABORATORY INVESTIGATION OF BENZO[b]THIOPHENE

## 11.1 SYNOPSIS

The results of the laboratory investigations suggest that benzo[b]thiophene (BT) is not likely to accumulate in an aqueous environment and that volatilization is the major environmental pathway of BT in aquatic systems. However, under some conditions, such as a deep lake where volatilization is slow because the turbulence is also low, photolysis and perhaps biodegradation may be significant.

The half-lives of BT in solution, as predicted by the one-compartment environmental exposure model, and the steady-state concentrations of BT in solution, on suspended solids, and on sediments near a point source in the presence of a continuous discharge of 1 $\mu$g ml$^{-1}$ (1 ppm), as predicted by the nine-compartment model are given below.

| | Half-life[*] in solution (hour) | Concentration in solution ($\mu$g ml$^{-1}$) | Concentration on suspended solids ($\mu$g g$^{-1}$) | Concentration[†] on sediments ($\mu$g g$^{-1}$) |
|---|---|---|---|---|
| River | 0.8 | 0.98 | 49 | 48 |
| Pond | 19 | 0.024 | 1.16 | 1.16 |
| Eutrophic lake | 19 | 0.047 | 2.32 | 0.60 |
| Oligotrophic lake | 140 | 0.119 | 6.00 | 2.15 |

The laboratory procedures used to estimate volatilization, photolysis, and oxidation rates, and the partition coefficients on a natural sediment and on a mixture of microorganisms were applied to BT. Biodegradation was a problem because BT degradation occurred only in the presence of naphthalene by what appeared to be a co-metabolic process. We know of no mathematical formalism that can be used to express the rate of a co-metabolic process. The upper limit for the biodegradation rate of BT was estimated to be one-half that of quinoline (see Section 7.6.2).

---

[*] Predicted by one-compartment model.

[†] Average concentration in sediments.

## 11.2 BACKGROUND

Thiophenes and benzothiophenes are present as minor constituents of petroleum crudes, coal tars, shale oil, and synthetic fuels. Concentrations as high as 5.4% have been found in Kuwait crudes. Since sulfur-containing compounds represent a major processing and air pollution problem, BT and dibenzothiophene (Part II, Section 12) were selected as examples of the general class of thiophenes.

The general physical properties of BT that were found in the literature are given in Table 11.1.

TABLE 11.1. PHYSICAL PROPERTIES OF BENZO[b]THIOPHENE

| | |
|---|---|
| Structure | 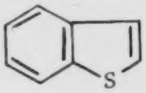 |
| Molecular weight | 134.19 |
| Melting point (°C) | 31.3 |
| Boiling point (°C) | 219.9 |
| Solubility[a] (μg ml$^{-1}$) | 130 ± 5 |
| Vapor pressure at 20°C (torr)[b] | 0.2 |
| UV spectrum [$\lambda_{max}$ nm(log ε)] [c]<br>in cyclohexane | 289 (3.36)<br>291 (3.36)<br>298 (3.57) |

1 μg ml$^{-1}$ (1 ppm) BT = 7.45 x 10$^{-6}$ M

[a] Measured in this study, Section 11.4.1.

[b] Estimated from the vapor pressure of naphthalene.

[c] Haines et al. (1956).

Literature data were not available on the solubility or ultraviolet absorption spectrum of BT in water, the vapor pressure at room temperature, the volatility from water, sorption by soil or sediments, chemical oxidation or photolysis in water, or environmental concentrations. Mackay and Wolkolf (1973) estimated that the half-life for volatilization of naphthalene from a typical lake is 2.2 hours. Therefore, we assumed by analogy that volatilization of BT might also be fast and that careful volatilization measurements would probably be required in this study.

Hydrogen peroxide, peracids, and hydroperoxides are reported to oxidize BT to the sulfoxide and subsequently to the sulfone derivative (Anashkina et al., 1972; Ponec and Prochazka, 1974; Ford and Young, 1965). Oxidation of BT in alkaline permanganate solution gives *o*-carboxylic acid and benzenesulfonic acid (Erickson, 1954).

BT absorbs strongly at 297 nm (log $\varepsilon$ 3.5) with a sharp decrease in the absorption spectrum going to the longer wavelengths (Haines et al., 1956). In the absence of air, purified neat BT is reported to be unstable to both daylight and mercury lamp irradiation and to form hydrogen sulfide, hydrogen, and condensed ring products.

Early studies by Maliyantz (1935), Strawinski (1950, 1951), and Zobell (1953) involved primarily anaerobic removal of organic sulfur from petroleum as $H_2S$. Kirshenbaum (1961) used aerobic conditions to convert the sulfur in petroleum into sulfate. However, these investigations were of a general type and did not deal with specific types of compounds. More pertinent to the current studies are those with dibenzothiophene (Yamada et al., 1968; Nakatani et al., 1968; Kodama et al., 1970, 1973; Gibson, 1975; and Hou and Laskin, 1975), or the studies with 2-thiophenecarboxylic acid and the studies with BT (Sagardia et al., 1975). Walker and Colwell (1974) and Walker et al. (1976) reported what may be biodegradations of benzothiophenes. These reports demonstrated that aerobic bacterial degradative processes were generally complex and frequently required the presence of other assimilable nutrients; in many cases, there was incomplete conversion of the substrate.

In most of the above investigations with thiophene compounds, petroleum hydrocarbons were present and they served as organic nutrients. Sagardia et al. (1975) used a light petroleum oil. They could not conclude whether the oil functioned to reduce the amount of benzothiophene in the aqueous phase and in this way reduced the toxicity of BT, or if it was the classical type of cometabolism first designated by this term in the studies of Leadbetter and Foster (1959).

While we anticipated that volatilization might be an important environmental pathway for BT, the literature data were insufficient for estimating the importance of adsorption by sediments, chemical oxidation, photolysis, or biodegradation. Therefore, screening studies were conducted for each of these processes.

## 11.3 ENVIRONMENTAL ASSESSMENT

### 11.3.1 Summary of Laboratory Data

The constants obtained in the laboratory investigations of the transformation and transport processes for BT are summarized in Table 11.2.

### 11.3.2 Environmental Assessment Using the One-Compartment Model

The half-lives of BT calculated for transformations and transport by individual environmental processes are listed in Table 11.3. Although the half-lives of BT vary fivefold among water bodies, the half-life for volatilization is the shortest in all standing waters and only dilution and sorption are faster in streams. Since volatilization occurs at the air-water interface and is linearly correlated with the oxygen reaeration rate constant at low turbulence (Part I), loss of BT from natural water bodies is expected to be roughly three times slower from sparingly mixed systems, such as deep stratified lakes, than from fast flowing streams.

TABLE 11.2. SUMMARY OF BENZO[b]THIOPHENE LABORATORY DATA

| Process | Sorption equilibrium | Partition coefficient |
|---|---|---|
| Sorption | $S_s = K_p S_w$ | $K_p = 59 \pm 2$[a]<br>$= 200$[b] |
| | Rate expression | Rate constant at 25°C |
| Volatilization[c] | $k_v[BT]$ | $k_v = (0.38 \pm 0.08)k_v^0$ |
| Photolysis[d] | $k_p[BT] = \Phi(\Sigma Z_\lambda \varepsilon_\lambda)[BT]$ | $k_p = (6.9 \pm 0.7) \times 10^{-7}\ \text{sec}^{-1}$ |
| Oxidation | $k_{ox}[RO_2\cdot][BT]$ | $k_{ox} = 83\ M^{-1}\ \text{sec}^{-1}$ |
| Hydrolysis | NA | $k_h = 0$ |
| Biodegradation | $k_{b_2} = \frac{\mu_{max}}{YK_s}$ | $k_{b_2} \sim 1.6 \times 10^{-6}\ \text{ml cell}^{-1}\ \text{hr}^{-1}$[e] |

[a] On Coyote Creek sediment.

[b] On laboratory mixture of microorganisms.

[c] See discussion in Part I, Section 5.3, and Appendix B.

[d] Assuming 12 hours sunlight per day in late May.

[e] BT degradation was not observed under our experimental conditions unless naphthalene was also present. This appeared to be a cometabolic process, but there is no kinetic expression that can be used to express the rate for this type of biodegradation. A rate constant one-half that of quinoline (Section 7.6.2) was used.

The photolysis half-life or BT is 25 to 120 days in surface waters (Table 11.3), assuming 12 hours of sunlight per day at the latitudes of San Francisco, Denver, and New York. These half-lives are nearly minimum for direct photolysis in natural waters during the late spring insolation. The minimum half-life of six days suggested by the experiments with humic acid (Section 11.5.1) is probably more realistic. Photolysis in clear lakes and small streams should be twice as fast as in turbid waters.

Oxidation and sorption are relatively unimportant as means of removing BT in natural waters. The oxidation rate was very slow in laboratory experiments, and extrapolation to environmental conditions suggests that oxidation in aquatic systems will be unimportant compared with other processes. Similarly, sorption is expected to generally remove less than 1% of the BT from solution, and even a significant increase of the sediment loading of natural waters would not change its relative role.

TABLE 11.3. TRANSFORMATION AND TRANSPORT OF BENZO[b]THIOPHENE PREDICTED BY THE ONE-COMPARTMENT MODEL

| Process | River | Eutrophic pond | Eutrophic lake | Oligotrophic lake |
|---|---|---|---|---|
| Photolysis, half-life (hr) | 1,200 | 2,900 | 3,500 | 600 |
| Oxidation, half-life (hr) | $10^5$ | $10^5$ | $10^5$ | $10^5$ |
| Volatilization, half-life (hr) | 45 | 230 | 180 | 180 |
| Hydrolysis | NA | NA | NA | NA |
| Biodegradation, half-life (hr)[a] | >20 | <20 | 20 | Very long |
| Half-life for all processes, except dilution (hr) | 14 | 19 | 19 | 140 |
| Half-life for all processes, including dilution (hr) | 0.8 | 19 | 19 | 140 |
| Amount BT adsorbed (mg $m^{-3}$)[b] | <5 | <15 | <2.5 | <0.5 |
| Percentage BT sorbed | 0.5 | 1.5 | 0.2 | 0.2 |

[a] Based on the assumption that the biodegradation rate of BT in the presence of alternative carbon sources will be one-half the biodegradation rate of quinoline when quinoline is the only carbon source.

[b] 1 μg $ml^{-1}$ BT is assumed in solution.

Although an enrichment culture for degradation of BT was developed in less than a week when naphthalene was present, enrichment cultures were not obtained in the absence of naphthalene. This result suggests that cometabolism of BT may be rapid, perhaps as rapid as volatilization.

In summary, the half-lives attributable to individual degradation mechanisms summarized in Table 11.3 suggest that volatilization and perhaps biodegradation will dominate the removal processes in typical ponds and lakes, but will be a factor of 10 less important than dilution in short stream segments. Indeed, the effects of dilution are only important in streams where the half-lives are 0.5 and 3.3 hours with and without dilution, respectively. The net effect in all water bodies is a rapid movement of undegraded BT either downstream or into the atmosphere.

### 11.3.3 Persistence

BT is unlikely to be persistent in the sense that this term has been used in pesticide research. Even the extremely low concentrations predicted in the computer simulations (next section) are improbable since BT biodegrades so rapidly.

### 11.3.4 Mass and Concentration Distributions Calculated Using Computer Models

The distributions of mass and concentration of BT expected at steady state during chronic discharge to each of four types of water bodies, as calculated with the aid of the computer model, are summarized in Table 11.4. The pseudo-first-order rate constants used in these simulations are presented in Appendix A.

The mass retained in each of these systems represents less than 1% of the BT in the inflowing waters, but of that 1%, 30% to 80% is retained in the sediments. The highest retention of BT in sediments occurs in the oligotrophic lake (0.78% of the total inflow) where biodegradation is minimal. The lowest percentage of retention in the sediments occurs in the eutrophic lake (0.32% of the total inflow). Because of the relatively small mass of suspended particulates, the soluble fraction dominates within the water columns of each system.

The interesting patterns with respect to the concentration of BT are best seen in Figures 11.1 through 11.4. Concentrations rapidly attain steady-state values in the well-mixed waters of the pond and river simulations and in the surface waters of the lake simulations, but change relatively slowly in the bottom waters of the lakes. Indeed, the concentrations in the deeper waters of the oligotrophic lake (Figure 11.4) scarcely change in the three to four weeks of simulated time following stoppage of discharge. Changes in sediment concentrations are extremely slow in all water bodies, because of the long times for scouring of sediments and exchange with the water column.

Concentrations of BT are highest in the suspended solids component of all the simulations although, for simplicity, this is shown only in Figure 11.1. Changes in concentration of suspended solids parallel changes in the concentrations of dissolved BT. Except in the river simulation, in which the sediment concentrations were still increasing at a significant rate when the simulated discharge was stopped, the concentrations of BT in the sediments were as much as twice as high as the concentrations of BT in solution.

TABLE 11.4. DISTRIBUTION OF BENZO[b]THIOPHENE IN VARIOUS AQUATIC SYSTEMS AT STEADY STATE (input concentrations of 1 μg ml$^{-1}$ benzo[b]thiophene

| | Pond | | River | | Eutrophic lake | | Oligotrophic lake | |
|---|---|---|---|---|---|---|---|---|
| | Mass (kg) | Conc. (μg ml$^{-1}$) | Mass (kg) | Conc. (μg ml$^{-1}$) | Mass (kg) | Conc. (μg ml$^{-1}$) | Mass (kg) | Conc. (μg ml$^{-1}$) |
| Compartment 1 (surface water) | | | | | | | | |
| Solution | 0.49 | 0.024 | 294 | 0.98 | 18.9 | 0.047 | 29.9 | 0.119 |
| Suspended solids | 0.007 | 1.16 | 1 | 49 | 0.029 | 2.32 | 0.075 | 6.00 |
| Compartment 2 (surface water) | | | | | | | | |
| Solution | -- | -- | 289 | 0.96 | 10.6 | 0.004 | 120 | 0.0478 |
| Suspended solids | -- | -- | 1.44 | 48 | 0.026 | 0.20 | 0.299 | 2.39 |
| Compartment 3 (surface water) | | | | | | | | |
| Solution | -- | -- | 285 | 0.95 | 0.548 | 0.002 | 10.7 | 0.0428 |
| Suspended solids | -- | -- | 1.42 | 47.5 | 0.0013 | 0.10 | 0.0267 | 2.14 |
| Compartment 5 (bottom water) | | | | | | | | |
| Solution | -- | -- | -- | -- | 0.242 | $9.7 \times 10^{-5}$ | 13.0 | 0.0052 |
| Suspended solids | -- | -- | -- | -- | 0.0006 | 0.0048 | 0.0326 | 0.260 |
| Compartments 7-9 (sediment)[a] | | | | | | | | |
| Solution | 0.006 | 0.024 | 0.72 | 0.96 | 0.105 | 0.012 | 0.0375 | 0.0430 |
| Solids | 0.78 | 1.16 | 97.2 | 48 | 8.2 | 0.60 | 29.2 | 2.15 |
| Total mass | 1.28 | | 969.8 | | 31.65 | | 203.38 | |

[a] The amounts given for solid and solution phases in the sediment compartments are estimated from the adsorption partition coefficient for suspended solids and may be overestimated because it was assumed that biodegradation of sorbed material does not occur.

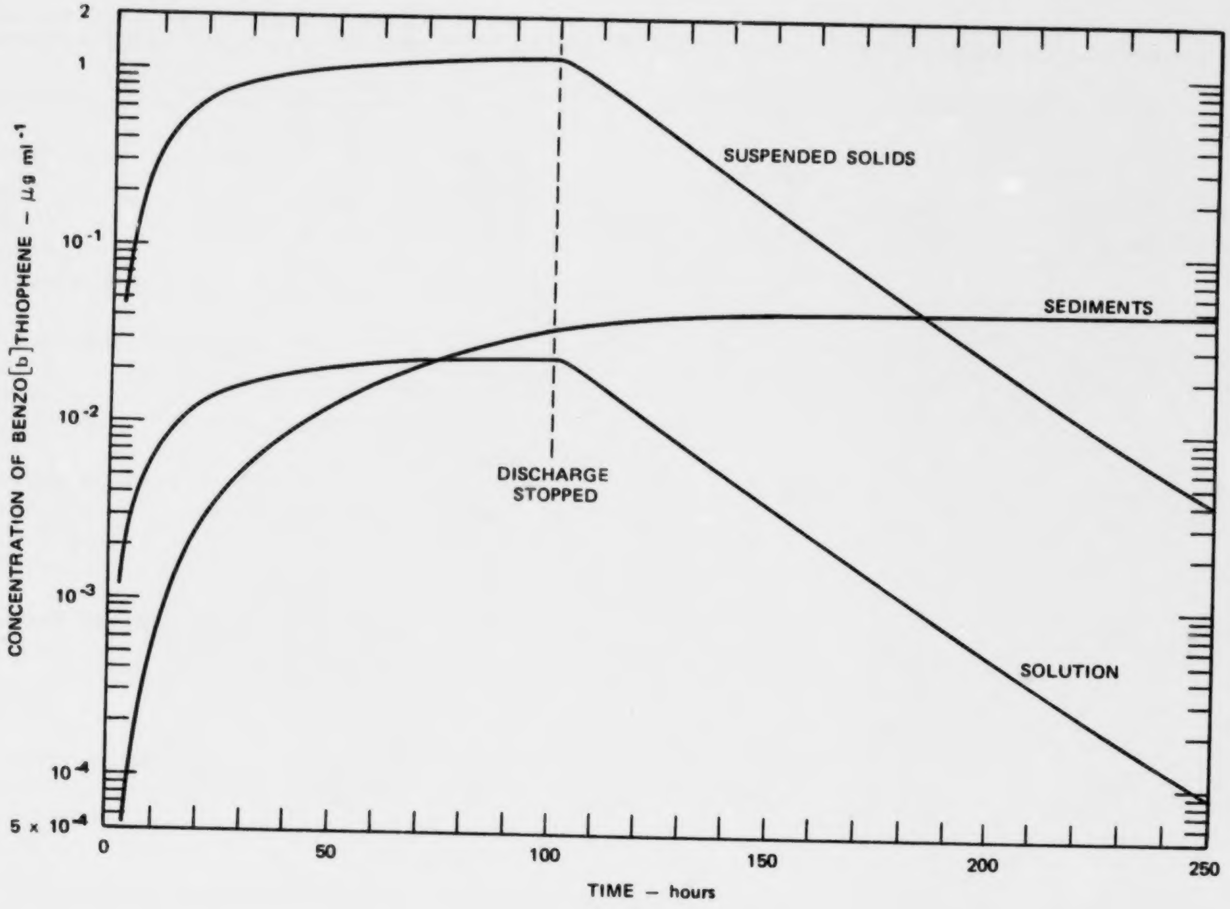

FIGURE 11.1 PERSISTENCE OF BENZO[b]THIOPHENE IN A PARTIALLY MIXED TWO-COMPARTMENT POND SYSTEM

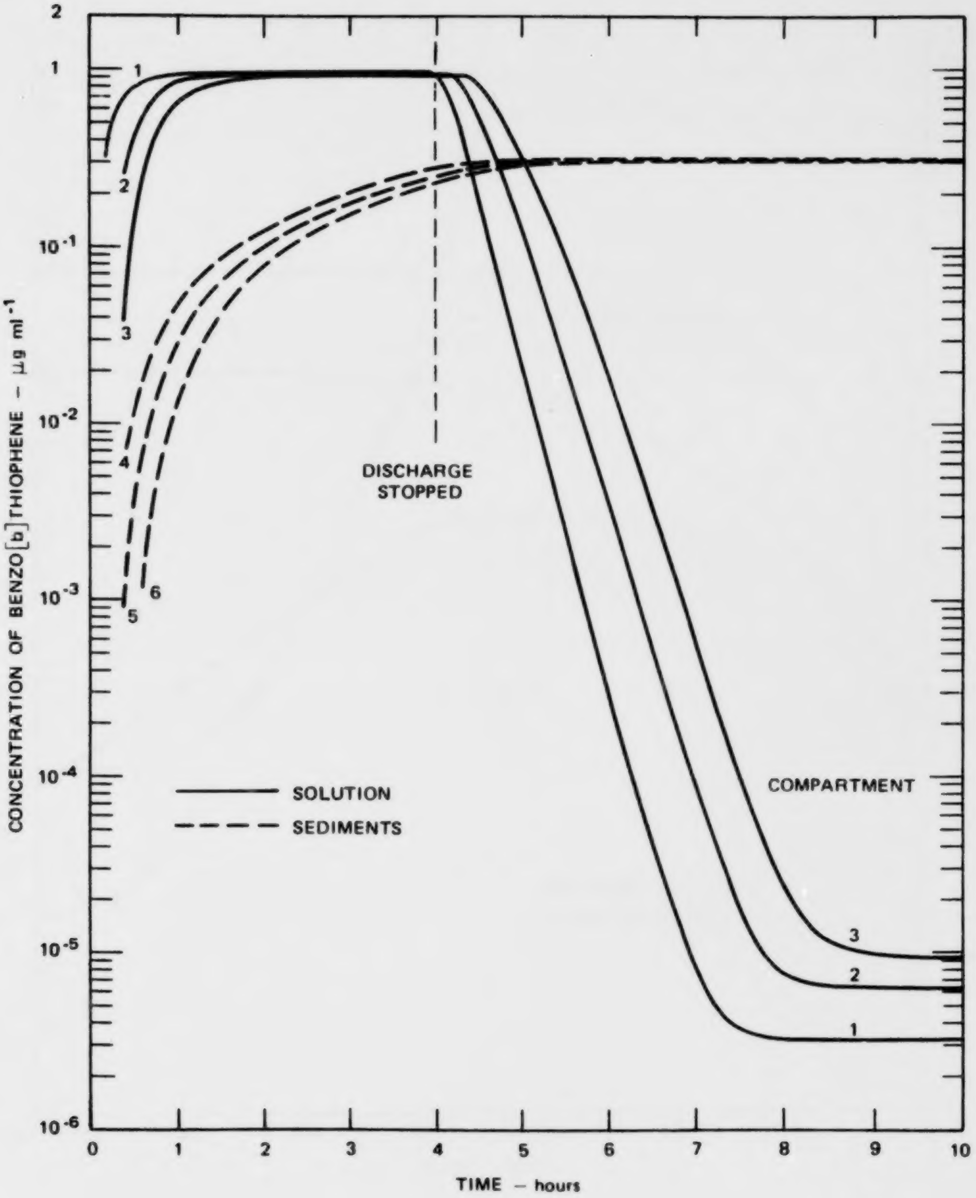

FIGURE 11.2 PERSISTENCE OF BENZO[b]THIOPHENE IN A PARTIALLY MIXED RIVER SYSTEM

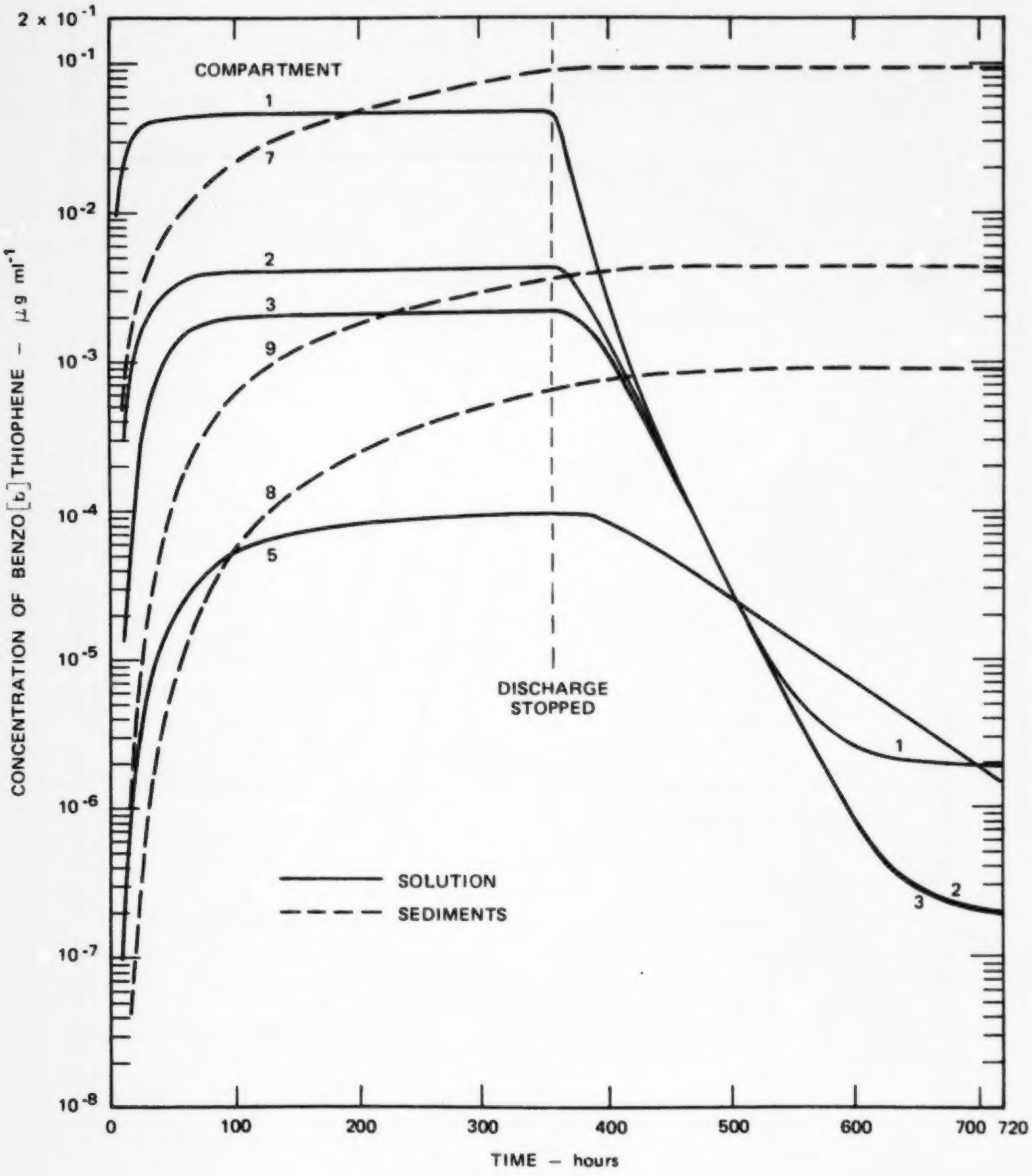

FIGURE 11.3 PERSISTENCE OF BENZO[b]THIOPHENE IN A PARTIALLY MIXED EUTROPHIC LAKE

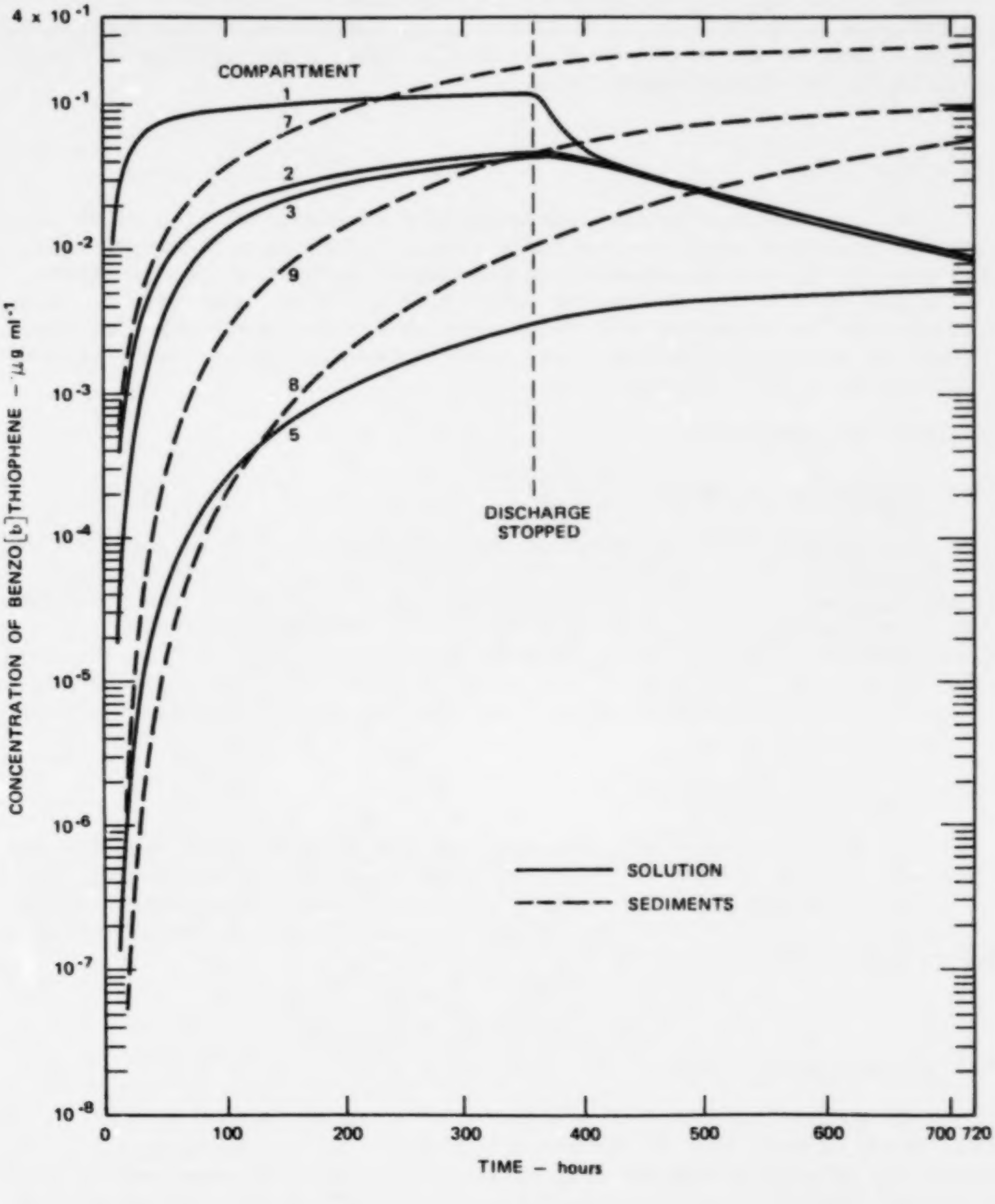

FIGURE 11.4 PERSISTENCE OF BENZO[b]THIOPHENE IN A PARTIALLY MIXED OLIGOTROPHIC LAKE

As expected, the highest concentrations both in solids and in solution occur near the sources (compartment 1 in each simulation), where values range from about $10^{-2}$ $\mu g\ ml^{-1}$ in the pond simulation to roughly 0.9 $\mu g\ ml^{-1}$ in the river simulation when the concentration in the waste stream is 1 $\mu g\ ml^{-1}$. Concentrations on solids and in solution in the lake simulations tend to be noticeably less in the deeper portions of the lake, although this is least pronounced in the oliogotrophic lake.

### 11.3.5 Discussion

The significance of the concentrations simulated in this study cannot be readily appraised with the available toxicological data; however, thiophene and by analogy BT, can be expected to be roughly equivalent to a p-cresol with respect to toxicity (McKee and Wolf, 1963). If so, some risk to aquatic organisms might be expected near discharges under the conditions simulated, but the risk to these organisms would appear generally to be low because of the rapid loss of BT from solution.

## 11.4 PHYSICAL PROPERTIES

### 11.4.1 Solubility in Water

The solubility of BT in water at 20.0°C was determined for five samples that were at room temperature before immersion and for six samples that had been warmed to 32°C before equilibration at 20.0°C. The solubility of the room temperature samples was 127.3 ± 2.5 (standard deviation) $\mu g\ ml^{-1}$, and the solubility of the warmed samples was 132.9 ± 4.6 $\mu g\ ml^{-1}$. The average solubility for all samples was 130.3 ± 4.6 $\mu g\ ml^{-1}$ ($9.7 \times 10^{-4}$ M). Thus, BT is slightly soluble in water (about five times as soluble as naphthalene).

### 11.4.2 Absorption Spectrum

Preliminary measurements showed that the UV absorption spectrum of BT in water is independent of pH in the range found in the environment (pH 5 to 9 was investigated). The absorption coefficients at wavelength intervals above 297.5 nm in distilled, deionized water at pH 6.6 (nonadjusted) are reported in Table 11.5.

### 11.4.3 Volatilization Rate

The volatilization of BT was measured using the method of Hill et al. (1976), which is described in Appendix B, Section B.1.3. Table 11.6 contains the BT volatilization data obtained at seven different oxygen reaeration rates. The BT volatilization rate constant $k_v^{BT}$ is plotted versus the oxygen reaeration rate $k_v^O$ in Figure 11.5.

TABLE 11.5. ABSORPTION SPECTRUM OF BENZO[b]THIOPHENE IN WATER AT pH 6.6[a]

| Center of wavelength interval[b] (nm) | Absorption coefficient (l mole$^{-1}$ cm$^{-1}$) |
|---|---|
| 297.5 | 1793 |
| 300.0 | 395 |
| 302.5 | 130 |
| 305.0 | 30 |
| 307.5 | 13 |
| 310.0 | 7 |
| 312.5[c] | 3 |
| 315.0 | 0 |

[a] Benzo[b]thiophene concentration is 18.7 μg ml$^{-1}$ (1.39 x 10$^{-4}$ M) in a 1-cm cell.

[b] The wavelength intervals are given in Appendix B, Table B.1.

[c] The absorption coefficient at 313.0 nm is 1.

In Part I, Section 5.3, it was shown that at low reaeration rates, the liquid film resistance is the rate controlling factor. Under these conditions, it was shown that the ratio $k_v^{BT}/k_v^0$ is equal to the ratio of the molecular diffusion constants D or the inverse of the ratio of the molecular diameters (equation 11.1).

$$\frac{k_v^{BT}}{k_v^0} = \frac{D_{BT}}{D_0} = \frac{d_0}{d_{BT}} \qquad (11.1)$$

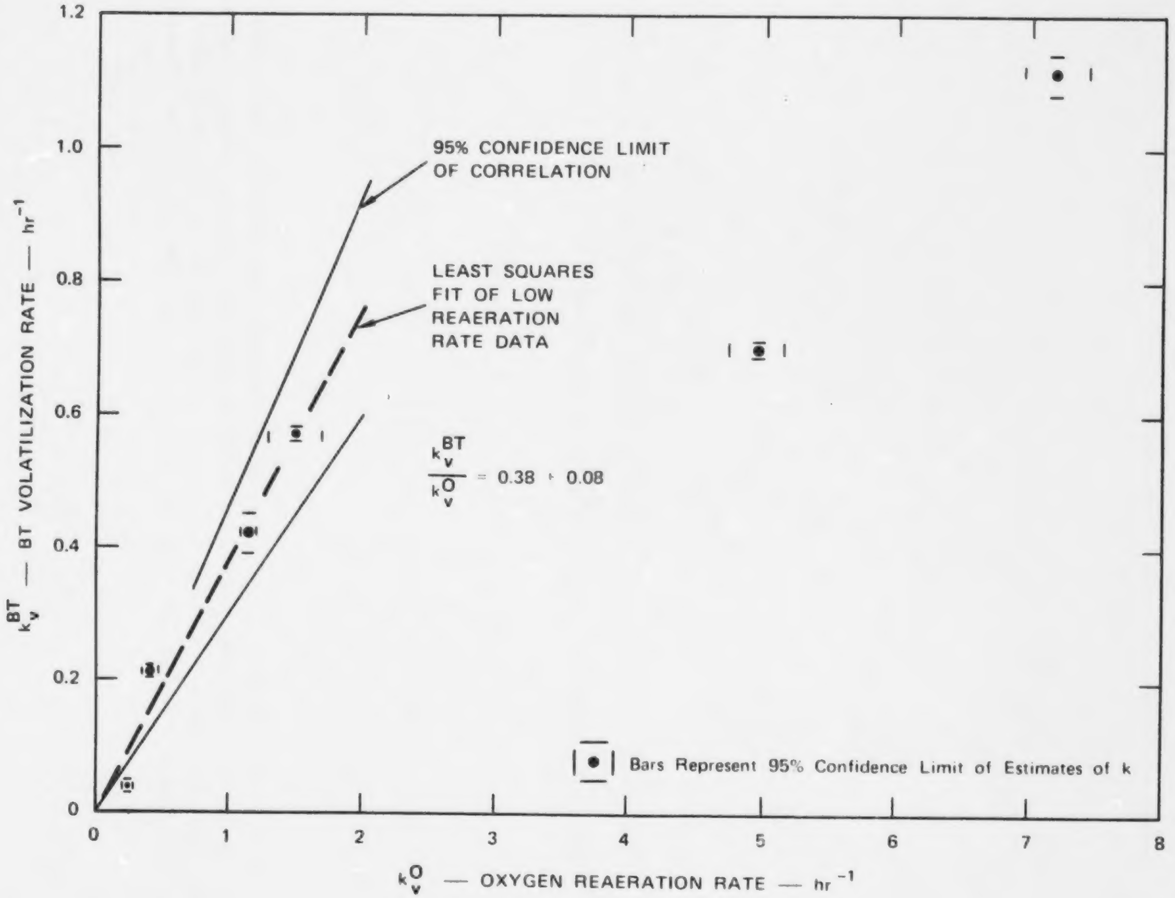

SA-4396-3

FIGURE 11.5 VOLATILIZATION OF BENZO[b]THIOPHENE FROM AQUEOUS SOLUTION

TABLE 11.6. VOLATILIZATION RATE DATA FOR BENZO[b]THIOPHENE

| Oxygen reaeration rate $k_v^O(hr^{-1})$ | BT volatilization rate $k_v^{BT}(hr^{-1})$ | $k_v^{BT}/k_v^O$ |
|---|---|---|
| 0.062 ± 0.002[a] | 0.087 ± 0.001[a] | 1.40 ± 0.06[a] |
| 0.26 ± 0.01 | 0.04 ± 0.004 | 0.15 ± 0.02 |
| 0.40 ± 0.03 | 0.21 ± 0.002 | 0.53 ± 0.04 |
| 1.16 ± 0.03 | 0.42 ± 0.015 | 0.36 ± 0.02 |
| 1.48 ± 0.09 | 0.57 ± 0.003 | 0.38 ± 0.02 |
| 4.97 ± 0.07 | 0.70 ± 0.007 | 0.14 ± 0.004 |
| 7.19 ± 0.11 | 1.11 ± 0.015 | 0.15 ± 0.008 |

[a] Standard deviation.

A value of d for BT may be estimated from the kinetic theory of gases (Present, 1958), in which the molecular volume (based on hard spheres) of a compound is between 1/3 to 1/2 of the critical volume. Using Lydersen's critical property increments (Reid and Sherwood, 1966), we estimate the critical volume to be 379 ml mole$^{-1}$. From this critical volume, the molecular diameter is estimated to be from 7.4 to 8.4 Å. Since the molecular diameter of oxygen is 2.98 Å (Tsivoglou, 1965), the expected ratio from equation (11.1) falls between 0.40 and 0.35. The experimental ratio of 0.38, obtained from a least squares regression of the $k_v^{BT}/k_v^O$ ratio for experimental data obtained when $k_v^O$ is less than 1.5 hr$^{-1}$ (see Figure 11.5), is in good agreement with the theoretical estimate.

At higher reaeration rates, the gas-film resistance becomes important. The data in Table 11.6 include only two high reaeration points. The experimental error of these points is only a few percent, and it is unlikely that the two high reaeration points also fall on the line that fits the data obtained at reaeration rates less than 1.5 hr$^{-1}$ (see Figure 11.5). However, since there are only two data points, we are reluctant to estimate a value for $k_v^{BT}/k_v^O$. It is therefore difficult to determine whether the limiting equation

$$\frac{k_v^{BT}}{k_v^O} = \frac{d_O H^{BT}}{d_{BT} H^O} \qquad (11.2)$$

where H is the Henry's law constant, applies for the data. If this limiting form does apply to the data, the two points suggest that the Henry's law constant for BT is less than the Henry's law constant for oxygen, $H^0$ ($3 \times 10^7$ torr). The value of the Henry's law constant for BT, $H^{BT}$, can be estimated by using equations (4) and (5) of Mackay and Wolkolf (1973). Using the measured solubility of 130 μg $ml^{-1}$ and assuming that the vapor pressure of BT is the same as naphthalene (0.23 torr at 20°C), we can calculate that the Henry's law constant for BT is $1.3 \times 10^4$ torr (230 torr $M^{-1}$). Therefore, at high reaeration, the ratio of $k_v^{BT}/k_v^0$ should be

$$\frac{k_v^{BT}}{k_v^0} \sim 0.38 \, \frac{1.3 \times 10^4}{3 \times 10^7} = 2 \times 10^{-4} \qquad (11.3)$$

The ratio for the two high reaeration rate data points is about 0.15. The cause of the lack of agreement is probably that the volatilization rate ratio is in an intermediate turbulence range and should be expressed by a more complex form (see Part I, Section 5.3). It is difficult to use this expression because we do not have a good way to estimate either the diffusivity of BT or the film thickness. It is also possible that the estimate of $H^{BT}$ is incorrect, but it is not likely to be underestimated by three orders of magnitude.

### 11.4.4 Sorption on Clay and Sediments

Two sorption isotherms were measured with a calcium montmorillonite clay and two with a natural sediment collected from Coyote Creek, San Jose, California. The isotherms were measured at two sediment or clay loadings and with initial BT concentrations of about 4 and 8 μg $ml^{-1}$. Precautions were taken to minimize exposure to light and volatilization. The results of these experiments are summarized in Table 11.7.

Very little sorption of BT took place on the calcium montmorillonite clay. A small but statistically significant difference existed between the concentration of BT in the blanks and the concentration in the supernatant from the clay. However, there was no statistically significant difference between the BT concentrations in the supernatant in the low and high clay loading samples. This was true for both clay isotherms.

The data from the two calcium montmorillonite clay experiments were used to estimate an upper bound of $K_p = 17$ for the sorption partition coefficient. It is possible that the small differences in BT concentration between blanks and clay samples could be attributed to a volatilization loss, since the workup of the clay samples involved one extra transfer and centrifugation that was not carried out during the workup of the blanks. The fact that the loss of BT in the clay samples was independent of clay loading would seem to support this possibility. This loss (expressed as percentage difference from blanks) remained relatively constant (9.9%, 11.2%, 11.2%, and 7.5%) over a wide range of clay loadings (100:1, 1000:1, 2000:1, and 5000:1 clay:BT by

TABLE 11.7. SORPTION OF BENZO[b]THIOPHENE ON SEDIMENTS

| Sediments | Total organic carbon (percent) | Sediment concentration (mg $ml^{-1}$) | BT concentration in supernatant (mg $ml^{-1}$)[a] | BT concentration on sediment ($\mu g\ g^{-1}$)[b] | Partition coefficient, $K_p$[c] | |
|---|---|---|---|---|---|---|
| | | | | | $a_o = 0$ | $a_o \neq 0$ |
| Ca-montmorillonite clay sorption | 0.06 | 6.0 | 2.0 ± 0.1 | 36.0 ± 21 | 11 ± 6 | -170 ± 50<br>($a_o$ = 374 ± 96) |
| | | 15 | 2.1 ± 0.1 | 8.9 ± 5.2 | | |
| Coyote Creek sorption | 1.4 | 8.2 | 2.3 ± 0.0 | 130.0 ± 10 | 59 ± 2 | 57 ± 8<br>($a_o$ = 3 ± 20) |
| | | 16 | 3.7 ± 0.2 | 220.0 ± 10 | | |
| | | 19 | 1.5 ± 0.1 | 100.0 ± 10 | | |
| | | 41 | 2.3 ± 0.0 | 120.0 ± 10 | | |

[a] Concentration measured in supernatant with population standard deviation.

[b] Concentration on sediment calculated from supernatant concentration with population standard deviation.

[c] Calculated by linear least squares method; see Appendix B, Section B.1.4 for description of regressions. Limits are 95% confidence limit.

weight, respectively). It is also possible that the clay:BT loadings that were used in the isotherms were not in the optimal range for measuring adsorption.

Good sorption data were obtained, however, with Coyote Creek sediment loadings of 2000:1 and 5000:1 sediment:BT by weight in those isotherms. The partition coefficient of 59 estimated from these experiments with Coyote Creek sediment suggests that sorption of BT was not strong, and comparisons with volatilization and biodegradation (Section 11.6) supported this conclusion. Since the environmental assessment suggested that less than 1% of the BT would be sorbed, no additional isotherm measurements using other natural sediments were made.

### 11.4.5 Biosorption

The sorption data obtained with 100 and 300 ng ml$^{-1}$ solutions of BT with living as well as heat-killed mixed populations of *Azotobacter beijerinckii* ATCC 19366, *Bacillus cereus* ATCC 11778, *Escherichia coli* ATCC 9637, and *Serratia marcescens* ATCC 13880 are presented in Table 11.8. The sorption partition coefficients for heat-killed cells are more than twice as large as for living cells.

TABLE 11.8. BIOSORPTION OF BENZO[b]THIOPHENE BY MIXED BACTERIAL CULTURES

| Condition of cells | Initial level of BT (ng ml$^{-1}$) | Sorption coefficient[a] |
|---|---|---|
| Viable cells | 100 | 122 ± 17 |
| Viable cells | 300 | 130 ± 22 |
| Heat-killed cells | 100 | 284 ± 92 |
| Heat-killed cells | 300 | 275 ± 71 |

[a] (μg/g)/(μg/ml), based on dry weights of cells, average coefficients ± standard deviation. Dry weights of viable cells = 1.02 ng ml$^{-1}$; heat-killed cells, 0.838 ng ml$^{-1}$.

The sorption of BT by heat-killed cells is not surprising and is probably associated with the lipid content of these cells. The sorption coefficient of heat-killed cells, as compared with viable cells, appears to be somewhat higher, as is indicated by the recoveries. These differences in recovery yields could readily account for the differences in sorption coefficients, which are of a relatively low order and not of great significance for a pollutant.

## 11.5 CHEMICAL TRANSFORMATION

### 11.5.1 Photolysis Rate

Data for the photolysis of BT in pure water and in water containing 9.5 μg $ml^{-1}$ humic acid are given in Table 11.9.

TABLE 11.9. RATE CONSTANTS FOR PHOTOLYSIS OF 1.0 μg $ml^{-1}$ BENZO[b]THIOPHENE[a]

| Irradiation source | Solution | Extent of reaction (%) | Rate constant $k_p \times 10^6$ $sec^{-1}$ |
|---|---|---|---|
| Borosilicate filter only | Pure water, pH 6.9 | 39 | 3.50 ± 0.22[b] |
| | | 84 | 5.12 ± 0.28 |
| Sunlight, late May | Pure water, pH 6.9 | 11 | 0.689 ± 0.072[c,d] |
| 313 nm | 9.5 μg $ml^{-1}$ humic acid, pH 5.4 | 22 | 0.851 ± 0.013 |

[a] 1.0 μg $ml^{-1}$ benzothiophene in water = $7.45 \times 10^{-6}$ M.

[b] Standard deviation.

[c] Calculated on basis of 12 hours of sunlight per day; to obtain average rate constant for full calendar day (24 hours), divide rate constant by two.

[d] Half-life of 23 calendar days.

Direct photolyses using only the borosilicate lamp well as a light filter to eliminate wavelengths below 290 nm were carried out to 39% and 84% consumption of BT; good first-order kinetic behavior was observed. Since BT has only a very small absorption coefficient at 313 nm, the borosilicate glass filter system was used since it provides greater light intensity than the 313-nm filter system for these screening experiments. The reason for the difference in the two rate constants in Table 11.9 is not known, but may be due to a change in the light flux. With the first-order photolysis behavior demonstrated by these experiments, direct photolysis of BT in sunlight was carried out to 11% loss of BT, and the rate constant in Table 11.9 was calculated from a first-order plot of the sunlight photolysis data.

A quantum yield was not measured for the direct photolysis of BT because volatilization of BT with a half-life of just a few hours appears to be the dominant pathway of BT (see Section 11.3); sunlight photolysis is only

1/100 as fast. Moreover, to measure the quantum yield of direct photolysis at 313 nm would require several hundred hours irradiation time because of the very small and uncertain value for the absorption coefficient for BT at this wavelength. The time and effort required for this experiment did not seem justified in view of the lesser importance of photolysis of BT as an environmental pathway.

It was, however, of interest to estimate how the photolysis half-life would vary as a function of the time of year by calculating the half-life of BT in sunlight as a function of season using the procedure of Zepp and Cline (1977). To make this calculation, a quantum yield for direct photolysis must either be measured or estimated. The direct photolysis in late May sunlight was found to have a measured half-life of 23 days. If a quantum yield of 0.1 is assumed, half-lives of 32 days in midspring and 17 days in midsummer are calculated using the procedure of Zepp and Cline. The agreement between the calculated and measured half-lives indicates that direct photolysis of BT has a quantum yield of $\sim$ 0.1.

The annual variation of half-life for direct photolysis of BT using a quantum yield of 0.1 is given in Figure 11.6. The figure shows that the half-life will vary from about 17 days during summer to over 350 days in winter.

The data in Table 11.9 show that the presence of humic acid promotes the photolytic transformation of BT. If we assume, based on the previous discussion, that direct photolysis of BT at 313 nm has a quantum yield of 0.1 and that the absorption coefficient at 313 nm has a maximum value of unity, the photolysis half-life of BT at 313 nm is greater than 950 hours. Thus, the acceleration of photolysis rate at 313 nm in the presence of humic acid may then be as much as fourfold: the half-life for BT, when photolyzed for 12 hours per day in sunlight in the presence of humic acid, may be about 6 days. Although the sensitized photolysis is a rapid process, volatilization will still be dominant under most environmental conditions, and for this reason no humic-acid-sensitized photolysis of BT was conducted in sunlight.

### 11.5.2 Oxidation Rate

The susceptibility of 1.2 $\mu$g ml$^{-1}$ ($8.8 \times 10^{-6}$ M) BT to free radical oxidation was examined using the AA-initiated oxidation reaction (see Part I, Section 6.3 of this report and Appendix B for discussion and procedure). This experiment was carried out at 50°C in pure water containing $1.0 \times 10^{-4}$ M AA. At the end of 100 hours reaction time, 60% of the BT had been consumed, corresponding to a first-order rate constant ($k_{ox}[RO_2\cdot]$) of $2.5 \times 10^{-6}$ sec$^{-1}$. Under these conditions (see Part I, Section 6.3) this value corresponds to a second-order rate constant $k_{ox}$ of 750 M$^{-1}$ sec$^{-1}$. At 25°C, $k_{ox}$ would be 83 M$^{-1}$ sec$^{-1}$, and with the assumption that $[RO_2\cdot] = 10^{-9}$ M in the environment, the half-life for BT toward oxidation in the aquatic environment is 96 days. The free radical oxidation of BT by $RO_2\cdot$ is clearly not competitive with volatilization in aquatic systems.

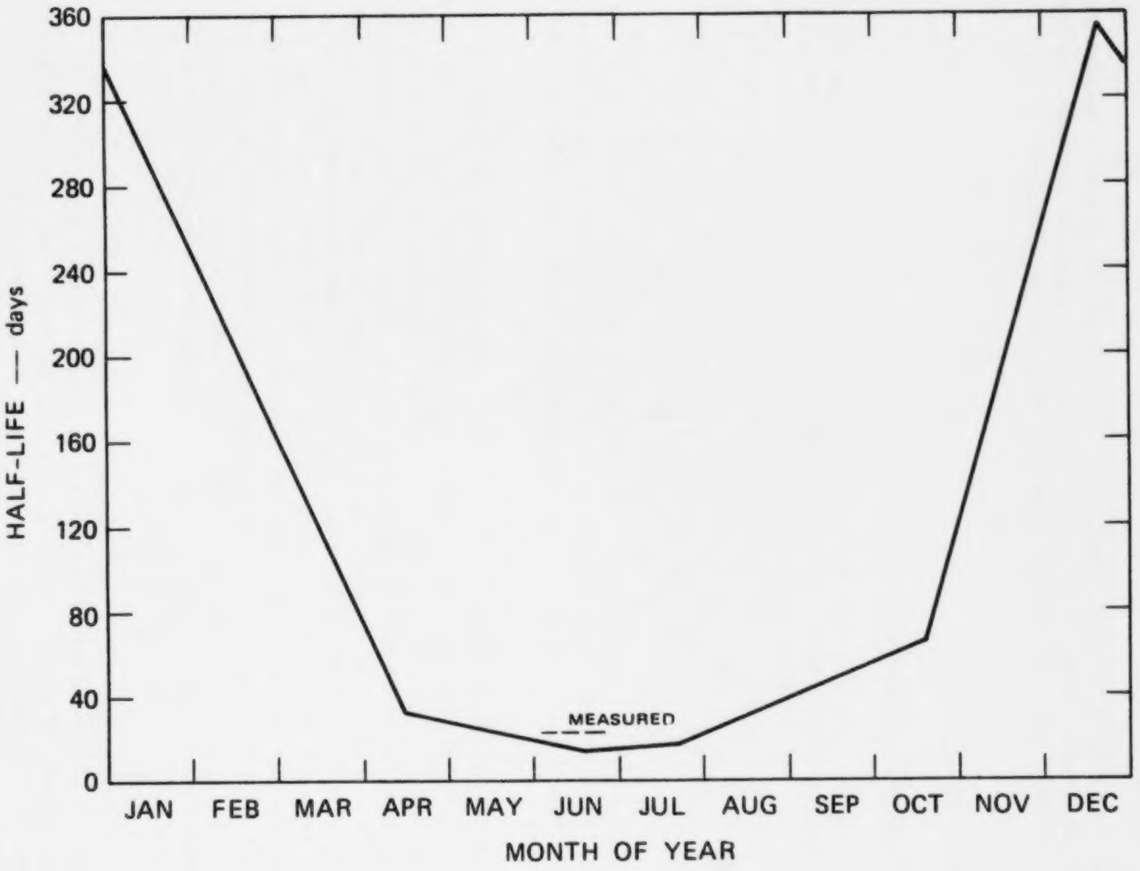

SA-4396-68

FIGURE 11.6 ANNUAL VARIATION OF PHOTOLYSIS HALF-LIFE FOR BENZO[b]THIOPHENE

### 11.5.3 Hydrolysis Rate

BT contains no functional groups that are hydrolyzable; therefore, no hydrolysis studies were carried out.

### 11.5.4 Products from Chemical Transformation

Since screening studies indicated that chemical transformation processes were not competitive with volatilization in aquatic systems, detailed kinetic and product identification studies were not carried out.

## 11.6 BIODEGRADATION

### 11.6.1 Development of Enrichment Cultures

Samples of Coyote Creek water and aeration effluent from the Palo Alto Sewage Plant, which were aerated and buffered in our 9-liter fermentors, did not produce BT-degrading systems when BT was the only carbon source added.* Because of the volatility of BT from aqueous solutions that are aerated, BT was added equivalent to 10, 10, 50, and 50 $\mu g\ ml^{-1}$ at days 0, 2, 4, and 7, respectively. Aliquots from the 5-liter volumes in the 9-liter fermentors were transferred at 3, 7, 10, and 14 days to media composed of basal inorganic salts, BT (50 $\mu g\ ml^{-1}$), glucose (50 $\mu g\ ml^{-1}$), and Difco Bacto yeast extract (50 $\mu g\ ml^{-1}$). This medium (100 ml) was contained in 500-ml Erlenmeyer flasks, which were capped with aluminum foil or screw-on caps to prevent loss of BT by aeration. BT-biodegradation was also not observed in these shaker flasks.

BT-biodegrading systems were, however, obtained in the 9-liter bottle fermentors after five to eight days if BT and naphthalene (each equivalent to 10 $\mu g\ ml^{-1}$) were added at two-day intervals. Transfers from the 9-liter fermentors were made to shaker flasks with media containing BT, naphthalene, and basal salts. Degrading systems were obtained with waters from Coyote Creek and from the eutrophic pond near Searsville Lake in Woodside, California, as well as with aeration effluents from the Palo Alto, South San Francisco, and Shell Oil Refinery wastewater treatment plants. These mixed cultures could be readily adapted to grow on media containing BT and naphthalene, each at 50 $\mu g\ ml^{-1}$. The Lake Tahoe water sample did not yield a BT-degrading system after six weeks of aerobic incubation and addition of BT and naphthalene (10 $\mu g\ ml^{-1}$ of each).

With all the above BT/naphthalene enrichment cultures, there was generally 70% to 80% decomposition of BT in two to three days when the media initially contained 50 $\mu g\ ml^{-1}$ each of BT and naphthalene. It soon became apparent that BT degradation was dependent on the presence of naphthalene. In an effort to develop a system without this dependency on naphthalene (that is, a system that would degrade BT when BT was the sole carbon source),

---

[*] These data were obtained using a UV assay, as described in Appendix B.

we attempted to develop a biodegrading system with aeration effluents from the Shell Oil Refinery. The following observations were made.

- When a transfer was made from a medium containing BT and naphthalene each at 30 $\mu$g ml$^{-1}$ to a medium containing only 30 $\mu$g ml$^{-1}$ BT as the sole carbon source, no BT degradation took place.

- When the culture mixture was grown in a medium containing BT and naphthalene each at 50 $\mu$g ml$^{-1}$, more than 80% of the BT was decomposed in 76 hours, but if tryptone (50 $\mu$g ml$^{-1}$), or a mixture of glucose (50 $\mu$g ml$^{-1}$) and Difco Yeast Extract (10 $\mu$g ml$^{-1}$) was substituted for the naphthalene, no BT degradation occurred.

- When the culture mixture was grown with naphthalene (50 $\mu$g ml$^{-1}$) as the sole carbon source, it developed an optical density of 0.05 at 24 hours, but when BT and naphthalene were present (50 $\mu$g of each ml$^{-1}$) the optical density was 0.03.

- When transfers were made to mineral salts/BT (5 and 10 $\mu$g ml$^{-1}$) no BT degradation took place in 64 hours. If at this time, naphthalene (10 $\mu$g ml$^{-1}$) was added, more than 90% of the BT was degraded in 24 hours.

- Growth was observed when the basal salts medium was supplemented with BT (20 $\mu$g ml$^{-1}$) and quinoline (50 $\mu$g ml$^{-1}$), but no BT degradation occurred in 7 days. The control with BT (20 $\mu$g ml$^{-1}$) and naphthalene (50 $\mu$g ml$^{-1}$) had more than 90% destruction of BT in 36 hours.

- The culture mixtures grown in salts/naphthalene (100 $\mu$g ml$^{-1}$) and in salts/BT (20 $\mu$g ml$^{-1}$) plus naphthalene (100 $\mu$g ml$^{-1}$) media for 22 hours were centrifuged, washed, and suspended in 0.05% phosphate buffer (pH 7.0). Cells were rested at RT for 20 hours, centrifuged again, and resuspended in salts media containing BT (20 $\mu$g ml$^{-1}$), or BT (20 $\mu$g ml$^{-1}$) plus naphthalene (20 $\mu$g ml$^{-1}$). The following results were obtained:

| Additives to growth media ($\mu$g ml$^{-1}$) | | Additives to test media ($\mu$g ml$^{-1}$) | | Residual BT (%) | |
|---|---|---|---|---|---|
| BT | N | BT | N | 7 hr | 22 hr |
| 0 | 100 | 20 | 0 | 96 | 88 |
| 0 | 100 | 20 | 20 | 72 | 1 |
| 20 | 100 | 20 | 0 | 98 | 92 |
| 20 | 100 | 20 | 20 | 37 | 0 |

- Cultures grown on salts media supplemented with BT (50 $\mu$g ml$^{-1}$) and naphthalene (50 $\mu$g ml$^{-1}$) for 64 and 70 hours had residual BT values of 25 and 1 $\mu$g ml$^{-1}$, and cell counts of $7.2 \times 10^7$ and $13.2 \times 10^7$ cells ml$^{-1}$, respectively.

- A BT-degrading system without dependency on the presence of naphthalene could not be developed by repeated subtransfers on media with gradual sequentially reduced naphthalene concentrations. When naphthalene was reduced to 10 μg ml$^{-1}$, 80% of the initial 30 μg ml$^{-1}$ of BT was decomposed; but when naphthalene was at 5 μg ml$^{-1}$, only 40% to 70% of the initial 30 μg ml$^{-1}$ BT was degraded.

- Replacing $(NH_4)_2SO_4$ with $NH_4NO_3$ to reduce $SO_4^{=}$ in the basal salts medium did not affect the results.

In our final attempt to develop cultures that could degrade BT when it was the only carbon source in an inorganic salts medium, we incubated aeration effluent from the Palo Alto Sewage Plant in our 9-liter aerobic fermentors with initial additions of BT and naphthalene (10 μg ml$^{-1}$ of each), BT and quinoline (10 μg ml$^{-1}$ of each), BT and glucose (10 μg ml$^{-1}$ of each) with Difco Bacto Yeast Extract (1 μg ml$^{-1}$), and BT and Difco Bacto tryptone (10 μg ml$^{-1}$ of each). At day 2, additional quantities of all the above components except quinoline were added to the respective bottles. Subsequently, all compounds or preparations as originally present were added at two-day intervals. Periodically, aliquots from the 9-liter fermentors were transferred to capped shaker flasks containing inorganic salts media and the corresponding additives. After 6 days, a BT-degrading system was obtained only in the bottle with BT and naphthalene as additives. After 26 days of incubation of the 9-liter fermentors and 13 days of incubation of the subtransfers in shaker flasks, no other BT-degrading systems were observed.

### 11.6.2 Biodegradation Kinetics

Because no culture system was developed that could utilize BT as the sole carbon source, no kinetic studies were conducted.

### 11.6.3 Identification of Metabolites

Six BT metabolites were tentatively identified by gas chromatography/mass spectrometry analysis of ethyl acetate extracts of acidified fermentations in which BT and naphthalene were the only carbon substrates. The products were assigned the following structures:

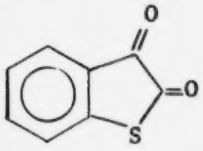
I

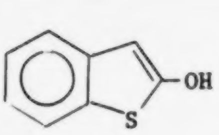
II

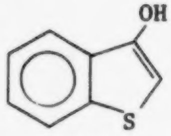
III

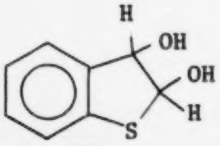
IV
(cis and trans
isomers)

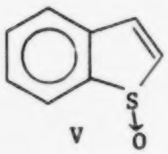
V

Subsequent studies have shown that products II and III are artifacts of the analytical procedure.

### 11.6.4 Discussion

The fact that all our BT degrading systems depended on naphthalene does not necessarily indicate that if we had used other hydrocarbons we could not have obtained BT decomposition. Naphthalene was selected in our studies because we felt it might be an inducer of enzymes that could also degrade BT and because naphthalene would usually be present in larger amounts if BT were discharged into aquatic systems.

In the enrichment studies it was apparent that BT had a toxic effect on microorganisms, and this may be an important factor in our failure to develop a culture system that would utilize BT as a sole carbon source. Although our studies involved reservoirs of many types of organisms, as is the realistic situation in nature, this does not preclude the possibility that microorganisms exist or may be developed that could utilize BT as a sole source of carbon. More realistic, however, is the fact that in the environment many other pollutants coexist that could function in cooxidative mechanisms to decompose BT.

The structures of the metabolites observed in these studies indicate that the thiophene ring is susceptible to biological oxidation. These compounds represent nearly all primary oxidations that could be expected on the carbons and sulfur in the thiophene ring.

# 12. LABORATORY INVESTIGATION OF DIBENZOTHIOPHENE

## 12.1 SYNOPSIS

The results of the laboratory investigation suggest that biodegradation is the major environmental pathway for dibenzothiophene (DBT) in eutrophic waters, while volatilization and photolysis dominate in oligotrophic waters. Dilution is competitive with biodegradation in eutrophic lakes and ponds and is several times faster in rivers. Sorption is important only in ponds where heavy sediment loading is assumed.

The nine-compartment environmental exposure model predicted the following steady-state concentrations of DBT in solution, suspended solids, and sediments near point sources in the presence of a continuous discharge of 1 $\mu g\ ml^{-1}$ (1 ppm) DBT:

|  | Half-life* (hr) | Solution ($\mu g\ ml^{-1}$) | Suspended solids ($\mu g\ g^{-1}$) | Sediments ($\mu g\ g^{-1}$) |
|---|---|---|---|---|
| River | 0.5 | $8.50 \times 10^{-3}$ | $1.19 \times 10$ | $1.15 \times 10$ |
| Pond | 13 | $1.32 \times 10^{-4}$ | $1.84 \times 10^{-1}$ | $1.84 \times 10^{-1}$ |
| Eutrophic lake | 13 | $3.72 \times 10^{-4}$ | $5.20 \times 10^{-1}$ | $1.32 \times 10^{-1}$ |
| Oligotrophic lake | 140 | $1.06 \times 10^{-3}$ | 1.48 | $5.10 \times 10^{-1}$ |

## 12.2 BACKGROUND

Dibenzothiophene is found in coal tars and petroleum and is probably in the effluent streams from coal gasification or liquefaction. Dibenzothiophene is also representative of the large class of organic sulfur compounds, including thiophenes, thienylsulfides, benzo(b)thiophenes, dibenzothiophenes, and benzo(b)naphthothiophenes, which could present particular problems in the environment. The physical properties of dibenzothiophene (DBT) are listed in Table 12.1.

The dibenzothiophenes present in coal and bitumens have recently been discussed by Hayatsu et al. (1975) and Clugston et al. (1976), respectively.

---

*Predicted by the one-compartment model.

### TABLE 12.1. PHYSICAL PROPERTIES OF DIBENZOTHIOPHENE

| | |
|---|---|
| Structure | 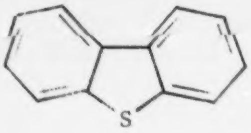 |
| Molecular weight | 184.27 |
| Melting point (°C)[a] | 99-100 |
| Boiling point (°C)[a] | 332-3 |
| Vapor pressure at 20° (torr)[b] | $2 \times 10^{-3}$ |
| Solubility in water ($\mu g\ ml^{-1}$)[c] | 1.11 ± 0.09 |
| UV spectrum (in ethanol) [$\lambda_{max}$ nm (log $\varepsilon$)][a] | 234 (4.9)<br>256 (4.3)<br>262 (4.1)<br>303 (3.5)<br>325 (3.6) |
| 1 $\mu g\ ml^{-1}$ DBT = $5.43 \times 10^{-6}$ M | |

[a] *CRC Handbook of Chemistry and Physics*, 57th Ed., 1976.

[b] Estimated from empirical equation for temperature range 110° to 330°C (Aubry et al., 1975).

[c] Measured in this study (Section 12.4.1).

Concentration data for dibenzothiophenes in coal, coal tars, and petroleum crude oils are somewhat controversial because thermal degradation of the national sulfur-containing polycyclic compounds may occur during analysis. However, there is ample evidence that many of these compounds are polyalkylated. In American Petroleum Institute studies on some crude oils, no dibenzothiophenes were reported (C. T. Hou, personal communication), but Kuwait and South Louisiana crude oils contained 3.3% and 0.4% dibenzothiophenes, respectively. These crudes also contained 5.9% and 0.7% naphthalenes, respectively.

Data on the water solubility, volatilization, or sorption of DBT could not be found in the literature.

Dibenzothiophene will not hydrolyze under the conditions prevailing in environmental aquatic systems.

Data were not available for evaluating the importance of chemical oxidation of DBT under environmental conditions. However, benzothiophene is oxidized to the sulfoxide and sulfone by hydrogen peroxide, peracids, and hydroperoxides (Anashkina et al., 1972; Ponec and Prochazka, 1974; Ford and Young, 1965), and similar processes should occur with DBT. In our study of the oxidation of benzothiophene by peroxy radicals (see Section 11), the half-life for oxidation in the aquatic environment was estimated to be over 10 years.

DBT absorbs strongly in the solar spectrum up to about 340 nm. No information on the photolysis of DBT was found in the literature. Benzothiophene, which has a long wavelength cutoff of about 310 nm (absorption coefficient of 7 $M^{-1}$ $cm^{-1}$) in the solar spectrum, was found to photolyze in pure water with a half-life of about 23 days.

The literature gave considerable evidence that Knecht (1962) obtained a mixture of organisms that could utilize dibenzothiophene as a sole carbon source in a medium lacking inorganic sulfur. These organisms belonged to the Arthrobacter and Pseudomonas genera and were obligately synergistic. Sulfate was one of the end products of metabolism, and the addition of organic nitrogen sources to the medium reduced the desulfurizing activity. Kuwait residuum, a fraction high in organic sulfur, supported growth of the organisms but no detectable reducible-sulfur accumulated in the medium. Knecht postulated that the initial attack on the DBT was at the thioether linkage and cleavage of one of the benzene rings. Walter et al. (1975) in studying microbial degradation of petroleum hydrocarbons concluded that aromatic nuclei containing sulfur were twice as refractory as nonsulfur analogs.

Yamada et al. (1968) reviewed microbiological studies used to desulfurize petroleum products and reported their first studies on the biodegradation of DBT. They isolated six biodegrading strains: one was identified as Pseudomonas jianii. In a later report from this laboratory (Nakatini et al., 1968), three more DBT degrading isolates were reported. In studies with mixtures of these isolates, a decrease in biodegradation activity of DBT was noted with some mixtures of active isolates. Their optimal medium contained 8.78% light oil, 0.4% meat extract, and 0.46% DBT, at an initial pH of 7.3, and they used a mixture of four isolates.

In two subsequent publications, Kodama et al. (1970, 1973) reported the isolation and identification of 3-hydroxy-2-formyl-benzothiophene, dibenzothiophene-5-oxide, 3-oxo-2[3'-hydroxy-thianaphthenyl-(2)-methylene]dihydrothianaphthalene, trans-4[2-(3-hydroxy)-thianaphthenyl]-2-oxo-3-butenoic acid, and the hemiacetal of this last product, as metabolites produced from DBT by P. abikonensis or P. jianii. Their medium contained 4.0 g meat extract in an inorganic salts medium that did not include any sulfates.

Laborde and Gibson (1975) used a Beijerinckia species mutant B836. The parent strain, obtained by enrichment procedures with biphenyl, could completely metabolize this compound when it was the sole carbon source. The mutant, obtained by exposure of the parent to a mutating agent, had restricted diphenyl metabolizing capabilities. When the mutant was grown on inorganic salts medium to which DBT and Na succinate were added, it produced cis-1,2-dihydroxy-1,2-dihydrodibenzothiophene. This is consistent with Gibson's position that microbes produce cis-dihydrodiols and mammalian systems produce trans isomers when aromatic compounds are converted to dihydrodiols. Gibson (1975), in studies with the parent and mutant strains, reported that in addition to the above cis-dihydrodiol DBT was transformed to 1,2-dihydroxydibenzothiophene, trans-4[2-(3-hydroxy)-thianaphthenyl]-2-oxo-3-butenoic acid, 3-hydroxy-2-formylbenzothiophene, and dibenzothiophene-5-oxide.

Hou and Laskin (1975) isolated a strain of Pseudomonas aeruginusa (ECR-8) that, in the presence of dodecane and tetradecane as hydrocarbons to solubilize DBT (and perhaps as cometabolites), resulted in the formation of 4[2-(3-hydroxy)-thianaphthenyl]-2-hydroxy-3-butenoic acid and two other compounds--probably a tetradecane ester of this acid and probably a chromophoric derivative of this acid.

Walker and Colwell (1974) used sediments collected from an oil-polluted creek at Baltimore Harbor in Chesapeake Bay to inoculate media contained 2 vol % motor oil or mixed hydrocarbon substrate. They reported aerobic degradation of benzothiophenes, dibenzothiophenes, and naphthobenzothiophenes in the range of 90% to 97%.

Kuritz et al. (1971) isolated four kinds of bacteria that produced $H_2S$ from organic sulfur compounds such as thiophene, dimethylsulfide, 1-butanethiol, polysulfides, crude oil, residue oil, and asphaltene when the organisms were grown in the presence of polypeptone and $FePO_4$ under anaerobic conditions. It is very probable that DBT adsorbed on sediments may also be decomposed by these types of organisms in fresh water systems.

Although the above cited studies clearly indicated that DBT is biodegradable, no kinetic constants were available that could be used in our environmental assessment procedures.

## 12.3 ENVIRONMENTAL ASSESSMENT

### 12.3.1 Summary of Laboratory Data

The rate constants obtained in the laboratory investigations of the transformation and transport processes for DBT are summarized in Table 12.2.

### 12.3.2 Environmental Assessment Using the One-Compartment Model

The half-lives of dissolved DBT calculated for individual transformation or removal processes in the one-compartment model are given in Table 12.3. Biotransformation (biodegradation) is clearly the dominant transformational pathway in eutrophic waters, but is roughly 2000 times slower than volatilization in oligotrophic waters. Dilution is very nearly as important as biotransformation in eutrophic lakes and ponds, and several times faster in rivers. Sorption is important only in the pond simulation, which assumes heavy sediment loading.

### 12.3.3 Persistence

Dibenzothiophene is not persistent in eutrophic waters, where half-lives are predicted to be half a day. In oligotrophic waters, however, half-lives should be about a week. The half-life of DBT in entire river segments will not differ from the half-life of DBT in ponds and eutrophic lakes because biodegradation is the dominant process in all these waters. However, DBT concentration in individual segments of a river will drop rapidly after a spill because of dilution from incoming water.

TABLE 12.2. SUMMARY OF LABORATORY DATA FOR DIBENZOTHIOPHENE

| Process | Sorption equilibrium | Partition coefficient |
|---|---|---|
| Sorption[a] | $S_s = K_p S_w$ | $K_p = 1380$ |
|  | Rate expression | Rate constant at 25°C |
| Volatilization[b] | $k_v^{DBT}$ | $k_v = (0.12 \pm 0.04) k_v^O$ |
| Photolysis[c] | $k_p[DBT] = \Phi(\Sigma Z_\lambda \varepsilon_\lambda [DBT]$ | $k_p = (2.04 \pm 0.08) \times 10^{-6} \text{sec}^{-1}$ |
| Oxidation | $k_{ox}[RO_2\cdot][DBT]$ | $k_{ox} < 7.5\ M^{-1}\ \text{sec}^{-1}$ |
| Hydrolysis | NA | --- |
| Biodegradation | $k_{b2} = \frac{\mu_m}{Y\ K_s}$ | $k_{b2} = (5.3 \pm 0.4) \times 10^{-7}\ \text{ml cell}^{-1}\ \text{hr}^{-1}$ |

[a] Measured on Coyote Creek sediment.

[b] See Part I, Section 5.3, and Appendix B.

[c] Assumes 12 hours sunlight per day in early March.

TABLE 12.3. TRANSFORMATION AND TRANSPORT OF DIBENZOTHIOPHENE PREDICTED BY THE ONE-COMPARTMENT MODEL

|  | River | Eutrophic pond | Eutrophic pond | Oligotrophic pond |
|---|---|---|---|---|
| Photolysis, half-life (hr)[a] | 380 | 950 | 950 | 190 |
| Oxidation, half-life (hr) | $>10^5$ | $>10^5$ | $>10^5$ | $>10^5$ |
| Volatilization, half-life (hr) | 140 | 720 | 580 | 580 |
| Hydrolysis, half-life (hr) | -- | -- | -- | -- |
| Biodegradation, half-life (hr) | 13 | 13 | 13 | $>10^4$ |
| Half-life for all processes except dilution (hr) | 13 | 13 | 13 | 140 |
| Half-life for all processes including dilution (hr) | 0.5 | 13 | 13 | 140 |
| Amount DBT sorbed (mg $m^{-3}$)[b] | 1.4 | 4.2 | 0.7 | 0.7 |
| Percentage DBT sorbed | 12% | 42% | 6.5% | 6.5% |

[a] Estimates are the average photolysis rates on a summer day at 40° latitude. Photolysis rates in midwinter are at least three times slower.

[b] Assumes 10 ng $ml^{-1}$ of dibenzothiophene in aqueous phase and a partition coefficient of 1400.

### 12.3.4 Mass and Concentration Distributions Calculated Using Computer Models

The pseudo-first-order rate constants used in these simulations are presented in Appendix A. The distributions of mass and concentration of DBT expected at steady state during chronic discharge to each of four types of water bodies are given in Table 12.4. The changes in concentration during and after discharge of DBT into the water bodies are shown in Figures 12.1 through 12.4.

The concentrations of DBT predicted to be in solution at steady state are on the order of $10^{-3}$ to $10^{-5}$ μg $ml^{-1}$, with concentrations on the order of $10^{-4}$ μg $ml^{-1}$ being most common (Table 12.4). The patterns of variation in concentration within and between simulations generally resemble those for the previously studied compounds (Figures 12.1-12.4). Changes in concentrations on suspended sediments parallel changes in the concentrations of dissolved DBT (Figure 12.1).

Concentrations of dissolved DBT in the computer simulations generally reach steady state, or very close to steady state, within 2 to 10 days of start of discharge. Declines from those relatively high concentrations to the lower steady states, which maintained by desorption from contaminated sediments after simulated discharges stop, is slower, perhaps 2 to 5 times slower (Figures 12.1-12.4). The concentrations in the sediments build up slowly during exposure and decline slowly when the input ceases. However, the corresponding increases and decreases in the aqueous compartments are rapid. The oligotrophic lake, where biodegradation is slow, differs from this pattern and the concentration in compartments that are relatively far from the point of contamination declines rather slowly.

### 12.3.5 Discussion

In eutrophic systems, biodegradation appears to be the dominant process and the half-lives of DBT are similar in the river, pond, and lake. The concentrations of DBT in various locations of water bodies decrease at approximately the same rate after the discharge stops, except in the oligotrophic lake, where decreases in different compartments are substantially different because biodegradation is very slow. For instance, the concentration in the lower part of the oligotrophic lake (Compartment 5) shows an insignificant decrease after discharge stops, yet the concentrations in the upper part of the oligotrophic lake show observable decreases due to the losses from photolysis and volatilization. The relatively slow decline in the concentration of dissolved DBT is a result of the relatively low microbial population in the oligotrophic lake.

In conclusion, DBT is expected to persist longer in oligotrophic waters than in eutrophic waters. In the lower part of the oligotrophic lake, DBT has a half-life of 15 days. During spring and fall turnovers in the lake, DBT may be brought up to the surface where photolysis and volatilization are important, and half-lives will be shorter.

TABLE 12.4. DISTRIBUTION OF DIBENZOTHIOPHENE IN VARIOUS AQUATIC SYSTEMS AT STEADY STATE (input concentrations of 1 ng $ml^{-1}$ dibenzothiophene)

| | Pond | | River | | Eutrophic lake | | Oligotrophic lake | |
|---|---|---|---|---|---|---|---|---|
| | Mass (kg) | Conc. (μg $ml^{-1}$) | Mass (kg) | Conc. (μg $ml^{-1}$) | Mass (kg) | Conc. (μg $ml^{-1}$) | Mass (kg) | Conc. (μg $ml^{-1}$) |
| Compartment 1 (surface water) | | | | | | | | |
| Solution | $2.64 \times 10^{-3}$ | $1.32 \times 10^{-4}$ | 2.55 | $8.50 \times 10^{-3}$ | $9.31 \times 10^{-2}$ | $3.72 \times 10^{-4}$ | $2.65 \times 10^{-1}$ | $1.06 \times 10^{-3}$ |
| Suspended solids | $1.10 \times 10^{-3}$ | $1.84 \times 10^{-1}$ | 0.35 | $1.19 \times 10$ | $6.51 \times 10^{-3}$ | $5.20 \times 10^{-1}$ | $1.85 \times 10^{-2}$ | 1.48 |
| Compartment 2 (surface water) | | | | | | | | |
| Solution | -- | -- | 2.48 | $8.26 \times 10^{-3}$ | $6.67 \times 10^{-2}$ | $2.66 \times 10^{-5}$ | 1.10 | $4.40 \times 10^{-4}$ |
| Suspended solids | -- | -- | 0.34 | $1.15 \times 10$ | $4.67 \times 10^{-3}$ | $3.73 \times 10^{-2}$ | $7.70 \times 10^{-2}$ | $6.16 \times 10^{-1}$ |
| Compartment 3 (surface water) | | | | | | | | |
| Solution | -- | -- | 2.41 | $8.03 \times 10^{-3}$ | $2.91 \times 10^{-3}$ | $1.16 \times 10^{-5}$ | $9.20 \times 10^{-2}$ | $3.68 \times 10^{-4}$ |
| Suspended solids | -- | -- | 0.33 | $1.12 \times 10$ | $2.05 \times 10^{-4}$ | $1.64 \times 10^{-2}$ | $6.44 \times 10^{-3}$ | $5.15 \times 10^{-1}$ |
| Compartment 5 (surface water) | | | | | | | | |
| Solution | -- | -- | -- | -- | $5.91 \times 10^{-4}$ | $2.36 \times 10^{-7}$ | $5.80 \times 10^{-2}$ | $2.32 \times 10^{-5}$ |
| Suspended solids | -- | -- | -- | -- | $4.14 \times 10^{-5}$ | $3.31 \times 10^{-4}$ | $4.06 \times 10^{-3}$ | $3.24 \times 10^{-2}$ |
| Compartments 7-9 (sediment)[a] | | | | | | | | |
| Solution | $3.30 \times 10^{-5}$ | $1.32 \times 10^{-4}$ | $6.17 \times 10^{-2}$ | $8.23 \times 10^{-3}$ | $8.24 \times 10^{-4}$ | $9.42 \times 10^{-5}$ | $3.19 \times 10^{-3}$ | $3.64 \times 10^{-4}$ |
| Solids | $1.24 \times 10^{-1}$ | $1.84 \times 10^{-1}$ | $2.32 \times 10^{2}$ | $1.15 \times 10$ | 1.81 | $1.32 \times 10^{-1}$ | 6.95 | $5.10 \times 10^{-1}$ |

[a] The amounts given for solid and solution phases in the sediment compartments are estimated from the sorption partition coefficient for suspended solids and may be overestimated because it was assumed that biodegradation of sorbed material does not occur.

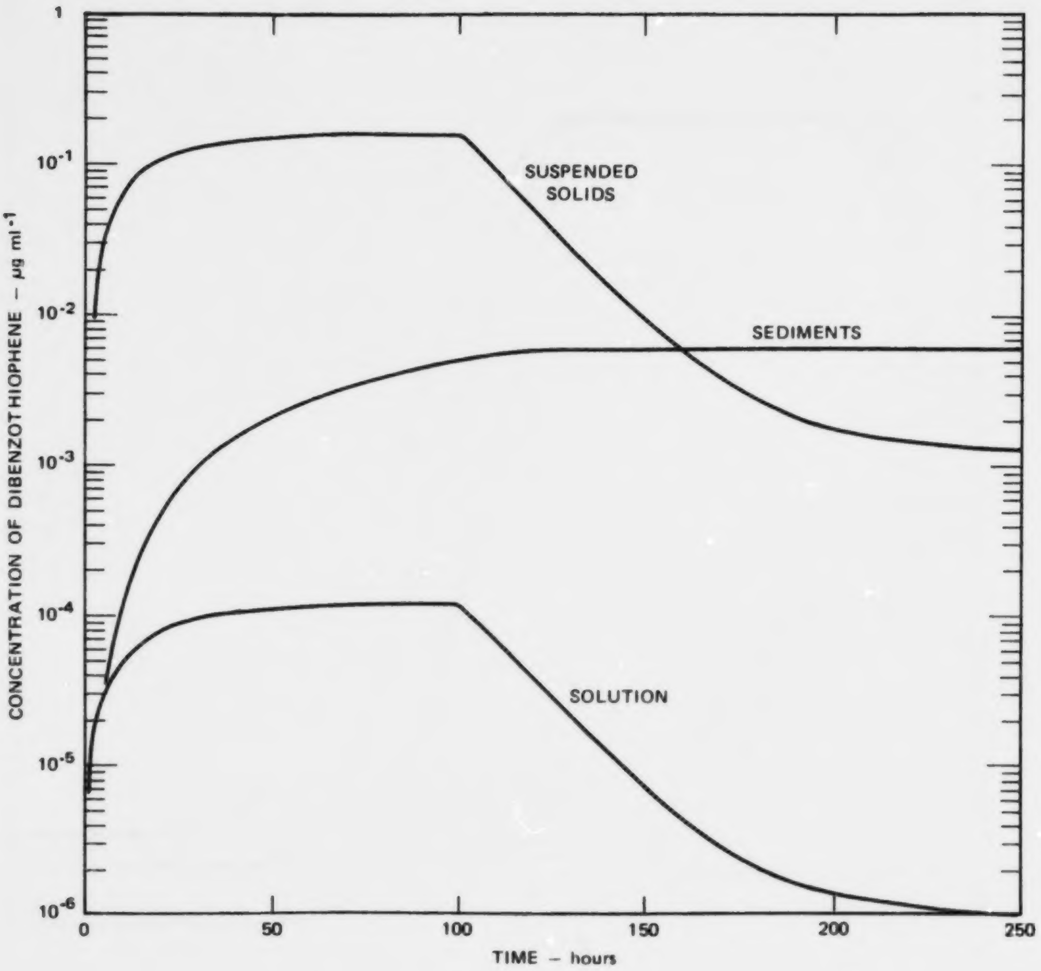

FIGURE 12.1. PERSISTENCE OF DIBENZOTHIOPHENE IN A TWO-COMPARTMENT POND SYSTEM

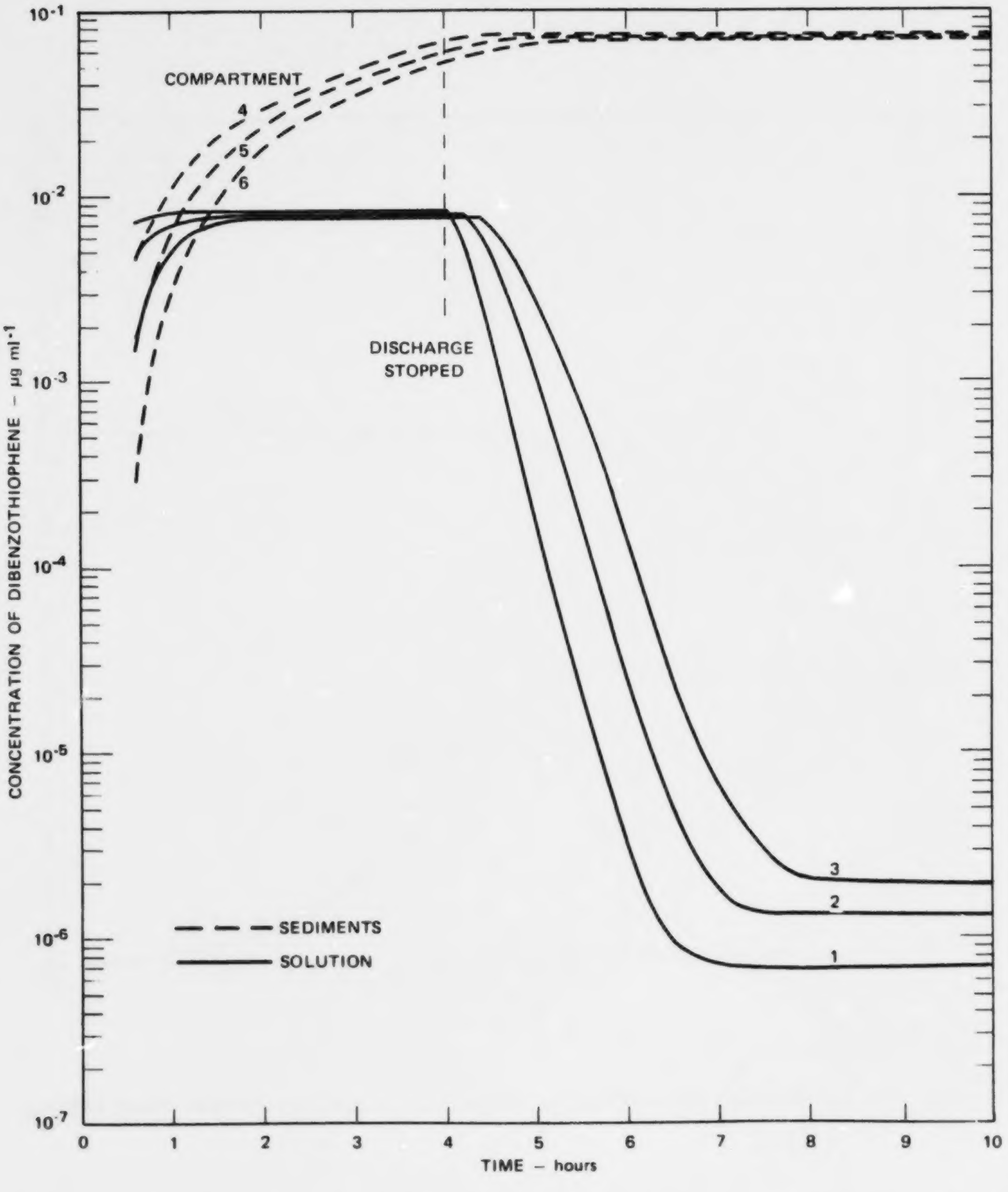

FIGURE 12.2. PERSISTENCE OF DIBENZOTHIOPHENE IN A PARTIALLY MIXED RIVER SYSTEM

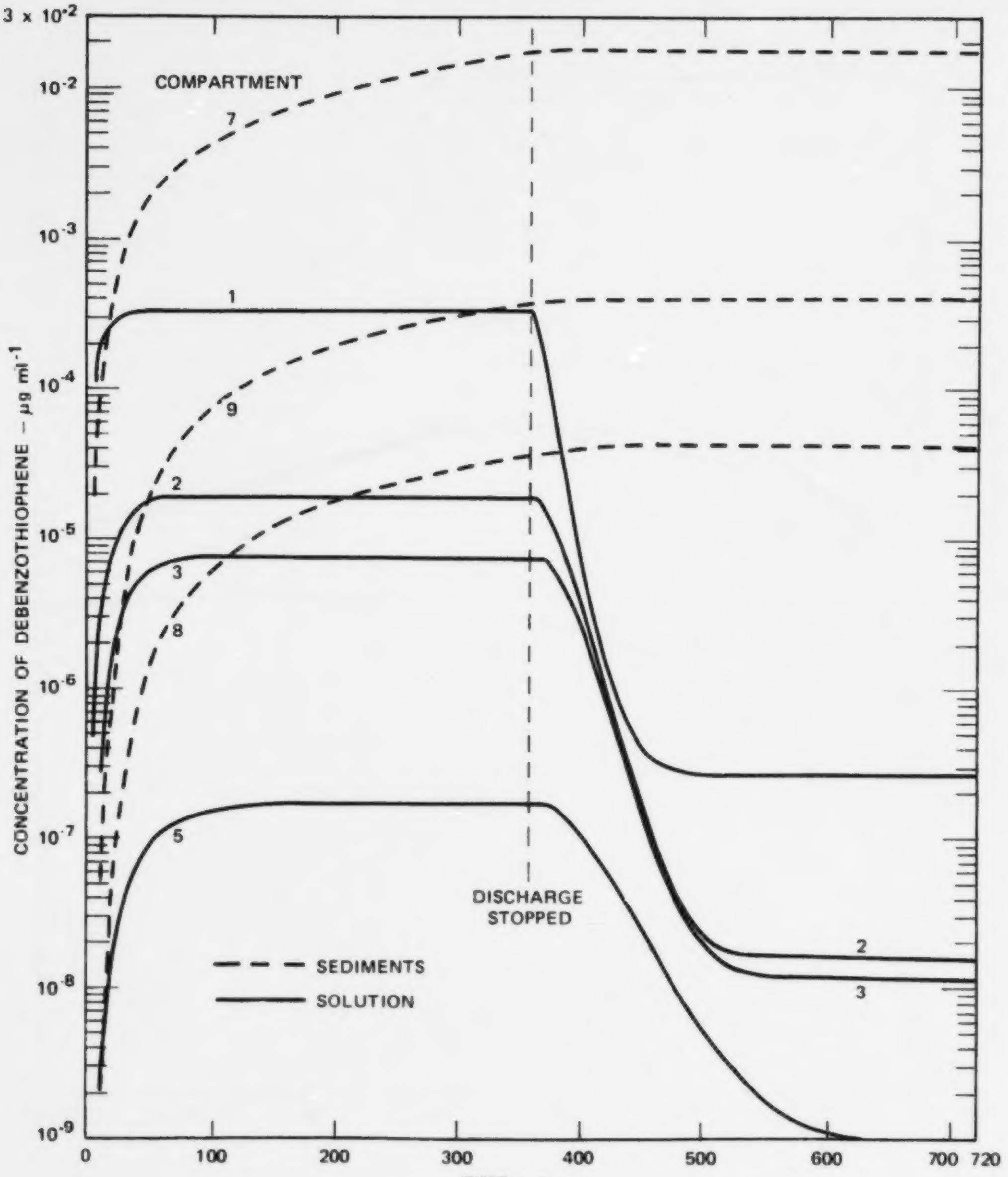

FIGURE 12.3. PERSISTENCE OF DIBENZOTHIOPHENE IN A EUTROPHIC LAKE

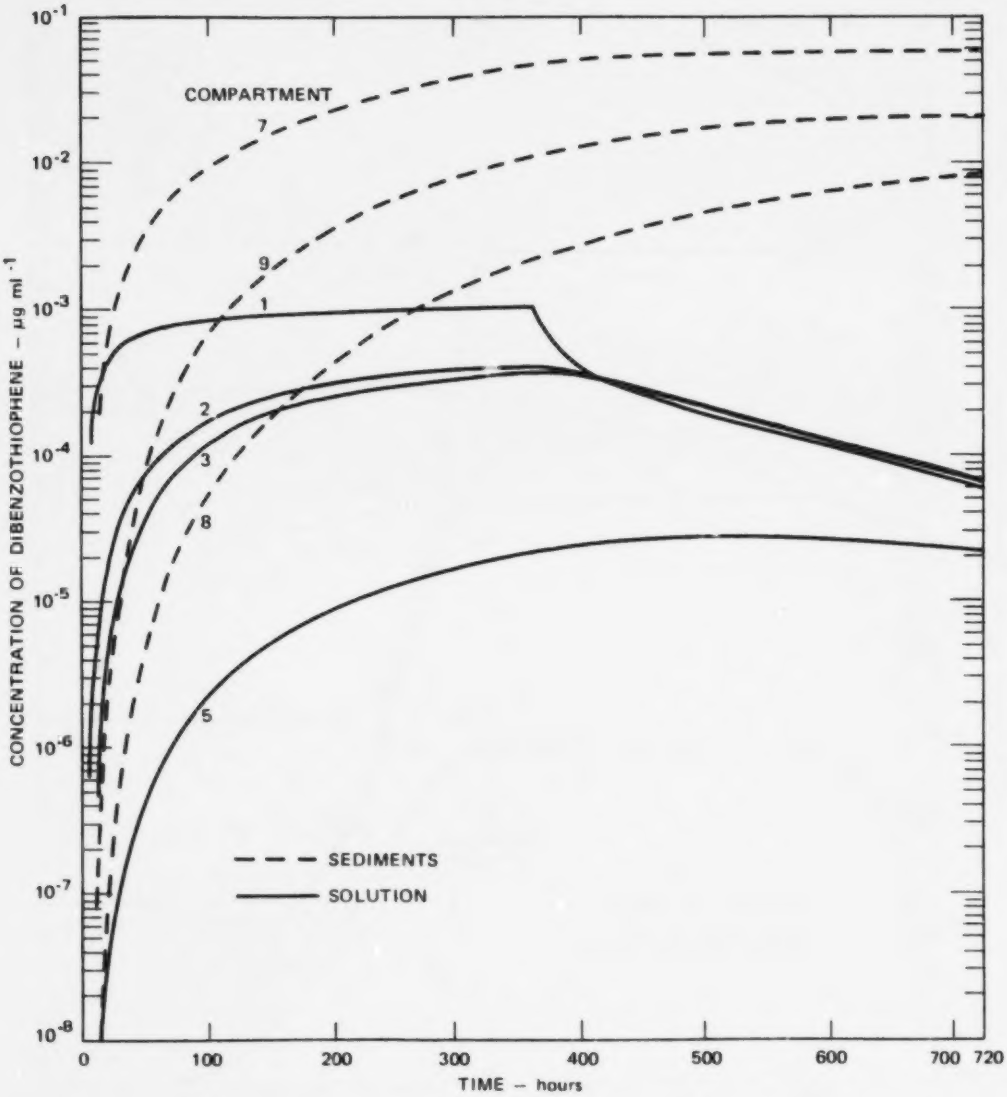

FIGURE 12.4. PERSISTENCE OF DIBENZOTHIOPHENE IN AN OLIGOTROPHIC LAKE

## 12.4 PHYSICAL PROPERTIES

### 12.4.1 Solubility in Water

The solubility of DBT in water at 28 ± 1°C was measured using the method of Campbell (1930). The solubility was 1.11 ± 0.09 μg ml$^{-1}$, based on replicate determinations.

### 12.4.2 Absorption Spectra

DBT absorbs light strongly in the solar region to 350 nm. The absorption spectrum of DBT in 30% acetonitrile-70% water was measured from 210 nm to 350 nm and in 80% acetonitrile-20% water from 320 nm to 380 nm. The pH of the first solution was 7.1; the pH of the second solution was not measured. The absorption coefficients at wavelength intervals from 297.5 to 360 nm and at wavelengths of 313 and 366 nm are reported in Table 12.5.

TABLE 12.5 ABSORPTION SPECTRUM OF DIBENZOTHIOPHENE IN 30% ACETONITRILE-70% WATER AT pH 7[a]

| Center of wavelength interval[b] (nm) | Average absorption coefficient[c] (M$^{-1}$ cm$^{-1}$) |
|---|---|
| 297.5 | 1154 |
| 300.0 | 1224 |
| 302.5 | 1327 |
| 305.0 | 1499 |
| 307.5 | 1782 |
| 310.0 | 2025 |
| 312.5 | 2080 |
| 315.0 | 1939 |
| 317.5 | 1892 |
| 320.0 | 2119 |
| 323.1 | 2394 |
| 330 | 526[d] |
| 340 | 13.1[d] |
| 350 | 7.5[d] |
| 360 | 0[d] |

[a] Dibenzothiophene concentration was 23.5 μg ml$^{-1}$ ($1.27 \times 10^{-4}$ M).

[b] The wavelength intervals are given in Appendix B, Table B.1.

[c] The absorption coefficients at 313.0 and 366 nm are 2080 and 0 M$^{-1}$ cm$^{-1}$, respectively.

[d] Values were determined from a solution of dibenzothiophene in 80% acetonitrile-20% water at a concentration of 98.2 μg ml$^{-1}$ ($5.33 \times 10^{-4}$ M).

### 12.4.3 Volatilization Rate

The volatilization rate of dibenzothiophene was measured using the method of Hill et al. (1976), which is described in Part I, Section 5.3. The DBT volatilization data obtained at four different oxygen reaeration rates are shown in Table 12.6. The DBT volatilization rate constant $k_v^{DBT}$ is plotted versus the oxygen reaeration rate constant $k_v^O$ in Figure 12.5.

TABLE 12.6. VOLATILIZATION DATA FOR DIBENZOTHIOPHENE

| Oxygen reaeration rate, $k_v^O$ ($hr^{-1}$) | DBT volatilization rate, $k_v^{DBT}$ ($hr^{-1}$) | $k_v^{DBT}/k_v^O$ |
|---|---|---|
| 4.49 ± 0.07 | 0.107 ± 0.001 | 0.024 ± 0.002 |
| 2.19 ± 0.43 | 0.0651 ± 0.0025 | 0.030 ± 0.008 |
| 0.432 ± 0.012 | 0.0474 ± 0.011 | 0.11 ± 0.03 |
| 0.199 ± 0.014 | 0.0318 ± 0.0037 | 0.16 ± 0.03 |

The critical volume of DBT was estimated using the critical volume increments of Lydersen (Reid and Sherwood, 1966) to be 525 ml/g-mole. Since the molecular volume is 1/2 to 1/3 of the critical volume (Present, 1955), this critical volume yields molecular diameter estimates of 9.4 to 8.2 Å. If volatilization were completely controlled by liquid phase resistence, then Equation (5.7) in Part I [Equation (12.1) below] can be used to estimate the ratio $k_v^{DBT}/k_v^O$. Using the value of $k_v^O$ = 2.98 Å (Tsivoglou, 1965),

$$\frac{k_v^{DBT}}{k_v^O} = \frac{d^O}{d^{DBT}} \simeq 0.34 \pm 0.02 \qquad (12.1)$$

For oxygen, mass transport is limited by liquid phase resistance for all $k_v^O < 0.6\ hr^{-1}$. There are only two points on Figure 12.5 where $k_v^O < 0.6$. Using these two points $k_v^{DBT}/k_v^O = 0.12 \pm 0.04$, which is significantly different from the prediction of equation (12.1).

The reason for the discrepancy is probably that the Henry's law constant for DBT, which is estimated to be 335 torr $M^{-1}$ using the method of Mackay and Wolkoff (1973), is low compared with the constant for $H^O$ ($3 \times 10^4$ torr $M^{-1}$). Since DBT has such a low Henry's law constant with respect to oxygen, the gas phase resistance to volatilization becomes important for DBT at turbulence levels where reaeration is still controlled by the liquid phase. The addition of the gas phase resistance slows the volatilization rate of DBT and yields a volatilization rate lower than predicted by the simple theory of equation (12.1).

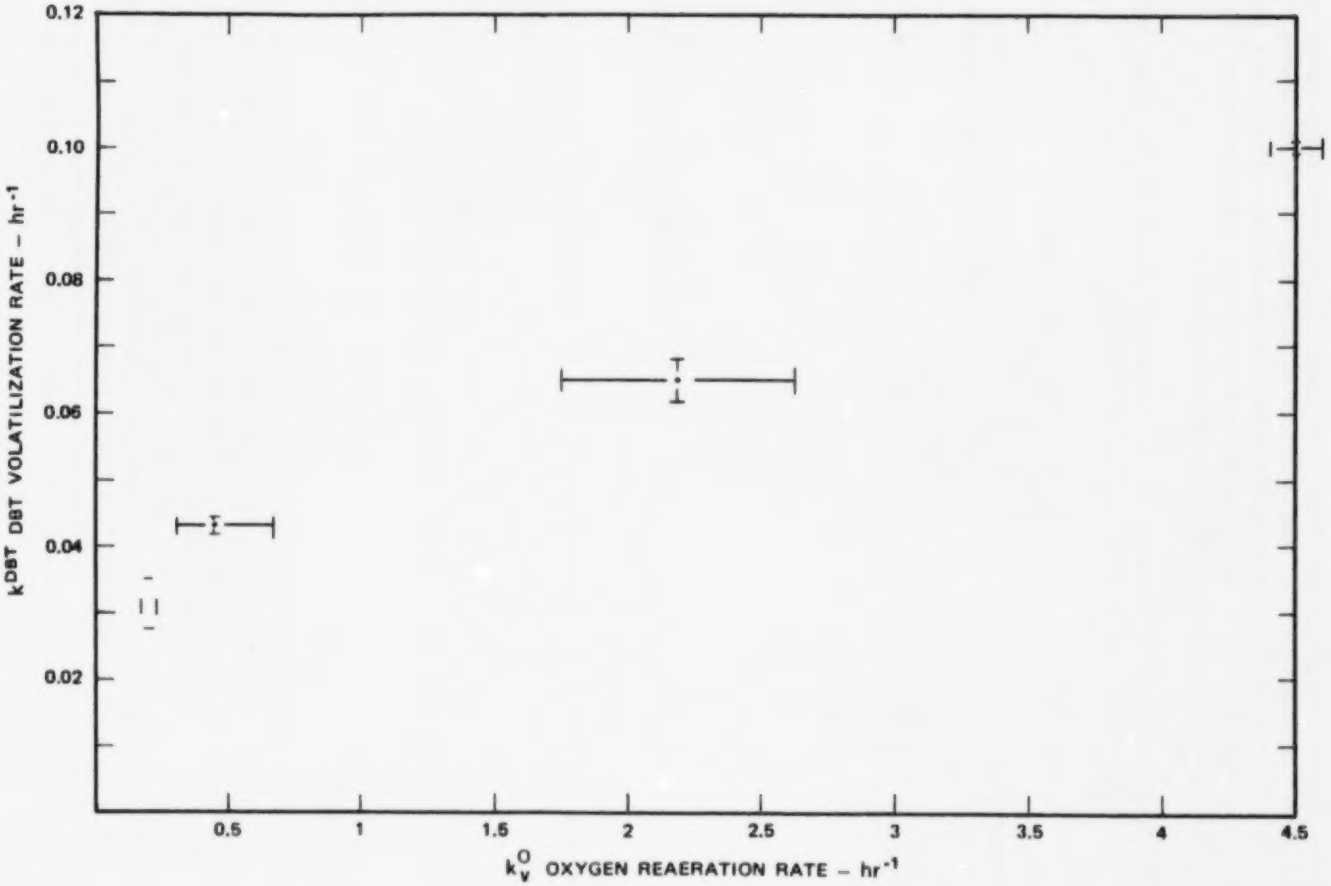

FIGURE 12.5. VOLATILIZATION OF DIBENZOTHIOPHENE FROM AQUEOUS SOLUTION

### 12.4.4 Sorption on a Sediment

The sorption partition coefficient of dibenzothiophene on Coyote Creek sediment was measured; the data are shown in Table 12.7. The experiment consisted of duplicate samples at two DBT concentrations and three sediment loadings, in addition to blanks containing DBT only and sediment only. The concentrations of DBT on the sediment were calculated from the concentration difference between the supernatants and the appropriate blanks.

Additional isotherm measurements were not conducted since sorption should not be an important pathway for dibenzothiophene.

TABLE 12.7. DIBENZOTHIOPHENE SORPTION ON COYOTE CREEK SEDIMENT[a]

| Sediment concentration (mg ml$^{-1}$) | DBT concentration in supernatant ($\mu$g ml$^{-1}$ x $10^3$)[b] | DBT concentration on sediment ($\mu$g g$^{-1}$)[c] | Partition coefficient, $K_p$ LLS[d] | |
|---|---|---|---|---|
| | | | $a_o = 0$ | $a_o \neq 0$ |
| 0.47 | 103 ± 2 | 120 ± 5 | | |
| 0.16 | 129 ± 5 | 193 ± 31 | 1380 ± 130 | 1580 ± 540 |
| 0.78 | 64 ± 2 | 71 ± 3 | | $a_o = -2 \pm 54$ |
| 0.16 | 95 ± 4 | 153 ± 27 | | |

[a] Total organic content = 1.4%.

[b] Concentration measured in supernatant with population standard deviation.

[c] Concentration on sediment calculated from supernatant concentration with population standard deviation.

[d] LLS = linear least squares regression; see Appendix B, Section B.1.4, for explanation of regressions; limits are 95% confidence limits.

### 12.4.5 Biosorption

A saturated solution of DBT in water was prepared by coating the inside of a clear 9-liter bottle with a solution of DBT in acetone and evaporating the acetone with a stream of $N_2$. Highly purified water was added to this bottle, and the resultant suspension was shaken. The suspension was centrifuged to provide a clear supernatant solution of DBT. The biosorption portion coefficient was measured using this solution and our mixture of four types of bacteria. Biosorptions were conducted in Corex tubes placed in a rotor drum. The centrifuged cell pellet and clear supernatant were extracted with ethyl acetate, and the sorption coefficients were calculated for both viable and heat-killed cells (Table 12.8).

The sorption coefficient with heat-killed cells was significantly higher than with viable cells. No data are available to explain this phenomenon at this time, but it is apparent that the sorption is not necessarily dependent on metabolic processes.

TABLE 12.8. BIOSORPTION OF DIBENZOTHIOPHENE

| Exp. No. | Cell type | Concentration[a] (g liter$^{-1}$) | Initial DBT concentration (ng ml$^{-1}$) | Sorption coefficient |
|---|---|---|---|---|
| 1 | Viable cells | 1.108[a] | 59 | $(1.54 \pm 0.20) \times 10^3$ |
| | Viable cells | 1.100[a] | 118 | $(1.55 \pm 0.37) \times 10^3$ |
| | Heat-killed cells | 0.92 | 118 | $(2.81 \pm 0.60) \times 10^3$ |
| 2 | Viable cells | 1.054 | 120 | $(1.64 \pm 0.42) \times 10^3$ |
| | Viable cells | 1.054 | 350 | $(1.35 \pm 0.21) \times 10^3$ |
| | Heat-killed cells | 0.847 | 350 | $(2.99 \pm 0.47) \times 10^3$ |

[a] Dry weight of cell suspension.

## 12.5 CHEMICAL TRANSFORMATION

### 12.5.1 Photolysis Rate

Photolysis of DBT is slow in the solar region with a half-life of greater than 5 days in summer. The photolysis rate of DBT is unaffected by oxygen but is accelerated by the presence of humic acid. Photolysis experiments were conducted with 0.50 μg ml$^{-1}$ ($2.71 \times 10^{-6}$ M) DBT in pure water and in natural waters from several sources; these waters also contained 1% added acetonitrile to increase the solubility of DBT. Data for the photolysis of DBT in sunlight and at 313 nm are given in Table 12.9. First-order kinetic behavior was found for photolyses carried out to beyond one half-life. The quantum yield at 313 nm for direct phototransformation of DBT in pure water is $5.0 \times 10^{-4}$.

The data in Table 12.9 show that photolysis rates of DBT at 313 nm in the three natural waters are about the same (within experimental error) as the rate in pure water. Two additional photolysis experiments (not shown in Table 12.9) were carried out to 50% conversion at 313 nm on a pure water solution of 0.5 μg ml$^{-1}$ DBT. One of the solutions had been degassed by three freeze-thaw cycles. The absence of oxygen did not affect the photolysis rate. The experiment at 313 nm in the water containing 810 μg ml$^{-1}$ humic acid absorbance of 0.46 at 313 nm theoretically should have reduced the rate 38% due to a light screening effect, the humic acid is in fact weakly promoting photolysis of DBT at 313 nm.

The sunlight photolysis experiments confirm this conclusion since DBT in the humic acid solution is photolyzed over twice as fast as in pure water. DBT photolyses in sunlight are more rapid in humic acid solution than in pure

TABLE 12.9. RATE CONSTANTS FOR PHOTOLYSIS OF 0.5 μg ml$^{-1}$ DIBENZOTHIOPHENE[a]

| Irradiation source | Solution[b] | Extent of reaction (%) | Rate constant ($K_p \times 10^6$ sec$^{-1}$) |
|---|---|---|---|
| 313 nm | Pure water | 60% | 2.32 ± 0.22[c,d] |
| 313 nm | Lake Tahoe water | 37 | 2.55 ± 0.34 |
| 313 nm | Searsville pond water | 33 | 2.38 ± 0.27 |
| 313 nm | Coyote Creek water | 37 | 2.92 ± 0.66 |
| 313 nm | Humic acid (8 μg ml$^{-1}$) in pure water | 55 | 1.93 ± 0.11 |
| Sunlight, early March | Pure water | 35 | 2.04 ± 0.08[e,f] |
| Sunlight, early March | Humic acid (8 μg ml$^{-1}$) in pure water | 63 | 4.60 ± 0.04[e,g] |

[a] 1.00 μg ml$^{-1}$ Dibenzothiophene in water = $5.43 \times 10^{-6}$ M.

[b] Solutions contained 1% acetonitrile as cosolvent.

[c] Standard deviation.

[d] Quantum yield for disappearance of dibenzothiophene was $5.0 \times 10^{-4}$.

[e] Calculated assuming 12 hours of sunlight per day in early March; to obtain average rate constant for full calendar day (24 hours), divide rate constant by two.

[f] Half-life of 7.9 days.

[g] Half-life of 3.5 days.

water because humic acid absorbs more extensively in the solar spectrum than DBT and transfers some fraction of the energy to DBT. The humic acid photosensitized process then dominates over any screening effect of humic acid in the less extensive absorption of DBT in the solar spectrum.

The half-life for direct photolysis of DBT in sunlight as a function of the time of year was calculated by the procedure of Zepp and Cline (1977) using the quantum yield of $5.0 \times 10^{-4}$ measured at 313 nm and the measured UV spectrum of DBT. The data are plotted in Figure 12.6. The half-life of about 12 days calculated for direct photolysis in sunlight in early March is in good agreement with the measured half-life of about 8 days.

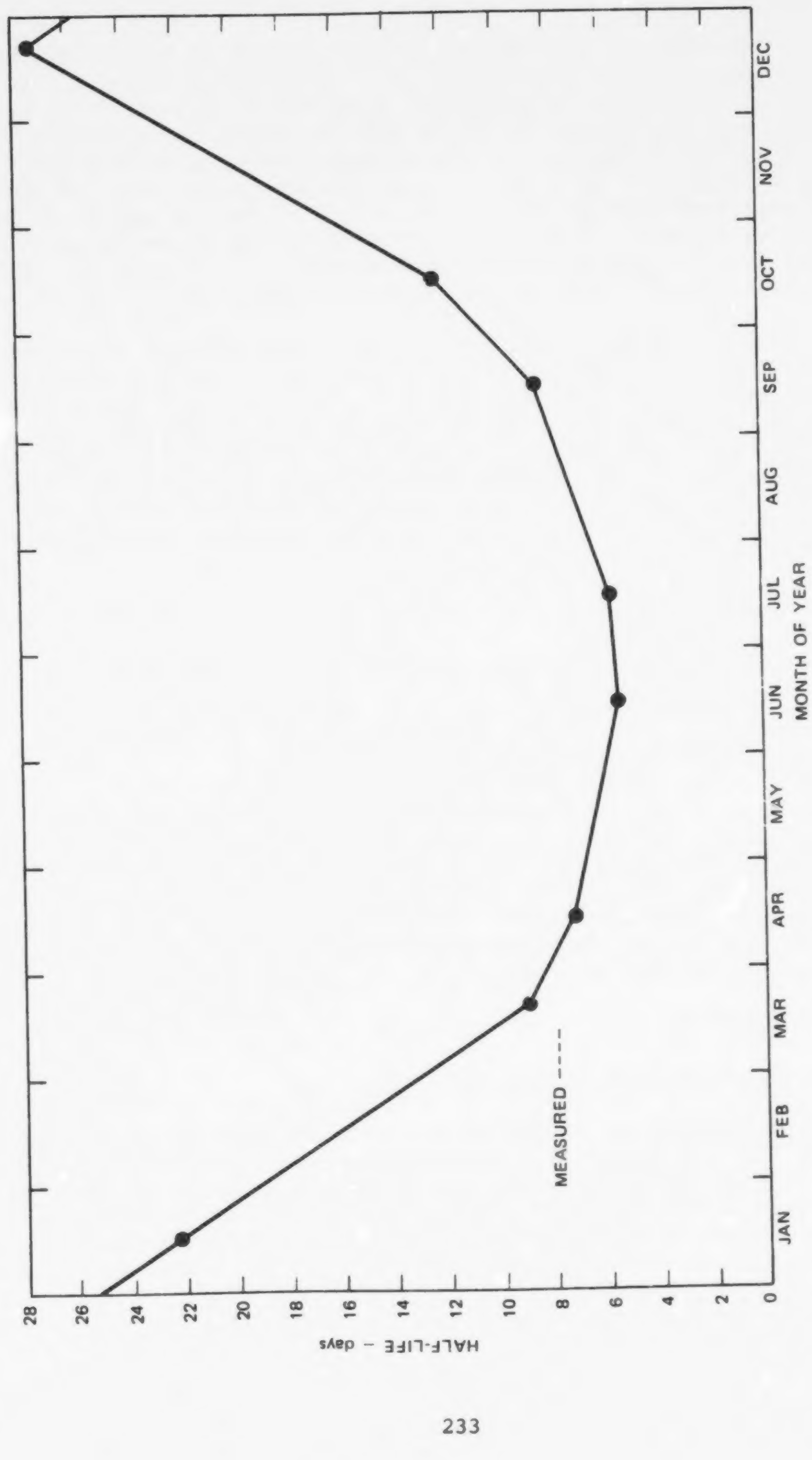

FIGURE 12.6. ANNUAL VARIATION OF PHOTOLYSIS HALF-LIFE OF DIBENZOTHIOPHENE

### 12.5.2 Oxidation Rate

The susceptibility of 0.50 $\mu g\ ml^{-1}$ ($2.7 \times 10^{-6}$ M) DBT to free radical oxidation was examined using the AA-initiated oxidation reaction. (See Part I, Section 5.4.2 of this report and Appendix B for discussion and procedure.) The experiment was carried out at 50.0°C in 1% acetonitrile in water containing $1.0 \times 10^{-4}$ M AA. A solution of DBT without AA was maintained under identical reaction conditions as a control. At the end of 70 hours reaction time, analyses of both solutions showed that about 50% of the DBT had been lost, and no early-eluting (polar) products were observed in the reverse-phase HPLC analysis, as were found in the photolysis experiments. We conclude that DBT did not oxidize and that the observed losses were probably due to volatilization.

In order to estimate a maximum value for the oxidation rate constant $k_{ox}$, it was assumed that the experimental error in the analysis was ±5%. A first-order rate constant for oxidation of DBT is then less than $2 \times 10^{-7}\ sec^{-1}$ at 50°C. Under our reactions, this corresponds to a second-order rate constant $k_{ox}$ of $<68\ M^{-1}\ sec^{-1}$. At 25°C, $k_{ox}$ is then $<7.5\ M^{-1}\ sec^{-}$ , and with the assumption that $[RO_2\cdot] = 10^{-9}$ M in the aquatic environment, the oxidation half-life of DBT is over 3 years. The free radical oxidation of DBT is clearly not competitive with volatilization or photolysis under environmental conditions.

### 12.5.3 Hydrolysis Rate

Since DBT contains no groups that are hydrolyzable, no hydrolysis studies were carried out.

### 12.5.4 Products from Chemical Transformations

Photolysis of DBT gave five early-eluting, primary products in the HPLC analysis. Attempts to characterize these products using GC/MS were unsuccessful. However, when the reaction solution was degassed using freeze-thaw cycles before photolysis, the yield of the third eluting product was diminished and the fifth eluting product was increased. These results suggest that both water and oxygen may be involved in some product-determining steps. The photolysis reaction products require further study.

## 12.6 BIODEGRADATION

### 12.6.1 Development of Biodegrading Cultures

Because naphthalene and anthracene could be expected to be present in natural materials containing DBT, enrichment studies were initiated with DBT, naphthalene in combination with DBT, and anthracene plus DBT as the organic substrates added to the six water samples used in most of these studies. These compounds were added at 10 $\mu g\ ml^{-1}$. $NH_4NO_3$ was used in place of $(NH_4)_2SO_4$ with the phosphate buffers to dilute water samples 4:5. All enrichments were initiated with 5-liter volumes of diluted waters in the 9-liter fermentors. Incubations were at 25°C, except for studies with Lake Tahoe water and cultures, which were conducted at 15°C.

Table 12.10 indicates the times (days) at which biodegradation of DBT was observed and the successes in developing cultures that would grow on basal salts medium containing DBT as the sole carbon source. Biodegrading cultures were developed successfully in all 9-liter fermentors containing DBT with naphthalene or anthracene. When DBT was the only substrate added, biodegradation of DBT was observed within six weeks for all but two waters (Coyote Creek and Lake Tahoe). Where degrading cultures developed with DBT as the sold carbon substrate in these 9-liter fermentors, breakdown of DBT was observed much later than in the samples containing naphthalene.

Transfers from the 9-liter fermentors were made to screw-capped Erlenmeyer flashs containing basal-inorganic-salts medium containing DBT, DBT plus naphthalene, or DBT plus anthracene, to correspond with the additives to the 9-liter fermentors. The basal salts medium was modified by substituting nitrate or chloride salts where sulfates were customarily used. Flasks were incubated in rotary action shakers. Subtransfers were made at two- or three-day intervals to media with decreasing amounts of naphthalene or anthracene, if these were used originally, and to media with increasing levels of DBT (up to 30-50 $\mu$g ml$^{-1}$).

Degradation of DBT was accompanied by color changes in the media to colorless to yellow to orange to a red insoluble product or products. Cell counts in these media after two to three days incubation were $(0.8 \sim 2) \times 10^5$ cells $\mu$g$^{-1}$ DBT. These yields were approximately 10% of those obtained with methyl parathion or quinoline as the sole carbon source.

With the effluent from the Shell Oil refinery in the 9-liter fermentor with DBT as the only added carbon source, degradation of DBT was observed within four days. Transfers made at four, six, and ten days to basal salts/DBT media did not result in DBT degradation in the shaker-flask fermentations. At 13 days, DBT equivalent to 10 $\mu$g ml$^{-1}$ was again added to the 9-liter fermentor, and a transfer made at 17 days resulted in a mixed-culture system that could degrade DBT in the basal salts/DBT medium.

With cultures that grew on basal salts/DBT plus naphthalene media and that were derived from Coyote Creek, aeration effluent from the South San Francisco sewage plant, and the effluent from the Shell Oil Refinery, several transfers were necessary in these media before cultures could be obtained that would utilize DBT as a sole carbon source.

Cultures were preserved in the vapor phase of liquid nitrogen after suspension in 5% DMSO.

### 12.6.2 Biodegradation Kinetics

Pseudo-first-order kinetic studies were conducted with a DBT degrading culture system derived from the eutrophic pond in Woodside, California. Two liters of two-day-old fermentation broth developed in three transfers on basal salts/30 $\mu$g ml$^{-1}$ DBT medium were used. The final broth prepared by a 100% dilution of the prior culture with 30 $\mu$g DBT ml$^{-1}$ medium was incubated only 18 hours and, at harvest, it contained 0.8 $\mu$g DBT ml$^{-1}$. The combined broths

### TABLE 12.10. DEVELOPMENT OF DIBENZOTHIOPHENE BIODEGRADING ENRICHMENT CULTURES

| Source of water sample | Compounds added to water sample | Days for first biodegradation | Development of culture on salts medium with DBT |
|---|---|---|---|
| Aeration effluent from Palo Alto Sewage Plant | DBT + naphthalene | 5 | Yes |
| | DBT + anthracene | 8 | Yes |
| Eutrophic pond, Wood, CA | DBT + naphthalene | 4 | Yes |
| | DBT | 17 | Yes |
| Coyote Creek, San Jose, CA | DBT + naphthalene | 8 | Yes |
| | DBT | -- | No[a] |
| Aeration effluent from South San Francisco plant | DBT + naphthalene | 2 | Yes |
| | DBT | 21 | Yes[a] |
| Aeration effluent from Shell Oil Refinery, Martinez, CA | DBT + naphthalene | 3 | Yes |
| | DBT | 17 | Yes |
| Lake Tahoe, CA | DBT + naphthalene | 32 | No[b] |
| | DBT | -- | No |

[a] Two attempts at transfers from 9-liter fermentors.

[b] Grew on salts medium with DBT plus naphthalene.

were filtered through sterile Whatman No. 4 filter paper to remove insoluble red metabolite(s). The filtrate was centrifuged, cells were washed twice with basal salts medium, the final cell pellet was suspended in 0.05 volume of basal salts medium, incubated on a shaker for 4 hours, centrifuged and again resuspended in 0.05 volume of basal salts medium. The stock suspension was used at two dilutions in the kinetic studies with initial concentrations of 1000 ng DBT $ml^{-1}$. The stability in viable cell counts during the kinetic studies is indicated in Table 12.11.

TABLE 12.11. VIABLE CELL COUNTS (cells $ml^{-1}$)
DURING PSEUDO-FIRST-ORDER BIODEGRADATION
KINETIC STUDIES WITH DIBENZOTHIOPHENE

| Time (hr) | Series 1 | Series 2 |
|---|---|---|
| 0 | $3.7 \times 10^6$ | $1.9 \times 10^6$ |
| 60 | $3.5 \times 10^6$ | $1.8 \times 10^6$ |
| 120 | $3.6 \times 10^6$ | $1.8 \times 10^6$ |
| 150 | $3.8 \times 10^6$ | -- |
| 180 | -- | $1.9 \times 10^6$ |
| 220 | -- | $2.0 \times 10^6$ |

There was a short lag period before biodegradation of DBT was optimally developed (Figure 12.7). The pseudo-first-order rate constants ($k_{b1}$) calculated from the slopes of the plots of ln DBT concentrations versus time were 1.85 $hr^{-1}$ and 1.05 $hr^{-1}$ for degradations initiated with $3.7 \times 10^6$ and $1.9 \times 10^6$ cells $ml^{-1}$, respectively. Consequently, the respective second-order rate constants were $5.0 \times 10^{-7}$ and $5.5 \times 10^{-7}$ ml $cell^{-1}$ $hr^{-1}$. Average $k_{b2}$ value equals $(5.3 \pm 0.4) \times 10^{-7}$ ml $cell^{-1}$ $hr^{-1}$.

### 12.6.3 Metabolites

The residues from the above kinetic studies were refrigerated for two days before they were extracted under neutral and acidic conditions with ethyl acetate. The concentrated extracts were analyzed by GC and HPLC. Preliminary observations indicated better resolution in our GC system and more products in the extract made from acidified broths than from the neutral broth. By GC, at least 10 products were observed in the acid-extracted fraction. This fraction was converted to the trimethylsilyl (TMS) derivatives and analyzed by GC-MS.

Structures for seven metabolites are indicated in Figure 12.8 and the mass spectra for Compounds A, B, C, D, E, F, and G or their TMS derivatives are presented in Figures 12.9 through 12.15. Compound A has been confirmed as dibenzothiophene-5-oxide by comparison of the mass spectrum with that of a reference sample. The identification of Compound B as 1,2-dihydroxy-1,2,3,4-tetrahydrodibenzothiophene is suggested from our MS data, from the structures

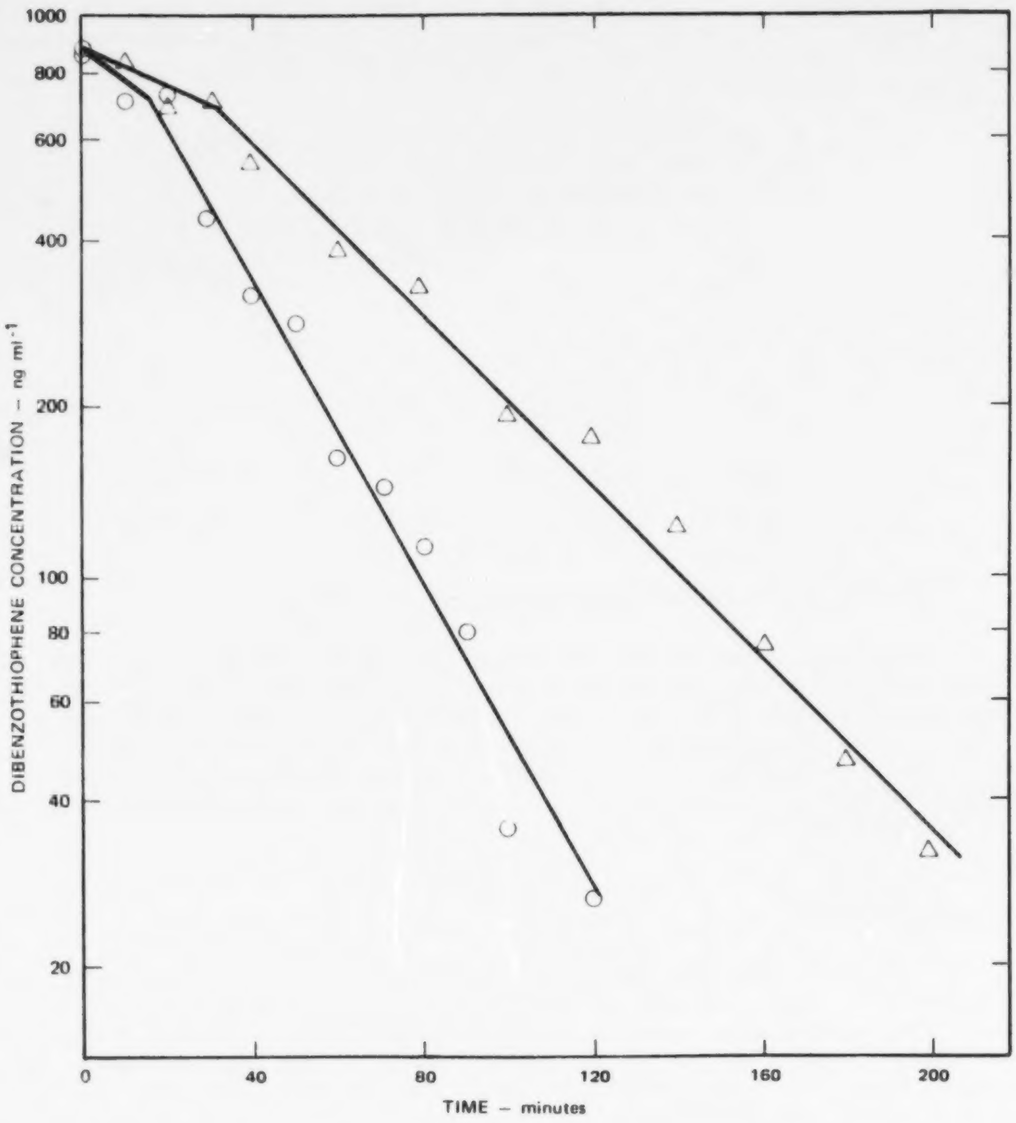

FIGURE 12.7. DIBENZOTHIOPHENE BIODEGRADATION IN BATCH FERMENTATION WITH HIGH CELL COUNTS

Initial cell concentrations: ○ $3.6 \times 10^6$ cells ml$^{-1}$

△ $1.9 \times 10^6$ cells ml$^{-1}$

of Compounds C, D, E, and F, and from the observation by Gibson (1975) that cis-1,2-dihydroxy-1,2-dihydrobenzothiophene was a metabolite of DBT.

Compounds C and D were converted to their bis TMS derivatives and the mass spectra of the separate GC fractions were interpreted as those from the cis and trans isomers of 4[2-(3-hydroxy)-thianaphthenyl]-2-oxo-3-butenoic acid. Compounds E, F, and G were assigned the structures 3-hydroxy-2-formylbenzothiophene, 3-hydroxy-benzothiophene, and 2,3-diketobenzothiophene, respectively.

The insoluble red product removed by filtration on Whatman No. 4 filter paper in the process of preparing the culture for kinetic evaluations was not studied.

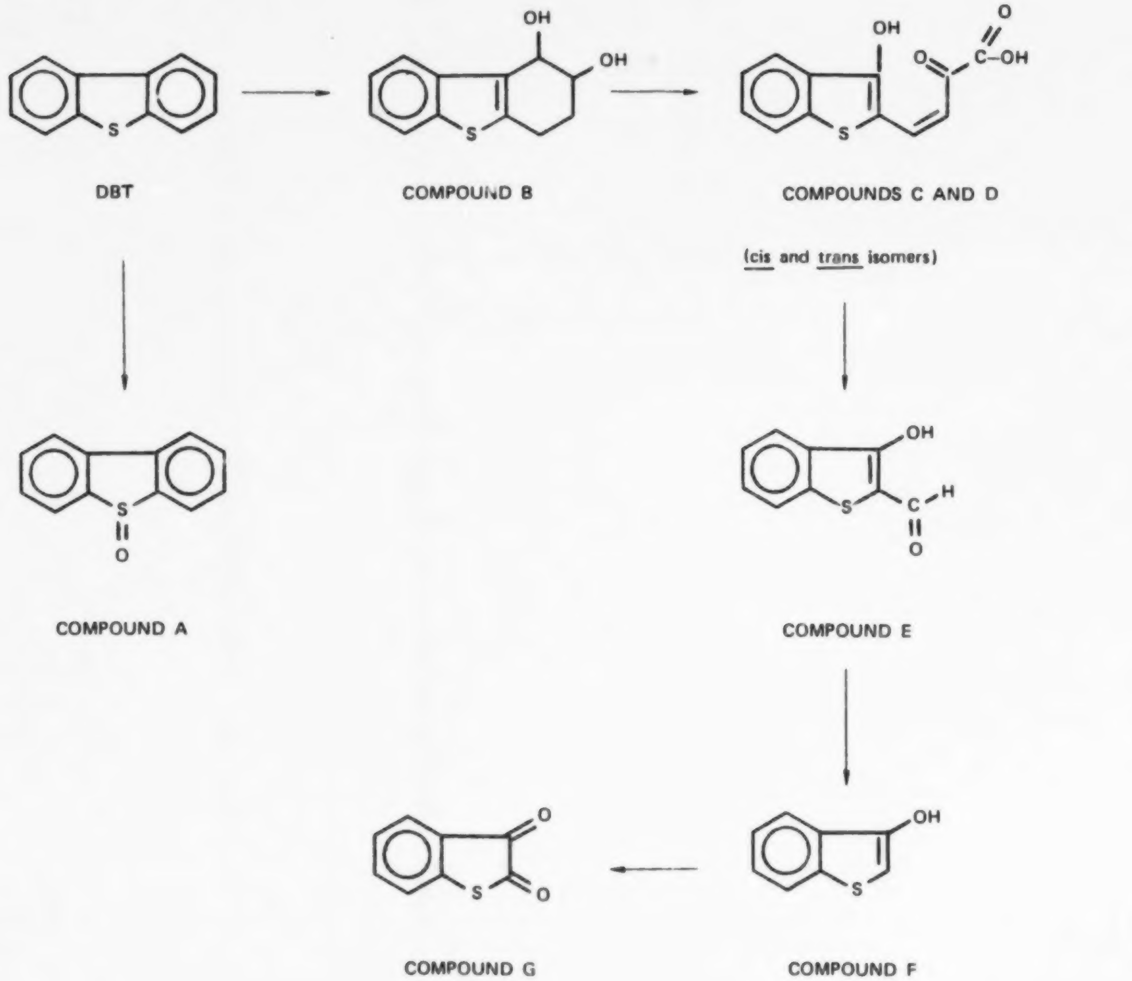
DBT
COMPOUND B
COMPOUNDS C AND D
(cis and trans isomers)
COMPOUND A
COMPOUND E
COMPOUND G
COMPOUND F

FIGURE 12.8 METABOLISM OF DIBENZOTHIOPHENE

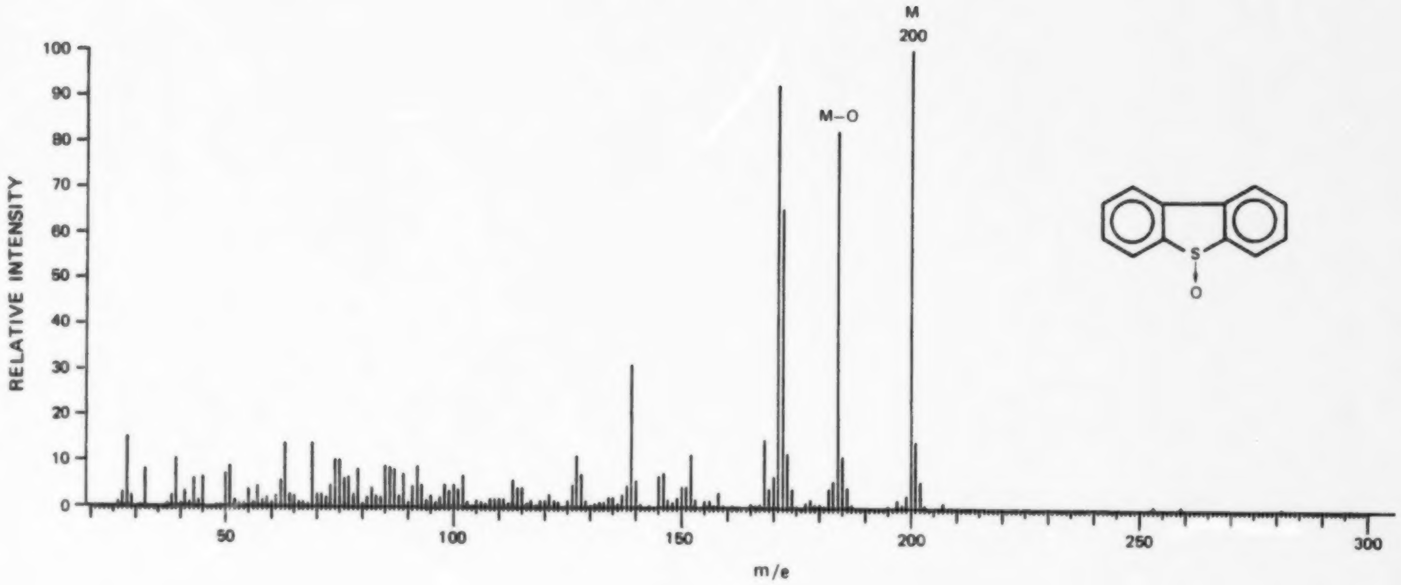

FIGURE 12.9 MASS SPECTRUM OF COMPOUND A, DIBENZOTHIOPHENE-5-OXIDE

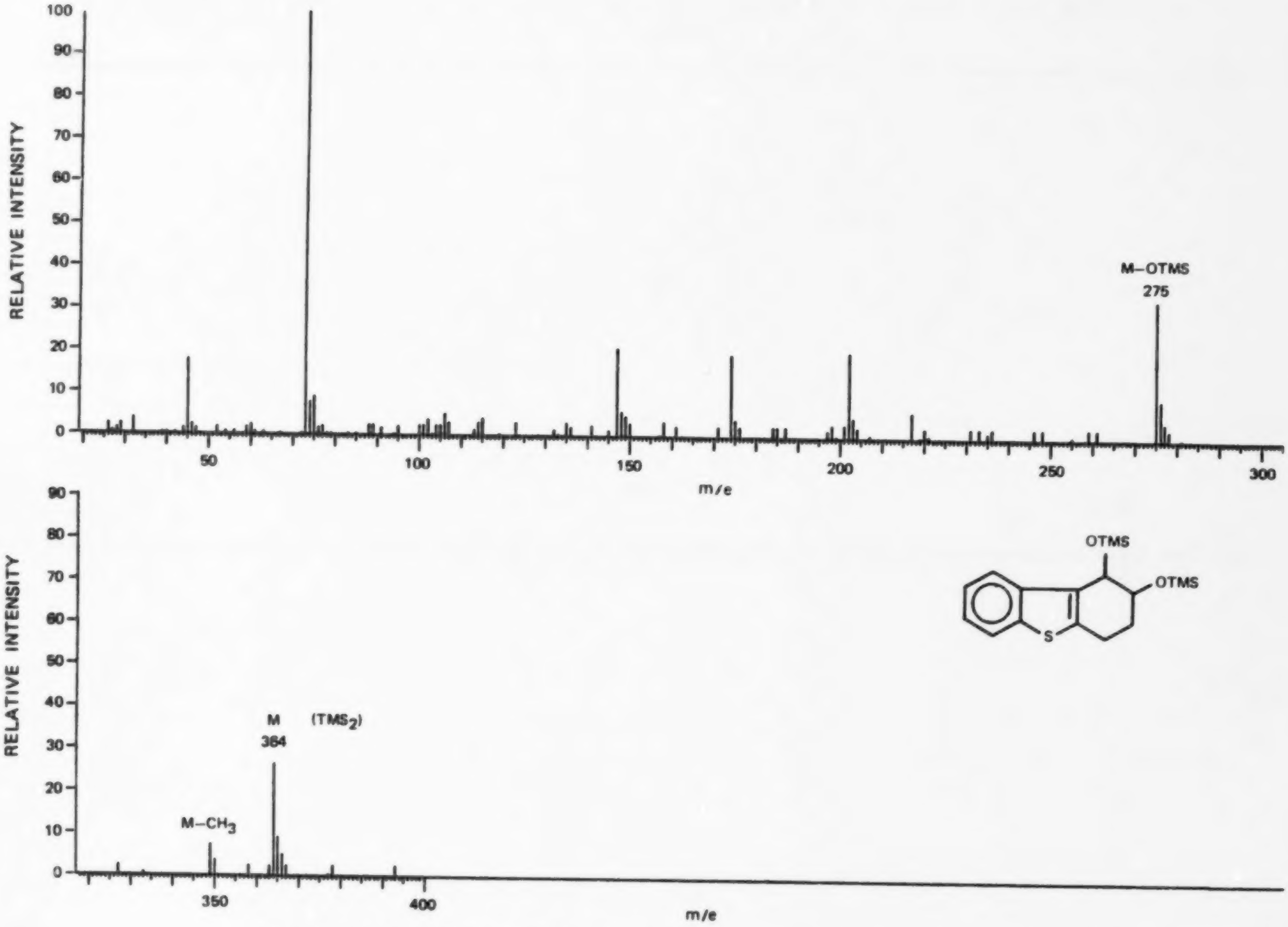

FIGURE 12.10 MASS SPECTRA OF COMPOUND B, BIS-TRIMETHYLSILYL ETHER

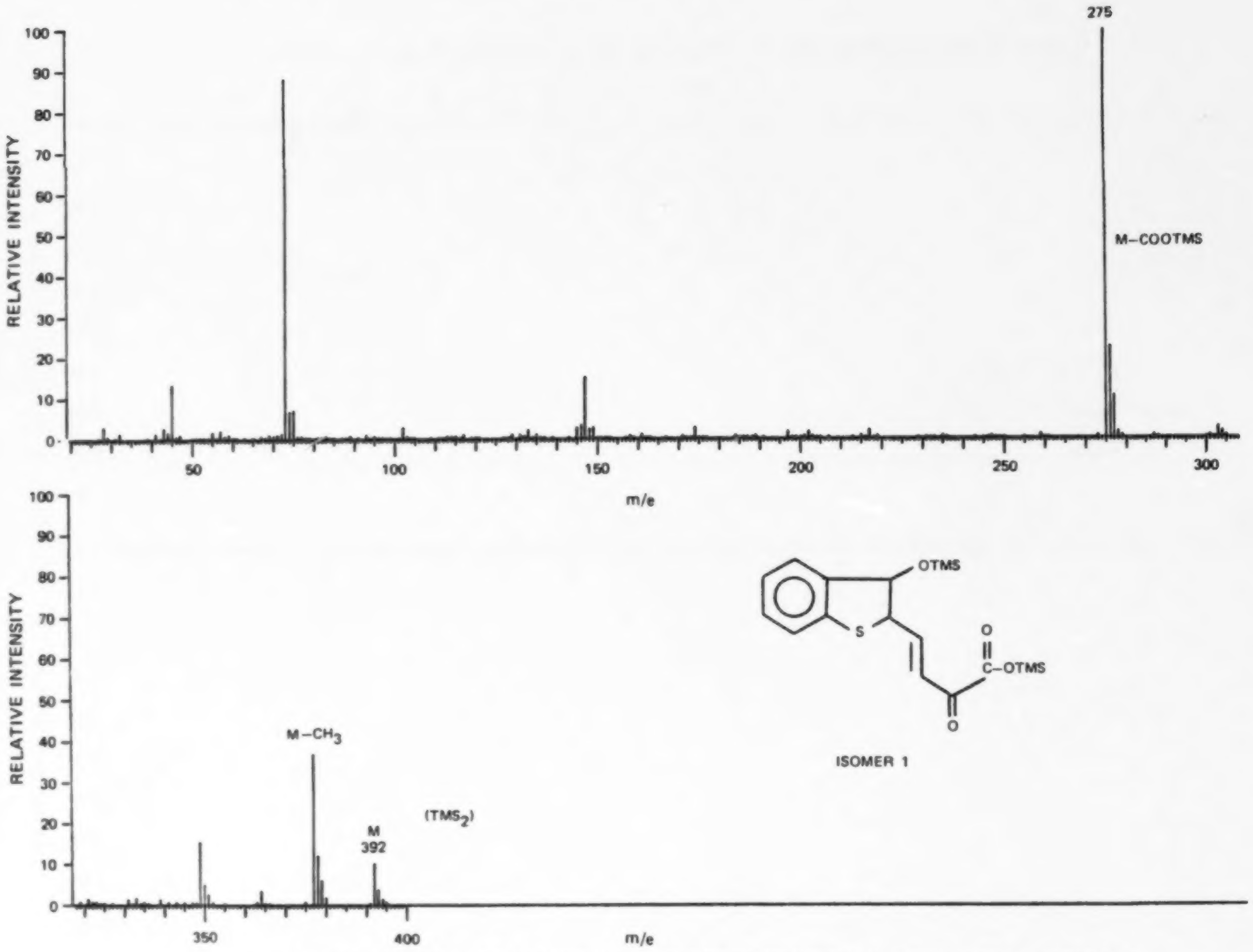

FIGURE 12.11 MASS SPECTRA OF COMPOUND C, BIS-TRIMETHYLSILYL DERIVATIVE, ISOMER 1

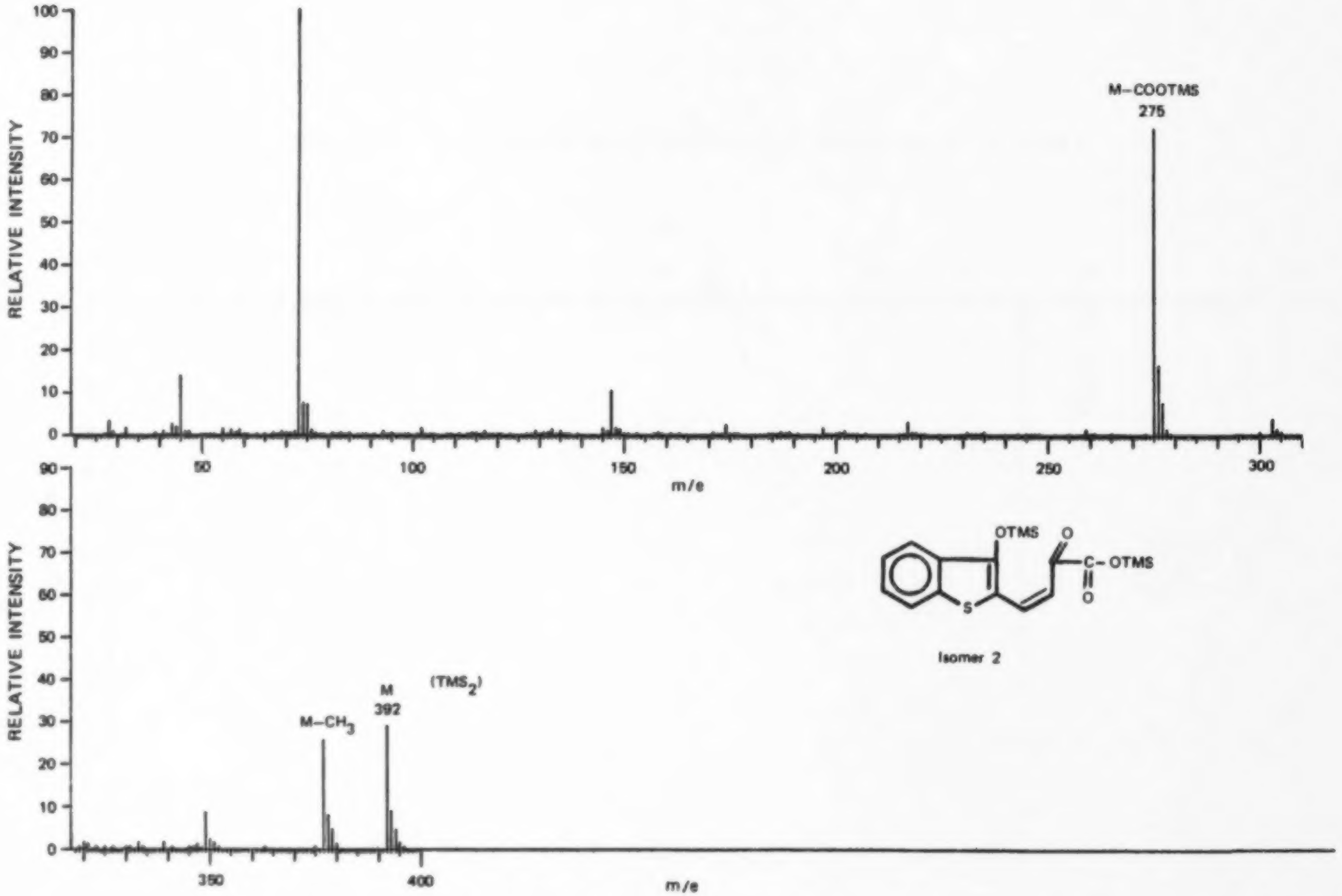

FIGURE 12.12 MASS SPECTRA OF COMPOUND D, BIS-TRIMETHYLSILYL DERIVATIVE, ISOMER 2

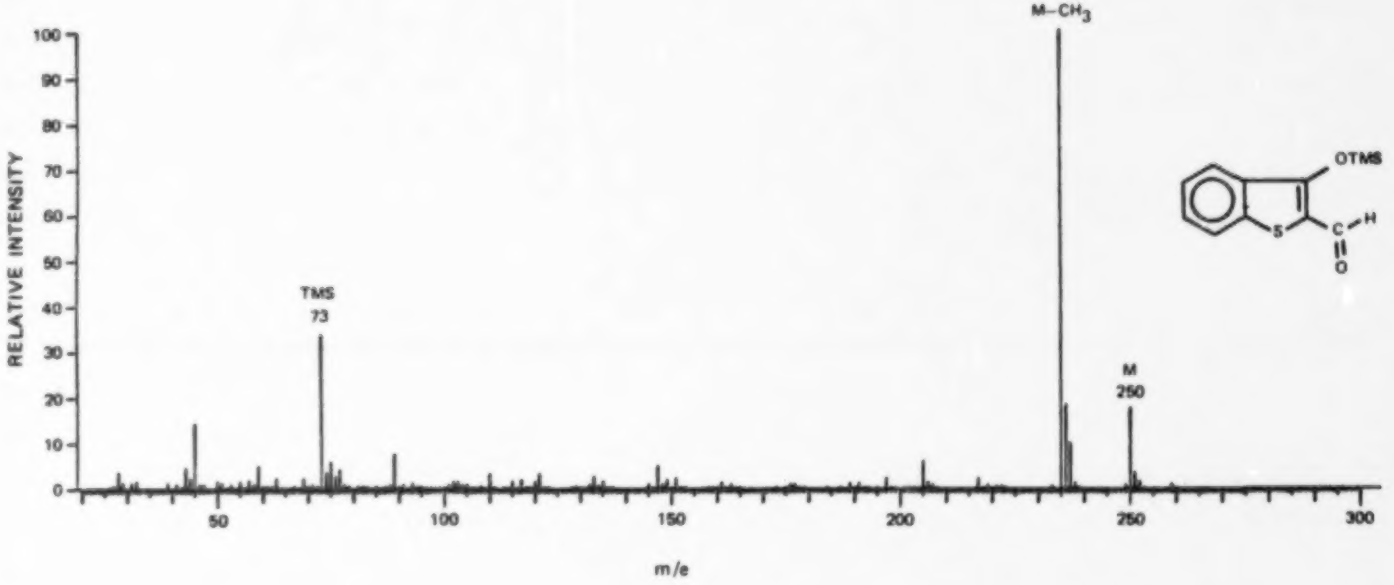

FIGURE 12.13 MASS SPECTRUM OF COMPOUND E, TRIMETHYLSILYL ETHER

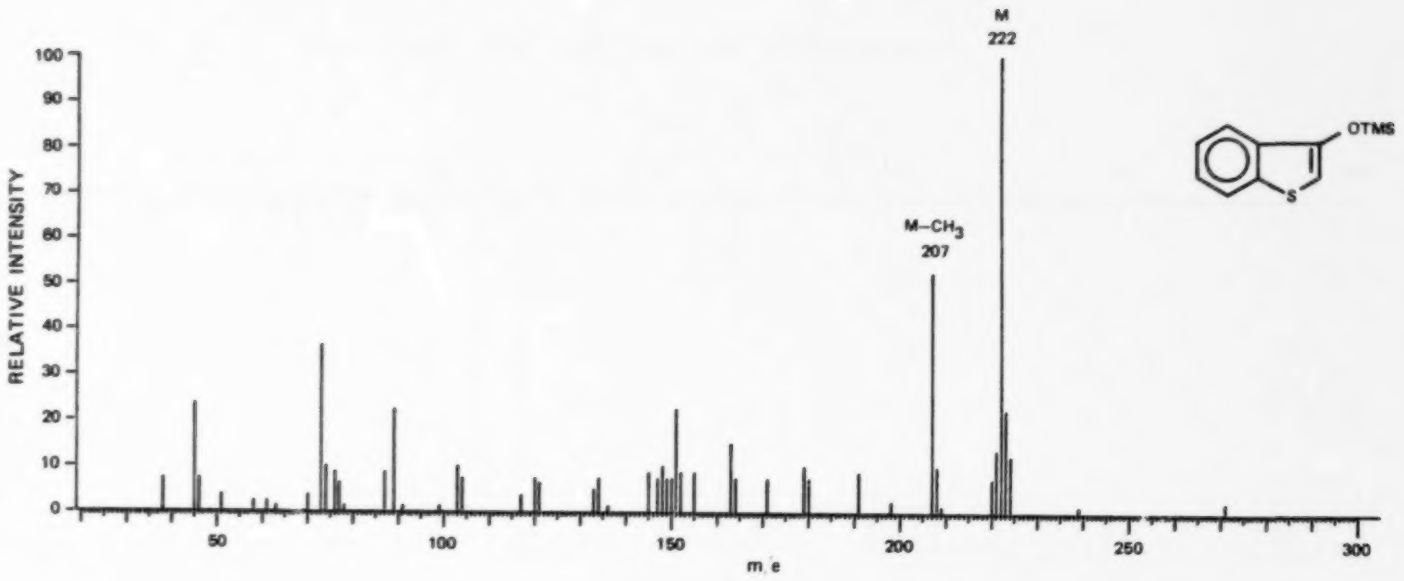

FIGURE 12.14 MASS SPECTRUM OF COMPOUND F, TRIMETHYLSILYL ETHER

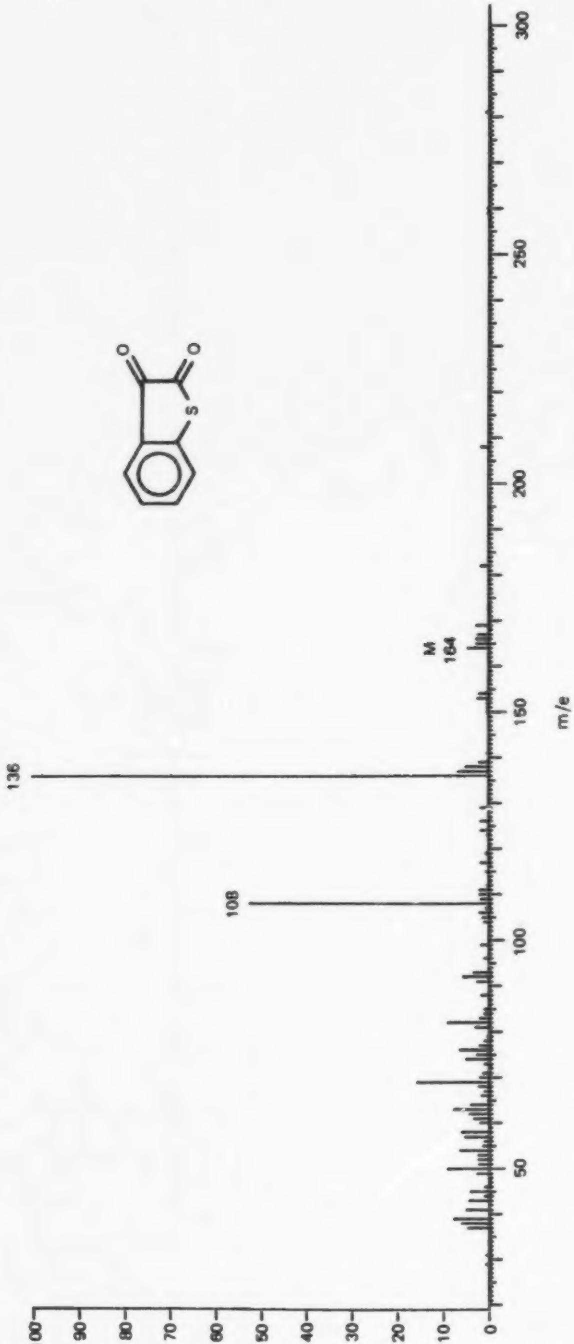

FIGURE 12.15 MASS SPECTRUM OF COMPOUND G

### 12.6.4 Discussion

The development of DBT biodegrading mixtures of cultures by our enrichment process revealed several interesting features that may exist when contaminants containing DBT are introduced into aquatic systems. When more readily biodegradable and chemically related compounds that coexist with DBT in petroleum or coal tar products were added, DBT biodegrading culture systems were more readily developed. In two cases, the addition of only DBT to the water sample did not result in DBT biodegradation. The difficulties encountered in several instances in developing cultures that could degrade DBT when transfers were made from media containing DBT plus naphthalene also indicate the complexity of evaluating the biodegradability of a compound. Undoubtedly, induction and cometabolism are important phenomena that operate in natural waters.

The kinetic rate constants developed with a mixed culture system indicate that if such cultures exist or can be developed, DBT is readily degraded.

Since the thiophenes exhibit toxic and phyiological activities, a knowledge of the characteristics of the metabolites can be of considerable significance. Although not all the observed metabolites have been studied, six chemical entities have been tentatively identified and the structure of one product has been confirmed by comparing its mass spectrum with a reference sample.

Basically, our data are in agreement or related to those of Kodama et al. (1970, 1973), Laborde and Gibson (1975), Gibson (1975), and Hou and Laskin (1975). Our determination of Compound B as a 1,2-dihydroxy-1,2,3,4-tetrahydrodibenzothiophene as compared with the 1,2-dihydroxy-1,2-dihydrobenzothiophene reported by Gibson (1975) may be due to differences in the cultures involved or to possible reduction at the 3,4 positions occurring between the time of the kinetic study and the extraction, when the 1,2-dihydro compound may have functioned as a hydrogen acceptor. The observation of the *cis* and *trans* forms of 4[2-(3-hydroxy)-thianaphthenyl)-2-oxo-butenoic acid] may be due to a *cis-trans* isomerase (Kodama et al., 1973) or to conversion under GC conditions. Bioconversions to Compounds E, F, and G are logical. It is possible that 2,3-dihydroxybenzothiophene is formed as an intermediate between Compounds F and G and that this dihydroxy compound or Compound G may undergo ring fission. Compound G was not previously reported as a metabolite of DBT. The insoluble red product present at these high dilutions of substrate may be similar to the Compounds A and B reported by Hou and Laskin (1975) or may be dimeric forms of DBT metabolites.

Many questions remain regarding DBT degradation pathways and these could be examined by using mixed cultures, pure cultures, or mutant cultures; by isolating metabolites at ambient temperatures; and by conducting material balances. The naturally occurring alkylated derivatives of DBT would of course have different metabolic pathways because of the influences of the alkyl groups. In some cases, the alkyl groups would be attacked first and such compounds could be more readily removed from water columns. On the other hand, branched alkyl substituents on both benzene rings could increase the resistance of such compounds to biodegradation.

# 13. LABORATORY INVESTIGATION OF METHYL PARATHION

## 13.1 SYNOPSIS

The results of our laboratory studies suggest that biodegradation is the major environmental pathway for methyl parathion (MP) in eutrophic systems. Sorption, photolysis, and hydrolysis are important and perhaps dominant transformation processes in oligotrophic systems. There is some evidence that the rate of hydrolysis of MP is accelerated by suspended sediments, but conclusive measurements were not conducted. The rate of volatilization of dissolved MP is not significant compared with the rates of chemical and biodegradation processes.

*p*-Nitrophenol was identified as a biodegradation product but was rapidly degraded in the one mixed culture system examined. O-Methyl-O-*p*-nitrophenylthiophosphoric acid and *p*-nitrophenol are the major products from neutral- (pH <8) and base-catalyzed hydrolysis (pH >8), respectively; the same products were found in the photohydrolysis of MP. Transformation of MP to paraoxon was not observed.

The results obtained from the nine-compartment computer model supported the conclusions reached on the basis of the laboratory rate data. They also suggested that physical sorption and biodegradation may be significant in bottom sediments. The model predicted the following steady-state concentrations of MP in solution, suspended solids, and sediments near point sources in the presence of a continuous discharge of 1 $\mu g\ ml^{-1}$ (1 ppm) methyl parathion.

| | Half-life* (hr) | Solution ($\mu g\ ml^{-1}$) | Suspended solids ($\mu g\ g^{-1}$) | Sediments ($\mu g\ g^{-1}$) |
|---|---|---|---|---|
| River | 0.6 | 0.989 | 49.46 | 49.1 |
| Pond | 27.3 | $1.2 \times 10^{-2}$ | 0.60 | 0.60 |
| Eutrophic lake | 28.3 | 0.06 | 3.00 | 0.51 |
| Oligotrophic lake | 151.6 | 0.098 | 4.90 | 1.40 |

---

*Predicted by one-compartment model.

## 13.2 BACKGROUND

Table 13.1 gives the physical properties and nomenclature of methyl parathion, which is a broad spectrum insecticide widely used in cotton cultivation in the United States. It is highly toxic to humans and most other nontarget organisms and may be sorbed by ingestion, by skin contact, or by inhalation. It is nonpersistent, requiring 3 to 10 applications per season on cotton and 1 to 4 applications per season on other crops. It is a serious hazard to persons or animals entering treated areas within 48 hours of application (von Rumker et al., 1974). However, methyl parathion disappears rapidly in both soils and water and does not appear to have had significant environmental impacts away from the sites of use.

TABLE 13.1. PHYSICAL PROPERTIES OF METHYL PARATHION

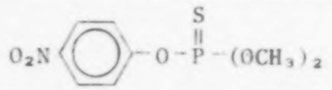

| | |
|---|---|
| Molecular weight | 263.12 |
| Melting point | 36°C |
| Vapor pressure at 20°C | $9.1 \times 10^{-3}$ torr |
| Solubility in water, $\mu g\ ml^{-1}$ | 50 $\mu g\ ml^{-1}$ or $2.1 \times 10^{-4}$ M |
| Chemical name | O,O-Dimethyl-O-p-nitrophenyl-phosphorothioate |
| Tradenames | Dalf, Folidol M., Metron, Nitox 80, Putron M, Tekovaisa |

Previous assessments of the environmental fate of methyl parathion have relied heavily on analogies to ethyl parathion and have consisted of a simple documentation of the apparent rate of disappearance from fields and selected water samples. King and McCarty (1968) reported sorption data on soils for both MP and parathion. Saltzman and Yaron (1972) reported sorption data for parathion on both clays and soils. All these workers found that the sorption partition coefficient, $K_p$, varied from 5 to 30, that $K_p$ was roughly proportional to the soil organic content, and that n in the Freundlich isotherm equation was approximately 1.

Limited information was available for assessing the chemistry of methyl parathion in aquatic environments. However, these data, along with those reported on parathion indicated that chemical transformation might be important under some environmental conditions.

The hydrolysis of methyl parathion has been studied under a variety of conditions as summarized below.

| Conditions | Half-life | Reference |
|---|---|---|
| "pH about 6," room temperature | 1.7 weeks | Cowart et al. (1971) |
| pH 12, 37.5°C | 2.1 hours | Jaglan and Gunther (1970) |
| pH 6 buffer, 70°C, 20% ethanol | 8.4 hours | Ruzicka et al. (1967) |

Low concentrations of copper ion have been reported to catalyze the hydrolysis of parathion and paraoxon (Ketalaar et al., 1956). The hydrolysis products of methyl parathion itself are reported to be p-nitrophenol and dimethyl phosphoric acid. It was recently reported that hydrolysis of parathion in acidic or neutral solutions also gives the dealkylated ester, O-ethyl-O-p-nitrophenylthiophosphoric acid, and ethanol (Weber, 1976).

Oxidation of parathion esters using permanganate, chlorine, silver oxide, ozone, and other chemicals has been reported (Gunther et al., 1968, 1970; Gomma and Faust, 1972). The latter paper reports an acceleration of the oxidation rate with increased pH values. The products identified in these reactions were paraoxon and p-nitrophenol.

While no work on the photochemistry of methyl parathion in aqueous solution has been reported, literature on the phototransformation of parathion is relevant because the structures are similar and the UV spectra of the two compounds are almost identical (the UV spectra of both parathion and methyl parathion show $\lambda_{max}$ 274 nm, log $\epsilon$ 4.0 and $\lambda_{max}$ 350 nm, log $\epsilon$ 2.4) (Sandi, 1959). Paraoxon and p-nitrophenol have been reported to result from photolysis of parathion (Cook and Pugh, 1957; Grunwell and Erickson, 1973). The latter paper also reported that parathion did not oxidize in the presence of photogenerated singlet oxygen. Contrary to the above findings, paraoxon was not found in a study on the photolysis of methyl parathion on soils (Baker and Applegate, 1970).

Although the above information indicated that methyl parathion would undergo hydrolysis, photolysis, and possibly oxidation, no reliable data were available for evaluating the rates or kinetics of these reactions in aquatic environments. Furthermore, the information available was both incomplete and confusing with regard to the identity and yields of products obtained in the respective transformation reactions. Since paraoxon and methyl paraoxon are more toxic than the parent thioesters themselves, particular attention was directed toward determining whether methyl paraoxon is formed from oxidation or photolysis of methyl parathion.

Recent research studies conducted in the laboratories of Hsieh[*] and Sethunathan[†] clearly indicate the biodegradability of parathion. Lichtenstein and Schulz (1964) in studies with soils and Graetz et al. (1970) using pure cultures concluded that the breakdown of parathion involves reduction of nitro groups to aminoparathion (0,0-diethyl-0-*p*-aminophenylphosphorothioate).

In their publication on pathways of microbial metabolism of parathion, Munnecke and Hsieh (1976) discussed the many potential intermediate aromatic products and diethylthiophosphoric acid formed in the decomposition of parathion by a mixed bacterial culture (minimum of nine isolates) fermentation with technical parathion. The intermediates were determined largely by the degree of the aerobic state of the fermentation. *p*-Nitrophenol and diethylthiophosphoric acid were primary degradation products in the oxidative pathway. Munnecke and Hsieh (1976) indicated that, in most studies on biodegradative mechanisms, insufficient substrate was used for identification of metabolites. A characteristic of their parathion degradation system was the release of small amounts of parathion hydrolase into the medium. They also observed that their hydrolase preparation had an optimal pH of 9.2. All studies with mixed cultures indicated that biodegradation of parathion proceeded until no aromatic ultraviolet-absorbing material remained. The parathion hydrolase was studied in greater detail by Munnecke (1976) for possible pesticide disposal in plant operations. This investigation included MP and five other pesticides.

The correlation of parathion fixation on soils with the soil organic content (Kliger and Yaron, 1973; D. P. H. Hsieh, private communications, 1976) suggest that methyl parathion may be sorbed by cellular material, including microbial cells. This is environmentally important because if a substance is sorbed by nonbiodegrading organisms (or sediment), its availability for decomposition by organisms that are capable of biodegrading it is decreased. Also, digestion of free floating cellular material containing the substance by cells that only partially degrade it, or do not degrade it, could result in food chain magnification. The alga *Chlorella pyrenoidosa* has been reported to biodegrade parathion (Zuckerman et al., 1970). The very fact that algae can sorb parathion poses a problem for food chain magnification or the deposition of the pesticide in the detritus and eventual degradation in the sediment. Gregory et al. (1969) reported the uptake of parathion by *Euglena gracilis* (a "flagellate"), two species of algae, and two species of ciliates. Their data implied a sorption partition coefficient of $2.2 \times 10^3$ when their *Euglena* were exposed to $1\ \mu g\ ml^{-1}$ parathion for 7 days. Kortus et al. (1971) studied the uptake of $^{32}P$-labelled parathion by *Euglena gracilis* and observed 69% uptake of the pesticide in 15 minutes.

A Midwest Research Institute report to the EPA (1975) reviewed the sorption of parathion by microbes and indicated that parathion sorption may be independent of life processes since the sorption characteristics of live and dead organisms showed little difference. This report also reviewed the effects of parathion on microorganisms and parathion biodegradation.

---

[*] Munnecke and Hsieh (1974, 1975, 1976), Hsieh and Munnecke (1972).

[†] Siddaramappa et al. (1973), Sethunathan (1973), Sethunathan and Yoshida (1973).

Several reports were previously published on the biodegradation of MP (Lichtenstein and Schulze, 1964; Yasuno et al., 1965; Maleszewska, 1974; Naumann, 1967). These include studies on waters and soils. However, these studies are not of the type that could be used in a multidisciplinary overall assessment of the fate of MP in oligotrophic, eutrophic, and waste waters.

## 13.3 ENVIRONMENTAL ASSESSMENT

### 13.3.1 Summary of Laboratory Data

The rate constants obtained in the laboratory investigations of the transformation and transport processes for MP are summarized in Table 13.2.

TABLE 13.2. SUMMARY OF METHYL PARATHION LABORATORY DATA

| Process | Sorption equilibrium | Partition coefficient |
|---|---|---|
| Sorption | $S_s = K_p S_w$ | $K_p = 50^a$ |
| | Rate expression | Rate constant at 25°C |
| Volatilization[b] | $k_v[MP]$ | $k_v < 6 \times 10^{-5}\ k_v^0$ |
| Photolysis[c] | $k_p[MP] = \phi(\Sigma Z_\lambda \varepsilon_\lambda)[MP]$ | $k_p = 2.7 \times 10^{-7}\ \mathrm{sec}^{-1}$ |
| Oxidation | $k_{ox}[RO_2\cdot][MP]$ | $k_{ox} = 3\ M^{-1}\ \mathrm{sec}^{-1}$ |
| Hydrolysis[d] | $k_h[MP]$ | $k_h = 9 \times 10^{-8}\ \mathrm{sec}^{-1}$ |
| Biodegradation | $k_{b2} = \frac{\mu_{max}}{YK_s}$ | $k_{b2} = 1.7 \times 10^{-7}\ \mu\mathrm{g\ cell}^{-1}\ \mathrm{hr}^{-1}$ |

[a] Average for all sediments

[b] See discussion in Part I, Section 5.3, and Appendix B.

[c] Early January.

[d] At pH < 8.

### 13.3.2 Environmental Assessment Using the One-Compartment Model

The half-lives of dissolved MP calculated for individual transformation or removal processes following a spill are listed in Table 13.3. Virtually all the MP is predicted to remain in solution and is predicted to be rapidly transformed by microbes in eutrophic waters. Photolysis is predicted to dominate transformations in oligotrophic waters. Half-lives of roughly 6.5 days and 1 day are expected in oligotrophic and eutrophic waters, respectively. Dilution effects are important only in rivers.

### 13.3.3 Persistence

Methyl parathion is not a "persistent" compound in eutrophic waters because it is rapidly transformed in solution. In clear, biologically unpro-

TABLE 13.3. TRANSFORMATION AND TRANSPORT OF METHYL PARATHION PREDICTED BY THE ONE-COMPARTMENT MODEL

| | River | Eutrophic pond | Eutrophic lake | Oligotrophic lake |
|---|---|---|---|---|
| Photolysis, half-life (hr)[a] | 340 | 850 | 850 | 170 |
| Oxidation, half-life (hr) | $>2 \times 10^5$ | $>2 \times 10^5$ | $>2 \times 10^5$ | $>2 \times 10^5$ |
| Volatilization, half-life (hr) | $>4 \times 10^5$ | $>5 \times 10^6$ | $>2 \times 10^6$ | $>2 \times 10^6$ |
| Hydrolysis, half-life (hr) | 1700 | 1700 | 1700 | 1700 |
| Biodegradation, half-life (hr) | 40 | 40 | 40 | >10,000 |
| Half-life for all processes except dilution (hr) | >7 | 28.5 | 28.5 | 157.5 |
| Half-life for all processes including dilution | 0.6 | 27.3 | 28.3 | 151.6 |
| Amount methyl parathion sorbed ($mg\ m^{-3}$)[b] | 5 | 15 | 2.5 | 2.5 |
| Percentage methyl parathion sorbed | 0.5% | 1.5% | 0.25% | 2.25% |

[a] Estimates are the average photolysis rates on a summer day at 40° latitude. Photolysis rates in midwinter are at least three times slower.

[b] 1 $\mu g\ ml^{-1}$ of methyl parathion in aqueous phase and partition coefficient of 50 are assumed.

ductive (oligotrophic) waters, however, MP will be more persistent because of the small microbial populations.

### 13.3.4 Mass and Concentration Distributions Calculated Using the Nine-Compartment Computer Model

The pseudo-first-order rate constants used in these simulations are presented in Appendix A. The distributions of mass and concentration of MP expected at steady state during chronic discharge to each of four types of water bodies are given in Table 13.4. Figures 13.1 to 13.4 show the dynamics of changes in concentration for the pond, river, and lake simulations. Changes in the MP concentrations in suspended solids parallel changes in concentration of dissolved MP, and consequently are shown only for the pond simulation to simplify the figures.

Despite the marked tendency of MP to remain in solution, roughly half of the MP is in the sediments at steady state (Table 13.4), under conditions of continuous discharge, with the possible exception of oligotrophic lakes. In all simulations, concentrations are 10 to 100 times higher on the suspended solids and in the sediments than in solution. After discharges are stopped in the simulations, MP concentrations decline most rapidly in the aqueous phases of the river and eutrophic lake simulations. The concentrations scarcely change in the sediments of any of the simulations because the scouring rate of the sediments is low ($t_{1/2} \sim 1700$ hr).

### 13.3.5 Discussion

The major influx of MP into natural waters should occur shortly after application either as sprays, drift, or run-off, possibly with a large fraction sorbed to soil particles. If so, the degradation rates should most nearly resemble the pond simulation, which assumes large populations of metabolically active microbes and high turbidity (Figure 13.1). The much smaller influx of MP that can be expected in winter, when biodegradation rates are suppressed, probably enters mainly in the sorbed form. If so, most of the MP is probably removed from the water column by sedimentation before undergoing substantial degradation, and then degrades slowly by hydrolysis or biodegradation.

The fraction that enters as a solution during the winter months probably undergoes moderate degradation by photolysis and hydrolysis before being transported to the sediments. If so, degradation in eutrophic waters during the winter should roughly approximate the rates for compartment 1 of the oligotrophic lake simulation, which shows the maximum contribution of abiotic degradation mechanisms (Figure 13.4). Given these assumptions, biodegradation should account for roughly 1000 times more degradation of MP in actual waters than any other form of degradation, and most of the degradation should occur in the summer.

The rapid attainment of steady-state values with respect to degradation rates and MP accumulation in solution and on solids shown by the simulations is surely excessive, perhaps a factor of ten too rapid, because of the assumption of frequent mixing with each compartment. However, the sequence in which

TABLE 13.4. DISTRIBUTION OF METHYL PARATHION IN VARIOUS AQUATIC SYSTEMS AT STEADY STATE (input concentrations of 1 $\mu g\ ml^{-1}$ Methyl Parathion)

| | Pond | | River | | Eutrophic Lake | | Oligotrophic Lake | |
|---|---|---|---|---|---|---|---|---|
| | Mass (kg) | Conc. ($\mu g\ g^{-1}$) | Mass (kg) | Conc. ($\mu g\ g^{-1}$) | Mass (kg) | Conc. ($\mu g\ g^{-1}$) | Mass (kg) | Conc. ($\mu g\ g^{-1}$) |
| Compartment 1 (surface water) | | | | | | | | |
| Solution | 0.75 | $0.38 \times 10^{-1}$ | $2.96 \times 10^{2}$ | $9.87 \times 10^{-1}$ | $1.51 \times 10$ | $6.06 \times 10^{-2}$ | $3.0 \times 10$ | $1.20 \times 10^{-1}$ |
| Suspended solids | $0.10 \times 10^{-1}$ | 1.74 | 1.47 | $4.90 \times 10$ | $3.79 \times 10^{-2}$ | 3.03 | $0.75 \times 10^{-1}$ | 6.00 |
| Compartment 2 (surface water) | | | | | | | | |
| Solution | -- | -- | $2.93 \times 10^{2}$ | $9.79 \times 10^{-1}$ | $2.08 \times 10$ | $1.00 \times 10^{-2}$ | $1.30 \times 10^{2}$ | $5.20 \times 10^{-2}$ |
| Suspended solids | -- | -- | 1.46 | $4.80 \times 10$ | $0.62 \times 10^{-1}$ | 0.50 | 0.32 | 2.60 |
| Compartment 3 (surface water) | | | | | | | | |
| Solution | -- | -- | $2.91 \times 10^{2}$ | $9.71 \times 10^{-1}$ | 1.31 | $5.24 \times 10^{-3}$ | $1.12 \times 10$ | $4.50 \times 10^{-2}$ |
| Suspended solids | -- | -- | 1.45 | $4.83 \times 10$ | $0.32 \times 10^{-2}$ | 0.26 | $0.28 \times 10^{-1}$ | 2.25 |
| Compartment 5 (bottom water) | | | | | | | | |
| Solution | -- | -- | -- | -- | 0.60 | $2.40 \times 10^{-6}$ | $1.05 \times 10$ | $4.20 \times 10^{-3}$ |
| Suspended solids | -- | -- | -- | -- | $0.15 \times 10^{-2}$ | 0.012 | $0.26 \times 10^{-1}$ | 0.21 |
| Compartments 7-9 (sediment)[a] | | | | | | | | |
| Solution | $0.95 \times 10^{-2}$ | $0.38 \times 10^{-1}$ | 7.34 | $9.79 \times 10^{-1}$ | 0.14 | $0.16 \times 10^{-2}$ | 0.37 | $4.42 \times 10^{-1}$ |
| Solids | 1.14 | 1.74 | $9.84 \times 10^{2}$ | $4.86 \times 10$ | $1.11 \times 10$ | 0.82 | $2.92 \times 10$ | 2.14 |

[a] The amounts given for solid and solution phases in the sediment compartments are estimated from the sorption partition coefficient for suspended solids and may be overestimated because it was assumed that biodegradation of sorbed material does not occur.

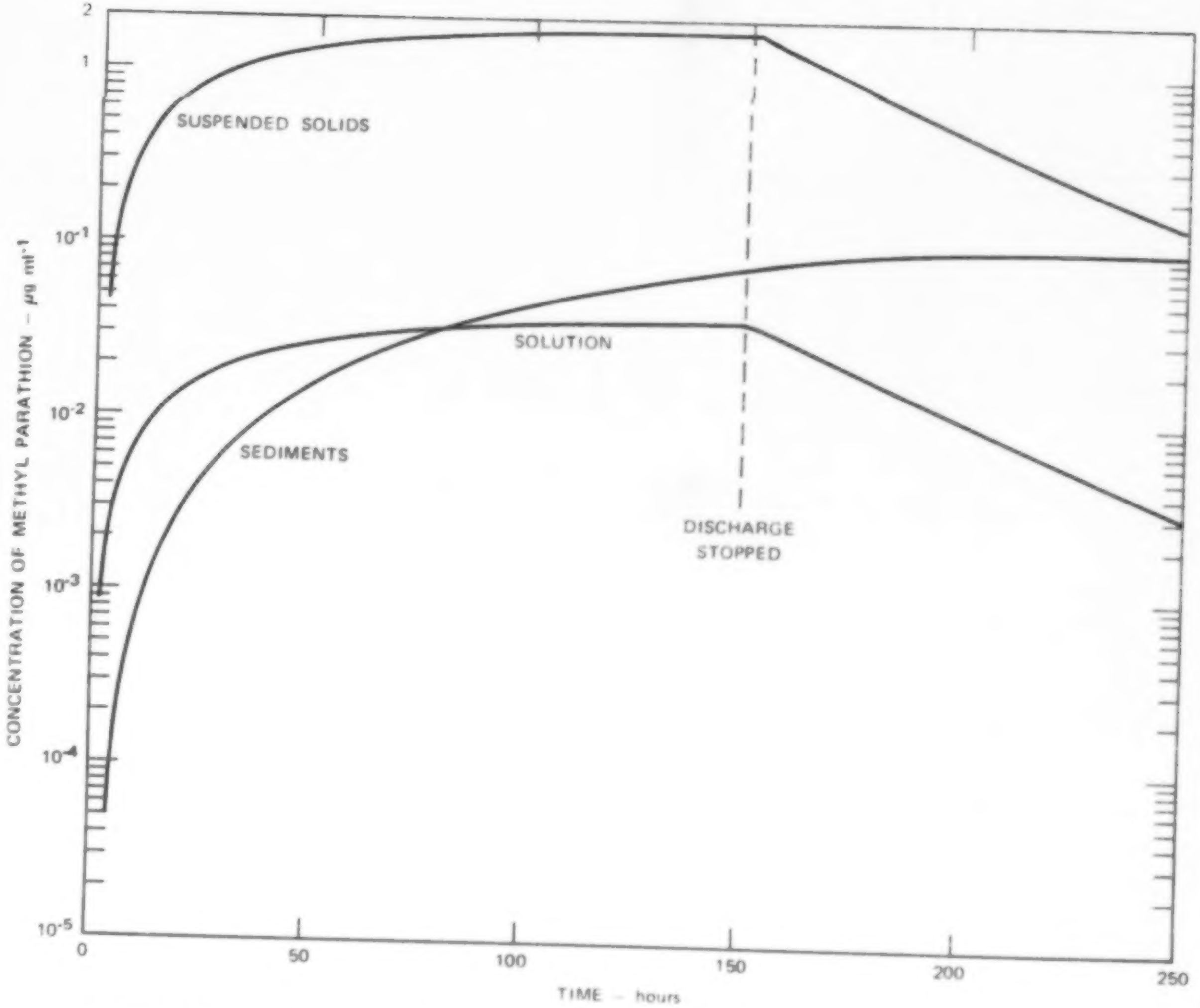

FIGURE 13.1 PERSISTENCE OF METHYL PARATHION IN A TWO-COMPARTMENT POND SYSTEM

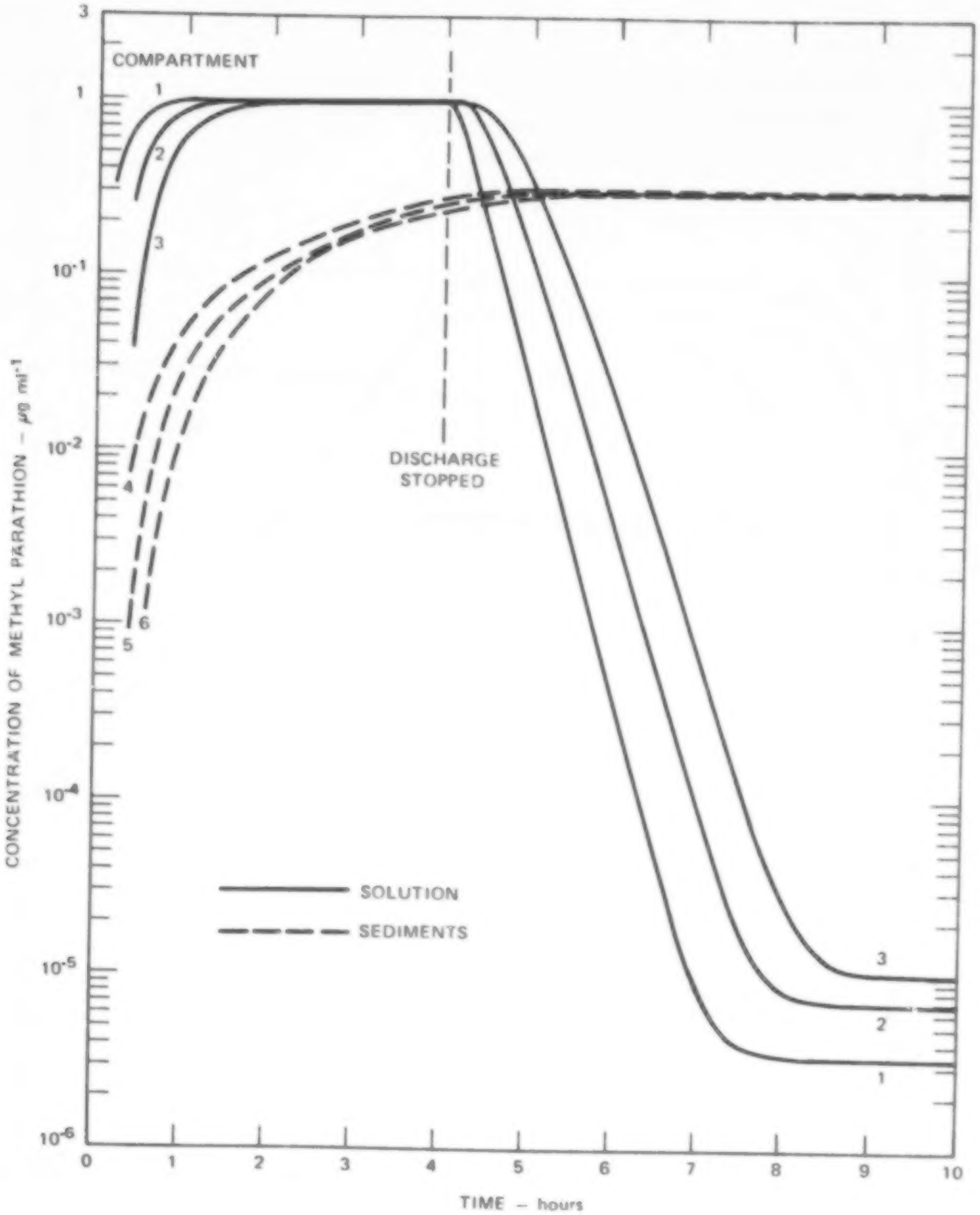

FIGURE 13.2 PERSISTENCE OF METHYL PARATHION IN A PARTIALLY MIXED RIVER SYSTEM

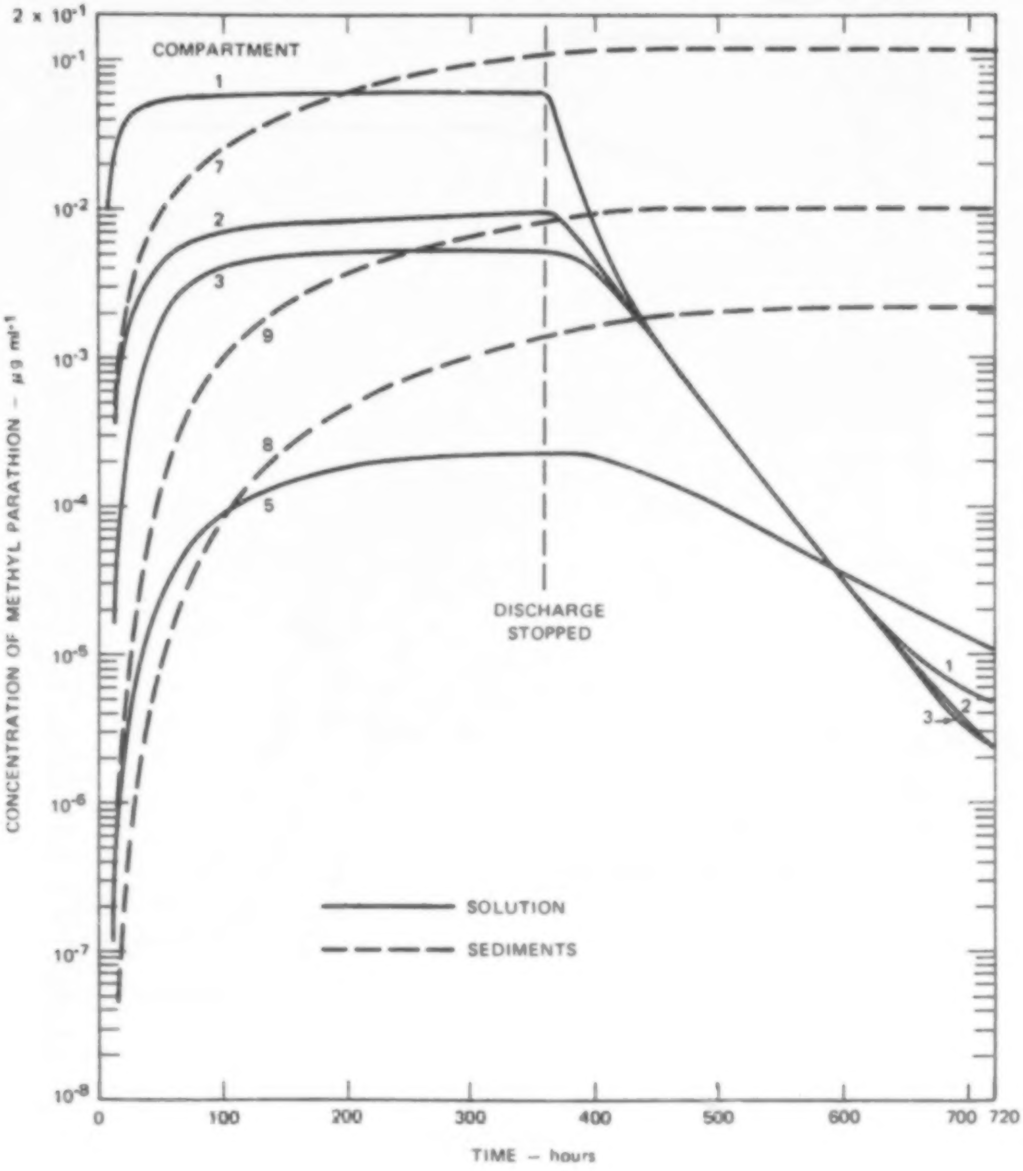

FIGURE 13.3 PERSISTENCE OF METHYL PARATHION IN A EUTROPHIC LAKE

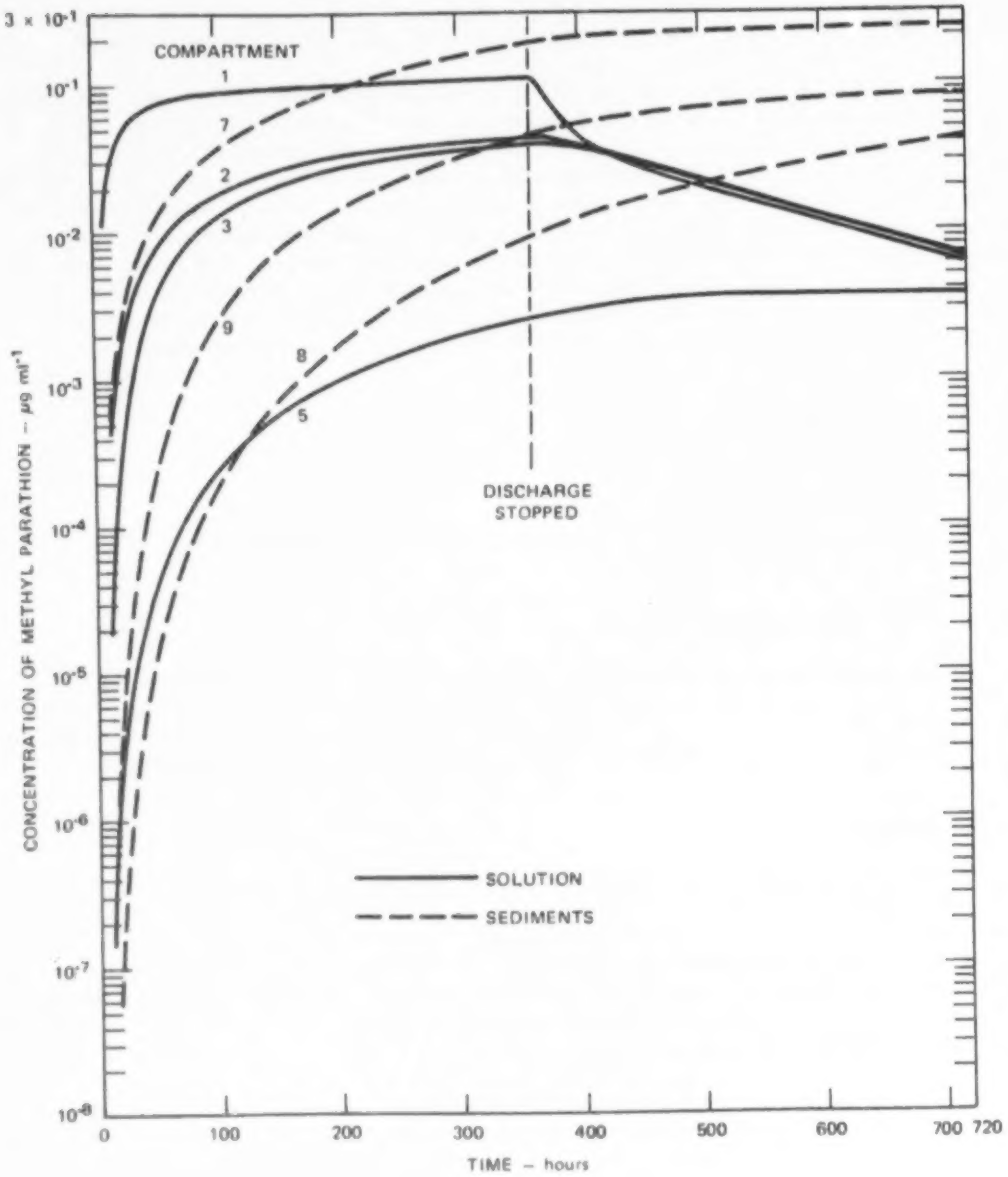

FIGURE 13.4 PERSISTENCE OF METHYL PARATHION IN AN OLIGOTROPHIC LAKE

the contents of MP, and hence the degradation rates of MP, in the various compartments reach steady state in the simulations should be accurate. The predicted sequence shows steady states appearing first in the well-mixed aqueous compartments near the source, then in the more remote aqueous compartments, and last in the sediments, which are not only remote from the source, but are characterized by a high mass of solids and hence change slowly.

On balance it is probable that MP concentrations under the chronic, low influx conditions assumed will be below toxic levels for vertebrates ($LC_{50}$ generally greater than 5 $\mu g\ ml^{-1}$) except in oligotrophic lakes, or possibly, in eutrophic lakes during winter when microbial activity is depressed by low temperatures. However, concentrations in all waters may be toxic to invertebrates ($LC_{50}$ of 2 $ng\ ml^{-1}$ to 1 $\mu g\ ml^{-1}$) under the conditions assumed. The risk should be consistently greater in shallow waters, but even here it should be fairly small since degradation appears to be virtually complete within weeks in both soil (Knutson et al., 1971) and contaminated waters (Yasuno et al., 1965; Hirakoso, 1968; Eichelberger and Lichtenberg, 1971).

## 13.4 PHYSICAL PROPERTIES

### 13.4.1 Solubility in Water

The solubility of MP in water is 50 $\mu g\ ml^{-1}$ (AAPCO, 1959).

### 13.4.2 Absorption Spectrum

The absorption spectrum was measured in the solar region (295 to 800 nm). The spectra at pH 5.1, 6.8, and 8.9 were identical within experimental error (± 2%). The data reported in Table 13.5 are the average absorption coefficients as described in Part I, Section 5.2, and Appendix B.

### 13.4.3 Volatilization

The volatilization rate of MP was measured by the method of Hill et al. (1976), which is described in Appendix B. The oxygen reaeration rate ranged from 5 to 23 $hr^{-1}$, which corresponds roughly to the turbulence of a waterfall. Each experimental point for the MP concentration is the average of replicate analyses of replicate samples and was corrected for evaporation of water. Within experimental error, which is about 5%, there was no decrease in MP concentration in 148 hours.

The MP volatilization data were fit to an exponential decay equation, using the Hewlett-Packard Model 65 routine. The volatilization rate constants were $-0.013\ day^{-1}$ for beaker A and $+0.0017\ day^{-1}$ for beaker B. Since these rate constants are equal to zero within experimental error and since the ratio of the volatilization rate constant to the oxygen reaeration rate constant is less than $4 \times 10^{-4}$, we concluded that volatilization was not an important environmental pathway for MP.

TABLE 13.5. ABSORPTION SPECTRUM OF METHYL PARATHION IN WATER[a]

| Center of wavelength interval[b] (nm) | Average absorption coefficient[c] ($M^{-1}$ $cm^{-1}$) |
|---|---|
| 297.5 | 6040 |
| 300.0 | 5460 |
| 302.5 | 4930 |
| 305.0 | 4310 |
| 307.5 | 3700 |
| 310.0 | 3210 |
| 312.5 | 2760 |
| 315.0 | 2290 |
| 317.5 | 1920 |
| 320.0 | 1630 |
| 323.1 | 1310 |
| 330.0 | 933 |
| 340.0 | 568 |
| 350.0 | 374 |
| 360.0 | 244 |
| 370.0 | 145 |
| 380.0 | 82 |
| 390.0 | 45 |
| 400.0 | 9 |
| 410.0 | 0 |

[a] Methyl parathion concentration 7.81 x $10^{-5}$ mole $liter^{-1}$.

[b] Wavelength intervals are given in Appendix B, Table B.1.

[c] The absorption coefficients at 313.0 nm and 366.0 nm are 2670 and 185, respectively.

### 13.4.4 Sorption on Clay and Sediments

Methyl parathion sorption isotherms were measured on six natural sediments and Ca-montmorillonite. Preliminary kinetic experiments were conducted using sediments from Coyote Creek, Navarro River, and Searsville Pond with no pH adjustment. In measuring isotherms starting from 7.5 and 8 $\mu g\ ml^{-1}$ sediment, we measured concentrations of MP in the supernatant after 16 and 22 hours of equilibration with the sediment. For all three sediments, no significant difference in supernatant concentration was detected at 16 and 22 hours, and it was concluded that sorption was complete in 16 hours. All subsequent isotherm measurements used 16-hour contact times to determine sorption partition coefficients.

The partition coefficient data, calculated by linear least squares regression using supernatant concentrations only, are summarized in Table 13.6. The partition coefficient for MP on Searsville sediment was also calculated using the nonlinear least squares regression (see Appendix B ) giving essentially the same value for $K_p$. Some parathion data have been included for comparison (Saltzman and Yaron, 1972). There are no striking differences in the sorption characteristics of these sediments. The Spearman rank correlation test (Langley, 1971) showed no correlation of the partition coefficient with either total organic carbon (TOC) or cation exchange capacity (CEC). Also, these sediments came from different regions of the United States and from several types of water bodies. The TOC and CEC values also vary over a wide range.

Saltzman and Yaron (1972) observed that the value of $K_p$ in the Freundlich isotherm for parathion increased as the organic content of the sediment increased. Therefore, our observation that the partition coefficient was fairly constant and independent of the organic content of the sediments studied here (Table 13.6) was surprising. However, the concentrations of MP used in this study were considerably lower than the parathion concentrations reported by Saltzman and Yaron (1972) and this may explain the differences.

In one experiment, a sorption isotherm of MP on Coyote Creek sediment was measured in the same way as above except that the sediment was subjected to three freeze-thaw cycles before exposure to MP. The freeze-thaw cycle breaks up cellular material that might be contained in the sediment. No effect on the partition coefficient was observed, suggesting that the effect of cellular material on the overall value of the partition coefficient is small with Coyote Creek sediment.

Sorption Kinetics--A study of the rate of sorption of MP was conducted with Coyote Creek sediment. Initial conditions were 3.5 $\mu g\ ml^{-1}$ MP and sediment levels of 5.9 $mg\ ml^{-1}$ and 11.9 $mg\ ml^{-1}$. The pH was adjusted to 6 at the beginning of the experiment. The concentration of MP in the supernatant was measured every 15 minutes for the first 2 hours and then less frequently for a total contact period of 27 hours. Replicate samples and replicate analyses were used for each measurement.

The data illustrated in Figure 13.5 show a rapid drop in MP followed by a slower drop that continues for at least 24 additional hours. It is not possible to determine from these data whether the drop continues after 24 hours or whether an equilibrium is established. The concentrations in the supernatant measured at 1 hour and estimated for 16 hours of contact give partition coefficients of 39 and 83, respectively, which are comparable to the Coyote Creek sediment isotherm run previously ($K_p$ = 51 ± 5, Table 13.6).

The slowly decreasing part of the curve in Figure 13.5 was analyzed assuming that the decay was first order in MP and sediment concentration,

TABLE 13.6. METHYL PARATHION SORPTION ON SEDIMENTS

| Sediments | Total organic carbon (%) | Sediment conc. (mg ml$^{-1}$) | MP concentration in supernatant[a] (μg ml$^{-1}$) | MP concentration on sediment[b] (μg g$^{-1}$) | Partition coefficient, $K_p$ | | |
|---|---|---|---|---|---|---|---|
| | | | | | LLS[c] | | NLLS[c] |
| | | | | | $a_o = 0$ | $a_o \neq 0$ | $S_w$ only |
| Ca-Montmorillonite clay sorption | 0.06 | 8.0 | 5.7 ± 0.3 | 280 ± 40 | 46 ± 2 | 49 ± 6<br>($a_o$ = -11 ± 27) | -- |
| | | 16 | 4.7 ± 0.2 | 200 ± 10 | | | |
| | | 4.2 | 3.2 ± 0.1 | 160 ± 20 | | | |
| | | 13 | 2.6 ± 0.1 | 100 ± 10 | | | |
| Coyote Creek sorption | 1.4 | 7.5 | 5.5 ± 0.4 | 270 ± 50 | 51 ± 5 | 28 ± 12<br>($a_o$ = 99 ± 49) | -- |
| | | 15 | 4.5 ± 0.1 | 200 ± 10 | | | |
| | | 3.7 | 3.2 ± 0.1 | 210 ± 40 | | | |
| | | 11 | 2.3 ± 0.2 | 140 ± 20 | | | |
| Des Moines River sorption | 0.6 | 7.7 | 5.8 ± 0.2 | 230 ± 20 | 42 ± 2 | 29 ± 4<br>($a_o$ = 59 ± 19) | -- |
| | | 15 | 4.7 ± 0.1 | 190 ± 10 | | | |
| | | 3.8 | 3.2 ± 0.1 | 160 ± 20 | | | |
| | | 12 | 2.4 ± 0.1 | 120 ± 10 | | | |
| Navarro River sorption | 0.4 | 8.1 | 6.2 ± 0.5 | 310 ± 60 | 48 ± 3 | 41 ± 12<br>($a_o$ = 30 ± 59) | -- |
| | | 16 | 4.9 ± 0.3 | 230 ± 20 | | | |
| | | 3.7 | 3.5 ± 0.3 | 160 ± 70 | | | |
| | | 11 | 2.6 ± 0.1 | 130 ± 10 | | | |
| Oconee River sorption | 0.6 | 7.9 | 6.3 ± 0.2 | 140 ± 20 | 51 ± 5 | 17 ± 3<br>($a_o$ = 34 ± 3) | -- |
| | | 17 | 5.3 ± 0.1 | 120 ± 3 | | | |
| | | 4.7 | 3.2 ± 0.0 | 89 ± 9 | | | |
| | | 13 | 2.7 ± 0.0 | 73 ± 3 | | | |
| Searsville Pond sorption | 3.8 | 7.7 | 5.5 ± 0.4 | 310 ± 50 | 60 ± 4 | 38 ± 8<br>($a_o$ = 100 ± 30) | 65 ± 4 |
| | | 16 | 3.7 ± 0.1 | 270 ± 10 | | | |
| | | 4.2 | 3.1 ± 0.1 | 190 ± 30 | | | |
| | | 13 | 1.9 ± 0.2 | 160 ± 10 | | | |
| Montmorillonite[d] | -- | -- | -- | -- | 100 | | |
| Soil[d] | -- | -- | -- | -- | 12 | | |

[a] Concentration measured in supernatant with population standard deviation.

[b] Concentration on sediment calculated from supernatant concentration with population standard deviation.

[c] LLS = linear least squares; NLLS = non linear least squares. See Appendix B, Section B.1.4 for description of regressions. Limits are 95% confidence limit.

[d] Data for parathion (Saltzman and Yaron, 1972).

$$-\frac{d[MP]}{dt} = k_a[MP](Sed) \qquad (13.1)$$

where:

$[MP]$ = MP concentration ($\mu g\ ml^{-1}$)
$(Sed)$ = sediment concentration ($mg\ liter^{-1}$)

The result of the analysis was $k_a = 2.0\ (\pm\ 0.2) \times 10^{-6}\ ml\ \mu g^{-1}\ MP\ hr^{-1}$. This yields a pseudo-first-order decay constant for MP of $0.012\ hr^{-1}$ when the sediment concentration is $5900\ mg\ liter^{-1}$ and $0.022\ hr^{-1}$ when the sediment concentration is $11{,}900\ mg\ liter^{-1}$. The half-lives are 58 hours and 29 hours, respectively.

The slow disappearance of MP could be caused by biological activity, sediment-catalyzed hydrolysis, or continued sorption by a mechanism different from the one that obtains in the first hour. Biodegradation is unlikely since MP solutions inoculated with Coyote Creek water show a lag of 5 days for adaptation before any degradation occurs (Section 13.6).

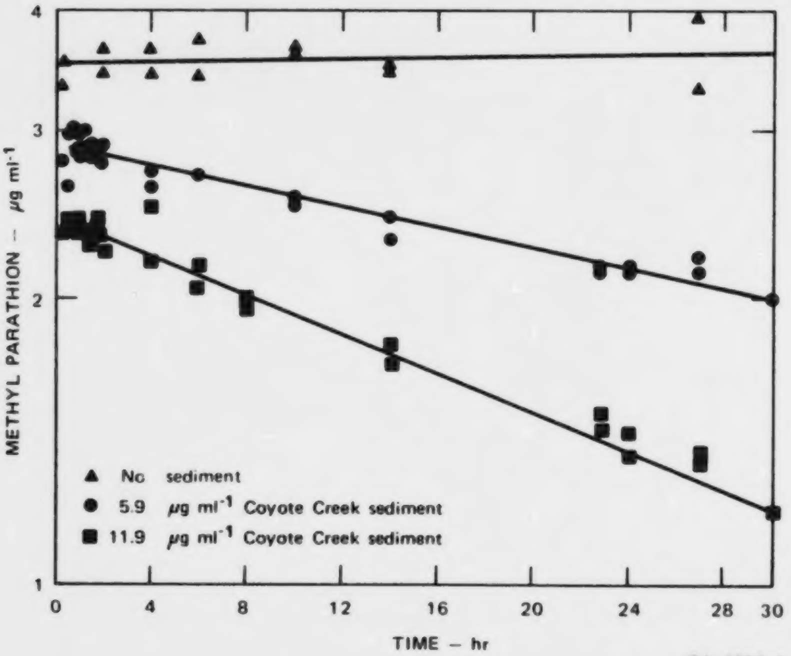

SA-4396-5

FIGURE 13.5 CONCENTRATION OF METHYL PARATHION IN SUPERNATANT

The following observations indicate that clay-catalyzed hydrolysis is also unlikely.* Although no analyses for hydrolysis products were performed during our kinetic experiment, evidence for hydrolysis in other experiments permits an estimate of sediment-catalyzed hydrolysis rates. In the experiment to measure a desorption isotherm (described below), MP (26 μg $ml^{-1}$) was in contact for 70 hours with Coyote Creek sediment at 12,100 mg $liter^{-1}$. An analysis of the supernatant showed, at most, 10% hydrolysis of MP to a single product, O-methyl-O-_p_-nitrophenylthiophosphoric acid ester.† _p_-Nitrophenol was not observed in the supernatant. If we assume that the hydrolysis rate is first order in both sediment and MP, this is equivalent to a half-life of 980 hours if the sediment concentration were 5900 mg $liter^{-1}$ or 490 hours for a concentration of 11,900 mg $liter^{-1}$. These half-lives are much longer than the half-lives for MP disappearance observed during the adsorption kinetic experiment (58 and 29 hours). The half-life for the solution-phase neutral hydrolysis was shown to be about 2100 hours (Section 13.5). There does appear to be about a fourfold increase in the neutral hydrolysis rate of MP in the presence of Coyote Creek sediment under the conditions of the experiment. However, neither neutral nor clay-catalyzed hydrolysis seems to be fast enough to account for all the observed slow decrease in MP. The data suggest that about 95% of the decrease in MP is due to continued sorption. The rapid initial sorption could be due to organic material and readily accessible clay surfaces. The slow sorption may involve diffusion into the interlaminar portion of the clay fraction of the sediment.

_Desorption_--Desorption of MP was measured by first contacting Coyote sediment at 12,100 mg $liter^{-1}$ with MP at 26 μg $ml^{-1}$ at pH 6. A 70-hour contact time was chosen in an attempt to ensure full sorption equilibrium. The partition coefficient that resulted from this contact was 60, based on the assumption that all MP that had disappeared from the supernatant was adsorbed into the sediment. Analysis of the supernatant indicated that approximately 10% hydrolysis to O-methyl-O-_p_-nitrophenylthiophosphoric acid ester occurred during the contact period. If the hydrolysis is included but we assume that the monoester is not strongly sorbed, then the MP partition coefficient is 47. Either of these estimates is consistent with previous determinations for MP sorption onto Coyote Creek sediment.

The sediment containing its sorbed MP was washed and then resuspended in water and shaken for eight hours. No significant hydrolysis would occur in this brief contact period. Figure 13.6 shows the supernatant concentrations determined during the contact period. Desorption equilibrium was obtained in 4 hours of contact. The data do not show any changes in supernatant concentration after four hours, indicating that desorption is complete.

---

*Satlzman, Mingelgrin, and Yaron (1976) demonstrated that oven-dried kaolinite accelerates the hydrolysis of both parathion and methyl parathion. Although the presence of small amounts of sorbed water increased the hydrolysis rates, larger amounts of water reduced the effect. No experiments on clay suspended in water containing dissolved MP were reported.

†This product should not be strongly sorbed because it is an acid and should be very soluble in water.

Figure 13.6 also shows the supernatant concentrations that would be expected if desorption had the same partition coefficient as sorption ($K_p$ = 51 ± 5) and if all the sorbed MP could be desorbed (corrections have been made for material lost during the washing operation). Sorption-desorption of MP on this sediment is not reversible. If we assume that the partition coefficient for sorption and desorption is the same, and about 50, these results suggest that approximately 50% of the sorbed MP was irreversibly sorbed and unavailable for desorption.

### 13.4.5 Biosorption

The results of three experiments with viable heat-killed (100°C for 15 minutes) bacterial cell mixtures are given in Table 13.7. The bacterial mixtures contained equal optical densities (2) of *Azotobacter beijerinckii* ATCC 19366, *Bacillus cereus* ATCC 11778, *Escherichia coli* ATCC 9637, and *Serratia marcesens* ATCC 13880. The recoveries of MP in sorptions with viable cell mixtures incubated at 25°C averaged 76%. Since no yellow coloration due to *p*-nitrophenol was observed, the degradation by this cell mixture was not restricted to a hydrolysis to *p*-nitrophenol. With viable cells incubated at 2°C and with heat-killed cells incubated at 25°C, recoveries of 100% were

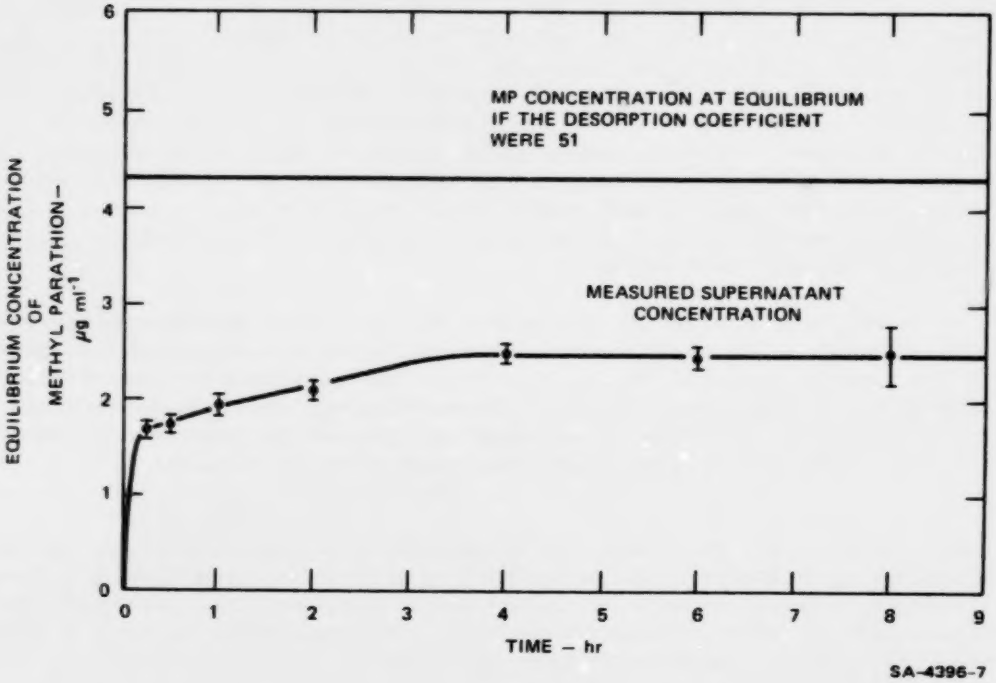

FIGURE 13.6 DESORPTION OF METHYL PARATHION FROM COYOTE CREEK SEDIMENT.
Loss of MP due to hydrolysis is included in the calculations.

obtained. With viable and heat-killed cells incubated at 25°C, the sorption coefficients were comparable, indicating that sorption by these organisms was not enzymatically mediated.

TABLE 13.7. SORPTION PARTITION COEFFICIENTS[a] OF METHYL PARATHION ON A MIXED BATERIAL POPULATION

| Initial MP in mixture ($ng\ ml^{-1}$) | Viable cells at 25°C | Heat-killed cells at 25°C | Viable cells at 2°C |
|---|---|---|---|
| 100 | 502 ± 30 | 359 ± 90 | 200 ± 86 |
| 300 | 468 ± 20 | 384 ± 47 | 242 ± 95 |

[a] The values of $K_p$ are the averages plus or minus standard deviation for three experiments and are based on the dry weight of cells, which were 916, 1037, and 1027 $\mu g\ ml^{-1}$ in the three experiments.

These sorption coefficients are considerably higher than those obtained in the sediment studies. This suggests that, after the algae "bloom" of eutrophic lakes, the sediments may sorb more MP because of the increased microbial counts and detritus in the sediment. Both the MP levels and the bacterial-cell concentrations used in these studies were much higher than would be expected in the natural state, and the levels of MP in microbial cells would be much lower.

## 13.5 CHEMICAL TRANSFORMATION

Methyl parathion was transformed by both hydrolysis and photolysis to give the same two products: p-nitrophenol (pNP) and O-methyl-O-p-nitrophenolthiophosphoric acid (MNTP). Although not identified in our HPLC analytical procedure, dimethylthiophosphoric acid and methanol are expected to be the complementary products to pNP and MNTP, respectively. In the hydrolysis studies, MNTP was the major product from reactions at less than pH 8, with increased yields of pNP at higher pHs. The products from photolysis MP were the same as those from hydrolysis in the same waters, but the yields of pNP were higher. Details of product yields and the chemistry are presented in Section 13.5.4.

### 13.5.1 Photolysis Rate

Data for the photolysis of MP in buffered and natural waters containing 1% acetonitrile are given in Table 13.8. Although the data are insufficient to make a firm conclusion, it appears that the photolysis rate is slightly accelerated by the presence of phosphate and borate salts in moderate concentrations, especially at pH 8. Similar buffer catalysis effects were also found in the hydrolysis studies (Section 13.5.3). The apparent acceleration of photolysis rate in buffer solutions is probably not important for an environmental assessment, however, since ionic strengths in most natural freshwater systems are quite low. The data in Table 13.8 indicate that 1.7 x $10^{-4}$ is a best value for the quantum yield for photolysis of MP in aqueous solution.

The photolysis rate constants of MP in natural waters are only slightly smaller than those in the lightly buffered distilled waters, the maximum decrease being 40% for the Aucilla River water. As discussed in Part I, Section 6.2 of this report, the presence of natural materials in waters may retard photolysis rates by light screening or by quenching processes. The natural materials may also promote phototransformations by photosensitization or photoinitiated free radical processes.

On the basis of the limited number of experiments and the data in Table 13.8, it is impossible to give definitive reasons for the rate constant decreases found. Thus, the rate constants for Searsville Pond and Lake Tahoe

TABLE 13.8. RATE CONSTANTS FOR PHOTOLYSIS OF 26 µg $ml^{-1}$ METHYL PARATHION[a]

| Irradiation source | Solution[b] (buffer or source) | Extent of reaction (%) | $k_p$ x $10^7$ $sec^{-1}$ |
|---|---|---|---|
| 313 nm | pH 8.0, 0.01 M borate | 82 | 73.8 ± 3.1[c] |
| 313 nm | pH 5.0, 0.01 M acetate | 64 | 32.3 ± 2.0[d] |
| 313 nm | pH 8-7, 0.001 M phosphates[e] | 37 | 46.7 ± 2.9[f] |
| 313 nm | pH 5.0-5.4, 0.001 M phosphates[e] | 20 | 45.1 ± 5.0[f] |
| 313 nm | pH 5.25, 9.5 µg $ml^{-1}$ humic acid in pure water | 59 | 36.2 ± 1.1 |
| 313 nm | pH 7.6, Lake Tahoe water | 67 | 33.3 ± 1.4 |
| 313 nm | pH 7.8, Coyote Creek water | 69 | 46.8 ± 1.7 |
| 313 nm | pH 7.5, Searsville Pond water | 57 | 32.1 ± 1.0 |
| 313 nm | pH 6.07 Aucilla River water | 60 | 28.0 ± 0.7 |
| 366 nm | pH 8.0, 0.067 M phosphates | 91 | 128.0 ± 1.6 |
| 366 nm | pH 5.0, 0.067 M phosphates | 54 | 50.2 ± 4.7[g] |
| Sunlight, early January | pH 5.0, 0.067 M phosphates | 57 | 7.89 ± 0.54[h] |

[a] 1.0 µg $ml^{-1}$ methyl parathion in water = 3.80 x $10^{-6}$ M.

[b] Solutions contain added 1% acetonitrile; composition of buffer solutions are described in Appendix B.

[c] Standard deviation.

[d] Quantum yield for MP disappearance at 313 nm is 1.2 x $10^{-4}$.

[e] pH shifted due to insufficient buffer concentration.

[f] Quantum yield for MP disappearance at 313 nm is 1.7 x $10^{-4}$.

[g] Quantum yield for MP disappearance at 366 nm is 2.5 x $10^{-4}$.

[h] Calculated assuming 8 hours of sunlight per day in early January; to obtain average rate constant for full calendar day (24 hours), divide rate constant by three. Rate constant corresponds to half-life of 30 calendar days.

waters (absorbances at 313 are 0.07 and 0, respectively) are about 75% of those calculated after taking into account a light screening effect. On the other hand, the photolysis rate constants for the distilled water-humic acid, Coyote Creek and Aucilla River experiments (absorbances of 0.56, 0.06, and 0.65 at 313 nm, respectively) are 45%, 10%, and 18% greater than those rate constants obtained after correcting for light screening.

While more experiments are required to confirm these results, these data along with the variations in product yields found in the experiments (see Section 13.5.4) indicate that the chemistry occurring may be quite complex. Further investigations of the photochemistry of these systems should be revealing and valuable for a better understanding of the effects of natural materials in aquatic photochemistry.

The half-life for the direct photolysis of MP as a function of the time of year was calculated by the procedure of Zepp and Cline (1977), using the quantum yield of $1.7 \times 10^{-4}$ and the measured UV spectrum of MP (Section 13.4.2). Allowing for a slight buffer effect on the rate constant (and therefore the quantum yield) at 366 nm in Table 13.8, the quantum yield is assumed to be independent of wavelength. The variation in half-life over the year, summarized in Figure 13.7, shows that the half-life will vary from 8 days in summer to about 38 days in winter. The latter is in excellent agreement with a 30-day half-life measured in an experiment conducted in early January sunlight.

### 13.5.2 Oxidation Rate

The susceptibility of 26.0 μg $ml^{-1}$ ($1.0 \times 10^{-4}$ M) methyl parathion to free radical oxidation was examined using the AA-initiated oxidation reaction (see Part I, Section 6.3 and Appendix B for discussion and procedure). The data for the experiments carried out for 100 hours at 50.0°C in 1% acetonitrile in water at pH 5 and pH 8 are given in Table 13.9.

TABLE 13.9. FREE RADICAL OXIDATION OF METHYL PARATHION AT 50°C

| Solution | Initial conc.[a] ($\times 10^5$ M) | MP consumed with added AA[b] ($\times 10^5$ M) | MP consumed without AA ($\times 10^5$ M) |
|---|---|---|---|
| Buffered pH 5 | 10.0 | 4.9 | 4.7 |
| Buffered pH 8 | 10.0 | 5.8 | 6.0 |

[a] 26.0 μg $ml^{-1}$ MP = $1.00 \times 10^{-4}$ M.

[b] $1.00 \times 10^{-4}$ M 4,4'-azobis(4-cyanovaleric acid) in 1% acetonitrile in buffered water (0.01 M acetate or borate). Reaction time was 100 hours.

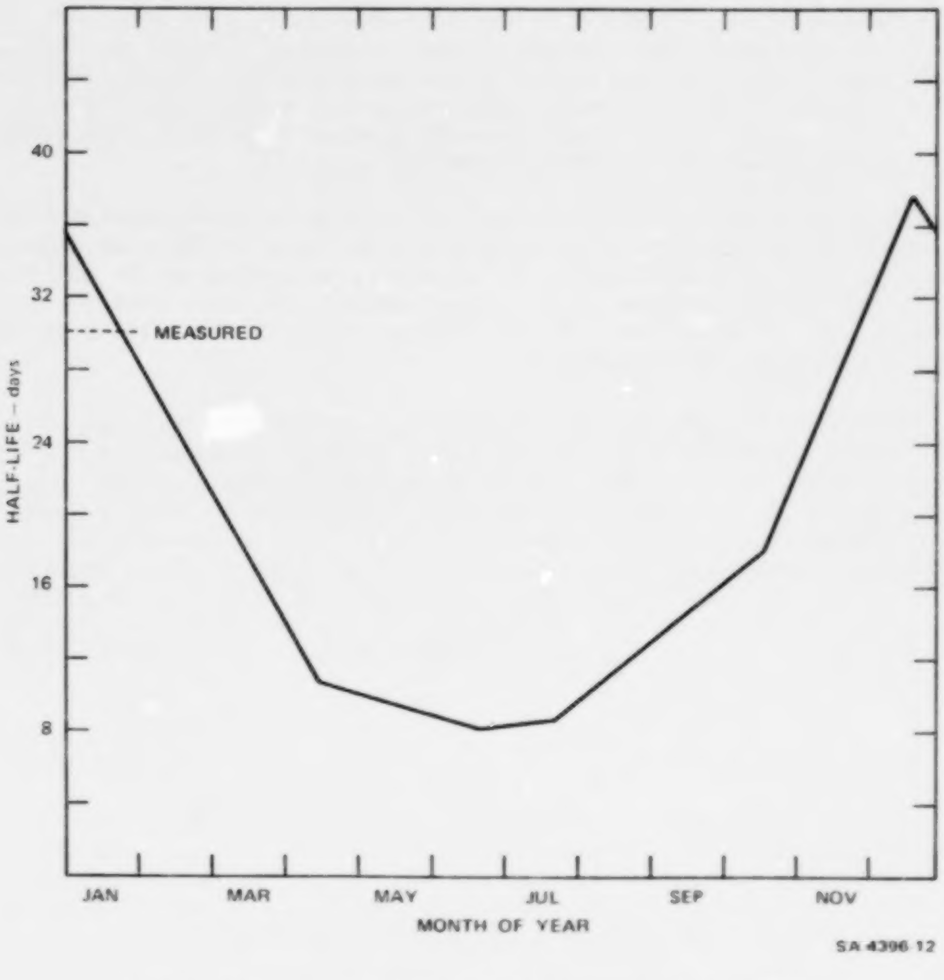

FIGURE 13.7 ANNUAL VARIATION OF PHOTOLYSIS HALF-LIFE OF METHYL PARATHION

These experiments demonstrated that the free radical oxidation of MP is not competitive with hydrolysis at 50°C. The loss of MP shown in Table 13.9 can be completely accounted for by hydrolysis processes (see Section 13.5.3). As in the photolysis experiments, no methyl paraoxon was detected. If we assume that less than 3% of MP consumed was oxidized in 100 hours (based on the precision of the measurements), then the second-order rate constant $k_{ox}$ is $<3$ $M^{-1}$ $sec^{-1}$ at 25°C (see Part I, Section 6.3).

The absence of oxidation products is fully consistent with the relative unreactivity of esters and pentavalent phosphorus toward oxyradicals. Lack of formation of methyl paraoxon in this experiment suggests that some other circumstances are necessary to convert a phosphorus-sulfur bond to a phosphorus-oxygen bond and that reports of its formation need to be examined carefully to clarify the special oxidizing conditions apparently necessary for this reaction. In this regard, it is interesting that oxidation of thiophosphoric acid esters to phosphoric acid esters by ozone has been reported (Gunther et al., 1970). Such a reaction could account for the field observations of the formation of paraoxon, which may then leach to ground and surface waters.

### 13.5.3 Hydrolysis Rate

Rate constants for the hydrolysis of MP at 40.0°C as a function of pH are given in Table 13.10. These data show that the hydrolysis rate is independent of pH to about pH 8 where the hydroxyl anion catalyzed reaction (also referred to as specific base catalysis; Frost and Pearson, 1961) becomes important. Buffer solutions at 0.067 M in total phosphate were used in initial studies but were replaced when catalysis by hydrogen phosphate dianion became evident. Acetate and borate buffers were then used successfully with no catalysis problems (see Table 13.10 for data and Appendix B for buffer compositions).

The rate constants for the hydrolysis of MP in several natural waters are listed in Table 13.11. The data from experiments in distilled water containing 9.5 $\mu$g ml$^{-1}$ humic acid and the four natural waters are in good agreement (in all of these exepriments the pH was less than 8). The data in Tables 13.10 and 13.11 show no catalysis in these natural waters when compared with experiments in buffered solutions. The satisfactory agreement among the first-order rate constants at the different methyl parathion concentrations (Table 13.11) verified that the hydrolysis reaction is first order in methyl parathion. The pH rate profile for methyl parathion at 40°C in the buffered and natural waters is given in Figure 13.8.

The detailed kinetics of hydrolysis have been discussed in Part I, Section 6.4, of this report. Figure 13.8 shows that MP hydrolysis is not an acid-catalyzed process above pH2 and that the OH$^-$ catalyzed reaction is important only above pH 8. The first-order rate constant $k_H$ is then given by

$$k_H = k_N + k_B[OH^-] \qquad (13.2)$$

To determine a value of $k_H$ at any pH and temperature, we determined the temperature dependence of $k_N$ and $k_B$ independently. Rates of hydrolysis were measured at pH 5 and 10, where the respective neutral and base-promoted processes are dominant (see Figure 13.8). These data are given in Table 13.12. The measured rate constant $k_H$ at pH 10 still required a slight adjustment for a contribution from $k_N$ before $k_B$ could be calculated. Table 13.12 also gives the Arrhenius expression (temperature dependence) for $k_N$ and $k_B$ calculated from this data.

TABLE 13.10. FIRST-ORDER RATE CONSTANTS $k_H$ FOR HYDROLYSIS OF METHYL PARATHION[a] AS A FUNCTION OF pH

| pH | $k_H \times 10^7$ ($sec^{-1}$) |
|---|---|
| 3.00 | 6.80 (± 0.26)[b] |
| 5.00 | 6.45 (± 0.33)[c] |
| 6.00 | 8.08 (± 0.52)[d] |
| 7.00 | 7.44 (± 0.24)[e] |
| 8.00 | 9.27 (± 0.17)[f] |
| 9.00 | 16.37 (± 1.39) |
| 10.00 | 67.70 (± 1.1) |
| 11.25 | 747 (± 166) |

[a] Experiments used 26 μg $ml^{-1}$ ($1.0 \times 10^{-4}$ M) methyl parathion at 40°C. Solvent was 1% acetonitrile in buffered distilled water. See Appendix B for composition of buffer solutions; pH buffer solutions designated (b) in footnotes c, e, and f were used in experiments where 0.076 M total phosphate buffers, designated (a), were found to show buffer catalysis.

[b] Standard deviation.

[c] Solution pH 5(b) used; rate constant in solution pH 5(a) was $8.47 \times 10^{-7}$ $sec^{-1}$.

[d] High value probably due to buffer catalysis (see footnotes c, e, f).

[e] Solution pH 7(b) used; rate constant in solution pH 7(a) was $14.3 \times 10^{-7}$ $sec^{-1}$.

[f] Solution pH 8(b) used; rate constant in solution pH 8(a) was $16.6 \times 10^{-7}$ $sec^{-1}$.

The rate parameters for the neutral hydrolysis ($k_N$) are $E_a = 23.4 \pm 0.9$ kcal mole$^{-1}$ log(A/sec$^{-1}$) = 10.10 ± 0.64; for the specific base catalyzed process ($k_B$), $E_a = 22.0 \pm 0.2$ kcal mole$^{-1}$ with log(A/M$^{-1}$ sec$^{-1}$) = 14.13 ± 0.17. From the Arrhenius expression for $k_N$ (Table 13.12), $k_N$ at 25°C is $9 \times 10^{-8}$ sec$^{-1}$, corresponding to a half-life of 89 days for MP in aqueous solutions below pH 8. The calculated half-life at 15°C is about 1 year in the same pH region. At pH 9, which is found in some lakes and ponds, half-lives of 45 and 180 days are calculated from the data in Table 13.12 at 25° and 15°C, respectively.

### 13.5.4 Products From Chemical Transformation

Hydrolysis and photolysis of methyl parathion produce two sets of common products, which are detected in our LC analysis scheme by the *p*-nitrophenyl moiety. These products are O-methyl-O'-*p*-nitrophenylthiophosphoric acid (MNTP) and *p*-nitrophenol (*p*NP). The *p*NP product, which has been reported in previous studies, was identified by its HPLC retention time compared with an authentic sample. An early eluting product was found in experiments under acid reaction conditions. To identify this product, we conducted a large-

TABLE 13.11. FIRST-ORDER RATE CONSTANTS $k_H$ FOR HYDROLYSIS OF METHYL PARATHION IN NATURAL WATERS[a]

| Natural water source | pH | $k_H \times 10^7$ (sec$^{-1}$) |
|---|---|---|
| Lake Tahoe | 7.6 | 12.41 (± 1.44)[b,c] |
| Lake Tahoe | 7.6 | 6.31 (± 0.36) |
| Coyote Creek | 7.8 | 7.54 (± 0.21) |
| Distilled water with 9.5 ppm humic acid[d] | 5.25 | 5.99 (± 0.53)[d] |
| Aucilla River | 6.07 | 6.10 (± 0.81) |
| Searsville Pond | 7.5 | 6.83 (± 0.08) |

[a] Except where noted, experiments used 26 μg ml$^{-1}$ ($1.0 \times 10^{-4}$ M) methyl parathion at 40°C. Solvent was 1% acetonitrile in filtered natural water.

[b] Standard deviation.

[c] 0.26 μg ml$^{-1}$ methyl parathion was used.

[d] 2.60 μg ml$^{-1}$ methyl parathion was used.

scale hydrolysis at pH 5.5 and 50.0°C and analyzed the mixture at 5 half-lives of methyl parathion. The reaction mixture contained 95% of the early eluting product with very small amounts of p-nitrophenol and methyl parathion. The reaction mixture was lyophilized to concentrate the reaction products. The mass spectrum of the product corresponded to that of the monodemethylated methyl parathion (parent m/e = 249). The NMR spectrum of this product in $D_2O$ confirmed the assigned structure as O-methyl-O-p-nitrophenylthiophosphoric acid, 3.65 δ (d, 3 protons), 7.6 δ (q, 4 protons). Although they were not identified in our HPLC analyses, dimethylthiophosphoric acid and methanol are expected to be the complementary products to pNP and MNTP, respectively.

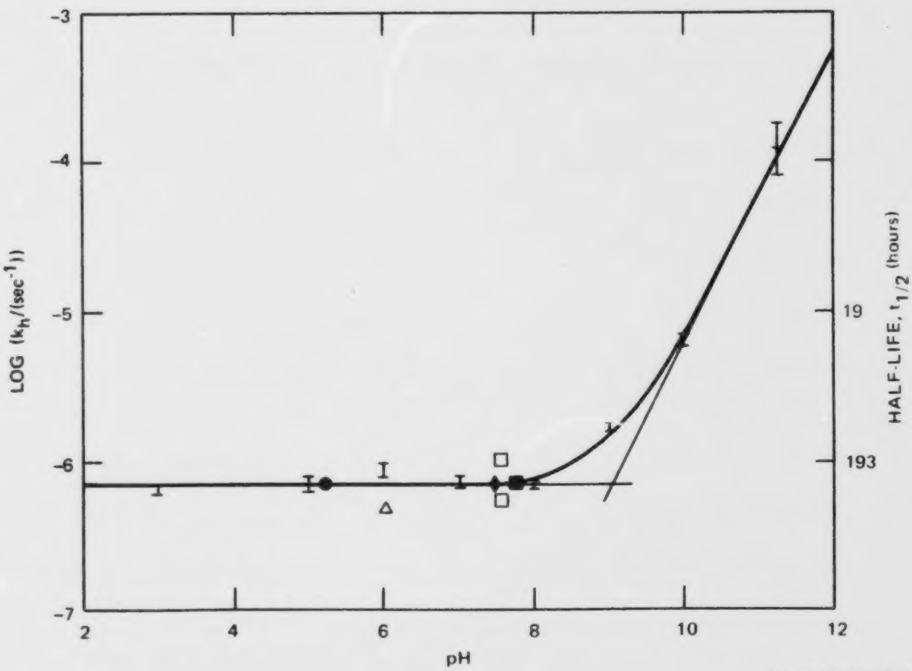

TA-327522-28R1

FIGURE 13.8 pH PROFILE FOR METHYL PARATHION AT 40°C. Points with bars: buffered distilled water (Table 13.11); other points (Table 13.10), ● distilled $H_2O$ with humic acid, △ Aucilla River, □ Lake Tahoe, ♦ Searsville Pond, ■ Coyote Creek.

TABLE 13.12. TEMPERATURE DEPENDENCE OF RATE CONSTANTS FOR NEUTRAL ($k_N$) AND BASE CATALYZED ($k_B$) HYDROLYSIS OF METHYL PARATHION

| Reaction | Temp. (°C) | Rate constants |  | Arrhenius expression |
|---|---|---|---|---|
|  |  | $k_H \times 10^7$ ($sec^{-1}$) | $k_N \times 10^7$ ($sec^{-1}$) |  |
| Neutral (measured at pH 5.00) | 40.0 | 6.45 (± 0.33) | 6.45 |  |
|  | 50.0 | 18.2 | 18.2 | $\log k_N = 10.10 - 23400/4.58T$ |
|  | 70.0 | 170.0 (± 2.8) | 170.0 |  |
|  |  |  | $k_B \times 10^3$ ($M^{-1}$ $sec^{-1}$) |  |
| Base-catalysed (measured at pH 10.00) | 20.0 | 5.83 (± 0.41) | 5.36[a] |  |
|  | 40.0 | 67.7 (± 1.1) | 61.6[a] | $\log k_B = 14.13 - 22000/4.58T$ |
|  | 51.0 | 220 (± 3.4) | 198[a] |  |

[a] Rate constant is corrected for the contribution of $k_N$ at the given temperature; the value of $k_N$ is calculated from the Arrhenius expression.

TABLE 13.13. PRODUCT BALANCE FOR HYDROLYSIS AND PHOTOLYSIS OF METHYL PARATHION

| Reaction solution | Hydrolysis yield[a] |  |  |  | Photolysis yield[a] (313 nm) |  |  |  |
|---|---|---|---|---|---|---|---|---|
|  | % Rxn | pNP[b] | MNTP[c,d] | Total[d] | % Rxn | pNP[b] | MNTP[c,d] | Total[d] |
| Buffer sol. pH 3.00 | 69 | 0 | 1.51 (2.26) | 1.51 (2.26) |  |  |  |  |
| Buffer sol. pH 5.00 | 42 | 0.01 | 0.40 (0.60) | 0.41 (0.61) | 46 | 0.15 | 0.07 (0.10) | 0.22 (0.25) |
| Buffer sol. pH 6.00 | 51 | 0.05 | 0.56 (0.84) | 0.61 (0.89) |  |  |  |  |
| Buffer sol. pH 7.00 | 88 | 0.10 | 0.69 (1.04) | 0.79 (1.14) |  |  |  |  |
| Buffer sol. pH 7.00 | 66 | 0.02 | 0.69 (1.04) | 0.71 (1.06) |  |  |  |  |
| Buffer sol. pH 8.00 | 75 | 0.36 | 0.61 (0.92) | 0.97 (1.29) | 64 | 0.83 | 0.19 (0.29) | 1.02 (1.12) |
| Buffer sol. pH 9.00 | 63 | 0.33 | 0.41 (0.62) | 0.74 (0.95) |  |  |  |  |
| Buffer sol. pH 10.00 | 68 | 0.50 | 0.04 (0.06) | 0.54 (0.56) |  |  |  |  |
| Buffer sol. pH 11.25 |  | 0.31 | - ( -- ) | 0.31 (0.31) |  |  |  |  |
| Lake Tahoe | 66 | 0.05 | 0.62 (0.93) | 0.67 (0.98) | 38 | 0.71 | 0.17 (0.26) | 0.88 (0.97) |
| Coyote Creek | 73 | 0.06 | 0.66 (0.99 | 0.72 (1.05) | 58 | 0.30 | 0.63 (0.95) | 0.96 (1.25) |
| Aucilla River | 24 | 0.05 | 0.58 (0.87) | 0.63 (0.92) | 58 | 0.11 | 0.44 (0.66) | 0.55 (0.77) |
| Searsville Pond | 27 | 0.03 | 0.35 (0.53) | 0.38 (0.56) | 54 | 0.41 | 0.19 (0.29) | 0.66 (0.70) |

Note: Product yield data are from HPLC analysis (UV detector) optimized for separation of methyl parathion during kinetic experiments. The *p*NP and MNTP elute earlier in the chromatogram and in some cases the baselines for *p*NP and MNTP are not well resolved; the MNTP data may also include other material that elutes at the same time. The MNTP and *p*NP may then be in error by ± 50% of the values listed.

[a] Based on methyl parathion consumed = 1.

[b] *p*NP = *p*-nitrophenol.

[c] MNTP = O-methyl-O-*p*-nitrophenylthiophosphoric acid.

[d] Since a pure reference sample of MNTP was not available, the yield of MNTP was calculated by assuming that the HPLC response factor ($R_f$) was the same as that of methyl parathion; the values in ( ) assume that the $R_f$ for MNTP is 1.5 times that of methyl parathion.

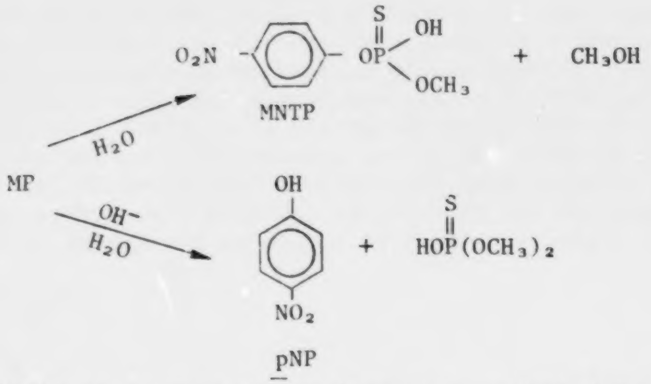

Although no specific studies were conducted to determine the conditions favoring the selective formation of either set of products, some information on this matter is available from analysis of the data obtained during kinetic measurements. Yields of pNP and MNTP calculated from these data are given in Table 13.13. These data are considered only semiquantitative inasmuch as the analytical separation was optimized for MP. While the precision of the pNP yield data is a few percent, the precision of the MNTP yield data may be ± 20% in some instances due to poor baseline resolution. However, MNTP is definitely a primary product because the MNTP peak is observed to increase as the reactions proceed. In the reaction in which MNTP was isolated, it was found to be the major product (>95%) in agreement with the low yields of pNP actually measured in the hydrolysis kinetic experiments below pH 8 (Table 13.13).

While pNP has been reported as a product from hydrolysis of MP, MNTP has not been reported. Recently the monoethyl ester analog to MNTP was reported to result from the hydrolysis and biodegradation of parathion (Weber, 1976). The data in Table 13.13 indicate that the MNTP is produced mainly by neutral hydrolysis and pNP is produced by base-catalyzed hydrolysis (> pH 8). These results are consistent with results for other phosphate esters in which hydroxide effects displacement on phosphorus with loss of the most acidic alcohol, whereas water displaces on carbon with loss of the phosphate group (Hilgetag and Teichman, 1965; Hudson, 1965; Vernon, 1957; Kirby and Warren, 1965).

From the data in Table 13.12 it is evident that photolysis of methyl parathion produces greater yields of pNP than hydrolysis in water from the same source. As in the hydrolysis experiments, a higher pH seems to favor formation of pNP. The yield data for MNTP and pNP in the natural water photolysis experiments also suggest that more subtle effects on the selectivity of product formation may be operative. From the data available it appears that the photolytic process involves a light-catalysed hydrolysis in which both water and hydroxide preferentially displace a p-nitrophenoxy group through an excited state in which displacement at phosphorus or at the Ar-O bond is possible. If MNTP is shown to be a significant environmental hazard, some studies directed toward the selective product formation may be warranted.

Since paraoxon is known to be more toxic than parathion, considerable effort was directed toward determining whether methyl paraoxon was a product from the chemical transformation of MP. The HPLC analytical procedure used would have detected methyl paraoxon formed in greater than 4% yield based on original MP present. No methyl paraoxon was found in the experimental work undertaken. Since paraoxon is more stable to hydrolysis than parathion at pHs less than 7, it is unlikely that this result was due to instability of paraoxon under the reaction conditions (Gomma and Faust, 1972). Although the data of Grunwell and Erickson (1973) are suspect for a number of reasons, their reported yield of paraoxon from photolysis of parathion is 3%, which is below the detectable limits of the experiments reported here. Thus, while methyl paraoxon may be a product, it must be formed in low yields (<4%).

## 13.6 BIODEGRADATION

### 13.6.1 Development of Biodegrading Cultures

Water samples used included all of those listed in Part I, Section 7.2. With all samplings of eutrophic water bodies and sewage effluents, enrichment systems that could rapidly decompose MP were developed in the 9-liter bottle fermentors. These were generally subtransferred several times to basal salts/MP/glucose/yeast extract, and they were finally able to grow on media in which the only added organic carbon was MP. Up to 300 $\mu g\ ml^{-1}$ MP could be completely metabolized per day, as determined by the disappearance of the UV absorbance of the p-nitrophenol moiety.

The development of enrichment systems generally followed the pattern of no change in MP concentrations for 3 to 10 days and then, within 24 to 36 hours, there was total disappearance of MP. In subtransfers, there were transient periods when the fermentation liquor would become yellow for 1 to 3 hours. (The yellow color was probably due to p-nitrophenol, which was identified as an intermediate product of MP, as described below.) In contrast to other water samples, the initial fermentation mixture of sewage effluent from the Monsanto Plant in Anniston, Alabama, with 100 $\mu g\ ml^{-1}$ MP became yellow within 20 to 30 seconds after addition of MP.

In three instances, when the first 9-liter bottle fermentations were set up with 5-liter volumes of water sample, buffer, and MP, 50-ml aliquots of these mixtures were removed and incubated at 25°C in 250-ml shaker flasks. Invariably, the initial breakdown of MP was markedly delayed in the shaker flasks and, in one instance with a Coyote Creek sample, no MP degradation was observed after three weeks of shaker flask incubation. Aeration was not a limiting problem because dissolved oxygen concentrations were essentially all at saturation levels in all fermentations. In an attempt to obtain a better understanding of this phenomenon, we diluted the contents in a 9-liter bottle fermentor 100-fold with centrifuged Coyote Creek water (to reduce bacterial counts) plus phosphates and $(NH_4)_2SO_4$ to represent the same total number of organisms that would be present in 50-ml aliquots for the 250-ml Erlenmeyer shaker flasks. In this instance, the diluted mixture, which contained 10 $\mu g\ ml^{-1}$ MP, developed a biodegradative system before the undiluted fermentations containing 1 or 10 $\mu g\ ml^{-1}$ MP. Considering that the 50 ml of mixture in each Erlenmeyer flask contained 40 ml of water sample, these observations suggest caution in classifying a chemical as nonbiodegradable when small scale studies are involved with perhaps 0.5% water or small soil additions as sources of natural microbial flora.

The 24-hour growth of the Coyote Creek enrichment cultures on basal salts/100 μg ml$^{-1}$ MP medium generally resulted in complete loss of MP (determined by the decrease of the UV absorption of MP) and an optical density (OD) of approximately 0.02. This OD is much lower than would be obtained with the same level of a good carbon nutrient. The culture mixture had a tendency to aggregate and viable counts were difficult to obtain, but were on the order of $10^7$ to $10^8$ cells ml$^{-1}$. Also, these cells were very small. The ability of these cultures to degrade MP was affected by transfers to fresh nutrient broth containing MP. In one case, a transfer in 0.1 diluted nutrient broth/ 50 μg ml$^{-1}$ MP resulted in a cell population that, when used as a 1% inoculum, produced a more rapid degradation of 100 μg ml$^{-1}$ MP in the inorganic salts medium. However, after three transfers in 0.1 nutrient broth/50 μg ml$^{-1}$ MP, the resultant culture complex did not degrade MP in 24 hours in the 100 μg ml$^{-1}$ MP basal salts medium.

With Lake Tahoe water (containing some sediment), no MP degradation was observed in a fermentor containing MP at 10 μg ml$^{-1}$ and incubated at 15°C for 6 weeks.

### 13.6.2 Biodegradation Kinetics

Biodegrading culture systems developed with Coyote Creek water were used in four types of kinetic studies: batch fermentations with low-count inocula of rested cells, continuous-feed fermentations in chemostats, cascade fermentations with freshly developed biodegrading systems sequentially transferred into buffered freshwater samples, and batch fermentations with high microbial populations.

The enrichment "culture" used in the kinetic experiments was streaked out on agar plates containing only basal salts plus MP. Many types of cultures were observed, and some were selected and streaked radially, from the outer edge of 50 μg ml$^{-1}$ MP/salts agar plates to the center of the plate. On incubation some colonies grew well, the entire length of the streak, some grew only close to the center, and some did not grow. These types of results would be expected if mixtures of biodegrading organisms contained cultures that could not metabolize MP directly but could grow on metabolic products released in total or in part by organisms capable of digesting MP or products closer to MP in the biodegradative pathways. It is also possible that the growth of some of the secondary organisms may be due to their ability to grow on products excreted by other organisms and is not directly related to the MP biodegradative pathway.

Another indication of the complexity of these mixed culture systems was that generally, after three washings with 0.05% phosphate pH 7 buffer to prepare resting cells, viable counts were stable over 18 to 27 hours at room temperature, but when an aliquot of one resting cell lot was gently shaken at 4°C during the 20- to 27-hour period, the viable count increased from $3 \times 10^9$ to $1.4 \times 10^{11}$ cells ml$^{-1}$. This nearly fiftyfold increase could be attributed to the autolysis or release of some metabolites that readily served as substrates for psychrophilic organisms in the culture mixture. Between 27 and 43 hours, the number of viable cells in the resting cell mixture maintained at room temperature also increased from $2.4 \times 10^9$ to $2.5 \times 10^{11}$

cells $ml^{-1}$. It is possible that the psychrophilic or other organisms eventually increased in numbers at room temperature, utilizing excreted or autolysis nutrients from other organisms, but this interpretation has no experimental support at this time.

Batch Fermentations with Low-Count Inocula of Rested Cells--Experimental results obtained with diluted inocula of rested cells in batch fermentations are presented in Tables 13.14 and 13.15 and in Figure 13.9. During the first 16 to 20 hours, there was no utilization of MP, but as is indicated in Figure 13.9, the increases in viable cell counts were essentially the same for flasks containing 0, 1, and 30 $\mu g\ ml^{-1}$ MP. The data for flasks containing 3, 10, and 20 $\mu g\ ml^{-1}$ MP were similar. These increases in bacterial counts are attributed to microbial interactions in mixed culture systems. It is also possible that carbon nutrients were introduced from the atmosphere or from the distilled water (Kayser et al., 1975). After this first phase of growth, MP degradation was initiated and there was a second growth phase that was most evident for flasks containing initial concentrations of 10, 20, and 30 $\mu g\ ml^{-1}$ MP.

TABLE 13.14. CELL COUNTS IN BATCH FERMENTATIONS WITH LOW COUNT INOCULA OF RESTED CELLS

| Time | Cell counts x $10^{-3}$ at different MP levels ($\mu g\ ml^{-1}$) | | | | | |
|---|---|---|---|---|---|---|
| (hr) | 0 | 1 | 3 | 10 | 20 | 30 |
| 0 | 9.0 | 9.0 | 9.0 | 9.0 | 9.0 | 9.0 |
| 4 | 9.8 | 6.0 | 6.3 | 6.5 | 6.4 | 5.9 |
| 8 | 15 | 13 | 14 | 14 | 12 | 14 |
| 12 | 74 | 53 | 73 | 63 | 63 | 210 |
| 16 | 1300 | 1700 | 1300 | 2000 | 1800 | 3800 |
| 20 | -- | 2100 | 2000 | 2400 | 2600 | 3900 |
| 24 | 2000 | 2000 | 2000 | 2900 | 2600 | 4300 |
| 28 | -- | 2900 | 2600 | 3000 | 3300 | 6800 |
| 32 | -- | 2900 | 2300 | 2900 | 3000 | 7400 |
| 36 | 1500 | 1500 | 1900 | 3100 | 3500 | 8000 |
| 40 | -- | 2400 | 2400 | 5700 | 8600 | 16000 |

TABLE 13.15. MP UTILIZATION IN BATCH FERMENTAITONS WITH LOW COUNT INOCULA OF RESTED CELLS

| | Methyl parathion concentration ($\mu g\ ml^{-1}$) | | | | | | | | | |
|---|---|---|---|---|---|---|---|---|---|---|
| Time | 1 | | 3 | | 10 | | 20 | | 30 | |
| (hr) | S | $\Delta S$[a] | S | $\Delta S$ | S | $\Delta S$ | S | $\Delta S$ | S | $\Delta S$ |
| 0 | 1.0 | 0.0 | 3.0 | 0.0 | 10.0 | 0.0 | 20.0 | 0.0 | 30.0 | 0.0 |
| 24 | -- | -- | -- | -- | 9.8 | 0.2 | 19.0 | 1.0 | 29.0 | 1.0 |
| 28 | -- | -- | -- | -- | 9.2 | 0.8 | 17.9 | 2.1 | 27.8 | 2.2 |
| 32 | -- | -- | -- | -- | 8.5 | 1.5 | 17.6 | 2.4 | 24.3 | 5.7 |
| 36 | 0.96 | 0.04 | 2.8 | 0.2 | 6.3 | 3.7 | 14.8 | 5.2 | 22.1 | 7.9 |
| 40 | 0.86 | 0.14 | 1.6 | 1.4 | 4.1 | 5.9 | 11.7 | 8.3 | 19.0 | 11.0 |
| 44 | 0.43 | 0.57 | 0.3 | 2.7 | 0.9 | 9.1 | 7.5 | 12.5 | 7.0 | 23.0 |

[a] $\Delta S$ = initial MP concentration ($S_o$) minus the MP concentration at time t (S).

From the MP biodegradations ($\Delta S$) given in Table 13.15, ln $\Delta S$ was plotted versus time, and linear relations were obtained (Figure 13.10). Table 13.16 presents values for MP utilizations ($\Delta S$) and viable cell counts (X) at 40 hours, as well as calculated values for the slopes at the curves ($\mu_m$) and $k_b$. The X and $\Delta S$ values at 40 hours were determined from plots of the data in Tables 13.14 and 13.15. Data for flasks initiated with 1 and 3 $\mu g\ ml^{-1}$ were not included because the $\mu_m$ and $k_b$ values were of questionable significance.

Although this procedure did not correct for the initial growth phase without MP utilization, this was not considered in the average $k_b$ value of $(1.7 \pm 0.3) \times 10^{-7}$ $\mu g$ MP $cell^{-1}\ hr^{-1}$. If X were determined at the time of initiation of MP utilization, $\Delta S/\Delta X = Y$ would be lower and the $k_b$ values would be somewhat higher. For example, in the 30 $\mu g\ ml^{-1}$ studies, $k_b$ would be approximately 30% higher.

Figure 13.11 presents MP degradation versus time in these batch shaker flask studies. The points at which $\Delta S$ was equal to 5 $\mu g\ ml^{-1}$ are indicated, and the slopes of the curves at these points along with corresponding S values were used to determine $K_s$ by equation (7.18), Part I. For degradations of 5 $\mu g\ ml^{-1}$ of MP in flasks originally containing 30, 20, and 10 $\mu g\ ml^{-1}$, the times were 32.4, 35.2 and 38.5 hours, respectively. The rates of decompositions or slopes corresponded to -0.72, -0.70, and -0.62 $hr^{-1}$,

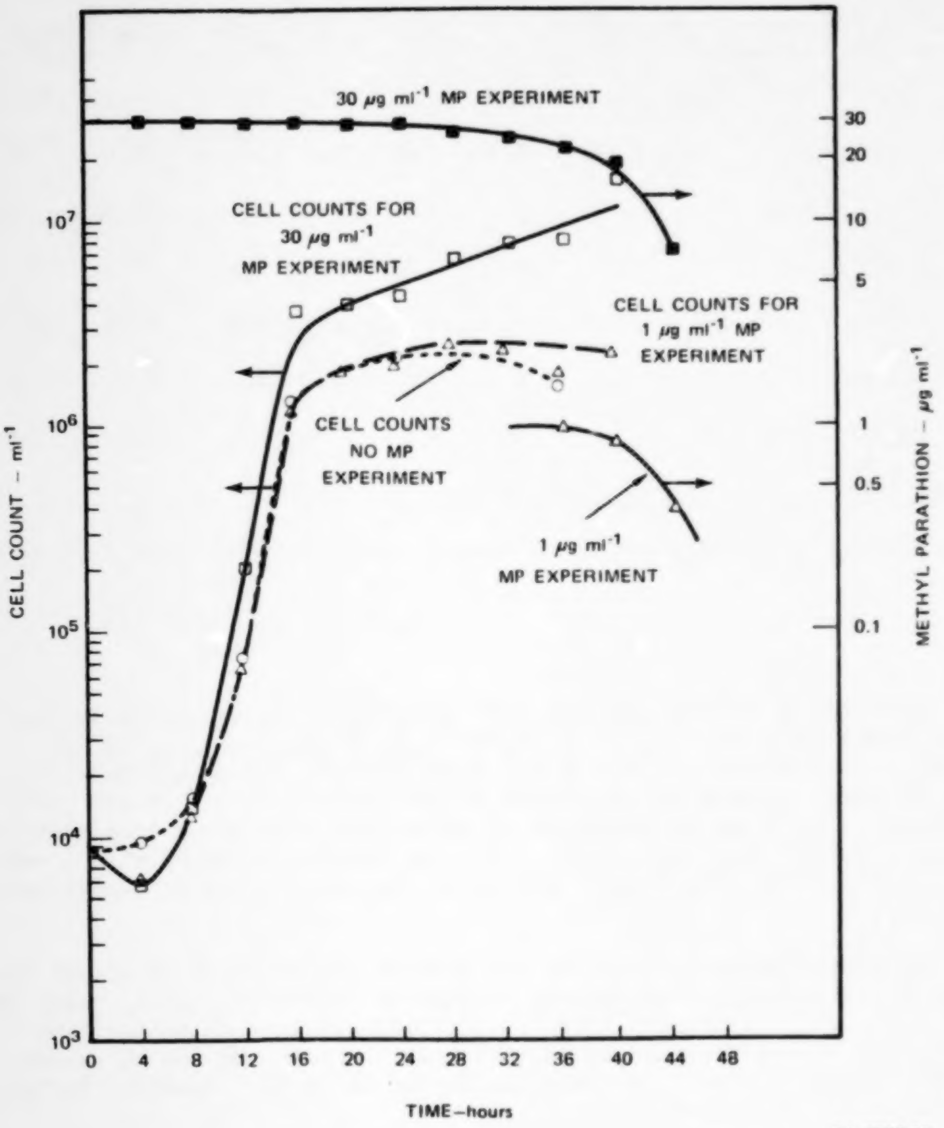

FIGURE 13.9 CELL COUNTS AND MP CONCENTRATIONS IN BATCH FERMENTATIONS WITH LOW COUNT INOCULA OF RESTED CELLS

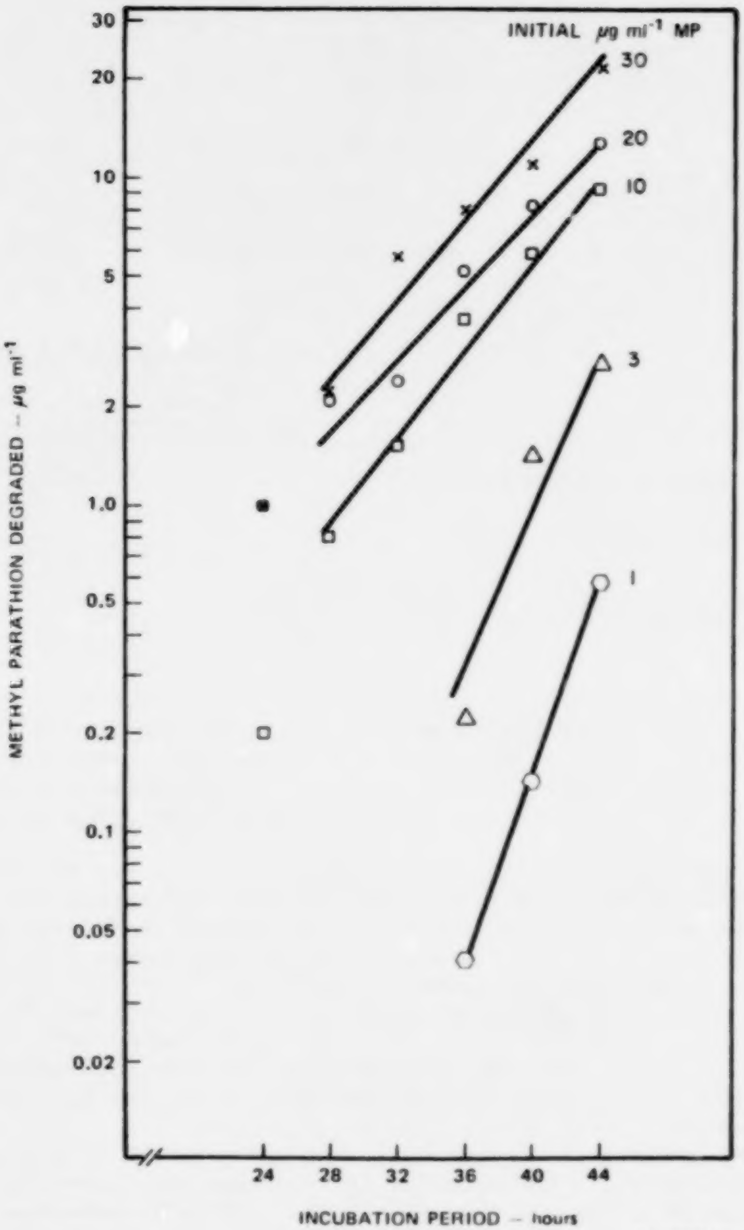

SA-4396-26

FIGURE 13.10 METHYL PARATHION UTILIZATION IN BATCH FERMENTATIONS WITH LOW COUNT INOCULA OF RESTED CELLS

TABLE 13.16. SUMMARY OF DATA AND KINETIC CONSTANTS IN BATCH FERMENTATIONS WITH LOW COUNT INOCULA OF RESTED CELLS

| Zero time MP concentration ($\mu$g ml$^{-1}$) | $\Delta$S at 40 hr[a] ($\mu$g ml$^{-1}$) | X at 40 hr[b] (cells ml$^{-1}$) | $\mu_m$ (hr$^{-1}$) | $k_b$ ($\mu$g cell$^{-1}$ hr$^{-1}$) |
|---|---|---|---|---|
| 30 | 12.5 | $1.3 \times 10^7$ | 0.144 | $1.4 \times 10^{-7}$ |
| 20 | 8.2 | $5.4 \times 10^6$ | 0.133 | $2.0 \times 10^{-7}$ |
| 10 | 5.8 | $5.0 \times 10^6$ | 0.139 | $1.6 \times 10^{-7}$ |
|  |  |  |  | Average $(1.7 \pm 0.3) \times 10^{-7}$ |

[a] From plots of data in Table 13.15.

[b] From plots of data in Table 13.14.

[c] Calculated by the equation, $k_b = \mu_m \frac{\Delta S}{X}$.

respectively. The $K_s$ values were 1.1, 1.1, and 1.0 (average 1.1) $\mu$g ml$^{-1}$, using the combined data from the 30 and 10, 30 and 20, and 20 and 10 $\mu$g ml$^{-1}$ fermentations, respectively. This calculated value of $K_s$ justifies the assumption that $K_s$ is significantly less than S for the above calculations of $k_b$ in the 10, 20, and 30 $\mu$g ml$^{-1}$ degradations reported in Table 13.16. The $k_{b2}$ was $1.3 \times 10^{-7}$ ml cell$^{-1}$ hr$^{-1}$.

Continuous-Feed Chemostat Fermentations--The data for MP biodegradation studies conducted in a chemostat under continuous fermentation conditions are presented and analyzed in Table 13.17. The average cell yield was $(5.9 \pm 5.1) \times 10^5$ cells $\mu$g$^{-1}$ MP. When S/$\mu$ was plotted versus S in Figure 13.12, $K_s$ and $\mu_m$ values were calculated as 2.6 $\mu$g ml$^{-1}$ and 0.61 hr$^{-1}$, respectively (Lineweaver-Burk procedure described in Part I, Section 7.3). The calculated value $k_b = \mu_m/Y = (2.0 \pm 1.7) \times 10^{-6}$ $\mu$g MP cell$^{-1}$ hr$^{-1}$. The variations in cell yields are understandable because even more complexities were involved than in the batch studies described above. The $k_{b2}$ value was $7.7 \times 10^{-7}$ ml cell$^{-1}$ hr$^{-1}$.

In these studies, chemostats were thoroughly shaken to dislodge organisms attached to solid surfaces and the contents were transferred daily to sterile chemostats. The problem of the effect of cells adhering to the reaction vessel walls and to the associated hardware on the kinetics has been well recognized in the past* and has led to the development or

---

* Zobell (1943), Larsen and Dimmick (1964), Atkinson and Fowler (1974), Pawlowsky and Howell (1973a,b), Pawlowsky et al. (1973), Gaudy et al. (1967), and Williamson and McCarty (1976a,b).

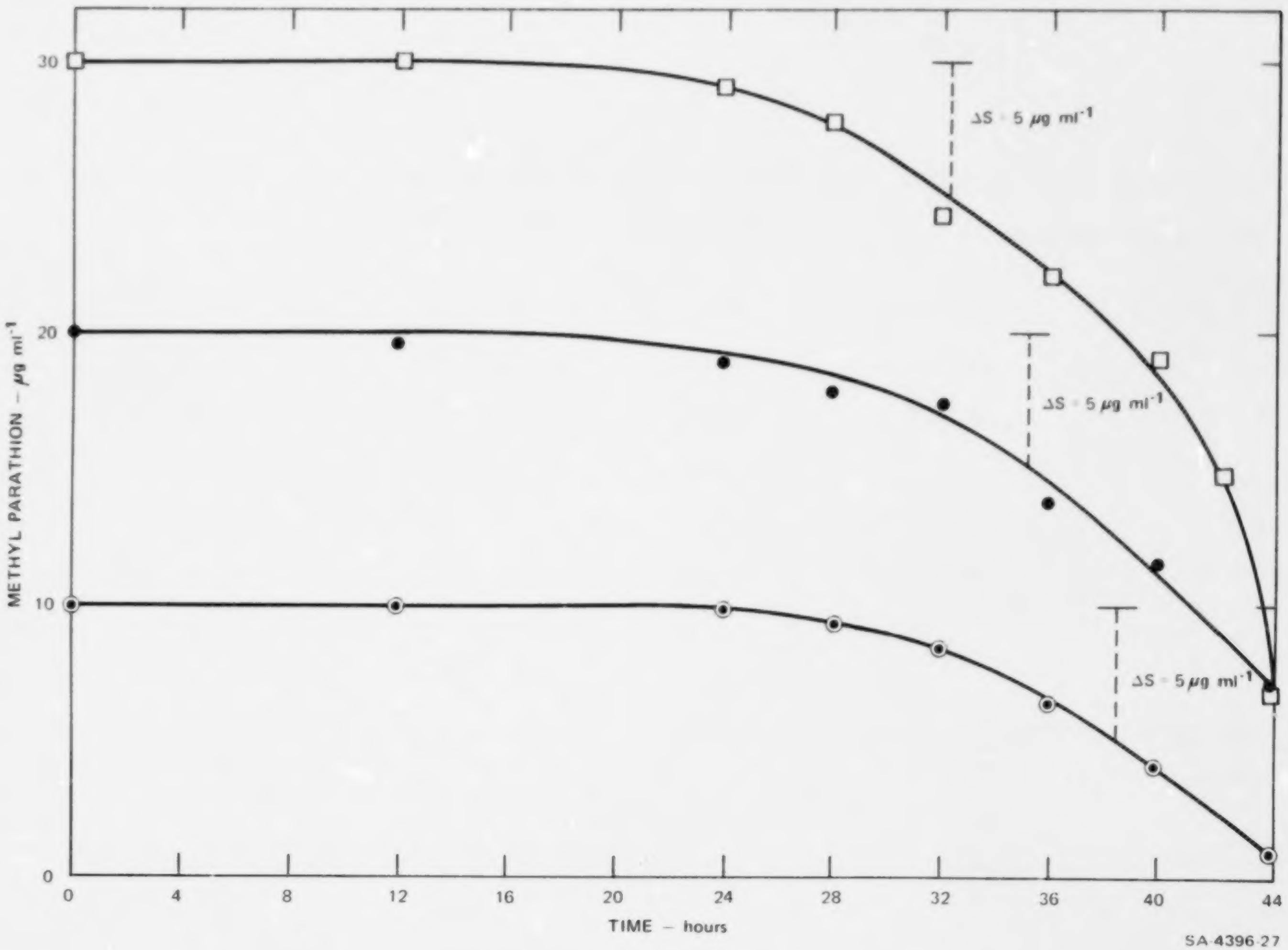

SA-4396-27

FIGURE 13.11 METHYL PARATHION DEGRADATION IN BATCH FERMENTATIONS WITH LOW INOCULUM OF RESTED CELLS. Initial MP concentrations at 10 (◉), 20 (●) and 20 (□) μg ml$^{-1}$

## TABLE 13.17. DATA FROM CONTINUOUS FEED CHEMOSTAT FERMENTATIONS

| Specific growth rate ($\mu$) (hr) | Outflow MP concentration (S) ($\mu$g ml$^{-1}$) | Microbial count (cells ml$^{-1}$) | $\frac{S}{\mu}$ (calculated) | Cell yield (Y) (cells $\mu$g$^{-1}$ MP) | $k_b$ ($\mu$g MP cell$^{-1}$ hr$^{-1}$) |
|---|---|---|---|---|---|
| 0.5 | 12.7 | | 25.4 | | -- |
| 0.45 | 5.97 | | 13.3 | | -- |
| 0.3 | 2.96 | $2.7 \times 10^7$ | 9.9 | $7.3 \times 10^5$ | $8.4 \times 10^{-7}$ |
| 0.38 | 4.58 | $4.7 \times 10^6$ | 12.05 | $1.3 \times 10^5$ | $4.7 \times 10^{-6}$ |
| 0.4 | 4.84 | | 12.1 | | -- |
| 0.4 | 6.63 | $1.45 \times 10^7$ | 12.05 | $4.3 \times 10^5$ | $1.4 \times 10^{-6}$ |
| 0.53 | 13.2 | $6.6 \times 10^6$ | 24.0 | $2.5 \times 10^5$ | $2.5 \times 10^{-6}$ |
| 0.2 | 0.98 | $5.6 \times 10^7$ | 4.9 | $14 \times 10^5$ | $4.4 \times 10^{-7}$ |
| | | | | Average | $(2.0 \pm 1.7) \times 10^{-6}$ |

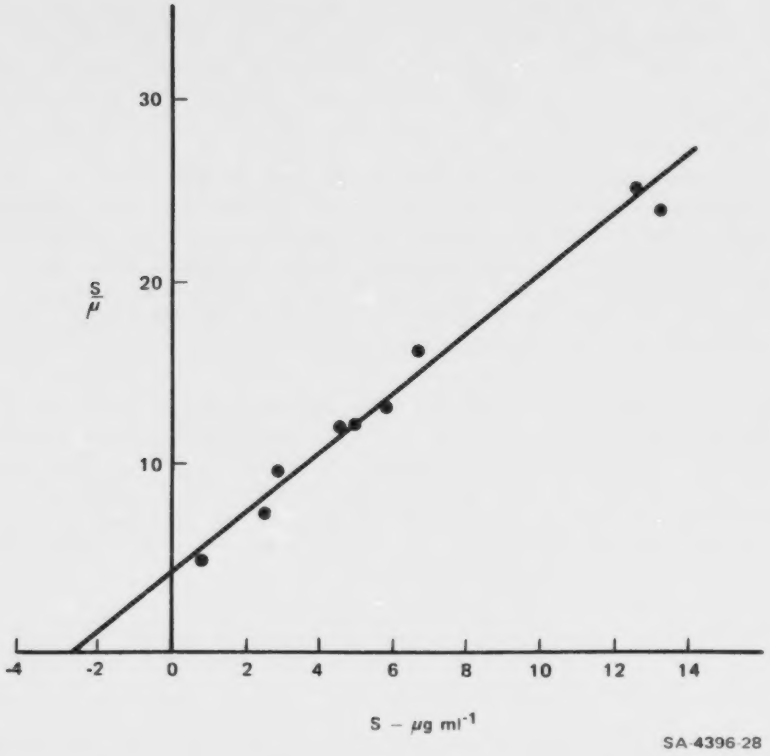

FIGURE 13.12 LINEWEAVER-BURK PLOT OF SPECIFIC GROWTH RATES AND SUBSTRATE CONCENTRATIONS FOR CONTINUOUS FEED CHEMOSTAT FERMENTATIONS OF METHYL PARATHION

adaptation of a "wall growth factor" parameter in kinetic evaluations.* This fermentation phenomena can play an important role in biodegradation. The degree to which MP is completely converted to cellular material can be affected by the feed rate. At higher feed rates some excreted metabolites may be washed out that can be utilized for growth by other organisms. Pawlowsky and Howell (1973a,b) in studies on mixed culture biooxidations of phenol observed that different organisms were favored at different dilution rates. Because the times involved in chemostat experiments were so much greater than division times of the organisms, more opportunities were available for changes in the character of microbial populations. It was difficult to replicate cell counts because of the continuous appearance of small colonies that became more obvious with increased incubation of plate count agar plates.

---

*Pawlowsky and Howell (1973a,b), Howell et al. (1972), Topiwala and Hamer (1971), and Chi et al. (1974).

Cascade Batch Fermentations with Fresh Coyote Creek Water Medium and a Freshly Developed Biodegradation System--Figure 13.13 includes the data for the initial adaptation of an MP biodegradation system and the subsequent sequential cascade transfer of this system into flasks containing fresh Coyote Creek water media. In this experiment the 1% (vol) inoculum was adequate for complete degradation of MP in 24 hours in the first two series of flasks, but it was inadequate in the third and fourth series. This could be attributed to interactions within the crude MP biodegrading system and to interactions among the bacteria present in the fresh Coyote Creek water media. These fresh waters would also contain protozoa that could prey on bacteria effective in MP degradation. The data in Figure 13.13 are typical. In other studies where larger inocula were used, no decrease in MP biodegradation at 24 hours was observed in the fourth series of flasks.

The rate constant $k_b$ was determined to be $(0.83 \pm 0.49) \times 10^{-7}$ μg MP $cell^{-1}$ $hr^{-1}$, using the procedure used for calculating the rate constant on batch fermentations with low count inocula of rested cells. The counts used in these calculations were undoubtedly high because the biodegrading system had not been subtransferred on media containing MP as the only carbon source and contained organisms not involved in MP degradation. For this reason, the $k_b$ value is undoubtedly low.

It must be recognized that in addition to the predator-prey relationships, the water from this eutrophic stream contains other compounds and diauxic growth may have occurred.

Batch Fermentation with Large Microbial Populations--The data obtained in this batch fermentation, starting with $1.8 \times 10^8$ cells $ml^{-1}$ ($X_o$) and 20 μg $ml^{-1}$ MP (S) are presented in Figure 13.14. Since the plot of ln S versus t is a straight line function with a decreasing slope, the decrease in MP concentration is first order in MP. In one hour, 97.5% of the MP was degraded.

The pseudo-first-order biodegradation rate constant calculated from the plot of ln S versus t was 3.69 $hr^{-1}$ (see Part I, Section 7.3). When this rate constant is divided by the cell numbers ($X_o = 1.8 \times 10^8$ cells $ml^{-1}$), a second-order biodegradation rate constant, $k_{b2}$, dependent on both S and X can be calculated. Under these conditions

$$k_{b2} = \frac{3.69}{1.8 \times 10^8} = 2 \times 10^{-8} \text{ ml cell}^{-1} \text{ hr}^{-1} \qquad (13.3)$$

In this experiment, it was assumed that $X_o \gg YS_o$. That these conditions have been met in this experiment is substantiated by calculating $YS_o = 1.2 \times 10^7$ cells $ml^{-1}$, using the yield factor $5.9 \times 10^5$ cells μg $MP^{-1}$ derived in continuous fermentations in a chemostat. This yield of cells is more than one order lower than the concentration of cells at the initiation of the experiment, and with conventional techniques it would not be possible to detect increased cell growth.

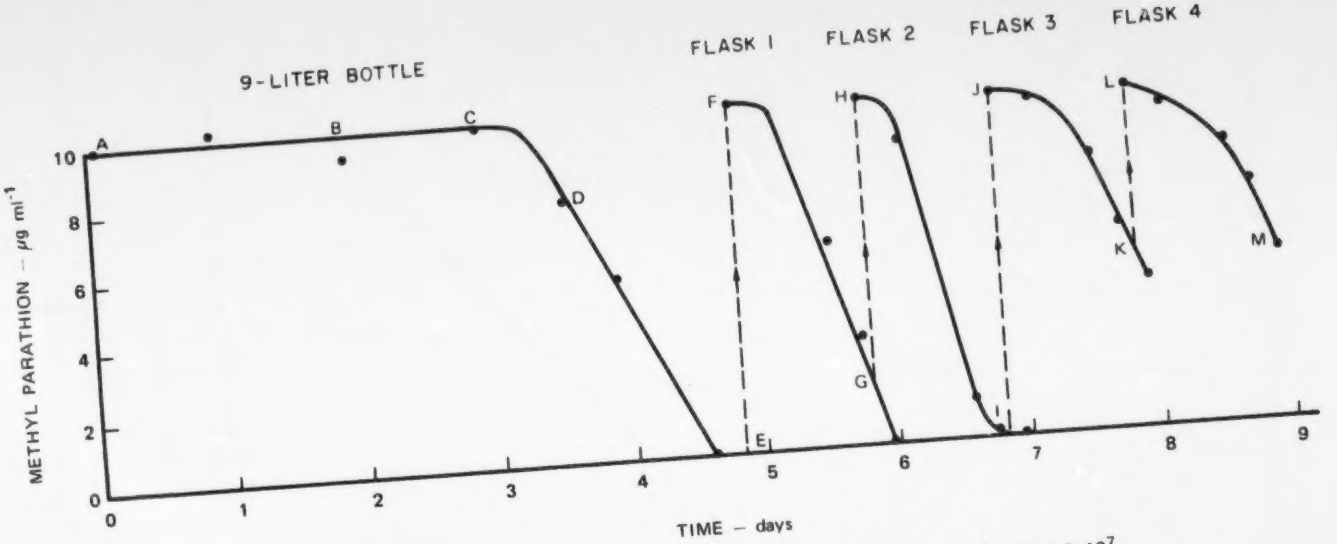

Viable Bacterial Counts: A, $5.0 \times 10^3$, B, $4.6 \times 10^5$, C, $8.3 \times 10^5$, D, $1.0 \times 10^6$, E, $4.4 \times 10^6$, F, $5.0 \times 10^4$, G, $1.2 \times 10^7$, H, $1.3 \times 10^5$, I, $2.3 \times 10^7$, J, $2.6 \times 10^5$, K, $1.2 \times 10^7$, L, $1.3 \times 10^5$, M, $1.7 \times 10^7$

SA-4396-29

FIGURE 13.13 CASCADE BATCH FERMENTATION OF METHYL PARATHION

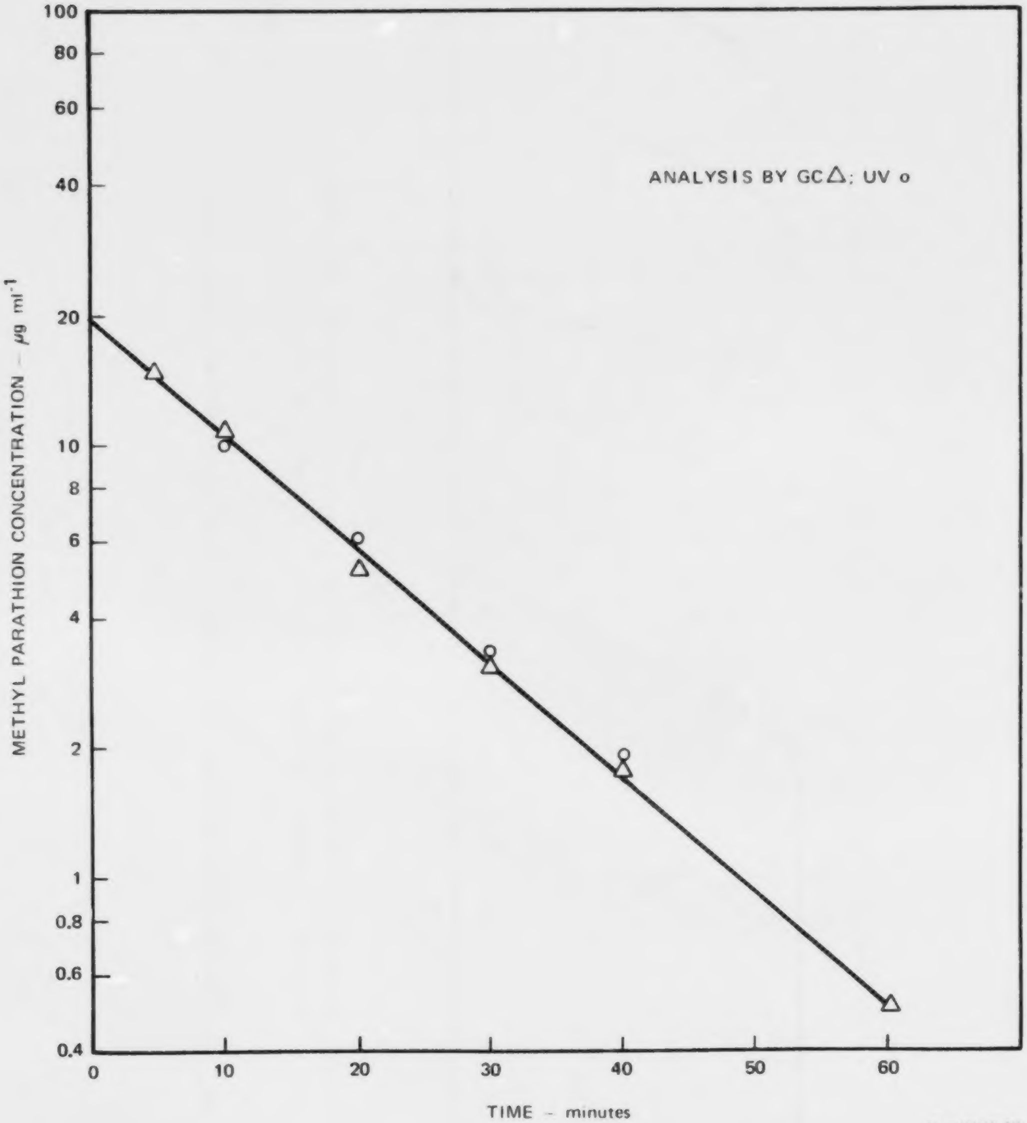

FIGURE 13.14 BATCH FERMENTATION WITH A HIGH POPULATION OF MP-DEGRADING ORGANISMS

The kinetic data obtained for MP biodegradation are summarized in Table 13.18. Considering the diversity of techniques and the fact that these were heterogenous mixtures of organisms, the agreement is good.

### 13.6.3 Identification of p-Nitrophenol as a Metabolite

During the growth of enrichment culture systems capable of biodegrading MP on basal salts/MP media, there was generally a variable period in which the solutions became yellow and then became colorless. Also, as was indicated previously, when MP was added to aeration effluent from the Monsanto Plant in Anniston, Alabama, the suspension quickly became a clear yellow. These observations suggested that p-nitrophenol was an intermediate in the biodegradation of MP as had been observed in the biodegradation of parathion (Munnecke and Hsieh, 1976).

The trimethylsilyl derivative of p-nitrophenol was isolated from an ethyl acetate extract of a Coyote Creek enrichment culture and identified by GC/MS (Figure 13.15) by comparison with the spectrum obtained from an authentic sample of p-nitrophenol. The relatively low levels of MP in the fermentation and the complexity of our microbial populations may account for our not detecting other aromatic metabolites or the other primary hydrolysis product, dimethylthiophosphoric acid.

Recently, Daughton and Hsieh (1976) reported the toxicity and resistance to biodegradation of diethylthiophosphoric acid formed in the microbial degradation of parathion; with the organisms used in these studies, p-nitrophenol was totally mineralized.

### 13.6.4 Discussion

The development of MP biodegrading cultures by enrichment procedures utilizing eutrophic waters and aeration effluents from sewage or wastewater treatment plants indicates that MP can be biodegraded by organisms present in many areas. The failure to develop a biodegrading system with waters from Lake Tahoe does not prove that the lake lacks any MP biodegrading organisms. It may be related to the results obtained with small samplings of microflora. It is also possible that our particular enrichment process did not favor development of other types of organisms that could degrade MP.

The very rapid development of the yellow color attributed to p-nitrophenol when MP was added to aeration effluent from the Monsanto Company's parathion MP manufacturing facility and the development of the yellow color when some cultures were subtransferred on MP/inorganic salts media suggest that the esterase involved in the hydrolysis of the phosphate-O-p-nitrophenol can be an exoenzyme. This had been reported for parathion by Munnecke and Hsieh (1976).

The high kinetic rate constants determined in these biodegradation studies also support the concept that MP should not be considered a serious

TABLE 13.18. SUMMARY OF KINETIC CONSTANTS FOR METHYL PARATHION BIODEGRADATION

| | $k_b$ (µg MP cell$^{-1}$ hr$^{-1}$) | $K_s$ (µg MP ml$^{-1}$ = µg ml$^{-1}$) | $k_{b2}$ (ml cell$^{-1}$ hr$^{-1}$) |
|---|---|---|---|
| Batch fermentation with low count inocula of rested cells | $(1.7 \pm 0.3) \times 10^{-7}$ | 1.1 | $1.3 \times 10^{-7}$ |
| Continuous feed chemostat fermentation | $(20 \pm 17) \times 10^{-7}$ | 2.6 | $7.7 \times 10^{-7}$ |
| Cascade batch fermentation | $(0.83 \pm 0.49) \times 10^{-7}$ | 1.8[a] | $0.46 \times 10^{-7}$ |
| Batch fermentation with a high population of MP-degrading organisms | -- | -- | $0.2 \times 10^{-7}$[b] |
| | | Average | $2.4 \times 10^{-7}$ |

[a] Average value of $K_s$ from first two experiments.

[b] Calculated from a first-order rate constant measured at a microbial poplation of $1.8 \times 10^{-8}$ cells ml$^{-1}$.

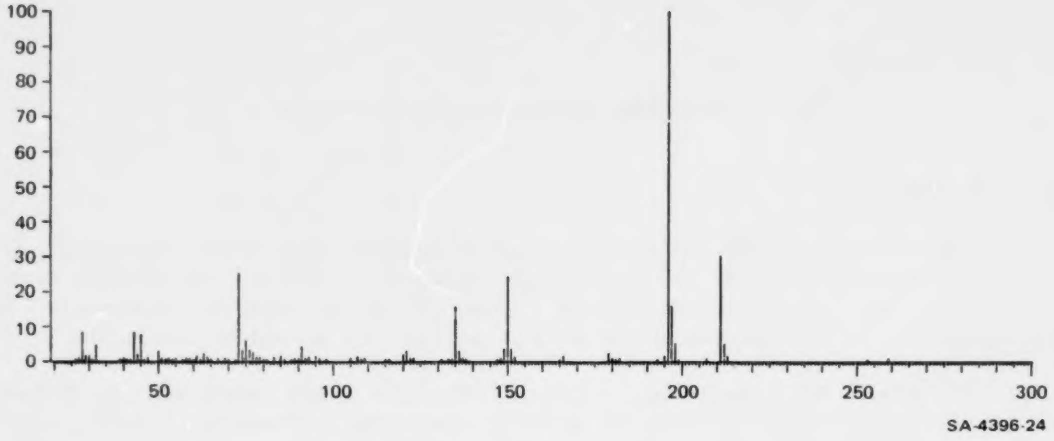

FIGURE 13.15 MASS SPECTRUM OF THE TRIMETHYLSILYL DERIVATIVE OF p-NITROPHENOL

environmental pollutant, provided the natural flora of a water body does not sorb the pesticide to a significant degree for biomagnification up the food chain. Munnecke (1976) recently reported that a crude cell extract from a mixed bacterial culture grown on parathion hydrolyzed this pesticide 2450 times faster than 0.1N sodium hydroxide at 40°C and suggested that this product could be used for disposal treatment of a number of organophosphate insecticides.

The lack of observation of any aromatic degradation product other than p-nitrophenol and the rapid degradation of this metabolite by aerobic mixed culture systems in aqueous systems suggest minimal possibilities for aromatic MP biodegradation products creating serious pollution problems.

# 14. LABORATORY INVESTIGATION OF MIREX

## 14.1 SYNOPSIS

The results of our laboratory studies suggest that volatilization and sorption are the dominant environmental pathways of mirex. Photolysis of mirex occurs only very slowly; hydrolysis and oxidation were not observed. Biodegradation was not observed under either aerobic or anerobic conditions.

The nine-compartment environmental exposure model predicted the following steady-state concentrations of mirex in solution, suspended solids, and sediments near point sources in the presence of a continuous discharge of $1 \times 10^{-5}$ μg ml$^{-1}$ (10 ppt) mirex.

| | Half-life in the aqueous phase* (hours) | Predicted steady-state concentrations | | |
|---|---|---|---|---|
| | | Solution (pg ml$^{-1}$) | Suspended solids (μg g$^{-1}$) | Sediments (μg g$^{-1}$) |
| River | 0.83 | 0.29 | $8.6 \times 10^{-2}$ | $7.7 \times 10^{-2}$ |
| Pond | 420 | 0.29 | $7.6 \times 10^{-4}$ | $1.6 \times 10^{-4}$ |
| Lake | 1480 | 0.05 | $1.4 \times 10^{-2}$ | $1.7 \times 10^{-3}$ |

## 14.2 BACKGROUND

Mirex is the generic name for 1,1A,2,2,3,3A,4,5,5,5A,5B,6-dodecachlorooctahydro-1,3,4-methano-2H-cyclobuta[c,d]pentalene, which is shown in Table 14.1. The general physical properties are also given in Table 14.1.

Mirex is used as a pesticide to control the fire ant in the southeastern United States and the big-headed ant in Hawaiian pineapple fields, and as a fire retardant in polymers. The term mirex has been applied to both the pure chemical as well as the fire ant bait. It has also been used as a trade name by Allied Chemical Company and Hooker Chemical Corporation. Dechlorane is the name used by Hooker Chemical Corporation for its fire retardant. All references to mirex in this report will refer to the pure chemical, which is assumed to have been leached from the bait into the aqueous environment.

Significant concentrations of mirex have been found in the sediment of Lake Ontario as a result of previous manufacturing activities by Hooker

---

*Predicted by one-compartment model.

Chemical. It has been found in Spring Creek, Pennsylvania, as a result of manufacturing by Nease Chemical Company. An excellent review of the chemistry and toxicology of mirex was published by Alley (1972). More recent research has shown that bioaccumulation in organisms can be significant (Cripe and Livingstone, 1977; Tagatz et al., 1976).

Average mirex concentrations in fish from contaminated waters generally appear to be less than 1 $\mu g\ g^{-1}$ but may be as high as 4 $\mu g\ g^{-1}$ (Suta, 1977). While the significance of these concentrations to animals in the wild is unclear (National Academy of Sciences, 1972), there is reason to suspect that mirex may be a source of Kepone, which is a reported carcinogen. The established tolerances for mirex in foods are 0.1 $\mu g\ g^{-1}$ in meats, eggs, and milk fat and 0.01 $\mu g\ g^{-1}$ in all other agricultural commodities (Suta, 1977).

TABLE 14.1. PHYSICAL PROPERTIES OF MIREX

| | |
|---|---|
| Structure | 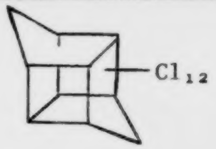 |
| Molecular weight | 546.0 |
| Melting point (°C) | 485 (decomposition) |
| Vapor pressure at 50°C (torr) | $6 \times 10^{-6}$ |
| Solubility in water at 22°C ($pg\ ml^{-1}$) | 70 ± 10[a] |

1.00 $pg\ ml^{-1}$ (1 ppt) mirex in water = $1.83 \times 10^{-12}$ M

[a] Measured in this study, see Section 14.3.1.

Recently, agreements have been made to phase out aerial applications of mirex bait (Chem. Eng. News, 1976; Holden, 1976), and the use of mirex may be sharply reduced in the near future. However, its extremely long persistence in the environment suggests that it may continue to be an environmental problem.

The low chemical reactivity of mirex is described in the 1972 review by Alley. Several papers have been published describing the products from photolysis of mirex, but it is not known how environmentally relevant these studies were and no data were given to assess how fast photolysis occurs in the aqueous environment (see Sections 14.5.1 and 14.5.4 for discussion). While mirex has been generally found to be resistant to biodegradation, it has been reported to be biodegraded under anaerobic conditions in sewage sludge (Andrade and Wheeler, 1974; Andrade et al., 1975). A mirex metabolite in monkeys has also been identified (Stein et al., 1976). Recently products of mirex have been identified in samples from field locations where large amounts of mirex were deposited and left exposed in the environment for 12 and 5 years (Carlson et al., 1976). Hollister et al. (1975) reported that several genera of algae concentrated mirex from very dilute solutions. A *Chlorococcum* sp. concentrated mirex 10,000-fold from a 10 ppt solution. Biomagnification into flatfish from mirex-containing sediment was reported by Koblinski and Livingston (1975).

While the chemical and physical characteristics of mirex suggest that it should be highly resistant to biological and chemical transformation in aqueous environments and be strongly sorbed on bacteria, algae, and sediments, a careful study and integrated assessment of the environmental pathways of mirex is required. Our study was designed to measure the physical properties of mirex and to obtain limiting estimates of the rate constants for chemical and biological transformation processes of mirex in solution in aquatic environments.

## 14.3 ENVIRONMENTAL ASSESSMENT

### 14.3.1 Summary of Laboratory Data

The rate constants obtained in the laboratory investigations of mirex are summarized in Table 14.2. The sorption partition coefficient measured on our test mixture of four bacteria species is $(4.8 \pm 0.5) \times 10^5$.

TABLE 14.2. SUMMARY OF MIREX LABORATORY DATA

| Process | Sorption equilibrium | Partition coefficient |
|---|---|---|
| Sorption | $S_s = K_p S_w$ | $K_p = 460,000 \pm 110,000^2$ |
| | Rate expression | Rate Constant at 25°C |
| Volatilization[b] | $k_v$[mirex] | $k_v = (6.3 \pm 1.8) \times 10^{-2}\ k_v^0$ |
| Photolysis[c] | $k_p[\text{mirex}] = \Phi\ (\Sigma Z_\lambda \varepsilon_\lambda)[\text{mirex}]$ | $k_p = < 5 \times 10^{-8}\ \text{sec}^{-1}$ |
| Oxidation | $k_{ox}[RO_2\cdot][\text{mirex}]$ | $k_{ox} < 30\ M^{-1}\ \text{sec}^{-1}$ |
| Hydrolysis | $k_h$[mirex] | $k_h < 1 \times 10^{-10}\ \text{sec}^{-1}$ |
| Biodegradation[d] | $k_{b2} = \frac{\mu\text{max}}{Y\ K_s}$ | $k_{b2} = 0$ |

[a] On Coyote Creek sediment.

[b] See discussion in Part I, Section 5.3, and Appendix B.

[c] First-order rate constant; see discussion in Section 14.5.1.

[d] Biodgradation was not observed in the enrichment procedures.

## 14.3.2 Environmental Assessment Using the One-Compartment Model

The half-lives of dissolved mirex calculated for individual transformation or removal processes following a spill are listed in Table 14.3. Volatilization and sorption appear to be the only important processes. Photolysis of mirex in solution was found to be much slower than sorption or volatilization and will not affect the transport of mirex by other processes. No biodegradation was detected in experiments that lasted up to six months. While this implies that acclimated cultures are improbable, species that can degrade mirex may yet be found.

TABLE 14.3. TRANSFORMATION AND TRANSPORT OF MIREX PREDICTED BY THE ONE-COMPARTMENT MODEL[a]

| Process | Stream | Eutrophic pond | Eutrophic lake | Oligotrophic lake |
|---|---|---|---|---|
| Photolysis, half-life (hr) | > 8,000 | > 8,000 | > 8,000 | > 8,000 |
| Oxidation, half-life (hr) | > 10,000 | > 10,000 | > 10,000 | > 10,000 |
| Volatilization, half-life (hr) | 500 | 700 | 1,980 | 1,980 |
| Hydrolysis, half-life (hr) | -- | -- | -- | -- |
| Biodegradation, half-life (hr) | -- | -- | -- | -- |
| Half-life for all processes, except dilution (hr) | 500 | 700 | 2,000 | 2,000 |
| Half-life for all processes, including dilution (hr) | 0.83 | 420 | 1,480 | 1,480 |
| Amount mirex sorbed ($mg\ m^{-3}$) | 0.3 | 0.9 | 0.15 | 0.15 |
| Percentage mirex sorbed | 97% | 99% | 94% | 94% |

[a] The initial concentration of mirex was assumed to be 10 pg $ml^{-1}$ (10 ppt).

Sorption half-lives have not been measured, but the times needed to reach equilibrium are generally less than half an hour, roughly two orders of magnitude faster than volatilization. Since the partition coefficient of mirex is greater than $10^5$, the amount of mirex removed from the water by sorption is expected to be high, with 93% to 98% of total mirex in the various systems located in the sediments even if one assumes that mirex enters only in the dissolved form. However, volatilization may cause significant losses of dissolved mirex from laboratory containers during stirring or transfer.

### 14.3.3 Persistence

Sorption is expected to significantly affect the persistence of concentrations of dissolved mirex after release to natural waters, rapidly bringing the concentrations of dissolved mirex below the limits of detection. While desorption will maintain relatively low concentrations of dissolved mirex in ensuing weeks, the concentrations should be well below 6 x $10^{-5}$ $\mu$g $g^{-1}$, the limit of solubility. Since these low concentrations will be present until the contaminated solids are buried by uncontaminated sediments and may later be uncovered by dredging or natural scouring, any statements regarding the persistence of mirex should be made very carefully.

Although variations in the persistence of mirex in eutrophic and oligotrophic waters should be scarcely measurable, concentrations will initially decline more rapidly in eutrophic waters. However, since eutrophic waters have higher concentrations of suspended solids than oligotrophic waters, the amount of mirex subject to eventual desorption should be greater in eutrophic waters.

### 14.3.4 Mass and Concentration Distributions Calculated Using Computer Models

Table 14.4 summarizes the distributions of mass and concentration of mirex expected at steady state during chronic discharge to each of four types of water bodies, as calculated with the aid of the computer model. The pseudo-first-order rate constants used in these simulations are presented in the appendix.

The steady-state concentrations of mirex in solution in the simulated stream segments imply a removal from solution of approximately 10% per kilometer. The reduction of concentrations of dissolved mirex in the stream simulation is due primarily to sorption followed by sedimentation. Hence, even in smaller and thus more slowly flowing and less turbulent rivers than we have assumed in the simulation, very nearly the same amount of mirex will be removed within the same river reach.

The steady-state concentrations of mirex in solution are roughly $10^{-7}$ to $10^{-9}$ $\mu$g $ml^{-1}$ in pond and lake simulations. This is roughly 100 to 10,000 times less than the input concentrations (Table 14.4). In the pond simulation, the steady-state concentration of mirex is estimated to be 0.01% of the concentration in inflowing waters. Within the lake simulations, the concentrations of mirex in the surface waters are about 100 times lower than the concentrations in inflowing waters.

The model predicts that virtually all the mirex is in the bottom sediments at steady state, a pattern in agreement with the available field data (Suta, 1977). Since the model assumes that mirex does not degrade in the sediments, the estimated values of mirex in sediment are probably upper limits

TABLE 14.4. DISTRIBUTION OF MIREX IN VARIOUS AQUATIC SYSTEMS AT STEADY STATE (input concentrations of 10 pg ml$^{-1}$ mirex)

| | Pond | | River | | Lake | |
|---|---|---|---|---|---|---|
| | Mass (kg) | Conc. (μg ml$^{-1}$) | Mass (kg) | Conc. (μg ml$^{-1}$) | Mass (kg) | Conc. (μg ml$^{-1}$) |
| Compartment 1 (surface water) | | | | | | |
| Solution | $5.7 \times 10^{-8}$ | $2.9 \times 10^{-9}$ | $8.7 \times 10^{-5}$ | $2.9 \times 10^{-7}$ | $1.2 \times 10^{-7}$ | $4.9 \times 10^{-8}$ |
| Suspended solids | $4.5 \times 10^{-6}$ | $7.6 \times 10^{-4}$ | $2.6 \times 10^{-3}$ | $8.6 \times 10^{-2}$ | $1.8 \times 10^{-4}$ | $1.4 \times 10^{-2}$ |
| Compartment 2 (surface water) | | | | | | |
| Solution | -- | -- | $7.9 \times 10^{-5}$ | $2.6 \times 10^{-7}$ | $7.0 \times 10^{-5}$ | $2.7 \times 10^{-8}$ |
| Suspended solids | -- | -- | $2.3 \times 10^{-3}$ | $7.6 \times 10^{-2}$ | $1.0 \times 10^{-3}$ | $8.0 \times 10^{-3}$ |
| Compartment 3 (surface water) | | | | | | |
| Solution | -- | -- | $7.2 \times 10^{-5}$ | $2.4 \times 10^{-7}$ | $4.2 \times 10^{-6}$ | $1.7 \times 10^{-8}$ |
| Suspended solids | -- | -- | $2.1 \times 10^{-3}$ | $7.0 \times 10^{-2}$ | $6.3 \times 10^{-5}$ | $5.0 \times 10^{-3}$ |
| Compartment 5 (bottom water) | | | | | | |
| Solution | -- | -- | -- | -- | $7.8 \times 10^{-7}$ | $3.1 \times 10^{-10}$ |
| Suspended solids | -- | -- | -- | -- | $1.1 \times 10^{-5}$ | $8.8 \times 10^{-5}$ |
| Compartments 7-9 (sediment)[a] | | | | | | |
| Solution | $7.2 \times 10^{-11}$ | $2.9 \times 10^{-9}$ | $2.0 \times 10^{-6}$ | $2.6 \times 10^{-7}$ | $8.4 \times 10^{-8}$ | $9.6 \times 10^{-9}$ |
| Solids | $1.7 \times 10^{-3}$ | $7.6 \times 10^{-4}$ | $1.5 \times 10^{-1}$ | $7.7 \times 10^{-2}$ | $6.5 \times 10^{-2}$ | $4.7 \times 10^{-3}$ |
| Total mass | $1.7 \times 10^{-3}$ | | $1.5 \times 10^{-1}$ | | $6.5 \times 10^{-2}$ | |

[a] The amounts given for solid and solution phases in the sediment compartments are estimated from the sorption partition coefficient for suspended solids and may be overestimated because it was assumed that biodegradation of sorbed material does not occur.

for the concentrations that may be expected in natural environments. However, this is unlikely to be a significant source of error and should be less than the uncertainties introduced by variations in the properties of actual water bodies.

The most significant patterns are seen in the pond and lake simulations (Figures 14.1 and 14.2), where concentrations of mirex in the solution, suspended solids, and sediment phases are predicted to be insensitive to termination of discharge following a period of chronic pollution since most of the mirex would be concentrated on the sediments. The exception is the concentration of dissolved mirex in streams (Figure 14.3), which is essentially controlled by dilution.

### 14.3.5 Discussion

Despite the uncertainties inherent in extrapolating laboratory data to the field, it is evident that approximately 95% of mirex should be rapidly trapped in suspended solids and sediments after discharges to the water are started. The mirex concentrations in the water column are too low to be detected in practice but are expected to be insensitive to the stoppage of discharge. Therefore, field sampling and control efforts should be focused on the sediments where mirex is accumulated.

Although volatilization has been observed in the laboratory, it is believed that the rate of escape of mirex into the atmosphere from natural waters as a result of volatilization will be very low because the amount of mirex predicted to be in solution is so much lower than the amount that is sorbed.

The most significant uncertainties lie in the potential biological effects and in the estimation of the ultimate concentration of the mirex, since this is determined largely by the properties of the sediments and dilution rates. Since the partition coefficient of mirex is probably sensitive to the organic content of the sediments, the ultimate concentration of mirex in water bodies with a long history of pollution with mirex may vary by one or two orders of magnitude among water bodies. However, the significance of the variations cannot be appraised with the available toxicological data. We can only say that the solution concentrations will be quite low shortly after discharges stop.

## 14.4 PHYSICAL PROPERTIES

### 14.4.1 Solubility in Water

The solubility of mirex in pure water at room temperature (22 ± 2°C) was measured using the procedure for low solubility substrates described in Appendix B, Section B.1.1. Saturated solutions of mirex were prepared in a 5-gallon carboy by coating the walls with mirex, filling it with water, and equilibrating for several days.

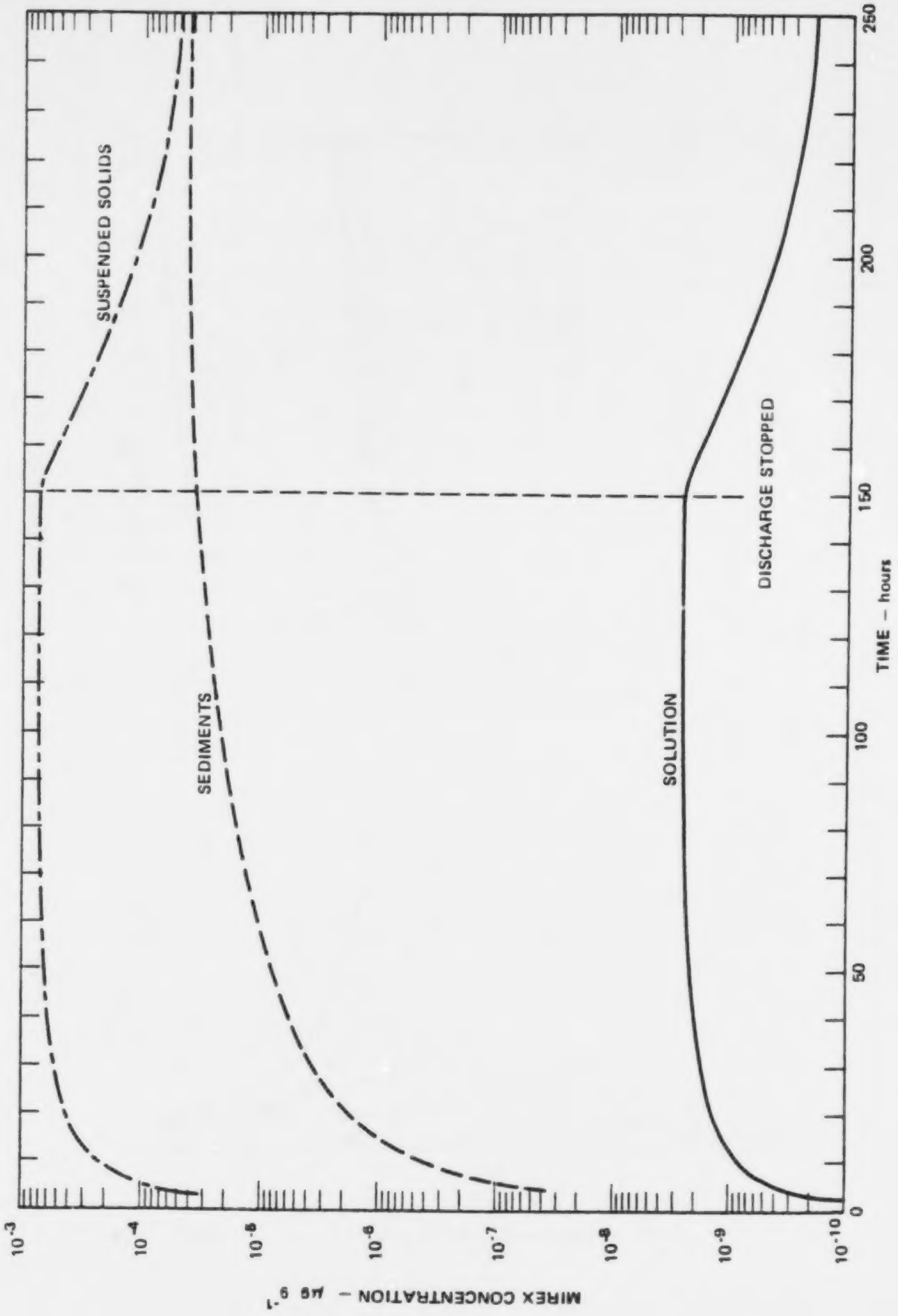

FIGURE 14.1 PERSISTENCE OF MIREX IN A TWO-COMPARTMENT POND SYSTEM

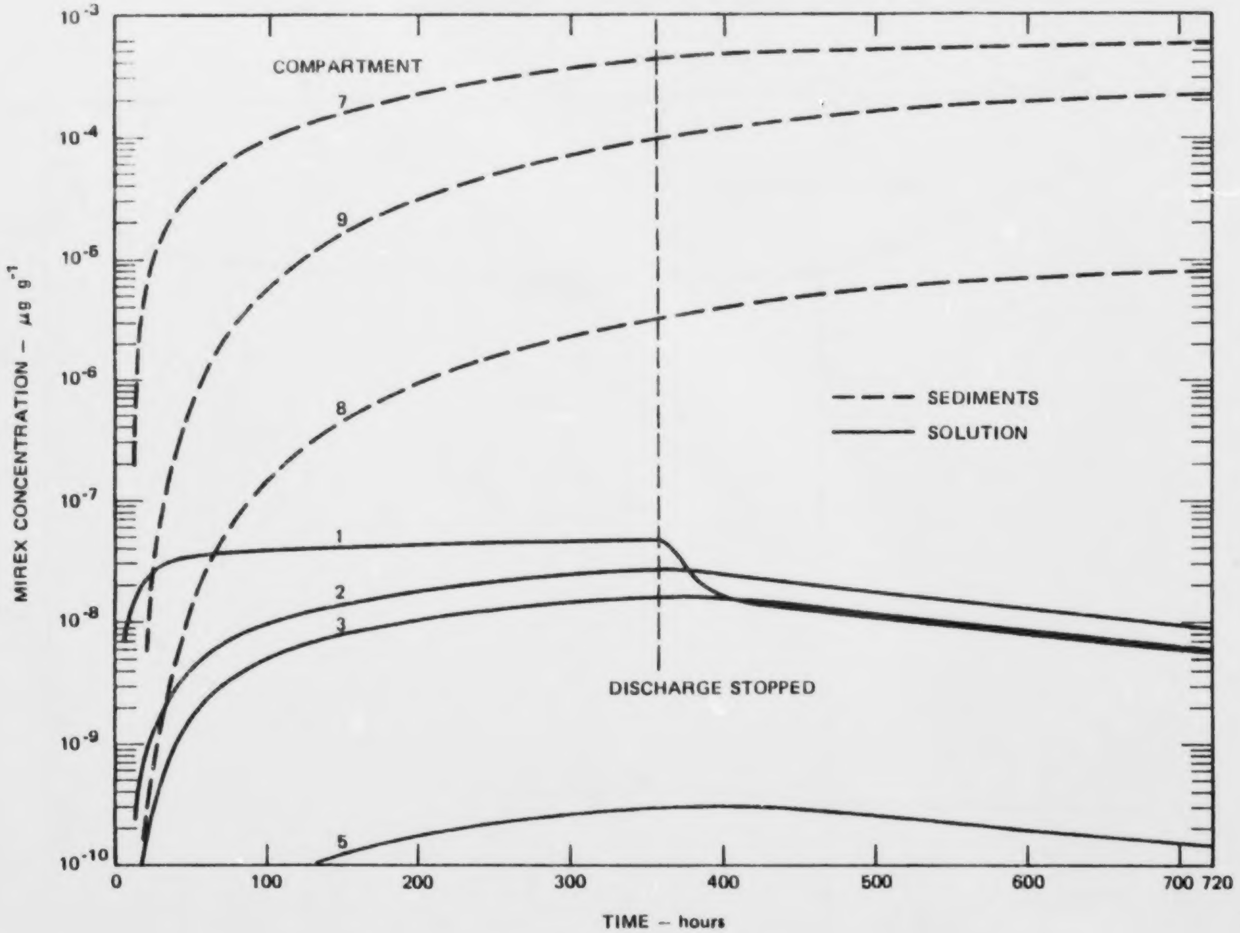

FIGURE 14.2 PERSISTENCE OF MIREX IN A PARTIALLY MIXED LAKE

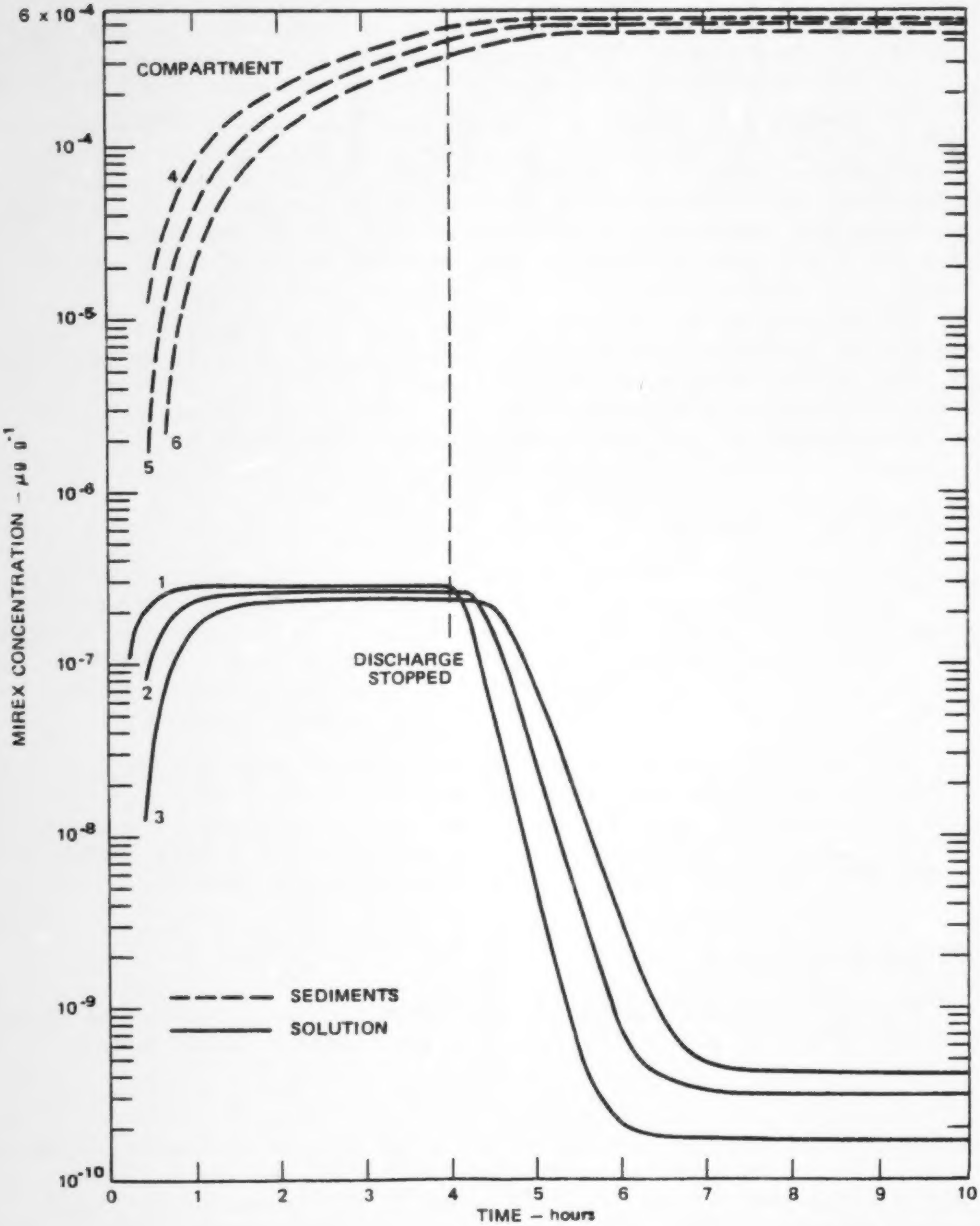

FIGURE 14.3 PERSISTENCE OF MIREX IN A PARTIALLY MIXED RIVER SYSTEM

Several experimental problems were encountered during the analysis of these solutions as well as the solutions from the volatilization and sorption studies. Solutions prepared in the carboy contained suspended solid mirex, which could be removed by centrifugation at 7500 rpm for 60 minutes. We also showed that a signifcant amount of the mirex will volatilize from the solution into the available air space.* This loss was minimized by keeping the carboys full (i.e., replacing volume removed with water and allowing reequilibration).

All samples were extracted with 15% methylene chloride in hexane, dried over $Na_2SO_4$, and concentrated by a factor of about 1000 on a steam bath, resulting in removal of the methylene chloride as an azeotrope. The remaining hexane solution was analyzed by electron capture GC. Considerable interferences from impurities in both the solvent and the water made the analysis difficult. No interfering peaks occurred at the elution time of the mirex.

The samples for the solubility study were equilibrated for 1 week, centrifuged at 7500 rpm for 60 minutes, extracted, and analyzed as described above. The solubility of mirex in pure water is 70 ± 10 pg $ml^{-1}$ ($1.3 \times 10^{-11}$ M), based on three determinations. In another experiment, a single sample equilibrated for two weeks gave the same value (70 pg $ml^{-1}$).

### 14.4.2 Absorption Spectrum

The solubility of mirex in water, 50% water/50% acetonitrile, 100% acetonitrile, and 100% methanol was so low that no absorption could be detected above 295 nm, even in 10-cm cells. However, since there were several reports in the literature that mirex photolyzed under various conditions (see Section 14.5.1), we decided to measure the uv absorption spectrum of mirex in a solvent (hexane) where the solubility would be significantly higher.

At a concentration of $5 \times 10^{-2}$ M, the absorption above 290 nm was still below our detection limit of 0.005 absorbance unit. Therefore, the absorption coefficient is less than 0.1 $M^{-1}cm^{-1}$ in the wavelength region greater than 290 nm. There is the possibility of a solvent shift between hexane and water, but since mirex is nonpolar, this shift should be minimal.

### 14.4.3 Volatilization Rate

The rate of volatilization of mirex from pure water was measured using the method of Hill et al. (1976), which is described in detail in Part I and Appendix B of this report. The solutions of mirex were prepared and analyzed in pure water using the procedures described in Section 14.4.1. The mirex solution was centrifuged before the experiment was initiated. The initial mirex concentration was 86 ± 10 pg $ml^{-1}$*.

---

*We estimated a Henry's law constant $H_c \sim 8 \times 10^3$ torr $M^{-1}$ using an estimate of the vapor pressure of mirex at 20°C of $1 \times 10^{-6}$ torr, and the solubility of mirex in water given in Table 14.1 (70 pg $ml^{-1}$), following the method of Mackay and Wolkoff (1973). Using this value, it can be shown that if a volume of saturated mirex solution is equilibrated with an equal volume of mirex-free air, approximately 40% of the mirex will volatilize into the air space.

Since there was a good possibility that the mirex would sorb onto the membrane and probe of the oxygen analyzer, our basic volatilization procedure was modified. The oxygen reaeration rate was measured in a separate beaker that was prepared at the same time except that it contained no mirex. It was stirred at the same rate as the mirex-containing beaker, as measured by the depth of the vortices. Each time a sample was withdrawn for mirex analysis, an equal volume was withdrawn from the second beaker. The oxygen-reaeration rate was measured in the second beaker in the usual way; the mirex-containing beaker was not subjected to the nitrogen purge. At the end of the experiment the beaker was emptied and extracted; 11% of the amount of mirex originally present was found sorbed to the beaker walls. This amount was within the experimental error of the procedure.

The average oxygen reaeration rate, $k_v^O$, over 2.5 days was 0.86 ± 0.13 $hr^{-1}$. The rate constant for volatilization of mirex, $k_v^M$, over the same time period was $(5.39 \pm 0.65) \times 10^{-2}$ $hr^{-1}$. The ratio, $k_v^M/k_v^O$, is $6.3 \pm 1.8) \times 10^{-2}$.

### 14.4.4 Sorption on Natural Sediment

The sorption partition coefficient of mirex was measured on Coyote Creek sediment. All solutions containing mirex were centrifuged before the isotherm measurements. The concentration of mirex in the supernatants after sorption and centrifugation was measured as described in Section 14.4.1. The sediment was extracted with two 10-ml portions hexane, and the hexane was concentrated and analyzed as before. The initial concentration of mirex was always less than the saturation concentration of 70 pg $ml^{-1}$. Duplicate samples at two mirex concentrations and two sediment concentrations plus blanks were prepared. The results are summarized in Table 14.5.

The wide range of recoveries is explained in part by the experimental difficulties discussed in Section 14.4.1, interferences introduced with the addition of sediment, and extra handling involved in the isotherm measurements. The second point is very high, however, for reasons that are not apparent. In the linear least squares (LLS) regression analysis, elimination of this point reduces the 95% confidence interval by one-half, but the partition coefficient is virtually unchanged. The nonlinear least squares (NLLS) regression, which compensates for flask effects (Appendix B, Section B.1.4) allows use of all the data and gives the best estimate of $K_p$ with the narrowest confidence interval. Even the lower bound of this value shows very strong sorption of mirex by sediments.

---

*This concentration is within the experimental error of the solubilility limit.

## TABLE 14.5. SORPTION OF MIREX ON COYOTE CREEK SEDIMENT

| Sorbent concentration ($\mu g\ ml^{-1}$) | Mirex concentration in supernatant ($pg\ ml^{-1}$) | Mirex concentration on sediment ($\mu g\ g^{-1}$) | Recovery (%) | Partition coefficients ($K_p \times 10^{-5}$) LSS[a] $a_o = 0$ | LSS[a] $a_o \neq 0$ | NLLS[a] $S_w$ and $S_s$ |
|---|---|---|---|---|---|---|
| 3.0 | 0.33 ± 0.5 | 0.91 ± 0.09 | 69 | 3.7 ± 3.6 | 1.1 ± 4.1 | 4.6 ± 1.0 |
| 3.0 | 0.33 ± 0.5 | 2.3 ± 0.43 | 180 | | ($a_o$ = 0.98 ± 1.1) | |
| 12 | 1.0 ± 0.5 | 0.41 ± 0.07 | 130 | | | |
| 3.0 | 4.5 ± 1.4 | 1.7 ± 0.53 | 84 | 3.6 ± 1.5[b] | 2.4 ± 1.6[b] | |
| 3.0 | 5.2 ± 0.71 | 1.6 ± 0.37 | 88 | | ($a_o$ = 0.46 ± 0.47)[b] | |
| 12 | 1.0 ± 0.5 | 0.53 ± 0.05 | 70 | | | |
| 12 | 1.0 ± 0.5 | 0.69 ± 0.05 | 81 | | | |

[a] LLS = linear least squares; NLLS = nonlinear least squares; see Appendix B, Section B.1.4 for explanation of regression.

[b] Recalculated excluding the data reported in the second line of this table.

### 14.4.5 Biosorption

Because of the very low solubility of mirex in water, the concentration used in biosorptions was reduced to 50 pg $ml^{-1}$ and the microbial mixture of four bacteria was used at an optical density of 0.01. This concentration of bacteria corresponded to a dry weight of 6 $\mu g\ ml^{-1}$. To facilitate analyses, sorptions were conducted in 100-ml Corex bottles, and contents from two bottles were combined for extractions. The correction factors applied for sorptions of mirex and bacterial cells containing mirex onto the glassware were 18% and 14% for the 1-hour sorptions and 3-hour desorptions, respectively. The results in Table 14.6 clearly indicate the affinity of bacterial cells for mirex. The sorption coefficients are of the same order as those obtained with benzo[a]pyrene.

TABLE 14.6. MIREX SORPTION AND DESORPTION ON A MIXED BACTERIAL POPULATION[a]

| | Amount in supernatant (%) | Amount in cells (%) | Sorption coefficient (x $10^{-5}$) |
|---|---|---|---|
| Sorption | 22 ± 1 | 63 ± 7 | 4.8 ± 0.5 |
| Desorption | 23 ± 4 | 45 ± 7 | 3.3 ± 0.5 |

[a] Dry weight of bacterial cells was equivalent to 6 $\mu g\ ml^{-1}$; sorptions were initiated with 50 pg mirex $ml^{-1}$.

## 14.5 CHEMICAL TRANSFORMATION

### 14.5.1 Photolysis Rate

While the UV absorption of mirex above 290 nm was found to be weak ($\varepsilon < 0.1\ M^{-1}\ cm^{-1}$), the reported photolyses of mirex (Alley et al., 1974a,b) and the apparent slowness of other processes justified some photochemical studies. Solutions of 33 ng $ml^{-1}$ ($6.0 \times 10^{-8}$ M) mirex in 1% acetonitrile in pure water were placed outdoors (Menlo Park, California) from November 1, 1976, to May 9, 1977. These solutions were analyzed for mirex at reactions times of 22, 63, 100, and 190 days by GC using an electrolytic conductivity detector operating in the halogen mode.

A progressive loss of mirex was found in each analysis, with a first-order rate constant of $(3.7 \pm 0.8) \times 10^{-3}$ $days^{-1}$ calculated from these data. This rate constant corresponds to a half-life of about 1 year.

A solution of 33 ng $ml^{-1}$ mirex in 1% acetonitrile in water from Coyote Creek was also exposed to sunlight over the same six-month period, with analyses for mirex carried out at 83 and 190 days. Including the initial concentration data point, a first-order rate constant for photolysis of $(4.2 \pm 0.2) \times 10^{-3}$ $days^{-1}$ was calculated.

Extraction of the glass in the head space and in contact with the solution showed that no significant loss of mirex had occurred through volatilization or adsorption in these experiments. Analyses of the mirex solutions showed that four products were formed in the photolyses; the gc retention times of two of these products correspond to those of Kepone and a monohydromirex (see Section 14.5.4 for further discussion of products).

Measurement of a quantum yield for mirex photolysis above 290 nm was not practical since the absorption coefficients in water (or other solvents) could not be reliably measured. To determine whether the 1-year half-life measured for mirex photolysis was plausible, we calculated the photolysis half-life according to the procedure of Zepp and Cline (1977), using hypothetical values of the quantum yield and the absorption coefficients. As described in Part I, Section 6.1, the photolysis rate constant in sunlight is a function of the solar irradiance $Z_\lambda$ the average absorption coefficients of the chemical $\varepsilon_\lambda$, and the quantum yield, $\phi$:

$$k_p = \frac{2.303}{6.02 \times 10^{20}} \phi \Sigma Z_\lambda \varepsilon_\lambda$$

Using the $Z_\lambda$ data for the summer season in the wavelength region 297.5 to 310 nm and assuming that the absorption coefficients over this region are equal to a value of 0.01 and that the quantum yield is 1.0, we calculated a minimum half-life of about 130 days for the direct photolysis of mirex. The calculated minimum half-lives for the winter and spring season are 850 and 190 days, respectively.

Any other combination of quantum yield and absorption coefficient that gives a product of 0.01 over the same wavelength region would give the same calculated half-lives. While reliable data for both $\phi$ and $\varepsilon_\lambda$ are still needed, these calculations indicate that for a compound like mirex, which has very weak absorption in the solar spectrum, photolysis may still occur with a half-life of about a year if the quantum yield is about unity.

Although the above calculation indicates that the measured half-life may be completely accounted for by the photolysis of mirex in solution, other processes could also contribute to the transformation rate of mirex in our experiments. The formation of products does show, however, that transformations are taking place. Since microbiological studies failed to develop any biodegrading cultures (see Section 14.6), such processes are not likely to occur in our filter-sterilized solutions, even after a 6-month reaction time.

A photoprocess that could have occurred in our photolysis experiments is photolysis of the mirex that was adsorbed on the glass of the reaction tube. Although it is not known whether it would catalyze the photolysis over that in solution, the sunlight photolysis of mirex on silica gel plates has been reported (Ivie et al., 1974), and one of the products was reported to be a monohydromirex. On the basis of our experiments we cannot say whether photolysis of mirex sorbed on glass is important. To rule out such an artifact in the data applied to the environmental assessment, further research is clearly required. Since the calculation performed according to the procedure of Zepp and Cline (1977) indicates that the solution phase photolysis may entirely account for the observed half-life, a priority in such additional research should be to determine the quantum yield for direct photolysis. Experiments near 280 nm ($\varepsilon$ for mirex is 0.15 at 280 nm) may be acceptable for this purpose since the absorption band that has a $\varepsilon_{max}$ at $\sim$ 228 nm is the one that tails into the solar spectrum region.

### 14.5.2 Oxidation Rate

Mirex was expected to show very low reactivity toward free radical oxidation since an initial process of chlorine atom abstraction from mirex by alkylperoxyl or alkyoxyl radical is a highly endothermic reaction.* To demonstrate this low reactivity and to ensure that no other radical reaction pathways would lead to transformation of mirex, we conducted a free radical oxidation experiment as described in Part I, Section 5.4.2, and Appendix B, Section B.2.

A solution of 33 ng $ml^{-1}$ ($6.0 \times 10^{-8}$ M) mirex in 1% acetonitrile in water containing $1.0 \times 10^{-4}$ M AA was heated at 52°C for 164 hours. At the end of this time all the mirex was found to be unreacted within the ±5% experimental error of the analysis, and no product peaks were found in the gc trace. Under the conditions of our free radical oxidation experiment, the slowest reaction that can be quantitatively evaluated has a rate constant of 30 $M^{-1}$ $sec^{-1}$ at 25°C. With the assumption that $[RO_2\cdot] = 10^{-9}$ M in the environment, this rate constant corresponds to a half-life of 0.7 year. The half-life for oxidation of mirex must then be greater than 0.7 year, and in fact is probably several orders of magnitude greater.

### 14.5.3 Hydrolysis Rate

Experiments to determine the susceptibility of mirex to chemical hydrolysis were conducted in sealed tubes at 100°C using 33 ng $ml^{-1}$ mirex in 1% acetonitrile in water. In tubes where an air space was present above the reaction solution, some volatilization of mirex was found with condensation and sorption onto the glass in the head space. Without an air space in the sealed tube, all the mirex was found to be present in solution, within the analytical experimental error of ±5%, after one month at 100°C.

---

*The bond dissociation energy for a C-Cl bond is about 80 kcal $mole^{-1}$ (Benson, 1968), whereas that for O-Cl is about 48 kcal $mole^{-1}$ (based on the O-Cl bond of t-butyl hypochlorite; Walling and Papaionnou, 1968), making the reaction at least 30 kcal $mole^{-1}$ endothermic.

No products were found in the GC analyses of any hydrolysis experiment. Kepone, which we considered to be the most likely hydrolysis product, was repeatedly sought in all analyses, but none was found. All reactions were carried out at a pH of about 7. The literature indicates that hydrolysis of halides by hydroxyl ion substitution would not be important below pH 10 and that there is no significant acid-catalyzed reaction (Mabey and Mill, 1977).

Although no evidence for hydrolysis at 100°C was found after one month, if we assume that the experimental error of ±5% is a loss due to hydrolysis of mirex, we can calculate an upper limit for a first-order rate constant of $2 \times 10^{-8}$ $sec^{-1}$. Allowing for a factor of two in rate for each 10°C interval (see Part I, Section 6.4) we estimate an upper limit for the hydrolysis rate constant of $1 \times 10^{-10}$ $sec^{-1}$ at 25°C. This rate constant corresponds to a half-life of over 250 years, confirming that hydrolysis of mirex will be a very slow process in the aquatic environment.

## 14.5.4 Products from Chemical Transformation

No loss of mirex or appearance of new GC peaks was observed in the hydrolysis or oxidation studies. Analysis of the sunlight photolysis reactions showed the loss of mirex and the appearance of four products. These products appeared in the GC analysis as one major peak and three minor peaks. It was calculated, however, that if these products were assumed to have GC response factors similar to that of mirex, they represented less than 40% of the total mirex consumed in the photolysis. One of the minor mirex photoproducts showed the same retention time as that of an authentic sample of Kepone (I).

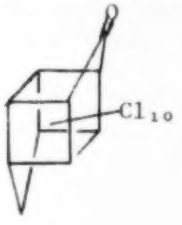

I

By comparing the mass spectrum of the major product peak (∼ 25% yield) with the data reported by Carlson et al. (1976), we identified the product as a monohydromirex. Insufficient material was available to identify any of the other mirex products by GC-MS or to confirm the presence of Kepone by other than its GC retention time.

Photolyses of 33 ng $ml^{-1}$ ($6.0 \times 10^{-8}$ M) mirex in solutions of 1% acetonitrile in pure water were also carried out in sealed Pyrex tubes irradiated with high intensity mercury lamps. Analysis of solutions irradiated for 24 and 48 hours using a 1000-watt lamp gave GC product peaks similar in retention time and in product proportions to those of the sunlight photolysis experiments. Photolysis of the 33 ng $ml^{-1}$ mirex solution with a 2500-watt lamp for 100 hours led to complete loss of mirex but without detection of products.

Although extensive product studies could not be pursued in this work, some discussion of products is relevant for the environmental assessment. Studies of Alley et al. (1973, 1974a) found the monohydromirex (II) to be a major product of mirex photolysis in cyclohexane or isooctane.

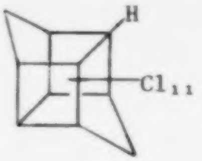

II

This monohydro product was also the major product when mirex was photolyzed on silica gel plates (Ivie et al., 1974). The monohydro product III is reported to be the major product from photolysis of mirex in triethylamine solvent (Alley et al., 1974b).

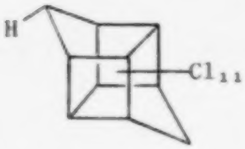

III

The change in products was attributed to photolysis of a charge transfer complex formed between the amine and mirex. In both solution photolyses, formation of the monohydro products can be explained by initial photodissociation of a C-Cl bond followed by hydrogen abstraction from solvent; it is difficult to explain, however, the formation of II on silica gel, which has no obvious hydrogen donor capability.

The formation of a monohydromirex product in our studies can be explained by photodissociation of C-Cl followed by hydrogen transfer from acetonitrile, which was necessarily present in all reactions as a cosolvent. Based on the work of Alley and coworkers, it is reasonable to assign II as our monohydromirex product from solution photolysis. Kepone, which was tentatively identified in this work, may be derived from mirex by the following photooxidative process:

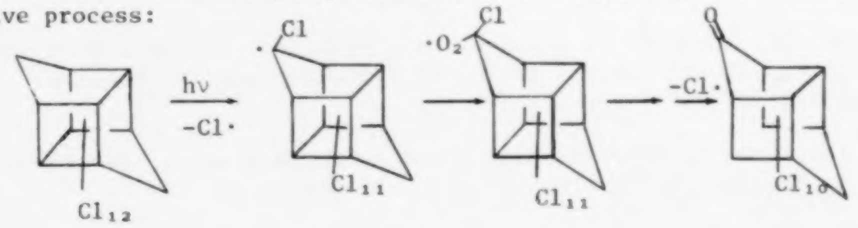

The failure to obtain a good product balance in our studies may be due to other photooxidative reactions that compete successfully with hydrogen transfer and loss of chlorine radical.

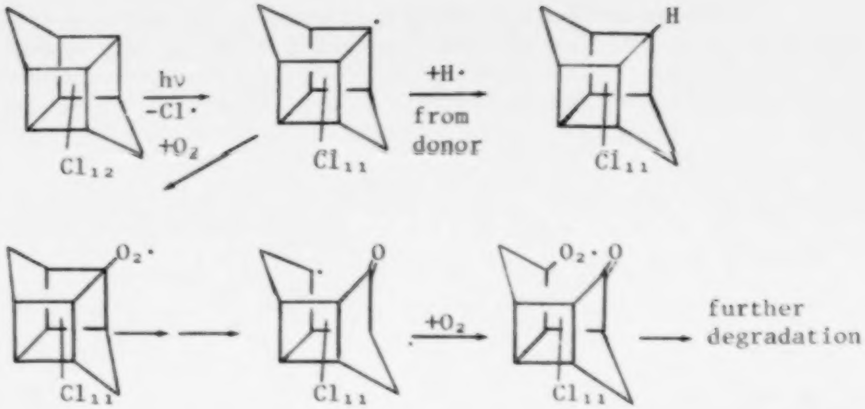

Oxidation products such as Kepone and other carbonyl-containing products may be as photolabile as mirex itself and further degraded to acidic, water-soluble compounds, which would not be extracted into hexane for subsequent analysis.

Experiments to study and identify the potentially numerous and complicated products in reaction mixtures from such photooxidations are beyond the resources of this project, but evidence for such extensive degradation is provided in the experiment with the 2500-watt lamp where neither mirex nor products were found after 100 hours of photolysis, but where some gas, possibly $CO_2$, was generated. Kepone itself has been reported to be exhaustively photolyzed in aqueous solution to give carbon dioxide and HCl as products (Knoevenagel and Himmelreich, 1973). In an aqueous environment, solution-phase photolysis of mirex could then lead to extensive photodegradation of the mirex structure. The monohydromirex or further reduced mirex structures may also be formed if sufficient concentrations of hydrogen species are available.

## 14.6 BIODEGRADATION

### 14.6.1 Development of Enrichment Cultures

In attempts to develop mirex-biodegrading systems, the following studies were conducted:

- Aerobic incubations of mirex with aeration effluents from sewage plants of the city of South San Francisco and the Shell Oil Company Refinery (Martinez, California).
- Anaerobic aqueous incubations of subsurface soils exposed to mirex in Florida and Mississippi with $^{14}C$-mirex.
- Anaerobic digestion of mirex with an inoculum obtained from an anaerobic sewage digester in the South San Francisco Sewage Plant.

Because mirex has such low solubility in water, 40 μg of mirex dissolved in methylene chloride was distributed on 1 g of 0.2-mm glass beads. The solvent was evaporated, and 200 ml of 4:5 diluted aeration effluent or anaerobic digester fluid was added to 500- or 250-ml Erlenmeyer flasks, respectively. It was anticipated that, with the greater relatively inert surface of the glass beads, solution of mirex would take place more readily if decomposition occurred. Appropriate additional sewage plant liquors (50 ml) were added at three weeks to the flasks containing South San Francisco sewage samples.

The results of the six-week aerobically incubated flasks are presented in Table 14.7. No significant degradation of mirex (as detected by GC) was observed in these flasks, which contained an equivalent of 200 μg mirex liter$^{-1}$.

TABLE 14.7. AEROBIC MIREX ENRICHMENT STUDIES WITH AERATION EFFLUENTS

| Source and treatment of aeration effluent[a] | % Recovery of mirex[b] |
|---|---|
| South San Francisco sewage plant | 92 ± 2 |
| South San Francisco sewage plant plus 50 μg ml$^{-1}$ Johnson's baby oil[c] | 100 ± 3 |
| South San Francisco sewage plant, autoclaved | 93 ± 2 |
| Shell Oil Refinery wastewater treatment plant | 97 ± 17 |
| Shell Oil Refinery wastewater treatment plant, autoclaved | 100 ± 1 |

[a] All effluents diluted with 0.25 vol of pH 7 phosphate-buffered $(NH_4)_2SO_4$ solution.

[b] Results are an average of GC analyses of duplicate flasks incubated in a rotary shaker at 25°C for 6 weeks.

[c] To provide n-paraffins, which are frequently good substrates and provide a good supply of H donors for substitution reactions.

The soil samples that had previously been exposed to mirex were from an experimental plot (#602025) in Gulfport, Mississippi, and a sample (#602038) of the muck from a pond at the site of an airplane crash near Sebring, Florida. Mirex was introduced into these samples in 1962 and 1968, respectively, and their mirex contents were reported as 0.096 and 2.5 μg g$^{-1}$, respectively (samples , analytical data, and analytical procedures were kindly provided by

Dr. J. H. Ford, USDA, Gulfport, Mississippi). Because these samples also contained Kepone and related products, $^{14}$C-mirex (California Bionuclear Corporation) was used to determine any possible change of mirex in suspension of 20 g soil, 30 ml $H_2O$, and 36 nCi (sp. act. 5.76 mCi/mmole) of $^{14}$C-mirex (added in 10 µl acetone). These suspensions were prepared in 50-ml (25 x 150 mm) Teflon-lined screw-capped tubes. Tubes were thoroughly sparged with nitrogen before they were sealed and they were shaken daily.

Extracts from individual tubes after thin layer chromatography (TLC) on silica gel (Andrade and Wheeler, 1974) when examined by x-ray film radioautography did not indicate any other radioactive component other than $^{14}$C-mirex. The x-ray radioautography would have detected less than 1% of conversion product to a 10-carbon compound if it had been separated by the TLC system. Band widths on the TLC plates corresponded to $R_f$ values of 0.63 to 0.68, and there was no discernible difference in intensity in the band of the radioautographs to suggest more than one component.

The anaerobic incubations with 200 ml of 80% anaerobic digester suspension from anaerobic digesters at the South San Francisco sewage plant were conducted at 37°C for up to 12 weeks, in standard tapered ground joint 250-ml Erlenmeyer flasks on which were 150 mm standard tapered extension tubes with aluminum-foil-covered rubber stoppers at the distal ends. These rubber stoppers were fitted with small-diameter Bunsen pressure relief valves. Half of the flasks had the equivalent of 50 µg succinic acid $ml^{-1}$ added weekly, and in each case the contents were sparged with nitrogen gas. Control recoveries obtained with the anaerobic digester sample added to the $^{14}$C-mirex deposited on glass beads were 97 ± 7% in four flasks. Recoveries of mirex after 12 weeks of anaerobic digestion averaged 93% and 92% (GC analyses) in duplicate flasks with and without added succinic acid, respectively.

### 14.6.2 Discussion

The above screening tests under aerobic conditions with aeration effluents from two sewage plants, the anaerobic studies with subsurface soil samples that were exposed to mirex for a long time, and the studies with anaerobic digester contents from a sewage plant clearly support the position that mirex, when added to natural waters, could resist biodegradation for long periods.

Our high recoveries of "mirex" may not in fact be absolutely indicative of lack of biodegradation. As has been reported by others, some undecachloromonohydromirex analogs may have similar GC retention times (Carlson et al., 1976) and may have $R_f$ values in TLC very close to those of mirex (Andrade and Wheeler, 1974). In this latter reference, the ratio of mirex:metabolite from anaerobic sludge digestion was 88:1 with $R_f$ values of 0.74 and 0.65, respectively. No explanation was presented for the differences in the mirex:metabolite ratios with the anaerobic sludge control and the mirex stock solution. In a subsequent paper relating to this metabolite (Andrade et al., 1975), the same $R_f$ by TLC was observed with the acetone:n-hexane (1:9 v/v) developing solvent they used previously, but with a double development with n-heptane, as we have used, the $R_f$ was 0.69. By comparison, our $R_f$ for mirex with a double development with n-heptane on silica gel plates was 0.65 (band width 0.63 to 0.68).

The difference in results obtained in the two laboratories may be attributed to experimental conditions. It is also questionable that we would have detected a second zone with an $R_f$ difference of 0.09 if we had a mirex:metabolite ratio greater than 100.

In the report on the characterization of a mirex metabolite from rhesus monkeys (Stein et al., 1976), a metabolite was observed at about two and five weeks after one single oral dose of $^{14}$C-mirex. The production of this metabolite after this prolonged period was attributed to bacterial action in the lower gut or in the feces. It was believed to be a monohydromirex. Jones and Hodges (1974) tested the activity of a variety of soil fungi, some bacteria, nine aerobic soils, and four anaerobic lake sediments and did not observe degradation of $^{14}$C-mirex.

It is apparent that, if microbial degradation of mirex can take place in a location, it will be very slow and it would form other polychlorinated monohydro analogs that would be expected to be toxic and biomagnified.

# 15. REFERENCES

Albersmeyer, W. 1958. Quantitative Determination of Aromatic Hydrocarbons in Aqueous Solutions. Gas-U. Wasserfach 99:269.

Alley, E. G. 1972. The Use of Mirex in Control of the Imported Fire Ant. J. Environ. Quality 2(1):52-61.

Alley, E.G., D. A. Dollar, B. R. Layton, and J. P. Minyard, Jr. 1973. Photochemistry of Mirex. J. Agr. Food Chem. 21(1):138-139.

Alley, E.G., B. R. Layton, and J. P. Minyard, Jr. 1974a. Identification of the Photoproducts of the Insecticides Mirex and Kepone. J. Agr. Food Chem. 22(3):442-445.

Alley, E.G., B. R. Layton, and J. P. Minyard, Jr. 1974b. Photoreduction of Mirex in Aliphatic Amines. J. Agr. Food Chem. 22(4):727-729.

Anashkina, N. P., S. M. Maksimov, and V. M. Dzyuba. 1972. Spectrophotometric Study of the Oxidation of Benzothiophene and 3-Methylbenzothiophene. Khim. Seraorg. Soedin., Soderzh. Neft. Nefteprod. 9:160-162; Chemical Abstracts 80:59814y (1974).

Andelman, J. B., and J. E. Snodgrass. 1974. Incidence and Significance of Polynuclear Aromatic Hydrocarbons in the Water Environment. CRC Critical Reviews in Environmental Control 4:69-83.

Andelman, J. B., and M. J. Suess. 1970. Polynuclear Aromatic Hydrocarbons in the Water Environment. Bull. World Health 43:479-508.

Andelman, J. B., and M. J. Suess. 1971. Photodecomposition of 3,4-Benzpyrene Sorbed on Calcium Carbonate. In: Organic Compounds in Aquatic Environments, Rudolfs Research Conference, Fifth 1969. pp. 439-468.

Andrade, Jr., P.S.L., and W. B. Wheeler. 1974. Biodegradation of Mirex by Sewage Sludge Organisms. Bull. Environ. Contamin. Toxicol. 11:415-416.

Andrade, Jr., P., W. B. Wheeler, and D. A. Carlson. 1975. Identification of a Mirex Metabolite. Bull. Environ. Contamin. Toxicol. 14:473-479.

American Pesticide Control Officials, Inc. 1959. Pesticide Chemicals Official Compendium. University of Maryland, College Park, Maryland.

Atkinson, B., and H. W. Fowler. 1974. The Significance of Microbial Film in Fermenters. Adv. Biochem. Eng. 3:224-227.

Aubry, M., M. N. Mayoral, and P. Villardry (1975), Bull. Soc. Chim. Fr., (3-4, Pt. 1), 500-2.

Baker, R. D., and H. G. Applegate. 1970. Effect of Temperature and Ultraviolet Radiation on the Persistence of Methyl Parathion and DDT in Soils. Agron. J. 62:509-512.

Ball, J. S. 1962. Nitrogen Compounds in Petroleum. Proc. Amer. Pet. Institute 42(8):27-30.

Bayly, R.C., S. Dagley, and D. T. Gibson. 1966. The Metabolism of Cresols by Species of *Pseudomonas*. Biochem. J. 101:293-301.

Ben'kovskii, V. G., A. Ya. Baikova, N. S. Lyubopytova, Y. N. Popov, E. A. Kruglov, A. I. Stekhun, and F. N. Latypova. 1974. Nitrogenous Bases of Diesel Fuel Produced by the Hydrogen Cracking of Arlam Petroleum Tar. Neftekhimiya 14:891-898; Chemical Abstracts 82:127279w (1975).

Benson, S. W. 1968. Thermochemical Kinetics. John Wiley and Sons, Inc. New York.

Braids, O. P., F. L. Hines, and G. W. Volk. 1967. The Occurrence of Carbazole in a Peat Soil. Soil Sci. Amer. Proc. 31:435-436.

Brocco, D., et al. 1973. Determination of Aza-heterocyclic Compounds in Atmospheric Dust by Combinations of Thin-layer and Gas Chromatography. J. Chromat. 84:361-367.

Brodeskii, E. S., V. S. Stopskii, N. V. Rasumov, and E. V. Gusinskaya. 1975. Refinement of the Structure-Group Characteristics of Nitrogenous Bases from Sakhalia Petroleums. Neftekhimiya 15:464-469: Chemical Abstracts 83:16666n (1975).

Calvert, J. G., and J. N. Pitts, Jr. 1966. Photochemistry, John Wiley & Sons, Inc., New York, pp. 780-782, 795-798.

Campbell, A. N. 1930. An Apparatus for the Determination of Solubility. J. Chem. Soc. London, Part I:179-180.

Carlson, D. A., K. D. Konyha, W. B. Wheeler, G. P. Marshall, and R. G. Zaylskie. 1976. Mirex in the Environment: Its Degradation to Kepone and Related Compounds. Science 194:939-941.

Castellano, A., J. P. Catteau, and A. Lablache-Combier. 1975. Mechanism of the Photochemical Substitution of 6-Membered Ring Monoazoaromatic Compounds by Methanol and Neutral and HCl Acidified Medium. Tetrahedron 31:2255-2261.

Chem. Eng. News 1976. Page 9. September 13, 1976.

Chi, C. T., J. A. Howell, and V. Pawlowsky. 1974. The Regions of Multiple Stable Steady States of a Biological Reactor with Wall Growth, Utilizing Inhibitory Substrates. Chem. Eng. Sci. 29:207-211.

Christensen, H. E., and T. T. Luginbyhl (eds.). 1975. Registry of Toxic Effects of Chemical Substances. U.S. Dept. of Health, Education and Welfare, National Institute for Occupational Safety and Health, Rockville, Maryland.

Christensen, H. E., E. J. Fairchild, B. S. Carroll, and R. J. Lewis, Sr. 1976. Registry of Toxic Effects of Chemical Substances, 1976 Edition. National Institute for Occupational Safety and Health, Rockville, Maryland. p. 404.

Claus, D. 1964. The Decomposition of Toluene by Soil Bacteria. J. Gen. Microbiol. 36:107-122.

Clemo, G. R. 1973. Some Aromatic Basic Constituents of Coal Soot. Tetrahedron 29:3987-3990.

Clugston, D. M., A. E. George, D. S. Montgomery, G. T. Smiley, and H. Sawatzky. 1976. Sulfur Compounds in Oils from the Western Canada Tar Belt. In: Shale Oil, Tar Sands, and Related Fuel Sources, T. F. Yen, ed. Advances in Chemistry Series 151, American Chemical Society, Washington, D.C. pp. 11-27.

Cobb, H. E., R. Atherton, and W. Olive. 1974. An Ecological Approach to the Problem of Biodegradation of Phenolic Wastes. Second Year Progress Report on AFOSR Grant 72-2356. University of Texas, San Antonio, Department of Biology, July 1974, 81 p.

Cook, J. W., and N. D. Pugh. 1957. A Quantitative Study of Cholinesterase-inhibiting Decomposition Products of Parathion Formed by Ultraviolet Light. J. Assoc. Offic. Agr. Chem. 40:227.

Cowan, C. T., and D. White. 1962. "Adsorption by Organo-Clay Complexes," Clays and Clay Minerals, Vol. 9, Proceedings of the Ninth Conferences on Clays and Clay Minerals. Pergamon Press, pp. 459-467.

Cowart, R. P., F. L. Bonner, and E. A. Epps, Jr. 1971. Rate of Hydrolysis of Seven Organophosphate Pesticides. Bull. Environ. Cont. Tox. 6:231-234.

CRC Handbook. 1974. 54th ed., R. C. Weast, Ed. in Chief. CRC Press, Cleveland, Ohio.

Cripe, C. R., and R. J. Livingston. 1977. Dynamics of Mirex and Its Principal Photoproducts in a Simulated Marsh System. Arch. Environ. Contam. Toxicol. 5:295-303.

Dagley, S., and M. D. Patel. 1957. Oxidation of *p*-Cresol and Related Compounds by a *Pseudomonas*. Biochem. J. 66:227-233.

Daughton, C. G., and D.P.H. Hsieh. 1976. Fate of the Dialkyl Thiophosphoryl Moiety of Parathion in a Bacterial Chemostat. Div. of Microb. and Biochem. Technol., 172nd National Meeting, American Chemical Society. Abstract 5.

Davis, W. W., and T. V. Parke, Jr. 1942. Determination of Solubilities of Extremely Low Order. J. Amer. Chem. Soc. 64:101-7.

Doehler, R. W., and W. A. Young. 1960. Some Conditions Affecting the Absorption of Quinoline by Clay Minerals in Aqueous Suspensions. Natl. Conf. on Clays and Clay Minerals. 9:468-483.

Dreisback, R. R. 1955. Physical Properties of Chemical Compounds. In: Advances in Chemistry, Series 15. American Chemical Society.

Eichelberger, J. W., and J. L. Lichtenberg. 1971. Persistence of Pesticides in River Water. Environ. Sci. Tech. 5:541-544.

Erickson, F. B. 1954. 2-Sulfobenzoic Acid. U.S. Patent 2,642,458, June 16, 1953; Chemical Abstracts 48:5219.

Fedoseeva, G. E., A. Y. Khesina, M. N. Poglazova, L. M. Shabad, and M. N. Meisel. 1968. Oxidation of Various Aromatic Polycyclic Hydrocarbons by Microorganisms. Dokl. Akad. Nauk SSSR 183:208-211.

Filatova, A. S., A. L. Koz'minykh, and V. B. Kapitul'skii. 1973. Determination of Some Aromatic Hydrocarbons in the Air of Coal Tar Processing Shops. Gig. Tr. Prof. Zabol. 17:49-52; Biol. Abstracts 58:5208 (1974).

Ford, J. F., and V. O. Young. 1965. Effect of Structure on the Rate of Reaction of Organosulfur Compounds with Peracetic Acid and tert-Butyl Hydroperoxide. Amer. Chemical Soc., Div. Petrol. Chem. Preprints 10(2):C111-122.

Friello, D. A., J. R. Mylroie, and A. M. Chakrabarty. 1975. Use of Genetically Engineered Multi-Plasmid Microorganisms for Rapid Degradation of Fuel Hydrocarbons. In: Proceeding of the Third International Biodegradation Symposium. J. Miles Sharpley and Arthur M. Kaplan, eds. Applied Science Publishers Ltd., London. pp. 205-214.

Frost, A. A., and R. G. Pearson. 1961. Kinetics and Mechanisms, 2nd ed. John Wiley and Sons, Inc., New York.

Funchess, M. J. 1917. The Nitrification of Pyridine, Quinoline, Quanidine Carbonate, etc., in Soils. Alabama Agric. Expt. Sta., Bull. 196; Tech. Bull. 3:65-82; Chemical Abstracts 11:3362 (1917).

Gaudy, A. F. Jr., M. Ramanathan, and B. S. Rao. 1967. Kinetic Behavior of Heterogeneous Populations in Completely Mixed Reactors. Biotechnol. Bioeng. 9:387-411.

Gibson, D. T. 1975. The Microbial Degradation of Aromatic Petroleum Products, Annual Report No. 2, prepared for Office of Naval Research Under Contract No. N00014-67-A-0126-0020, University of Texas at Austin, Austin, Texas (30 June 1975).

Gibson, D. T. 1975. Microbial Degradation of Polycyclic Aromatic Hydrocarbons. In: Proceedings of the Third International Biodegradation Symposium, J. M. Shapley and A. M. Kaplan, eds. Applied Science Publishers, Ltd., London. pp. 57-66.

Gibson, D. T. 1976. Microbial Metabolism of Polycyclic Aromatic Hydrocarbons. Preprints of the Division of Petroleum Chemistry, Inc., 172nd Annual Meeting of the Americal Chemical Society 21(3):409.

Gibson, D.T., V. Mahadevan, D. M. Jerina, H. Yagi, and H.J.C. Yeh. 1975. Oxidation of the Carcinogens Benzo[a]pyrene and Benzo[a]anthracene to Dihydrodiols by a Bacterium. Science 189:295-297.

Gibson, D. T., R. E. Roberts, M. C. Wells, and V. M. Kobal. 1973. Oxidation of a Biphenyl by a Beijerinckia species. Biochem. Biophys. Res. Comm. 50:211-219.

Gomma, H. M., and S. D. Faust. 1972. Chemical Hydrolysis and Oxidation of Parathion and Paraoxon in Aquatic Environments in "Fate of Organic Pesticides in Aquatic Environments." Amer. Chem. Soc. Publ. III:189-209.

Graetz, D., G. Chesters, T. C. Daniel, L. W. Newland, and G. B. Lee. 1970. Parathion Degradation in Lake Sediments. J. Water Pollut. Contr. Fed. 42:R76-R94.

Gregory, W. W., J. K. Reed, and L. E. Priester, Jr. 1969. Accumulation of Paration and DDT by Some Algae and Protozoa. J. Protozool. 16:69-71.

Grunwell, R. R., and R. H. Erickson. 1973. Photolysis of Parathion. New Products. J. Agr. Food Chem. 21:929-931.

Gunther, F. A., D. E. Ott, and F. E. Hearth. 1968. The Oxidation of Parathion to Paraoxon in Aqueous Media by Silver Oxide. Bull. Environ. Cont. Tox. 3:49-57.

Gunther, F. A., D. E. Ott, and M. Ittig. 1970. The Oxidation of Parathion to Paraoxon II by Use of Ozone. Bull. Environ. Cont. Tox. 5:87-94.

Haines, W. E., R. V. Helm, G. L. Cook, and J. S. Ball. 1956. Purification and Properties of Ten Organic Sulfur Compounds--Second Series. J. Phys. Chem. 60:549-555.

Haque, R., and D. Schmedding. 1975. A Method of Measuring the Water Solubility of Hydrophobic Chemicals: Solubility of Five Polychlorinated Biphenyls. Bull. Environ. Contam. Toxicol. 14:13-18.

Harrison, R. M., R. Perry, and R. A. Wellings. 1975. Polynuclear Aromatic Hydrocarbons in Raw, Potable and Waste Waters. Water Research 9:331-346.

Hartung, G. K., and D. M. Jewell. 1962. Carbazole, Phenazines and Dibenzofuran in Petroleum Products: Methods of Isolation and Determination. Anal. Chim. Acta 26:514-528.

Harwood, J. H., and S. J. Pirt. 1972. Quantitative Aspects of Growth of the Methane Oxidizing Bacterium *Methylococcus capsulatus* on Methane in Shake Flask and Continuous Chemostat Culture. J. Appl. Bact. 35:597-607.

Hashimoto, K. 1973. Oxidation of Phenols by Yeast. II. Oxidation of Cresols by *Candida tropicalis*. J. Gen. Appl. Microbiol. 19:171-187.

Hayatsu, R., R. G. Scott, L. P. Moore, and M. H. Studier. 1975. Aromatic Units in Coal. Nature 257:378-380.

Haynes, C. G., A. H. Turner and W. A. Waters. 1956. The Oxidation of Monohydric Phenols by Alkaline Ferricyanide. J. Chem. Soc., 2823.

Hesse, P. R. 1971. A Textbook of Soil Chemical Analysis. Chemical Publishing Company, Inc., New York. Chapter 11.

Hilgetag, G., and H. Teichman. 1965. The Alkylating Properties of Alkyl Thiophosphates. Angew Chem. 4:914-922.

Hill IV, J., et al. 1976. Dynamic Behavior of Vinyl Chloride in Aquatic Ecosystems. U.S. Environmental Protection Agency, EPA-600/3-76-011.

Hirakoso, S. 1968. Inactivation of Some Insecticides by Bacteria in Mosquito Breeding Polluted Water. Japan. J. Exp. Med. 38:327-334.

Hoffmann, D., G. Rathkamp, and S. Nesnow. 1969. Quantitative Determination of 9-Methylcarbazoles in Cigarette Smoke. Anal. Chem. 41:1256-1259.

Hoffmann, D., G. Rathkamp, and H. Wuziwodzki. 1968. Studies on Tobacco Smoke. VI. Determination of Carbazoles in Cigaret Smoke. Beitr. Tabakforsch. 4:253-263; Chem. Abstracts 71:196432 (1969).

Holden, C. 1976. Mirex: Persistent Pesticide on Its Way Out. Science 194:301-303.

Hollister, T. A., G. E. Walsh, and J. Forester. 1975. Mirex and Marine Unicellular Algae: Accumulation, Population Growth and Oxygen Evolution. Bull. Environ. Contamin. Toxicol. 14:753-759.

Holm-Hansen, O., C. R. Goldman, R. Richards, P. M. Williams. 1976. Chemical and Biological Characteristics of a Water Column in Lake Tahoe. Limn. Ocean. 21(4):548-562.

Hou, C. T., and A. I. Laskin. 1975. Microbial Conversion of Dibenzothiophene. Developments Indust. Microbiol. 17:351-362.

Howard, J. A. 1972. Absolute Rate Constants for Reactions of Oxyl Radicals. Adv. in Free Radical Chemistry 4:49-173.

Howell, J. A., C. T. Chi, and U. Pawlowsky. 1972. Effect of Wall Growth on Scale-Up Problems and Dynamic Operating Characteristics of the Biological Reactor. Biotechnol. Bioeng. 14:253-265.

Hsieh, D.P.H., and M. Munnecke. 1972. Accelerated Microbial Degradation of Concentrated Parathion. Proc. IV. Ferm. Symp. Ferment. Technol. 551-554.

Hudson, R. F. 1965. Structure and Mechanism in Organic Phosphorous Chemistry. Academic Press, New York.

International Agency for Research on Cancer. 1973. Monograph on the Evaluation of Carcinogenic Risk of the Chemical to Man: Certain Polycyclic Aromatic Hydrocarbons and Heterocyclic Compounds. World Health Organization, Geneva, Switzerland. Vol. 3.

Ivie, G. W., H. W. Dorough, and E. G. Alley. 1974. Photodecomposition of Mirex on Silica Gel Chromatoplates Exposed to Natural and Artificial Light. J. Agr. Food Chem. 22(6):933-935.

Jaglan, P. S., and F. A. Gunther. 1970. Comparison of Hydrolysis Rates of Methyl Parathion and Methyl Paraoxon by Gas Liquid Chromatography and Spectrometry. J. Chrom. Sci. 8:483-485.

Jones, A. S., and C. S. Hodges. 1974. Persistence of Mirex and Its Effects on Soil Microorganisms. J. Agr. Food Chem. 22:435-439.

Joussot-Dubien, J., and J. Houdard. 1967. Reversible Photolysis of Pyridine in Aqueous Solution. Tetrahedron Letters 44:4389-4391.

Kaplin, V. T., L. V. Semenchenko, and E. G. Ivanov. 1968. Decomposition of a Phenol Mixture in Natural Waters Miniature-scale Operation. Gidrokhim. Mater. 45:199-202; Chemical Abstracts 69:69508h.

Karr, C. and L-C. Ta-chuang. 1958. Spectrophotometric Analysis of the Distillable Low-Temperature Tar Bases. J. Inst. Eng. 31:522-527.

Karr, C., Jr., P. A. Estep, T.-C. L. Chang, and J. R. Comberiati. 1967. Identification of Distillable Paraffins, Olefins, Aromatic Hydrocarbons, and Neutral Heterocyclics from a Low-Temperature Bituminous Coal Tar. Bureau of Mines Bulletin 637. pp. 59-61.

Kataoka, N., A. Imanura, Y. Kawazoe, G. Chihara, and C. Nagata. 1966. Electron Spin Resonance Study on the Photo-induced Radicals from Related Compounds to Carcinogenic 4-Nitroquinoline 1-Oxide. Chem. Pharm. Bull. (Tokyo) 14:1171.

Kaywer, W. V., K.C.D. Hickman, W. W. Bond, M. S. Favero, and L. A. Carson. 1975. Bacteriological Evaluation of an Ultra-Pure Watertilling System. Appl. Microbiol. 30:704-706.

Ketelaar, J. A., H. R. Gersmann, and M. M. Beck. 1956. Metal-Catalysed Hydrolysis of Thiophosphoric Esters. Nature. 177:392.

Khesina, A. Y., N. P. Shcherbak, and L. M. Shabad. 1969. Destruction of Benzo[a]pyrene by Soil Microflora. Byull. Eksp. Biol. Med. 68:70-73. Chem. Abstracts 72:44240V, 1970.

King, P. H., and P. L. McCarty. 1968. A Chromatographic Model for Predicting Pesticide Migration in Soils. Soil Sci. 106:248-261.

Kirby, A. J. , and S. G. Warren. 1965. The Organic Chemistry of Phosphorous. Elsevier, New York.

Kirschenbaum, I. 1961. Bacteriological Desulfurization of Petroleum. U.S. Patent 2,975,103.

Kirso, U., and M. Gubergrits. 1972. Kinetics and Macromechanism of Oxidation of Phenols of Various Structures by Molecular Oxygen in Aqueous Alkali. J. Appl. Chem. (USSR) 45:847-851.

Klevens, H. B. 1950. Solubilization of Polycyclic Hydrocarbons. J. Phys. Colloid. Chem. 54:283-298.

Kliger, L., and B. Yaron. 1973. Parathion Recovery from Soils after a Short Contact Period. Bull. Environ. Cont. Tox. 13:714-719.

Knecht, Jr., A. T. (1962), Microbial Oxidation of Dibenzothiophene and Its Possible Application in the Desulfurization of Coal and Petroleum, Dissertation Absts. 22:3350.

Knoevenagel, K. and R. Himmelreich. 1973. Photolysis of Kepone and Kelevan. Z. Pflanzenkr. Pflanzenschutz 80(3-4):155-159; Chem Abstr. 80:70044t.

Knutson, H., A. M. Kadoum, T. L. Hopkins, G. F. Swoyer, and T. L. Harvey. 1971. Insecticide Usage and Residues in a Newly Developed Great Plains Irrigation District. Pesticides Monitor. J. 5:17-27.

Kobylinski, G. J., and R. J. Livingston. 1975. Movement of Mirex from Sediment and Uptake by the Hogchoker, Trinectes maculatus. Bull. Environ. Contamin. Toxicol. 14:692-698.

Kodama, K., S. Nakatani, K. Umehara, K. Shimizu, Y. Minoda, and K. Yamada. 1970. Microbial Conversion of Petro-sulfur Compounds, Part III, Isolation and Identification of Products from Dibenzothiophene. Agr. Biol. Chem. 34:1320-1324.

Kodama, K., K. Umehara, K. Shimizu, S. Nakatani, Y. Minoda, and K. Yamada. 1973. Identification of Microbial Products from Dibenzothiophene and Its Proposed Oxidation Pathway. Agr. Biol. Chem. 37:45-50.

Kortus, J., P. Macuch, J. Mayer, K. Durcek, and V. Kremery. 1971. Uptake of 32p-Parathion and 32p Imidan. J. Hyg. Epidemiol. Microbiol. Immunol. (Prague) 15:101-103.

Kostenbader, P. D., and J. W. Flecksteiner. 1968. Biological Oxidation of Coke Plant Weak Ammonia Liquor. Blast Furnace Steel Plant 56:475-480.

Kurita, S., T. Endo, H. Nakamura, T. Yaai, and N. Tamiya (1971), Decomposition of Some Organic Sulfur Compounds in Petroleum by Anaerobic Bacteria, J. Gen. Appl. Microbiol. 17:185-198.

Laborde, A., and D. T. Gibson (1975), Bacterial Oxidation of Dibenzothiophene, Abstracts of the Annual Meeting of the Amer. Soc. Microb. Q-45

Land, E. J., and G. Porter. 1963. Primary Photochemical Processis in Aromatic Molecules. Trans. Far. Soc. 59:2016-2026.

Landa, S., V. Solin, K. Burianek, and B. Pisecka. 1953. Biological Degradation of Phenols. I. Biological Oxidation of Monobasic Phenols. Chem. Listy. 47:622-629.

Lange's Handbook of Chemistry. 1973. John A. Dean, Ed. McGraw-Hill Book Company.

Langley, R. 1971. Practical Statistics Simply Explained. Dover Publications, New York 199-211.

Larsen, D. H., and R. L. Dimmick. 1964. Attachment and Growth of Bacteria on Surfaces of Continuous-Culture Vessels. J. Bact. 88:1380-1387.

Leadbetter, E. R., and J. W. Foster. 1959. Oxidation Products Formed from Gaseous Alkanes by the Bacterium Pseudomonas methanica. Archiv. Biochem. Biophys. 82:491-492.

Leaver, I. H. 1971. Semiquinone Radical Intermediates in the Eosin-Sensitized Photooxidation of Phenols. Austral. J. Chem. 24:891.

Lichtenstein, E. P., and K. R. Schulz. 1964. The Effects of Moisture and Microorganisms on the Persistence and Metabolism of Some Organophosphorous Insecticides in Soils with Special Emphasis on Parathion. J. Econ. Entomol. 57:618-627.

Lohrbacher, H., H. D. Puels, and H. W. Schlipkoeter. 1971. Studies on the Storage and Metabolism of 3,4-Benzpyrene (Benzo[a]pyrene) in Microorganisms. Zentralbl. Bakteriol. Parasitenkd. Infectionskr. Hyg. Erste Abt. Orig. Reihe B. Hyg. Praev. Med. 155:168-174. (Biol. Abs. 56:436. 1973).

Mabey, W., and T. Mill. 1978. Critical Review of Hydrolysis of Organic Compounds in Water Under Environmental Conditions. To be published in J. Phys. Chem. Ref. Data 7:000.

Mackay, D., and A. W. Wolkoff. 1973. Rate of Evaporation of Low Solubility Contaminants from Water Bodies to the Atmosphere. Environ. Sci. Tech. 7:611-614.

Maczynski, A., and Z. Maczynska. 1965. Vapor-Liquid Equilibrium in Binary System Quinoline-Water. Bull. Acad. Pol. Sci. 13:299-302.

Malaney, G. W., P. A. Lutin, J. J. Cibulka, and L. H. Hickerson. 1967. Resistance of Carcinogenic Organic Compounds to Oxidation by Activated Sludge. J. Water Pollution Control Adm. 39:2020-2029.

Maleszewska, J. 1974. Degradation of Methyl Parathion by Microorganisms Occurring in Surface Water and Sewage. Pol. Arch. Hydrobiol. 21:163-171.

Maliyantz, A. A. 1935. Desulfurizing Crude Oil by Microbiological Methods. Azerbaidzhanskoe Neftyanoe Khozyaistvo 6:89-93.

McEachern, D. M., et al. 1975. Enthalpies of Combustion and Sublimation and Vapor Pressures of Three Benzoquinolines. J. Chem. Eng. Data 20:226-228.

McGinnes, P. R., and V. L. Snoeyink. 1974. Determination of the Fate of Polynuclear Aromatic Hydrocarbons in Natural Water Systems. WRC Report No. 80, PB 232 168.

McKee, J. E., and H. W. Wolf (eds.). 1963. Water Quality Criteria, 2nd edition. The Resources Agency of California, State Water Resources Control Board, Sacramento, California.

McLafferty, F. W. 1973. Interpretation of Mass Spectra. 2nd ed. W. A. Benjamin, Inc., Reading, Massachusetts. p. 118.

Medvedev, V. A., and V. D. Davydov. 1973. Transformation of Individual Coal-Tar-Chemical-Industry Organic Products in a Chermozen Soil. Poehvodenie pp. 22-28; Chem. Abstracts 78:706185 (1973).

Merck Index, The, 7th Edition. 1960. Merck and Co., Inc. Rahway, New Jersey.

Merkel, P. B., and D. R. Kearns. 1972. Remarkable Solvent Effects on the Lifetime of $^1\Delta_g$ Oxygen. J. Amer. Chem. Soc. 94:1029-1030.

Midwest Research Institute and RvR Consultants. 1975. Initial Scientific and Minieconomic Review of Parathion. EPA-540/1-75-001 (PB-241 819/2WP), U.S. Environmental Protection Agency, Office of Pesticide Programs.

Mill, T., D. G. Hendry, W. R. Mabey, H. Richardson, B. Y. Lan, and A. Baraze. 1977. Oxidation of Organic Compounds in Dilute Aqueous Solution. Abstract. 173rd Meeting of the American Chemical Society, New Orleans, March 20-25. PHYS. 222.

Monod, J. 1949. The Growth of Bacterial Cultures. Am. Rev. Microbiol. 3:371-394.

Moriconi, E. J., B. Rakoczy, and W. F. O'Connor. 1961. Ozonolysis of Polycyclic Aromatics. VIII. Benzo[a]pyrene. J. Amer. Chem. Soc. 83:4618-4623.

Munnecke, D. M. 1976. Enzymatic Hydrolysis of Organophosphate Insecticides, A Possible Pesticide Disposal Method. Appl. Environ. Microbiol. 32:7-13.

Munnecke, D. M., and D.P.H. Hsieh. 1974. Microbial Decontamination of Parathion and p-Nitrophenol in Aqueous Media. Appl. Microbiol. 28(2):212-217.

Munnecke, D. M., and D.P.H. Hseih. 1975. Microbial Metabolism of a Parathion-Xylene Pesticide Formulation. Appl. Microbiol. 30(4):575-580.

Munnecke, D. M., and D.P.H. Hsieh. 1976. Pathways of Microbial Metabolism of Parathion. Appl. Environ. Microbiol. 31(1):63-69.

Musso, H. 1967. "Phenol Coupling" in Oxidative Coupling of Phenols, W. I. Taylor and A. R. Battersby (eds.). Marcel-Dekker, Inc., New York, pp. 1-94.

Nakatani, S., T. Akasaki, K. Kodama, Y. Minoda, and K. Yamada. 1968. Microbial Conversion of Petro-sulfur Compounds Part II, Culture Conditions of Dibenzothiophene--Utilizing Bacteria. Agr. Biol. Chem. 32:1205-1211.

National Academy of Science. 1972. Report of the Mirex Advisory Committee to William D. Ruckelshaus, Administrator, Environmental Protection Agency. National Academy of Science, Washington, D.C.

National Academy of Sciences. 1972. Particulate Polycyclic Organic Matter. National Academy of Sciences, Washington, D.C.

Naucke, W., H. V. Laaser, and F. Tarkmann. 1972. Water-Soluble Organic Substances in Slightly Decomposed Sphagnum Peats. Fourth Proceedings of Intern. Peat Congress 4:45-60.

Naumann, K. 1967. Decomposition of Parathion by Soil Bacteria. Phytopathol. Z. 60:343-357.

Niaussat, P., and J. Ottenwalder. 1969. Apparation of Benzo (3,4) pyrene in Cultures of Marine Phyto-plankton; Incidence of Associate Bacteria. Rev. Hyg. Med. Soc. 17:487-496. (Biol. Abstracts 53:26642, 1972).

Oka, S. 1962. Transfer of Antiseptics of Microorganisms and Their Toxic Effects. VI. Toxic Effect and Adsorption of Phenols and Esters of Acid Antiseptics on Bacterial Cells. Agr. Biol. Chem. (Tokyo) 20:515-525.

Pawlowsky, V., and J. A. Howell. 1973a. Mixed Culture Bioxidation of Phenol. I. Determination of Kinetic Parameters. Biotechnol. and Bioeng. 15(5):889-896.

Pawlowsky, V., and J. A. Howell. 1973b. Mixed Culture Biooxidation of Phenol. II. Steady State Experiments in Continuous Culture. Biotechnol. Bioeng. 15(5):897-903.

Lawlowsky, V., J. A. Jowell, and C. T. Chi. 1973. Mixed Culture Biooxidation of Phenol. III. Existence of Multiple Steady States in Continuous Culture with Wall Growth. Biotechnol Bioeng. 15(5):905-916.

Perrin, D. D. 1965. Dissociation Constants of Organic Bases in Aqueous Solution. Butterworth, London.

Pfoertner, K., and D. Boese. 1970. Die Photosensibilisierte Oxydation einwertiger Phenols zu Chinonen. Helv. Chim. Acta 53:1553-1566.

Phillips, L. S., and C. Hinshelwood. 1953. Adaption of Aerobacter aerogenes to Resist Phenols and Various Phenols. J. Chem. Soc., 3679-3683.

Pitts, J. N., Jr., J.K.S. Wan, and E. A. Schuck. 1964. Photochemical Studies in an Alkali Halide Matrix. I. An o-Nitrobenzaldehyde Actinometer and Its Application to a Kinetic Study of the Photoreduction of Benzophenone by Benzhydrol in a Pressed Potassium Bromide Disk. J. Amer. Chem. Soc. 86:3606-3610.

Poglazova, M. N., and M. N. Meisel. 1971. Localization of Benzo[a]pyrene in Bacterial Cells. Mikrobiologiya 40:1050-1053.

Poglazova, M. N., G. E. Fedoseeva, A. Y. Khesina, M. N. Meisel, and L. M. Shabad. 1966. Modification of Benzpyrene by Soil Microorganisms. Dokl. Akad. Nauk. SSSR 169:1174-1177.

Poglazova, M. N., G. E. Fedoseeva, A. J. Khesina, M. N. Meissei, and L. M. Shabad. 1967a. Destruction of Benzo[a]pyrene by Soil Bacteria. Life Sciences 6:1053-1062.

Poglazova, M. N., G. E. Fedoseeva, A. J. Khesina, M. N. Meissei, and L. M. Shabad. 1967b. Further Investigations of the Decomposition of Benzo[a] pyrene by Soil Bacteria. Dokl. Biol. Sci. 176:1165-1167.

Poglazova, M. N., G. E. Fedoseeva, A. J. Khesina, M. N. Meissei, and L. M. Shabad. 1968. The Oxidation of Benzo[a]pyrene by Microorganisms in Relation to Its Concentration in the Medium. Dokl. Biol. Sci. 179:1460-1462.

Poglazova, M. N., G. E. Fedoseeva, A. Y. Khesina, M. N. Meisel, and L. M. Shabad. 1971. Benzo[a]pyrene Metabolism by Microflora of Various Soils and Separate Species of Microorganisms. Dokl. Akad. Nauk SSSR 198:1211-1213.

Poglazova, M. N., A. Y. Khesina, G. E. Fedoseeva, M. N. Meisel, and L. M. Shabad. 1972. Destruction of Benzo[a]pyrene in Waste Waters by Microorganisms. Dokl. Akad. Nauk SSSR 204:222-225.

Ponec, R., and M. Prochazka. 1974. Effect of Substitution on Oxidation of Sulfides. Coll. Czech. Chem. Commun. 39:2088-2098. Chem. Abstr. 82:111295n (1975).

Poulson, R. E., C. M. Frost, and H. B. Jensen. 1974. Characteristics of Synthetic Crude from Crude Shale Oil Producted by in situ Combustion Retorting. Amer. Chem. Soc., Div. Fuel Chem., Prepr. 19(2):175-182.

Present, D. 1958. Kinetic Theory of Gases. McGraw-Hill Book Company, New York. 280pp.

Pupp, C., R. C. Lao, J. J. Murray, R. F. Pottie. 1974. Equilibrium Vapor Concentrations of Some Polycyclic Aromatic Hydrocarbons, Arsenic Trioxide ($As_4O_6$) and Selenium Dioxide, and the Collection Efficiencies of these Air Pollutants. Atmos. Environ. 8:915-25.

Radding, S. B., T. Mill, C. W. Gould, D. H. Liu, H. L. Johnson, D. C. Bomberger, and C. V. Fojo. 1976. The Environmental Fate of Selected Polynuclear Aromatic Hydrocarbons. EPA 560/2-75-009, Environmental Protection Agency, Washington, D.C., February 1976. 122pp.

Ray, S., and R. W. Frei. 1972. Separation of Polynuclear Aza-heterocyclics by High Speed Liquid Chromatography on a Chemically Bonded Stationary Phase. J. Chromatography. 71:451-457.

Reid, R. C., and T. K. Sherwood. 1966. The Properties of Gases and Liquids. 2nd ed. McGraw-Hill Book Company, New York.

Robbins, W. J. 1916. The Cause of the Disappearance of Coumarin, Vanillin, Pyridine and Quinoline in the Soil. Science 44:894-895.

Robbins, W. J. 1917. The Cause of the Disappearance of Coumarin, Pyridine, and Quinoline in the Soil. Alabama Agric. Expt. Station, Bull. 195; Tech. Bull. 2:49-64; Chemical Abstracts 11:3362 (1917),

Robbins, W. R. 1971. Student Projects on the Oxidation by Marine Bacteria of Aromatic Compounds Found in Oil. Massachusetts Institute of Technology, Report No. MITSG 71-10, Cambridge, Mass., June 28, 1971.

Ruzicka, J. H., J. H. Thomson, and B. B. Wheals. 1967. The Gas Chromatographic Determination of Organophosphorous Pesticides. II. A Comparative Study of Hydrolysis Rates. J. Chromatog. 31:37-47.

Sagardia, F., J. J. Rigau, A. Martinez-Lahoz, F. Fuentes, C. Lopez, and W. Flores. 1975. Degradation of Benzothiophene and Related Compounds by a Soil Pseudomonas in an Oil Aqueous Environment, Applied Microbiol. 29:722-725.

Sawicki, E. et al. 1965. Use of Gas-liquid and Thin-layer Chromatography in Characterizing Air Pollutants by Fluorimetry. Talania. 13:619-629. Chemical Abstracts.

Saltzman, S., U. Mingelgrin, and B. Yaron. 1976. Role of Water in the Hydrolysis of Parathion and Methyl Parathion on Kaolinite. J. Agric. Food Chem. 24(4):739-743.

Saltzman, S., and B. Yaron. 1972. Parathion Adsorption from Aqueous Solutions as Influenced by Soil Components. Pestic. Chem., Proc. Int. Congr. Pestic. Chem. 2nd. 6:87-100.

Sandi, E. 1959. Beitrage zur Analyse einiger insecticider Thiophosphorsäureester. Beit. Anal. Chem. 167:241-245.

Schmidt, C. E., A. F. Sharkey, Jr., and R. A. Friedel. 1974. Mass Spectrometric Analysis of Product Water from Coal Gasification. Bureau of Mines Advancing Energy Utilization Technology Program, Technical Progress Report 86, December 1974.

Sethunathan, N. 1973. Parathion Degradation in Submerged Rice Soils in the Philippines. J. Agr. Food Chem. 21:504-506.

Sethunathan, N., and T. Yoshida. 1973. Parathion Degradation in Submerged Rice Soils in the Philippines. J. Agr. Food Chem. 21:504-506.

Shabad, L. M. 1968. The Distribution and the Fate of the Carcinogenic Hydrocarbon Benzo[a]pyrene. Z. Krebsforsch. 70:204-210.

Shabad, L. M., Y. L. Cohan, A. P. Ilnitsky, A. Y. Khesina, N. P. Shcherbak, and G. A. Smirnov. 1971. The Carcinogenic Hydrocarbon Benzo[a]pyrene in the Soil. J. Natl. Cancer Inst. 47:1179-1192.

Sidderamappa, R., K. P. Rajaram, and N. Sethunathan. 1973. Degradation of Parathion by Bacteria Isolated from Flooded Soil. Appl. Microbiol. 26(6):846-849.

Silvey, J.K.G., and A. W. Roach. 1975. The Taste and Odor Producing Aquatic Actinomycetes. CRC Critical Reviews in Environmental Control 5:233-273.

Sisler, F. D., and C. Zobell 1947. Microbial Utilization of Carcinogenic Hydrocarbons. Science 106:521-522.

Slater, J. H., A. T. Bull, and E. Senior. 1976. Microbial Interaction-Competition. Proceed. Soc. Gen. Microbiol. 3:103.

Smith, L. D. 1976. Inhibition of *Clostridium betulinum* by Strains of *Clostridium perfringens* Isolated from Soil. Appl. Microbiol. 30:319-323.

Snyder, L. R. 1969. Nitrogen and Oxygen Compound Types in Petroleum. Total Analyses of a 400-700°F Distillate from a California Crude Oil. Anal. Chem. 41:314-324.

Stein, V. B., K. A. Pittman, and M. W. Kennedy. 1976. Characterization of a Mirex Metabolite from Monkeys. Bull. Environ. Contam. Toxicol. 15:140-146.

Stevens, B., and B. E. Alger. 1968. The Photoperoxidation of Unsaturated Organic Molecules; II. The Autoperoxidation of Aromatic Hydrocarbons. J. Phys. Chem. 72:3468-3474.

Stevens, B., S. R. Perez, and J. A. Ors. 1974. Photoperoxidation of Unsaturated Organic Molecules: XIV. $O_2\ {}^1\Delta_g$ Acceptor Properties and Reactivity. J. Amer. Chem. Soc. 96:6846-6850.

Strawinski, R. J. 1950. Method of Desulfurizing Crude Oil, U.S. Patent 2,521,761.

Strawinski, R. J. 1951. Purification of Substances by Microbial Action. U.S. Patent 2,574,070.

Suess, M. J. 1972. Aqueous Solutions of 3,4-Benzpyrene. Water Research 6:981-985.

Suess, M. J. 1976. The Environmental Load and Cycles of Polycyclic Aromatic Hydrocarbons. In: International Conference on Environmental Screening and Assessment, Las Vegas, Nevada, September 14-19, 1975. Institute of Electrical and Electronic Engineers, Inc.

Suta, B. E. 1977. Human Population Exposures to Mirex and Kepone. Discussion Draft under EPA ORD Contract 68-01-4314.

Tagatz, M. E., P. W. Bothwick, J. M. Ivey, and J. Knight. 1976. Effects of Leached Mirex on Experimental Communities of Estaurine Animals. Arch. Environ. Contam. Toxicol. 4(4):435-442.

Topiwala, H. H., and G. Hamer. 1971. Effect of Wall Growth in Steady State Continuous Cultures. Biotechnol. Bioengin. 13(6):919-922.

Tsivoglou, E. C., et al. 1965. Tracer Measurements of Atmospheric Reaeration-I. Laboratory Studies. J. Water Pollution Control Federation 37:1343-1362.

Utkina, L. F. 1965. Identification of Some Aromatic Hydrocarbons in Coal Tar on the Basis of Quasilinear Luminescence and Absorption Spectra at Low Temperatures. Tr. Mezhvuz. Konf. Peddgog. Inst. Radiofiz. Specktrosk. 1st Moscow. 53-8; Chem. Abstracts 66:67743a (1967).

Vernon, C. A. 1957. Phosphoric Esters and Related Compounds. The Chem. Soc., Spec. Publ. 8, London.

von Rumker, R., E. W. Lawless, A. F. Meiners, K. A. Lawrence, G. L. Kelar, and F. Horay. 1974. Production, Distribution, Use and Environmental Impact Potential of Selected Pesticides. EPA 540/1-74-001, U.S. Environmental Protection Agency, Office of Pesticide Programs.

Vymetal, J. 1974a. Quinoline Bases in Black Coal Tar. Chem. Listy 68:1234-1253; Chemical Abstracts 82:75217c (1975).

Vymetal, J. 1974b. Separation by Rectification of Pyridine Bases from Products of High Temperature Carbonization of Coal. Erdoel Kohle, Erdgas, Petrochem. Brennst.-Chem. 27:8-12; Chemical Abstracts 81:138391g (1974).

Walker, J. D., and R. R. Colwell. 1974. Microbial Petroleum Degradation: Use of Mixed Hydrocarbon Substrates. Applied Microbiol. 27:1053-1060.

Walker, J. D., and R. R. Colwell. 1975. Effects of Petroleum on Estuarine and Marine Microorganisms. Can. J. Microbiol. 21:305-13.

Walker, J. D., R. R. Colwell and L. Petrakis (1975), Microbial Petroleum Degradation: Application of Computerized Mass Spectrometry, Can. J. Microbiol. 21:1760-1767.

Walker, J. D., R. R. Colwell, and L. Petrakis. 1976. Biodegradation of Petroleum by Chesapeake Bay Sediment Bacteria. Can. J. Microbiol. 22:423-428.

Walling, C., and C. G. Papaioannou. 1968. Bond Dissociation Energies of t-Butyl Hypohalites. J. Phys. Chem. 72:2260-2262.

Waters, W. A. 1964. Mechanism of Oxidation of Organic Compounds. Methuen and Co., Ltd., London, 152 pages.

Weber, K. 1976. Degradation of Parathion in Seawater. Water Research 105: 237-241.

Wiberg, K. B. 1965. Oxidation in Organic Chemistry. Academic Press, New York, 443 pages.

Wilkinson, T. G., H. H. Topiwala, and G. Hamer. 1974. Interactions in a Mixed Bacterial Population Growing on Methane in Continuous Culture. Biotechnol. and Bioengin. 16:41-59.

Williamson, K., and P. L. McCarty. 1976a. A Model of Substrate Utilization by Bacterial Films. J. Water Pollut. Control Fed. 48(1):9-24.

Williamson, K., and P. L. McCarty. 1976b. Verification Studies of the Biofilm Model for Bacterials Substrate Utilization. J. Water Pollut. Control Fed. 48(2):281-296.

Wise, J. 1975. The Lake Tahoe Study, as Requested by the 92nd Congress in Section 114 of The Federal Water Pollution Control Act Amendments of 1972. U.S. Environmental Protection Agency.

Wodzinski, R. S., and D. Bartolini. 1972. Physical State in Which Naphthalene and Bibenzyl are Utilized by Bacteria. Appl. Microbiol. 23:1077-1081.

Wodzinski, R. S., and J. E. Coyle. 1074. Physical State of Phenanthrene for Utilization by Bacteria. Appl. Microbiol. 27:1081-1084.

Wodzinski, R. S., and M. J. Johnson. 1968. Yields of Bacterial Cells from Hydrocarbons. Appl. Microbiol. 16:1886-1891.

Wodzinski, R. S., and D. Larocca. 1977. Bacterial Growth Kinetics on Diphenylmethane and Naphtharene-Heptamethylnonane Mixtures. Appl. Microbiol. 33:660-665.

Wolfe, N. L., R. G. Zepp, G. L. Baughman, R. C. Fincher, and J. A. Gordon. 1976. Chemical and Photochemical Transformation in Selected Pesticides in Aquatic Systems. U.S. Environmental Protection Agency, EPA-600/3-76-067.

Wu, W.R.K., and H. H. Storch. 1967. Hydrogenation of Coal and Tar. Bulletin 633, U.S. Dept. of the Interior, Bureau of Mines, pp. 154.

Yamada, K., Y. Minoda, K. Kodama, S. Nakatani, and T. Akasaki. 1968. Microbial Conversion of Petroleum Compounds Part I, Isolation and Identification of Dibenzothiophene Utilizing Bacteria. Agr. Biol. Chem. 32:840=845.

Yang, R. D., and A. E. Humphrey. 1975. Dynamic and Steady State Studies of Phenol Biodegradation in Pure and Mixed Cultures. Biotechnol. Bioeng. 17:1211-1235.

Yasuno, M., S. Hirakoso, M. Sasa, and M. Uchida. 1965. Inactivation of Some Organophosphorous Insecticides by Bacteria in Polluted Water. Jap. J. Exp. Med. 35(6):545-563.

Zepp, R. G., and D.M. Cline. 1977. Rates of Direct Photolysis in Aquatic Environments. Environ. Sci. Technol. 11:359-366.

Zobell, E. 1943. The Effect of Solid Surfaces upon Bacterial Activity. J. Bact. 46:39-56.

Zobell, C. E. 1953. Process of Removing Sulfur from Petroleum Hydrocarbons and Apparatus. U.S. Patent 2,641,564.

Zherebtsov, I. P., and V. P. Lopatinskii. 1970. Izv. Tomsk. Politekh. Inst. 163:12-17; Chem. Abstracts 75:117862x (1971).

Zuckermann, B. M., K. Deubert, M. Mackiewicz, and H. Gunner. 1970. Studies on Biodegradation of Parathion. Plant Soil. 33(2):273-281.

Appendix A

## INPUT DATA FOR NINE-COMPARTMENT MODEL

The nine-compartment computer model was used to simulate the transport and transformation of eleven compounds in a pond, a river, a eutrophic lake, and an oligotrophic lake. The sorption partition coefficients and the rate constants used as input to the computer model are given in Tables A.1 through A.43. All rate and equilibrium values are at 25°C.

### TABLE A.1. NINE-COMPARTMENT COMPUTER MODEL INPUTS FOR *p*-CRESOL: POND SIMULATION

| | Water (compartment 1) | Sediment (compartment 7) |
|---|---|---|
| Sorption partition coefficient | 10 | 10 |
| Pseudo-first-order rate constants | | |
| Volatilization ($hr^{-1}$) | 0 | 0 |
| Photolysis ($hr^{-1}$) | $2 \times 10^{-4}$ | 0 |
| Oxidation ($hr^{-1}$) | 0 | 0 |
| Hydrolysis ($hr^{-1}$) | 0 | 0 |
| Kinetic constants for biodegradation | | |
| Bacterial population (cells $ml^{-1}$) | $10^6$ | $10^7$ |
| Active bacterial population (cells $ml^{-1}$) | $10^5$ | $10^5$ |
| Maximum growth rate ($hr^{-1}$) | 0.56 | 0.28 |
| Half-saturation constant ($\mu g\ ml^{-1}$) | 0.99 | 1.98 |
| Yield factor (cells $\mu g^{-1}$) | $10^6$ | $10^6$ |

TABLE A.2. NINE-COMPARTMENT COMPUTER MODEL INPUTS
FOR *p*-CRESOL:
RIVER SIMULATION

| | Water compartments | | | Sediment compartments | | |
|---|---|---|---|---|---|---|
| | 1 | 2 | 3 | 7 | 8 | 9 |
| Sorption partition coefficient | 10 | 10 | 10 | 10 | 10 | 10 |
| Pseudo-first-order rate constants | | | | | | |
| Volatilization ($hr^{-1}$) | 0 | 0 | 0 | 0 | 0 | 0 |
| Photolysis ($hr^{-1}$) | $5 \times 10^{-4}$ | $5 \times 10^{-4}$ | $5 \times 10^{-4}$ | 0 | 0 | 0 |
| Oxidation ($hr^{-1}$) | 0 | 0 | 0 | 0 | 0 | 0 |
| Hydrolysis ($hr^{-1}$) | 0 | 0 | 0 | 0 | 0 | 0 |
| Kinetic constants for biodegradation | | | | | | |
| Bacterial population (cells $ml^{-1}$) | $10^6$ | $10^6$ | $10^6$ | $10^7$ | $10^7$ | $10^7$ |
| Active bacterial population (cells $ml^{-1}$) | $10^5$ | $10^5$ | $10^5$ | $10^5$ | $10^5$ | $10^5$ |
| Maximum growth rate ($hr^{-1}$) | 0.56 | 0.56 | 0.56 | 0.28 | 0.28 | 0.28 |
| Half-saturation constant ($\mu g\ ml^{-1}$) | 0.99 | 0.99 | 0.99 | 1.98 | 1.98 | 1.98 |
| Yield factor (cells $\mu g^{-1}$) | $10^6$ | $10^6$ | $10^6$ | $10^6$ | $10^6$ | $10^6$ |

TABLE A.3. NINE-COMPARTMENT COMPUTER MODEL INPUTS
FOR p-CRESOL:
EUTROPHIC LAKE SIMULATION

| | Water compartments | | | | Sediment compartments | | |
|---|---|---|---|---|---|---|---|
| | 1 | 2 | 3 | 5 | 7 | 8 | 9 |
| Sorption partition coefficient | 10 | 10 | 10 | 10 | 10 | 10 | 10 |
| Pseudo-first-order rate constants | | | | | | | |
| Volatilization ($hr^{-1}$) | 0 | 0 | 0 | 0 | 0 | 0 | 0 |
| Photolysis ($hr^{-1}$) | $2 \times 10^{-4}$ | $2 \times 10^{-4}$ | $2 \times 10^{-4}$ | $2 \times 10^{-5}$ | 0 | 0 | 0 |
| Oxidation ($hr^{-1}$) | 0 | 0 | 0 | 0 | 0 | 0 | 0 |
| Hydrolysis ($hr^{-1}$) | 0 | 0 | 0 | 0 | 0 | 0 | 0 |
| Kinetic constants for biodegradation | | | | | | | |
| Bacterial population (cells $ml^{-1}$) | $10^6$ | $10^6$ | $10^6$ | $10^6$ | $10^7$ | $10^7$ | $10^7$ |
| Active bacterial population (cells $ml^{-1}$) | $10^5$ | $10^5$ | $10^5$ | $10^5$ | $10^5$ | $10^5$ | $10^5$ |
| Maximum growth rate ($hr^{-1}$) | 0.56 | 0.56 | 0.56 | 0.38 | 0.28 | 0.28 | 0.28 |
| Half-saturation constant ($\mu g\ ml^{-1}$) | 0.99 | 0.99 | 0.99 | 1.5 | 1.98 | 1.98 | 1.98 |
| Yield factor (cells $\mu g^{-1}$) | $10^6$ | $10^6$ | $10^6$ | $10^6$ | $10^6$ | $10^6$ | $10^6$ |

TABLE A.4. NINE-COMPARTMENT COMPUTER MODEL INPUTS FOR p-CRESOL: OLIGOTROPHIC LAKE SIMULATION

| | Water compartments | | | | Sediment compartments | | |
|---|---|---|---|---|---|---|---|
| | 1 | 2 | 3 | 5 | 7 | 8 | 9 |
| Sorption partition coefficient | 10 | 10 | 10 | 10 | 10 | 10 | 10 |
| Pseudo-first-order rate constants | | | | | | | |
| Volatilization ($hr^{-1}$) | 0 | 0 | 0 | 0 | 0 | 0 | 0 |
| Photolysis ($hr^{-1}$) | $1 \times 10^{-2}$ | $1 \times 10^{-3}$ | $1 \times 10^{-3}$ | $1 \times 10^{-4}$ | 0 | 0 | 0 |
| Oxidation ($hr^{-1}$) | 0 | 0 | 0 | 0 | 0 | 0 | 0 |
| Hydrolysis ($hr^{-1}$) | 0 | 0 | 0 | 0 | 0 | 0 | 0 |
| Kinetic constants for biodegradation | | | | | | | |
| Bacterial population (cells $ml^{-1}$) | $10^2$ | $10^2$ | $10^2$ | $10^2$ | $10^7$ | $10^7$ | $10^7$ |
| Active bacterial population (cells $ml^{-1}$) | 10 | 10 | 10 | 10 | 10 | 10 | 10 |
| Maximum growth rate ($hr^{-1}$) | 0.56 | 0.56 | 0.56 | 0.38 | 0.28 | 0.28 | 0.28 |
| Half-saturation constant ($\mu g\ ml^{-1}$) | 0.99 | 0.99 | 0.99 | 1.5 | 1.98 | 1.98 | 1.98 |
| Yield factor (cells $\mu g^{-1}$) | $10^6$ | $10^6$ | $10^6$ | $10^6$ | $10^6$ | $10^6$ | $10^6$ |

### TABLE A.5. NINE-COMPARTMENT COMPUTER MODEL INPUTS FOR BENZ[a]ANTHRACENE: POND SIMULATION

| | Water (compartment 1) | Sediment (compartment 7) |
|---|---|---|
| Sorption partition coefficient | $2.5 \times 10^4$ | $2.5 \times 10^4$ |
| Pseudo-first-order rate constants | | |
| Volatilization ($hr^{-1}$) | $7.0 \times 10^{-6}$ | 0 |
| Photolysis ($hr^{-1}$) | $1.4 \times 10^{-2}$ | 0 |
| Oxidation ($hr^{-1}$) | 0 | 0 |
| Hydrolysis ($hr^{-1}$) | 0 | 0 |
| Biodegradation ($hr^{-1}$) | 0 | 0 |

## TABLE A.6. NINE-COMPARTMENT COMPUTER MODEL INPUTS FOR BENZ[a]ANTHRACENE: RIVER SIMULATION

| | Water compartments | | | Sediment compartments | | |
|---|---|---|---|---|---|---|
| | 1 | 2 | 3 | 7 | 8 | 9 |
| Sorption partition coefficient | $2.5 \times 10^4$ | $2.5 \times 10^4$ | $2.5 \times 10^4$ | $2.5 \times 10^4$ | $2.5 \times 10^4$ | $2.5 \times 10^4$ |
| Pseudo-first-order rate constants | | | | | | |
| Volatilization ($hr^{-1}$) | $7.0 \times 10^{-6}$ | $7.0 \times 10^{-6}$ | $7.0 \times 10^{-6}$ | 0 | 0 | 0 |
| Photolysis ($hr^{-1}$) | $3.4 \times 10^{-2}$ | $3.4 \times 10^{-2}$ | $3.4 \times 10^{-2}$ | 0 | 0 | 0 |
| Oxidation ($hr^{-1}$) | 0 | 0 | 0 | 0 | 0 | 0 |
| Hydrolysis ($hr^{-1}$) | 0 | 0 | 0 | 0 | 0 | 0 |
| Biodegradation ($hr^{-1}$) | 0 | 0 | 0 | 0 | 0 | 0 |

TABLE A.7. NINE-COMPARTMENT COMPUTER MODEL INPUTS FOR BENZ[a]ANTHRACENE: EUTROPHIC LAKE SIMULATION

| | Water compartments | | | | Sediment compartments | | |
|---|---|---|---|---|---|---|---|
| | 1 | 2 | 3 | 5 | 7 | 8 | 9 |
| Sorption partition coefficient | $2.5 \times 10^4$ | $2.5 \times 10^4$ | $2.5 \times 10^4$ | $2.5 \times 10^4$ | $2.5 \times 10^4$ | $2.5 \times 10^4$ | $2.5 \times 10^4$ |
| Pseudo-first-order rate constants | | | | | | | |
| Volatilization ($hr^{-1}$) | $7.0 \times 10^{-6}$ | $7.0 \times 10^{-6}$ | $7.0 \times 10^{-6}$ | 0 | 0 | 0 | 0 |
| Photolysis ($hr^{-1}$) | $1.4 \times 10^{-2}$ | $1.4 \times 10^{-2}$ | $1.4 \times 10^{-2}$ | $1.4 \times 10^{-3}$ | 0 | 0 | 0 |
| Oxidation ($hr^{-1}$) | 0 | 0 | 0 | 0 | 0 | 0 | 0 |
| Hydrolysis ($hr^{-1}$) | 0 | 0 | 0 | 0 | 0 | 0 | 0 |
| Biodegradation ($hr^{-1}$) | 0 | 0 | 0 | 0 | 0 | 0 | 0 |

TABLE A.8. NINE-COMPARTMENT COMPUTER MODEL INPUTS FOR BENZ[a]ANTHRACENE: OLIGOTROPHIC LAKE SIMULATION

| | Water compartments | | | | Sediment compartments | | |
|---|---|---|---|---|---|---|---|
| | 1 | 2 | 3 | 5 | 7 | 8 | 9 |
| Sorption partition coefficient | $2.5 \times 10^4$ | $2.5 \times 10^4$ | $2.5 \times 10^4$ | $2.5 \times 10^4$ | $2.5 \times 10^4$ | $2.5 \times 10^4$ | $2.5 \times 10^4$ |
| Pseudo-first-order rate constants | | | | | | | |
| Volatilization ($hr^{-1}$) | $7.0 \times 10^{-6}$ | $7.0 \times 10^{-6}$ | $7.0 \times 10^{-6}$ | 0 | 0 | 0 | 0 |
| Photolysis ($hr^{-1}$) | $6.9 \times 10^{-2}$ | $6.9 \times 10^{-2}$ | $6.9 \times 10^{-2}$ | $6.9 \times 10^{-3}$ | 0 | 0 | 0 |
| Oxidation ($hr^{-1}$) | 0 | 0 | 0 | 0 | 0 | 0 | 0 |
| Hydrolysis ($hr^{-1}$) | 0 | 0 | 0 | 0 | 0 | 0 | 0 |
| Biodegradation ($hr^{-1}$) | 0 | 0 | 0 | 0 | 0 | 0 | 0 |

## TABLE A.9. NINE-COMPARTMENT COMPUTER MODEL INPUTS FOR BENZO[a]PYRENE: POND SIMULATION

| | Water (compartment 1) | Sediment (compartment 7) |
|---|---|---|
| Sorption partition coefficient | $5 \times 10^4$ | $5 \times 10^4$ |
| Pseudo-first-order rate constants | | |
| Volatilization ($hr^{-1}$) | $2.0 \times 10^{-5}$ | 0 |
| Photolysis ($hr^{-1}$) | $9.2 \times 10^{-2}$ | 0 |
| Oxidation ($hr^{-1}$) | 0 | 0 |
| Hydrolysis ($hr^{-1}$) | 0 | 0 |
| Biodegradation ($hr^{-1}$) | 0 | 0 |

TABLE A.10. NINE-COMPARTMENT COMPUTER MODEL INPUTS
FOR BENZO[a]PYRENE:
RIVER SIMULATION

| | Water compartments | | | Sediment compartments | | |
|---|---|---|---|---|---|---|
| | 1 | 2 | 3 | 7 | 8 | 9 |
| Sorption partition coefficient | $5.0 \times 10^4$ | $5.0 \times 10^4$ | $5.0 \times 10^4$ | $5.0 \times 10^4$ | $5.0 \times 10^4$ | $5.0 \times 10^4$ |
| Pseudo-first-order rate constants | | | | | | |
| Volatilization ($hr^{-1}$) | $5.0 \times 10^{-3}$ | $5.0 \times 10^{-3}$ | $5.0 \times 10^{-3}$ | 0 | 0 | 0 |
| Photolysis ($hr^{-1}$) | $2.3 \times 10^{-1}$ | $2.3 \times 10^{-1}$ | $2.3 \times 10^{-1}$ | 0 | 0 | 0 |
| Oxidation ($hr^{-1}$) | 0 | 0 | 0 | 0 | 0 | 0 |
| Hydrolysis ($hr^{-1}$) | 0 | 0 | 0 | 0 | 0 | 0 |
| Biodegradation ($hr^{-1}$) | 0 | 0 | 0 | 0 | 0 | 0 |

TABLE A.11. NINE-COMPARTMENT COMPUTER MODEL INPUTS
FOR BENZO[a]PYRENE:
EUTROPHIC LAKE SIMULATION

| | Water compartments | | | | Sediment compartments | | |
|---|---|---|---|---|---|---|---|
| | 1 | 2 | 3 | 5 | 7 | 8 | 9 |
| Sorption partition coefficient | $5.0 \times 10^4$ | $5.0 \times 10^4$ | $5.0 \times 10^4$ | $5.0 \times 10^4$ | $5.0 \times 10^4$ | $5.0 \times 10^4$ | $5.0 \times 10^4$ |
| Pseudo-first-order rate constants | | | | | | | |
| Volatilization ($hr^{-1}$) | $1.0 \times 10^{-3}$ | $1.0 \times 10^{-3}$ | $1.0 \times 10^{-3}$ | 0 | 0 | 0 | 0 |
| Photolysis ($hr^{-1}$) | $9.2 \times 10^{-2}$ | $9.2 \times 10^{-2}$ | $9.2 \times 10^{-2}$ | $9.2 \times 10^{-3}$ | 0 | 0 | 0 |
| Oxidation ($hr^{-1}$) | 0 | 0 | 0 | 0 | 0 | 0 | 0 |
| Hydrolysis ($hr^{-1}$) | 0 | 0 | 0 | 0 | 0 | 0 | 0 |
| Biodegradation ($hr^{-1}$) | 0 | 0 | 0 | 0 | 0 | 0 | 0 |

TABLE A.12. NINE-COMPARTMENT COMPUTER MODEL INPUTS
FOR BENZO[a]PYRENE:
OLIGOTROPHIC LAKE SIMULATION

| | Water compartments | | | | Sediment compartments | | |
|---|---|---|---|---|---|---|---|
| | 1 | 2 | 3 | 5 | 7 | 8 | 9 |
| Sorption partition coefficient | $5.0 \times 10^4$ | $5.0 \times 10^4$ | $5.0 \times 10^4$ | $5.0 \times 10^4$ | $5.0 \times 10^4$ | $5.0 \times 10^4$ | $5.0 \times 10^4$ |
| Pseudo-first-order rate constants | | | | | | | |
| Volatilization ($hr^{-1}$) | $1.0 \times 10^{-3}$ | $1.0 \times 10^{-3}$ | $1.0 \times 10^{-3}$ | 0 | 0 | 0 | 0 |
| Photolysis ($hr^{-1}$) | $4.6 \times 10^{-1}$ | $4.6 \times 10^{-1}$ | $4.6 \times 10^{-1}$ | $4.6 \times 10^{-2}$ | 0 | 0 | 0 |
| Oxidation ($hr^{-1}$) | 0 | 0 | 0 | 0 | 0 | 0 | 0 |
| Hydrolysis ($hr^{-1}$) | 0 | 0 | 0 | 0 | 0 | 0 | 0 |
| Biodegradation ($hr^{-1}$) | 0 | 0 | 0 | 0 | 0 | 0 | 0 |

### TABLE A.13. NINE-COMPARTMENT COMPUTER MODEL INPUTS FOR QUINOLINE: POND SIMULATION

| | Water (compartment 1) | Sediment (compartment 7) |
|---|---|---|
| Sorption partition coefficient | 0 | 0 |
| Pseudo-first-order rate constants | | |
| Volatilization ($hr^{-1}$) | 0 | 0 |
| Photolysis ($hr^{-1}$) | $2 \times 10^{-4}$ | 0 |
| Oxidation ($hr^{-1}$) | 0 | 0 |
| Hydrolysis ($hr^{-1}$) | 0 | 0 |
| Kinetic constants for biodegradation | | |
| Bacterial population (cells $ml^{-1}$) | $10^6$ | $10^7$ |
| Active bacterial population (cells $ml^{-1}$) | $10^5$ | $10^5$ |
| Maximum growth rate ($hr^{-1}$) | 0.74 | 0.37 |
| Half-saturation constant ($\mu g$ $ml^{-1}$) | 0.16 | 0.32 |
| Yield factor (cells $\mu g^{-1}$) | $3.3 \times 10^6$ | $3.3 \times 10^6$ |

TABLE A.14. NINE-COMPARTMENT COMPUTER MODEL INPUTS
FOR QUINOLINE:
RIVER SIMULATION

| | Water compartments | | | Sediment compartments | | |
|---|---|---|---|---|---|---|
| | 1 | 2 | 3 | 7 | 8 | 9 |
| Sorption partition coefficient | 0 | 0 | 0 | 0 | 0 | 0 |
| Pseudo-first-order rate constants | | | | | | |
| Volatilization ($hr^{-1}$) | 0 | 0 | 0 | 0 | 0 | 0 |
| Photolysis ($hr^{-1}$) | $6 \times 10^{-4}$ | $6 \times 10^{-4}$ | $6 \times 10^{-4}$ | 0 | 0 | 0 |
| Oxidation ($hr^{-1}$) | 0 | 0 | 0 | 0 | 0 | 0 |
| Hydrolysis ($hr^{-1}$) | 0 | 0 | 0 | 0 | 0 | 0 |
| Kinetic constants for biodegradation | | | | | | |
| Bacterial population (cells $ml^{-1}$) | $10^6$ | $10^6$ | $10^6$ | $10^7$ | $10^7$ | $10^7$ |
| Active bacterial population (cells $ml^{-1}$) | $10^5$ | $10^5$ | $10^5$ | $10^5$ | $10^5$ | $10^5$ |
| Maximum growth rate ($hr^{-1}$) | 0.74 | 0.74 | 0.74 | 0.37 | 0.37 | 0.37 |
| Half-saturation constant ($\mu g\ ml^{-1}$) | 0.16 | 0.16 | 0.16 | 0.32 | 0.32 | 0.32 |
| Yield factor (cells $\mu g^{-1}$) | $3.3 \times 10^{-6}$ | $3.3 \times 10^{-6}$ | $3.3 \times 10^{-6}$ | $3.3 \times 10^{-6}$ | $3.3 \times 10^{-6}$ | $3.3 \times 10^{-6}$ |

## TABLE A.15. NINE-COMPARTMENT COMPUTER MODEL INPUTS FOR QUINOLINE: EUTROPHIC LAKE SIMULATION

| | Water compartments | | | | Sediment compartments | | |
|---|---|---|---|---|---|---|---|
| | 1 | 2 | 3 | 5 | 7 | 8 | 9 |
| Sorption partition coefficient | 0 | 0 | 0 | 0 | 0 | 0 | 0 |
| Pseudo-first-order rate constants | | | | | | | |
| Volatilization ($hr^{-1}$) | 0 | 0 | 0 | 0 | 0 | 0 | 0 |
| Photolysis ($hr^{-1}$) | $2 \times 10^{-4}$ | $2 \times 10^{-4}$ | $2 \times 10^{-4}$ | $2 \times 10^{-5}$ | 0 | 0 | 0 |
| Oxidation ($hr^{-1}$) | 0 | 0 | 0 | 0 | 0 | 0 | 0 |
| Hydrolysis ($hr^{-1}$) | 0 | 0 | 0 | 0 | 0 | 0 | 0 |
| Kinetic constants for biodegradation | | | | | | | |
| Bacterial population (cells $ml^{-1}$) | $10^6$ | $10^6$ | $10^6$ | $10^6$ | $10^7$ | $10^7$ | $10^7$ |
| Active bacterial population (cells $ml^{-1}$) | $10^5$ | $10^5$ | $10^5$ | $10^5$ | $10^5$ | $10^5$ | $10^5$ |
| Maximum growth rate ($hr^{-1}$) | 0.74 | 0.74 | 0.74 | 0.50 | 0.37 | 0.37 | 0.37 |
| Half-saturation constant ($\mu g\ ml^{-1}$) | 0.16 | 0.16 | 0.16 | 0.24 | 0.32 | 0.32 | 0.32 |
| Yield factor (cells $\mu g^{-1}$) | $3.3 \times 10^{-6}$ | $3.3 \times 10^{-6}$ | $3.3 \times 10^{-6}$ | $3.3 \times 10^{-6}$ | $3.3 \times 10^{-6}$ | $3.3 \times 10^{-6}$ | $3.3 \times 10^{-6}$ |

TABLE A.16. NINE-COMPARTMENT COMPUTER MODEL INPUTS
FOR QUINOLINE:
OLIGOTROPHIC LAKE SIMULATION

| | Water compartments | | | | Sediment compartments | | |
|---|---|---|---|---|---|---|---|
| | 1 | 2 | 3 | 5 | 7 | 8 | 9 |
| Sorption partition coefficient | 0 | 0 | 0 | 0 | 0 | 0 | 0 |
| Pseudo-first-order rate constants | | | | | | | |
| Volatilization ($hr^{-1}$) | 0 | 0 | 0 | 0 | 0 | 0 | 0 |
| Photolysis ($hr^{-1}$) | $1.2 \times 10^{-3}$ | $1.2 \times 10^{-3}$ | $1.2 \times 10^{-3}$ | $1.2 \times 10^{-4}$ | 0 | 0 | 0 |
| Oxidation ($hr^{-1}$) | 0 | 0 | 0 | 0 | 0 | 0 | 0 |
| Hydrolysis ($hr^{-1}$) | 0 | 0 | 0 | 0 | 0 | 0 | 0 |
| Kinetic constants for biodegradation | | | | | | | |
| Bacterial population (cells $ml^{-1}$) | $10^2$ | $10^2$ | $10^2$ | $10^2$ | $10^3$ | $10^3$ | $10^3$ |
| Active bacterial population (cells $ml^{-1}$) | 10 | 10 | 10 | 10 | 10 | 10 | 10 |
| Maximum growth rate ($hr^{-1}$) | 0.74 | 0.74 | 0.74 | 0.50 | 0.37 | 0.37 | 0.37 |
| Half-saturation constant ($\mu g\ ml^{-1}$) | 0.16 | 0.16 | 0.16 | 0.24 | 0.32 | 0.32 | 0.32 |
| Yield factor (cells $\mu g^{-1}$) | $3.3 \times 10^6$ | $3.3 \times 10^6$ | $3.3 \times 10^6$ | $3.3 \times 10^6$ | $3.3 \times 10^6$ | $3.3 \times 10^6$ | $3.3 \times 10^6$ |

## TABLE A.17. NINE-COMPARTMENT COMPUTER MODEL INPUTS FOR BENZO[f]QUINOLINE: POND SIMULATION

| | Water (compartment 1) | Sediment (compartment 7) |
|---|---|---|
| Sorption partition coefficient | $1.4 \times 10^{3}$ | $1.4 \times 10^{3}$ |
| Pseudo-first-order rate constants | | |
| Volatilization ($hr^{-1}$) | $1.6 \times 10^{-6}$ | 0 |
| Photolysis ($hr^{-1}$) | 0.1 | 0 |
| Oxidation ($hr^{-1}$) | $1.0 \times 10^{-7}$ | 0 |
| Hydrolysis ($hr^{-1}$) | 0 | 0 |
| Biodegradation ($hr^{-1}$) | $3.6 \times 10^{-3}$ | $3.6 \times 10^{-3}$ |

TABLE A.18. NINE-COMPARTMENT COMPUTER MODEL INPUTS FOR BENZO[f]QUINOLINE: RIVER SIMULATION

| | Water compartments | | | Sediment compartments | | |
|---|---|---|---|---|---|---|
| | 1 | 2 | 3 | 7 | 8 | 9 |
| Sorption partition coefficient | $1.4 \times 10^3$ | $1.4 \times 10^3$ | $1.4 \times 10^3$ | $1.4 \times 10^3$ | $1.4 \times 10^3$ | $1.4 \times 10^3$ |
| Pseudo-first-order rate constants | | | | | | |
| Volatilization ($hr^{-1}$) | $8.0 \times 10^{-6}$ | $8.0 \times 10^{-6}$ | $8.0 \times 10^{-6}$ | 0 | 0 | 0 |
| Photolysis ($hr^{-1}$) | 0.25 | 0.25 | 0.25 | 0 | 0 | 0 |
| Oxidation ($hr^{-1}$) | $1.0 \times 10^{-7}$ | $1.0 \times 10^{-7}$ | $1.0 \times 10^{-7}$ | 0 | 0 | 0 |
| Hydrolysis ($hr^{-1}$) | 0 | 0 | 0 | 0 | 0 | 0 |
| Biodegradation ($hr^{-1}$) | $3.6 \times 10^{-3}$ | $3.6 \times 10^{-3}$ | $3.6 \times 10^{-3}$ | $1.8 \times 10^{-3}$ | $1.8 \times 10^{-3}$ | $1.8 \times 10^{-3}$ |

TABLE A.19. NINE-COMPARTMENT COMPUTER MODEL INPUTS FOR BENZO[f]QUINOLINE: EUTROPHIC LAKE SIMULATION

| | Water compartments | | | | Sediment compartments | | |
|---|---|---|---|---|---|---|---|
| | 1 | 2 | 3 | 5 | 7 | 8 | 9 |
| Sorption partition coefficient | $1.4 \times 10^3$ | $1.4 \times 10^3$ | $1.4 \times 10^3$ | $1.4 \times 10^3$ | $1.4 \times 10^3$ | $1.4 \times 10^3$ | $1.4 \times 10^3$ |
| Pseudo-first-order rate constants | | | | | | | |
| Volatilization ($hr^{-1}$) | $2.0 \times 10^{-6}$ | $2.0 \times 10^{-6}$ | $2.0 \times 10^{-6}$ | 0 | 0 | 0 | 0 |
| Photolysis ($hr^{-1}$) | 0.10 | 0.10 | 0.10 | $1.0 \times 10^{-2}$ | 0 | 0 | 0 |
| Oxidation ($hr^{-1}$) | $1.0 \times 10^{-7}$ | $1.0 \times 10^{-7}$ | $1.0 \times 10^{-7}$ | $1.0 \times 10^{-7}$ | 0 | 0 | 0 |
| Hydrolysis ($hr^{-1}$) | 0 | 0 | 0 | 0 | 0 | 0 | 0 |
| Biodegradation ($hr^{-1}$) | $3.6 \times 10^{-3}$ | $3.6 \times 10^{-3}$ | $3.6 \times 10^{-3}$ | $2.5 \times 10^{-3}$ | $1.8 \times 10^{-3}$ | $1.8 \times 10^{-3}$ | $1.8 \times 10^{-3}$ |

TABLE A.20. NINE-COMPARTMENT COMPUTER MODEL INPUTS
FOR BENZO[*f*]QUINOLINE:
OLIGOTROPHIC LAKE SIMULATION

| | Water compartments | | | | Sediment compartments | | |
|---|---|---|---|---|---|---|---|
| | 1 | 2 | 3 | 5 | 7 | 8 | 9 |
| Sorption partition coefficient | $1.4 \times 10^3$ | $1.4 \times 10^3$ | $1.4 \times 10^3$ | $1.4 \times 10^3$ | $1.4 \times 10^3$ | $1.4 \times 10^3$ | $1.4 \times 10^3$ |
| Pseudo-first-order rate constants | | | | | | | |
| Volatilization ($hr^{-1}$) | $2.0 \times 10^{-6}$ | $2.0 \times 10^{-6}$ | $2.0 \times 10^{-6}$ | 0 | 0 | 0 | 0 |
| Photolysis ($hr^{-1}$) | 0.50 | 0.50 | 0.50 | $5.0 \times 10^{-2}$ | 0 | 0 | 0 |
| Oxidation ($hr^{-1}$) | $1.0 \times 10^{-7}$ | $1.0 \times 10^{-7}$ | $1.0 \times 10^{-7}$ | $1.0 \times 10^{-7}$ | 0 | 0 | 0 |
| Hydrolysis ($hr^{-1}$) | 0 | 0 | 0 | 0 | 0 | 0 | 0 |
| Biodegradation ($hr^{-1}$) | $3.6 \times 10^{-7}$ | $3.6 \times 10^{-7}$ | $3.6 \times 10^{-7}$ | $2.5 \times 10^{-7}$ | $1.8 \times 10^{-7}$ | $1.8 \times 10^{-7}$ | $1.8 \times 10^{-7}$ |

## TABLE A.21. NINE-COMPARTMENT COMPUTER MODEL INPUTS FOR CARBAZOLE: POND SIMULATION

| | Water (compartment 1) | Sediment (compartment 7) |
|---|---|---|
| Sorption partition coefficient | 200 | 200 |
| Pseudo-first-order rate constants | | |
| Volatilization ($hr^{-1}$) | 0 | 0 |
| Photolysis ($hr^{-1}$) | $4.6 \times 10^{-2}$ | 0 |
| Oxidation ($hr^{-1}$) | $2.9 \times 10^{-3}$ | 0 |
| Hydrolysis ($hr^{-1}$) | 0 | 0 |
| Biodegradation ($hr^{-1}$) | $2.3 \times 10^{-2}$ | $2.3 \times 10^{-3}$ |

## TABLE A.22. NINE-COMPARTMENT COMPUTER MODEL INPUTS FOR CARBAZOLE: RIVER SIMULATION

| | Water compartments | | | Sediment compartments | | |
|---|---|---|---|---|---|---|
| | 1 | 2 | 3 | 7 | 8 | 9 |
| Sorption partition coefficient | 200 | 200 | 200 | 200 | 200 | 200 |
| Pseudo-first-order rate constants | | | | | | |
| Volatilization ($hr^{-1}$) | 0 | 0 | 0 | 0 | 0 | 0 |
| Photolysis ($hr^{-1}$) | $1.1 \times 10^{-1}$ | $1.1 \times 10^{-1}$ | $1.1 \times 10^{-1}$ | 0 | 0 | 0 |
| Oxidation ($hr^{-1}$) | $2.9 \times 10^{-3}$ | $2.9 \times 10^{-3}$ | $2.9 \times 10^{-3}$ | 0 | 0 | 0 |
| Hydrolysis ($hr^{-1}$) | 0 | 0 | 0 | 0 | 0 | 0 |
| Biodegradation ($hr^{-1}$) | $2.3 \times 10^{-2}$ | $2.3 \times 10^{-2}$ | $2.3 \times 10^{-2}$ | $2.3 \times 10^{-3}$ | $2.3 \times 10^{-3}$ | $2.3 \times 10^{-3}$ |

TABLE A.23. NINE-COMPARTMENT COMPUTER MODEL INPUTS
FOR CARBAZOLE:
EUTROPHIC LAKE SIMULATION

| | Water compartments | | | | Sediment compartments | | |
|---|---|---|---|---|---|---|---|
| | 1 | 2 | 3 | 5 | 7 | 8 | 9 |
| Sorption partition coefficient | 200 | 200 | 200 | 200 | 200 | 200 | 200 |
| Pseudo-first-order rate constants | | | | | | | |
| Volatilization ($hr^{-1}$) | 0 | 0 | 0 | 0 | 0 | 0 | 0 |
| Photolysis ($hr^{-1}$) | $4.6 \times 10^{-2}$ | $9.2 \times 10^{-2}$ | $4.6 \times 10^{-2}$ | $4.6 \times 10^{-3}$ | 0 | 0 | 0 |
| Oxidation ($hr^{-1}$) | $2.9 \times 10^{-3}$ | $2.9 \times 10^{-3}$ | $2.9 \times 10^{-3}$ | $2.9 \times 10^{-3}$ | 0 | 0 | 0 |
| Hydrolysis ($hr^{-1}$) | 0 | 0 | 0 | 0 | 0 | 0 | 0 |
| Biodegradation ($hr^{-1}$) | $2.3 \times 10^{-2}$ | $2.3 \times 10^{-2}$ | $2.3 \times 10^{-2}$ | $1.6 \times 10^{-2}$ | $2.3 \times 10^{-3}$ | $2.3 \times 10^{-3}$ | $2.3 \times 10^{-3}$ |

## TABLE A.24. NINE-COMPARTMENT COMPUTER MODEL INPUTS FOR CARBAZOLE: OLIGOTROPHIC LAKE SIMULATION

| | Water compartments | | | | Sediment compartments | | |
|---|---|---|---|---|---|---|---|
| | 1 | 2 | 3 | 5 | 7 | 8 | 9 |
| Sorption partition coefficient | 200 | 200 | 200 | 200 | 200 | 200 | 200 |
| Pseudo-first-order rate constants | | | | | | | |
| Volatilization ($hr^{-1}$) | 0 | 0 | 0 | 0 | 0 | 0 | 0 |
| Photolysis ($hr^{-1}$) | $4.6 \times 10^{-2}$ | $9.2 \times 10^{-2}$ | $4.6 \times 10^{-2}$ | $4.6 \times 10^{-3}$ | 0 | 0 | 0 |
| Oxidation ($hr^{-1}$) | $2.9 \times 10^{-3}$ | $2.9 \times 10^{-3}$ | $2.9 \times 10^{-3}$ | $2.9 \times 10^{-3}$ | 0 | 0 | 0 |
| Hydrolysis ($hr^{-1}$) | 0 | 0 | 0 | 0 | 0 | 0 | 0 |
| Biodegradation ($hr^{-1}$) | $2.3 \times 10^{-6}$ | $2.3 \times 10^{-6}$ | $2.3 \times 10^{-6}$ | $1.6 \times 10^{-6}$ | $2.3 \times 10^{-7}$ | $2.3 \times 10^{-7}$ | $2.3 \times 10^{-7}$ |

## TABLE A.25. NINE-COMPARTMENT COMPUTER MODEL INPUTS FOR 7H-DIBENZO[c,g]CARBAZOLE: POND SIMULATION

| | Water (compartment 1) | Sediment (compartment 7) |
|---|---|---|
| Sorption partition coefficient | 0 | 0 |
| Pseudo-first-order rate constants | | |
| Volatilization ($hr^{-1}$) | 0 | 0 |
| Photolysis ($hr^{-1}$) | 0.462 | 0 |
| Oxidation ($hr^{-1}$) | 0.001 | 0.001 |
| Hydrolysis ($hr^{-1}$) | 0 | 0 |
| Biodegradation ($hr^{-1}$) | 0 | 0 |

## TABLE A.26. NINE-COMPARTMENT COMPUTER MODEL INPUTS FOR 7H-DIBENZO[c,g]CARBAZOLE: RIVER SIMULATION

| | Water compartments | | | Sediment compartments | | |
|---|---|---|---|---|---|---|
| | 1 | 2 | 3 | 7 | 8 | 9 |
| Sorption partition coefficient | 0 | 0 | 0 | 0 | 0 | 0 |
| Pseudo-first-order rate constants | | | | | | |
| Volatilization ($hr^{-1}$) | 0 | 0 | 0 | 0 | 0 | 0 |
| Photolysis ($hr^{-1}$) | 0.693 | 0.693 | 0.693 | 0 | 0 | 0 |
| Oxidation ($hr^{-1}$) | 0.001 | 0.001 | 0.001 | 0.001 | 0.001 | 0.001 |
| Hydrolysis ($hr^{-1}$) | 0 | 0 | 0 | 0 | 0 | 0 |
| Biodegradation ($hr^{-1}$) | 0 | 0 | 0 | 0 | 0 | 0 |

TABLE A.27. NINE-COMPARTMENT COMPUTER MODEL INPUTS
FOR 7H-DIBENZO[c,g]CARBAZOLE:
EUTROPHIC LAKE SIMULATION

| | Water compartments | | | | Sediment compartments | | |
|---|---|---|---|---|---|---|---|
| | 1 | 2 | 3 | 5 | 7 | 8 | 9 |
| Sorption partition coefficient | 0 | 0 | 0 | 0 | 0 | 0 | 0 |
| Pseudo-first-order rate constants | | | | | | | |
| Volatilization ($hr^{-1}$) | 0 | 0 | 0 | 0 | 0 | 0 | 0 |
| Photolysis ($hr^{-1}$) | 0.462 | 0.462 | 0.462 | 0.046 | 0 | 0 | 0 |
| Oxidation ($hr^{-1}$) | 0.001 | 0.001 | 0.001 | 0.001 | 0.001 | 0.001 | 0.001 |
| Hydrolysis ($hr^{-1}$) | 0 | 0 | 0 | 0 | 0 | 0 | 0 |
| Biodegradation ($hr^{-1}$) | 0 | 0 | 0 | 0 | 0 | 0 | 0 |

TABLE A.28. NINE-COMPARTMENT COMPUTER MODEL INPUTS FOR 7H-DIBENZO[c,g]CARBAZOLE: OLIGOTROPHIC LAKE SIMULATION

| | Water compartments | | | | Sediment compartments | | |
|---|---|---|---|---|---|---|---|
| | 1 | 2 | 3 | 5 | 7 | 8 | 9 |
| Sorption partition coefficient | 0 | 0 | 0 | 0 | 0 | 0 | 0 |
| Pseudo-first-order rate constants | | | | | | | |
| Volatilization ($hr^{-1}$) | 0 | 0 | 0 | 0 | 0 | 0 | 0 |
| Photolysis ($hr^{-1}$) | 1.4 | 1.4 | 1.4 | 1.4 | 0 | 0 | 0 |
| Oxidation ($hr^{-1}$) | 0.001 | 0.001 | 0.001 | 0.001 | 0.001 | 0.001 | 0.001 |
| Hydrolysis ($hr^{-1}$) | 0 | 0 | 0 | 0 | 0 | 0 | 0 |
| Biodegradation ($hr^{-1}$) | 0 | 0 | 0 | 0 | 0 | 0 | 0 |

## TABLE A.29. NINE-COMPARTMENT COMPUTER MODEL INPUTS FOR BENZO[b]THIOPHENE: POND SIMULATION

| | Water (compartment 1) | Sediment (compartment 7) |
|---|---|---|
| Sorption partition coefficient | 50 | 50 |
| Pseudo-first-order rate constants | | |
| Volatilization ($hr^{-1}$) | $3 \times 10^{-3}$ | 0 |
| Photolysis ($hr^{-1}$) | $2.4 \times 10^{-4}$ | 0 |
| Oxidation ($hr^{-1}$) | 0 | 0 |
| Hydrolysis ($hr^{-1}$) | 0 | 0 |
| Biodegradation ($hr^{-1}$) | $3.5 \times 10^{-2}$ | $1.7 \times 10^{-2}$ |

TABLE A.30. NINE-COMPARTMENT COMPUTER MODEL INPUTS
FOR BENZO[b]THIOPHENE:
RIVER SIMULATION

| | Water compartments | | | Sediment compartments | | |
|---|---|---|---|---|---|---|
| | 1 | 2 | 3 | 7 | 8 | 9 |
| Sorption partition coefficient | 50 | 50 | 50 | 50 | 50 | 50 |
| Pseudo-first-order rate constants | | | | | | |
| Volatilization ($hr^{-1}$) | $1.5 \times 10^{-2}$ | $1.5 \times 10^{-2}$ | $1.5 \times 10^{-2}$ | 0 | 0 | 0 |
| Photolysis ($hr^{-1}$) | $6.0 \times 10^{-4}$ | $6.0 \times 10^{-4}$ | $6.0 \times 10^{-4}$ | 0 | 0 | 0 |
| Oxidation ($hr^{-1}$) | 0 | 0 | 0 | 0 | 0 | 0 |
| Hydrolysis ($hr^{-1}$) | 0 | 0 | 0 | 0 | 0 | 0 |
| Biodegradation ($hr^{-1}$) | $3.5 \times 10^{-2}$ | $3.5 \times 10^{-2}$ | $3.5 \times 10^{-2}$ | $8.5 \times 10^{-3}$ | $8.5 \times 10^{-3}$ | $8.5 \times 10^{-3}$ |

TABLE A.31. NINE-COMPARTMENT COMPUTER MODEL INPUTS FOR BENZO[b]THIOPHENE: EUTROPHIC LAKE SIMULATION

| | Water compartments | | | | Sediment compartments | | |
|---|---|---|---|---|---|---|---|
| | 1 | 2 | 3 | 5 | 7 | 8 | 9 |
| Sorption partition coefficient | 50 | 50 | 50 | 50 | 50 | 50 | 50 |
| Pseudo-first-order rate constants | | | | | | | |
| Volatilization ($hr^{-1}$) | $3.8 \times 10^{-3}$ | $4.5 \times 10^{-3}$ | $3.8 \times 10^{-3}$ | 0 | 0 | 0 | 0 |
| Photolysis ($hr^{-1}$) | $2.4 \times 10^{-4}$ | $2.4 \times 10^{-4}$ | $2.4 \times 10^{-4}$ | $2.4 \times 10^{-5}$ | 0 | 0 | 0 |
| Oxidation ($hr^{-1}$) | 0 | 0 | 0 | 0 | 0 | 0 | 0 |
| Hydrolysis ($hr^{-1}$) | 0 | 0 | 0 | 0 | 0 | 0 | 0 |
| Biodegradation ($hr^{-1}$) | $3.5 \times 10^{-2}$ | $3.5 \times 10^{-2}$ | $3.5 \times 10^{-2}$ | $1.3 \times 10^{-2}$ | $4.0 \times 10^{-3}$ | $4.0 \times 10^{-3}$ | $4.0 \times 10^{-3}$ |

TABLE A.32. NINE-COMPARTMENT COMPUTER MODEL INPUTS
FOR BENZO[b]THIOPHENE:
OLIGOTROPHIC LAKE SIMULATION

| | Water compartments | | | | Sediment compartments | | |
|---|---|---|---|---|---|---|---|
| | 1 | 2 | 3 | 5 | 7 | 8 | 9 |
| Sorption partition coefficient | 50 | 50 | 50 | 50 | 50 | 50 | 50 |
| Pseudo-first-order rate constants | | | | | | | |
| Volatilization ($hr^{-1}$) | $3.8 \times 10^{-3}$ | $4.5 \times 10^{-3}$ | $3.8 \times 10^{-3}$ | 0 | 0 | 0 | 0 |
| Photolysis ($hr^{-1}$) | $1.2 \times 10^{-3}$ | $1.2 \times 10^{-3}$ | $1.2 \times 10^{-3}$ | $1.2 \times 10^{-4}$ | 0 | 0 | 0 |
| Oxidation ($hr^{-1}$) | 0 | 0 | 0 | 0 | 0 | 0 | 0 |
| Hydrolysis ($hr^{-1}$) | 0 | 0 | 0 | 0 | 0 | 0 | 0 |
| Biodegradation ($hr^{-1}$) | $3.5 \times 10^{-6}$ | $3.5 \times 10^{-6}$ | $3.5 \times 10^{-6}$ | $1.3 \times 10^{-6}$ | $4.0 \times 10^{-7}$ | $4.0 \times 10^{-7}$ | $4.0 \times 10^{-7}$ |

## TABLE A.33. NINE-COMPARTMENT COMPUTER MODEL INPUTS FOR DIBENZOTHIOPHENE: POND SIMULATION

| | Water (compartment 1) | Sediment (compartment 7) |
|---|---|---|
| Sorption partition coefficient | $1.4 \times 10^3$ | $1.4 \times 10^3$ |
| Pseudo-first-order rate constants | | |
| Volatilization ($hr^{-1}$) | $9.6 \times 10^{-3}$ | 0 |
| Photolysis ($hr^{-1}$) | $7.3 \times 10^{-4}$ | 0 |
| Oxidation ($hr^{-1}$) | 0 | 0 |
| Hydrolysis ($hr^{-1}$) | 0 | 0 |
| Biodegradation ($hr^{-1}$) | $5.3 \times 10^{-2}$ | $5.3 \times 10^{-2}$ |

TABLE A.34. NINE-COMPARTMENT COMPUTER MODEL INPUTS
FOR DIBENZOTHIOPHENE:
RIVER SIMULATION

| | Water compartments | | | Sediment compartments | | |
|---|---|---|---|---|---|---|
| | 1 | 2 | 3 | 7 | 8 | 9 |
| Sorption partition coefficient | $1.4 \times 10^3$ | $1.4 \times 10^3$ | $1.4 \times 10^3$ | $1.4 \times 10^3$ | $1.4 \times 10^3$ | $1.4 \times 10^3$ |
| **Pseudo-first-order rate constants** | | | | | | |
| Volatilization ($hr^{-1}$) | $4.8 \times 10^{-2}$ | $4.8 \times 10^{-2}$ | $4.8 \times 10^{-2}$ | 0 | 0 | 0 |
| Photolysis ($hr^{-1}$) | $1.8 \times 10^{-3}$ | $1.8 \times 10^{-3}$ | $1.8 \times 10^{-3}$ | 0 | 0 | 0 |
| Oxidation ($hr^{-1}$) | 0 | 0 | 0 | 0 | 0 | 0 |
| Hydrolysis ($hr^{-1}$) | 0 | 0 | 0 | 0 | 0 | 0 |
| Biodegradation ($hr^{-1}$) | $5.3 \times 10^{-2}$ | $5.3 \times 10^{-2}$ | $5.3 \times 10^{-2}$ | $5.3 \times 10^{-2}$ | $5.3 \times 10^{-2}$ | $5.3 \times 10^{-2}$ |

TABLE A.35. NINE-COMPARTMENT COMPUTER MODEL INPUTS
FOR DIBENZOTHIOPHENE:
EUTROPHIC LAKE SIMULATION

| | Water compartments | | | | Sediment compartments | | |
|---|---|---|---|---|---|---|---|
| | 1 | 2 | 3 | 5 | 7 | 8 | 9 |
| Sorption partition coefficient | $1.4 \times 10^3$ | $1.4 \times 10^3$ | $1.4 \times 10^3$ | $1.4 \times 10^3$ | $1.4 \times 10^3$ | $1.4 \times 10^3$ | $1.4 \times 10^3$ |
| Pseudo-first-order rate constants | | | | | | | |
| Volatilization ($hr^{-1}$) | $1.2 \times 10^{-2}$ | $1.4 \times 10^{-2}$ | $1.2 \times 10^{-2}$ | 0 | 0 | 0 | 0 |
| Photolysis ($hr^{-1}$) | $7.3 \times 10^{-4}$ | $7.3 \times 10^{-4}$ | $7.3 \times 10^{-4}$ | $7.3 \times 10^{-5}$ | 0 | 0 | 0 |
| Oxidation ($hr^{-1}$) | 0 | 0 | 0 | 0 | 0 | 0 | 0 |
| Hydrolysis ($hr^{-1}$) | 0 | 0 | 0 | 0 | 0 | 0 | 0 |
| Biodegradation ($hr^{-1}$) | $5.3 \times 10^{-2}$ | $5.3 \times 10^{-2}$ | $5.3 \times 10^{-2}$ | $3.5 \times 10^{-2}$ | $2.6 \times 10^{-2}$ | $2.6 \times 10^{-2}$ | $2.6 \times 10^{-2}$ |

TABLE A.36. NINE-COMPARTMENT COMPUTER MODEL INPUTS
FOR DIBENZOTHIOPHENE:
OLIGOTROPHIC LAKE SIMULATION

| | Water compartments | | | | Sediment compartments | | |
|---|---|---|---|---|---|---|---|
| | 1 | 2 | 3 | 5 | 7 | 8 | 9 |
| Sorption partition coefficient | $1.4 \times 10^3$ | $1.4 \times 10^3$ | $1.4 \times 10^3$ | $1.4 \times 10^3$ | $1.4 \times 10^3$ | $1.4 \times 10^3$ | $1.4 \times 10^3$ |
| Pseudo-first-order rate constants | | | | | | | |
| Volatilization ($hr^{-1}$) | $1.2 \times 10^{-2}$ | $1.4 \times 10^{-2}$ | $1.2 \times 10^{-2}$ | 0 | 0 | 0 | 0 |
| Photolysis ($hr^{-1}$) | $3.6 \times 10^{-3}$ | $3.6 \times 10^{-3}$ | $3.6 \times 10^{-3}$ | $3.6 \times 10^{-4}$ | 0 | 0 | 0 |
| Oxidation ($hr^{-1}$) | 0 | 0 | 0 | 0 | 0 | 0 | 0 |
| Hydrolysis ($hr^{-1}$) | 0 | 0 | 0 | 0 | 0 | 0 | 0 |
| Biodegradation ($hr^{-1}$) | $5.3 \times 10^{-6}$ | $5.3 \times 10^{-6}$ | $5.3 \times 10^{-6}$ | $3.5 \times 10^{-6}$ | $2.6 \times 10^{-6}$ | $2.6 \times 10^{-6}$ | $2.6 \times 10^{-6}$ |

## TABLE A.37. NINE-COMPARTMENT COMPUTER MODEL INPUTS FOR METHYL PARATHION: POND SIMULATION

| | Water (compartment 1) | Sediment (compartment 7) |
|---|---|---|
| Sorption partition coefficient | 50 | 50 |
| Pseudo-first-order rate constants | | |
| Volatilization ($hr^{-1}$) | 0 | 0 |
| Photolysis ($hr^{-1}$) | $8 \times 10^{-4}$ | 0 |
| Oxidation ($hr^{-1}$) | 0 | 0 |
| Hydrolysis ($hr^{-1}$) | $4 \times 10^{-4}$ | $4 \times 10^{-4}$ |
| Kinetic constants for biodegradation | | |
| Bacterial population (cells $ml^{-1}$) | $10^6$ | $10^7$ |
| Active bacterial population (cells $ml^{-1}$) | $10^5$ | $10^5$ |
| Maximum growth rate ($hr^{-1}$) | 0.61 | 0.2 |
| Half-saturation constant ($\mu g\ ml^{-1}$) | 2.6 | 5.2 |
| Yield factor (cells $\mu g^{-1}$) | $10^6$ | $10^6$ |

## TABLE A.38. NINE-COMPARTMENT COMPUTER MODEL INPUTS FOR METHYL PARATHION: RIVER SIMULATION

| | Water compartments | | | Sediment compartments | | |
|---|---|---|---|---|---|---|
| | 1 | 2 | 3 | 7 | 8 | 9 |
| Sorption partition coefficient | 50 | 50 | 50 | 50 | 50 | 50 |
| Pseudo-first-order rate constants | | | | | | |
| Volatilization ($hr^{-1}$) | 0 | 0 | 0 | 0 | 0 | 0 |
| Photolysis ($hr^{-1}$) | $2 \times 10^{-3}$ | $2 \times 10^{-3}$ | $2 \times 10^{-3}$ | 0 | 0 | 0 |
| Oxidation ($hr^{-1}$) | 0 | 0 | 0 | 0 | 0 | 0 |
| Hydrolysis ($hr^{-1}$) | $4 \times 10^{-4}$ | $4 \times 10^{-4}$ | $4 \times 10^{-4}$ | $4 \times 10^{-4}$ | $4 \times 10^{-4}$ | $4 \times 10^{-4}$ |
| Kinetic constants for biodegradation | | | | | | |
| Bacterial population (cells $ml^{-1}$) | $10^6$ | $10^6$ | $10^6$ | $10^7$ | $10^7$ | $10^7$ |
| Active bacterial population (cells $ml^{-1}$) | $10^5$ | $10^5$ | $10^5$ | $10^5$ | $10^5$ | $10^5$ |
| Maximum growth rate ($hr^{-1}$) | 0.61 | 0.61 | 0.61 | 0.2 | 0.2 | 0.2 |
| Half-saturation constant ($\mu g\ ml^{-1}$) | 2.6 | 2.6 | 2.6 | 5.2 | 5.2 | 5.2 |
| Yield factor (cells $\mu g^{-1}$) | $10^6$ | $10^6$ | $10^6$ | $10^6$ | $10^6$ | $10^6$ |

TABLE A.39. NINE-COMPARTMENT COMPUTER MODEL INPUTS FOR METHYL PARATHION: EUTROPHIC LAKE SIMULATION

| | Water compartments | | | | Sediment compartments | | |
|---|---|---|---|---|---|---|---|
| | 1 | 2 | 3 | 5 | 7 | 8 | 9 |
| Sorption partition coefficient | 50 | 50 | 50 | 50 | 50 | 50 | 50 |
| Pseudo-first-order rate constants | | | | | | | |
| Volatilization ($hr^{-1}$) | 0 | 0 | 0 | 0 | 0 | 0 | 0 |
| Photolysis ($hr^{-1}$) | $8 \times 10^{-4}$ | $1 \times 10^{-3}$ | $8 \times 10^{-4}$ | $8 \times 10^{-5}$ | 0 | 0 | 0 |
| Oxidation ($hr^{-1}$) | 0 | 0 | 0 | 0 | 0 | 0 | 0 |
| Hydrolysis ($hr^{-1}$) | $4 \times 10^{-4}$ | $4 \times 10^{-4}$ | $4 \times 10^{-4}$ | $4 \times 10^{-4}$ | $4 \times 10^{-4}$ | $4 \times 10^{-4}$ | $4 \times 10^{-4}$ |
| Kinetic constants for biodegradation | | | | | | | |
| Bacterial population (cells $ml^{-1}$) | $10^6$ | $10^6$ | $10^6$ | $10^6$ | $10^7$ | $10^7$ | $10^7$ |
| Active bacterial population (cells $ml^{-1}$) | $10^5$ | $10^5$ | $10^5$ | $10^5$ | $10^5$ | $10^5$ | $10^5$ |
| Maximum growth rate ($hr^{-1}$) | 0.61 | 0.61 | 0.61 | 0.4 | 0.2 | 0.2 | 0.2 |
| Half-saturation constant ($\mu g\ ml^{-1}$) | 2.6 | 2.6 | 2.6 | 0.4 | 0.52 | 0.52 | 0.52 |
| Yield factor (cells $\mu g^{-1}$) | $10^6$ | $10^6$ | $10^6$ | $10^6$ | $10^6$ | $10^6$ | $10^6$ |

### TABLE A.40. NINE-COMPARTMENT COMPUTER MODEL INPUTS FOR METHYL PARATHION: OLIGOTROPHIC LAKE SIMULATION

| | Water compartments | | | | Sediment compartments | | |
|---|---|---|---|---|---|---|---|
| | 1 | 2 | 3 | 5 | 7 | 8 | 9 |
| Sorption partition coefficient | 50 | 50 | 50 | 50 | 50 | 50 | 50 |
| Pseudo-first-order rate constants | | | | | | | |
| Volatilization ($hr^{-1}$) | 0 | 0 | 0 | 0 | 0 | 0 | 0 |
| Photolysis ($hr^{-1}$) | $4 \times 10^{-3}$ | $5 \times 10^{-3}$ | $4 \times 10^{-3}$ | $4 \times 10^{-4}$ | 0 | 0 | 0 |
| Oxidation ($hr^{-1}$) | 0 | 0 | 0 | 0 | 0 | 0 | 0 |
| Hydrolysis ($hr^{-1}$) | $4 \times 10^{-4}$ | $4 \times 10^{-4}$ | $4 \times 10^{-4}$ | $4 \times 10^{-4}$ | $4 \times 10^{-4}$ | $4 \times 10^{-4}$ | $4 \times 10^{-4}$ |
| Kinetic constants for biodegradation | | | | | | | |
| Bacterial population (cells $ml^{-1}$) | $10^2$ | $10^2$ | $10^2$ | $10^2$ | $10^3$ | $10^3$ | $10^3$ |
| Active bacterial population (cells $ml^{-1}$) | 10 | 10 | 10 | 10 | 10 | 10 | 10 |
| Maximum growth rate ($hr^{-1}$) | 0.61 | 0.61 | 0.61 | 0.4 | 0.2 | 0.2 | 0.2 |
| Half-saturation constant ($\mu g\ ml^{-1}$) | 0.26 | 0.26 | 0.26 | 0.4 | 0.52 | 0.52 | 0.52 |
| Yield factor (cells $\mu g^{-1}$) | $10^6$ | $10^6$ | $10^6$ | $10^6$ | $10^6$ | $10^6$ | $10^6$ |

## TABLE A.41. NINE-COMPARTMENT COMPUTER MODEL INPUTS FOR MIREX: POND SIMULATION

| | Water (compartment 1) | Sediment (compartment 7) |
|---|---|---|
| Sorption partition coefficient | $3 \times 10^5$ | $3 \times 10^5$ |
| Pseudo-first-order rate constants | | |
| Volatilization ($hr^{-1}$) | $1 \times 10^{-4}$ | 0 |
| Photolysis ($hr^{-1}$) | 0 | 0 |
| Oxidation ($hr^{-1}$) | 0 | 0 |
| Hydrolysis ($hr^{-1}$) | 0 | 0 |
| Biodegradation ($hr^{-1}$) | 0 | 0 |

## TABLE A.42. NINE-COMPARTMENT COMPUTER MODEL INPUTS FOR MIREX: RIVER SIMULATION

| | Water compartments | | | Sediment compartments | | |
|---|---|---|---|---|---|---|
| | 1 | 2 | 3 | 7 | 8 | 9 |
| Sorption partition coefficient | $3 \times 10^5$ | $3 \times 10^5$ | $3 \times 10^5$ | $3 \times 10^5$ | $3 \times 10^5$ | $3 \times 10^5$ |
| Pseudo-first-order rate constants | | | | | | |
| Volatilization ($hr^{-1}$) | $1.4 \times 10^{-3}$ | $1.4 \times 10^{-3}$ | $1.4 \times 10^{-3}$ | 0 | 0 | 0 |
| Photolysis ($hr^{-1}$) | 0 | 0 | 0 | 0 | 0 | 0 |
| Oxidation ($hr^{-1}$) | 0 | 0 | 0 | 0 | 0 | 0 |
| Hydrolysis ($hr^{-1}$) | 0 | 0 | 0 | 0 | 0 | 0 |
| Biodegradation ($hr^{-1}$) | 0 | 0 | 0 | 0 | 0 | 0 |

## TABLE A.43. NINE-COMPARTMENT COMPUTER MODEL INPUTS FOR MIREX: EUTROPHIC AND OLIGOTROPHIC LAKE SIMULATIONS

| | Water compartments | | | | Sediment compartments | | |
|---|---|---|---|---|---|---|---|
| | 1 | 2 | 3 | 5 | 7 | 8 | 9 |
| Sorption partition coefficient | $3 \times 10^5$ | $3 \times 10^5$ | $3 \times 10^5$ | $3 \times 10^5$ | $3 \times 10^5$ | $3 \times 10^5$ | $3 \times 10^5$ |
| Pseudo-first-order rate constants | | | | | | | |
| Volatilization ($hr^{-1}$) | $3.5 \times 10^{-4}$ | $3.5 \times 10^{-4}$ | $3.5 \times 10^{-4}$ | 0 | 0 | 0 | 0 |
| Photolysis ($hr^{-1}$) | 0 | 0 | 0 | 0 | 0 | 0 | 0 |
| Oxidation ($hr^{-1}$) | 0 | 0 | 0 | 0 | 0 | 0 | 0 |
| Hydrolysis ($hr^{-1}$) | 0 | 0 | 0 | 0 | 0 | 0 | 0 |
| Biodegradation ($hr^{-1}$) | 0 | 0 | 0 | 0 | 0 | 0 | 0 |

Appendix B

# EXPERIMENTAL PROCEDURES

The first four sections of this appendix supplement the descriptions of the general laboratory procedures that were given in Part I of this report. The remaining sections give the specific experimental conditions for each chemical studied. These sections are conveniently numbered to coincide with the section number for that chemical in the body of the report. For example, Section B.4 gives the specific experimental conditions for p-cresol, which is discussed in Section 4 of Part II.

## B.1 PHYSICAL TRANSPORT

### B.1.1 Solubility

The general procedure described by Campbell (1930) was used to measure the solubilities of solids in the μg ml$^{-1}$ range. A small amount of the solid substrate is placed in an all-glass apparatus, which is immersed in a water bath and shaken gently. This apparatus has two compartments separated by a glass frit. When the flask is inverted, the aqueous solution is filtered through the frit to remove solid substrate. The filtration step can be carried out without removing the apparatus from the water bath. After equilibration in the water for several days, the sample is filtered in the apparatus and the filtrate is analyzed for the substrate.

Generally, at least three measurements are made. Also, measurements are made on samples that have been heated to 35° to 40°C, allowed to equilibrate, and then cooled in the water bath. Since the concentrations are fairly high, potential problems that are encountered with low-solubility materials, such as adsorption onto the frit during filtration and the possibility that finely divided particulate substrate is not removed during filtration, are not likely to be significant.

Solutions of compounds having a solubility in the ng ml$^{-1}$ range were prepared by the procedure described by Haque and Schmedding (1975). The substrate is dissolved in an organic solvent and put on the walls of a 5-gallon (18.8 liter) carboy. The carboy is rotated slowly on its side while the solvent evaporates, so that a thin film of substrate coats the wall of the carboy. A large Teflon-coated magnetic stirring bar is added, and the carboy is filled with the purest water available. Care must be taken to prevent the substrate from coating the bottom of the carboy so that it is not dislodged by the stirring bar. The solution is allowed to stir gently for at least a week to assure that equilibration has taken place. Samples of water are withdrawn with a glass siphon and analyzed for the substrate.

In several cases, we found that even with these precautions particulate matter, presumably substrate, could be observed in the carboy, and the substrate concentration was reduced by centrifugation at 10,000 rpm. The solubility measurements of low-solubility (less than 0.1 $\mu$g ml$^{-1}$) compounds should be made on centrifuged samples.

### B.1.2 Absorption Spectra

Pure water was used as the solvent for measurement of absorption spectra whenever possible. However, it was often necessary to increase the solubility by adding a water-soluble cosolvent, such as acetonitrile. The general procedure was to prepare a substrate solution of a minimum of about $10^{-5}$ M in water, using acetonitrile to dissolve any solid, undissolved substrate. Some trial and error was required to minimize the amount of acetonitrile. The absorption spectra were measured in 1-cm and 10-cm cells on a Cary model 14 spectrophotometer. To obtain satisfactory spectra with 10-cm cells, we always ran solvent versus solvent to obtain a baseline. Then, the cell containing solvent in the sample beam was refilled with the substrate solution, and the absorption spectrum was measured. Suitable standards were prepared to assure that the same absorbance was obtained in the 10-cm cell with a solution that was one-tenth the concentration used in the 1-cm cell.

The molar extinction coefficients $\varepsilon_\lambda$ are obtained from Beer's law.

$$\text{Absorbance} = -\log \frac{I}{I_o} = \varepsilon_\lambda \ell S \qquad \text{(B-1)}$$

where $I_o$ is the incident light flux and I is the transmitted light flux in the spectrophotometer. If $\ell$, the cell path length, is in centimeters and if S, the substrate concentrations, is in M, then the molar extinction coefficient $\varepsilon_\lambda$ is in units of cm$^{-1}$ M$^{-1}$. The average molar extinction coefficient for each nominal wavelength is calculated from the average of the molar extinction coefficients at the lower and upper limits of the wavelength interval (Table B.1).

TABLE B.1. NOMINAL WAVELENGTHS AND WAVELENGTH INTERVALS FOR UV AND VISIBLE ABSORPTION SPECTRA

| Nominal wavelength (nm) | Wavelength interval (nm) |
|---|---|
| 297.5 | ± 1.25 |
| 300.0 to 320.0 | ± 1.25 |
| 323.1 | ± 1.9, - 1.85 |
| 330.0 | ± 5.0 |
| 340.0 and higher | ± 5.0 |

*The actual precision of a measured wavelength is about ± 0.5 nm.

### B.1.3 Volatilization Rates

Volatilization rates were measured using the method described by Hill et al. (1976). A solution of the substrate in pure water was prepared at a concentration that is below its saturation value. About 1 liter of this solution was placed in a 2-liter beaker equipped with a stirring bar. The solution was purged with nitrogen to remove most of the dissolved $O_2$. At the start of the experiment ($t = 0$), the concentration of substrate was measured and the $O_2$ concentration was measured with a Delta model 2010 $O_2$-analyzer. Successive substrate and $O_2$ measurements were made at regular time intervals.

The substrate concentration versus time data were then fit to an exponential decay curve of the form

$$[S_t] = [S_o]e^{-k_v^S t} \tag{B.2}$$

which is the integrated form of the first-order rate expression

$$-\frac{dS}{dt} = k_v^S[S] \tag{B.3}$$

The oxygen concentration data are fit to the integrated form of equation (B.4)

$$\frac{d[O_2]}{dt} = k_v^O\ ([O_2]_{sat} - [O_2]t) \tag{B.4}$$

which is

$$[O_2]_t = [O_2]_{sat} - \left( [O_2]_{sat} - [O_2]_o \right) e^{-k_v^O t} \tag{B.5}$$

where $[O_2]_{sat}$ is the saturation concentration of $O_2$ in water at the temperature of the measurement and is a constant because the concentration of $O_2$ in the air is constant.

The linear least squares routine supplied with the Hewlett-Packard Model 65 calculator was used to calculate values of $k_v^O$ and $k_v^S$. This program gives a linear least squares fit to lnS versus t, plus the variance of the parameter estimates. The value of $k_v^S/k_v^O$ was calculated from these values.

### B.1.4 Sorption

Preparation of Ca-Montmorillonite and Natural Sediments--The montmorillonite clay used in these studies was a Wyoming montmorillonite obtained from Dr. William John, Department of Geology, University of Missouri, Columbia, Missouri. Clay suspensions (about 1% by weight) were prepared by soaking a measured weight of clay in distilled-deionized water for at least one week. The clay suspension was then passed through an ion exchange column that had been presaturated with calcium ions to convert the clay from the sodium form to the calcium form. This was necessary because the Na-montmorillonite suspension could not be centrifugedbut the Ca-montmorillonite could. The particle size was less than 1 μm.

The procedures used to prepare and store the natural sediments were designed to preserve the sediments in their natural state as well as possible. Natural sediments were screened to remove large rocks, twigs, and other debris. The mesh sizes of the screens used were 4, 16, and 28 per 2.54 cm. Following the screening, the sediment was mixed, using a Humbolt splitter to be sure the sediment was uniform. A small volume of each sediment was mixed with two volumes of 0.1 M calcium chloride and the pH was recorded. The remainder of the screened and split sediment was stored in 100-ml Nalgene bottles at 4°C until use. The sediments were never allowed to dry out, and no attempts were made to kill or remove the bacteria in the sediments. Before use, the sediment was resuspended in water and allowed to settle for 30 seconds. The sediment was then transferred as a slurry using a pipet.

The characteristics of the Ca-montmorillonite clay and natural sediments used in these studies are given in Table B.2. The organic carbon (OC) values, expressed as percent carbon by weight, were determined using the Walkley and Black procedure, which involves oxidation of the organic material by chromate followed by back-titration with ferrous ammonium sulfate (Hesse, 1971).

TABLE B.2. SOURCES AND CHARACTERISTICS OF Ca-MONTMORILLONITE CLAY AND NATURAL SEDIMENTS

| Source | Location and description | Sediment pH | OC[a] (%) | Cation exchange capacity (meq/100 g) |
|---|---|---|---|---|
| Wyoming | Ca-montmorillonite clay | -- | 0.05 | 69.0 |
| Navarro River | Mendocino County, California An unpolluted river that drains redwood forests, orchards, and pasture | 6.7 | 0.5 | 4.5 |
| Des Moines River | Iowa | 7.1 | 0.8 | 10.5 |
| Oconee River | Georgia | 6.2 | 0.8 | 8.5 |
| Coyote Creek | San Jose, California A eutrophic, polluted stream | 6.5 | 1.9 | 13.5 |
| Searsville Pond | Woodside, California A small eutrophic but unpolluted pond | 6.7 | 5.0 | 34.5 |

[a] Organic carbon, Walkley and Black values, corrected for recovery by multiplying experimental value by 1.33.

Sorption isotherm measurements--In most cases, the clay and sediment isotherm measurements were made at two sediment loadings and two substrate concentrations. Replicate flasks were used at each level, and at least three analyses of each flask were made. Suitable blanks of both sorbent and substrate were carried through the experimental steps and analyzed. Contact times of 1 to 16 hours were used. There were no experimental problems in the sediment sorption studies with the 16-hour time, except for p-cresol, which biodegraded rapidly during the experiment. In that case, a 1-hour exposure was used. For the biosorption studies, the partitioning time was about 1 hour. At longer times, sorption by the glassware was a problem with low-solubility substrates.

As the experiments progressed, the experimental plan for the isotherm measurements evolved into the experimental plan described in Table B.3. We consider this to be the minimum number of data points that will permit a sound statistical analysis of the data.

TABLE B.3. RECOMMENDED EXPERIMENTAL PLAN FOR ISOTHERM MEASUREMENTS

| Substrate concentration | Number of flasks[a] | | |
|---|---|---|---|
| | No sediment | Low sediment | High sediment |
| None | 1 | 2 | 2 |
| Low | 2 | 2 | 2 |
| High | 2 | 2 | 2 |

[a] Four replicate measurements of the substrate concentration at equilibrium in each flask should be made.

The mechanics of the isotherm measurements were generally the same whether the sorbent was Ca-montmorillonite clay, a natural sediment, or our bacterial mixture. A solution* of the substrate in water was prepared. An aliquot of the substrate solution and an aliquot of a suspension of the sorbent were mixed and allowed to shake for a specified period of time. The mass of dry sorbent used was determined, normally by a gravimetric procedure, in a separate experiment. A portion of the mixture was centrifuged to separate the substrate remaining in solution and the sorbent. The supernatant and usually the sorbent were analyzed separately to measure the substrate concentration.

Statistical Analysis of Isotherm Data--The data were fit to the Freundlich isotherm equation with n = 1,

$$S_s = K_p S_w \tag{B.6}$$

---

* The importance of using true solutions below the substrate solubility limit cannot be overemphasized, especially with low-solubility substrates.

The value of $S_w$ was always measured. If $S_s$ was not measured independently, then it was claculated from

$$S_s = (S_o - S_w)V_w/m_s \tag{B.7}$$

where $S_o$ is the initial concentration of substrate used (determined from the concentration in flasks without sorbent), $V_w$ is the volume of solution (in ml), and $m_s$ is the mass of sediment (in grams) added to the flask. Preliminary estimates of $K_p$ were obtained by two methods: when only $S_s$ was measured, every concentration measurement was used, and when both $S_s$ and $S_w$ were measured, average $S_s$ and $S_w$ were calculated for each flask. In both cases the data were then fit to an equation of the form

$$y = bx \tag{B.8}$$

(notice the similarity to equation B.6, using a linear least squares regression method. The regression equations are:

$$b = \frac{\Sigma x_i y_i}{\Sigma x_i^2} \tag{B.9}$$

$$S_{yx} = \left\{\left[\Sigma y_i^2 - \frac{\left(\Sigma x_i y_i\right)^2}{\Sigma x_i^2}\right](n - 1)^{-1}\right\}^{\frac{1}{2}} \tag{B.10}$$

$$r^2 = \left[- \frac{1}{n}(\Sigma y_i)^2 + \frac{\left(\Sigma x_i y_i\right)^2}{\Sigma x_i^2}\right]\left[\Sigma y_i^2 - \frac{1}{n}(\Sigma y_i)^2\right]^{-1} \tag{B.11}$$

$$95\% \text{ confidence interval} = \left(t_{n-1,\alpha}\right) S_{yx}\left(\Sigma x_i^2\right)^{\frac{1}{2}} \tag{B.12}$$

where $b = K_p$ is the slope, $x_i$ and $y_i$ are the individual or average measurements from each flask of $S_w$ and $S_s$, respectively, $S_{yx}$ is the standard error, $r^2$ is the correlation coefficient, and $t_{n-1,\alpha}$ is the t-value from Student's t-test for n measurements at $\alpha - 0.05$ confidence. These expressions were programed and used on an Hewlett-Packard model 65 calculator.

To test that the linear Freundlich isotherm (n = 1, equation B.6) does pass through the origin, the data were fit to a linear equation of the form

$$S_s = K_p S_w + a_o \tag{B.13}$$

where $a_o$ is the intercept. The HP-65 Stat-Pac routine was used to estimate the 95% confidence intervals about $a_o$. If these confidence intervals include the origin, then equation (B.6) was used.

The limitations of the linear method can be removed by stating the problem as:

- When sorbent is present

$$S_w = \frac{S_i - \hat{a}_o}{1 + M_s \hat{K}_p / V_w} \; ; \; i = h \text{ or } \ell \qquad (B.14)$$

- When sorbent is not present

$$S_w = S_i \; ; \; i = h \text{ or } \ell \qquad (B.15)$$

The hat on a variable indicates that its value is estimated by the regression procedure. $\hat{S}_i$ is equivalent to $S_o$ and represents the original amount of substrate present in each flask, $\hat{S}_h$ being the concentration in flasks with the high amount of substrate and $\hat{S}_\ell$ being the concentration in flasks with the low amount of substrate. $M_s$ represents the amount (grams) of sorbent present. In this procedure, $\hat{S}_h$ or $\hat{S}_\ell$ was estimated using all the flasks as in the linear method.

Since each flask was handled separately and at a different time, the above procedure was modified to include "flask effects" as an estimated parameter. Flask effects include such things as biases due to instrument drift and systematic errors on the part of the analyst. The resulting problem formulation is suitable for input to a nonlinear regression program that estimates values for $S_h$, $S_\ell$, $a_o$, $K_p$, and the flask effects. The actual results of the nonlinear regressions are comparable to the estimates obtained from the linear least squares regressions, except that the nonlinear approach gives smaller confidence limits for the parameter estimates.

The Biomedical Statistical Series nonlinear regression program BMD07R performed the regression indicated above by equations (B.14) and (B.15). BMD07R executes a user-supplied FORTRAN subroutine to compute the estimate of the dependent variable and its first derivatives with respect to the regression parameters for each observation. The data available to the subroutine consisted of $S_w$ and $M_s/V_w$ augmented by dichotomous dummy variables indicating the presence or absence of sorbent, the amount (high or low) of substrate, and the flask measured (one of two flasks). These dummy variables controlled the computation of the dependent variable estimate for each observation by one of the two regression equations (B.14) or (B.15).

When both $S_s$ and $S_w$ were measured, the linear least squares procedures using average values for $S_s$ and $S_w$ are not statistically correct because again response variables appear on both sides of the regression equation. In addition, the averaging procedure throws away valuable information about experimental variance. To deal more correctly with this situation, eight simultaneous nonlinear regression equations were used. Four regressions use only the substrate concentrations measured on the sediment from the various flasks.

$$S_s = \hat{K}_p \hat{S}_i \qquad i = 1, 2, 3, 4 \qquad (B.16)$$

and four regressions use only the concentrations measured in the supernatant, $S_w$,

$$S_w = \hat{S}_i \qquad i = 1, 2, 3, 4 \qquad \text{(B.17)}$$

where $S_i$ is the estimated value of substrate concentration in a particular flask. With this formulation, the response variables appear only on the left-hand side of the regression equation. The subscript "i" on the right-hand side is the independent variable, since it indicates the conditions used to set up the flask. For example, i = 1 indicates the two duplicate flasks that contained high sediment and high substrate concentrations. The common parameters $\hat{K}_p$ and $\hat{S}_i$ tie the simultaneous regressions together and assure that the resulting estimate for $K_p$ is conditioned on both the sediment and supernatant concentrations measured.

The method is superficially similar to the simple linear least squares procedure used to estimate $K_p$. The regression equations (B.17) use the supernatant concentrations to estimate a single concentration that best represents the concentration in the flasks for each different substrate and sediment level. This representative concentration is then used with the concentration of substrate on the sediment in equations (B.16) to estimate $K_p$. An important difference between the two approaches, however, is that, with the nonlinear approach the supernatant concentration, $S_i$, that represents a particular substrate and sediment level is not necessarily the average supernatant concentration. The values of $\hat{S}_i$ determined by the method are almost always very close to the average except when concentration measurements are highly scattered.

BMD07R also performed the regression indicated by equations (B.16) and (B.17) above. In this case the data available to the dependent variable estimation subroutine was augmented by dichotomous dummy variables indicating substrate or supernate measurement of $S_i$, sediment levels (low or high), and a flask indicator (one of two flasks). These variables controlled the regression equation (B.16) or (B.17) used to estimate the dependent variable for each observation.

An important feature of nonlinear approach is that it does not require that the same number of observations of both $S_s$ and $S_w$ be made in each flask. The formulation also does not require that individual measured values of $S_s$ and $S_w$ from a particular flask be paired (see equation B.6). This is an important feature because any pairing of data points is artificial and could bias the estimate of $K_p$.

Biosorption and Desorption--Biosorption and desorption studies were conducted with mixtures of four species of gram-positive and gram-negative aquatic-origin bacteria. The mixtures contained equal optical densities of *Azotobacter beijerinckii* ATCC 19366, *Bacillus cereus* ATC 11778, *Escherichia coli* ATC 9637, and *Serratia marcescens* ATCC 13880. In the early stages of this program, *Flavobacterium capsulatum* ATCC 14666 was used, but because this organism was difficult to centrifuge to a compact pellet and clear supernatant, it was replaced with the above indicated *Serratia marcescens*.

The test organisms were transferred several times in Trypticase-Soy broth at 25°C before they were used for sorption studies. Sixteen-hour cultures were either in the late logarithmic or early stationary growth phases. At this stage, each culture was harvested by centrifuging, washed with 0.05% potassium phosphate buffer (pH 7.0), resuspended and diluted with this buffer until the suspension had an optical density of 2 to 4.

Appropriate aliquots of suspensions of each of the four organisms were combined and diluted with buffer to form a mixture containing equal optical densities of each organism and a mixture that, when mixed with the solution of the substrate, resulted in the desired concentration and organisms. With substrates having a low solubility, the density of the bacterial mixture was lower than with more soluble substrates.

In some instances, biosorption studies were also conducted with heat-killed cells. Consequently an aliquot of the above mixture of organisms was heated at 100°C for 15 minutes, cooled, and centrifuged. The resulting pellet was resuspended in fresh buffer to the original volume, and an appropriate volume of this suspension was diluted as above with a solution of the substrate under study to yield the corresponding cell densities and substrate concentrations.

Biosorption studies were conducted by incubating the viable and heat-killed cell mixtures in Corex centrifuge tubes or bottles for 1 hour at 25°C. Cells were maintained in suspension by placing the containers in roller drums or on a rotary shaker. The tubes or bottles were centrifuged for 10 minutes at 12,000 or 16,000 G, respectively, and the supernatants were carefully decanted. The supernatants were extracted with an organic solvent (usually ethyl acetate). The solvent extract was dried and then assayed directly or concentrated before assay. To assay sorbed substrate in the pellets, water was added and this suspension was solvent extracted as above. With some substrates that were tenaciously retained by the cell pellets, the water-suspended cells in the presence of some solvent were slowly frozen and thawed three times before extraction.

Desorptions were conducted only if the sorption partition coefficients were 10,000 or more. The cell pellets from replicate sorption studies were suspended in volumes of buffer or buffer and solvent equivalent to those used for sorptions, incubated with shaking at 25°C for 3 hours, and centrifuged. Both supernatants and pellets were analyzed by the procedures used for sorption determinations.

In some cases, corrections were made for sorption on glassware of substrate and cultures containing sorbed substrate. Separate controls consisted of extraction of tubes from which the incubated suspensions in test substrate solutions were decanted in lieu of separation of cells by centrifuging.

Dry weights of cells used in sorption studies were determined by weighing the pellet obtained after cells from aliquots of mixed viable or heat-killed bacterial suspensions were centrifuged, washed with distilled water, and dried for 16 hours at 90-95°C.

The biosorption partition coefficients of chemicals between bacteria and buffer were determined as

$$K_p = \frac{\mu\text{g substrate per g dry wt of cells}}{\mu\text{g substrate per ml in supernatant}} \qquad (B.18)$$

Purification of Humic Acid--The humic acid (Fluka AG, Buchs SG, distributed by Tridom Chemical, Inc.) was dissolved in 0.1 N NaOH and centrifuged 45 minutes at 10,000 rpm. The supernatant was decanted off; the solids were resuspended in 0.1 N NaOH and centrifuged again for 45 minutes at 10,000 rpm. The supernatant was added to the previous batch and the combined solution filtered twice through glass fiber filters, then through a 0.45-μm Millipore HA filter at 40 psig until a flow rate of 1 ml $\text{min}^{-1}$ was obtained. The filtrate was returned to the filter and refiltered at 350 psig. The filtrate was then placed in a presoaked 0.98-inch-diameter dialysis tube (Union Carbide) and put into running deionized water for 24 hours. The solution was then passed through an OH-saturated amberlite IRA-400 exchange column, then through an H-saturated amberlite IR-120 exchange column to neutralize the humic acid. This solution was stored in a refrigerator and diluted just prior to use in the photochemical studies (Section B.2.2 of this Appendix).

## B.2 CHEMICAL TRANSFORMATION

### B.2.1 Preparation of Reaction Solutions

Solutions of chemicals were prepared in pure water and natural waters. All glassware used was routinely baked out overnight at 580°C. Pure water was obtained from a Millipore water purification system. The first stage of this system purifies tap water by reverse osmosis (Milli-RO-4); the second stage uses a Milli-Q system in which the water is passed through a carbon filter, two ion exchange filters, and finally a 0.22-μm cellulose ester filter. The filter-sterilized water obtained typically shows greater than 18 Mohm-cm resistivity and less than 1 μg $\text{ml}^{-1}$ total organic carbon (below detectable limit of instrument).

Natural waters were obtained from Coyote Creek, Searsville Pond, and Lake Tahoe. These waters were filtered through 0.22-μm filters before preparation of the solutions to sterilize the waters and to remove any heterogeneous components from solution. The latter was a precaution to ensure that no adventitious processes due to heterogeneity occurred in the solution kinetics processes being measured. Some water quality parameters for these filtered waters are given in Table B.4.

Reaction solutions were usually prepared from a stock solution of the chemical in acetonitrile. An aliquot of this stock solution was diluted with an amount of water to give a 1% or 0.1% acetonitrile in water solution. Preparation of the stock solution and subsequent dilutions were made to obtain 1 μg $\text{ml}^{-1}$ or less concentration of chemicals. As discussed in Part I of this report, 1% acetonitrile does not have any significant effect on the kinetic processes under study; the presence of 1% acetonitrile was sufficient to produce usable concentrations of chemicals for our kinetics experiments. When the solubility of the chemical in water was high enough, water was used as the sole solvent. When the solubility of a chemical in a solution was uncertain, the absence of light scattering from a beam of green light or a $CO_2$ laser passed through the solution was interpreted as indicating a homogeneous solution (i.e., free of particulates).

TABLE B.4. SOME WATER QUALITY PARAMETERS[a] FOR 0.22-μm FILTERED WATER FROM SEARSVILLE POND, COYOTE CREEK, AND LAKE TAHOE

| | Total organic carbon (mg ml$^{-1}$) | Total inorganic carbon (mg ml$^{-1}$) | Iron (mg ml$^{-1}$) | Copper (mg ml$^{-1}$) | Total Hardness (mg ml$^{-1}$) |
|---|---|---|---|---|---|
| Searsville Lake | 10 | < 10 | 0.010 | 0.024 | 700 |
| Coyote Creek | 7 | < 7 | 0.030 | 0.014 | 280 |
| South Lake Tahoe | 2 | < 2 | 0.020 | < 0.005 | 28 |

[a] Analyses were made by LFE Environmental Analysis Laboratories, Richmond, CA.

Except for the experiments with quinoline and p-cresol, all analyses were performed by high pressure liquid chromatography (HPLC) on a Waters Associates chromatograph apparatus (Model 6000A pump, MV6K injector, and a M440 absorbance detector). Separations were made with a 30 cm x 4 mm μBondapak $C_{18}$ column (reverse phase). The solvent eluent composition, UV detector wavelength, and internal standard, if any, are given below in the sections for the specific chemical. Peak areas in the HPLC traces were determined on a SpectraPhysics Autolab Minigrator.

Data for concentration as a function of time were fit to a first-order kinetic rate law using a computer least squares program. The first-order kinetic rate constants and the standard deviations are presented in the respective sections on the chemicals in the body of the report.

### B.2.2 Photochemical Studies

Laboratory Photolyses--Reaction mixtures of the chemical (4 ml) were placed in 10-mm-O.D. borosilicate tubes (Pyrex 7740) and photolyzed on a merry-go-round reactor (Ace Glass). The irradiation source was a Hanovia 450-watt, medium-pressure Hg lamp contained in a borosilicate immersion well. The distance between the irradiation source and tubes was about 10 cm. The reaction temperature was at the ambient operating temperature of the system (~28°C).

The photolyses were carried out using several different filter systems, which were placed between the Hg lamp and reaction mixtures. In all laboratory photolyses, the borosilicate glass immersion well (8-mm total glass path length) served as a filter to screen out all light below 290 nm. The filter systems used in the photolyses are described below.

- 313 nm filter system: Corning CS 7-54 glass filter with a 0.001 M potassium chromate solution in 3% aqueous sodium carbonate circulated in the immersion well. This system transmitted primarily the 313.2 and 312.6 nm Hg lines, which represented greater than 95% of the light incident on the reaction solutions (a small Hg line at 302.2 nm was also present).*
- 366 nm filter system: Corning glass CS 0-52 and CS 7-60 glass filters. This pair of glass filters transmitted only the 365.1, 365.6, and 366.4 nm lines of the Hg lamp, with no other lines observed (less than 1% of light outside the 366 nm band).*
- Borosilicate glass only: This system used only the immersion well as filter and was employed only for p-cresol and benzo[b]thiophene experiments. Examination of the transmitted light showed that, in the region where these compounds absorb (less than 330 nm), the same two Hg lines were present as described above for the 313 nm system, but the filters did affect the relative intensities of the lines.*

Sample tubes were removed from the merry-go-round reactor at appropriate times and immediately analyzed.

The quantum yield ($\phi$) was calculated from the photolysis rate constant $k_p$, obtained from the slope of the first-order plot of photolysis data using the following equation:

$$k_p = 2.303\, \varepsilon_\lambda\, I_\lambda \phi \ell = d(\ln C_o/C)/dt \tag{B.19}$$

where $\varepsilon_\lambda$ is the absorption coefficient of chemical at wavelength $\lambda$, $\ell$ is the pathlength, and $I_\lambda$ is measured as above. The value of $I_\lambda$ is constant for the system since the same tubes were used in both the actinometry and in the chemical photolyses. Any differences produced by reflection effects in using the tubes should be negligible.

The photochemical system was calibrated at 313 nm and at 366 nm wavelengths using the o-nitrobenzaldehyde actinometer system (Pitts et al., 1968; Calvert and Pitts, 1966). In these calibration experiments, a solution of approximately $1 \times 10^{-2}$ M o-nitrobenzaldehyde in acetonitrile was photolyzed in the borosilicate tubes for reaction times of up to 10 minutes at either wavelength in the merry-go-round photochemical reactor. The solutions were analyzed for starting aldehyde using reverse phase HPLC with 50% acetonitrile in water as eluent. The light incident on the tubes was then calculated according to the method of Calvert and Pitts (1966), using a quantum yield for o-nitrobenzaldehyde photolysis of 0.50.

The light flux ($I_\lambda$) incident on the samples in the 10-mm-O.D. tubes at 313 nm was about $1 \times 10^{18}$ photons $sec^{-1}$ $liter^{-1}$, and at 366 nm about $6 \times 10^{18}$ photons $sec^{-1}$ $liter^{-1}$. It was necessary to check $I_\lambda$ frequently using the actinometer because the walls of the immersion well became dirty and diminished the light from the Hg lamp. Precautions were especially necessary when using the 313 nm filter system since the chromate solutions decomposed after irradiation times of several days.

---

*Light transmitted by the filters was determined with a grating monochromator.

The natural waters used in laboratory photolysis studies were not characterized with regard to the natural organic substances in them. Photolyses were carried out for each compound in a "synthetic" natural water made with pure water and the humic acid prepared as described in Section B.1.4. Several different humic acid solutions were used in these studies over the two years work. The absorbancies of these solutions at the particular wavelengths of interest (either 313 or 366 nm) are given in the sections on the individual chemicals in the body of the report.

As discussed in Part I of this report, the presence of light-absorbing natural materials in waters has a screening effect that makes the photolysis rate slower than in pure water solutions. To determine whether the natural substances exerted any other effect in the photolyses (such as photosensitization or excited state quenching), a screening factor was calculated using the expression (R.G. Zepp, private communication, 1977):

$$S_\lambda = \frac{1 - 10^{-\alpha\ell}}{2.303\ \alpha\ell} \qquad \text{(B.20)}$$

where $\alpha\ell$ is the absorbance when a 1-cm cell is used and $S_\lambda$ is the ratio of the rate when $\alpha\ell > 0.02$ to the rate when $\alpha\ell < 0.02$ (taken as pure water in this study). The product of $S_\lambda$ and the rate constant in pure water then gives the rate constant that should be observed if only a screening effect is operative, and with which the rate constant in natural waters should be compared. UV spectral data for the 0.22-μm filtered natural waters are given in Table B.5.

TABLE B.5. UV ABSORBANCE OF 0.22-μm FILTERED NATURAL WATERS

| | Absorbance in 1-cm cell, at wavelength λ(nm) | | | | | | | |
|---|---|---|---|---|---|---|---|---|
| Source | 280 | 300 | 313 | 325 | 350 | 366 | 375 | 400 |
| Coyote Creek (Collected July 1976) | 0.11 | 0.08 | 0.06 | 0.05 | 0.04 | 0.03 | 0.03 | 0.01 |
| Lake Tahoe (Collected April 1976) | ← | | | < 0.01 | | | | → |
| Searsville Pond | 0.14 | 0.09 | 0.07 | 0.05 | 0.02 | 0.02 | 0.01 | 0.01 |
| Aucilla River[a] | 0.95 | 0.76 | 0.65 | 0.56 | 0.41 | -- | 0.29 | 0.21 |

[a] Water from the Aucilla River in Florida was provided by Dr. R. G. Zepp and was used only in methyl parathion studies.

Sunlight Photolyses--Outdoor photolyses using sunlight were carried out with pure water solutions of each chemical to validate the computer calculation of half-life in sunlight based on measured values of $\varepsilon_\lambda$ and $\phi$. Sunlight photolyses require attention to placement of apparatus. Photolysed solutions were placed in a location free of excessive reflections from walls and windows and without morning and afternoon shadows. We used 11-mm-O.D. borosilicate tubes held in a rack at a 60° angle to the horizon; the tubes were made from the same glass stock used in the laboratory photolyses. These tubes are much more readily sealed for long exposure and, judging from the good agreement between computed and measured values for the half-life ($t_{1/2}$) in sunlight for most chemicals, are quite satisfactory for this purpose.

### B.2.3 Free Radical Oxidation

To screen the susceptibility of chemicals to free radical oxidation, the chemical was oxidized using 4,4'-azobis(4-cyanovaleric acid) (AA) as the source of free radicals. Solutions of chemicals of concentrations 1 $\mu$g ml$^{-1}$ or less were prepared in pure water that contained 1.00 x $10^{-4}$ M AA. The solutions, saturated with air by shaking, were placed in a 50°C water bath for 100 hours. Solutions of the chemical at the same concentration without AA were run simultaneously as controls under identical reaction conditions. The 100-hour reaction time corresponds to one half-life for AA. The solutions were then analyzed for starting chemical and products.

For chemicals that showed significant oxidation at 100 hours, the same experiment was repeated at shorter reaction times and to lower conversions. Data for the disappearance of the chemical as a function of time were then fit to a first-order rate law using a computer least squares program. This rate constant was used to estimate rate constants for free radical oxidation of chemicals in aquatic environments (see Section 6.3 in Part I of this report).

### B.2.4 Hydrolysis

Screening reactions for hydrolysis were carried out for mirex, as discussed in Section 14. The detailed hydrolysis studies of methyl parathion are described in B.13 and Section 13.

## B.3 BIODEGRADATION

The basic procedures used in evaluating biodegradability are described in Part I of this report and the minor variations are designated in the appropriate sections dealing with biodegradability studies on specific compounds.

The principal natural aquatic reservoirs used as representative sources for cultures were:

- A eutrophic pond near Searsville Lake in Woodside, California.
- Coyote Creek, a eutrophic stream in San Jose, California.

- Aeration effleunt from the Palo Alto, California, sewage treatment facility. The organic matter treated is primarily of domestic origin.
- Aeration effluent from the treatment plant in the Shell Oil Refinery, Martinez, California. This plant treats wastes that could have a great similarity to those that might be expected from a coal liquefaction plant.
- Aeration effluent from the sewage plant of the Monsanto Chemical Company installation in Anniston, Alabama, where parathion and methyl parathion are produced.
- Lake Tahoe, California, a large, deep, cold oligotrophic lake between California and Nevada.

The water quality from the two eutrophic sources varied considerably with the season but there is no means of avoiding this problem. In fact, this can be a positive factor in the results of our investigations when the results are compared with those obtained with the more regulated sewage or wastewater treatment plants. Arbitrarily, incubation temperatures of 25°C were selected for all incubations associated with waters other than Lake Tahoe. Samples from Lake Tahoe were all incubated at 15°C. The selection of the media for enrichment studies was also arbitrary. The high phosphate level (0.2%) was necessary to maintain a constant pH with many water sample that were incubated without any added substrate.

All enrichment processes were conducted under aerobic conditions with the initial water samples diluted 4:5 to provide a $KH_2PO_4$-$K_2HPO_4$ mixture (equivalent to 0.2%) for buffering at pH 7.0 and $(NH_4)_2SO_4$ or $NH_4NO_3$ (equivalent to 0.01%) nitrogen supplement. The concept was to use samples as large as possible. Enrichments were generally initiated with 5-liters of diluted water samples in 9-liter bottle fermentors, but where preliminary observations indicated a rapid development of biodegrading organisms, 1.2 liter of diluted samples was used in 2.6-liter Fernbach flasks incubated in rotatory action shakers with temperature control.

Rapid estimations of pollutant degradation were made by extracting with two volumes of solvent at acidic or neutral pH and then determining the UV absorption characteristics of the solvent extracts. The details of the procedures are indicated in each section dealing with a specific chemical in the body of the report. In some cases, this method was not applicable to the first incubations with water samples because of interfering UV absorbing compounds in the water sample.

The periods between transfers differed with the development of biodegrading cultures. Generally, subtransfers were made to basal salts/added compounds media in which test compounds were present at the original concentration and at an increased concentration.

## B.4 p-CRESOL

### B.4.1 Source

p-Cresol (99+% Aldrich "Gold Label") was used as received

### B.4.2 Physical Transport Experiments

Analysis--The 1-ml aqueous samples were extracted with 1 ml diethyl ether and analyzed directly by GC. Recovery was > 99%.

Instrument: Perkin-Elmer Model 3920, FID
Column: 3 m x 3 mm O.D. glass, packed with 10% FFAP on 80/100 mesh acid-washed Chromosorb W DCMS.
Column temperature: 190°C
Carrier gas: $N_2$ at 60 ml $min^{-1}$
Retention time: 4.75 min
Internal standard: o-cresol
Sensitivity: 1 ng

Volatilization rate--Solutions of p-cresol containing 5 μg $ml^{-1}$ were stirred in 2000-ml beakers. Aliquots were removed at suitable intervals over 121 hours and analyzed.

### B.4.3 Chemical Transformation Experiments

Analysis--Aqueous samples were extracted three times with equal volumes of ethyl acetate and analyzed directly by GC.

Instrument: Hewlett-Packard 700 GC, FID
Column: 3 m x 3 mm O.D. stainless steel packed with 10% FFAP on acid-washed Chromosorb W
Column temperature: 165°C
Carrier gas: $N_2$
Internal standard: p-nitrotoluene

### B.4.4 Biodegradation Experiments

Analysis--Aqueous samples and cells were extracted with two equal volumes of ethyl acetate, dried over $Na_2SO_4$, concentrated, and analyzed by GC.

Instrument: Hewlett-Packard 5711 GC, FID
Column: 1.8 m x 2 mm 10% DEGS on 80/100 mesh Chromosorb W(HP)
Column temperature: 175°C
Carrier gas: $N_2$ at 35 ml $min^{-1}$
Retention time: 6.36 min
Internal standard: 1,3,4,5,6,7,8-octahydroanthracene

## B.5 BENZ[a]ANTHRACENE

### B.5.1 Source

Benz[a]anthracene (Eastman) was used as received.

### B.5.2 Physical Transport Experiments

Analysis--Aqueous samples were analyzed by direct injection onto the HPLC column. The sample was first diluted by 25% with acetonitrile to minimize sorption onto the sample loop. The sample loop size was 3.5 ml.

Instrument: Du Pont Model 848; Aminco fluorescence detector
Column: 22 cm x 4.6 mm O.D. Du Pont Zorbax ODS
Mobile phase: 90% acetonitrile, 10% $H_2O$
Pressure: 2000 psig
Internal standard: phenanthrene

Sediments were extracted with ethyl acetate. A 20-μl sample was analyzed by HPLC using the above method, except that the mobile phase was 70% acetonitrile: 30% water at a pressure of 3000 psig.

Volatilization rate--A solution of benz[a]anthracene containing 4 ng $ml^{-1}$ was stirred in a 2000-ml beaker. Samples were removed at suitable intervals over a 24 hour period.

### B.5.3 Chemical Transformation Experiments

Analysis--Aqueous samples were analyzed by direct injection onto the HPLC column.

Instrument: Waters Associates Model 6000A; Model M440 UV detector at 280 nm
Column: 30 cm x 4 mm μBondapak $C_{18}$
Mobile phase: 80% acetonitrile, 20% water

### B.5.4 Biodegradation and Biosorption

Analysis--Aqueous samples and cells were extracted twice with equal volumes of ethyl acetate and analyzed by HPLC.

Instrument: Spectrophysics Model 3500 HPLC; fluorescence detector (Aminco) at 360 nm
Column: 30 cm x 4 mm μBondapak $C_{18}$
Mobile phase: 75% methanol, 25% water
Flow rate: 1.6 ml $min^{-1}$
Retention time: 280 seconds
Internal standard: benzo[a]pyrene
Detection limit: 9 ng

## B.6 BENZO[a]PYRENE

### B.6.1 Source

Benzo[a]pyrene (99+% Aldrich Gold Label) was used as obtained.

### B.6.2 Physical Transport Experiments

Analysis--For solubility studies, 1000 ml samples were extracted twice with 50 ml hexane and concentrated to 1 ml; 10 μl was analyzed by HPLC.

Instrument: Waters Associates Model 6000A; M440 UV detector at 254 nm
Column: 30 cm x 4 mm μBondapak $C_{18}$ (Waters Associates)
Mobile phase: 80% acetonitrile, 20% water
Flow rate: 3.6 ml $min^{-1}$
Internal standard: triphenylbenzene

Calcium montmorillonite clay isotherm supernatant solutions were extracted in the same manner and analyzed by HPLC using the following conditions:

Instrument: Du Pont Model 848; UV detector at 265 nm
Mobile phase: 99.5% hexane, 0.5% isopropanol
Pressure: 2000 psig
Column: 22 cm x 2 mm Zorbax SIL
Internal standard: triphenylbenzene
Sensitivity: 2 ng

Samples (100-ml) of the remaining sorption isotherm supernatant and volatilization solutions were extracted with 10 ml benzene and analyzed by HPLC:

Instrument: Du Pont Model 848; Aminco fluorometer detector
Column: 22 cm x 4.6 mm Zorbax ODS
Mobile phase: 100% methanol
Pressure: 800 psig
Internal standard: pyrene
Sensitivity: 500 pg

Volatilization rate--A solution containing 0.95 ng $ml^{-1}$ benzo[a]pyrene was stirred in a 2000-ml beaker for 72 hours; samples were removed periodically for analysis.

### B.6.3 Chemical Transformation Experiments

Analysis--Aqueous samples were analyzed by direct injection onto the HPLC column.

Instrument: Waters Associates Model 6000A; Model M440 UV detector at 254 nm
Column: 30 cm x 4 mm μBondapak $C_{18}$ (Waters Associates)
Mobile phase: 70% methanol, 30% water
Internal standard: 1,3,5-tris(4-methoxyphenyl)benzene

### B.6.4 Biodegradation and Biosorption Experiments

Analysis--Aqueous samples and cells were extracted with two equal volumes of ethyl acetate and analyzed by HPLC. Some samples were dried and concentrated before analysis.

Instrument: Spectraphysics Model 3500; Aminco fluorometer detector at 360 nm
Column: 30 cm x 4 mm μBondapak $C_{18}$ (Waters Associates)
Mobile phase: 85% methanol, 15% water
Flow rate: 1.6 ml $min^{-1}$
Retention time: 400 sec
Internal standard: chrysene
Sensitivity: 100 pg

## B.7 QUINOLINE

### B.7.1 Source

Quinoline (96% Aldrich) was purified by preparative gas chromatography before use.

### B.7.2 Physical Transport Experiments

Analysis--Aqueous 1-ml samples were extracted with 1 ml $CS_2$; 1-μl samples were analyzed by GC.

Instrument: Perkin-Elmer Model 3920, FID
Column: 6 ft x 1/8 in. 5% Carbowax 20M on 80/100 mesh Chromosorb W DCMS
Column temperature: 170°C
Carrier gas: $N_2$ at 60 ml $min^{-1}$
Retention time: 165 seconds
Internal standard: naphthalene (RT = 90 sec)

Volatilization rate--A solution containing 8 μg $ml^{-1}$ quinoline was stirred in a 2000-ml beaker. Samples were removed at suitable intervals over 100 hours.

### B.7.3 Chemical Transformation Experiments

Analysis--The pH of the aqueous samples was adjusted to be greater than 12; three extractions were made with equal volumes of ethyl acetate and analyzed by GC.

Instrument: Hewlett-Packard 5700; FID
Column: 300 cm x 0.32 cm 10% FFAP on A/W Chromosorb W
Column temperature: 165°C
Carrier gas: $N_2$
Internal standard: biphenyl

### B.7.4 Biodegradation and Biosorption Experiments

Analysis--Aqueous samples and cells were extracted with two equal volumes of ethyl acetate and analyzed by HPLC.

Instrument: SpectraPhysics Model 3500; Schoeffel Variable UV detector at 220 nm
Mobile phase: 60% methanol, 40% water
Column: 30 cm x 4 mm μBondapak $C_{18}$ (Waters Associates)
Flow rate: 1.6 ml $min^{-1}$
Retention time: 320 seconds
Sensitivity: 100 pg

## B.8 BENZO[f]QUINOLINE

### B.8.1 Source

Benzo[f]quinoline (Eastman) was used as received.

### B.8.2 Physical Transport Experiments

Analysis--The aqueous samples were diluted until they contained 57% acetonitrile; 0.75 ml was injected directly onto the HPLC column.

Instrument: Du Pont Model 848; UV detector at 254 nm
Column: 4.6 mm x 22 cm Zorbax ODS
Mobile phase: 90% methanol, 10% water
Pressure: 2000 psig
Internal standard: anthracene

Sediments were extracted with 15 ml ethyl acetate and concentrated to 1 ml. The extracts were analyzed under the conditions listed above.

Volatilization rate--A solution containing 12 μg $ml^{-1}$ benzo[f]quinoline was stirred in a 2000-ml beaker; samples were removed at suitable intervals over 104 hours.

### B.8.3 Chemical Transformation Experiments

Analysis--Aqueous samples were analyzed by direct injection onto the HPLC column.

Instrument: Waters Associates Model 660A; Model M440 UV detector at 254 nm
Column: 30 cm x 4 mm μBondapak $C_{18}$
Mobile phase: 75% methanol, 25% water

### B.8.4 Biodegradation and Biosorption Experiments

Analysis--Aqueous samples and cells were extracted twice with equal volumes of ethyl acetate and analyzed by HPLC.

Instrument: SpectraPhysics 3500; Schoeffel variable fluorescence detector at 360 nm
Column: 24 cm x 6 mm Spherisorb ODS (SpectraPhysics)
Mobile phase: 55% methanol, 45% water
Flow rate: 1.6 ml $min^{-1}$
Retention time: 190 seconds
Internal standard: anthracene
Sensitivity: 1 ng

## B.9 9H-CARBAZOLE

### B.9.1 Source

9H-Carbazole (99+% Aldrich) was recrystallized from methanol/ethyl acetate before use.

### B.9.2 Physical Transport Experiments

Analysis--In the solubility experiments, 5 ml of solution was extracted twice with 2 ml, and then 1 ml of ethyl acetate, and concentrated to 0.5 ml; 3-μl samples were analyzed by GC.

Instrument: Hewlett-Packard 5750; FID
Column: 10 ft x 1/8 in. 5% SE-30
Column temperature: programmed from 155° to 188°C at 8° $min^{-1}$
Carrier gas: helium at 45 ml $min^{-1}$
Retention time: 4 minutes
Internal standard: fluoranthene (RT = 6 minutes)
Sensitivity: 5 ng

Direct injection of 20-μl aqueous samples onto a HPLC column was used in the sorption isotherm and volatilization analyses.

Instrument: Du Pont Model 848; UV detector at 245 nm
Column: 4.6 mm x 25 cm Zorbax ODS
Mobile phase: 75% acetonitrile, 25% water
Pressure: 2000 psig (3.1 ml $min^{-1}$)

Volatilization rate--A solution of carbazole containing 0.6 $\mu g\,ml^{-1}$ was stirred in a 2000-ml beaker; samples were removed at suitable intervals over an 80-hour period.

### B.9.3 Chemical Transformation Experiments

Analysis--Aqueous samples were injected directly onto the HPLC column.

Instrument: Waters Associates Model 660A; Model M440 UV detector at 254 nm
Column: 30 cm x 4 mm μBondapak $C_{18}$ (Waters Associates)
Mobile phase: 55% acetonitrile, 45% water

### B.9.4 Biodegradation and Biosorption Experiments

Analysis--Aqueous samples and cells were extracted twice with equal volumes of ethyl acetate and analyzed by HPLC.

Instrument: SpectraPhysics Model 3500; SpectraPhysics UV detector at 254 nm and Aminco fluorometer at 254 nm
Column: 24 cm x 6 mm Spherisorb ODS (SpectraPhysics)
Mobile phase: 65% methanol, 35% water
Flow rate: 1.6 ml $min^{-1}$
Retention time: 360 seconds
Internal standard: anthracene
Sensitivity: 70 ng (UV), 6 ng (fluorometer)

## B.10 7H-DIBENZO[g,g]CARBAZOLE

### B.10.1 Source

7H-Dibenzocarbazole (98% Aldrich) was used as received.

### B.10.2 Physical Transport Experiments

Analysis--Solubility measurements were carried out by direct aqueous injection of 1 ml onto the HPLC column.

Instrument: Du Pont Model 848; Aminco fluorescence detector
Column: 24 cm x 6 mm Spherisorb ODS
Mobile phase: 95% methanol, 5% water

Volatilization and isotherm supernatant solutions were diluted until they contained 25% acetonitrile. They were analyzed by direct aqueous injection of 100 μl onto the HPLC column.

Instrument: Du Pont Model 848; Aminco fluorometer
Column: 4.6 mm x 22 cm Zorbax ODS

Mobile phase: 85% acetonitrile, 15% water
Pressure: 2000 psig

Sediments were extracted with 10 ml ethyl acetate and analyzed under the same conditions described above.

Volatilization rate--A solution of DBC containing 16 ng ml$^{-1}$ was stirred in a 2000-ml beaker; samples were removed at suitable intervals over a 5-day period.

### B.10.3 Chemical Transformation Experiments

Analysis--Samples were analyzed by direct aqueous injection onto the HPLC column.

Instrument: Waters Associates Model 660A; M440 UV detector at 254 nm
Column: 30 cm x 4 mm µBondapak $C_{18}$ (Waters Associates)
Mobile phase: 85% methanol, 15% water
Internal standard: triphenylbenzene

### B.10.4 Biodegradation and Biosorption Experiments

Analysis--Aqueous samples and cells were extracted with two equal volumes of ethyl acetate and analyzed by HPLC.

Instrument: SpectraPhysics Model 3500; Aminco fluorescence detector at 360 nm
Column: 30 cm x 4 mm µBondapak $C_{18}$ (Waters Associates)
Mobile phase: 80% methanol, 20% water
Flow rate: 1.6 ml min$^{-1}$
Retention time: 340 seconds
Internal standard: benzo[a]pyrene
Sensitivity: 50 pg

## B.11 BENZO[b]THIOPHENE

### B.11.1 Source

Benzo[b]thiophene (thianaphthene, Aldrich 97%) was recrystallized from methanol before use.

### B.11.2 Physical Transport Experiments

Analysis--Aqueous 2-ml samples were extracted twice with 0.9 ml $CS_2$ and the volume adjusted to 2 ml with $CS_2$; 4-µl injections were made onto the GC.

Instrument: Hewlett-Packard 5750; FID
Column: 6 ft x 1/8 in. 5% Carbowax 20M
Column temperature: 124°C
Carrier gas: He at 45.5 ml $min^{-1}$
Internal standard: naphthalene

Volatilization rate--Solutions of benzothiophene containing from 18 to 25 $\mu g\ ml^{-1}$ were stirred in 2000-ml beakers for 75 to 450 minutes. Samples were removed and analyzed at suitable intervals.

### B.11.3 Chemical Transformation Experiments

Analysis--Aqueous samples were injected directly onto the HPLC column.

Instrument: Waters Associates Model 6000A; M440 UV detector at 254 nm
Column: 30 cm x 4 mm μBondapak $C_{18}$ (Waters Associates)
Mobile phase: 55% acetonitrile, 45% water
Internal standard: phenanthrene

### B.11.4 Biodegradation and Biosorption Experiments

Analysis--In the biodegradation experiments, aqueous samples and cells were extracted with two equal volumes of ethyl acetate and analyzed by HPLC. Biosorption analyses were done in the same manner using hexane as extractant.

Instrument: SpectraPhysics Model 3500; Schoeffel variable UV detector at 228 nm
Column: 30 cm x 4 mm μBondapak $C_{18}$ (Waters Associates)
Mobile phase: 60% methanol, 40% water
Flow rate: 1.6 ml $min^{-1}$
Retention time: 380 seconds
Sensitivity: 500 pg

## B.12 DIBENZOTHIOPHENE

### B.12.1 Source

Dibenzothiophene (Aldrich 95%) was recrystallized from methanol before use.

### B.12.2 Physical Transport Experiments

Analysis--After adjustment to contain 25% acetonitrile, the aqueous samples were analyzed by direct injection onto the HPLC column. Sample size was 0.75 ml.

Instrument: Du Pont Model 848; UV detector at 254 nm
Column: 4.6 mm x 22 cm Zorbax ODS
Mobile phase: 80% acetonitrile, 20% water
Flow rate: 3.0 ml $min^{-1}$

Sediments were extracted with 15 ml ethyl acetate and concentrated to 1 ml before analysis using the above conditions.

Volatilization rate--Solutions of DBT ranging in concentration from 140 to 200 ng $ml^{-1}$ were stirred in 2000-ml beakers for 11 to 69 hours. Samples were removed at suitable intervals for analysis.

### B.12.3 Chemical Transformation Experiments

Analysis--Samples were analyzed by direct injection onto the HPLC column.

Instrument: Waters Associates Model 6000A; M440 UV detector at 254 nm
Mobile phase: 60% acetonitrile, 40% water
Column: 30 cm x 4 mm μBondapak $C_{18}$

### B.12.4 Biodegradation and Biosorption Experiments

Analysis--Aqueous samples and cells were extracted three times with equal volumes of ethyl acetate and analyzed by HPLC.

Instrument: SpectraPhysics Model 3500; SpectraPhysics 230 UV detector at 254 nm
Column: 24 cm x 6 mm Spherisorb ODS (SpectraPhysics)
Mobile phase: 55% methanol, 45% water
Flow rate: 1.6 ml $min^{-1}$
Retention time: 640 seconds
Internal standard: anthracene
Sensitivity: 20 ng

## B.13 METHYL PARATHION

### B.13.1 Source

Methyl parathion (Chem Services) was used as received.

### B.13.2 Physical Transport Experiments

Analysis--Aqueous 2-ml samples were extracted twice with 1 ml hexane; 5-μl samples were analyzed directly by GC. Recovery was 99+%.

Instrument: Perkin-Elmer Model 3920, FID
Column: 30% OV-1 on 100-120 mesh Gaschrom-Q
Column temperature: 190-195°C
Carrier gas: $N_2$ at 80 ml $min^{-1}$
Internal standard: Tributyl phosphate

Volatilization rate--A solution containing 7 $\mu g\ ml^{-1}$ methyl parathion was stirred in a 2000-ml beaker. Samples were removed at suitable intervals for analysis.

### B.13.3 Chemical Transformation Experiments

Analysis--Samples were analyzed by direct aqueous injection onto the HPLC column.

Instrumnet: Waters Associates Model 6000A; M440 UV detector at 280 nm
Column: 30 cm x 4 mm μBondapak $C_{18}$
Mobile phase: 50% acetonitrile, 50% water
Internal standard: *p*-nitrotoluene

Hydrolysis rate--One volume of methyl parathion in acetonitrile was diluted to 100 volumes with buffered or natural waters to give a $1.00 \times 10^4$ M (26.0 ppm) methyl parathion solution in 1% acetonitrile. More dilute solutions were prepared by an analogous procedure.

Buffered solutions were made using deionized-distilled water with buffer salts at the concentrations listed below. Buffers at 0.067 M in total phosphate salt were used in early studies but were replaced when catalysis by hydrogen phosphate dianion became evident. Acetate and borate buffers were used successfully with no catalysis problems. The following buffer solutions were used:

| | | |
|---|---|---|
| pH 3.00 | | 100 ml 0.067 M $NaH_2PO_4$, 0.50 ml 0.1 M $H_3PO_4$ |
| pH 5.00 | (a) | 100 ml 0.067 M $NaH_2PO_4$, 3.00 ml 0.067 M $K_2HPO_4$ |
| | (b) | 0.01 ml sodium acetate, acetic acid to adjust pH |
| pH 6.00 | | 88 ml 0.067 M $NaH_2PO_4$, 12.00 ml 0.067 M $K_2HPO_4$ |
| pH 7.00 | (a) | 39 ml 0.067 M $NaH_2PO_4$, 61.0 ml 0.067 M $K_2HPO_4$ |
| | (b) | Same solution diluted tenfold |
| pH 8.00 | (a) | 5.5 ml 0.067 M $NaH_2PO_4$, 94.5 ml 0.067 M $K_2HPO_4$ |
| | (b) | 0.01 ml $Na_2B_4O_7$ |
| pH 9.00 | (a) | 0.025 M $Na_2B_4O_7$, 0.001 ml acetic acid to adjust pH |
| pH 10.00 | | 0.010 M $Na_2B_4O_7$, 0.001 M NaOH to adjust pH |
| pH 11.25 | | 0.050 M $K_2CO_3$ |

All pH solutions were adjusted to the given pH values and were checked using a Coleman Model 39 pH meter calibrated against standard buffer solutions.

Reaction mixtures in volumetric flasks were immersed in a darkened, thermostated water bath at 20°, 40°, 50°, and 70°C. The solutions were prepared and the reactions were conducted in the dark, to prevent photolytic degradation, and were analyzed immediately after removal from the thermostated bath. Reactions were carried through at least two half-lives of methyl parathion to verify pseudo-first-order kinetics in each type of water and pH.

### B.13.4 Biodegradation and Biosorption Experiments

Analysis--Aqueous samples and cells were extracted with two equal volumes of ethyl acetate and analyzed directly by GC.

Instrument: Varian Associates Model 5711; AFIS (Varian Model 2740)
Column: 5 ft x 1/4 in. 4% SE-30 + 6% OV-210 on 80/160 mesh Gaschrom Q
Column temperature: 200°C
Carrier gas: $N_2$ at 33 ml $min^{-1}$
Retention time: 3.73 minutes
Internal standard: ethyl parathion
Sensitivity: 50 pg

## B.14 MIREX

### B.14.1 Source

Mirex (Chem Services) was purified by column chromatography through silica gel followed by sublimation.

### B.14.2 Physical Transport Experiments

Analysis--Aqueous 150-ml samples and sediments were extracted twice with 10 ml hexane, dried with sodium sulfate, and concentrated to 0.1 µl; 5-µl injections were analyzed by GC.

Instrument: Tracor Model 220; $Ni^{63}$ electron capture detector
Column: 5 ft x 1/8 in. OV-210
Temperature 180°C
Carrier and purge gas: 5% methane, 95% argon
Sensitivity: 10 pg

Special precautions were taken to avoid contamination of the samples: Glassware was cleaned by baking at 700°C and/or by multiple rinses in Milli-Q water and distilled-in-glass hexane.

For extraction, the distilled-in-glass hexane was further purified with fuming sulfuric acid, followed by neutralization with sodium bicarbonate, then redistillation over sodium sulfate. The sodium sulfate used to dry the extracts was purified by boiling 3 times for 10 minutes in excess distilled-in-glass hexane and drying at 100°C.

*Volatilization rate*--A solution of mirex containing 86 pg $ml^{-1}$ was stirred in a 2000-ml beaker for 60 hours; samples were removed at suitable intervals for analysis.

### B.14.3 Chemical Transformation Experiments

*Analysis*--Aqueous 100-ml samples were extracted twice with 50 ml distilled-in-glass hexane, dried with $Na_2SO_4$, and concentrated to 0.5 ml; 5-μl aliquots were analyzed by GC.

Instrument: Tracor Model 220, Coulson electrolytic conductivity detector
Column: 3 ft, 5% SE-30
Column temperature: 170°-220°C at 5° $min^{-1}$
Carrier gas: helium
Internal standard: aldrin

### B.14.4 Biodegradation and Biosorption Experiments

*Analysis*--Aqueous samples and cells were extracted twice with equal volumes of 40% isopropanol in hexane and analyzed by GC.

Instrument: Varian Model 5711, electron capture detector (Analog Technology, scandium foil)
Column: 5 ft x 2 mm 3% OV-17 on Gas Chrom-Q
Column temperature: 220°C
Carrier gas: $N_2$ at 30 ml $min^{-1}$
Internal standard: Methoxychlor
Sensitivity: 90 pg

Appendix C

# NATURAL WATER SOURCES

One goal of this research was to determine what comparisons can be made between experimental data obtained using several actual waters and sediments. To this end, screening and detailed studies were planned to include natural waters whenever possible. This appendix describes the sources of the natural waters and sediments to provide a more complete view of the types of waters our sources represent.

## C.1 LAKE TAHOE

Lake Tahoe is located in the Sierra Nevada at the California-Nevada border at 39° latitude. A recent article by Holm-Hansen et al. (1976) describes the chemical and biological characteristics of a water column in Lake Tahoe. This lake is large (499 $km^2$) and very oligotrophic. Surface temperatures vary from 7° to 20°C with season, with the temperature below 50 meters constant at about 6°C. Additional information regarding land use in the Tahoe watershed is available in an EPA study (Wise, 1975).

Water and sediment samples for our studies were taken about 30 meters offshore at Sugar Pine Point on the California side of the lake. Water samples were taken at several intermediate depths to 30 meters where the sediment sample was taken for biodegradation screening studies. Some water quality parameters for a sample of water that was filter-sterilized are given in Table B.4; UV spectral data for this water are given in Table B.5.

## C.2 COYOTE CREEK

Coyote Creek originates near the Blue Ridge and Pine Ridge areas of the coast mountain range in Santa Clara County, California. Fed by springs and runoff, Coyote Creek drains first into Coyote Reservoir and then into Anderson Reservoir. It continues below the reservoir and parallels U.S. Highway 101 for about 40 km until it enters the South San Francisco Bay delta system. The creek system runs through agricultural and light urban regions below the second reservoir until it passes through the City of San Jose near the bay. In the agricultural region, seasonal canning industries discharge some wastes into the creek.

Our samples were taken in a park near San Jose State University in San Jose, where the creek is about 3 meters wide and less than 1 meter deep. The water is eutrophic, and our water samples had a slight yellow coloration, much of which was removed by filtration. Water quality parameters for the filter-sterilized water are given in Table B.4; UV spectral data for this water are given in Table B.5. Characteristics of a sediment from Coyote Creek at our sampling point are given in Table 5.3 of Part I of this report.

## C.3 SEARSVILLE POND

Searsville Pond is an unofficial name that we assigned to our sampling location in a wetlands area near Searsville Lake. This is a light urban region about 6 km west of Menlo Park and the Stanford University campus. Most of the wetlands area was formerly a game refuge and is now part of the Jasper Ridge Biological Preserve of Stanford University. The wetlands area is fed by Alembique Creek, an intermittent, highly organic creek originating in the foothills of the coastal mountain range in San Mateo County.

Our sampling location was on the west side of a causeway over the wetlands area, where emergent vegetation surrounded about 2000 $m^2$ of open water, which we used as our sampling pond. After two years of low rainfall, this area dried up in the spring of 1977 after our laboratory studies had been completed. While the waters from this area were definitely eutrophic, there were no obvious anthropogenic discharges to either the pond or wetlands areas. The uplands surrounding the wetland are covered by a mosaic of oak-woodland, chaparral, and annual grassland vegetation.

Some water quality parameters and UV spectral data for a sample of filtered water are given in Tables B.4 and B.5, respectively. Characteristics of a sediment from this pond are given in Table 5.3 of Part I of this report.